

ABSTRACT

Title of Document: INVERSE FIRE MODELING TO ESTIMATE
THE HEAT RELEASE RATE OF
COMPARTMENT FIRES

Andrew Neviackas, Master of Science 2007

Directed By: Dr. Arnaud Trouvé
Department of Fire Protection Engineering

The objective of this research is to develop a new paradigm in fire-fighting techniques and demonstrate the feasibility of using fire imaging technology (*e.g.*, thermal imaging cameras to monitor smoke conditions from a burning building) combined with fire modeling software for real-time fire analysis to assist firefighter operations. This project focuses on the development of a prototype inverse fire modeling (IFM) algorithm. The IFM uses: MATLAB as the programming language; BRI2002 as the zone model; and a genetic algorithm for optimization. The IFM is tested as a stand-alone component in which the camera-based observations of smoke layer properties are replaced by data on the upper layer temperature (T_{UL}) coming from a reference BRI simulation with a certain heat release rate (HRR_{ref}). The objective of the IFM algorithm is then to provide an estimate of HRR_{ref} from the sole knowledge of T_{UL} . The performance of the IFM algorithm has been studied in a series of tests of gradually increasing complexity.

INVERSE FIRE MODELING TO ESTIMATE THE HEAT RELEASE RATE OF
COMPARTMENT FIRES

By

Andrew Neviackas

Thesis submitted to the Faculty of the Graduate School of the
University of Maryland, College Park, in partial fulfillment
of the requirements for the degree of
Masters of Science
2007

Advisory Committee:
Dr. Arnaud Trouvé (Advisor/Chair)
Dr. Marino di Marzo
Dr. James Milke

Acknowledgements

First of all I would like to express my deepest gratitude towards my advisor Dr. Arnaud Trouvé for all of his continuous assistance, supervision and support throughout the duration of this project. Without his guidance this research project would not have been possible. I would also like to thank the other members on my committee, Dr. Marino di Marzo for starting this project and for his encouragement and support throughout the entire process. I would like to thank Dr. James Milke the other member of the committee, for all of his dedication and time, and for all of his help throughout my education here at the University of Maryland. I would also like to recognize the following individuals for their help and assistance with this project: Kevin Lewy (Aerospace Engineering, UMD), Richard Peacock (NIST), Dr. Stuart Milner (Civil Engineering, UMD), Dr. Ken Matsuyama, and Tensei Mizukami. I would like to thank the rest of the staff of Fire Protection Engineering at the University of Maryland for everything through the years. Finally I would like to thank my parents, and my brother and sisters for all of their love, support and encouragement throughout this project and my entire education.

Table of Contents

Acknowledgements	iii
Table of Contents	iv
List of Tables.....	vi
List of Figures	vii
List of Figures	vii
1 Chapter 1: Introduction	1
1.1 Overview	1
1.2 Literature Review.....	3
1.2.1 History of Inverse Fire Modeling.....	3
1.2.2 Genetic Algorithms and Fire Protection Engineering	8
1.3 Stages of Research	10
2 Chapter 2: Approach.....	12
2.1 Introduction.....	12
2.2 Description of Compartment Fires.....	12
2.2.1 Pre-Flashover	12
2.2.2 Post-Flashover.....	14
2.3 Zone Modeling Approach.....	17
2.4 Selection of BRI2002	20
2.4.1 Important Features of BRI2002	21
3 Chapter 3: Inverse Fire Modeling.....	28
3.1 Introduction.....	28
3.2 Inverse Fire Modeling Background	28
3.3 Optimization	30
3.3.1 Background.....	30
3.3.2 Genetic Algorithms	32
3.3.3 Description of Inverse Fire Model Coupled with a Genetic Algorithm ...	36
3.4 Testing Procedure	37
3.4.1 Single Compartment Tests.....	38
3.4.2 Multiple Compartments	40
4 Chapter 4. Results	43
4.1 Introduction.....	43
4.2 Single Compartment Tests.....	49
4.2.1 Heat Release Rate as Only Parameter	49
4.2.2 Single Compartment, Door Vent Configuration as Parameters.....	60
4.2.3 Single Compartment, Door and Window Configuration as Parameters....	71
4.3 Multiple Compartment Tests	77
4.4 FDS Comparison.....	91
5 Chapter 5: Summary and Conclusion	104
5.1 Introduction.....	104
5.2 Summary.....	104
5.3 Future Work.....	106
Appendices.....	108
Appendix A1	113

Appendix A2	131
Appendix A3	181
Appendix A4	208
Appendix A5	250
Appendix A6	264
Appendix B.....	289
Bibliography.....	298

List of Tables

Table 1. Problem classes for optimization [23].....	31
Table 2. Key for simulations for single compartment tests. The letter labeling system is explained in Figure 13 to Figure 18.	44
Table 3. Key for simulations for multiple compartments.....	48
Table 4. Single parameter tests where the entire reference curve is analyzed from 1-6000s.....	50
Table 5. Steady and sloped reference curve results for a steady 500 kW fire. A vent of 1m x 2m is fully open throughout all simulations.....	56
Table 6. MQH estimate of the reference simulation v. IFM estimate.	60
Table 7. Single Compartment tests where the door width and door height are additional parameters.	62
Table 8. Simulation where the IFM overestimated the reference simulation.	66
Table 9. Results for a constant and sloped reference curve with door width and door height as additional parameters.	69
Table 10. Fire size, door and window configuration as parameters, where an exact reference curve is used.....	72
Table 11. Constant and Sloped reference curve results where window configuration is an additional parameter.	75
Table 12. Simulation MR_W1_10_11_a_4.*	79
Table 13. Simulation MR_W1:18_a_3.....	82
Table 14. Simulation MR_W1:18_a_1.....	84
Table 15. Simulation MR_W1_W10:18_b_3	86
Table 16. Simulation MR_W1_W10:18_b_2	89
Table 17. Simulation FDS_Room1_a1. FDS 1MW MLR used as input into IFM.....	94
Table 18. Simulation FDS_Room1_a2. FDS 3MW MLR used as input into IFM.....	94
Table 19. FDS and IFM comparison for the average total HRR on the floor. The IFM estimate is based on a temperature reading in room 1.....	98
Table 20. FDS and IFM comparisons of the average total HRR. The temperatures being analyzed were taken from the Fire Room and are therefore greater than those from room 1.	101

List of Figures

Figure 1. Overview of the stages of a pre-flashover compartment fire [17].	14
Figure 2. Overview of the physics of a compartment fire [17].	14
Figure 3. Depiction of over-ventilated and under-ventilated compartment fires [17].	16
Figure 4. Depiction of zone fire model with upper and lower layers [17].	17
Figure 5. Depiction of CFD model with many individual grid cells [17].	18
Figure 6. Depiction of the zone model structure for BRI2002 [2].	22
Figure 7. Iteration process used in BRI2002 to calculate equivalence ratio [2].	24
Figure 8. Depiction showing a transition to incomplete burning after an equivalence ratio of 0.3 [2].	25
Figure 9. Study performed in BRI2002 depicting a fall off in the fuel mass burning rate.	26
Figure 10. Study performed in BRI2002 showing that incomplete combustion occurs when the upper layer oxygen mass fraction falls below 14%.	26
Figure 11. Global Equivalence Ratio v. time for different fuel mass loss rates. As can be seen a mass loss rate of 800 kW produces a GER of 0.3 approximately.	27
Figure 12. Layout of the multiple compartment scenarios.	41
Figure 13. Simulation letter a. Exact reference curve is analyzed entirely from 1-6000s.	45
Figure 14. Simulation letter b. Exact reference curve is analyzed from 2000-6000s.	45
Figure 15. Simulation letter c. Approximate steady reference curve with the constant value taken at 4000s.	46
Figure 16. Simulation letter d. Approximate steady reference curve with value taken at 3000s.	46
Figure 17. Simulation letter f. Approximate sloped reference curve at 4000s.	47
Figure 18. Simulation letter g. Approximate sloped reference curve at 3000s.	47
Figure 19. Simulation letter MR_a. Exact reference curve analyzed 2000-3000s.	48
Figure 20. Simulation letter MR_b. Approximate steady reference curve with constant value taken at 2500s.	49
Figure 21. Simulation SR10_10_3_Fb_a_2. Evolution of the best fitness ever found and the average fitness of the population.	51
Figure 22. Simulation SR10_10_3_Fb_a_2. Plot of the upper layer temperature of the reference simulation and the GA best simulation.	52
Figure 23. Simulation SR3_3_3_NC_b_1 Evolution of the best fitness ever found and the average fitness of the population for a reference simulation of 200 kW steady fire. An exact solution was found.	54
Figure 24. Simulation SR3_3_3_NC_b_2 Evolution of the best fitness ever found and the average fitness of the population for a steady 600 kW reference simulation. An exact solution was found.	55
Figure 25. Simulation SR3_3_3_NC_d_1 evolution of the best fitness ever found and the average fitness of the population.	57
Figure 26. Simulation SR3_3_3_NC_d_1 upper layer temperature profile for the steady reference curve and the GA best.	58
Figure 27. Simulation SR3_3_3_NC_b_1 upper layer temperature profile of the reference simulation and the GA best.	63

Figure 28. Simulation SR3_3_3_NC_b_3 upper layer temperature profile of the reference simulation and the GA best.....	63
Figure 29. Simulation SR3_3_3_NC_b_5 upper layer temperature profile of the reference simulation and GA best.	64
Figure 30. Simulation SR3_3_3_Fb_b_3 evolution of the performance of the GA for a population size of 50 and 1000 generations.....	67
Figure 31. Simulation SR3_3_3_Fb_b_3 upper layer temperature profile of the reference simulation and the GA best.....	67
Figure 32. Simulation SR3_3_3_NC_d_1 evolution of the performance of the GA.	70
Figure 33. Simulation SR3_3_3_NC_d_1 temperature profile of the reference simulation and GA Best.	71
Figure 34. Simulation SR3_3_3_NC_b_1 temperature profile of the reference simulation and GA best.....	73
Figure 35. Simulation SR3_3_3_NC_b_3 temperature profile of the reference simulation and GA best.....	74
Figure 36. Simulation SR3_3_3_NC_b_5 temperature profile of the reference simulation and GA best.....	74
Figure 37. Simulation SR3_3_3_NC_g_1 evolution of the performance of the GA.	76
Figure 38. Simulation SR3_3_3_NC_g_1 upper layer temperature profile of the reference simulation and GA best.	77
Figure 39. Simulation MR_MR_W1_10_11_a_4 evolution of the performance of the GA.	80
Figure 40. Simulation MR_MR_W1_10_11_a_4 upper layer temperature profile for the reference simulation and GA best.	80
Figure 41. Simulation MR_MR_W1:18_a_1 profile of the upper layer temperature of the reference simulation and the GA best in room 1.....	85
Figure 42. Simulation MR_MR_W1_W10:18_b_3 evolution of the performance of the GA..	87
Figure 43. Simulation MR_MR_W1_W10:18_b_3 upper layer temperature profile of the reference curve and GA best.	87
Figure 44. Simulation MR_MR_W1_W10:18_b_2 upper layer temperature profile of the reference simulation and GA best in room 1.	90
Figure 45. Multiple compartment scenario where FDS was used to measure temperatures.	92
Figure 46. Sample reference curve for FDS multiple compartment tests.....	93
Figure 47. Upper layer temperature profile for a 1MW MLR fire for FDS and BRI2002.	95
Figure 48. Heat release rates in fire room, corridor and room 1 for a 1MW MLR as predicted by FDS and BRI2002.	96
Figure 49. Mass flow rates into and out of fire room as predicted by FDS and BRI2002.	97
Figure 50. FDS and IFM time evolution of the HRR for a 1MW and 3MW MLR. Analysis room is room 1.	99
Figure 51. FDS and IFM comparison of the time evolution of the total HRR. Analysis room is room 1.	99
Figure 52. FDS and IFM comparison of the time evolution of the HRR for 1MW and 3MW MLR scenario. Analysis room is the Fire Room.....	102

Figure 53. FDS and IFM comparison of the time evolution of the HRR for a 3MW and 6MW MLR. Analysis room is the Fire Room.....	103
Figure 54. Simulation letter a. Exact reference curve is analyzed entirely from 1-6000s.	110
Figure 55. Simulation letter b. Exact reference curve is analyzed from 2000-6000s. ..	110
Figure 56. Simulation letter c. Approximate steady reference curve with the constant value taken at 4000s.	111
Figure 57. Simulation letter d. Approximate steady reference curve with value taken at 3000s.....	111
Figure 58. Simulation letter f. Approximate sloped reference curve at 4000s.	112
Figure 59. Simulation letter g. Approximate sloped reference curve at 3000s.....	112
Figure 60. Simulation letter MR_a. Exact reference curve analyzed 2000-3000s.....	208
Figure 61. Simulation letter MR_b. Approximate steady reference curve with constant value taken at 2500s.	209
Figure 62. Sample reference curve for FDS multi-compartment tests.	264
Figure 63. Upper Layer Temperatures for BRI and FDS for 1MW MLR.....	285
Figure 64. HRR Comparisons for BRI and FDS 1MW MLR.	285
Figure 65. Mass Flow Rates through door for FDS and BRI.	286
Figure 66. Mass flow rates through window for BRI and FDS 1MW MLR.	286
Figure 67. Total Mass Flow Rates through door and window for FDS and BRI 1MW MLR.....	287
Figure 68. Upper layer temperature profile for BRI and FDS 3MW MLR.	287
Figure 69. HRR comparisons for FDS and BRI for 3MW MLR.....	288

1 Chapter 1: Introduction

1.1 Overview

The objective of this project is to develop an Inverse Fire Model (IFM) that is capable of estimating the average heat release rate inside a building in an attempt to aid fire-fighting operations. This project is a proof of concept. It is designed to demonstrate that by obtaining a profile of the upper layer temperature, an estimate can be made of the average heat release rate inside a building. Ideally, through the use of thermal imaging cameras strategically placed outside of a burning building, fire conditions coming out of broken windows can be recorded and analyzed at a fire scene. *Assuming this can be done*; the upper layer temperature coming out of the windows can be recorded and used as inputs into the Inverse Fire Model in an attempt to predict the average fire size. This information can be used to determine if the fire is growing in size, maintaining its size or declining.

The goal of this research is to support firefighter safety and better enable firefighters' decision making by backing out the average heat release rate of a fire. Each year over 100 firefighters are killed in the line of duty [1]. By providing information on the size of the fire, firefighters will have a better understanding of the conditions inside a burning building. This study uses an advanced optimization tool, a genetic algorithm, coupled with a two-layer zone fire model, BRI2002, to predict the average heat release rate of a fire. The genetic algorithm through an error analysis estimates the heat release rate that minimizes the error between a zone model prediction, and a previously established upper layer temperature profile.

This research focuses on developing an Inverse Fire Model, studying its robustness and verifying the proof of concept. The IFM uses a genetic algorithm, to provide the best estimate of the average fire size. The genetic algorithm is based on the principles of Social Darwinism, or the “survival of the fittest” theory. Using MATLAB as the programming language, the IFM couples the genetic algorithm with the Japanese zone model BRI2002 developed by the Building Research Institute in Tsukuba, Japan [2]. The IFM uses the genetic algorithm to sort through potentially thousands of different scenarios with varying vent configurations and fire sizes. This is done to back out the particular solution which minimizes the error between the upper layer temperature predicted in BRI2002 and the thermal imaging cameras. For the purpose of this research, however, upper layer temperatures potentially recorded by thermal imaging cameras outside of the building will be obtained from a reference BRI2002 simulation with a known fire size, HRR_{ref} . The IFM will then provide an estimate of the heat release rate that can be directly compared to HRR_{ref} .

The genetic algorithm uses an evaluation or fitness function that minimizes an error function. The fitness is a score assigned to a candidate solution and is a measure of the quality of that candidate. Based on a seeded initial population and its corresponding fitness, the genetic algorithm will create a subsequent population that in most cases has an improved fitness. Until the error is minimized, the genetic algorithm will keep producing subsequent and better fitted individuals. This research assumes that the heat release rate that will be backed out by the IFM will be an average value.

It is important to reiterate that this research is a proof of concept. By obtaining the upper layer temperatures from a simulation performed by BRI, this research is

designed to determine how accurately the genetic algorithm can estimate the HRR. After determining the validity of the algorithm to estimate the HRR from a reference BRI simulation, future work can focus on validating the model with actual experimental data and potentially coupling it with thermal imaging cameras or other devices.

1.2 Literature Review

1.2.1 History of Inverse Fire Modeling

For the purpose of fire modeling, it is generally accepted that the fire's heat release rate is a known input for the model. Most performance-based designs require the use of a fire model to support the conclusions that are made. These performance-based designs require a heat release rate for a typical fuel load present. These heat release rates are known, and are usually measured in full-scale cone calorimeter tests. Inverse fire modeling, however, uses information from the fire (i.e. temperatures, smoke concentrations etc.) to estimate the HRR and in some situations the location of the fire itself. Inverse fire modeling is important because it can provide an estimate as to how large a fire is. Firefighters can use this information to better understand the conditions with which they are dealing. A few studies have attempted to back out the heat release rate and/or the location of a fire through inverse fire modeling [3]-[8]. These studies have primarily focused on using sensors inside a building, and are extensively based on using theoretical velocity and temperature correlations. These studies are outlined below.

Forney and Davis, have developed a Sensor Driven Fire Model (SDFM) at the National Institute of Standards and Technology which uses sensor signals inside a building to estimate the fire size [3]. This model also attempts to estimate the location of the fire and predict its further development through the zone model CFAST [9]. The

SDFM uses ceiling jet algorithms for temperature and smoke concentrations to convert the analog data from a heat or smoke detector (on a ceiling) into a HRR. According to Davis, the basic equation that relates the convective heat release rate to the ceiling jet temperature and radial distance from the fire is [3]:

$$\dot{Q}_c = 0.172H^{5/2} \left(\frac{r}{.18H} \right)^{.345} \left(\frac{\Delta T_{cj}^{3/2}}{T_\infty^{1/2}} \right)$$

\dot{Q}_c = convective heat release rate
 H = ceiling height above fire surface
 r = radial distance from plume centerline
 ΔT_{cj} = excess ceiling jet temperature
 T_∞ = ambient temperature

(1)

Using heat or smoke detectors placed at the ceiling, an estimate of the ceiling jet temperature can be obtained. A calibration curve for the analog signal produced by the detector as a function of temperature/gas concentration must be known. Using this information the SDFM provides an estimate of the HRR of the fire based on either the temperature or smoke concentration through the use of modeling correlations, such as the one illustrated above. This HRR is then used as an input into the zone model CFAST to predict upper layer temperatures, layer height and to determine if fire spread and growth is likely [3].

The structure of the model works by having the user input information about the building geometry, and information about the sensors (location, calibration constants etc.). The SDFM initializes itself and then determines if a fire is occurring. If it detects a fire, the SDFM will predict the heat release rate and location and subsequently use these as inputs for CFAST. Tests were run to validate the model with experimental data, where only one detector is assumed to be in each room. These results showed good agreement

with the experimental measurements. In addition, the SDFM used in this study works very quickly and has a calculation cycle much quicker than real time. In order to speed up the calculation and iteration process, only the necessary fundamental equations in CFAST were used [3].

Lee and Lee have also studied inverse fire modeling through their work entitled “The Estimation of Fire Location and Heat Release Rate by Using Sequential Inverse Method [4].” Through the use of an optimization algorithm focusing on the sequential regularization approach, an estimate of the location and size of the fire can be made based on temperature readings inside a compartment. The premise of the research revolves around comparing temperature profiles inside a compartment by minimizing the residuals to determine fire location and size. The sequential inverse method is cost effective, non-iterative and is able to estimate the transient HRR [4].

FDS was used in their studies to provide experimental data of the temperature profile inside a compartment. This data was then used as inputs into their model. In order to account for the noise that an actual sensor would encounter, random errors were added to the temperature measurements calculated in FDS. Using these temperature profiles as inputs into Alpert’s velocity and temperature correlations, the inverse method estimates fire location and size. Their sequential inverse method utilizes the finite difference approach and assumes that several heat release rates in the future are constant [4].

Tests were run in a 10m x 10m x 3m compartment with a steady fire source of 100 kW. Results showed that the algorithm was able to estimate the HRR to within 11-31.5% difference of the actual value. In addition, the algorithm estimated the location of

the fire to an approximate difference of 1.27%. Lee and Lee also performed studies where the HRR changed, from a steady 100 kW fire to a steady 200 kW fire, the inverse method was able to track the change in fire size relatively well [4].

Richards et. al. have also studied inverse fire modeling through their work entitled “Fire Detection, Location, and Heat Release Rate Through Inverse Problem Solution” [5]. This research determined the location of the fire and its heat release rate based upon the times that individual temperature sensors on the ceiling reach their activation temperature. The algorithm compares the activation times of sensors on the ceiling to predictions of sensor activation times by a zone fire model. The algorithm measures residuals between measured and predicted activation times through the least squares method. The fire model used was the zone model Lavent. The forward problem consisted of using Lavent to predict the “transient temperature field across a ceiling [5].” Using this temperature profile, the time at which a particular sensor will activate can be calculated. For a particular compartment scenario, 528 fire scenarios of different heat release rates and locations were performed for the forward problem. For each one of these scenarios, an activation time of the temperature sensors on the ceiling was predicted [5].

The inverse problem is solved by comparing actual sensor activations to the predicted estimates calculated in the forward problem. Experiments were first run where the experimental data was replaced with Lavent simulations with systematic and random errors that had been added to compare to the original simulations without errors. A second set of tests used a prototype video detection system [6]. This video detection system monitors the times and locations that actual color changing temperature sensors

activated. The video system recorded these results and used them as inputs to solve the inverse problem. Results showed that the detection and location of the fire size was very dependent on systematic errors. Nevertheless the tests demonstrated that the location of the fire could be estimated to within one third the distance of sensors, and the fire size to a factor of three of its actual heat release rate.

Torero and Berry et al. are currently pursuing an area of active research known as the “FireGrid” project [7]. This current work proposes to integrate data collected from a number of sensors (Temperature, CO, smoke etc.) and have it instantaneously relay information to field models such as Computational Fluid Dynamics (CFD) models and Finite Element (FE) models. “In FireGrids ‘Emergency Response’ model, parallelization and on-demand Grids will allow the same CFD and FE models to be run faster than real time [7].” Field models use the information obtained from sensors, attempt to run in super real time and model the evolution of the fire and its impact on the building [7]. This information can be used to better defend against the fire and provide more information to fire-fighters.

Other research has focused on using signal processing algorithms to locate the fire in a single compartment [8]. Using temperature sensor arrays, a signal processing algorithm can estimate the location of a fire based on signal time delay estimates of these temperature sensors through a near field and a far field algorithm.

As seen above, there have been a few studies to estimate the heat release rate and location of a compartment fire through an inverse method. These studies primarily revolve around using sensors inside the building to establish a profile of temperatures inside a compartment. These temperature readings can act as input into theoretical

velocity and temperature correlations. These correlations can be inverted to solve for the heat release rate and/or fire location through a wide array of methods as discussed above. Some of these studies, in particular, those performed by Lee et al. and Richards et al. accounted for systematic errors of the sensors. These studies have produced fairly accurate results when compared to experimental data. They are, however, limited to sensors inside a building and often times to one compartment. In addition, these studies are limited to their assumptions that the ventilation characteristics inside a building are known. The proposed methodology presented in this document, assumes sensors outside of a building can be used to estimate the fire size inside. In addition, through the use of a genetic algorithm, many different unknown parameters such as ventilation characteristics can be handled and estimated.

1.2.2 Genetic Algorithms and Fire Protection Engineering

Genetic algorithms (GAs) are highly functional optimization tools, capable of solving a wide array of problems. They are particularly useful for problems where there are many local minima and maxima. They are also capable of handling multiple variables (parameters). A detailed description on the workings of genetic algorithms and the theory of optimization algorithms will be discussed in chapter 3. Genetic algorithms have been used extensively in mathematics and engineering problems. They have been used in particular applications of fire protection engineering and fire science.

GAs have been utilized to predict what parameters produce the least nitrogen oxide emissions of a large coal fired boiler [10]. Zhou et. al used an Artificial Neural Network to model the NO_x emissions from the boiler, and the genetic algorithm was used to find what parameters i.e. coal properties, boiler load, air distribution scheme will minimize the

NO_x emissions. The purpose of this study was to understand what parameters produce the cleanest and most efficient combustion of coal. Additional research has used a genetic algorithm to optimize airflow conditions inside a coal mine during a fire [11]. Mine fires are inherently dangerous to the miners due to the potential for release of highly poisonous and harmful gases. Ventilation control inside a mine can help limit these harmful side effects. Therefore, optimizing the ventilation control through the use of a genetic algorithm helps identify the parameters (fan working output, working air pressure etc.) that are most important to optimize the air current during a mine fire [11].

GA's have been used to optimize the location and number of fire stations in a town or city [12]. The genetic algorithm was used to find the solution that minimizes the “sum of losses from the fire and the cost of providing the service [12].” This information can be used to identify the ideal number of fire stations in a particular region while considering the balance between a cost-effective solution and one that still provides adequate protection. By optimizing the distance between fire stations and accident sites, reaction time from the fire station to the fire can also be reduced [12]. Zhao has utilized a GA as part of a hybrid neural network to model steel columns under fire conditions or elevated temperatures [13]. The GA was used to “provide effective and robust search algorithms to design artificial neural networks automatically [13].”

Other work has been performed in predicting the kinetics of polyurethane foam in smoldering combustion [14]. Lautenberger et al. demonstrated through the use of a genetic algorithm that the kinetic and stoichiometric parameters for smoldering polyurethane foam can be estimated. The genetic algorithm finds the parameters that provide the best agreement between a theoretical Arrhenius type model and actual

thermogravimetric measurements. Benchmark tests were run against the thermal degradation of cellulose, where experimental data is available. The genetic algorithm measured the difference of mass loss rates between the calculation estimated by the Arrhenius type model and the experimental data. Lautenberger's results showed excellent agreement between predictions based on parameters that were estimated through the GA and the experimental benchmark data.

A genetic algorithm was also used to estimate material properties for FDS modeling [15]. Lautenberger et al. simulated bench scale fire tests through the use of FDS's pyrolysis model and compared the results to experimental data. In order to utilize FDS to simulate fire growth and spread, it is important to have "material properties" as input for the FDS input file. The genetic algorithm finds the best set of material properties that provides optimal agreement between the FDS pyrolysis model and bench scale test data. The material properties needed for the FDS pyrolysis model included the thermal conductivity, specific heat, pre-exponential factor, activation energy, and the heat of pyrolysis. Experimental tests were first performed by running an idealized case using FDS's pyrolysis model to represent the known experimental data. The GA was then used to determine that the same properties could be backed out. The GA worked relatively well in backing out the similar properties. This study proved that the genetic algorithm is capable of estimating material properties needed for FDS input based on a comparison with bench scale tests.

1.3 Stages of Research

This particular project consists of two primary stages of research. The first stage, on which this report focuses, is the proof of concept stage. It discusses the development

and testing of the IFM and its ability to couple the genetic algorithm with the zone model BRI2002 to estimate the average heat release rate of a fire. This study focuses on verifying the robustness of the model in backing out the fire size through a number of stand alone computer studies. These studies include simulations of single, and multi-compartment scenarios along with multiple unknown parameters revolving around the ventilation profile inside the compartment.

After it is successfully shown that the average fire size inside a compartment can be reasonably estimated by studying the upper layer temperature through this research, stage 2 can commence. This second stage will focus on studying the accuracy of thermal imaging cameras in measuring the upper layer temperature of smoke coming out of broken windows, along with combining the camera's readings as input for the genetic algorithm. Stage 2 will also consist of validating the BRI model with experimental data, and reducing simulation time of the IFM. Stage 2 is not part of this present study and is considered as future work to be conducted after the proof of concept has been provided.

2 Chapter 2: Approach

2.1 Introduction

This section outlines the basic fundamentals of compartment fires from pre-flashover to post-flashover fires. It discusses the concept of the Global Equivalence Ratio (GER) and its relationship to under and over-ventilated fires. The theory behind zone fire modeling is also conveyed in this chapter. Zone models were selected because of their ability to provide relatively accurate simulations and still be computationally cheap. A justification of why BRI2002 was selected over other zone models such as CFAST is provided, as well as, a brief summary of the main features of BRI2002.

2.2 Description of Compartment Fires

2.2.1 Pre-Flashover

A compartment fire is defined by two main stages, a pre-flashover stage and a post-flashover stage. Flashover is a rapid transition in the development of a compartment fire to a situation where every combustible becomes involved. It is formally defined by the International Standards Organization as “the rapid transition to a state of total surface involvement in a fire of combustible material within an enclosure [16].” A pre-flashover fire is concerned with the ignition, and development of the fire plume, ceiling jet and the formation of the upper layer [16].

After ignition has occurred, the fire growth is primarily controlled by the flame spread, and the compartment itself has little effect on the fire’s development [16]. After flaming combustion has taken place, products of combustion are released (CO_2 , H_2O , CO , soot) into the air. These products of combustion are hotter, and less dense than ambient

air and subsequently rise to the ceiling. As a result, cooler air becomes entrained due to pressure differentials and mixes with these products of combustion. This rising of combustion products and the entrainment of air forms the fire plume. As the fire plume hits the ceiling the gases move across the ceiling until they come in contact with the wall. This initial spread of the gases across the ceiling is what is known as a ceiling jet. As the ceiling jet hits the wall, the smoke filling process begins and the establishment of an upper smoke layer takes place. This smoke layer descends towards the floor and rises in temperature as the fire continues to grow [17].

As smoke continues to rise and add to the volume of the upper layer, the smoke layer composition and temperature become approximately uniform due to turbulent mixing [17]. The temperature of the smoke layer is also affected by the compartment itself, as heat is lost to the neighboring walls and ceiling through convective and radiative heat transfer. As the smoke layer descends towards the floor, it may begin to flow out of an open vent. Eventually, what is known as a “quasi-steady vented period” may take place and a stable upper layer will form [17]. When this happens, the mass flow rate out of the vent (smoke) is approximately equal to the mass flow rate coming in through the vent (air). At this point in the fire development, the fire can take one of two paths. It can decline due to fuel depletion or oxygen starvation, or it can grow and experience a transition to flashover where all other combustibles become auto-ignited. These stages of pre-flashover growth can be seen in Figure 1 below, along with a fundamental overview of a compartment fire in Figure 2.

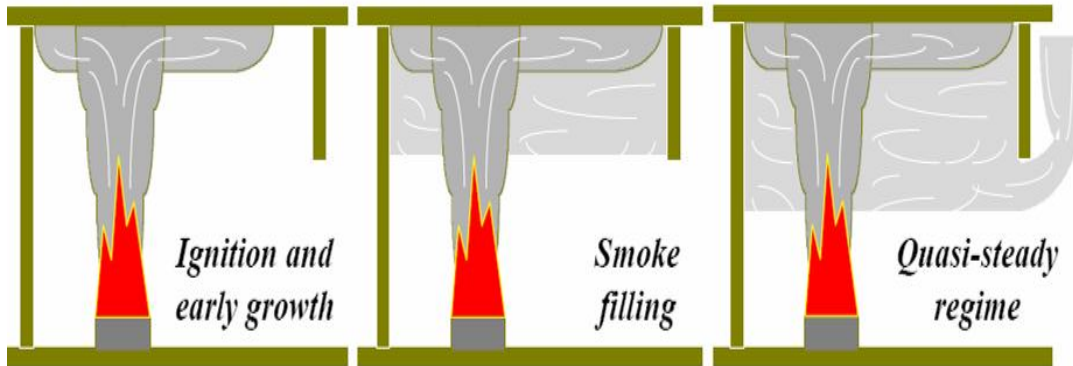


Figure 1. Overview of the stages of a pre-flashover compartment fire [17].

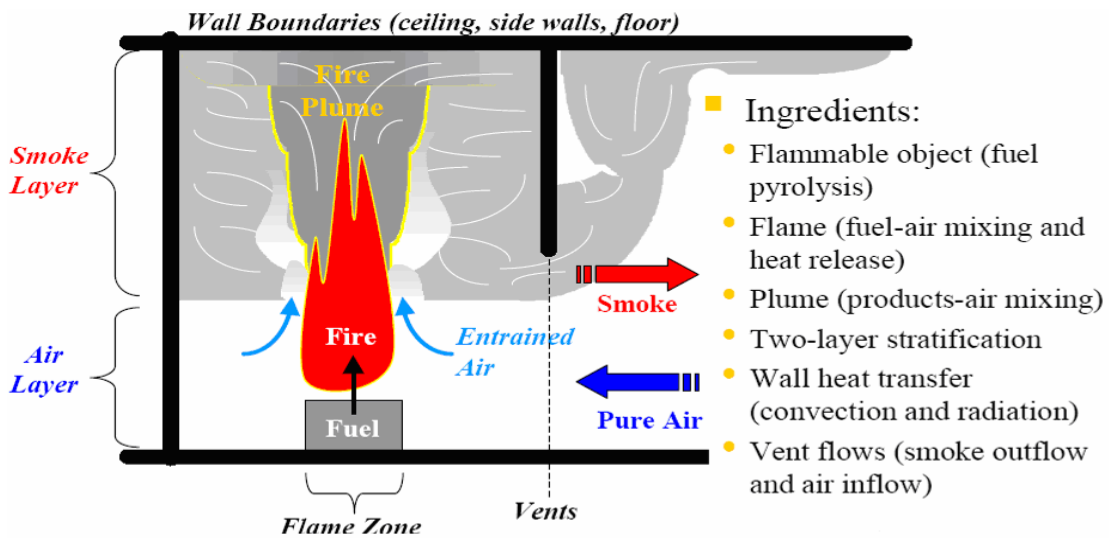


Figure 2. Overview of the physics of a compartment fire [17].

2.2.2 Post-Flashover

As discussed, a transition to flashover inside a compartment can take place. The critical thresholds for flashover to occur, are usually associated with an upper layer temperature of 500-600 °C, or a heat flux at the floor of 20-25 kW/m². It is believed that these parameters are capable of auto-igniting other combustibles inside the compartment. After flashover has occurred, the fire is considered to be in the post-flashover stage, and is called a fully developed fire [16]. At this point the fire is limited by the supply of

oxygen and is referred to as under-ventilated or fuel rich. In this situation, there is plenty of fuel but not enough oxygen to burn. At this point, due to the lack of oxygen, flames will extend out of the compartment in an attempt to burn (see Figure 3).

In the pre-flashover stage, the fire is considered to be over-ventilated or fuel lean. In this situation, there is plenty of oxygen to burn all of the fuel. This transition from an over-ventilated fire to an under-ventilated fire is characterized through the Global Equivalence Ratio (GER). The GER is defined below as follows:

$$GER = r_s \left(\frac{\dot{m}_f}{Y_{O_2, in} \dot{m}_{in}} \right) \quad (2)$$

If the GER is less than or equal to 1, the fire is considered to be over-ventilated. If the GER is above 1, the fire is under-ventilated. In the above equation, r_s is known as the stoichiometric oxygen to fuel mass ratio. This term is fuel dependent and describes the amount of oxygen needed per unit mass of fuel to burn at stoichiometric conditions.

$$r_s = \frac{\dot{m}_{O_2}}{\dot{m}_{fuel}} \quad (3)$$

The term, \dot{m}_{in} is the mass flow rate of air into the compartment. It is commonly accepted in the Fire Protection Engineering field, that an estimate of the air flow rate coming into the compartment can be estimated as follows for post flashover fires with a single vent subjected to natural ventilation:

$$\dot{m}_{in} \approx .5w_o H_o \sqrt{H_o}$$

$w_o = \text{width of vent}$

$H_o = \text{height of vent}$

(4)

The other term, \dot{m}_f is the fuel mass loss rate. If the GER is below 1, the fire is over-ventilated and the fuel mass loss rate is approximately equal to the mass burning rate \dot{m}_b .

$$GER \leq 1$$

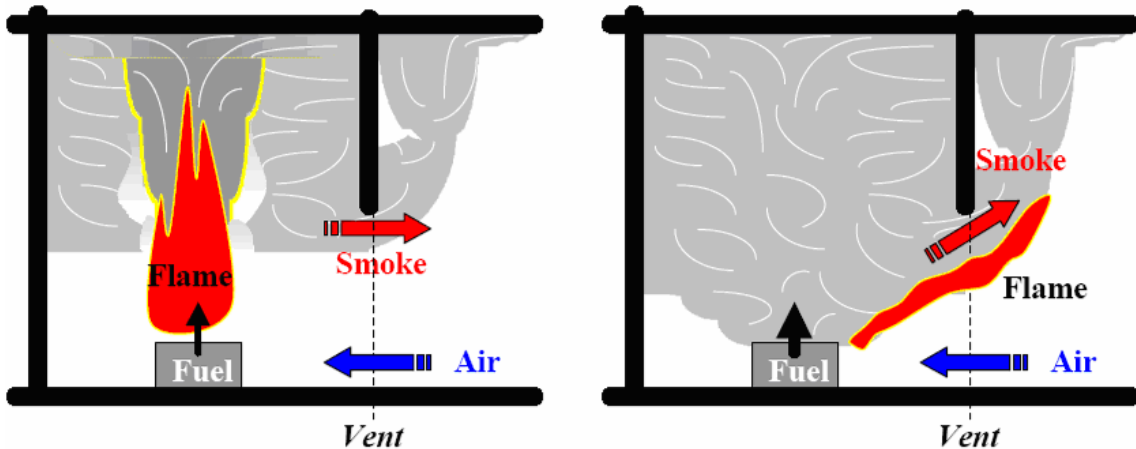
$$\dot{m}_f \approx \frac{\dot{Q}}{r_s \Delta H_{O_2}} \quad (5)$$

Where \dot{Q} is the heat release rate of the fire, and ΔH_{O_2} is the heat of combustion per unit mass of oxygen (13.1 MJ/kg-K). If the fire is under-ventilated, the fuel mass loss rate is not equal to the mass burning rate. The mass burning rate is less than the fuel mass loss rate because not all of the fuel can combust due to the lack of available oxygen. Instead the mass burning rate \dot{m}_b is defined below for under-ventilated combustion:

$$\dot{m}_b = \frac{\dot{m}_{in} Y_{O_2, in}}{r_s} \quad (6)$$

The following Figure 3 is a description of over-ventilated, and under-ventilated combustion in a compartment fire. Notice that in the post-flashover stage, due to the lack of oxygen, the fire extends outside of the vent as previously discussed and the smoke layer is near the floor.

■ Flame location: (1) near the fuel source; (2) near the vents



(1) Over-ventilated combustion, *i.e.* small values of the Global Equivalence Ratio: $GER \leq 1$

(2) Under-ventilated combustion, *i.e.* large values of the Global Equivalence Ratio: $GER \geq 1$

Figure 3. Depiction of over-ventilated and under-ventilated compartment fires [17].

2.3 Zone Modeling Approach

As discussed, in the case of a fire, a compartment naturally stratifies into two layers, a hot upper layer and cool lower layer. A zone model decomposes the fire compartment into two control volumes, consisting of the upper and lower layers. The upper layer is composed of the fuel source itself, the flame, the fire plume, ceiling jet and the hot smoke layer. The lower layer is composed of fresh air considered to be at ambient temperatures. It is this lower layer that adds the necessary oxygen to the fire and allows the fire to grow. This concept can be observed in Figure 4 below. The zone model relies on empirical correlations and conservation of energy statements. The primary differential equations that govern zone models revolve around the compartment bulk pressure (p), the volume of the upper layer (V_{UL}), the Temperature of the upper layer (T_{UL}), and the Temperature of the lower layer (T_{LL}).

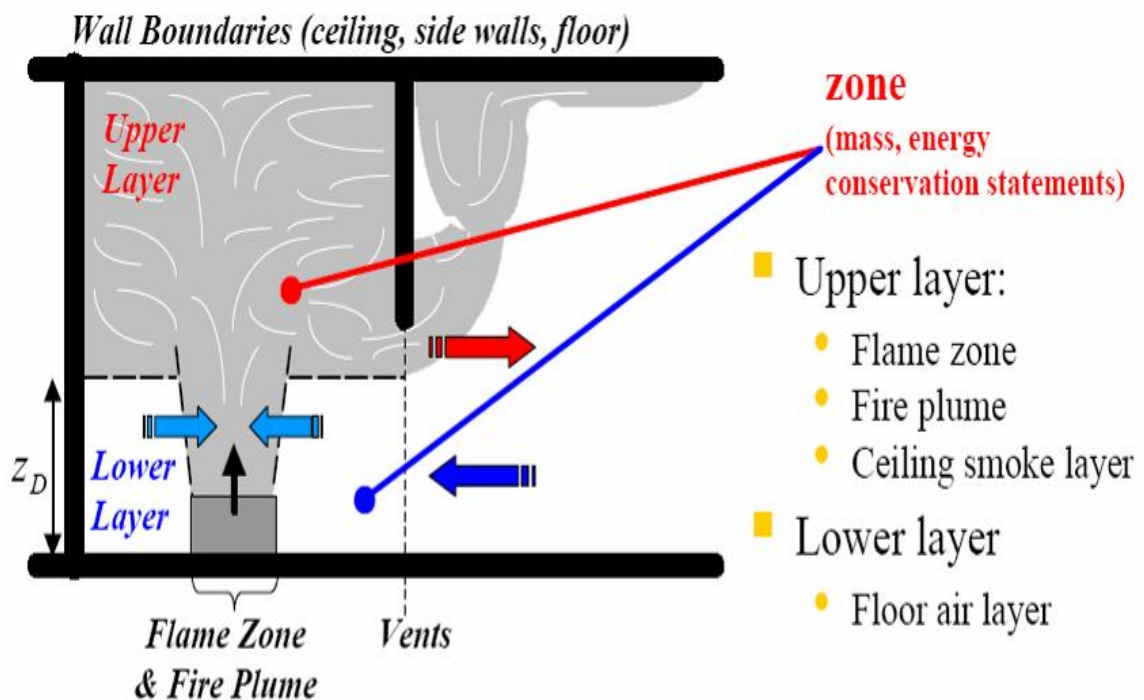


Figure 4. Depiction of zone fire model with upper and lower layers [17].

A Computational Fluids Dynamics (CFD) model such as the Fire Dynamics Simulator (FDS), however, decomposes the fire compartment into several hundred or even thousands of individual control volumes. Each individual grid cell (control volume) accounts for the physics including mass, momentum, and energy conservation statements (see Figure 5). Although CFD may be able to better resolve the fire compartment because of the large number of grid cells it is, however, computationally expensive and can take hours or even days to run a simulation depending on the number of grid cells.

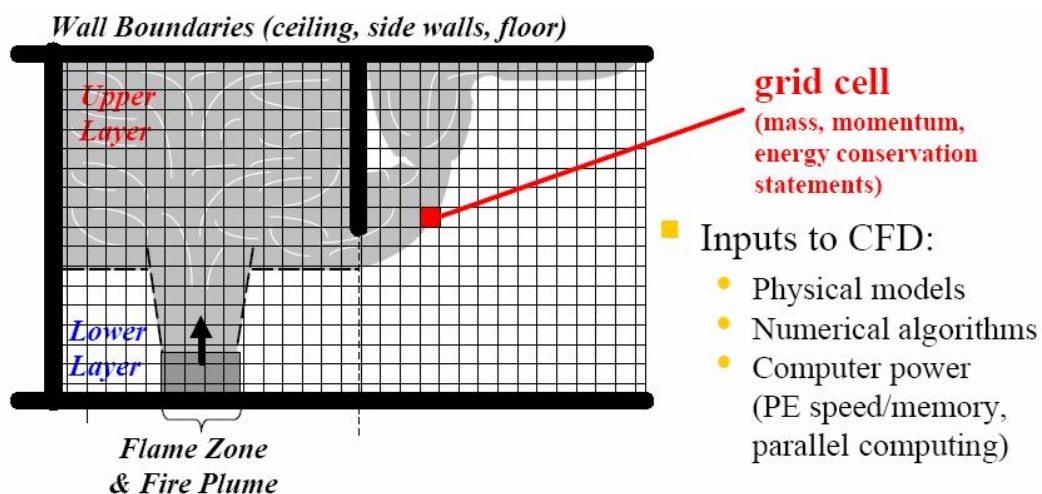


Figure 5. Depiction of CFD model with many individual grid cells [17].

For the purpose of this project it was imperative to analyze thousands of different simulations with varying fire sizes and vent configurations. Time is a very important issue in this project. Ideally this IFM should work in real time or faster than real time. The estimated heat release rate needs to be calculated in real time in order to quickly provide information to firefighters. Therefore, although CFD may be more accurate it is not computationally feasible to use FDS in this project. Zone models, because they are computationally cheap and relatively accurate were selected for this project. In addition, zone models have a very wide system level viewpoint and can handle problems large in

size and scope. They are also well suited for studies of the long time impact of a fire on a building [17]. This is important for this project because large time scales will be involved in order to study steady state.

2.4 Selection of BRI2002

In order to determine the best and most reliable model for this project, two primary zone models were analyzed in the initial stages of this research, CFAST (developed by National Institute of Standards and Technology, NIST) and the Japanese zone model BRI2002 (developed in Tsukuba, Japan at the Building Fire Research Laboratory). Both models use the similar fundamental conservation equations as described above to model fire conditions.

CFAST, however, has a number of advantages over BRI2002. Its primary advantages include the ability to have multiple fires in one or more compartments. It is also able to spread the fire from one compartment to another through the establishment of ignition temperatures. The current version of BRI2002 is unable to have multiple fires and account for fire spread. A multi-fire version of BRI has been developed, however, this model still does not allow the ability to spread the fire and only allows for one fire per compartment. In addition, this model is still in the testing stage and is unavailable to the public. Both models can, however, model the burning of excess fuel from the fire room in other compartments. CFAST is also more user friendly than BRI and has a pre-processor that allows input files to be made quickly and efficiently. In addition, CFAST's output can be visualized in a post-processor such as Smokeview as developed by NIST. This post-processor allows the geometry and the fire to be visualized.

The main advantage of BRI over CFAST, however, as determined through a number of preliminary tests is the robustness of the model. CFAST is known to become unstable in its calculations and stop well before its dedicated time, due to numerical instabilities. This is especially true when CFAST models rooms that become very under-

ventilated and has trouble calculating species yields of excess Carbon, CO and CO₂ [18]. BRI, on the other hand, is a much more reliable model in that it is less likely to stop due to numerical instabilities. Because potentially thousands of zone model simulations need to be run in order to adequately estimate the heat release rate, it is important to have a model that will not stop frequently. Therefore, because of its robustness, BRI was selected over CFAST.

2.4.1 Important Features of BRI2002

BRI2002 is a multi-story, multi-room zone model, which assumes that the fire naturally stratifies into two zones, an upper layer and a lower layer as can be seen below in Figure 6 [2]. The primary assumptions made in the model are as follows:

- a) “Any space in a building is filled with an upper and a lower gas layer
- b) The upper and lower layers are distinctly divided by a horizontal boundary plane (discontinuity)
- c) Each layer is uniform with respect to physical properties by virtue of vigorous mixing;
- d) Mass transfer across the boundary of a layer occurs only through a fire plume, doorjets and doorjet plumes;
- e) Heat transfer across a layer boundary occurs by radiative heat exchange among the layers and the boundary surface contacting with the layer, as well as that associated with the mass transfer referred in (d)
- f) All the heat released by a fire source is transported by the fire plume, in other words, the flame radiation loss is neglected

g) Radiative heat transfer between rooms is neglected [2].”

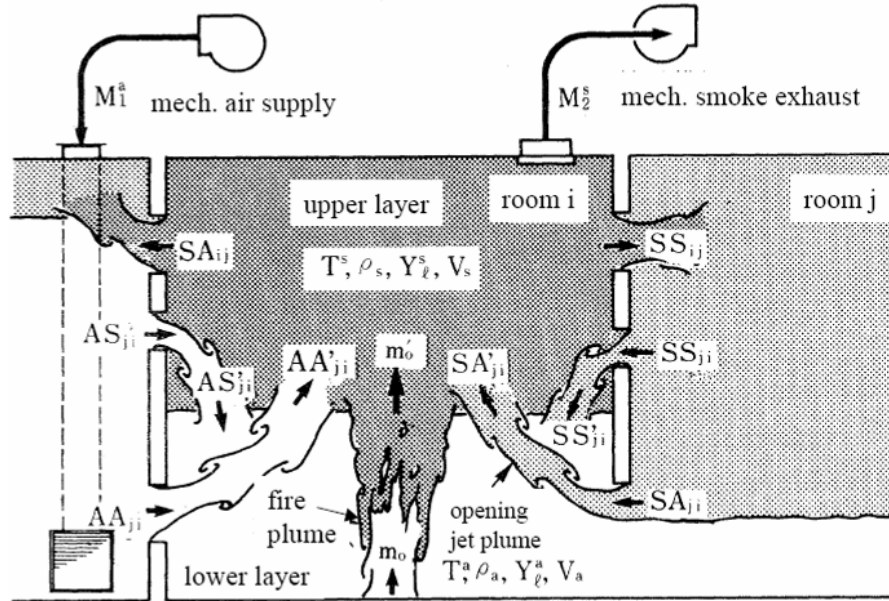


Figure 6. Depiction of the zone model structure for BRI2002 [2].

In BRI2002, attention must be placed on inputting the fire source conditions.

Creating a fire in BRI is done by specifying a fuel mass loss rate or heat release rate and the corresponding area of the fuel source. It is important that a very large mass loss rate compared with the size of the room opening or the fire source area not be specified [2].

If either occurs, an excessive production of unburned fuel can occur in the upper layer.

This can lead to numerical instabilities. It is tentatively recommended that the maximum

heat release rate in any compartment be: $HRR_{max} < 1,500AH^{1/2} (kW)$, and the maximum

heat release rate per unit area of fire source be $< 1,000 (kW/m^2)$. In most models run for

this research, the area of the fire source was specified so that the maximum heat release

rate per unit area (HRRPUA) of the fire source was $500 kW/m^2$. This value was

specified for two reasons. The first is that in several sample example files in the BRI

users guide, 500 kW/m² is used as the HRRPUA. Secondly, research was conducted to find typical heat release rate values per unit area of office configurations. A study performed by NIST for the Cook County Administration Building, burned full-scale workstations that one may encounter in a typical office configuration. This study showed that typical HRRPUA were on the order of 340-590 kW/m² [19]. NFPA92B recommends that a typical heat release rate per unit area of law offices be 290 kW/m² [20]. All of these values are similar and, therefore, 500 kW/m² was selected as a reasonable and representative estimate.

The mass burning rate in BRI is a function of the equivalence ratio. In ideal conditions, as discussed in section 2.2 of this report, a fire becomes under-ventilated for a global equivalence ratio above 1. For a GER less than 1, the fuel mass loss rate is approximately equal to the mass burning rate. BRI2002, however, considers a fire to be affected by ventilation effects if the equivalence ratio is greater than approximately 0.3. For an equivalence ratio less than or equal to 1.0 (fuel controlled burning) [2]:

$$\dot{m}_b = \sum (Y_{f,j} \dot{m}_{in,j} - Y_f \dot{m}_{out,j}) \quad (7)$$

For an equivalence ratio less than 0.3, $Y_{F,out} = 0$. However, for an equivalence ratio above 0.3, $Y_{F,out} > 0$ and the aforementioned fuel mass burning rate does not equal the fuel mass loss rate. For an equivalence ratio greater than 1.0 (oxygen controlled burning) the mass burning rate in BRI is specified as [2]:

$$\dot{m}_b = \frac{1}{r} \sum (Y_{O_2,j} \dot{m}_{in,j} - Y_{O_2} \dot{m}_{out,j}) \quad (8)$$

An iterative method is used in BRI to calculate the equivalence ratio and species yields of combustion products. This process is outlined below in Figure 7:

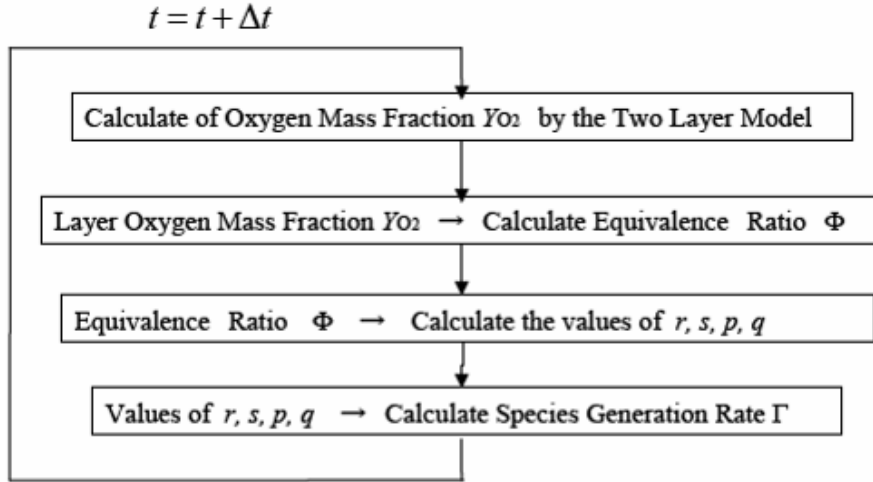


Figure 7. Iteration process used in BRI2002 to calculate equivalence ratio [2].

The implicit relationship in BRI that relates the oxygen mass fraction and the equivalence ratio is as follows [2]:

$$Y_{O_2} = \frac{Y_{O_2}^a}{1 + \phi_2 \Phi} \left[1 - \left[\left\{ r + (1-r)(1-s) \left(1 - \frac{p_1}{2} - p_2 \right) \right\} v_C + \left\{ r + (1-r)(1-s)(1-q_1) \right\} \frac{v_H}{4} - \left\{ 1 - (1-r)s \right\} \frac{v_O}{2} \right] \frac{\Phi}{v_{O_2}} \right] \quad (9)$$

Through the use of well calibrated data it has been shown that an equivalence ratio of greater than 0.3, can cause fuels to burn incompletely, and produce excess unburned fuel. This concept is demonstrated in the following Figure 8, and has been incorporated in the BRI2002 model.

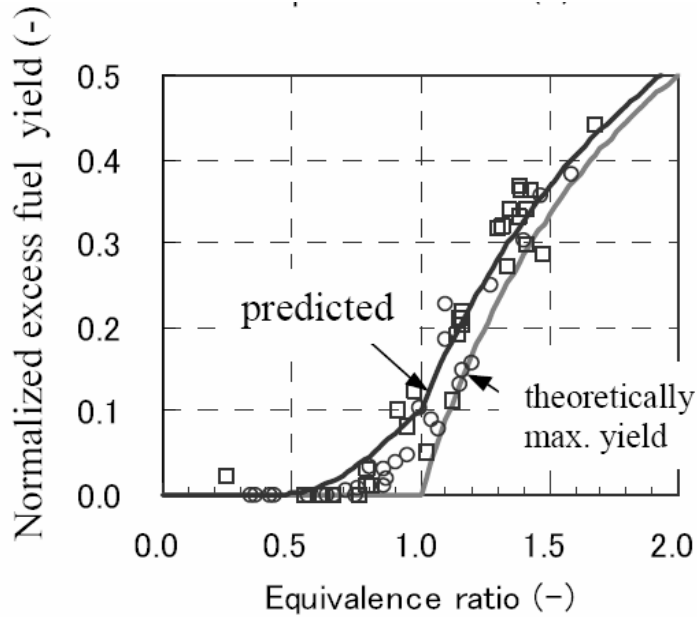


Figure 8. Depiction showing a transition to incomplete burning after an equivalence ratio of 0.3 [2].

Studies were performed in BRI to analyze the affect of this concept in a 3m x 3m x 3m room, with a 1m x 2m vent to the outside. The heat release rate per unit area was maintained at 500 kW/m² and the mass loss rate was specified to be steady starting throughout the simulation. The simulation time was 6000s, and the intended HRR was increased systematically until it was observed that control over the HRR was lost due to incomplete combustion. As can be seen in Figure 9 and Figure 10, a steady mass loss rate to produce a HRR of 800 kW shows signs of incomplete combustion. In addition, this study shows that the largest fire that can be supported in this compartment is around 1.0-1.5MW.

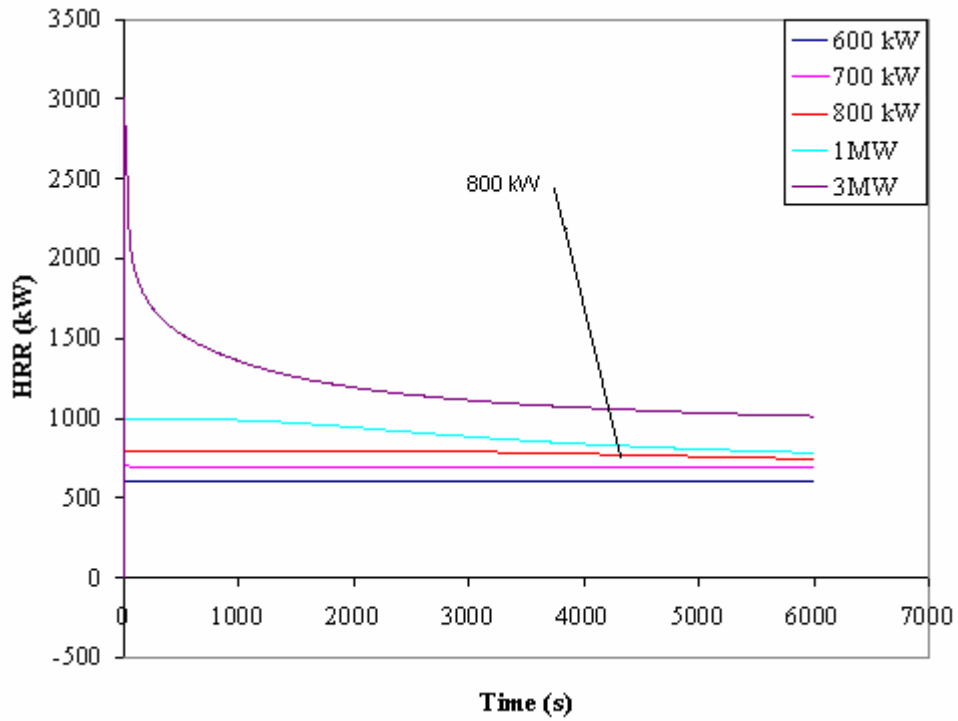


Figure 9. Study performed in BRI2002 depicting a fall off in the fuel mass burning rate.

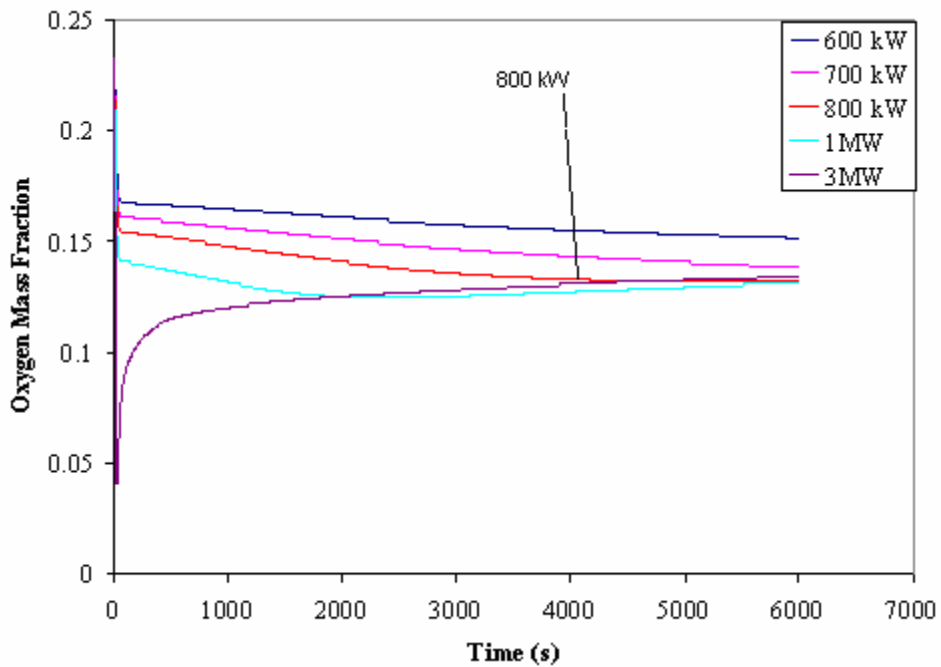


Figure 10. Study performed in BRI2002 showing that incomplete combustion occurs when the upper layer oxygen mass fraction falls below 14%.

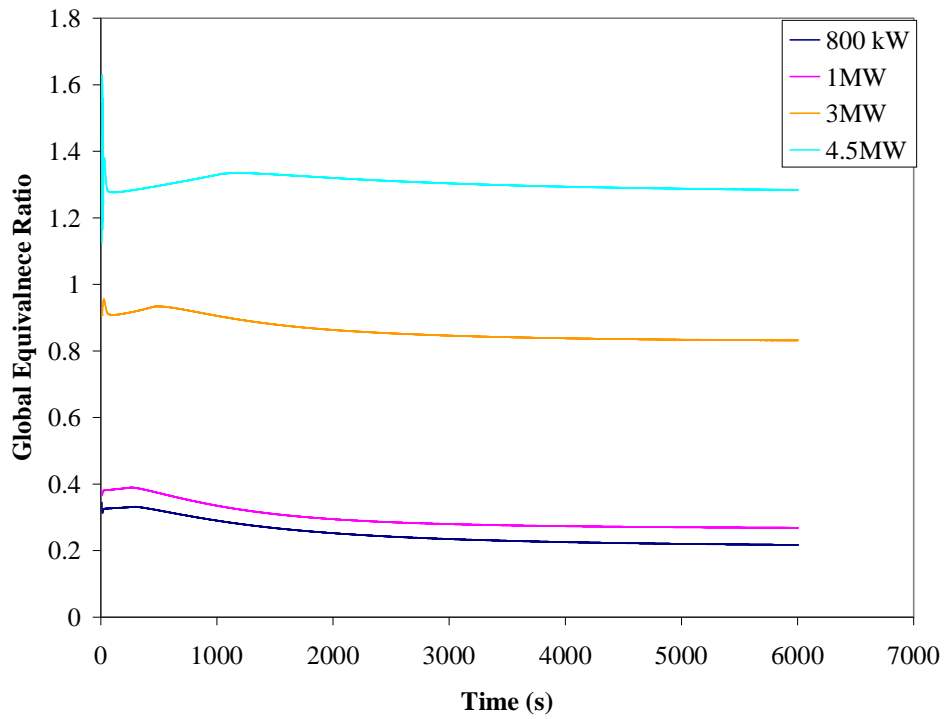


Figure 11. Global Equivalence Ratio v. time for different fuel mass loss rates. As can be seen a mass loss rate of 800 kW produces a GER of 0.3 approximately.

This study also depicts the oxygen mass fraction in the upper layer going below 14% for the 800 kW fire. BRI simulates fires to burn incompletely when this oxygen mass fraction drops below 14 %.

3 Chapter 3: Inverse Fire Modeling

3.1 Introduction

This chapter outlines the inverse modeling strategy used to estimate the heat release rate of compartment fires. It gives a background on the theory of optimization and describes the fundamental workings of a genetic algorithm, and how it is coupled with the zone model BRI2002. A discussion of why genetic algorithms are useful optimization tools is presented as well. This chapter also outlines the test procedure used to analyze the IFM.

3.2 Inverse Fire Modeling Background

As discussed in section 1.2 of this document, a few studies have been performed on inverse fire modeling in an attempt to estimate the heat release rate of a fire. The basic premise of inverse fire modeling is to use a temperature profile of the upper gas layer and subsequently estimate the fire size. A correlation developed by McCaffrey, Harkleroad and Quintiere known as the MQH correlation is a good representation of the relationship between the heat release rate, the temperature of the upper layer, vent configuration and wall properties [21]. This correlation is defined below.

$$\Delta T_g = 6.85 \left(\frac{\dot{Q}^2}{A_0 \sqrt{H_0} h_k A_T} \right)^{1/3}$$

$$h_k = k / \delta \text{ for } t > t_p$$

$$t_p = \left(\frac{\rho c}{k} \right) \left(\frac{\delta}{2} \right)^2$$

$$h_k = \left(\frac{k \rho c}{t} \right)^{1/2}$$

$$\text{for } t \leq t_p \tag{10}$$

ΔT_g = Temperature of upper gas layer above ambient (K)
 ρ = density of compartment surface (kg / m³)
 c = specific heat of compartment surface (kJ / kg – K)
 k = thermal conductivity of compartment surface (kW / m – k)
 t = exposure time
 t_p = thermal penetration time (s)
 δ = thickness of compartment surface

The above equation is the classical MQH equation for a pre-flashover compartment fire, i.e. temperatures up to 600 °C. As can be seen this correlation demonstrates that the temperature of the upper layer scales with the fire size to the power of (2/3), the ventilation factor to the power of (-1/3) and wall losses to the power (-1/3). By inverting this equation, the HRR as a function of upper gas layer, vent configuration and wall properties can be obtained:

$$\dot{Q} = \left[\left(\frac{\Delta T_g}{6.85} \right)^3 * \left(A_0 \sqrt{H_0} h_k A_T \right) \right]^{1/2} \tag{11}$$

In a single compartment where the vent configuration, wall properties and upper gas layer is known this equation provides a reasonable estimate of the fire size. The methodology presented in this document utilizes a similar approach. Using a profile of

the upper gas layer, an estimate of the fire size is estimated. This research, however, attempts to account for the fact that a particular vent configuration may not be known.

3.3 Optimization

3.3.1 Background

In the field of applied mathematics optimization revolves around finding a value x , such that a function, $f(x)$ is as small or as large as possible [22]. Engineering optimization refers to “the process of finding the ‘best’ possible values for a set of variables for a system while satisfying various constraints [23].” These best possible values refer to either minimizing or maximizing the design objectives, where design objectives are something to be made as high or as low as possible [23]. For example, they could be to minimize cost, or to maximize output. The basic form of an optimization problem revolves around minimizing or maximizing an objective function, such as [23]:

$$\underset{x \in D}{\text{Minimize}} \{f_1(x), f_2(x), \dots, f_m(x)\} \quad (12)$$

Where f_i , $i = 1, \dots, m$ is an objective function and x is a variable vector that is constrained to lie in a region D [23]. Optimization encompasses a wide array of problems from a simple linear function, to non-linear functions with multiple variables, or multi-objective problems where the goal is to optimize more than one design objective [23]. The optimization problem classes are summarized below in Table 1.

Table 1. Problem classes for optimization [23].

Problem Class
Linear Programming
Nonlinear Programming
Single-objective unconstrained
Multiple Variable
Curve Fitting
Least Squares
Single-objective constrained
Single Variable
Multiple Variable
Quadratic
Semi-infinite
Multiobjective

The particular type of problem class that this research falls under is the “nonlinear single-objective constrained single variable” and “multiple variable” problem class. When only the HRR of the compartment is optimized, it is a single variable problem. However, when the ventilation profile along with the HRR is included, it becomes a multiple variable problem. In both cases, however, it is a single objective problem because the end goal is to minimize the temperature residuals of the upper layer between a candidate solution and the reference curve. Optimization algorithms are numerical methods that are designed to solve these problem classes. There are many optimization techniques that are specifically designed for each type of problem. Some traditional optimization techniques that are used to solve nonlinear problems are trial and error, linearization, gradient method and the Monte Carlo simulation [14]. The genetic algorithm was selected because of its advantages over other these optimization techniques including “excellent performance in high dimensional problems, resistance to becoming trapped in local optima, wide exploration of the parameter space [14].” A further description on the workings of genetic algorithms is discussed in the next section.

3.3.2 Genetic Algorithms

Genetic algorithms (GAs) are an advanced optimization tool that are used to solve a wide array of optimization problems. A genetic algorithm is superior to other optimization functions because it can handle both linear and non-linear functions that may contain many local minima and maxima [14]. Due to its stochastic sampling technique, a genetic algorithm is less likely to get trapped in these local extrema and is successful at providing a global viewpoint [24]. “Genetic algorithms have been shown to solve linear and nonlinear problems by exploring all regions of the state space and exponentially exploring promising areas through mutation, crossover and selection operations applied to individuals in the population [24].” A GA was selected for this project because of its ability to handle multiple parameters and because it is less likely than other optimization functions as mentioned in section 3.3.1 to become trapped on a local extrema.

The GA works on the principles of Social Darwinism, or survival of the fittest theory. The process works by seeding the algorithm with an initial population. This population consists of a number of individuals, or potential candidate solutions. Each individual consists of a parameter set, where each parameter is referred to as a gene. For this project the parameters or genes are the mass loss rate, the door width, the door height, window width and window heights of compartments. The algorithm assigns each individual candidate a fitness, or a measure of the quality of the candidate solution. Through a number of genetic operations, a subsequent population is produced based on the previous population. Through the process of Social Darwinism better fitted individuals tend to survive and reproduce based on their fitness, however, individuals

with a lesser fitness can reproduce by chance as well [15]. The algorithm continues this process until a set number of generations or a specified fitness threshold is reached.

The intended methodology utilized in this research is to have BRI or FDS create a reference curve with known parameters that are exact. Then using the genetic algorithm, it will be determined how accurately a potential solution estimates the reference curve. The genetic algorithm is used because of its abilities to sort through multiple parameters. In this case, the ventilation inside a compartment and the fire size are unknown and will be parameters. The genetic algorithm will run through tens to thousands of different simulations with varying mass loss rates and vent sizes to determine the best individual. The final solution that is obtained through the genetic algorithm is not always the exact optimal solution. The solution that the genetic algorithm yields, however, will predict results that are very close to the reference simulation.

3.3.2.1 Workings of a Genetic Algorithm

As discussed above, the genetic algorithm begins its process with an initial population of individual candidates. Each individual candidate contains parameters i.e. heat release rate, door width, door height, window width, window height, depending on the particular problem. This initial population can either be manually inputted to the genetic algorithm, or it can be randomly generated as was done for this research. Each population can contain tens, hundreds or even thousands of individual candidate sets of parameters. For this study, the population size was varied but generally maintained between 20-100 individuals. A study analyzing the effect of population sizes and

generations can be seen in Appendix A5. This research demonstrated that typical population sizes around 20-100 produced accurate results. In the genetic algorithm it is specified that each parameter be maintained between user specified bounds. For example, the mass loss rate parameter can be specified to be between 200 – 6,000 kW for the entire simulation, and the door width between 0-2 m.

As mentioned, after an initial population has been generated, each individual candidate is assigned a fitness. The fitness is the backbone of the genetic algorithm and empowers all of the subsequent generations. The fitness function for this project is designed to measure a discrepancy (or error) between the upper layer temperature of the reference curve and the upper layer temperature created by a candidate solution (individual). The fitness function is defined below:

$$f = \left(\sqrt{\frac{\sum_{n=1}^N (T_{ref}(t_n) - T_{try}(t_n))^2}{N}} \right)^{-1} \quad (13)$$

This function is a form of the least squares error function. Here $T_{ref}(t_n)$ is the temperature of the upper layer of the reference curve at time n, and T_{try} is the temperature of the candidate solution generated by the genetic algorithm at time n, as well. The function is raised to the power of -1 so that near perfect solutions will yield a very large fitness. An exact solution will produce an infinite fitness. For example a candidate solution that produces an average temperature difference of 1 °C from the reference curve will yield a fitness of about 1. A candidate solution that produces an average temperature difference of 50 °C will yield a fitness of about .02. This fitness function is designed to assign a factor to the distance of how far on average the temperature of the candidate

solution is from the reference curve. This function measures the fitness of each individual and provides information to the genetic operator functions so that better individuals can survive and reproduce.

Operator functions allow the GA to search the space for better solutions [24]. These functions create new solutions based on the previous population. Two basic types of operator functions exist in the genetic algorithm that was used for this research. These are crossover functions, which take two individuals and produce two new individuals while a mutation function takes one individual and alters it to produce a new individual [24]. These new individuals are referred to as “children.” The genetic algorithm here uses seven different crossover and mutation functions for this research. These functions are the default operator functions and can be adjusted as needed. However, for the purpose of studying the algorithm, all default crossover and mutation functions were used in this research. *It is important to note*, however, that by adequately selecting which operator functions are used, the computational time can be greatly reduced because fewer mutations occur and fewer individuals are produced. However, the search space may not be as widely analyzed without all the functions. The particular use of crossover and mutation functions is an area that needs to be analyzed in more detail in the future.

After new individuals have been reproduced, a selection function is used to determine which of the individuals will survive to the next generation [24]. The selection function utilized in this research is the default function, entitled “Normalized Geometric Select”. It is a ranking selection function that is based on the normalized geometric distribution. It ranks the possible candidate solutions (individuals) based upon their fitness and selects new individuals accordingly [24]. Generally speaking better fitted

individuals survive and reproduce, therefore, improving the quality of the candidate solutions, however, by chance lesser fitted individuals can survive as well [15].

The genetic algorithm is terminated through one of two ways. It can either be stopped if any one individual ever reaches a specified fitness threshold, or it can be stopped if the specified number of generations is reached. For this research, all genetic algorithms were stopped after a certain number of generations occurred. This varied from simulation to simulation but was primarily between 25 and 100 generations. As can be seen in Appendix A5, a study analyzing the effects of the population size and number of generations demonstrated that 25-100 generations generally provided accurate results while conserving computational cost.

3.3.3 Description of Inverse Fire Model Coupled with a Genetic Algorithm

The IFM utilizes the genetic algorithm to sort through thousands of different zone model simulations in an attempt to find the optimal solution between the reference BRI simulation and the trial solution. Houck et al. of North Carolina State University created the genetic algorithm used for this research [24]. The package comes in the form of a Genetic Algorithm Optimization Toolbox (GAOT). The algorithm is freeware and is available at the following website

<http://www.ie.ncsu.edu/mirage/GAToolBox/gaot/papers/gaot.ps>. This toolbox is comprised of dozens of MATLAB m-files containing the genetic algorithm code itself, initialization functions, termination functions, selection functions and operator functions as discussed above.

In order for the IFM to solve the inverse problem at hand, the genetic algorithm needed to be coupled with the zone model BRI2002. The author is unaware of genetic algorithms ever having been coupled with zone models before, and as such the IFM needed to be built from scratch. The IFM combined Microsoft batch files to perform automatic operations of BRI. These batch files were called by MATLAB to run BRI2002 the specified number of times as designated in the GA. The data from every zone model simulation was subsequently analyzed in MATLAB and the corresponding fitness was calculated. New individuals were also automatically inserted into BRI simulations through MATLAB. This entire process encompasses the IFM.

3.4 Testing Procedure

In order to test the IFM, a number of individual tests of increasing difficulty were performed to challenge the GA to estimate the reference heat release rate. These tests revolved around a single compartment scenario and multiple compartment scenarios. In some scenarios, the only parameter was the heat release rate. In others, as will be described below, door widths, door heights and window areas were added as additional unknown parameters. It is important to note that the issue of time in this project has not been taken into account. When arriving at a fire scene it will be very difficult to have an understanding of when exactly the fire started. Therefore, this research takes time out of the equation and assumes that the BRI solutions can be compared to the reference temperatures during an arbitrary time window (corresponding usually to long time scales, for instance 2000s-6000s). The exact interpretation and determination of this time window is left for future work.

3.4.1 Single Compartment Tests

In order to prove that the IFM is a reliable and capable model, it needed to first be verified on a number of small-scale tests. Two separate compartments were made to represent a typical office that a firefighter might encounter. The first compartment was the larger of the two; it was designed to be 10m x 10m x 3m. It had a single door to the outside, sized at 1m x 2m. The wall materials were made of hard fiberboard and flexible fiberboard (wood composites). The second compartment was the smaller of the two at 3m x 3m x 3m, once again with a 1m x 2m door to the outside. The first set of tests focused on estimating the heat release rate as a single parameter. The second set of tests included the door width and the door height as additional parameters. In most practical applications, the door height of a compartment will be known. However, in order to challenge the genetic algorithm the door height was left as a parameter. In the final set of tests for both of these sized compartments, three additional parameters were included. These additional parameters were a window width, a window upper height and a window lower height. Once again, many or all of these parameters might be known, however, in order to challenge the GA once again it was necessary to incorporate these three as additional parameters.

In all of these cases the bounds on the parameters, i.e. MLR's and ventilation characteristics varied in order to test the IFM. As discussed in section 2.4.1 the ratio between HRR to area of the fire source is important to be maintained lower than 1000 kW/m² in BRI. The IFM attempted to maintain a MLR to fuel source area ratio of 500 kW/m². However, in order to explore a wider solution space of larger mass loss rates and further test the GA, sometimes based on the compartment configuration, the area of the

fire source could not be contained within the physical domains of the compartment. In these particular situations the MLR to fire source area burns according to the area of the compartment and can become greater than 500 kW/m^2 . In these situations, however, it is still lower than the recommended 1000 kW/m^2 value. Nevertheless, BRI2002 successfully completes all of the candidate simulations within the specified bounds. The bounds that were selected for every case were chosen to maintain a balance where the GA was adequately tested and BRI2002 did not stop due to numerical instabilities.

The GA was tested to estimate the fire size of a reference BRI or FDS simulation. Using these reference simulations instead of experimental data was done for two reasons. First of all, it needed to be proven that the IFM and the genetic algorithm worked. If the GA proved that it could successfully estimate the average HRR with reasonable certainty, the proof of concept can be validated. Secondly, experimental test data is difficult to come by, and if BRI or FDS is used correctly with proper inputs it should provide a reasonable estimate of the upper layer temperature. Further validation and verification of BRI is to be done as future work.

The GA was challenged to estimate fire sizes from several reference curves each with their own set of initial conditions (fire size and vent configurations). In some cases the reference curve was represented as a constant temperature at a particular point of time, or sloped as in the form of its steady state value. This was to challenge the GA in giving an estimate of a curve where there was no exact solution, and an entire temperature history is not known. In all of the cases it is assumed that the wall properties of the building are known. Wall materials will greatly impact the temperature of the upper layer, as different materials will affect the heat transfer balance between the upper

layer and the wall. For this research, however, it will be assumed that wall properties are identical between the reference and candidate solutions and the wall properties are currently not included as potential unknown parameters.

3.4.2 Multiple Compartments

In the second set of tests the genetic algorithm was tested to estimate the heat release rate of a potentially more realistic fire scenario. This consisted of two rows of 9 offices, separated by a single long corridor. Each office was spaced 4.5m x 4.5m x 3m. The corridor was 3.5m in width by 40.5m in length. All wall materials were composed of a plaster front and a “normal concrete” backing [2]. As defined in the BRI user’s guide, the properties of normal concrete are as follows: emissivity 0.9, thermal conductivity 1.63×10^{-3} kW/m-K, specific heat 0.895 kJ/kg-K, density 2250 kg/m³, and thickness 0.10m.

In this scenario, it is envisioned that a fire is occurring in a single compartment. A window on the opposite side of the corridor (non-fire side) is opened and allows smoke to pour out. Ideally, thermal imaging cameras will analyze smoke coming out of this open window. The logic behind this setup is to account for a fire scenario where the smoke being analyzed cannot be directly measured from the fire room itself. Instead it must cross multiple compartments, and therefore lose some of its energy to the neighboring compartments. This will be more challenging for the GA, as a lot more energy balance equations occur for this scenario.

The reference curve being analyzed will be the upper layer temperature of the compartment across the hall from the fire room. This room is designated as room 1, and the fire room is designated as room 10 as can be seen in Figure 12. It will be assumed

that all door widths inside the building will be unknown. The window ventilation, however, will be known and will not be included as parameters in this configuration. Various window configurations will change between tests and this will be discussed in the results section. It will be assumed that the door height is constant at 2.13 m for all rooms. The main assumption will be in relation to the location of the fire. Currently the algorithm is incapable of handling the location of the fire. The reason for this is due to the limitations in zone modeling, and the symmetry that exists. For example, if the ventilation configuration was the same in every room, it does not matter what room the fire is in, because the exact same results will occur. Therefore, it will be assumed the fire location is known, but the fire size is not. A depiction of the building can be seen below in Figure 12 (picture taken from CFAST input file in Smokeview).

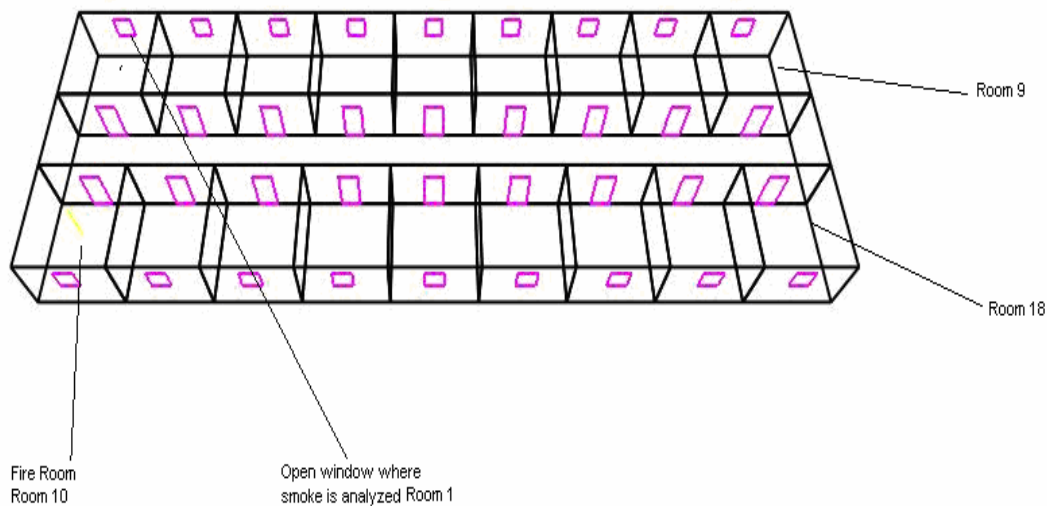


Figure 12. Layout of the multiple compartment scenarios.

In the final set of tests, the IFM was compared to an FDS simulation. Fire Dynamics Simulator was used to model the fire scenario in a similar configuration to the one described above. FDS was used as a further attempt to make a more realistic large scale fire scenario. FDS and BRI2002 would be directly compared in the same time

frame in order to compare the results. FDS was used to model the fire scenario, and then using a thermocouple placed in room 1, a profile of the upper layer temperature could be made. This was then used as an input into the IFM. The IFM would be tested to see if it could accurately estimate the fire size of different MLRs as predicted in FDS.

4 Chapter 4. Results

4.1 Introduction

This chapter describes the fundamental results obtained from the tests outlined in section 3.4. Every test run and its results are presented in Appendices A1-A6. In this chapter the words IFM and GA are inter-changeable. The first section of this chapter describes the results obtained from single compartment tests. Results analyzing the ability of the IFM to estimate the fire size for either a single parameter (HRR only) or multiple parameters (HRR and vent configurations) are discussed below. In some cases, the results are also compared to more classical expressions such as the McCaffrey Quintiere Harkleroad (MQH) Correlation for pre-flashover fires. The second half of this section outlines the tests performed for the multiple compartment scenarios. It is important to note the terminology used in these sections. *Mass Loss Rate* is the corresponding fire size in kW that is input into BRI. *Heat Release Rate* is the fire size in kW that *actually* burns inside a compartment based on the mass burning rate. The simulations are organized in the following manner in this section and the appendix:

Single Compartment Tests:

SR3_3_3_Fb_letter_#

Where:

SR (Single Room)

3_3_3 (3m x 3m x 3m single compartment)

10_10_3 (10m x 10m x 3m single compartment)

Fb (Compartment walls are composed of hard and flexible fiber board, all simulations are ramped up to 720 kW at 120s, and then its steady value from 240-6000s)

NC (Compartment walls are composed of normal concrete, all simulations are steady from 0-6000s)

Table 2. Key for simulations for single compartment tests. The letter labeling system is explained in Figure 13 to Figure 18.

Letter	Meaning
a	Exact reference curve and GA candidate solutions analyzed 1-6000s*. Exact reference curve.
b	Exact reference curve and GA candidate solutions analyzed at steady state (2000-6000s).
c	Approximate steady reference curve with the value taken at 4000s. Both curves analyzed 2000-6000s.
d	Approximate steady reference curve with the value taken at 3000s. Both curves analyzed 2000-6000s.
e	Approximate steady reference curve with the average value taken from 2000-6000s.
f	Approximate sloped reference curve with the instantaneous slope taken at 4000s. Both curves analyzed 2000-6000s.
g	Approximate sloped reference curve with the instantaneous slope taken at 3000s. Both curves analyzed 2000-6000s.
h	Approximate sloped reference curve with the slope being the average slope from 2000-6000s. Both curves analyzed 2000-6000s.

*For any simulations where the * symbol is shown, this means that the analysis period was 0-6000s, not 1-6000s. For these simulations the reference simulation was at 22°C at time 0, and all candidate solutions were at 0°C, because the dlmread command used in MATLAB recorded the first point as 0 °C and not 22 °C.

(Simulation number in that particular grouping)

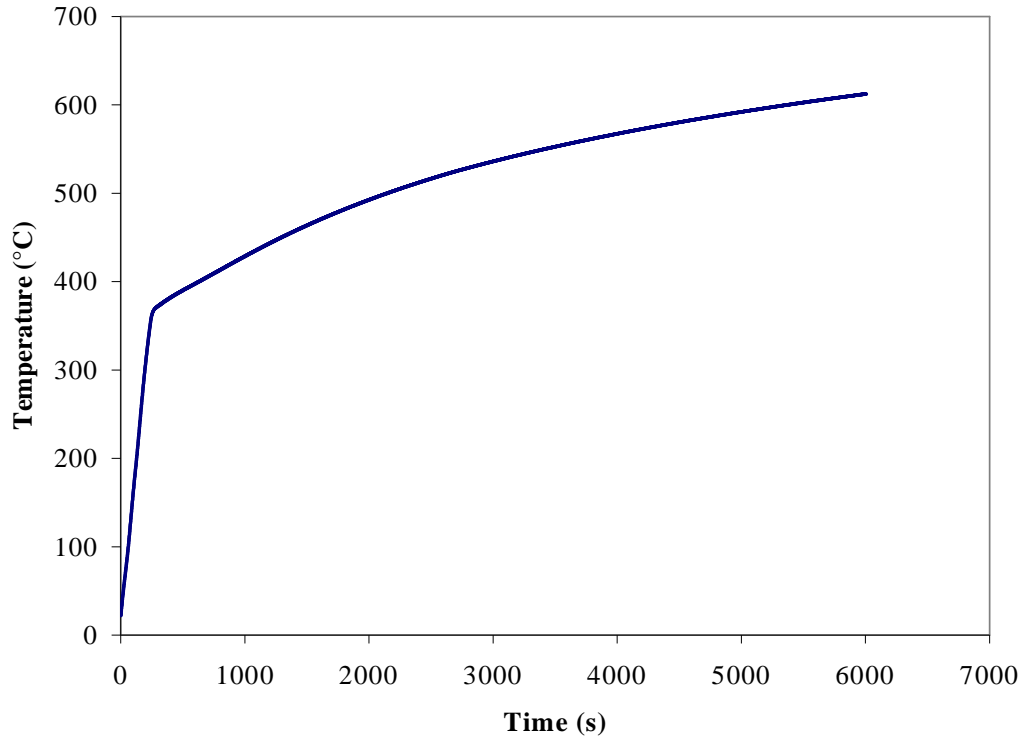


Figure 13. Simulation letter a. Exact reference curve is analyzed entirely from 1-6000s.

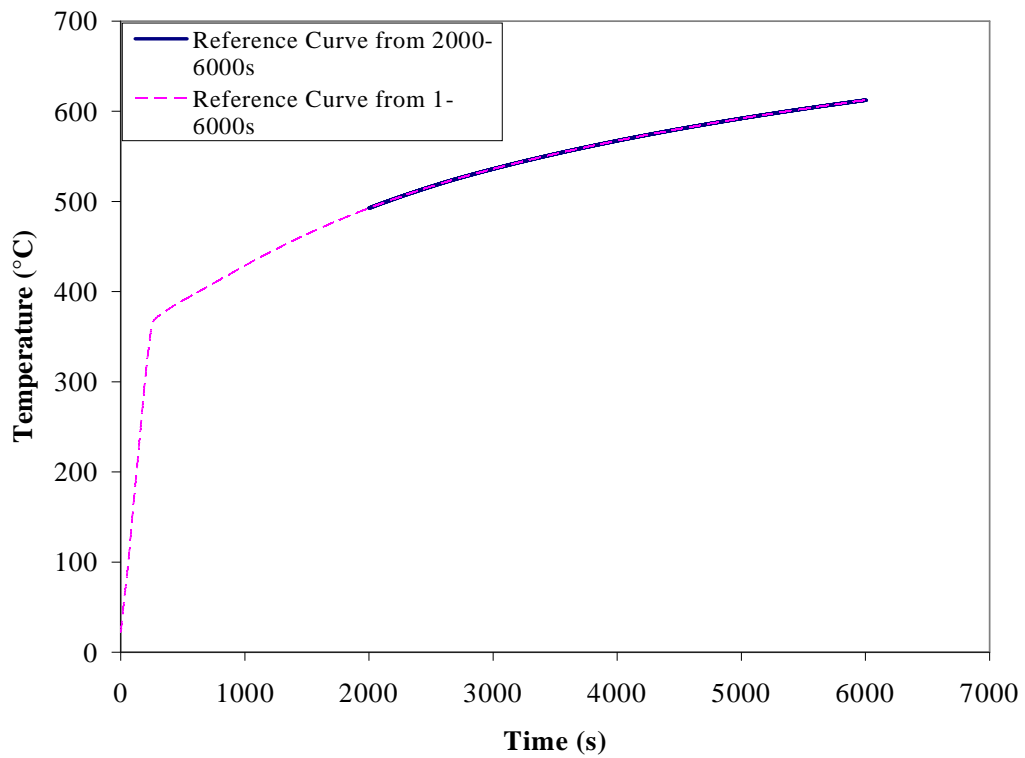


Figure 14. Simulation letter b. Exact reference curve is analyzed from 2000-6000s.

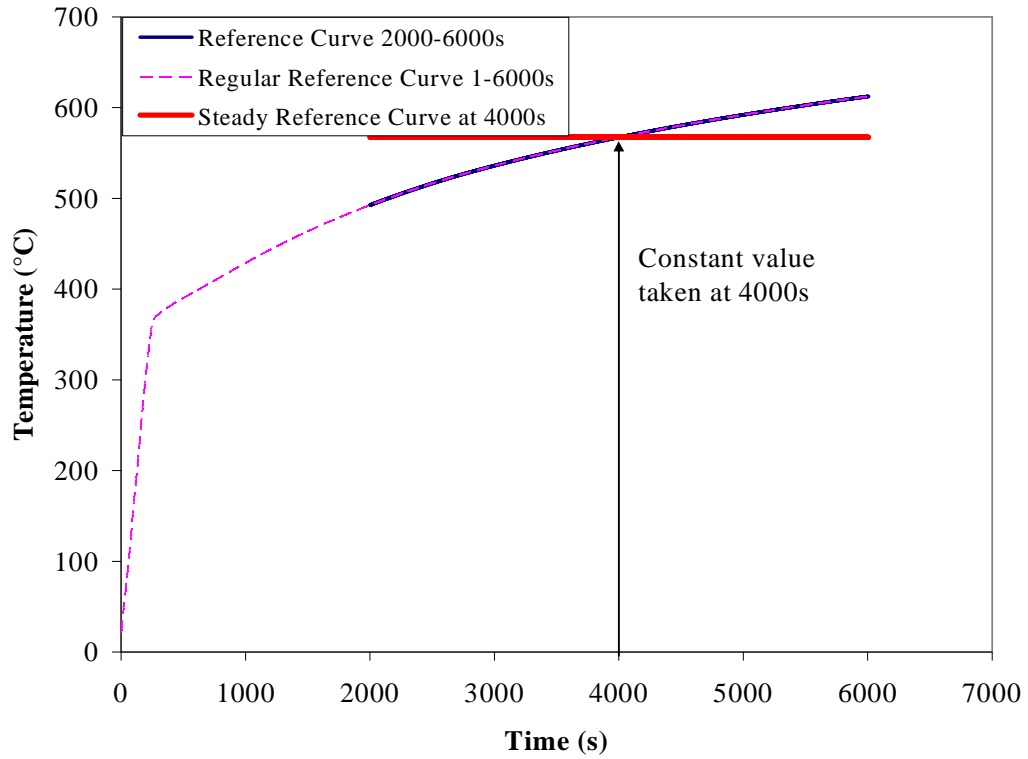


Figure 15. Simulation letter c. Approximate steady reference curve with the constant value taken at 4000s.

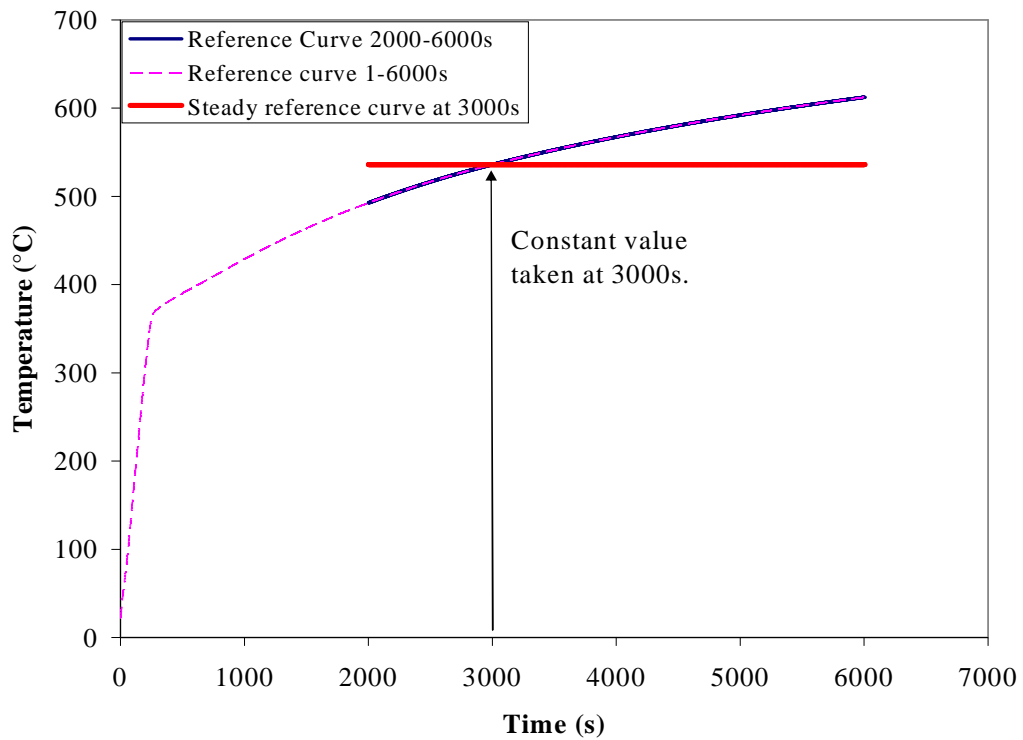


Figure 16. Simulation letter d. Approximate steady reference curve with value taken at 3000s.

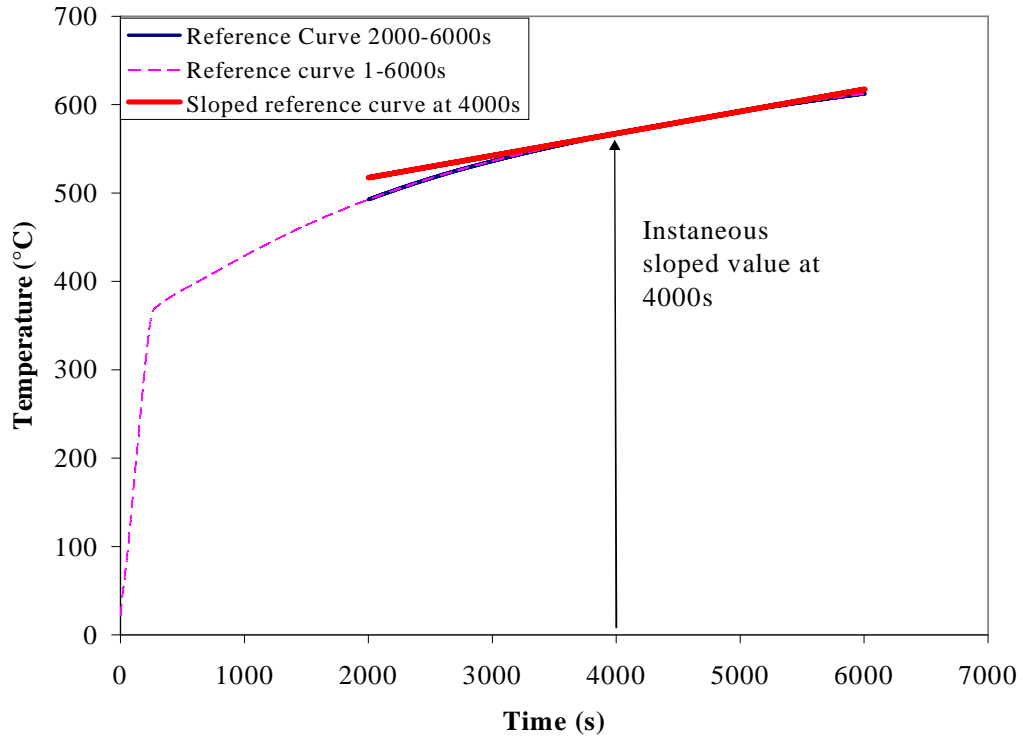


Figure 17. Simulation letter f. Approximate sloped reference curve at 4000s.

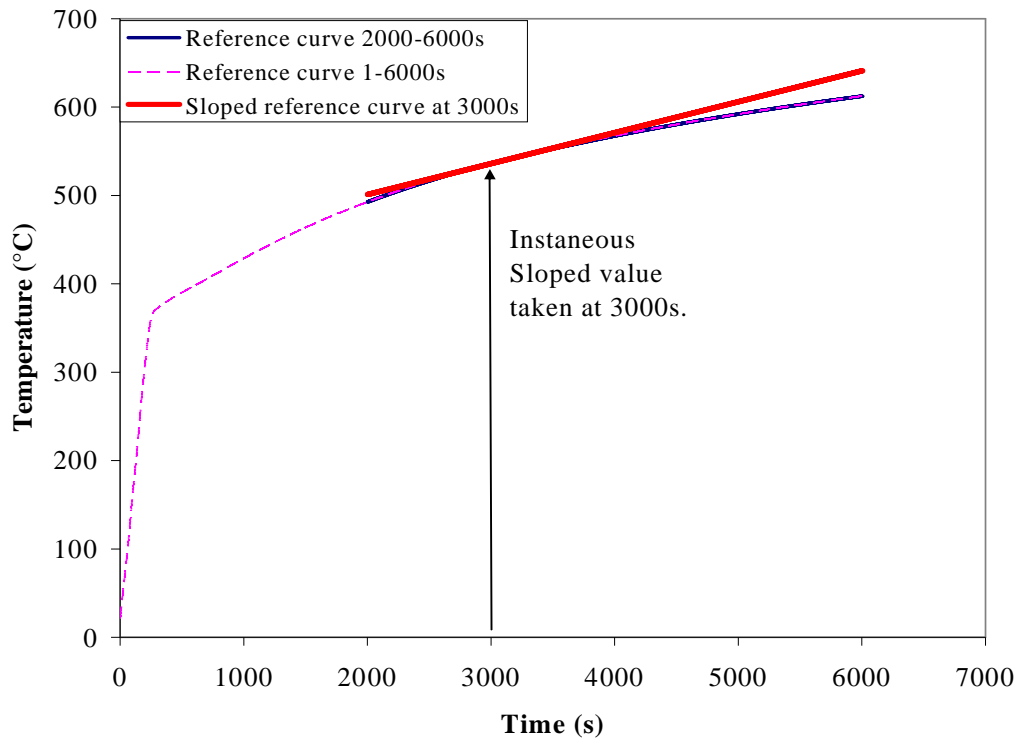


Figure 18. Simulation letter g. Approximate sloped reference curve at 3000s.

Multiple Compartment Tests:

MR_W#_letter_#

Where MR (multiple rooms/compartments)

W# (Number of outside windows that are open)

W1_10_11 (window 1, 10 and 11 are open)

W1_10:18 (window 1, windows 10 through 18 are open)

W1:18 (all windows are open)

Table 3. Key for simulations for multiple compartments.

Letter	Meaning
a	Exact reference curve and GA candidate solutions analyzed at steady state 2000-3000s from window W1.
b	Approximate steady reference curve with value taken instantaneously at 2500s. Both curves analyzed 2000-3000s. Approximate steady reference curve.

(Simulation number in that particular grouping)

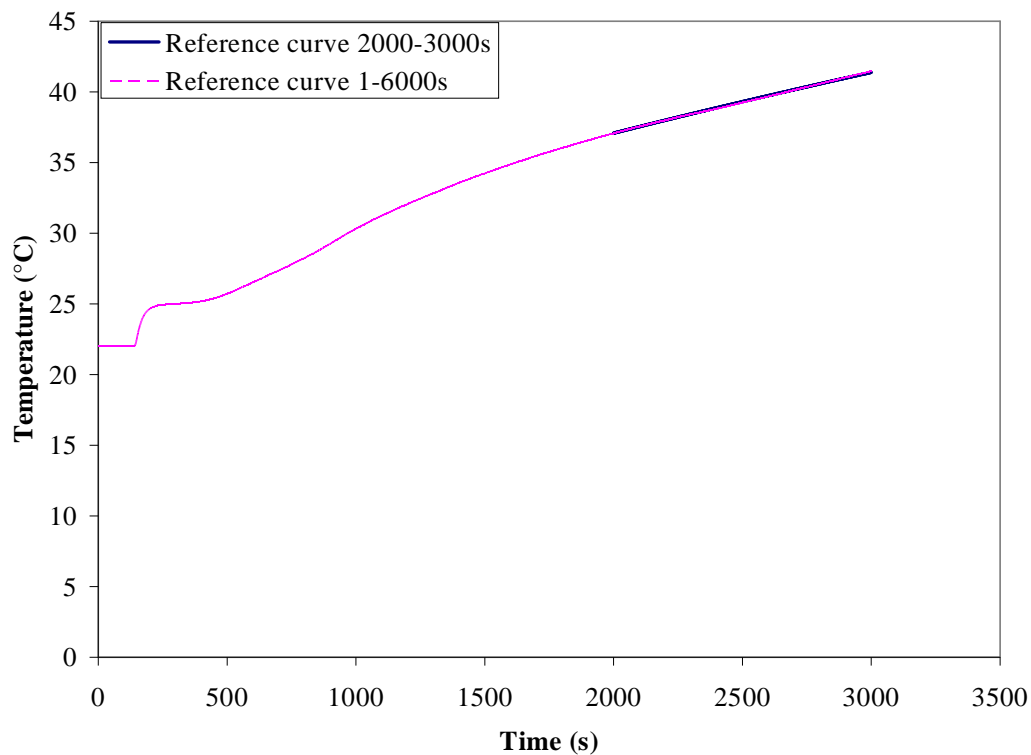


Figure 19. Simulation letter MR_a. Exact reference curve analyzed 2000-3000s.

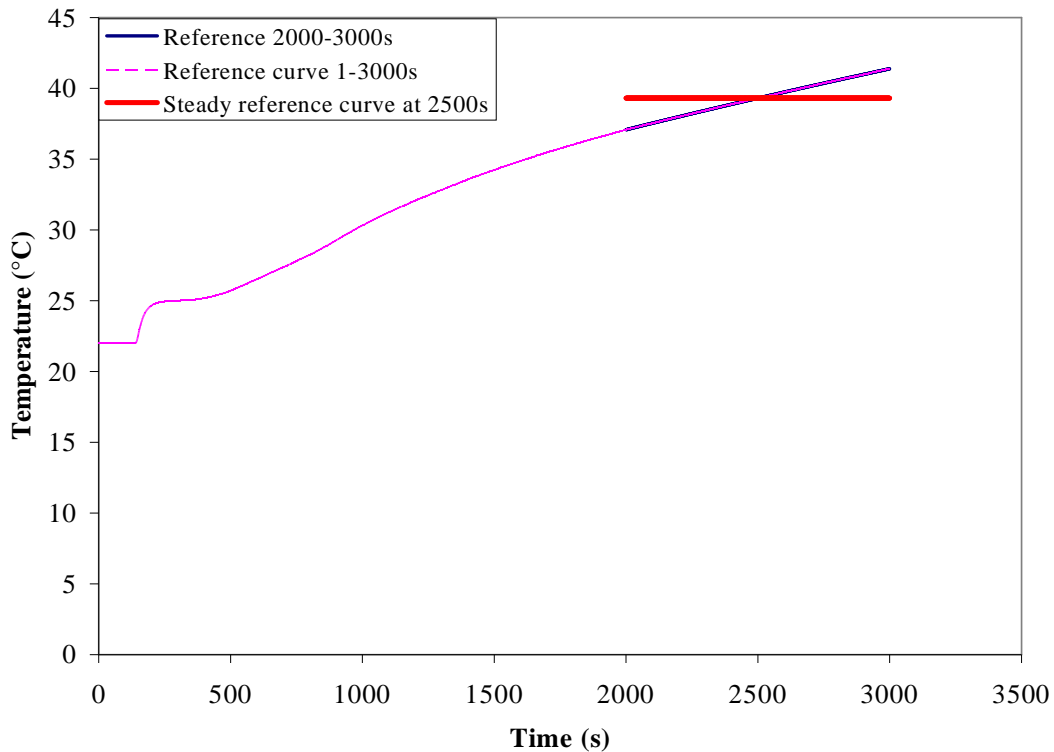


Figure 20. Simulation letter MR_b. Approximate steady reference curve with constant value taken at 2500s.

4.2 Single Compartment Tests

4.2.1 Heat Release Rate as Only Parameter

A large number of tests were run to determine if the heat release rate of the fire could successfully be estimated in a situation where the vent configuration was known. As a result, the only parameter that changed was the mass loss rate of the fire. For a single parameter, the IFM proved to be very effective in estimating the HRR of the reference simulation. All of these results can be seen in Appendix A1.

The first tests ever run analyzed a situation where the mass loss rate of a fire remained steady from 240-6000s. The fire was initially ramped up to 720 kW at 120s. This value was an arbitrary value in order to ramp the HRR from 0 kW. The IFM then analyzed a number of candidate solutions of different mass loss rates that remained

steady from 240-6000s. These candidate simulations were assumed to have the same initial ramping form of 720 kW at 120s. The curves were analyzed from 1-6000s to determine if the algorithm could back out the exact reference curve. The following results are for a reference curve where a steady mass loss rate was prescribed to yield a 1920 kW fire or a 2400 kW fire in the 10m x 10m x 3m compartment. The population size and the number of generations varied in each simulation. As can be seen, the results were nearly perfect for every simulation.

Table 4. Single parameter tests where the entire reference curve is analyzed from 1-6000s.

Simulation Number	Reference MLR	Reference Average HRR (240-6000s)	GA Best MLR	GA Best Average HRR (2000-6000s)	Bounds on Parameters	Notes About Simulation
SR10_10_3_Fb_a_1	1920 kW	1406 kW	1918.8 kW	1406 kW	1,000-10,000 kW	50 generations, population size of 10.*
SR10_10_3_Fb_a_2	2400 kW	1485 kW	2423 kW	1489 kW	1,000-10,000 kW	20 generations, population size of 10.
SR10_10_3_Fb_a_3	2400 kW	1485 kW	2400 kW	1485 kW	1,000-3,250 kW	10 generations, population size of 10.
SR10_10_3_Fb_a_4	2400 kW	1485 kW	2402 kW	1485 kW	1,000-5,000 kW	30 generations, population size of 10.

These tests were run in order to demonstrate that the genetic algorithm correctly optimizes the fitness function and is capable of extracting a perfect, if not a near perfect, solution in relatively few generations. Simulation 2's performance can be seen in Figure 21 below. The blue curve is the fitness of the best individual ever found, and the red curve is the average fitness of the population or a measure of the quality of the candidate solutions. As can be seen, the best solution is found very quickly and produces a result

that is only 4 kW away from the HRR of the reference simulation. Its mass loss rate is 23 kW from the reference simulation, but that is still very reasonable for only 20 generations. A plot of the reference curve's upper layer temperature with the GA's best estimate for simulation 2 can be observed in Figure 22. As demonstrated, the two temperature profiles are nearly identical. Even for the "worst" estimate of all 4 simulations above, the GA is able to find a solution that produces less than 1 °C difference between itself and the reference curve.

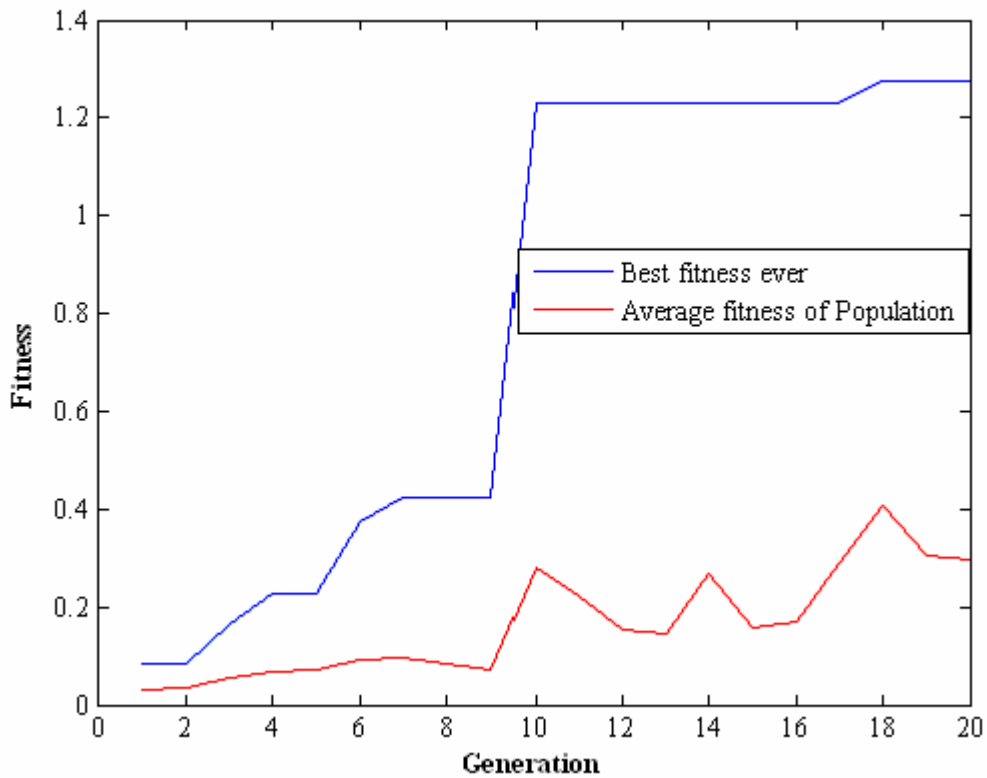


Figure 21. Simulation SR10_10_3_Fb_a_2. Evolution of the best fitness ever found and the average fitness of the population.

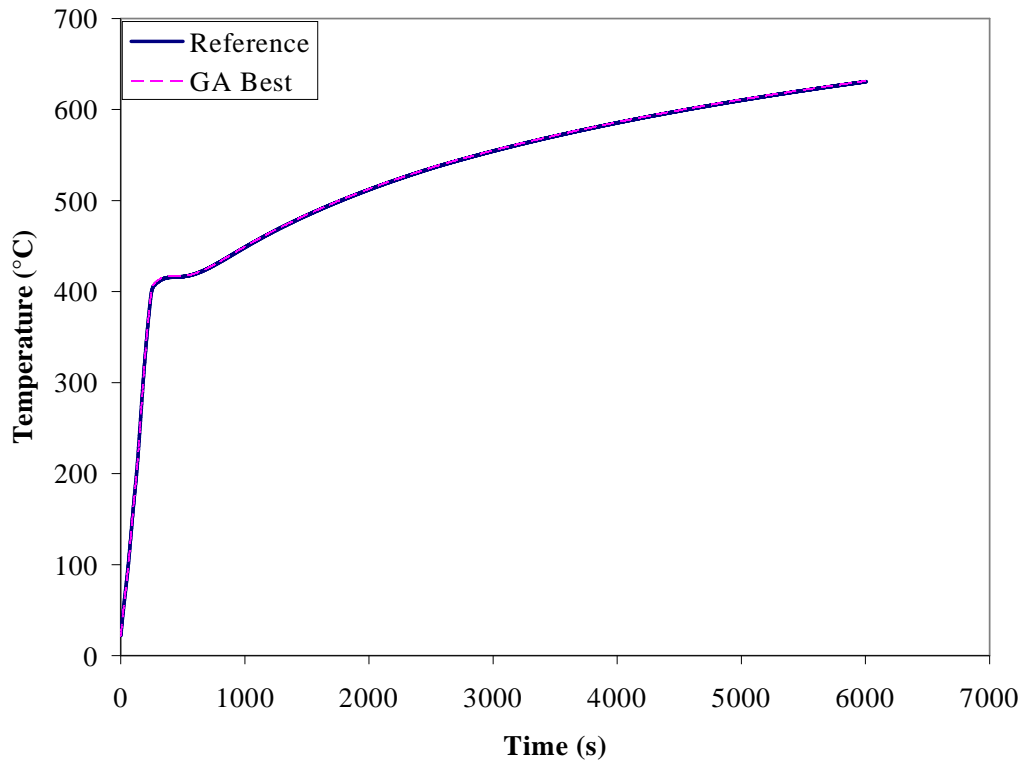


Figure 22. Simulation SR10_10_3_Fb_a_2. Plot of the upper layer temperature of the reference simulation and the GA best simulation.

As shown in Table 4, the prescribed mass loss rate of 2400 kW or 1920 kW is not equal to the HRR created by the mass burning rate. As discussed in chapter 2, this can be explained by the fact that BRI2002 starts to burn incompletely when the oxygen mass fraction drops below 14% or namely the equivalence ratio goes above 0.3. Therefore, this series of tests were extended to fire sizes that were completely over-ventilated, i.e. a MLR of less than 800 kW to determine if the results were repeatable.

The over-ventilated tests were run in a compartment 3m x 3m x 3m, and there was no initial ramping of the MLR curve. The fire sizes were steady from time 0-6000s. The compartment was also changed from a composite of hard and flexible fiberboard, to normal concrete as defined in the BRI user’s guide. Two simulations were run, one for a steady 200 kW fire and another for a steady 600 kW fire corresponding to simulations

SR3_3_3_NC_b_1 and SR3_3_3_NC_b_2 respectively in Appendix A1. The population sizes were equal to 20 and the number of generations equal to 50. The GA successfully backed out both heat release rates. In fact, the GA found an exact match of 200 kW for the 200 kW reference curve, and 600.2 kW for the 600 kW reference curve. The performance of their simulations can be seen in Figure 23 for the 200 kW reference curve and Figure 24 for the 600 kW reference curve.

In these simulations the GA only analyzed steady state conditions, i.e. a time period of 2000-6000s. Obtaining total steady state in a fire condition where the upper layer temperature does not change at all, with time is not possible. This is because the wall materials heat up very slowly and, as a result, causes the upper layer temperature to continue to change with time due to its decreasing wall heat losses. Therefore, based on the temperature curves, relative steady state was defined between 2000-6000s. In an actual fire, the exact starting time and duration may be unknown; therefore the current IFM is limited to making estimations in a known time period. In other words, these tests are designed to show at quasi-steady state, what value of the HRR provides the best estimate of the reference curve. As a result, this current research is limited in that it can only make comparisons assuming the time period is known.

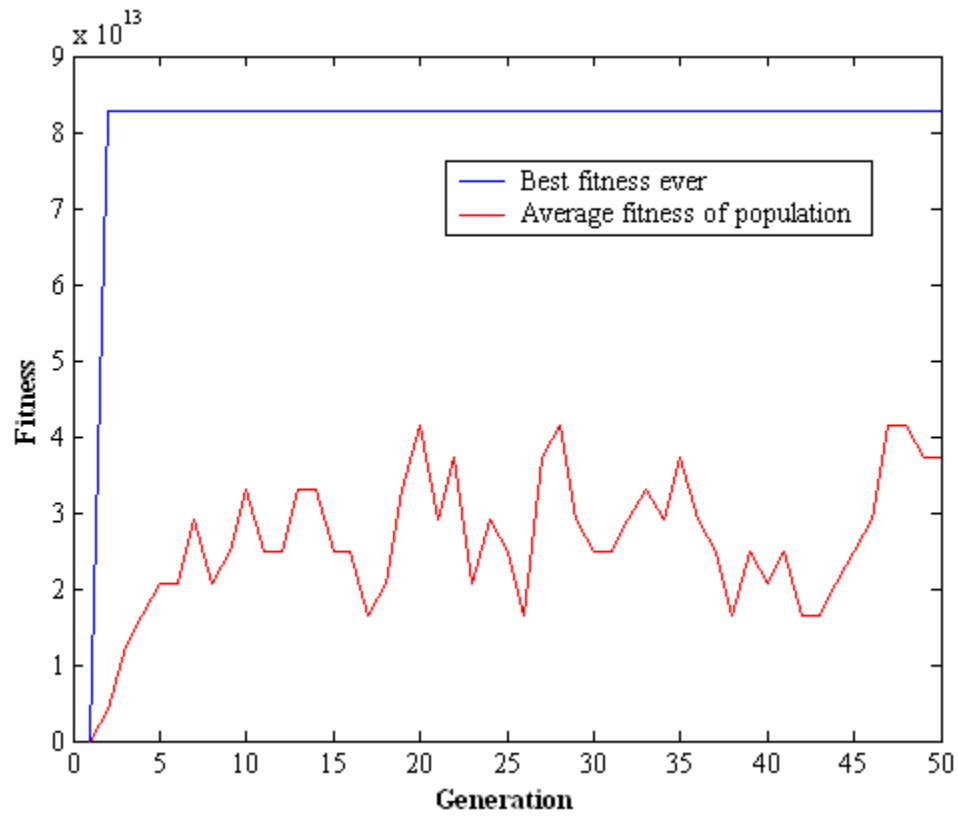


Figure 23. Simulation SR3_3_3_NC_b_1 Evolution of the best fitness ever found and the average fitness of the population for a reference simulation of 200 kW steady fire. An exact solution was found.

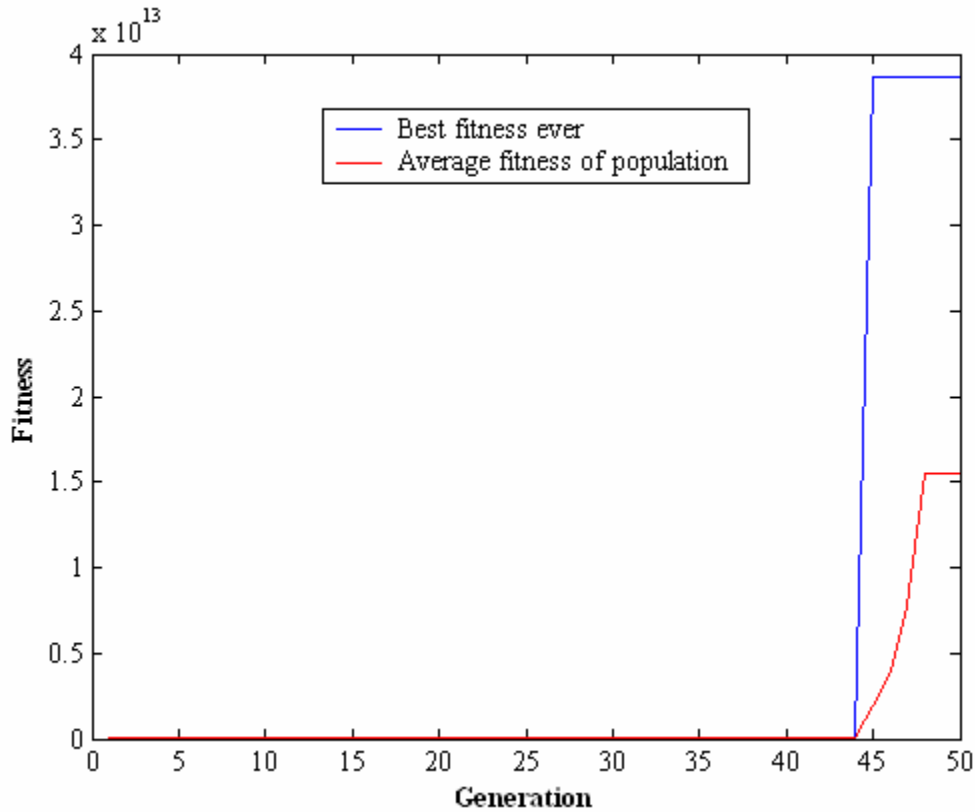


Figure 24. Simulation SR3_3_3_NC_b_2 Evolution of the best fitness ever found and the average fitness of the population for a steady 600 kW reference simulation. An exact solution was found

These simulations demonstrate once again the GA's ability to sort through several hundred simulations and estimate the reference HRR. Running these simulations for one parameter, for a population size of 20 and 50 generations takes on the order of 2 hours on a single 2.0 GHz processor. Ultimately this time needs to be reduced if it is to be used in real time applications.

In an actual fire situation, obtaining a profile of the upper layer temperature for a long time will not be feasible. Most likely, at a fire scene cameras will be setup and will record an instantaneous value of the temperature of the upper layer at a period of time or for a few seconds. In addition, in an actual scenario there will be no exact solution. In the tests outlined above, an exact solution could potentially be found because both the reference simulation and the candidate solutions were analyzed in the same time frame.

To account for this, the GA was tested where a single value of the reference curve was taken and used to represent a constant reference curve for a period of 2000-6000s. The IFM was then tested to determine if the GA could find a HRR that provided the least amount of error between this steady reference curve and the predictions. Other simulations were run where the reference curve was instantaneously sloped at a particular time (i.e. the reference curve is a linear function of time). This was done in an attempt to more directly mimic the shape of the reference curve at quasi-steady conditions. Currently, the temperatures that were taken from the reference curve were values somewhere defined in steady state i.e. 2000-6000s.

These sets of tests were run for fire scenarios that burned completely and incompletely. The incomplete burning cases can be seen in appendix A1. The cases presented below are when the MLR was prescribed to yield a 500 kW fire and are completely over-ventilated. A steady 500 kW fire was specified in a 3m x 3m x 3m room made of normal concrete. The results can be seen in Table 5 below

Table 5. Steady and sloped reference curve results for a steady 500 kW fire. A vent of 1m x 2m is fully open throughout all simulations

Simulation Number	Reference MLR	Reference Average HRR (2000-6000s)	GA Best MLR	GA Best Average HRR (2000-6000s)	Bounds on Parameters	Notes About Simulation
SR3_3_3_NC_c_1	500 kW	499 kW	500.1 kW	499 kW	200-9,000 kW	Population size 20, 50 generations.
SR3_3_3_NC_d_1	500 kW	499 kW	476 kW	475 kW	200-9,000 kW	Population size 20, 50 generations.
SR3_3_3_NC_f_1	500 kW	499 kW	503 kW	502 kW	200-9,000 kW	Population size 20, 50 generations.
SR3_3_3_NC_g_1	500 kW	499 kW	506 kW	505 kW	200-9,000 kW	Population size 20, 50 generations.

As demonstrated in Table 5, for this scenario the estimated results at steady state are very close to the reference simulation. The performance of simulation

SR3_3_3_NC_d_1 can be seen below, along with a plot of the GA best curve and the steady reference simulation.

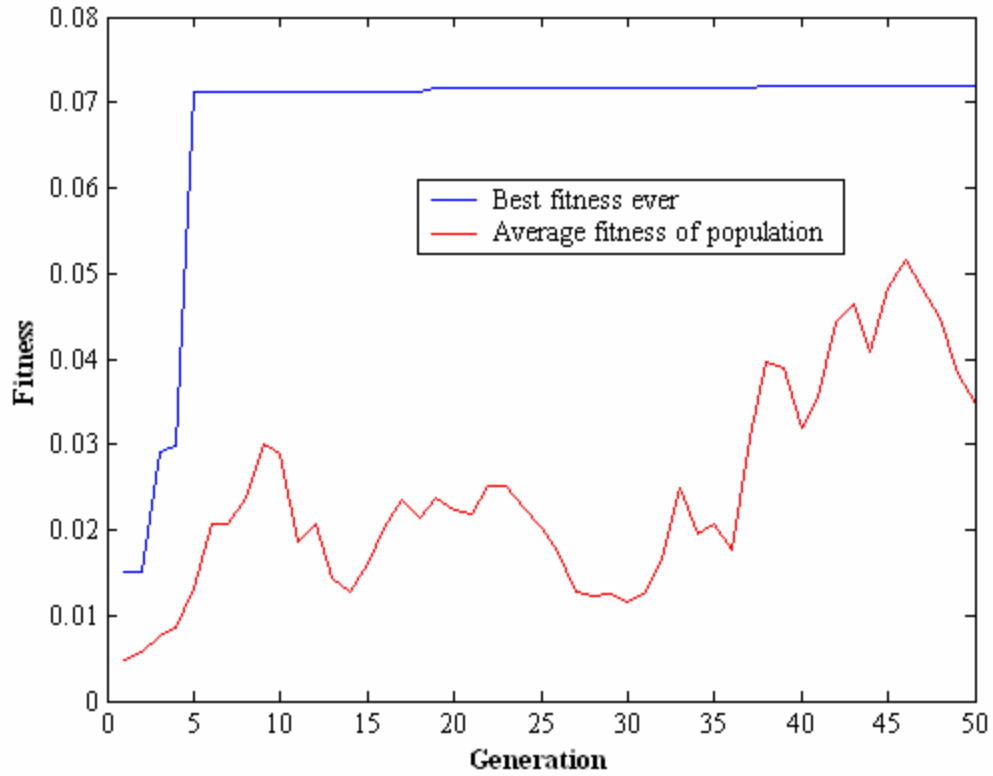


Figure 25. Simulation SR3_3_3_NC_d_1 evolution of the best fitness ever found and the average fitness of the population.

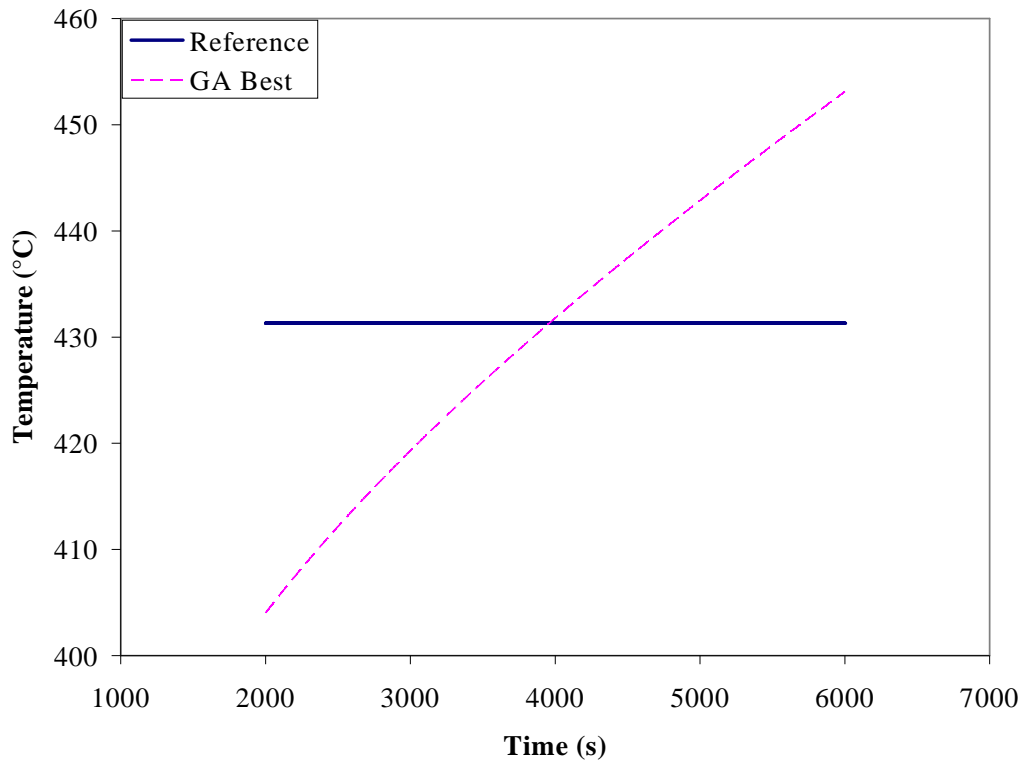


Figure 26. Simulation SR3_3_3_NC_d_1 upper layer temperature profile for the steady reference curve and the GA best.

As demonstrated in these results, the IFM is very successful in estimating the reference HRR if only one parameter is involved, the MLR itself. An alternative to this type of Inverse Fire Model would be to use a correlation such as the McCaffrey Quintiere Harkleroad Correlation which relates fire size to upper layer temperature, and compartment configuration as outlined in section 3.2. As previously discussed, the equation can be inverted if the upper gas layer is known to solve for the HRR, \dot{Q} :

$$\dot{Q} = \left[\left(\frac{\Delta T_g}{6.85} \right)^3 * \left(A_0 \sqrt{H_0} h_k A_T \right) \right]^{1/2}$$

The MQH correlation was compared against the IFM for the 500 kW fire scenarios summarized in Table 5. Using the temperature of the upper layer as calculated in BRI for a steady 500 kW fire at 3000s and 4000s into the simulation the comparison

can be made. This correlation, however, assumes that the vent configuration is known. As will be discussed in later sections, the IFM will account for an unknown vent configuration. However, since this set of tests assumes the vent configuration is known, the MQH correlation can be compared directly against the IFM. The following is a sample calculation of the MQH correlation where properties are taken from the BRI user's guide for normal weight concrete, and the temperature of the upper layer at 4000s was calculated in BRI to be 444 °C for a 500 kW fire:

$$\rho = 2250 \text{ kg} / \text{m}^3$$

$$c = .895 \text{ kJ} / \text{kg} - \text{K}$$

$$k = 1.63 \text{ W} / \text{m} - \text{K}$$

$$\delta = .10 \text{ m}$$

$$\Delta T_g = 422 \text{ K}$$

$$t_p = \left(\frac{2250 \text{ kg} / \text{m}^3 * .895 \text{ kJ} / \text{kg} - \text{K}}{.00163 \text{ kW} / \text{m} - \text{K}} \right) \left(\frac{.1 \text{ m}}{2} \right)^2 = 3089 \text{ s}$$

$$\text{because } t(4000 \text{ s}) > t_p(3089 \text{ s})$$

$$h_k = k / \delta$$

$$\Rightarrow h_k = (.00163 \text{ kW} / \text{m} - \text{K}) / .1 \text{ m} = .0163 \text{ kW} / \text{m} - \text{K}$$

$$\Rightarrow \dot{Q} = \left[\left(\frac{717 \text{ K} - 295 \text{ K}}{6.85} \right)^3 * \left(2 \text{ m}^2 * \sqrt{2 \text{ m}} * .0163 \text{ kW} / \text{m} - \text{K} * 52 \text{ m}^2 \right) \right]^{1/2} = 749 \text{ kW}$$

As shown, the MQH correlation estimates the 500 kW fire size to within the correct order of magnitude at 750 kW. With known properties of normal weight concrete used, as given in the BRI user's guide, the following estimates of the heat release rate based on the MQH correlation were made.

Table 6. MQH estimate of the reference simulation v. IFM estimate.

BRI MLR	MQH Correlation
200 kW (4000s)	290 kW
200 kW (3000s)	400 kW
200 kW (average temp)	289 kW
500 kW (4000s)	749 kW
500 kW (3000s)	1018 kW
500 kW (average temp)	746 kW
600 kW (4000s)	888.4 kW
600 kW (3000s)	1206 kW
600 kW (average temp)	885 kW

As can be seen for a steady 200 kW fire as predicted in BRI, the MQH correlation estimates a fire size of around 290 kW at a corresponding temperature value taken at 4000s into the simulation. For the 600 kW fire as predicted in BRI, the MQH correlation estimates a fire size of 890 kW for a corresponding temperature value at 4000s. For the simulated data as predicted in BRI, the MQH correlation has provided an estimate that has the correct order of magnitude and is quite reasonable to the BRI prediction. However, the IFM provides a better estimate to the reference simulation. The IFM incorporates a more fundamental formulation utilized in BRI and is very successful in estimating the fire size if the vent configuration is known. Where a vent configuration is fixed, only a single solution exists and the IFM maximizes the fitness function in only a few generations by successfully finding the optimal solution.

4.2.2 Single Compartment, Door Vent Configuration as Parameters

In the second series of tests, an attempt to account for an unknown vent configuration was studied. All of these results are summarized in Appendix A2. In most practical applications, the vent configuration inside a compartment will *not* be known, i.e. whether a door to the fire compartment is half open, fully open etc. The same series of

tests as outlined in section 4.2.1 were run for a configuration where the door width and door height were considered to be unknowns.

For the 3m x 3m x 3m compartment composed of normal concrete, a series of tests were run that analyzed fire scenarios that burned completely and incompletely. In these tests the reference and the trial simulations were analyzed at “steady state”, i.e. 2000-6000s, and as a result an exact solution could potentially be found. These results can be seen in Table 7 below.

Table 7. Single Compartment tests where the door width and door height are additional parameters.

Simulation Number	Reference MLR	Reference Average HRR (2000-6000s)	Reference Vent	GA Best MLR	GA Best Average HRR (2000-6000s)	GA Best Vent	Bounds on MLR	Bounds on Vent	Notes on Simulation
SR3_3_3_NC_b_1.	200 kW	200 kW	1m x 2m	205 kW	205 kW	1.28 m x 1.94 m	200-7,000 kW	Width: 0.25m-2m, Height: 1m-3m	Population size 20. 50 Generation
SR3_3_3_NC_b_2.	600 kW	599 kW	1m x 2m	608 kW	607 kW	0.61 m x 2.42 m	200-7,000 kW	Width: 0.25m-2m, Height: 1m-3m	Population size 20. 50 Generation
SR3_3_3_NC_b_3.	1000 kW	973 kW	1m x 2m	1078 kW	1071 kW	1.54 m x 2.12 m	200-7,000 kW	Width: 0.25m-2m, Height: 1m-3m	Population size 20. 50 Generation
SR3_3_3_NC_b_4.	2000 kW	1222 kW	1m x 2m	1762 kW	1193 kW	1.02 m x 1.99 m	200-7,000 kW	Width: 0.25m-2m, Height: 1m-3m	Population size 20. 50 Generation
SR3_3_3_NC_b_5.	3000 kW	1271 kW	1m x 2m	4536 kW	1420 kW	1.95 m x 1.53 m	200-7,000 kW	Width: 0.25m-2m, Height: 1m-3m	Population size 20. 50 Generation

A time history of the upper layer temperature profile for simulations

SR3_3_3_NC_b_1, SR3_3_3_NC_b_3, and SR3_3_3_NC_b_5 are depicted below.

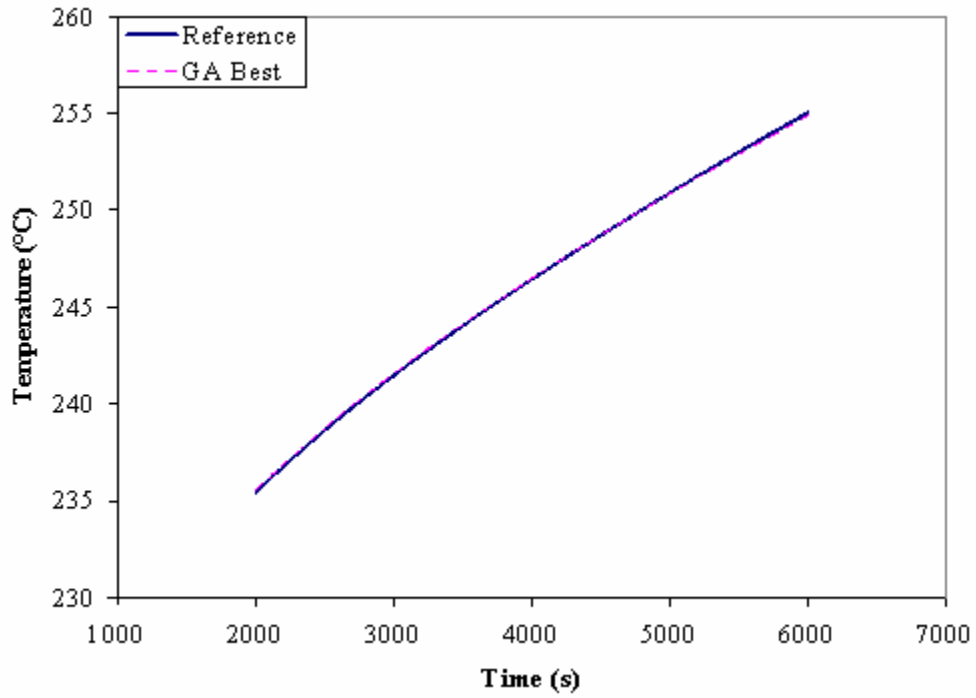


Figure 27. Simulation SR3_3_3_NC_b_1 upper layer temperature profile of the reference simulation and the GA best.

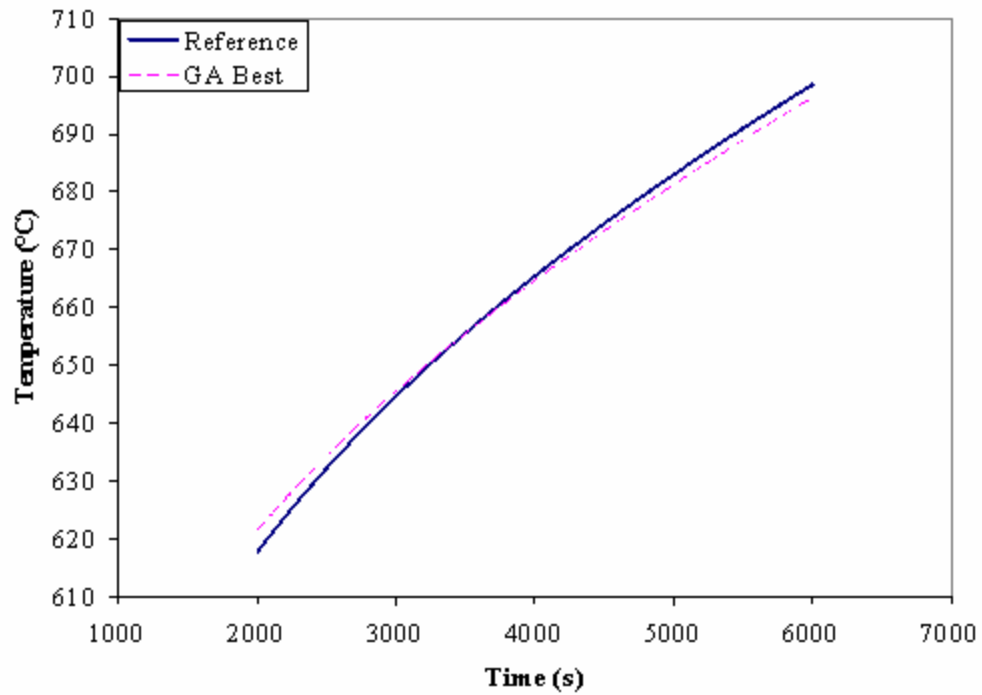


Figure 28. Simulation SR3_3_3_NC_b_3 upper layer temperature profile of the reference simulation and the GA best.

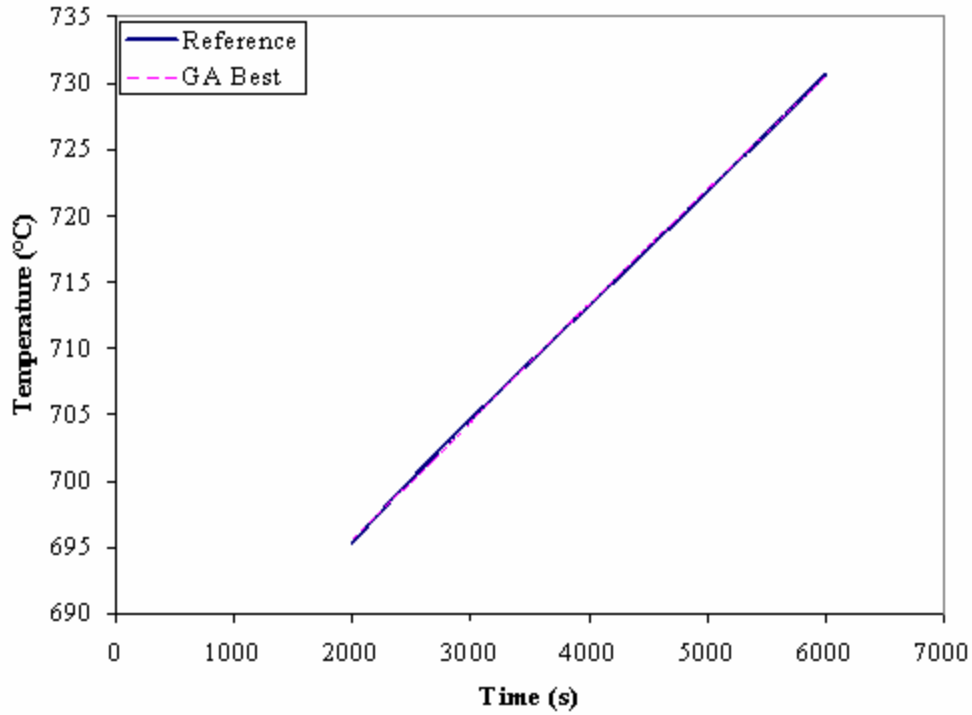


Figure 29. Simulation SR3_3_3_NC_b_5 upper layer temperature profile of the reference simulation and GA best.

As demonstrated in these plots, the GA has successfully run through 50 generations and found a solution that is very similar to the reference simulation. As can be seen in all of these results, the GA best solution does not converge towards the exact parameters that were used for the reference simulation. However, as demonstrated in the above figures, these GA best solutions produce differences in the temperatures on the order of .1 °C to 2 °C. This error in temperature range is negligible and further emphasizes that the GA is successful in finding a near optimal solution. As previously discussed, the problem that is being considered has the potential for multiple solutions. This point can be further emphasized through the MQH correlation.

$$\Delta T_g = 6.85 \left(\frac{Q^2}{A_0 \sqrt{H_0} h_k A_T} \right)^{1/3}$$

This basic equation shows that as long as the ratio of HRR to the power of 2 divided by the ventilation factor stays approximately the same, similar values of the upper layer temperature can be obtained. Therefore, the GA is much more likely to find a solution that is not the exact reference simulation, but still produces a similar temperature reading as the reference simulation. It is this basic ratio between HRR and ventilation that needs to be satisfied in order to achieve a similar temperature profile as the reference simulation. However, as illustrated in Table 7 the average HRR of the GA best simulation, which is the main parameter of interest, is always close and within a reasonable estimate of the reference simulation's HRR. For example, simulation SR3_3_3_NC_b_1 has a reference HRR from its mass burning rate of 200 kW, compared to the GA best simulation of 205 kW. These differences are negligible, and for all intensive purposes, the same. Simulation SR3_3_3_NC_b_5 estimated an average HRR of 1420 kW with a vent configuration of 1.95m x 1.53m compared to the reference simulation's HRR of 1271 kW with a vent configuration of 1m x 2m. The reference simulation's ventilation factor is approximately equal to $2.82\text{m}^{2.5}$. The GA best simulation's ventilation factor is approximately equal to $3.69\text{m}^{2.5}$. Therefore the larger ventilation factor brings in more cool air and counteracts the larger heat release rate. This produces a similar temperature profile to the reference simulation. Nevertheless, for practical applications, the average HRR of the GA best simulation is only 149 kW away from the reference simulation. For fire applications this estimate is very reasonable. Therefore, although the solution is not exact, the IFM still estimates a HRR that is on the correct order of magnitude to the reference simulation in nearly every simulation.

A particular case where the IFM greatly overestimated the reference simulation can be seen in Figure 30 and Figure 31 below. The GA estimated an average HRR of 1833 kW with a much larger vent configuration compared to an average HRR of 1074 kW with a smaller vent configuration. This difference of over 700 kW is large, and demonstrates a limitation in the IFM. Again the discrepancy between the reference and predicted HRR is simply due to the fact that the problem has multiple solutions and the IFM strategy correctly converges towards one of them.

Table 8. Simulation where the IFM overestimated the reference simulation.

Simulation Number	Reference MLR	Reference Average HRR (2000-6000s)	Reference Vent	GA Best MLR	GA Best Average HRR (2000-6000s)	GA Best Vent	Bounds on MLR	Bounds on Vent	Notes on Simulation
SR3_3_3_ Fb_b_3	2900kW	1074 kW	1m x 2m	2630 kW	1833 kW	1.80 m x 2.67 m	1,000-7,000 kW	Width: .75m-2m, Height: 1m-2.9m	Population size of 50 1000 generations

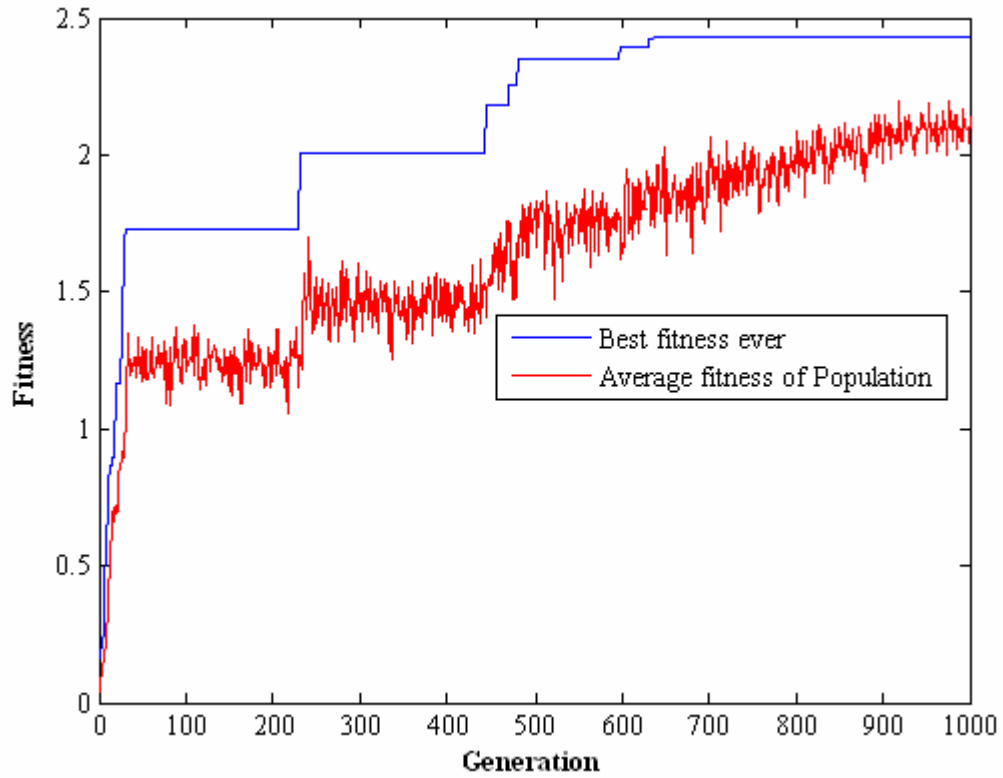


Figure 30. Simulation SR3_3_3_Fb_b_3 evolution of the performance of the GA for a population size of 50 and 1000 generations.

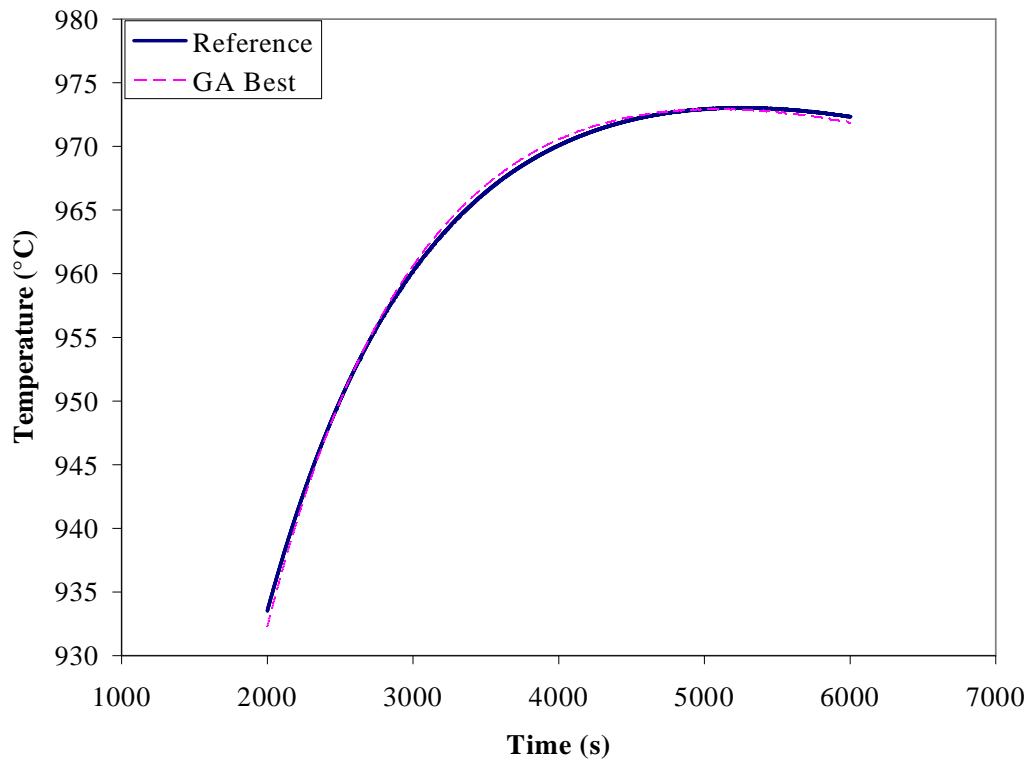


Figure 31. Simulation SR3_3_3_Fb_b_3 upper layer temperature profile of the reference simulation and the GA best.

These sets of tests were extended to a number of other configurations and are outlined in Appendix A2. All simulations, however, convey the same basic premise as depicted in Table 7 that the IFM is capable of providing a reasonable estimate of the HRR. These sets of tests were also extended to simulations where an exact solution is not known, i.e. the use of an approximate reference curve in the form of a steady or sloped reference curve as described in Table 2. As was the case with single parameter tests, these were run for MLRs that burn incompletely and completely. These results are summarized in Table 9.

Table 9. Results for a constant and sloped reference curve with door width and door height as additional parameters.

Simulation Number	Reference MLR	Reference Average HRR (2000-6000s)	Reference Vent	GA Best MLR	GA Best Average HRR (2000-6000s)	GA Best Vent	Bounds on MLR	Bounds on Vent	Notes on Simulation
SR3_3_3_Fb_c_1	3000 kW	1081 kW	1m x 2m	2657 kW	1417 kW	2.00 m x 1.99 m	200-4,500 kW	Width: .75m-2m, Height: 1m-3m	Population size of 25, 25 generations
SR3_3_3_Fb_d_1	3000 kW	1081 kW	1m x 2m	4497 kW	1385 kW	1.91 m x 1.75 m	200-4,500 kW	Width: .75m-2m, Height: 1m-3m	Population size of 25, 25 generations
SR3_3_3_Fb_f_1	3000kW	1081 kW	1m x 2m	2913 kW	1148 kW	1.14 m x 2.00 m	200-4,500 kW	Width: .75m-2m, Height: 1m-3m	Population size of 25, 25 generations
SR3_3_3_Fb_g_1	3000 kW	1081 kW	1m x 2m	2508 kW	1066 kW	.75m x 2.32 m	200-4,500 kW	Width: .75m-2m, Height: 1m-3m	Population size of 25, 25 generations
SR3_3_3_NC_c_1	500 kW	499 kW	1m x 2m	2036 kW	434 kW	.71m x 1.03 m	200-7,000 kW	Width: 0.25m-2m, Height: 1m-3m	Population size of 20, 50 generations
SR3_3_3_NC_d_1	500 kW	499 kW	1m x 2m	1465 kW	366 kW	0.44 m x 1.20 m	200-7,000 kW	Width: 0.25m-2m, Height: 1m-3m	Population size of 20, 50 generations
SR3_3_3_NC_f_1	500 kW	499 kW	1m x 2m	456 kW	456 kW	2.00 m x 1.17 m	200-7,000 kW	Width: 0.25m-2m, Height: 1m-3m	Population size of 20, 50 generations
SR3_3_3_NC_g_1	500 kW	499 kW	1m x 2m	1434 kW	438 kW	0.79 m x 1.00 m	200-7,000 kW	Width: 0.25m-2m, Height: 1m-3m	Population size of 20, 50 generations

These tests demonstrate that a reference curve that is instantaneously sloped to more directly mimic its steady state shape generally produces better results than a steady reference curve. For example, simulation SR3_3_3_Fb_c_1 produces an average HRR of 1417 kW, compared to the reference simulation of 1081 kW. SR3_3_3_Fb_f_1 produces

an average HRR of 1148 kW which is very close to 1081 kW considering that an approximate reference curve was used. The only difference between these two simulations is that the first simulation utilizes a constant temperature for its reference curve, and the second simulation utilizes a sloped reference curve. In all of these simulations, however, the GA estimates a HRR that is close to the reference simulation. The time evolution of simulation SR3_3_3_NC_d_1 can be seen below. As shown in its evolution of the fitness plot, the best fitness ever found is on the order of .38. This is consistent with an average error of approximately 2-3 °C between the GA best and reference curve. This is consistent with Figure 32 and Figure 33.

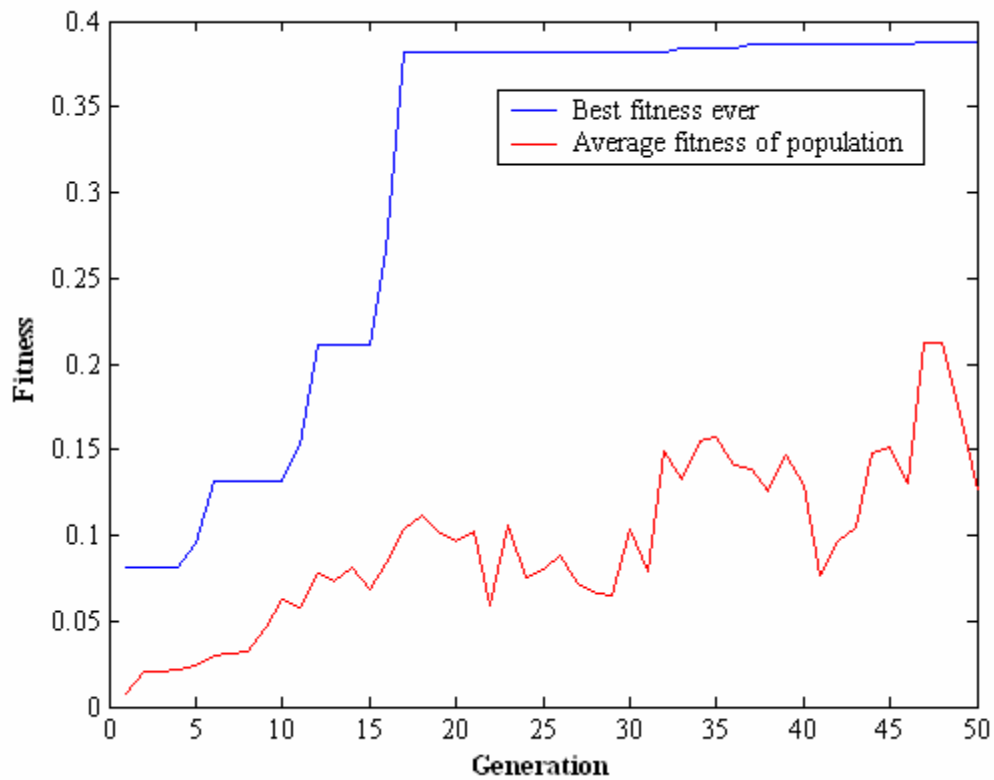


Figure 32. Simulation SR3_3_3_NC_d_1 evolution of the performance of the GA.

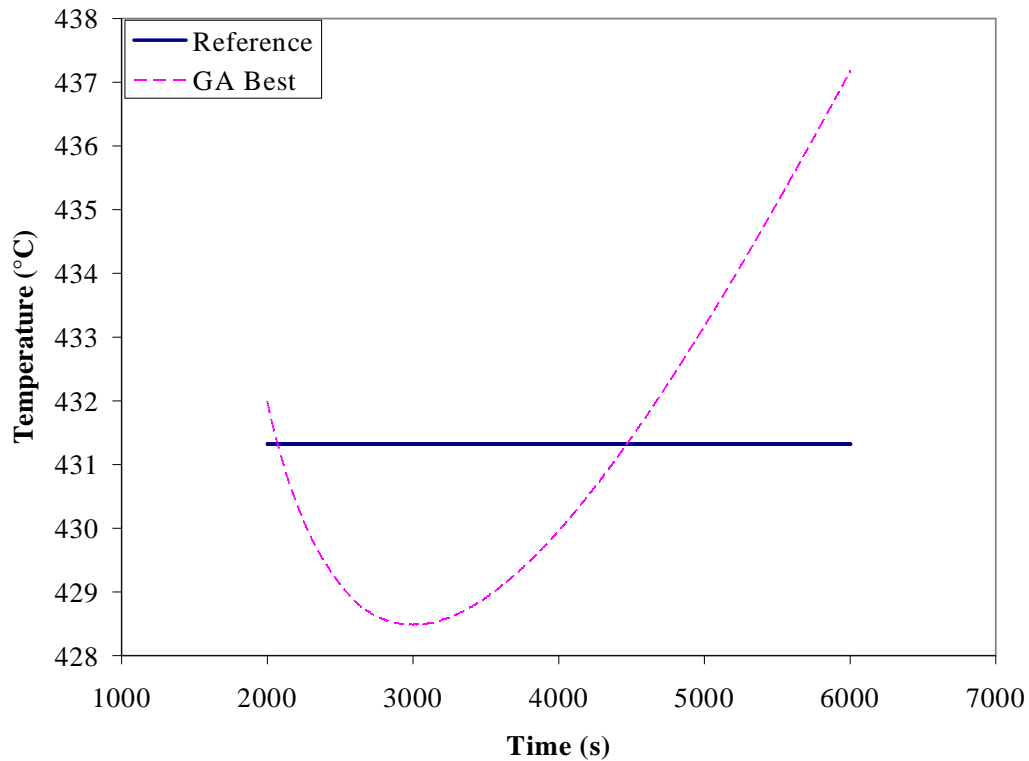


Figure 33. Simulation SR3_3_3_NC_d_1 temperature profile of the reference simulation and GA Best.

4.2.3 Single Compartment, Door and Window Configuration as Parameters

After it was demonstrated that the GA could reasonably estimate the fire size of a single compartment scenario where the door width and door heights were considered to be unknown parameters, the IFM was challenged to do the same with even more parameters. These parameters were in the form of an additional ventilation source, a window width, window upper height and window lower height. These results are summarized in appendix A3. As shown in section 4.2.2 the potential for multiple solutions exists once again. With additional ventilation parameters included, the same principle as described in section 4.2.2 still applies, and the potential for multiple solutions

still exists. Nevertheless, the IFM in all of its tests is able to find a solution that produces a similar temperature profile to the reference simulation. Once again, as will be demonstrated the average HRR of the GA best simulation is still in most cases a very reasonable estimate of the reference simulation.

Table 10. Fire size, door and window configuration as parameters, where an exact reference curve is used.

Simulation Number	Reference MLR	Reference Average HRR (2000-6000s)	Reference Door	Reference Window	GA Best MLR	GA Best Average HRR (2000-6000s)	GA Best Door	GA Best Window	Bounds on MLR	Bounds on Door	Bounds of Window	Notes on Simulation
SR3_3_3_NC_b_1	200 kW	200 kW	1m x 2m	1.0m wide. 1.5m-2.5m high	203 kW	203 kW	.65m x 1.85 m	1.86m wide 0.80m – 2.29m high.	200-6,000 kW	Width: 0.5m-2m, Height: 1m-2.5m	Width: 0m-2m, Upper end: 1.5m-3m, Lower end: 0m-1.5m	Population size 20, 50 generations
SR3_3_3_NC_b_2	600 kW	598 kW	1m x 2m	1.0m wide. 1.5m-2.5m high.	549 kW	548 kW	1.52 m x 2.10 m	1.13m wide. .61m - 1.92m high.	200-6,000 kW	Width: 0.5m-2m, Height: 1m-2.5m	Width: 0m-2m, Upper end: 1.5m-3m, Lower end: 0m-1.5m	Population size 20, 50 generations
SR3_3_3_NC_b_3	1000 kW	995 kW	1m x 2m	1.0m wide. 1.5m-2.5m high.	909 kW	788 kW	.96m x 1.21m	0.18m wide. 1.32m - 2.60m high.	200-6,000 kW	Width: 0.5m-2m, Height: 1m-2.5m	Width: 0m-2m, Upper end: 1.5m-3m, Lower end: 0m-1.5m	Population size 20, 50 generations
SR3_3_3_NC_b_4	2000 kW	1638 kW	1m x 2m	1.0m wide. 1.5m-2.5m high.	4263 kW	1952 kW	1.28 m x 1.93m	1.77m wide. 1.25m - 1.93m high.	200-6,000 kW	Width: 0.5m-2m, Height: 1m-2.5m	Width: 0m-2m, Upper end: 1.5m-3m, Lower end: 0m-1.5m	Population size 20, 50 generations
SR3_3_3_NC_b_5	3000 kW	1836 kW	1m x 2m	1.0m wide. 1.5m-2.5m high.	3396 kW	1890 kW	1.07m x 1.96m	1.36m wide. 1.32m - 2.25m high.	200-6,000 kW	Width: 0.5m-2m, Height: 1m-2.5m	Width: 0m-2m, Upper end: 1.5m-3m, Lower end: 0m-1.5m	Population size 20, 50 generations

A temperature profile for the reference simulation and the GA best for simulations SR3_3_3_NC_b_1, SR3_3_3_NC_b_3, and SR3_3_3_NC_b_5 can be seen in Figure 34, Figure 35 and Figure 36 respectively. As can be seen in these figures, the GA has found

an estimate that produces a similar temperature profile to the reference simulation. In addition, the average HRR is once again a reasonable estimate of the reference simulation's HRR. Simulations SR3_3_3_NC_b_3 and SR3_3_3_NC_b_4 produce the largest variations between the HRR of the GA best and the reference curve. However, the vent configuration is different and still produces similar temperature readings.

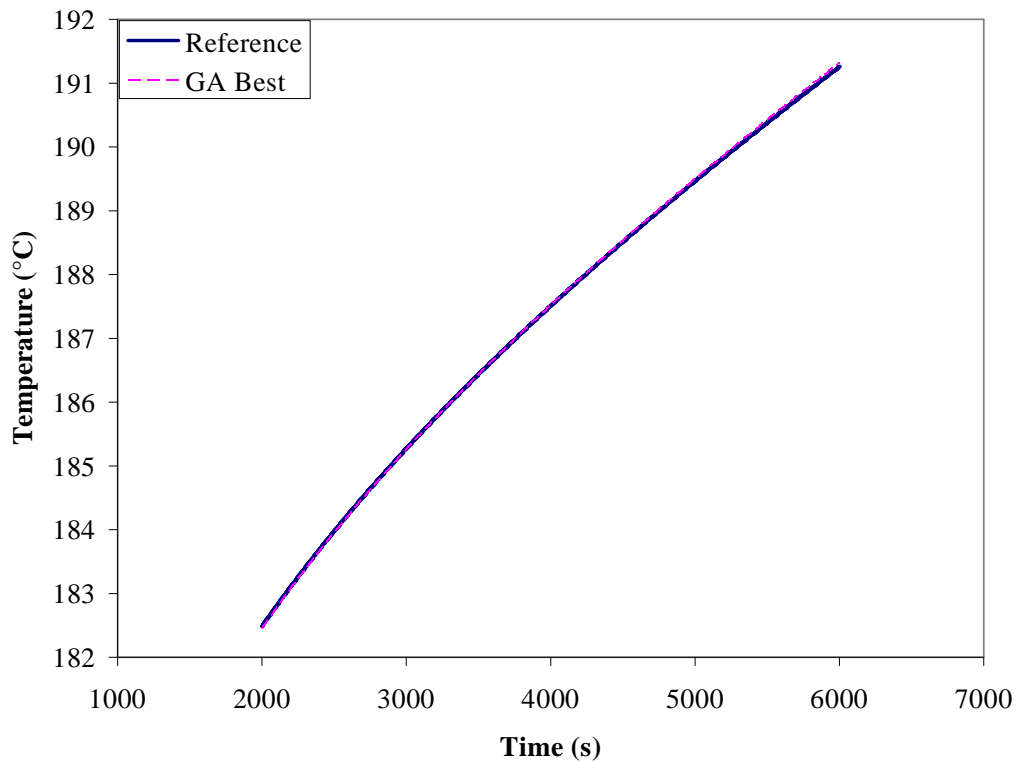


Figure 34. Simulation SR3_3_3_NC_b_1 temperature profile of the reference simulation and GA best.

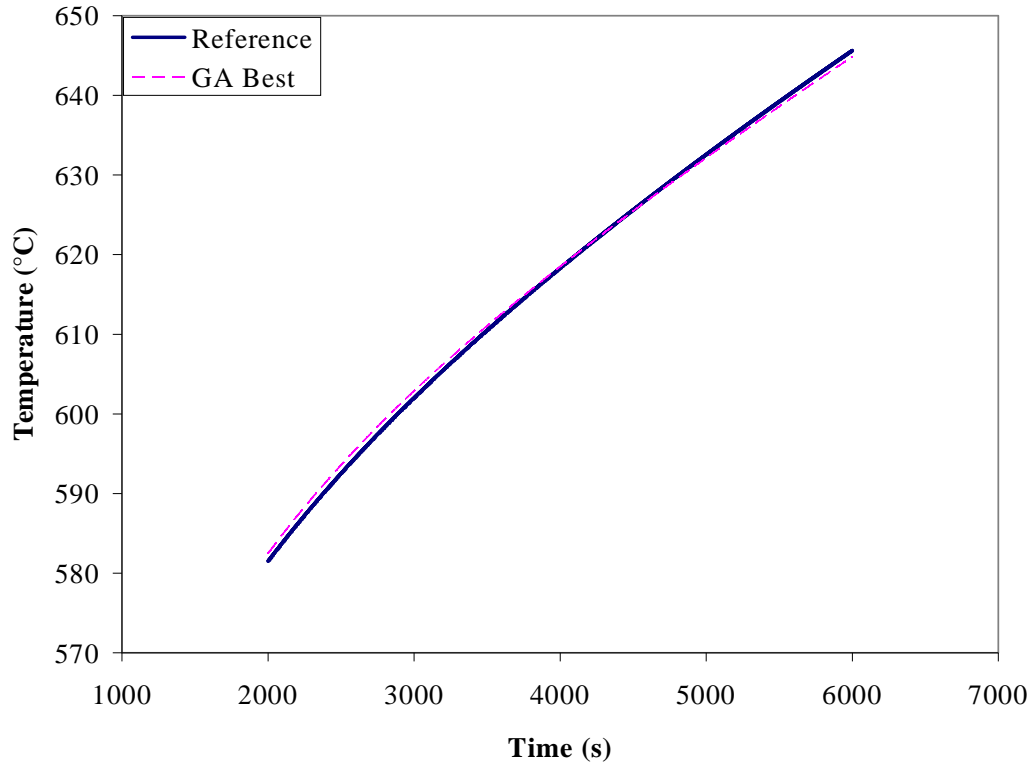


Figure 35. Simulation SR3_3_3_NC_b_3 temperature profile of the reference simulation and GA best.

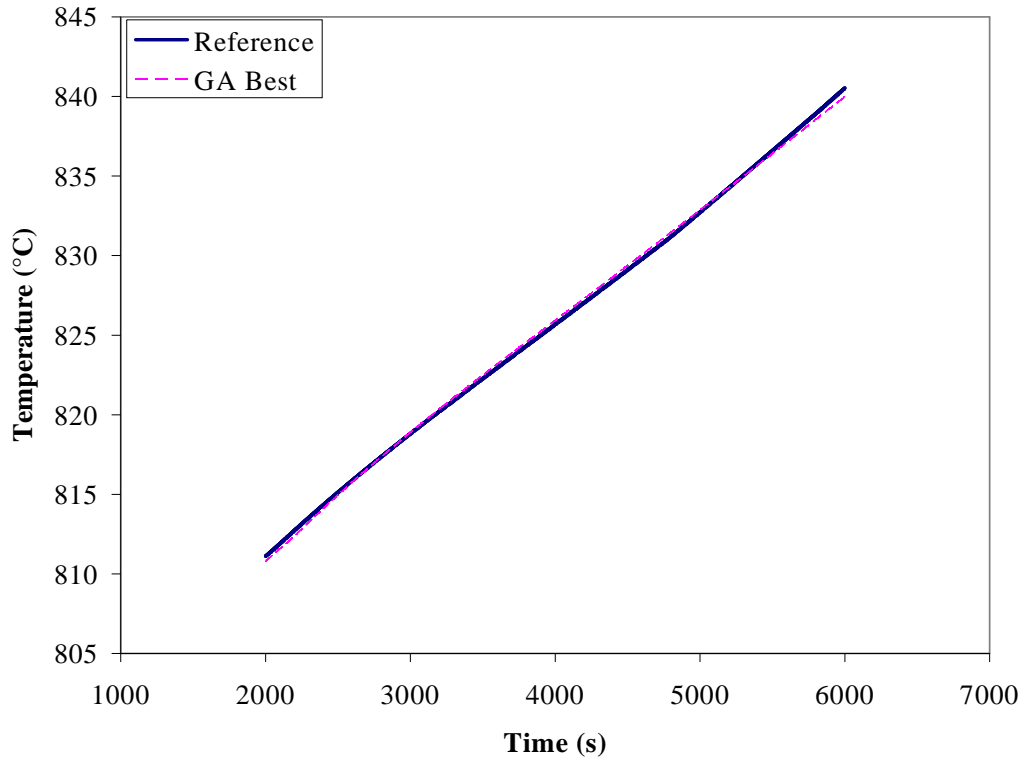


Figure 36. Simulation SR3_3_3_NC_b_5 temperature profile of the reference simulation and GA best.

Simulations were also run where an approximate reference curve was used. Once again, this implies that the reference curve was taken to be a sloped or steady value.

These results are illustrated in Table 11 below.

Table 11. Constant and Sloped reference curve results where window configuration is an additional parameter.

Simulation Number	Reference MLR	Reference Average HRR (2000-6000s)	Reference Door	Reference Window	GA Best MLR	GA Best Average HRR (2000-6000s)	GA Best Door	GA Best Window	Bounds on MLR	Bounds on Door	Bounds of Window	Notes on Simulation
SR3_3_3_Fb_c_1	3000 kW	1539 kW	1m x 2m	1.5m-2.5m high Width 1m	2786 kW	1421 kW	.69m x 2.15m	.72m wide. 1.08m-2.67m high	200-4500 kW	Width: 0.5m-2m, Height: 1m-2.5m	Width: 0m – 2.0m, Upper end: 1.5m-3m, Lower end: 0m-1.5m	Population size of 25, 25 generation
SR3_3_3_Fb_d_1	3000 kW	1539 kW	1m x 2m	1.5m-2.5m high Width 1m	3225 kW	1435 kW	.53m x 1.50m	1.24m wide. .96m -2.48m high	200-4500 kW	Width: 0.5m-2m, Height: 1m-2.5m	Width: 0m– 2.0m, Upper end: 1.5m-3m, Lower end: 0m-1.5m	Population size of 25. 25 generation
SR3_3_3_Fb_f_1	3000 kW	1539 kW	1m x 2m	1.5m-2.5m high Width 1m	3756 kW	1871 kW	1.22m x 2.26m	.67m wide. 1.02m - 2.90m high.	200-4500 kW	Width: 0.5m-2m, Height: 1m-2.5m	Width: 0 m– 2.0m, Upper end: 1.5m-3m, Lower end: 0m-1.5m	Population size of 25, 25 generation.
SR3_3_3_NC_c_1	500 kW	499 kW	1m x 2m	1.5m-2.5m high Width 1m	540 kW	538 kW	.52m x 2.50m	.51m wide. .24m - 2.98m high.	200-6,000 kW	Width: 0.5m-2m, Height: 1m-2.5m	Width: 0m-2m, Upper end: 1.5m-3m, Lower end: 0m-1.5m	Population size of 20, 50 generation
SR3_3_3_NC_d_1	500 kW	499 kW	1m x 2m	1.5m-2.5m high Width 1m	574 kW	572 kW	2.00m x 2.42m	.39m wide. .14m -2.39m high.	200-6,000 kW	Width: 0.5m-2m, Height: 1m-2.5m	Width: 0m-2m, Upper end: 1.5m-3m, Lower end: 0m-1.5m	Population size of 20. 50 generation
SR3_3_3_NC_f_1	500 kW	499 kW	1m x 2m	1.5m-2.5m high Width 1m	433 kW	432 kW	2.00m x 1.00m	.90m wide. 0m - 2.36m high.	200-6000 kW	Width: 0.5m-2m, Height: 1m-2.5m	Width 0-2m, Upper end: 1.5m-3m, Lower end: 0m-1.5m	Population size of 20, 50 generation
SR3_3_3_NC_g_1	500 kW	499 kW	1m x 2m	1.5m-2.5m high Width 1m	629 kW	626 kW	1.74m x 1.00m	1.35m wide. 1.13m - 2.82m high.	200-6,000 kW	Width: 0.5m-2m, Height: 1m-2.5m	Width 0-2m, Upper end 1.5m-3m, Lower end: 0m-1.5m	Population size of 20, 50 generation

A plot of the time evolution of the performance of the GA for simulation SR3_3_3_NC_g_1 and its final solution can be seen in Figure 37 and Figure 38 below. Even where an approximate reference curve is used, and there are an additional 3 parameters, the GA is able to sort through thousands of potential candidate solutions and extract a reasonable estimate of the reference HRR.

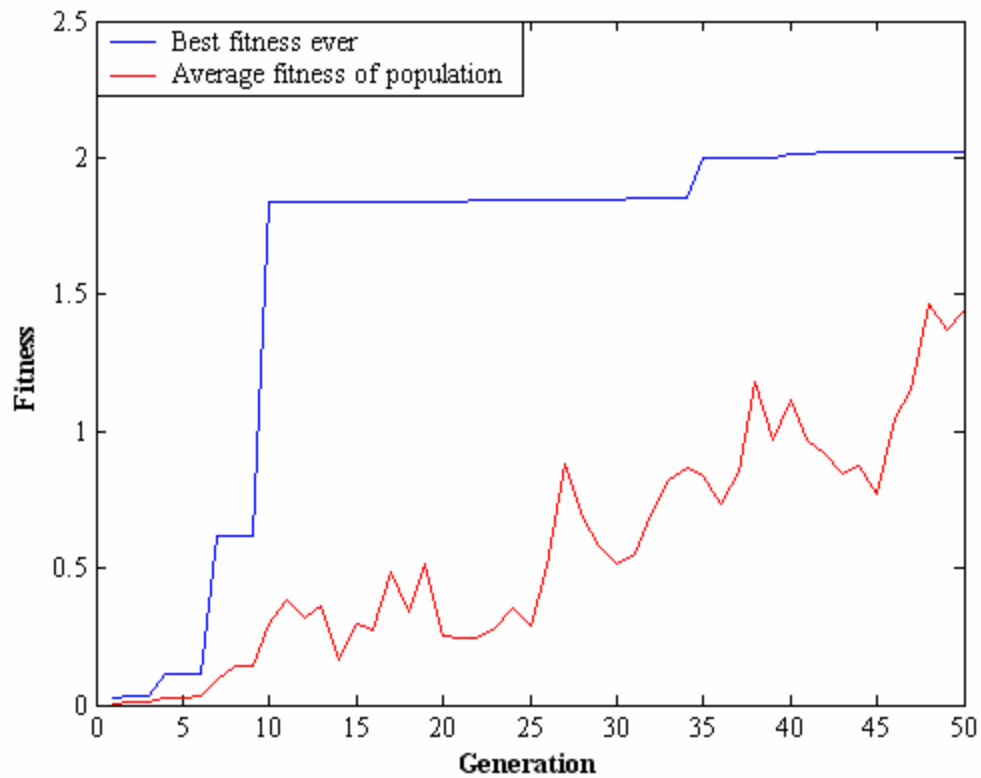


Figure 37. Simulation SR3_3_3_NC_g_1 evolution of the performance of the GA.

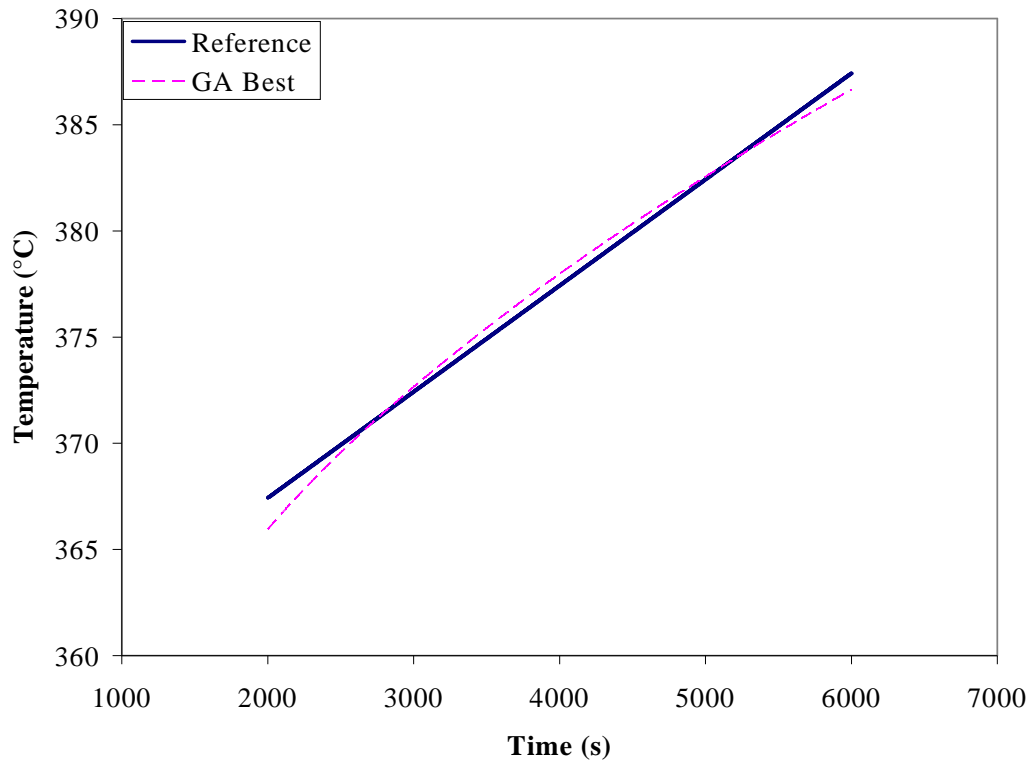


Figure 38. Simulation SR3_3_3_NC_g_1 upper layer temperature profile of the reference simulation and GA best.

4.3 Multiple Compartment Tests

After the series of robustness tests for single compartment scenarios were run and it was demonstrated that the IFM could successfully estimate the reference HRR under steady state conditions, the compartment configuration was changed to a more realistic large-scale fire scenario. The series of tests were extended to a multiple compartment configuration as shown in section 3.4.2. These results assumed that the window configuration was known, however, the door width of each compartment along with the fire size was unknown. This resulted in a total of 19 unknown parameters. These results are all summarized in Appendix A4. In this set of tests, steady state was considered to be 2000-3000s as opposed to 2000-6000s in order to cut down on simulation time and minimize instability issues with BRI. As discussed previously, it is anticipated the upper

layer that is being analyzed will not be the upper layer directly in the fire room. Instead, the upper layer will be from a room that is away from the fire room. In this case, room 1 as seen in Figure 12 will be considered to be the analysis room where the upper layer is studied.

The first set of multiple compartment tests analyzed a situation where only three windows were open, room 1, room 10 and room 11. A series of tests of different fire sizes were run. The results of MR_W1_10_11_a_4 are shown below in Table 12. As demonstrated, the total HRR on the floor of the building of the GA best is very similar to the reference simulation. The GA best estimate was 1702 kW compared to 1715 kW. This difference is negligible. This negligible difference is most likely due to the fact that the GA successfully estimated the ventilation characteristics of room 1, room 10 (fire room) and room 11 almost exactly (all of these rooms had open windows to the outside and are hence the most important in terms of capturing the physics). In addition, a fitness of around 54 was recorded for its best solution. This implies a negligible temperature difference of only around .01 °C.

This result shows that even with a large number of unknown parameters, 19, the GA is still able to find a solution that produces similar results to the reference simulation. In this set of tests, the smoke being analyzed is not in the fire room. It is in room 1 which is across the corridor of the building. This demonstrates that even if the direct smoke layer out of the fire room cannot be analyzed, a correct estimate of the fire size can still be made. An evolution of the performance of the GA and a plot of the temperature profile of the upper layer in room 1 for the reference simulation and GA best simulation can be seen in Figure 39 and Figure 40 respectively.

Table 12. Simulation MR_W1_10_11_a_4.*

Parameters	Reference Values	GA Best	Bounds	Notes
Mass Loss Rate	3000 kW	3050 kW	200- 5250 kW	Population size 25, 25 generations
Total HRR	1702 kW	1715 kW		
HRR Fire Room	1103 kW	1129 kW		
HRR Corridor	558 kW	546 kW		
HRR Room 1 (Analysis Window)	2 kW	2.5 kW		
HRR in all other rooms combined	40 kW	37 kW		
D1 width	1m	0.99m	0.25m – 1.5m	
D2 width	1m	0.65m	0.25m – 1.5m	
D3 width	1m	0.78m	0.25m – 1.5m	
D4 width	1m	0.97m	0.25m – 1.5m	
D5 width	1m	1.11m	0.25m – 1.5m	
D6 width	1m	0.38m	0.25m – 1.5m	
D7 width	1m	0.54m	0.25m – 1.5m	
D8 width	1m	1.08m	0.25m – 1.5m	
D9 width	1m	1.27m	0.25m – 1.5m	
D10 width	1m	0.94m	0.25m – 1.5m	
D11 width	1m	0.98m	0.25m – 1.5m	
D12 width	1m	1.44m	0.25m – 1.5m	
D13 width	1m	1.25m	0.25m – 1.5m	
D14 width	1m	0.25m	0.25m – 1.5m	
D15 width	1m	1.02m	0.25m – 1.5m	
D16 width	1m	1.23m	0.25m – 1.5m	
D17 width	1m	1.41m	0.25m – 1.5m	
D18 width	1m	0.94m	0.25m – 1.5m	

* It is important to note that the heat release rates shown in this table and every table in this section are the average values of the heat release rates from 2000-3000s taken at 200s increments.

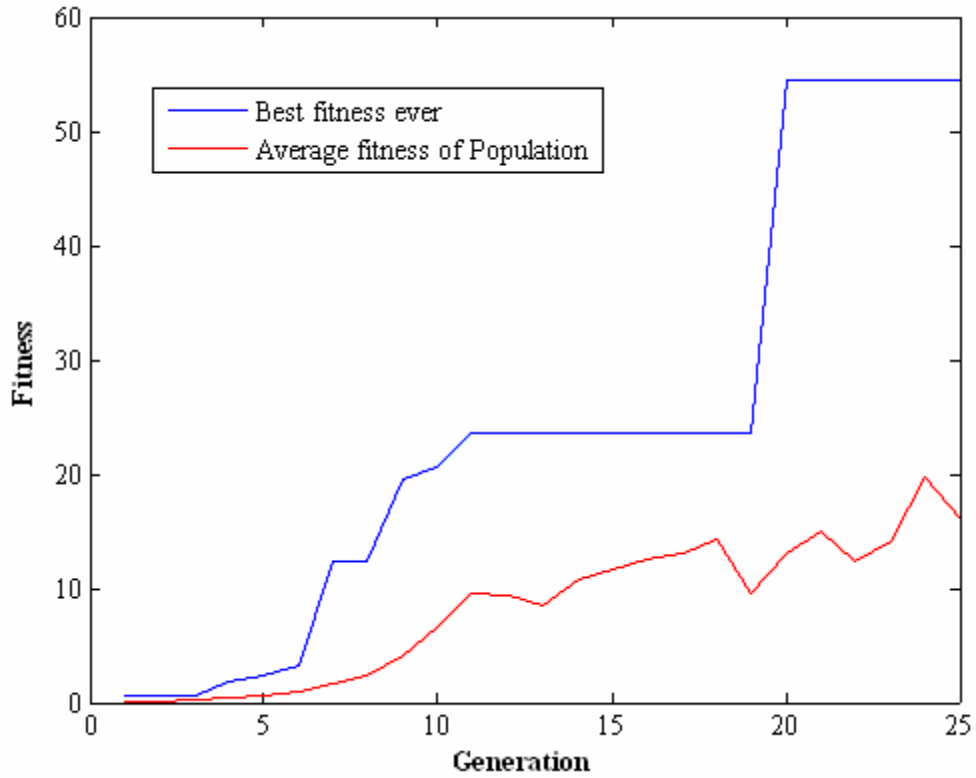


Figure 39. Simulation MR MR_W1_10_11_a_4 evolution of the performance of the GA.

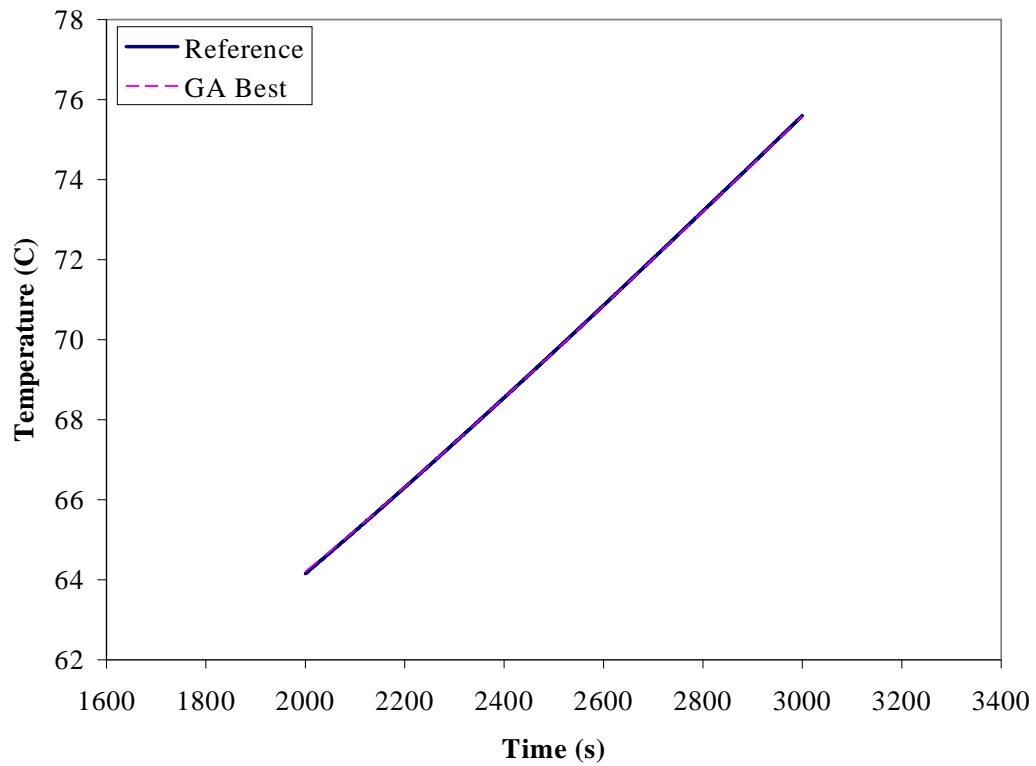


Figure 40. Simulation MR_W1_10_11_a_4 upper layer temperature profile for the reference simulation and GA best.

In the above simulation only three windows are open. The other rooms all have windows that are closed throughout the entire simulation. The door widths to these rooms that have closed windows are still included as parameters in the simulation. These door widths do have an impact because of the potential for more or less smoke to enter a room and hence affect the heat transfer balance. Nevertheless, the door widths that lead to a room with an open window play a much bigger role because these control the amount of fresh air that can come into the corridor. As a result, other simulations with different window configurations were run. These other simulations included a total of 11 windows or 18 windows being open. Simulation MR_W1:18_a_3 had a reference MLR of 7000 kW and every window was open. Its results are presented below in Table 13.

Table 13. Simulation MR_W1:18_a_3

Parameters	Reference Values	GA Best	Bounds	Notes
Mass Loss Rate	7000 kW	5863 kW	200- 7000 kW	Population size 25, 25 generations
Total HRR	3732 kW	3555 kW		
HRR Fire Room	2074 kW	2159 kW		
HRR Corridor	979 kW	910 kW		
HRR Room 1 (Analysis Window)	40 kW	36 kW		
HRR in all other rooms combined	639 kW	450 kW		
D1 width	1m	1.28m	0m – 1.5m	
D2 width	1m	1.31m	0m – 1.5m	
D3 width	1m	1.44m	0m – 1.5m	
D4 width	1m	0.53m	0m – 1.5m	
D5 width	1m	1.33m	0m – 1.5m	
D6 width	1m	0.31m	0m – 1.5m	
D7 width	1m	1.37m	0m – 1.5m	
D8 width	1m	0.86m	0m – 1.5m	
D9 width	1m	1.28m	0m – 1.5m	
D10 width	1m	1.29m	0m – 1.5m	
D11 width	1m	0.90m	0m – 1.5m	
D12 width	1m	1.14m	0m – 1.5m	
D13 width	1m	0.71m	0m – 1.5m	
D14 width	1m	0.97m	0m – 1.5m	
D15 width	1m	0.79m	0m – 1.5m	
D16 width	1m	0.44m	0m – 1.5m	
D17 width	1m	1.50m	0m – 1.5m	
D18 width	1m	1.03m	0m – 1.5m	

As shown in simulation MR_W1:18_a_3, even when all windows to the outside are open, the GA is once again successful in providing a reasonable estimate of the fire size. Simulation MR_W1:18_a_1, however, did not produce such good results. It is once again a scenario where every window is open; however, the prescribed MLR was 3000 kW for the reference simulation. These results are summarized in Table 14. In this

particular simulation the GA did not find as good of an estimate of the total HRR. The GA estimated the total HRR to be 2954 kW compared to the reference simulation of 2176 kW. This reminds us of the potential of the GA to find a fire size that is not as close to the reference fire size due to the varying venting configuration. Nevertheless, as shown in Figure 41 the two temperature curves are once again nearly identical and the GA's performance is excellent.

Table 14. Simulation MR_W1:18_a_1

Parameters	Reference Values	GA Best	Bounds	Notes
Mass Loss Rate	3000 kW	4472 kW	200- 7000 kW	Population size 25, 25 generations
Total HRR	2176 kW	2954 kW		
HRR Fire Room	1819 kW	2054 kW		
HRR Corridor	357 kW	772 kW		
HRR Room 1 (Analysis Window)	0 kW	5 kW		
HRR in all other rooms combined	0 kW	122 kW		
D1 width	1m	0.48m	0m – 1.5m	
D2 width	1m	0.87m	0m – 1.5m	
D3 width	1m	0.11m	0m – 1.5m	
D4 width	1m	0.33m	0m – 1.5m	
D5 width	1m	1.29m	0m – 1.5m	
D6 width	1m	0.36m	0m – 1.5m	
D7 width	1m	0.83m	0m – 1.5m	
D8 width	1m	0.79m	0m – 1.5m	
D9 width	1m	1.07m	0m – 1.5m	
D10 width	1m	1.33m	0m – 1.5m	
D11 width	1m	0.45m	0m – 1.5m	
D12 width	1m	1.17m	0m – 1.5m	
D13 width	1m	1.17m	0m – 1.5m	
D14 width	1m	0.49m	0m – 1.5m	
D15 width	1m	1.28m	0m – 1.5m	
D16 width	1m	0.99m	0m – 1.5m	
D17 width	1m	0.84m	0m – 1.5m	
D18 width	1m	0.81m	0m – 1.5m	

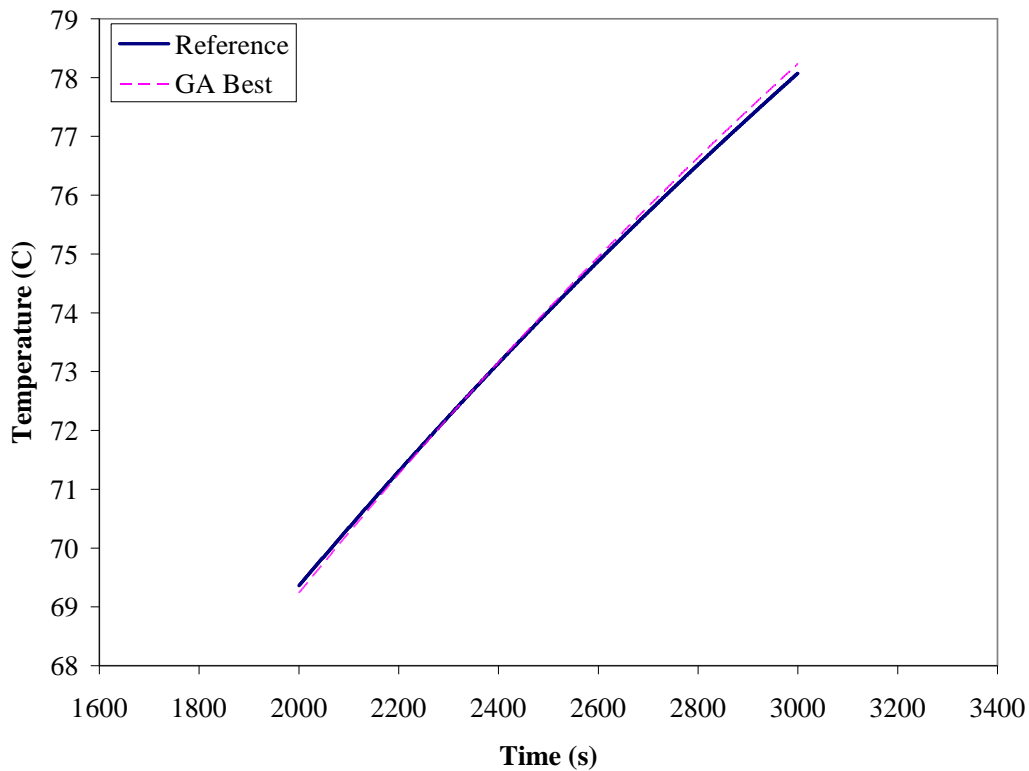


Figure 41. Simulation MR_W1:18_a_1 profile of the upper layer temperature of the reference simulation and the GA best in room 1.

In the aforementioned simulations there is the potential to achieve an exact solution with an infinite fitness because both the reference simulation and the candidate solutions are analyzed on the same time frame of 2000-3000s. Once again, obtaining an exact temperature profile such as the one described above will be unrealistic. Instead an instantaneous temperature value in the reference curve's steady state region was taken and used as a constant value for the 1000s analysis period. Simulation MR_W1_W10:18_b_3 took an instantaneous value at 2500s into the simulation of a 7000 kW mass loss rate and used it to make a constant reference curve.

Table 15. Simulation MR_W1_W10:18_b_3

Parameters	Reference Values	GA Best	Bounds	Notes
Mass Loss Rate	7000 kW	6037 kW	200- 7000 kW	Population size 25, 25 generations
Total HRR	3402 kW	3242 kW		
HRR Fire Room	1734 kW	1800 kW		
HRR Corridor	817 kW	868 kW		
HRR Room 1 (Analysis Window)	79 kW	73 kW		
HRR in all other rooms combined	771 kW	502 kW		
D1 width	1m	1.46m	0.25m – 1.5m	
D2 width	1m	1.40m	0.25m – 1.5m	
D3 width	1m	0.91m	0.25m – 1.5m	
D4 width	1m	0.25m	0.25m – 1.5m	
D5 width	1m	1.21m	0.25m – 1.5m	
D6 width	1m	0.27m	0.25m – 1.5m	
D7 width	1m	1.07m	0.25m – 1.5m	
D8 width	1m	0.88m	0.25m – 1.5m	
D9 width	1m	0.48m	0.25m – 1.5m	
D10 width	1m	1.15m	0.25m – 1.5m	
D11 width	1m	0.88m	0.25m – 1.5m	
D12 width	1m	1.27m	0.25m – 1.5m	
D13 width	1m	0.74m	0.25m – 1.5m	
D14 width	1m	0.76m	0.25m – 1.5m	
D15 width	1m	0.57m	0.25m – 1.5m	
D16 width	1m	0.55m	0.25m – 1.5m	
D17 width	1m	1.21m	0.25m – 1.5m	
D18 width	1m	1.01m	0.25m – 1.5m	

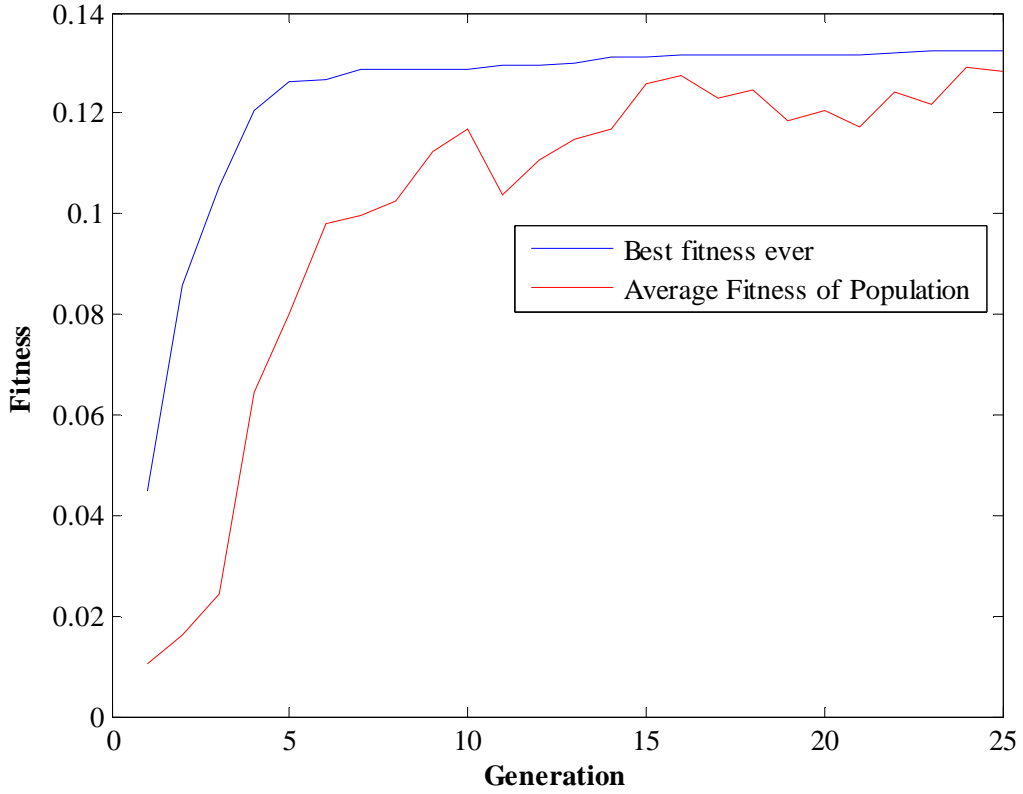


Figure 42. Simulation MR_W1_W10:18_b_3 evolution of the performance of the GA.

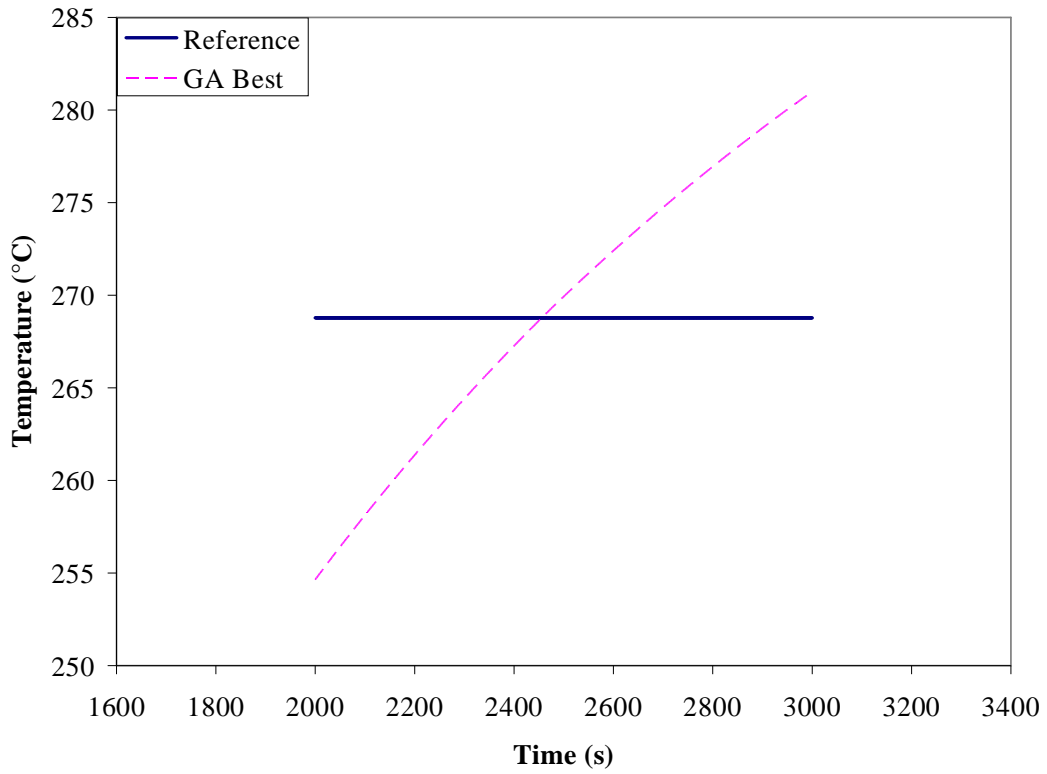


Figure 43. Simulation MR_W1_W10:18_b_3 upper layer temperature profile of the reference curve and GA best.

Simulation MR_W1_W10:18_b_3 demonstrated that the total HRR in the compartment for the GA best simulation was 3242 kW compared to 3402 kW for the reference simulation. This difference of 160 kW is a very reasonable estimate considering no exact solution can ever be obtained. Another simulation MR_W1_W10:18_b_2 utilized the same concept; however, a steady mass loss rate of 5000 kW was prescribed. The GA best estimate was found to be 3190 kW for the total HRR, compared to 2717 kW for the reference simulation. The GA best estimate is 473 kW larger than the reference simulation. However, due to the vent configuration as can be seen Table 16 the temperature of upper layer in room 1 is a good estimate of the reference simulation as demonstrated in Figure 44.

Table 16. Simulation MR_W1_W10:18_b_2

Parameters	Reference Values	GA Best	Bounds	Notes
Mass Loss Rate	5000 kW	5511 kW	200- 7000 kW	Population size 25, 25 generations
Total HRR	2717 kW	3190 kW		
HRR Fire Room	1626 kW	1828 kW		
HRR Corridor	800 kW	947 kW		
HRR Room 1 (Analysis Window)	23 kW	21 kW		
HRR in all other rooms combined	269 kW	394 kW		
D1 width	1m	0.72m	0.25m – 1.5m	
D2 width	1m	0.50m	0.25m – 1.5m	
D3 width	1m	0.28m	0.25m – 1.5m	
D4 width	1m	0.66m	0.25m – 1.5m	
D5 width	1m	0.97m	0.25m – 1.5m	
D6 width	1m	0.28m	0.25m – 1.5m	
D7 width	1m	1.04m	0.25m – 1.5m	
D8 width	1m	1.20m	0.25m – 1.5m	
D9 width	1m	0.72m	0.25m – 1.5m	
D10 width	1m	1.35m	0.25m – 1.5m	
D11 width	1m	1.38m	0.25m – 1.5m	
D12 width	1m	1.49m	0.25m – 1.5m	
D13 width	1m	1.36m	0.25m – 1.5m	
D14 width	1m	0.58m	0.25m – 1.5m	
D15 width	1m	1.39m	0.25m – 1.5m	
D16 width	1m	1.29m	0.25m – 1.5m	
D17 width	1m	0.99m	0.25m – 1.5m	
D18 width	1m	1.38m	0.25m – 1.5m	

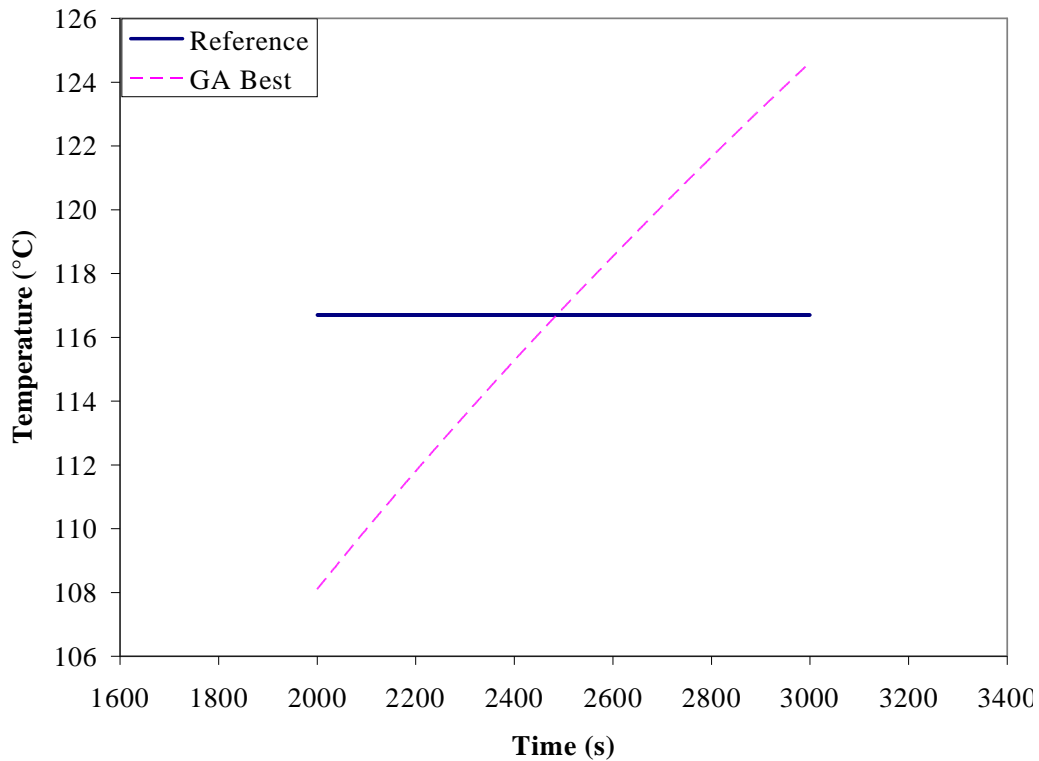


Figure 44. Simulation MR_W1_W10:18_b_2 upper layer temperature profile of the reference simulation and GA best in room 1.

In most cases the IFM will provide a very reasonable estimate of the reference fire size. However, due to the potential for multiple solutions, occasionally the IFM will find a solution which estimates a fairly different value of the fire size. Nevertheless, even in these situations where the estimate is less good, it is always has the correct order of magnitude.

In a practical application it may be impossible to provide a reasonable estimate of the actual fire size in a building. In addition, by limiting this analysis to only steady state, the transient nature of a fire cannot be captured. However, this research demonstrates that if a single value in its quasi-steady state region is captured, the IFM can track the fire size. Therefore, in an actual fire scenario, a temperature profile may be able to be compared qualitatively with the IFM. If a particular temperature profile is analyzed at a

certain time, the IFM can determine the relative fire size at steady state at that period of time. A short time later a second temperature profile can be recorded and a second estimate of the fire size at steady state can be made. A qualitative comparison can then be made which will demonstrate whether the fire has doubled in size, tripled in size etc. This information can then be passed on to firefighters.

4.4 FDS Comparison

An attempt to even further test the IFM in a more realistic scenario was performed. Using Fire Dynamics Simulator (FDS) as developed by NIST, the multi-compartment scenario was input into FDS. Slight changes were incorporated into the multi-compartment configuration to make it more compatible with the FDS structure. The main changes were that the door heights inside the compartment were changed from 2.13m to 2.0m to account for a grid of 0.25m cells to be used in FDS. In addition the wall materials were completely changed to normal weight concrete without the plaster front to allow for an easy and uniform input of material properties into the FDS model. FDS was then used to run steady fires of different MLRs. Using FDS a measure of the temperature of the upper layer in Room 1 could be made with a thermocouple placed in the middle of the room .25m from the ceiling. This temperature reading would then be used as an input into the IFM. A picture of the FDS layout of the compartment can be seen below in Figure 45.

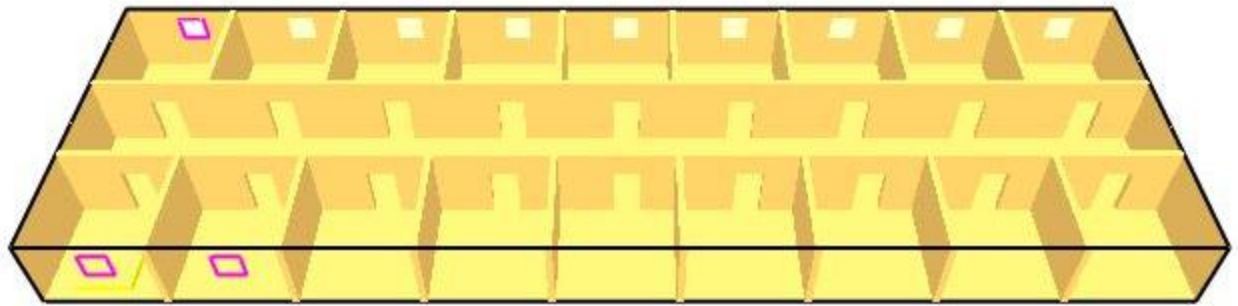


Figure 45. Multiple compartment scenario where FDS was used to measure temperatures.

Two separate tests were run using FDS. Both of these involved the situation where three windows were open, room 1, room 10 (fire room), and room 11. The first test had a steady fire size of 1MW for 800s that was ramped up to a steady 3MW fire for an additional 800s. The second test did the same thing except with a 3MW fire being ramped up to a 6MW fire. The 3MW fire produced very similar results for both cases, and as a result the IFM only ran once for the 3MW case (when the results for the 3MW case from FDS are given in the tables, it is for the scenario when a 3MW fire is steady from 0-800s). The IFM and the FDS simulations were analyzed in the same time frame from 400s-800s. Using this time period instead of steady state is different than the strategy described above. The purpose of this was to allow for a comparison of BRI2002 and FDS to be made under the same conditions. This would serve as a step to validate the zone model BRI against CFD tools. The goal of these tests was to determine how accurately the IFM estimates the HRR as predicted by FDS, and how well it can track the change in the fire size in this known time period.

The temperatures that were input into the IFM were taken instantaneously at either 600s or 1200s in FDS depending on whether or not the HRR had been ramped.

This concept is demonstrated in Figure 46 below. This single value was then used as a constant reference curve in the IFM for the 400-800s analysis period. All of these results are summarized in Appendix A6. These results showed that the IFM was very successful in tracking the temperatures that were recorded by FDS and input into the IFM. However, the IFM could not track the jump in fire sizes as predicted by FDS, or estimate the HRR as calculated by FDS very accurately.

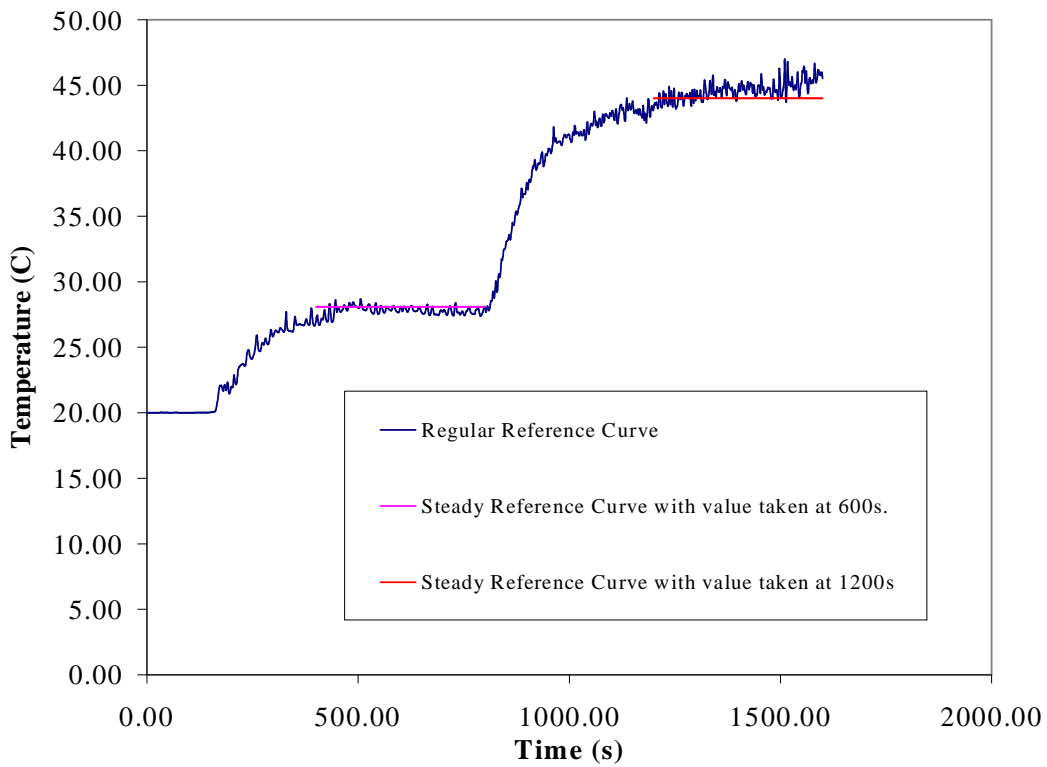


Figure 46. Sample reference curve for FDS multiple compartment tests.

The first test challenged the IFM to estimate the HRR of a steady 1MW fire and a steady 3MW fire assuming the ventilation inside the building is known. Therefore, the only parameter for these two tests was the MLR to be input into the model. These results are shown in Table 17 and Table 18.

Table 17. Simulation FDS_Room1_a1. FDS 1MW MLR used as input into IFM.

Parameters	Reference Values	GA Best	Bounds	Notes
Mass Loss Rate	FDS 1MW	2266 kW	200- 6000 kW	Population size 10, 20 generations. FDS temperature was 28 °C at 600s.
Total HRR	992 kW	2146 kW		
HRR Fire Room	988 kW	2101 kW		
HRR Corridor	0 kW	45 kW		
HRR Room 1 (Analysis Window)	0 kW	0 kW		
HRR in all other rooms combined	NA	0 kW		

Table 18. Simulation FDS_Room1_a2. FDS 3MW MLR used as input into IFM.

Parameters	Reference Values	GA Best	Bounds	Notes
Mass Loss Rate	3000 kW	3668 kW	200- 6000 kW	Population size 10, 20 generations. FDS temperature was 43°C at 600s
Total HRR	2476 kW	2782 kW		
HRR Fire Room	2301 kW	2402 kW		
HRR Corridor	78 kW	380 kW		
HRR Room 1 (Analysis Window)	0 kW	0 kW		
HRR in all other rooms combined	NA	0 kW		

As shown in Table 17 and Table 18 the IFM estimate of the total HRR is considerably larger than the FDS prediction. Considering that the only unknown

parameter is the MLR, this would imply that BRI and FDS are predicting different results for the same scenario. A further analysis emphasizes this point. The upper layer temperatures in the fire room, corridor and room 1 are different between models for the same scenario. This point is demonstrated in Figure 47 for a 1MW fire that was run in both models (the 3MW comparison between models can be seen in Appendix A6).

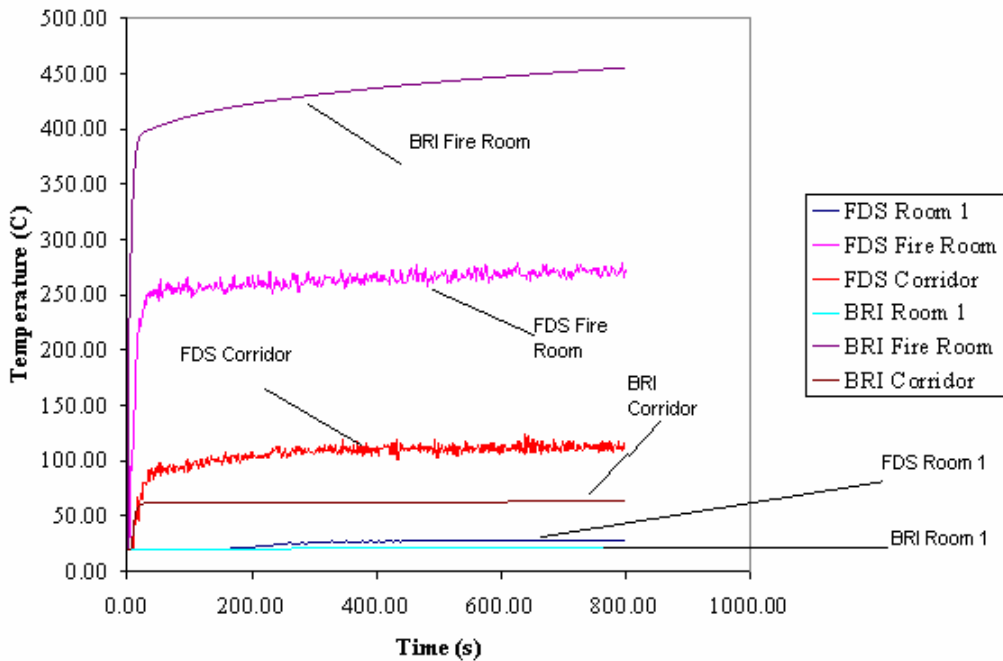


Figure 47. Upper layer temperature profile for a 1MW MLR fire for FDS and BRI2002.

As can be seen the upper layer temperature predicted in the fire room is far lower for the FDS calculation than the BRI2002 calculation. However, the temperature in the corridor and the room of interest (room 1) are higher in FDS than in BRI. For a 1MW fire the FDS temperature in room 1 is 28 °C, compared to 22 °C as predicted in BRI. For a 3MW fire, the FDS temperature in room 1 is 43 °C, compared to 38 °C in BRI. Although these temperature differences in room 1 between a 3MW and a 1MW fire are small, they are large enough to be detected by the IFM. In order for such a large temperature difference to occur between the models, either the HRRs are different, the

wall properties are different or the ventilation into the room must be different. The heat release rates as demonstrated in Figure 48 are basically the same for a 1MW MLR. The wall properties that were used in FDS are the same as those used in BRI2002. Therefore, the difference has to be because of the mass flow rates into and out of the fire room.

Figure 49 demonstrates that FDS calculates higher flow rates than BRI.

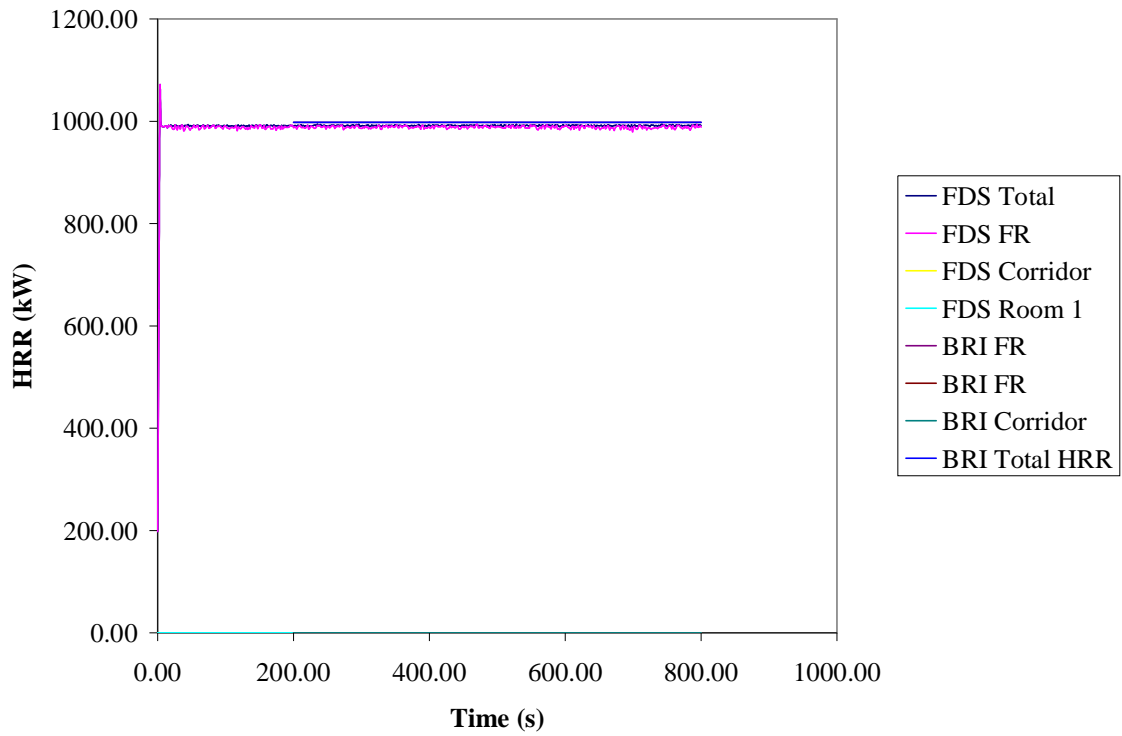


Figure 48. Heat release rates in fire room, corridor and room 1 for a 1MW MLR as predicted by FDS and BRI2002.

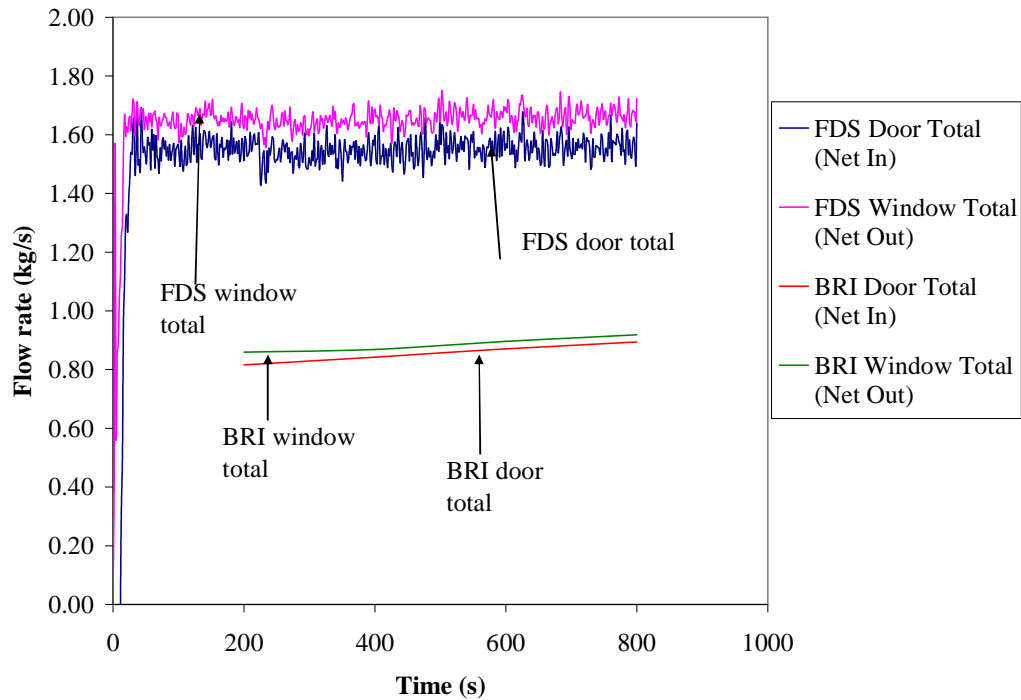


Figure 49. Mass flow rates into and out of fire room as predicted by FDS and BRI2002.

Therefore the larger mass flow rates as calculated in FDS, transport more of the hot smoke out of the room and into the corridor. This is consistent with Figure 47 in that the corridor temperatures calculated in FDS are higher than those calculated in BRI. The mass flow rates in FDS are about twice those calculated in BRI. This explains the 150 °C temperature difference in the fire room between the models, and the lower temperatures in the corridor and room 1 as calculated in BRI. Therefore, because the models calculate this scenario differently, the HRR that is estimated by the IFM for the 1MW MLR case is an overestimate. This larger HRR of 2146 kW in simulation FDS_Room1_a1 calculated by the IFM is expected because the simulation must produce more heat in order to achieve the higher temperature as calculated in room 1 by FDS. The IFM, however, has successfully done its job because it found a solution that produced minimum temperature differences between the reference simulation and the GA best simulation. This same

concept applies for the 3MW MLR case. A larger HRR is needed to achieve the higher temperatures as measured in room 1. The plots of the upper layer temperature profiles can be seen in Appendix A6.

Even though it was discovered that FDS and BRI2002 have calculated this fire scenario differently, the IFM was challenged to determine if it could estimate the fire size if the ventilation configurations were assumed to be unknown. By doing this, it could be determined how much of an impact the ventilation plays in this situation, and if the IFM would be susceptible to producing a result of a greatly different HRR. In addition, it can be determined how well the IFM tracks the change in fire size when ventilation is included. These results can be seen in Appendix A6. For the 1MW MLR scenario where ventilation was included, the IFM estimated a total average HRR of 2165 kW, and for the 3MW MLR scenario where ventilation was included as parameters, the IFM estimated a total average HRR of 2624 kW.

The average total fire size between the IFM and FDS estimate for the 1MW, 3MW and 6MW scenarios where ventilation is included as an unknown is summarized in Table 19. The time evolution of the HRR for the FDS and IFM comparison can be seen in Figure 50 and Figure 51.

Table 19. FDS and IFM comparison for the average total HRR on the floor. The IFM estimate is based on a temperature reading in room 1.

Actual Fire Size (MLR)	FDS HRR	IFM HRR (Room 1 temperature analysis)
1MW	992 kW	2165 kW
3MW	2476 kW	2624 kW
6MW	3654 kW	2988 kW

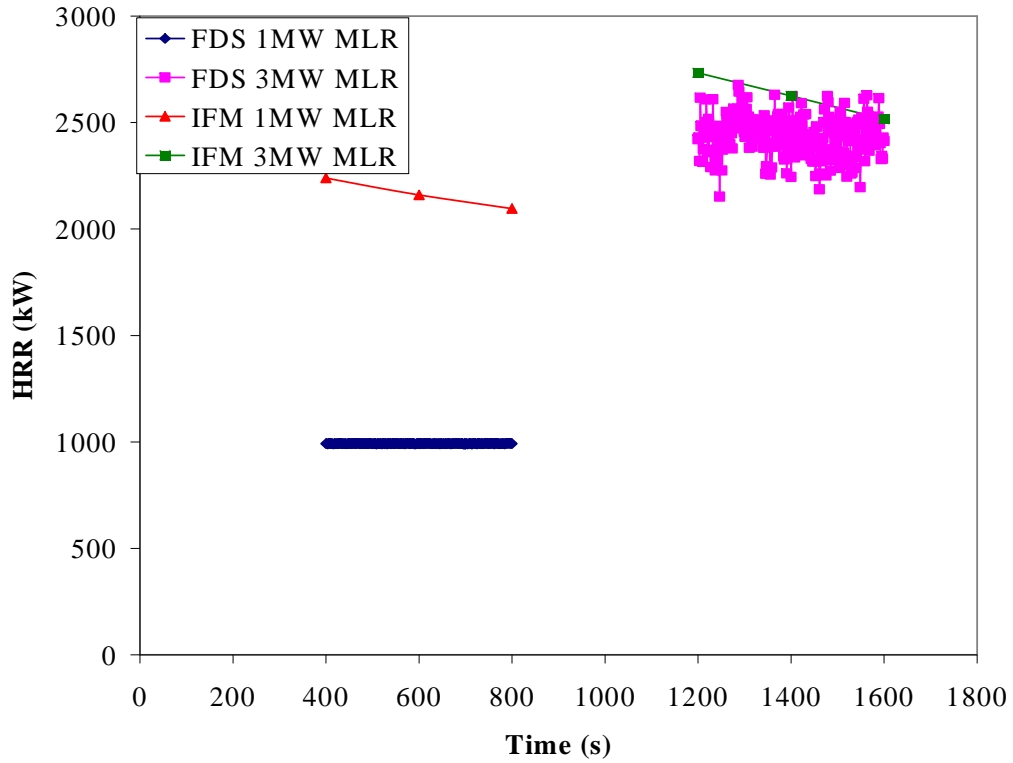


Figure 50. FDS and IFM time evolution of the HRR for a 1MW and 3MW MLR. Analysis room is room 1.

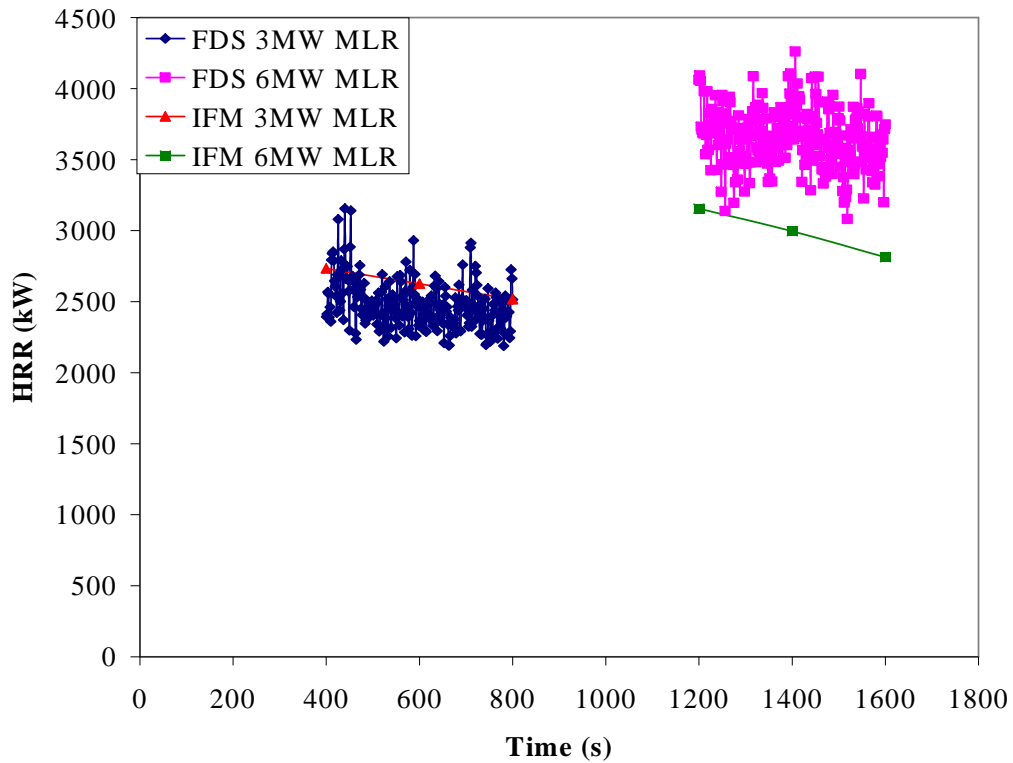


Figure 51. FDS and IFM comparison of the time evolution of the total HRR. Analysis room is room 1.

As can be seen in Table 19, the jump in fire size from a 1MW to a 3MW MLR as predicted in FDS is around 2.5 or 150%. The jump in fire size from a 3MW to a 6MW MLR as predicted in FDS is 1.48 or around 50%. By analyzing an instantaneous temperature value in room 1 from these different fire sizes, the IFM calculated a jump in fire size from a 1MW to a 3MW fire of 1.21 or around 20%. For the 3MW to 6MW fire increase, the IFM calculated a jump in the fire size of 1.13 or around 10%. By analyzing the upper layer temperature in room 1, the IFM is not very successful in qualitatively estimating the increase in fire size from a 1MW to a 3MW fire. The IFM predicts only around a 20% increase from a 3MW to a 6MW MLR, as compared to around 150% in FDS. FDS predicts a much larger increase in the fire size than BRI. This can be attributed to a couple of reasons, the first of which is the differences in the models as discussed previously. The second of which may be due to the fact that the temperatures recorded in room 1 are small, and as result the signal to noise ratio might be too low for qualitative differences to be measured.

Therefore, the same series of tests outlined above, were extended to the situation where the upper layer temperature of the fire room was analyzed. This concept is different than before, however, the temperatures in the fire room change much more significantly with a change in HRR and as a result the IFM may be better able to track the qualitative jump in fire size. All of these results are summarized in appendix A6 as well, under the label “FDS_FR.”

Table 20. FDS and IFM comparisons of the average total HRR. The temperatures being analyzed were taken from the Fire Room and are therefore greater than those from room 1.

Actual Fire Size (MLR)	FDS HRR	IFM HRR (Fire Room temperature analysis)
1MW	992 kW	429 kW
3MW	2476 kW	1434 kW
6MW	3654 kW	2516 kW

The heat release rate over time for FDS and the IFM estimates are plotted in Figure 52 and Figure 53. FDS's prediction of the change in fire size of about 150% is much more in line with the IFM estimate of a 230% increase in the average fire size. FDS's estimate of the change in fire size between a 3MW and a 6MW fire of around 50% is also better aligned with BRI's estimate of around a 75% increase. Therefore it appears that by using the upper layer temperature profile in the fire room, the IFM is more successful at qualitatively tracking the increase in fire size than when the upper layer temperature in room 1 was used.

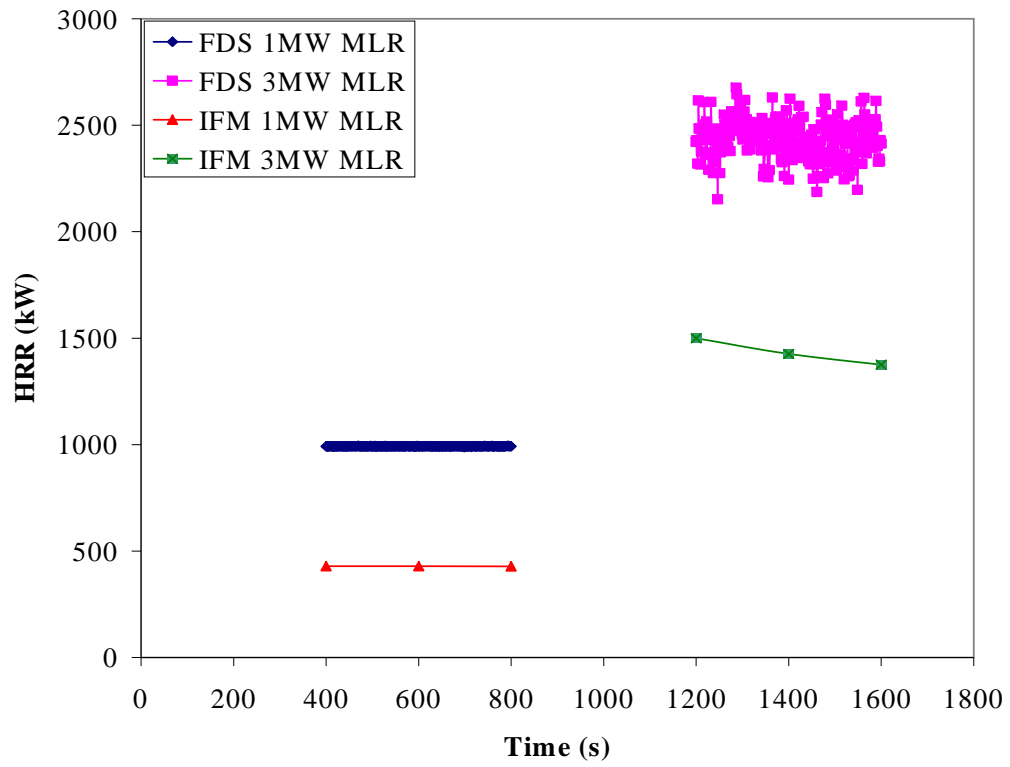


Figure 52. FDS and IFM comparison of the time evolution of the HRR for 1MW and 3MW MLR scenario. Analysis room is the Fire Room.

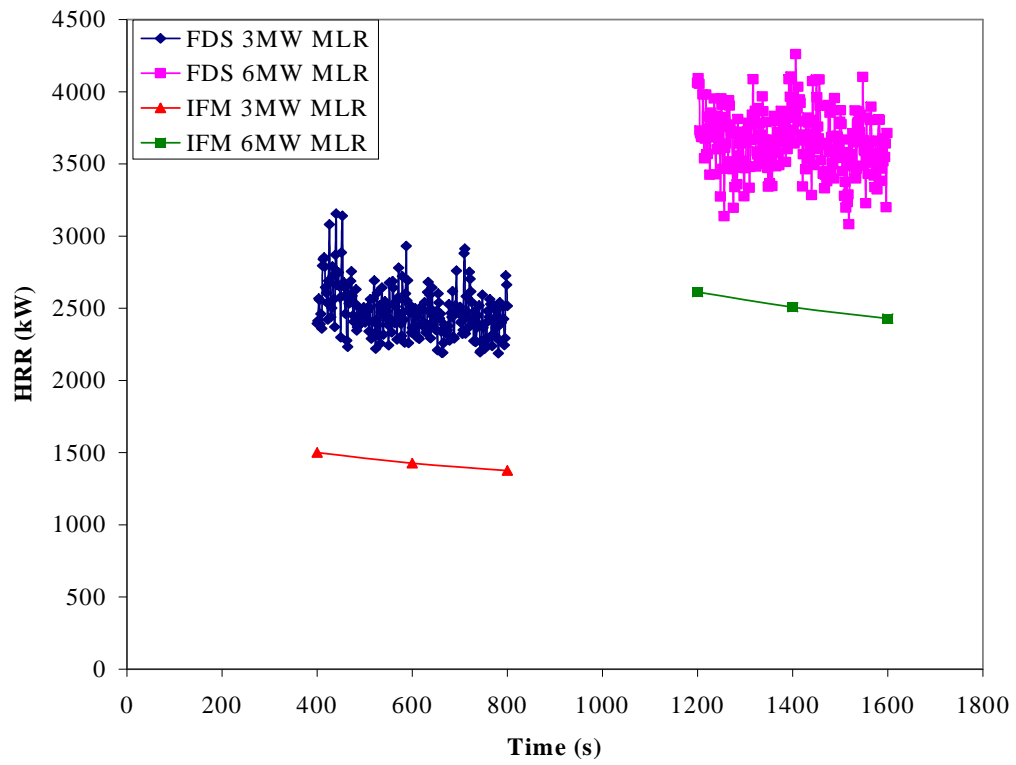


Figure 53. FDS and IFM comparison of the time evolution of the HRR for a 3MW and 6MW MLR. Analysis room is the Fire Room.

5 Chapter 5: Summary and Conclusion

5.1 Introduction

This chapter summarizes the research performed and presented above in Chapter 4. This chapter also outlines the future work that needs to be conducted. This future work revolves around further refinement and validation of the IFM, and the commencement of stage 2 of this project.

5.2 Summary

An Inverse Fire Model (IFM) was developed and analyzed in this research. The IFM coupled a GA with the Japanese zone model BRI2002 in an attempt to estimate the average fire size at quasi steady conditions, or at a known time period using a profile of the upper layer temperature coming out of open windows. This research challenged the IFM to estimate the fire size of a reference BRI2002 simulation. The IFM uses the GA to automatically run through thousands of potential candidate solutions to find a particular solution whose upper layer temperature most closely resembles a previously established reference curve from BRI2002. This IFM is different than other previous models because it is able to incorporate a large number of unknown parameters such as the ventilation profile inside a building through the use of the GA. A number of tests were performed of increasing difficulty for the IFM ranging from single compartment to multiple compartment scenarios.

For single compartment tests the IFM successfully converges and matches the predicted upper layer temperature with the reference temperature. The IFM is very successful in optimizing the single-objective problem utilized in this research in

relatively few generations. In scenarios where only the MLR is a parameter, the IFM is capable of providing excellent agreement between the HRR_{Ref} and the candidate HRR.

When additional parameters such as the door width, and door height were incorporated into the model the IFM is still capable of finding a solution that provides excellent agreement between the candidate's upper layer temperature and the reference simulation. In most of these cases, the estimated heat release rate is very similar to the reference HRR. In other cases, however, the estimated HRR is substantially different than the reference HRR. The reason for this is because when ventilation is incorporated as a parameter, no unique solution exists. The MQH correlation demonstrates that as long as the basic ratio of the HRR/ventilation is approximately the same, similar upper layer temperatures can be produced. In any case, the IFM still works and converges to one of the many solutions in every simulation.

For multiple compartment tests where up to 19 parameters were included, the IFM still successfully finds a solution that produces a similar upper layer temperature as the reference simulation. As was the case with single compartments a reasonable estimate of the HRR is made in most simulations. However, due to varying vent configurations the potential for the IFM to converge towards a solution with a considerably different HRR still exists. When the IFM was used to optimize inputs given from an FDS simulation, it was once again successful in optimizing the fitness function. The estimated HRR as predicted in BRI through the IFM was very different than the FDS prediction. The reason for this is due to a different representation of the fire scenario as predicted in BRI compared to FDS. Despite these differences, the IFM still demonstrated

that it could qualitatively track a change in fire size by analyzing the upper layer temperature in the fire room.

5.3 Future Work

This research has successfully demonstrated the ability of the IFM to track the temperatures of a reference simulation and in most cases provide a reasonable estimate of the reference HRR using a profile of the upper layer temperature. A number of further studies should be performed on this work. Further validation of the model must continue. The IFM should be extended to other compartment configurations. In order to determine if the IFM can make qualitative comparisons about the fire size, more multiple compartment tests and validation work must be done. In order to minimize the potential of the IFM to converge to a solution with a greatly different HRR, an attempt to make this problem multi-objective should be performed. Incorporating the upper layer temperature in more than one room or the upper layer height, the algorithm may be less susceptible to converge to one of these solutions.

In addition, an attempt to analyze transient fires and times other than steady state must also be researched. Further analysis of the zone model BRI2002 must take place. The IFM should also be compared to an actual fire scenario with known experimental data. The IFM must also drastically reduce the time of its simulation in order to run in real time, or faster than real time. Currently for a simulation where a single compartment is involved and a population size of 25 along with 25 generations is used, it takes on the order of 1-1.5 hours to run on a single 2.0 GHz processor. For the multiple compartment scenario used in this research at a population size of 25 and 25 generations, the simulation time of the IFM can be on the order of 6-7 hours for a single 2.0 GHz

processor. Further research must focus on adequately selecting the mutation and crossover functions to reduce simulation time and running the model on parallel processors.

Stage 2 of this project should also commence. This revolves around demonstrating that thermal imaging cameras can reasonably estimate the temperature of the hot smoke layer coming out of broken windows. Ultimately the IFM needs to be coupled with the sensor input and run as a cohesive unit.

Appendices

- Appendix A1: Single Compartment tests with HRR as only parameter
- Appendix A2: Single Compartment tests with HRR, door width, door height as parameters
- Appendix A3: Single Compartment tests with HRR, door width, door height, window width, window upper height, window lower height as parameters.
- Appendix A4: Multiple Compartment tests
- Appendix A5: Population and Generation studies.
- Appendix A6: FDS and BRI comparisons.
- Appendix B: Sample input files and IFM code structure for a single compartment and multiple compartment tests.

*For every simulation there are two plots. The first plot is a time evolution of the performance of the GA. In this plot if there are two curves then the top curve is the evolution of the best fitness ever, and the lower curve is the average fitness of the population. The average fitness is a representation of the quality of the “gene” pool. If this plot has only one curve, then it is the evolution of the **average fitness** of the population alone. The second plot is always a temperature profile of the hot upper gas layer for the reference simulation and the GA best simulation.

Key:

The appendix is organized in the following manner for single compartment studies:

SR3_3_3_Fb_letter_#

Where SR (Single Room)

3_3_3 (3m x 3m x 3m single compartment)

10_10_3 (10m x 10m x 3m single compartment)

Fb (Compartment’s walls are composed of hard and flexible fiber board, all simulations are ramped up to 720 kW at 120s, and then its steady value from 240-6000s)

NC (Compartment’s walls are composed of normal concrete, all simulations are steady from 0-6000s)

Letter	Meaning
a	Exact reference curve and candidate GA solutions analyzed 1-6000s*.
b	Exact reference curve and candidate GA solutions analyzed at steady state (2000-6000s).
c	Approximate steady reference curve with the value taken at 4000s. Both curves analyzed 2000-6000s.
d	Approximate steady reference curve with the value taken at 3000s. Both curves analyzed 2000-6000s.
e	Approximate steady reference curve with the average value taken from 2000-6000s. Both curves analyzed 2000-6000s.
f	Approximate sloped reference curve with the instantaneous slope taken at 4000s. Both curves analyzed 2000-6000s.
g	Approximate sloped reference curve with the instantaneous slope taken at 3000s. Both curves analyzed 2000-6000s.
h	Approximate sloped reference curve with the slope being the average slope from 2000-6000s. Both curves analyzed 2000-6000s.

*For any simulations where the * symbol is shown, this means that the analysis period was **0**-6000s, not 1-6000s. For these simulations the reference simulation was at 22°C at time 0, and all trial solutions were at 0°C, because the dlmread command used in MATLAB recorded the first point as 0 °C and not 22 °C.

(Overall simulation number)

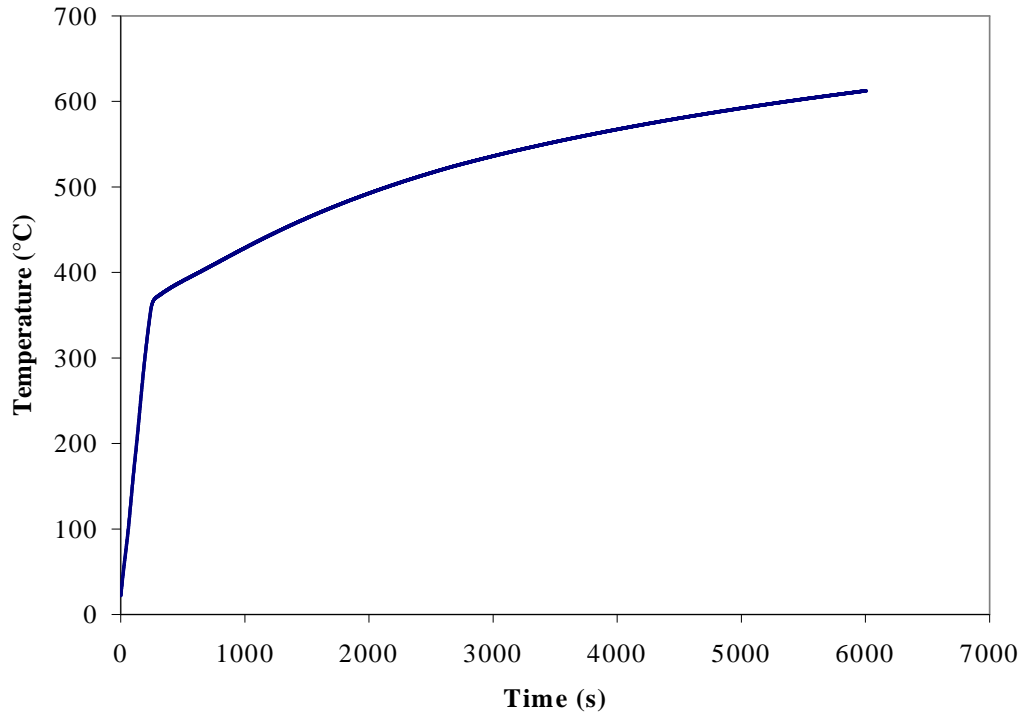


Figure 54. Simulation letter a. Exact reference curve is analyzed entirely from 1-6000s.

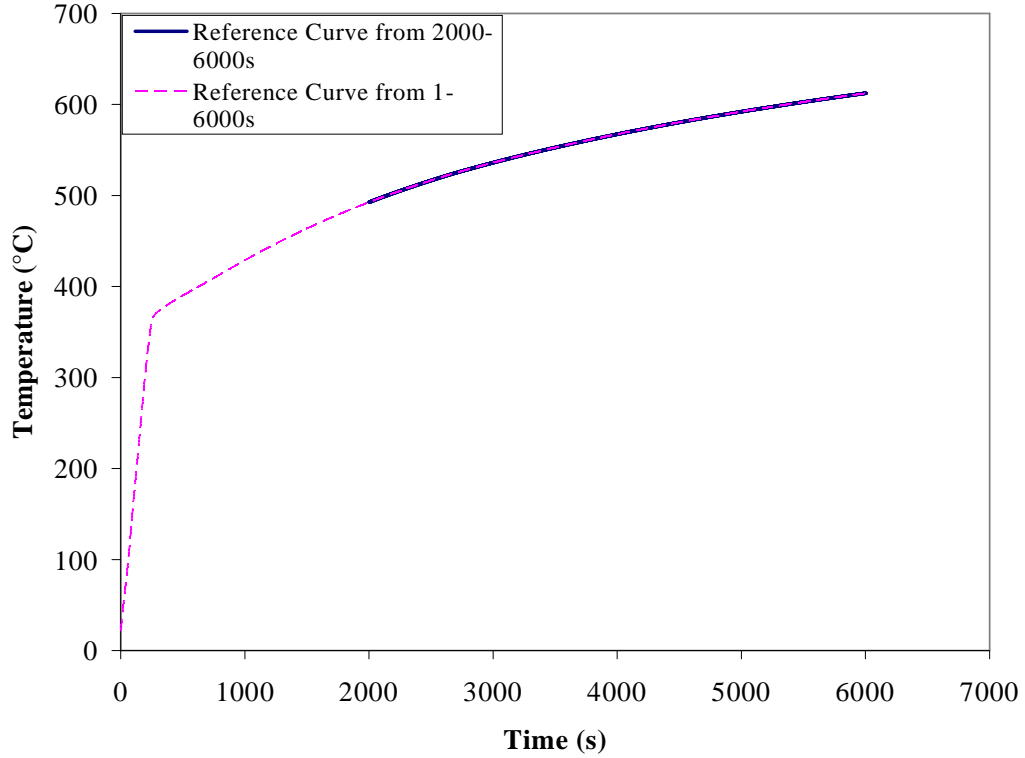


Figure 55. Simulation letter b. Exact reference curve is analyzed from 2000-6000s.

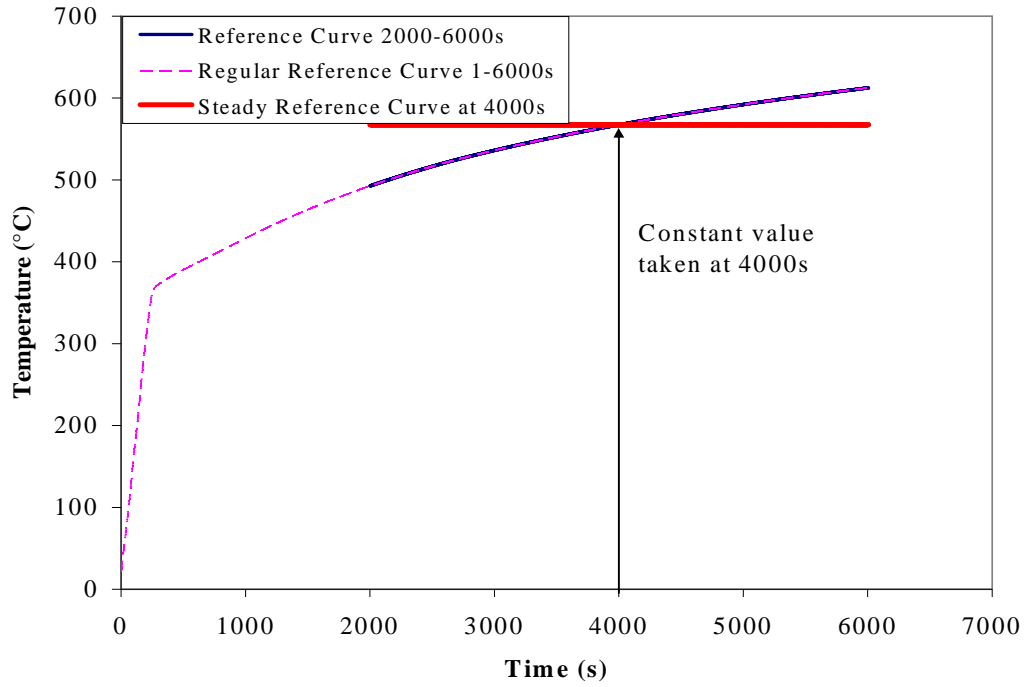


Figure 56. Simulation letter c. Approximate steady reference curve with the constant value taken at 4000s.

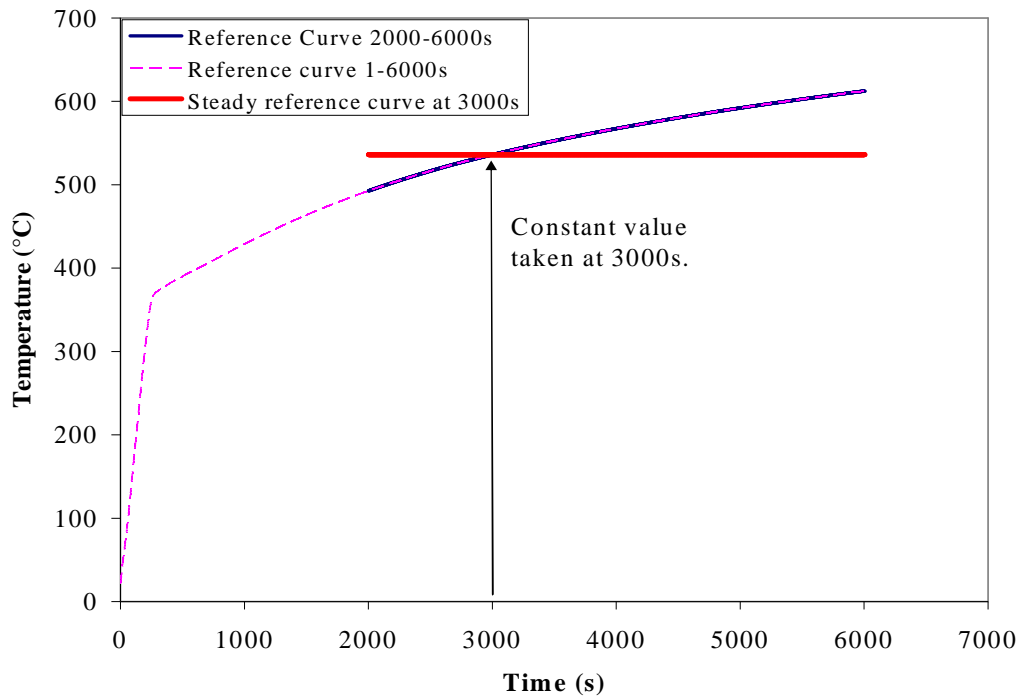


Figure 57. Simulation letter d. Approximate steady reference curve with value taken at 3000s.

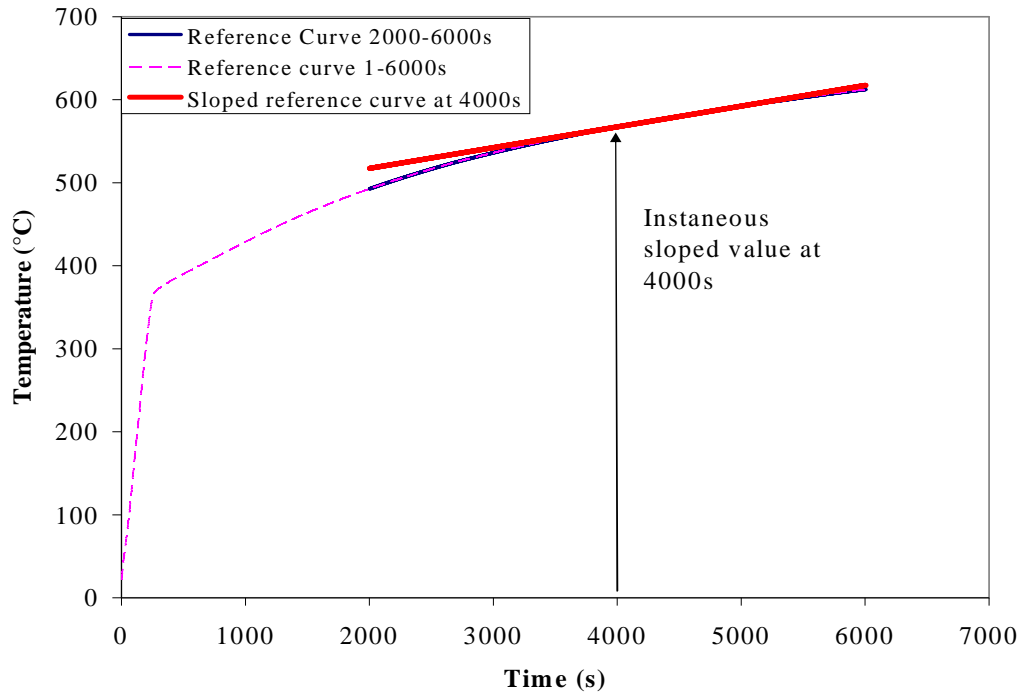


Figure 58. Simulation letter f. Approximate sloped reference curve at 4000s.

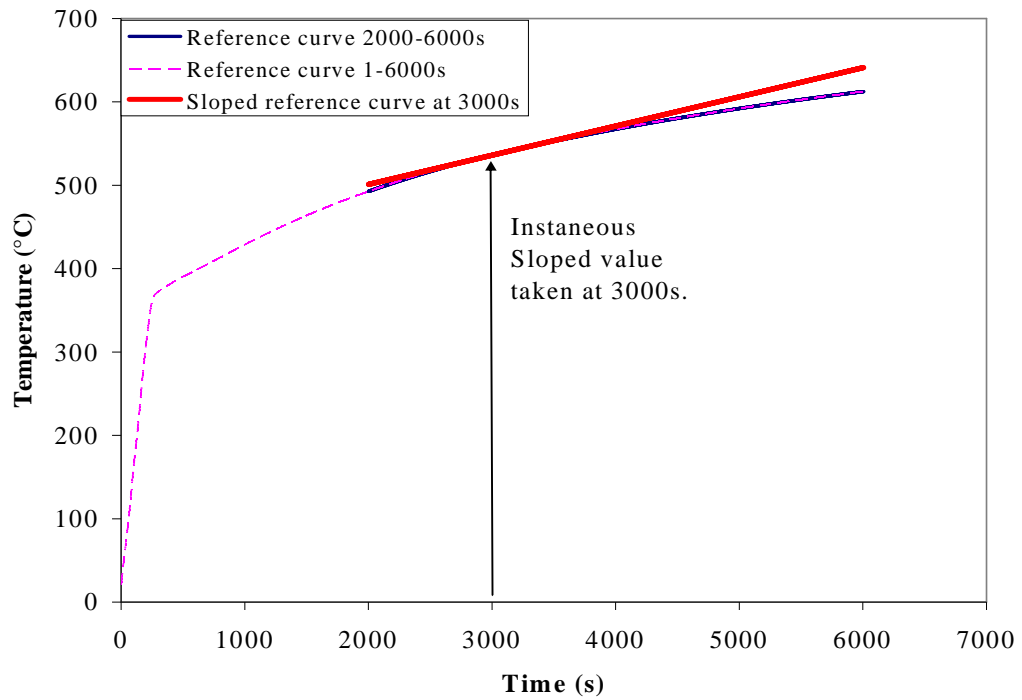
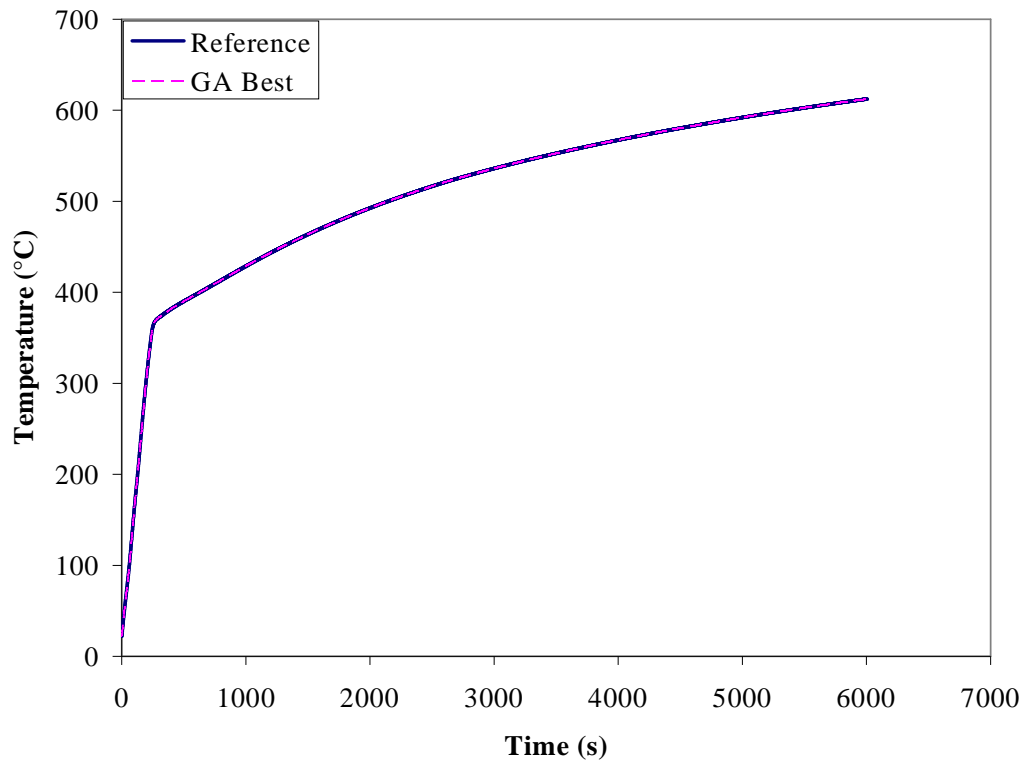
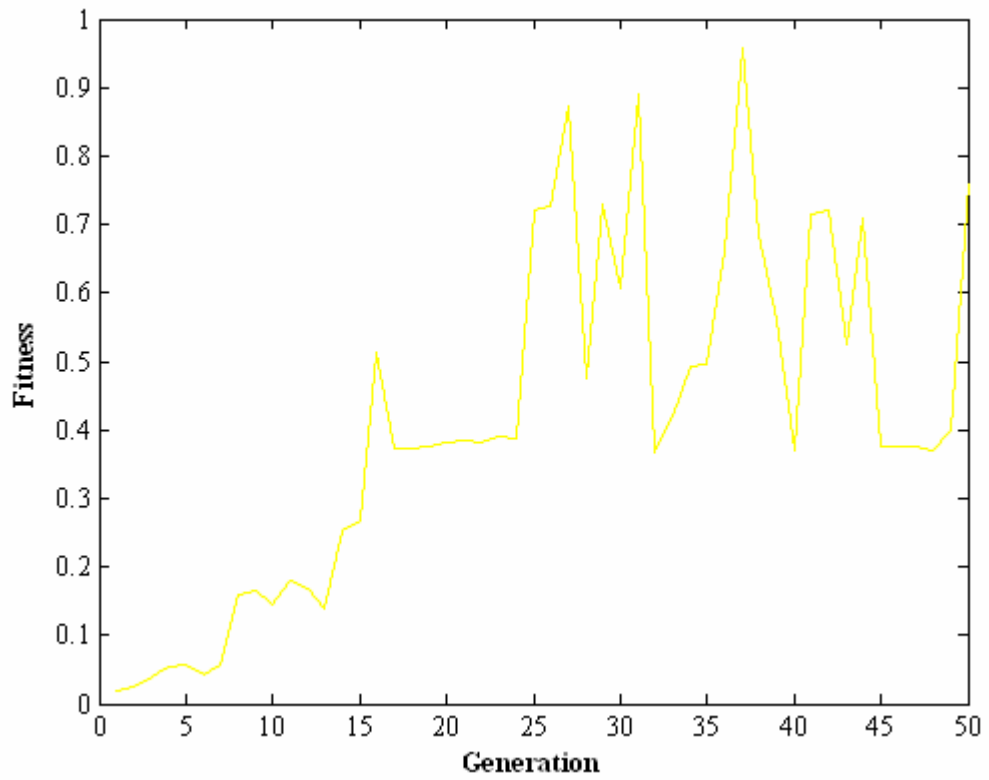


Figure 59. Simulation letter g. Approximate sloped reference curve at 3000s.

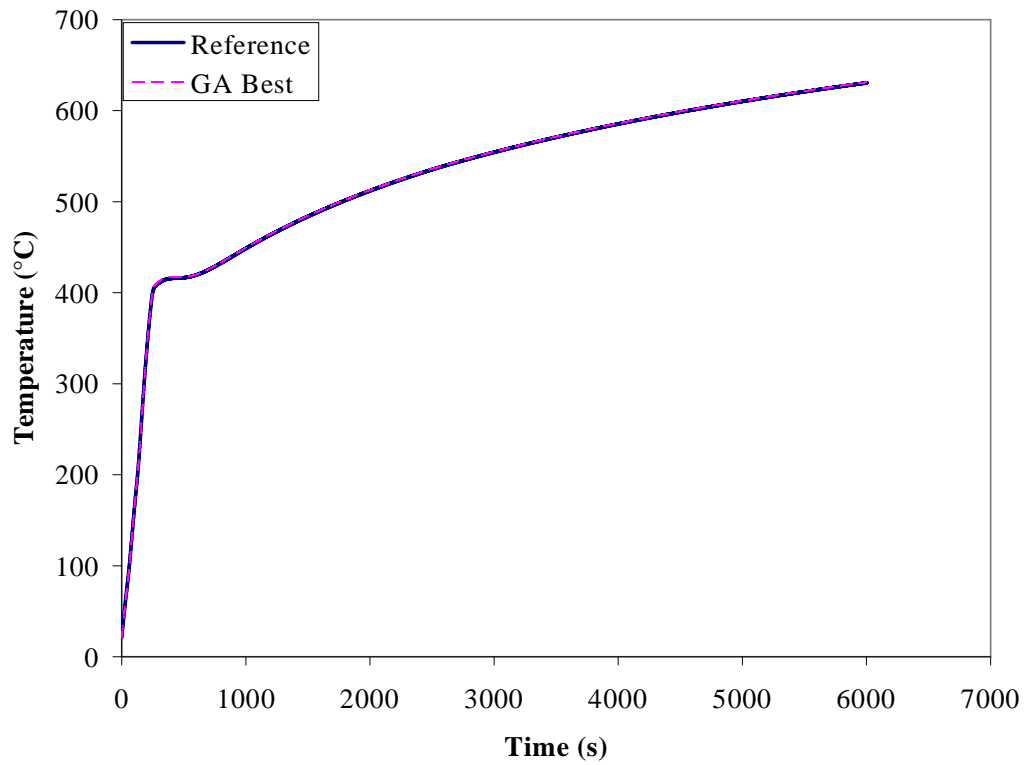
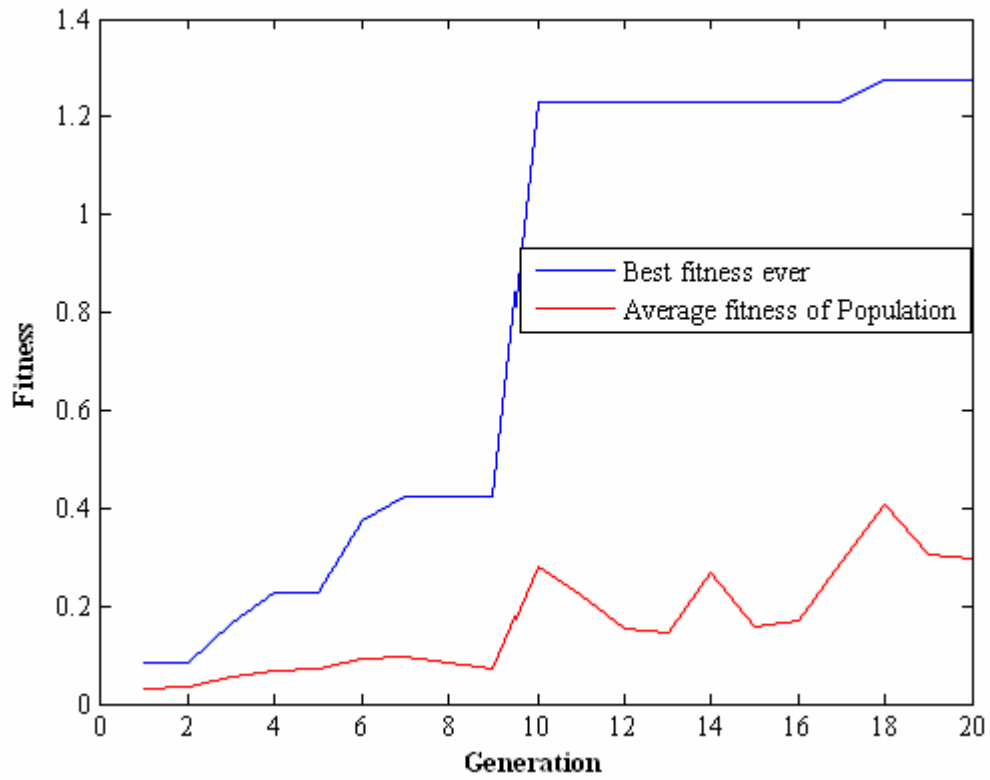
Appendix A1

Simulation Number	Reference MLR	Reference Average HRR	GA Best MLR	GA Best Average HRR	Bounds on Parameters	Notes About Simulation
SR10_10_3_Fb_a_1	1920 kW	1406 kW (240-6000s)	1918.8 kW	1406 kW (240-6000s)	1000-10,000 kW	50 generations, population size of 10.*
SR10_10_3_Fb_a_2	2400 kW	1485 kW (240-6000s)	2423 kW	1489 kW (240-6000s)	1000-10,000 kW	20 generations, population size of 10.
SR10_10_3_Fb_a_3	2400 kW	1485 kW (240-6000s)	2400 kW	1485 kW (240-6000s)	1000-3,250 kW	10 generations, population size of 10.
SR10_10_3_Fb_a_4	2400 kW	1485 kW (240-6000s)	2402 kW	1485 kW (240-6000s)	1000-5,000 kW	30 generations, population size of 10.
SR10_10_3_Fb_c_1	3000 kW	1337 kW (2000-6000s)	9797kW kW	1186 kW (2000-6000s)	1000-10,000 kW	Population size of 50, 50 generations.
SR10_10_3_Fb_d_1	3000 kW	1337 kW (2000-6000s)	9491kW kW	1077.6 kW (2000-6000s)	1000-10,000 kW	Population size of 50, 50 generations.
SR10_10_3_Fb_f_1	3000kW	1337 kW (2000-6000s)	3363kW	1349 kW (2000-6000s)	1000-10,000 kW	Population size of 50, 50 generations.
SR10_10_3_Fb_g_1	3000 kW	1337 kW (2000-6000s)	3378kW	1349 kW (2000-6000s)	1000-10,000 kW	Population size of 50, 50 generations.
SR3_3_3_NC_b_1	200 kW	200 kW (2000-6000s)	200 kW	200 kW (2000-6000s)	200-9,000 kW	Population size 20, 50 generations
SR3_3_3_NC_b_2	600 kW	599 kW (2000-6000s)	600.3 kW	599 kW (2000-6000s)	200-9,000 kW	Population size 20, 50 generations.
SR3_3_3_NC_b_3	1000 kW	973 kW (2000-6000s)	1018 kW	985 kW (2000-6000s)	200-9,000 kW	Population size 20, 50 generations.
SR3_3_3_NC_b_4	2000 kW	1222 kW (2000-6000s)	2000 kW	1222 kW (2000-6000s)	200-9,000 kW	Population size 20, 50 generations.
SR3_3_3_NC_b_5	3000 kW	1271 kW (2000-6000s)	3000 kW	1271 kW (2000-6000s)	200-9,000 kW	Population size 20, 50 generations.
SR3_3_3_NC_c_1	500 kW	499 kW (2000-6000s)	500.1 kW	499 kW (2000-6000s)	200-9,000 kW	Population size 20, 50 generations.
SR3_3_3_NC_d_1	500 kW	499 kW (2000-6000s)	476 kW	475 kW (2000-6000s)	200-9,000 kW	Population size 20, 50 generations.
SR3_3_3_NC_f_1	500 kW	499 kW (2000-6000s)	503 kW	502 kW (2000-6000s)	200-9,000 kW	Population size 20, 50 generations.
SR3_3_3_NC_g_1	500 kW	499 kW (2000-6000s)	506 kW	505 kW (2000-6000s)	200-9,000 kW	Population size 20, 50 generations.

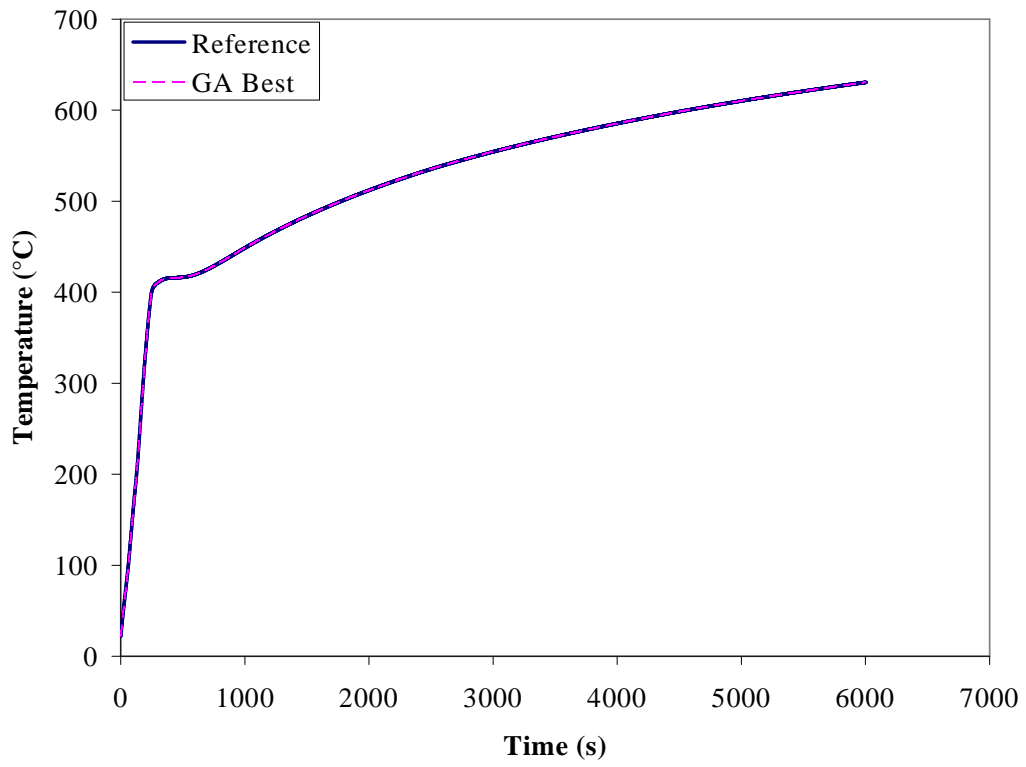
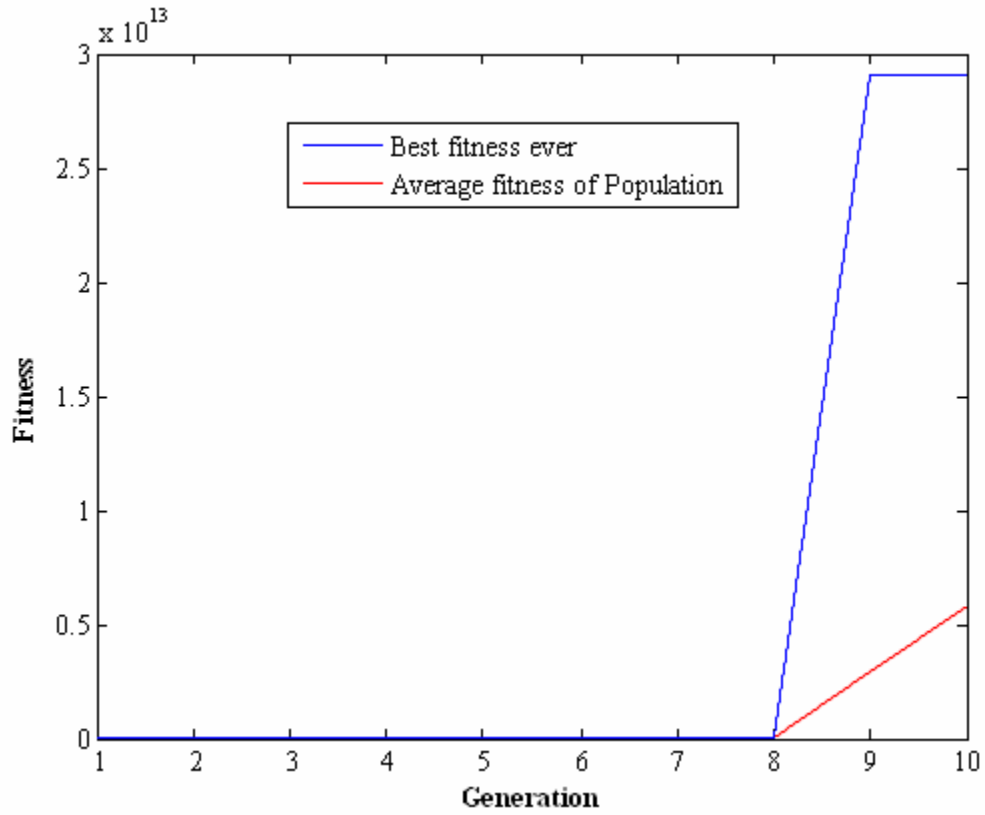
SR10_10_3_Fb_a_1



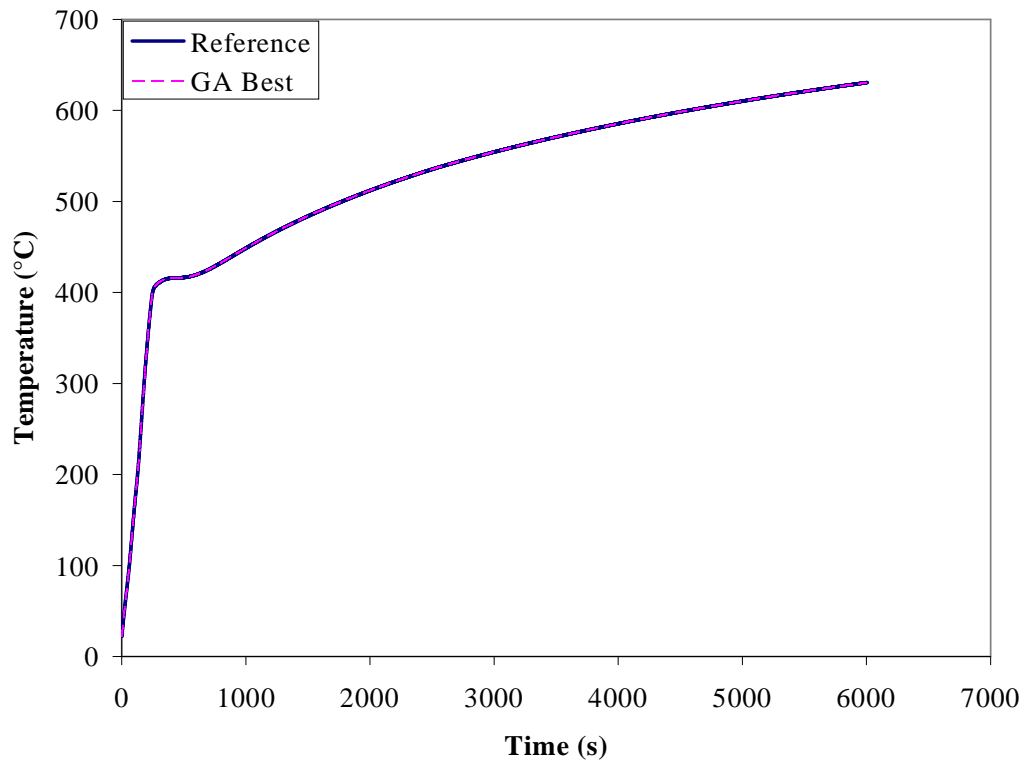
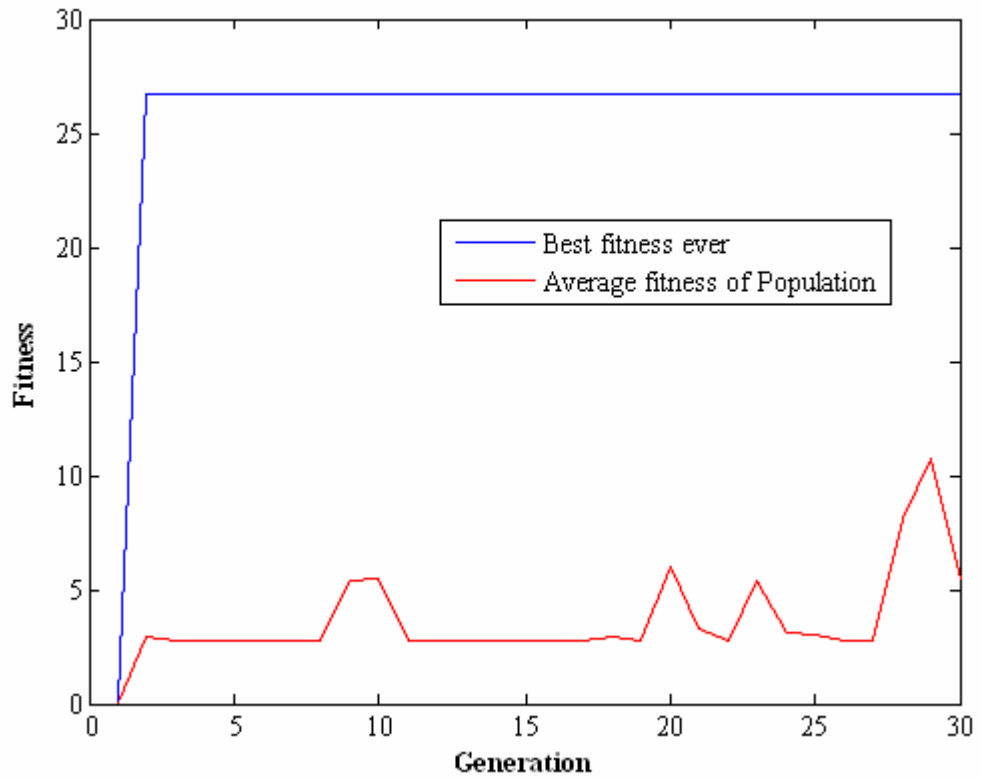
SR10_10_3_Fb_a_2



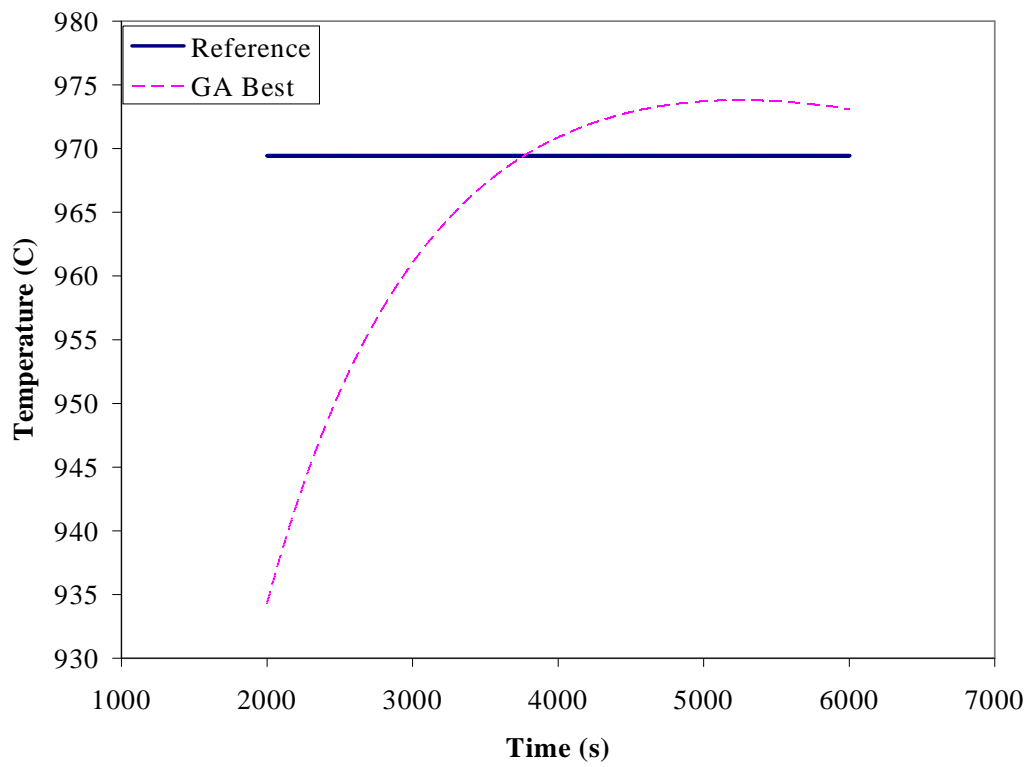
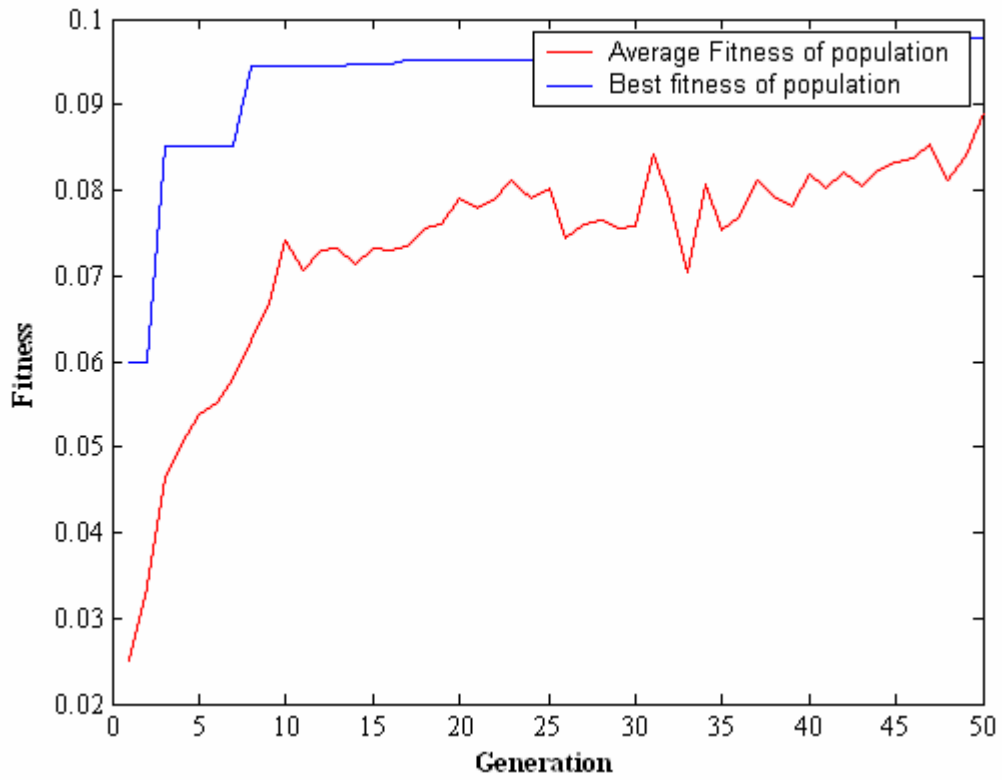
SR10_10_3_Fb_a_3



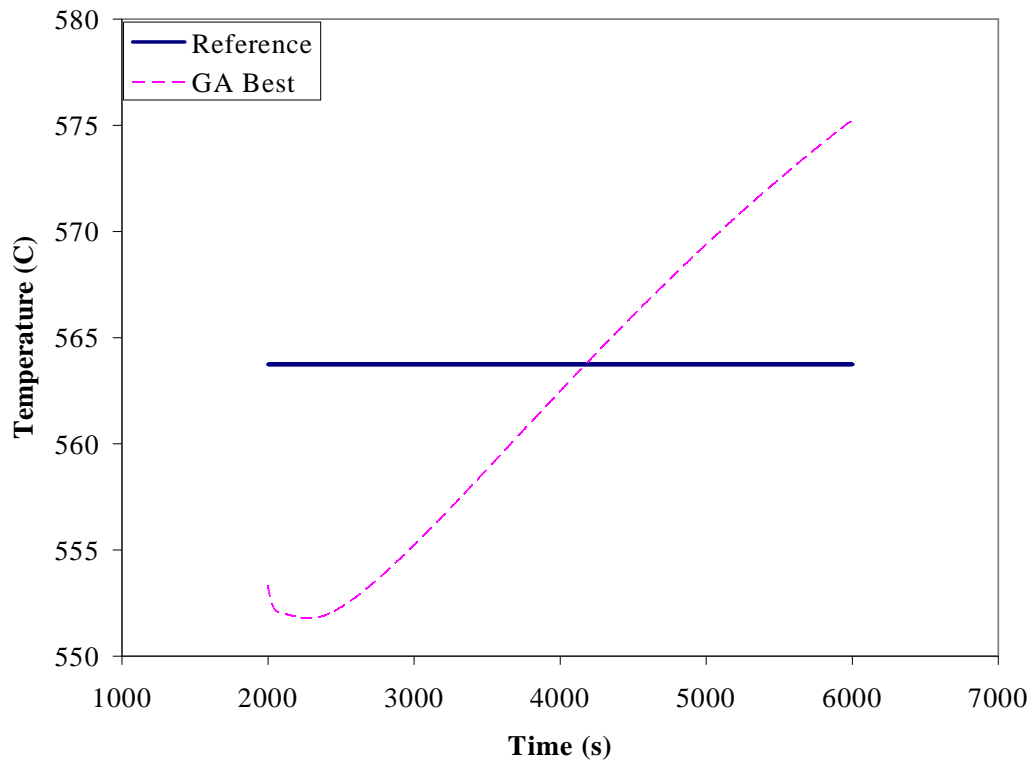
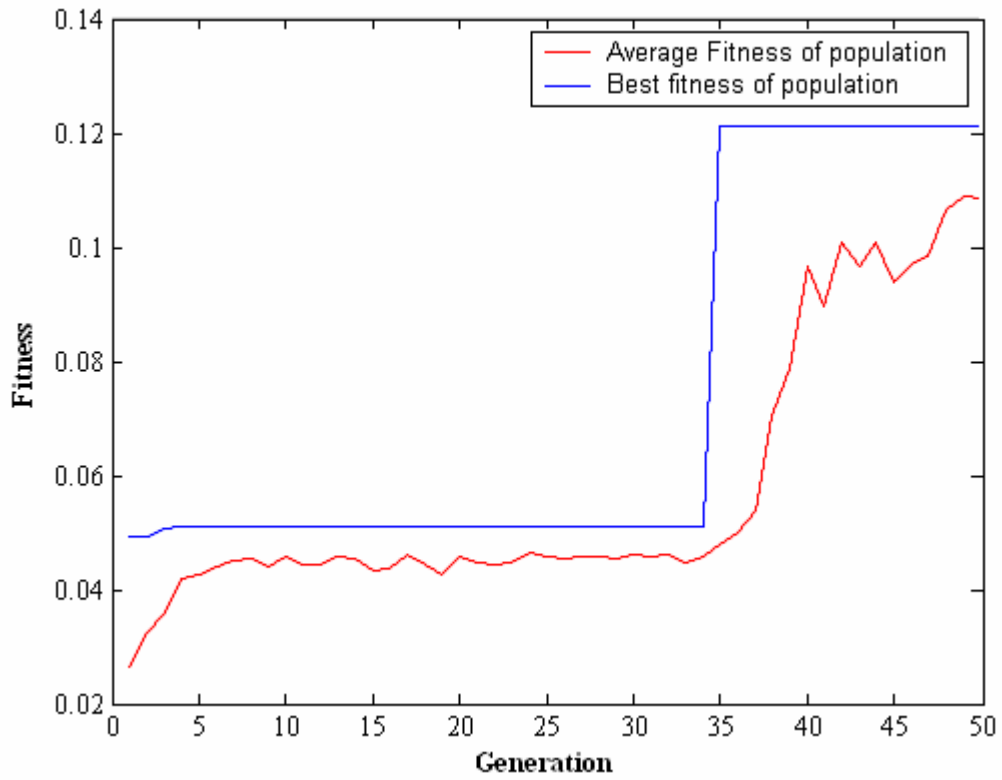
SR10_10_3_Fb_a_4



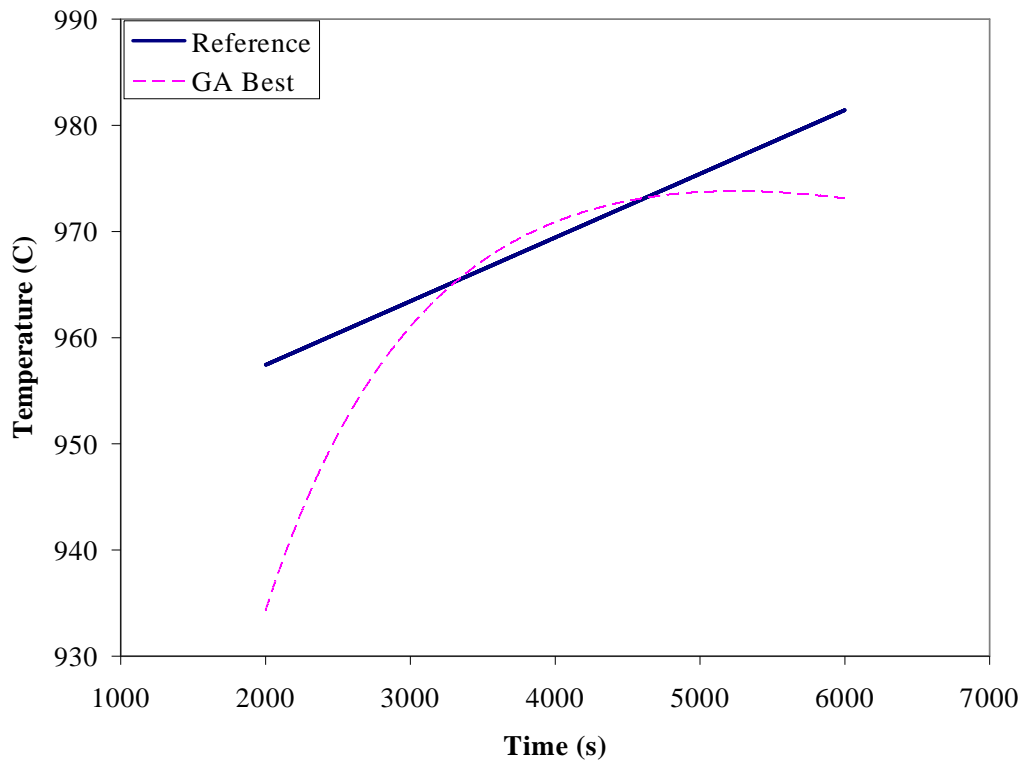
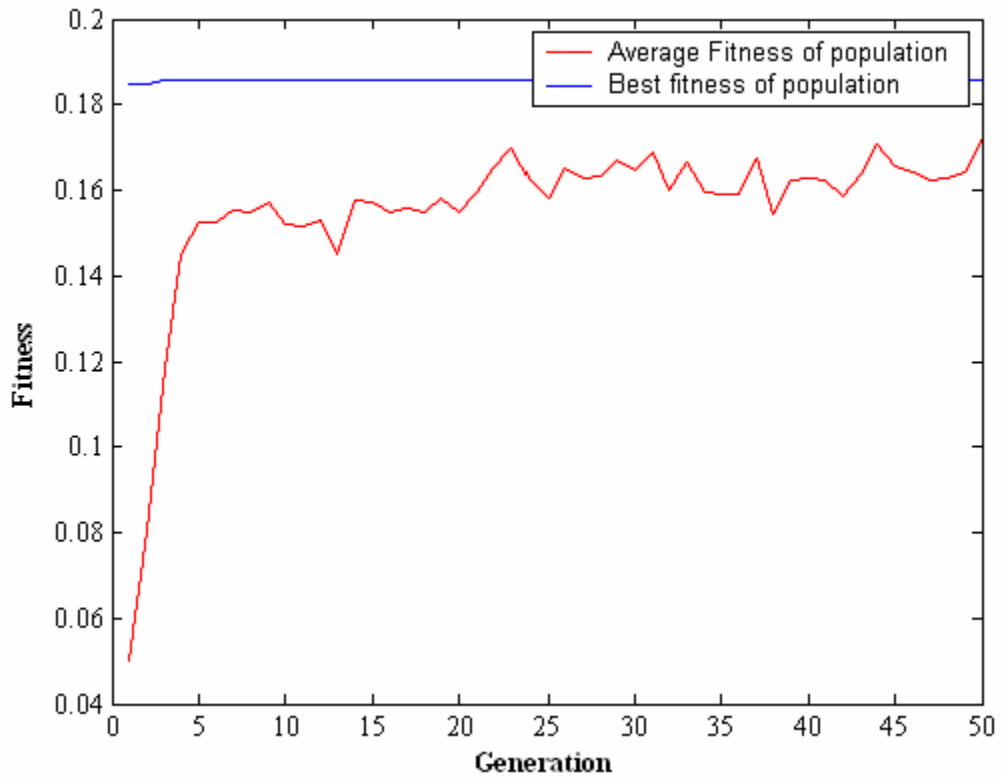
SR10_10_3_Fb_c_1



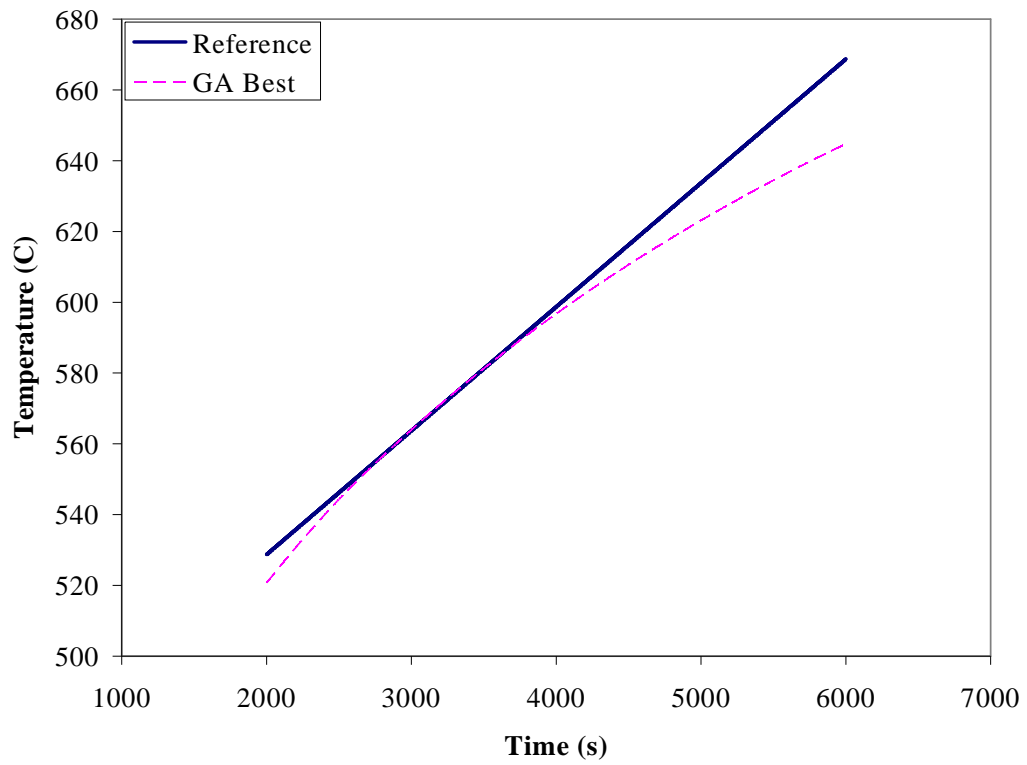
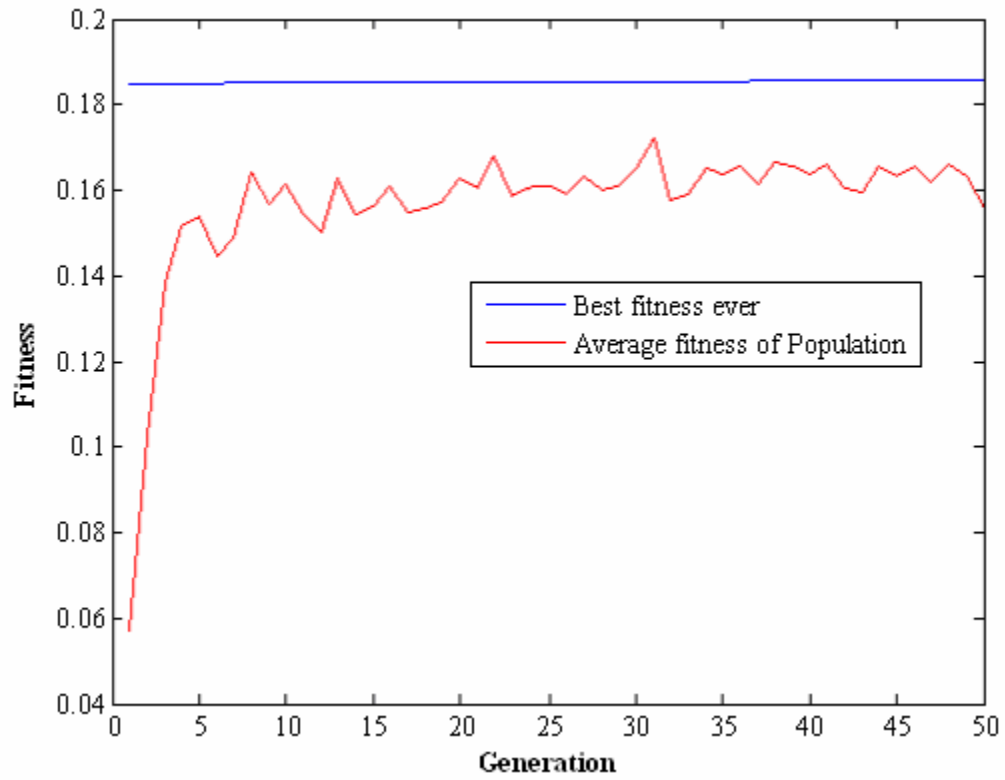
SR10_10_3_Fb_d_1



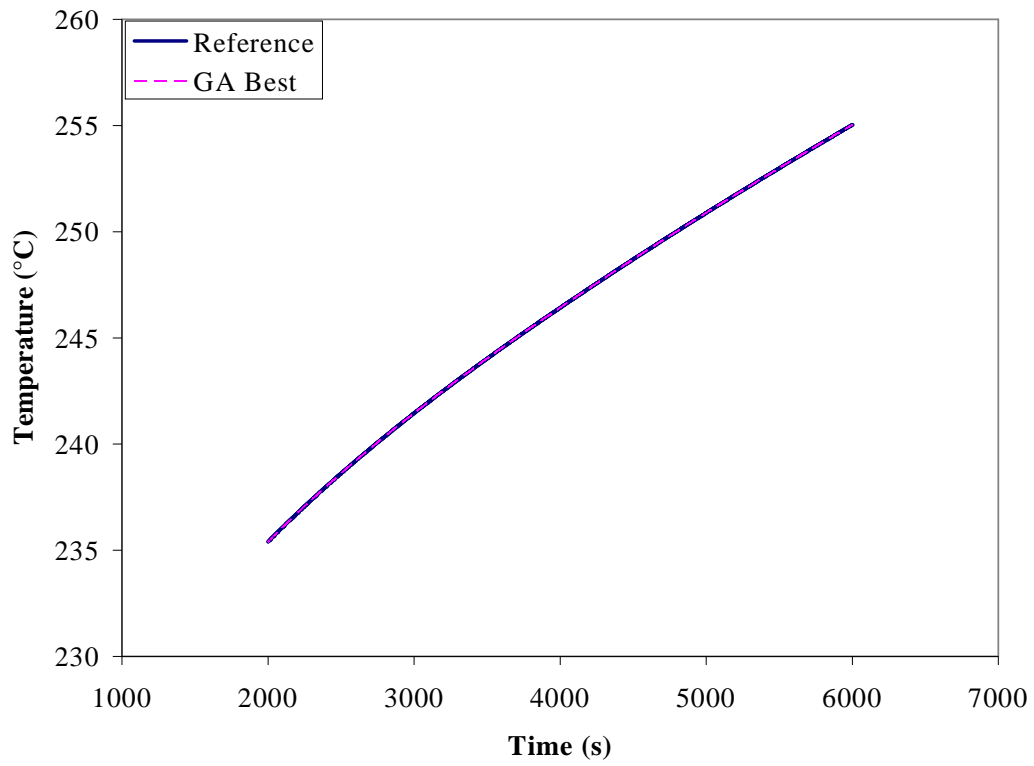
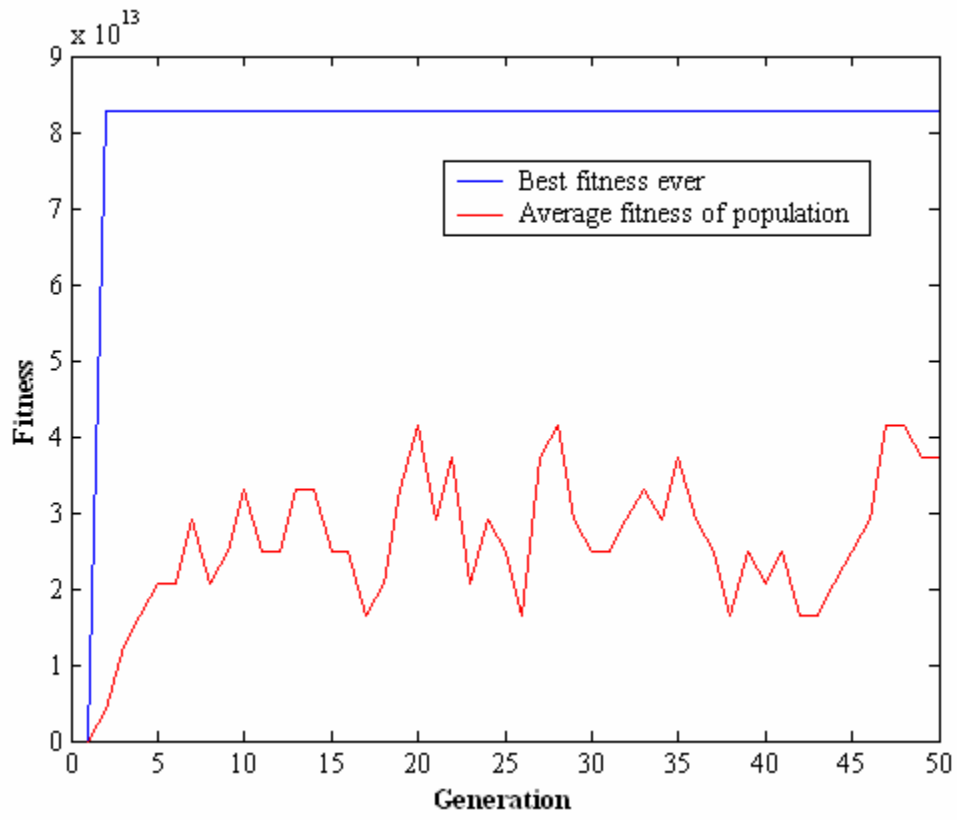
SR10_10_3_Fb_f_1



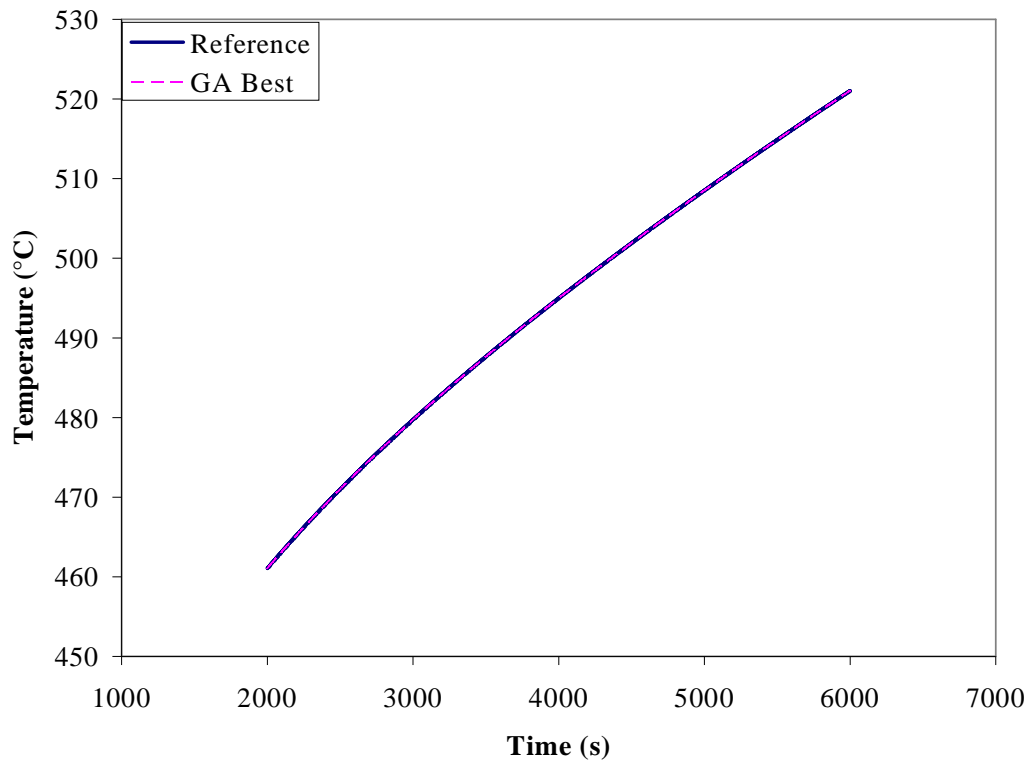
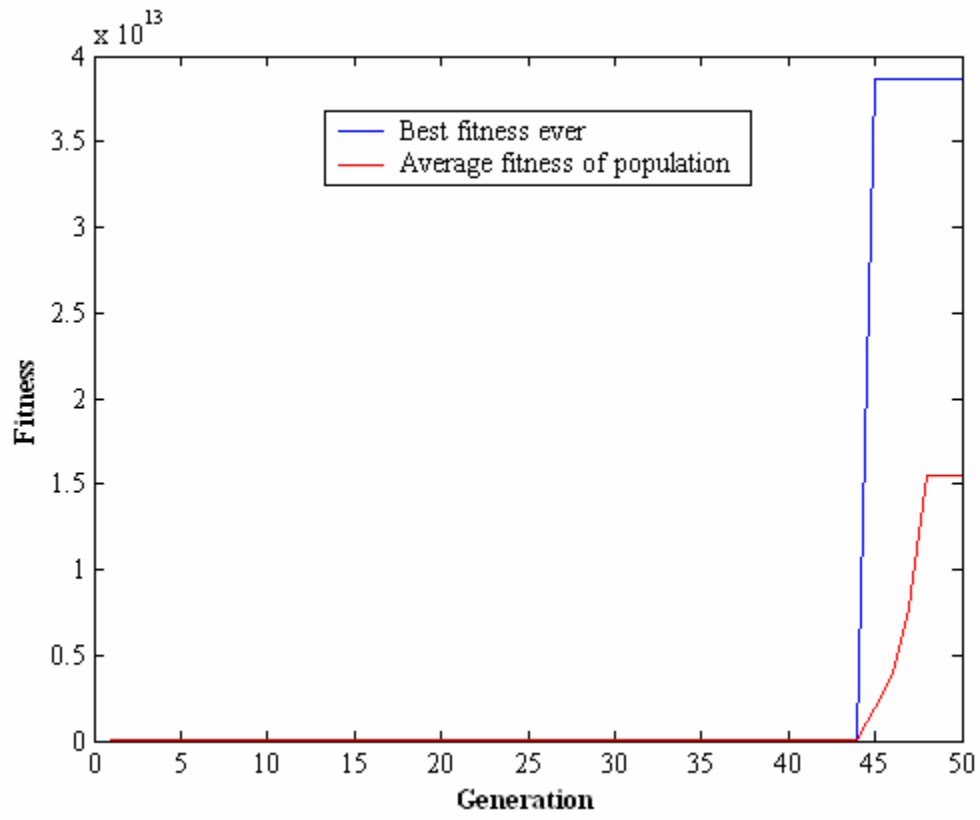
SR10_10_3_Fb_g_1



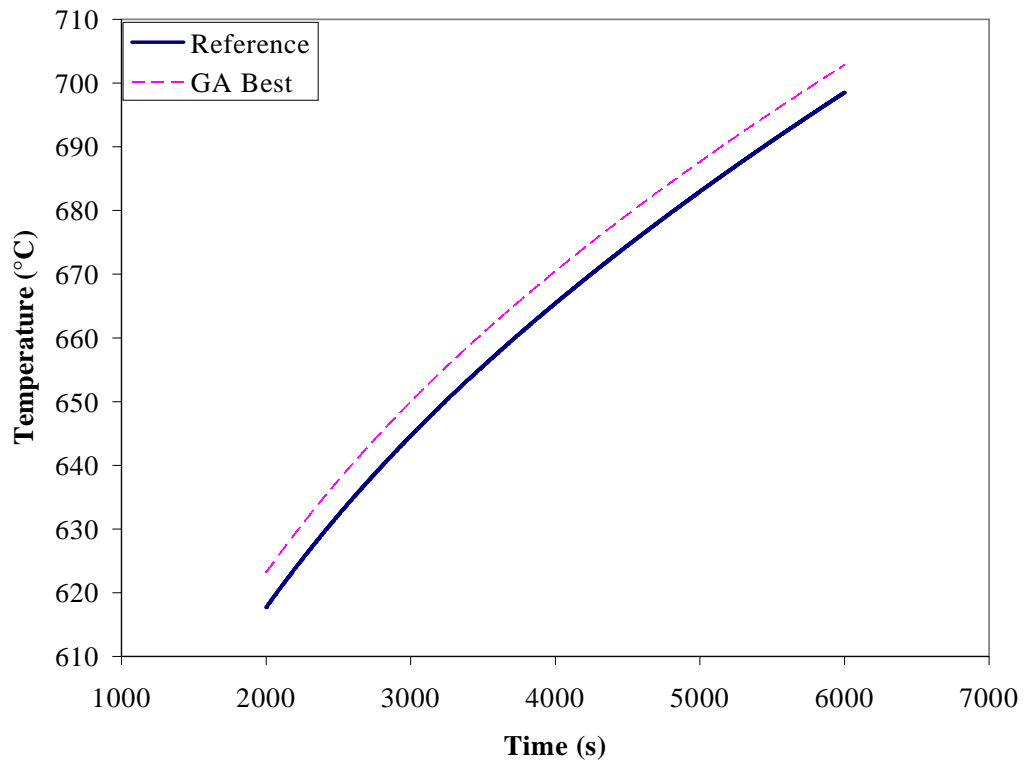
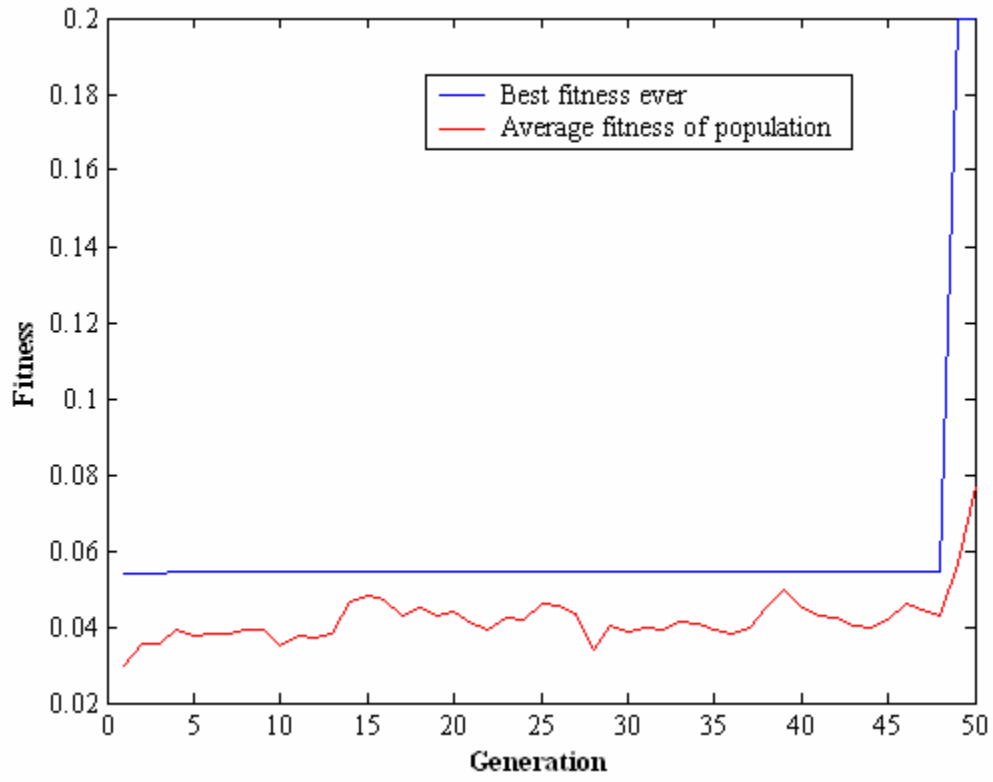
SR3_3_3_NC_b_1



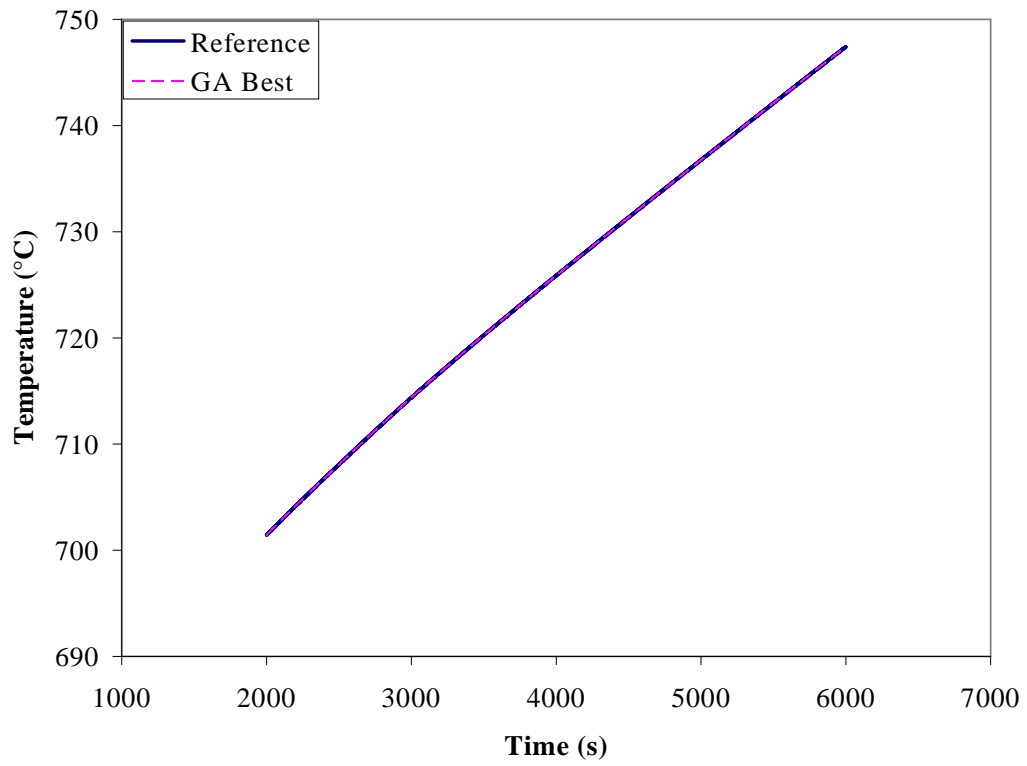
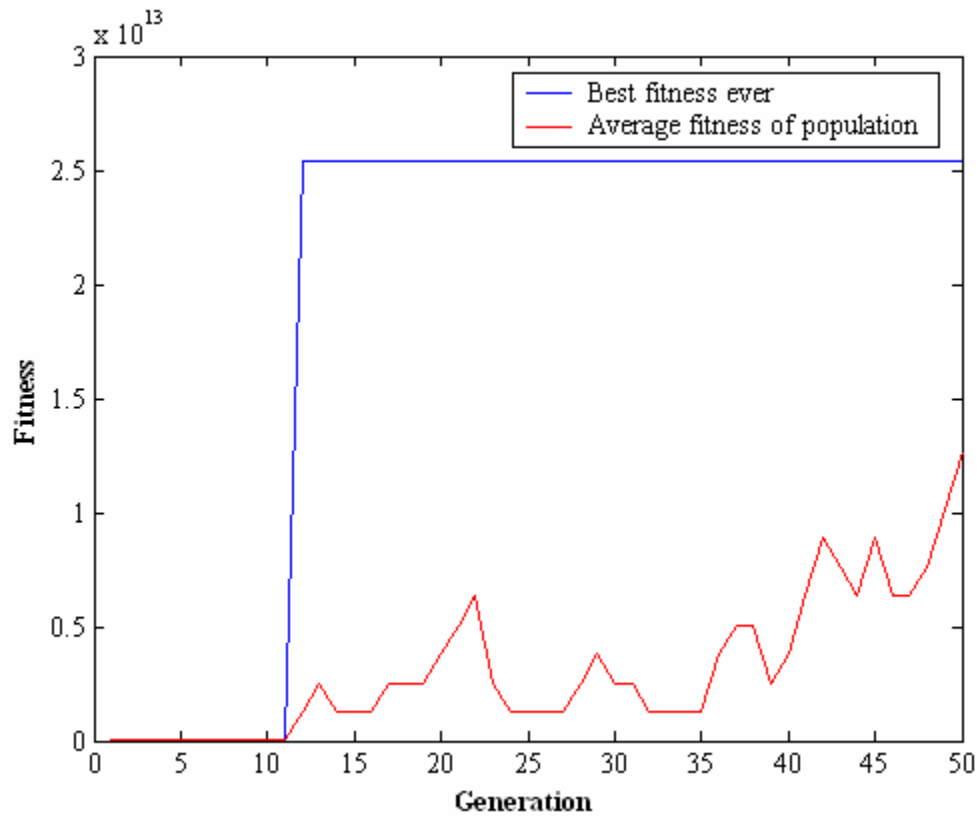
SR3_3_3_NC_b_2



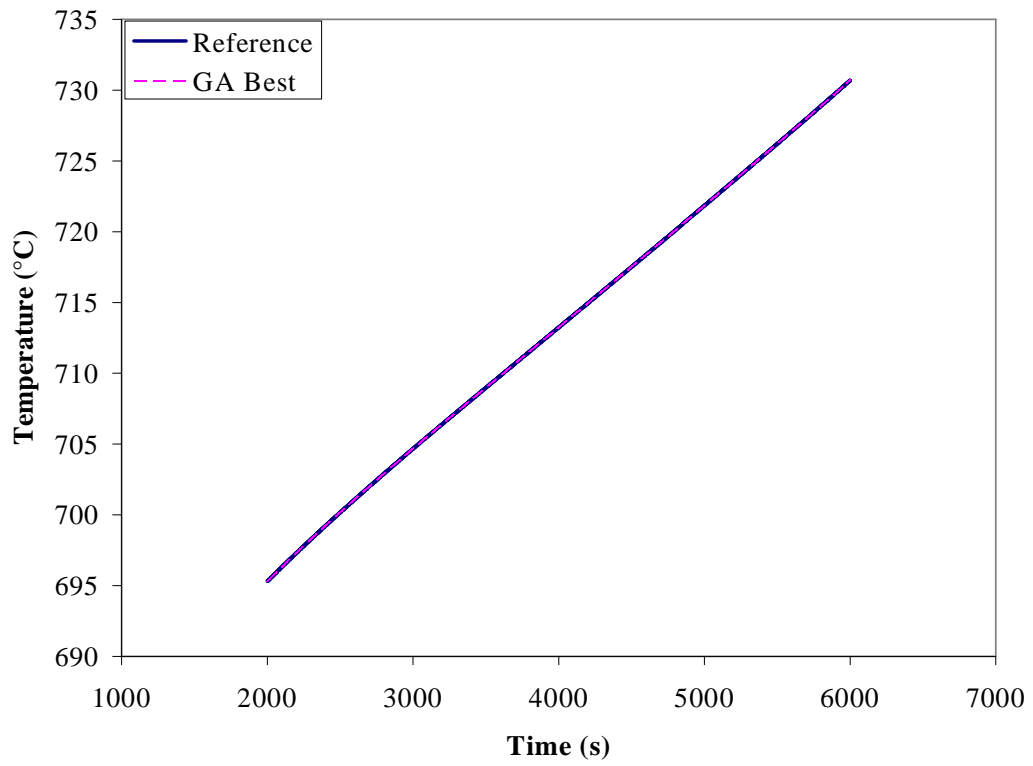
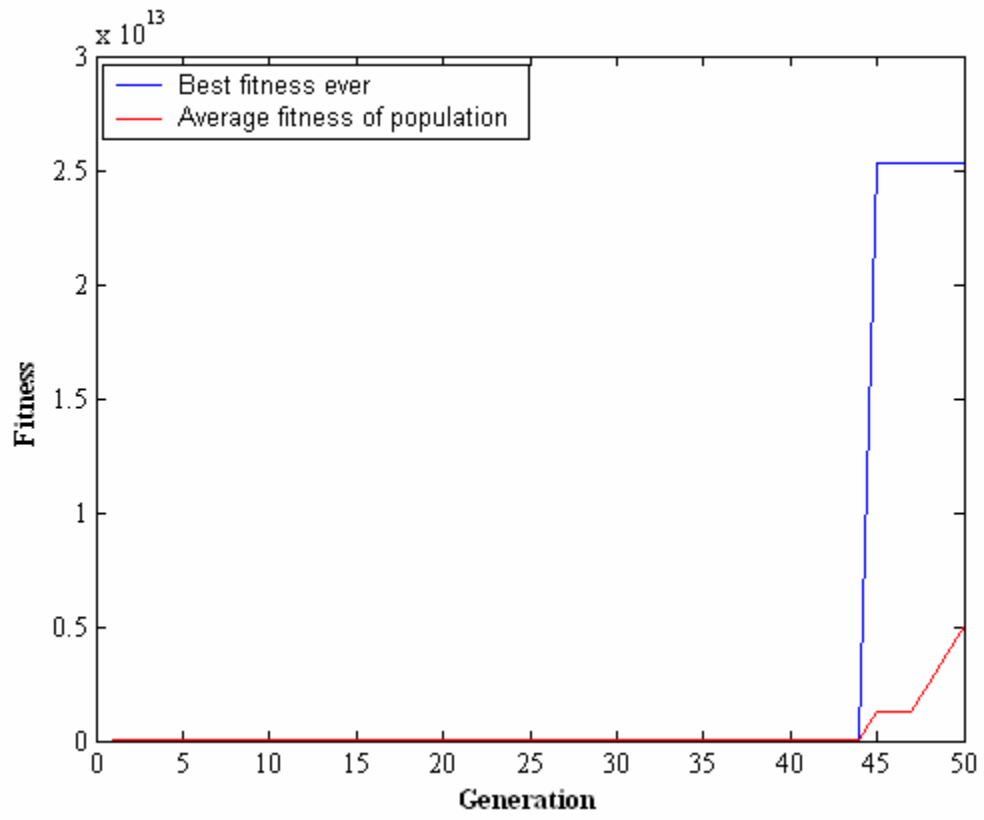
SR3_3_3_NC_b_3



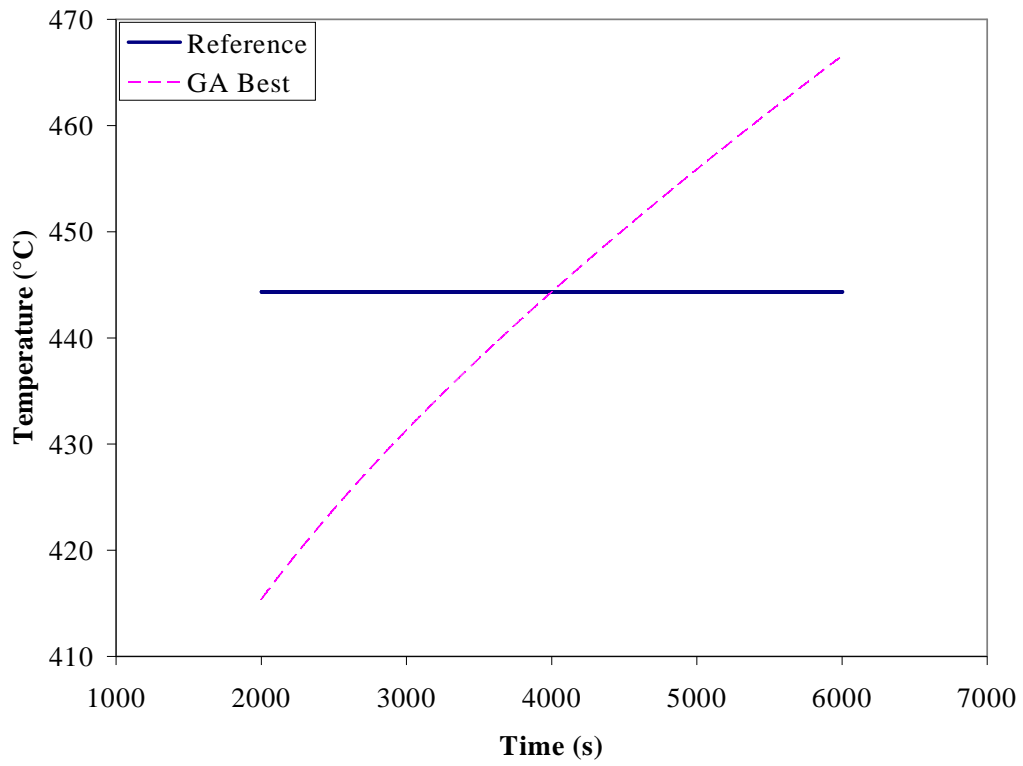
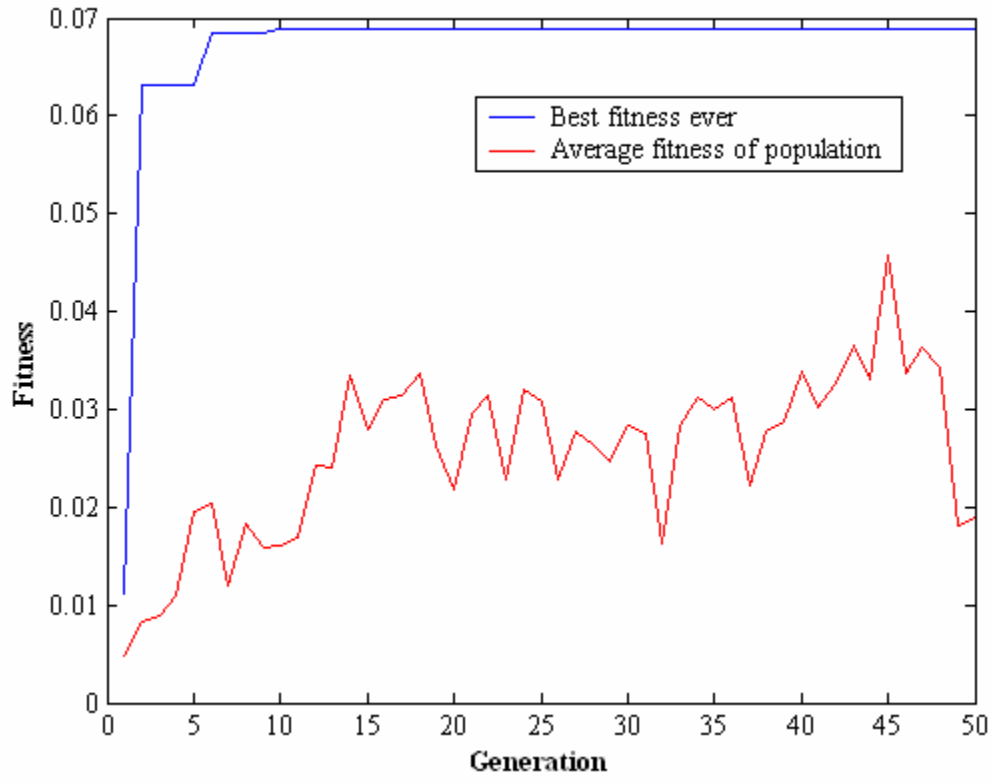
SR3_3_3_NC_b_4



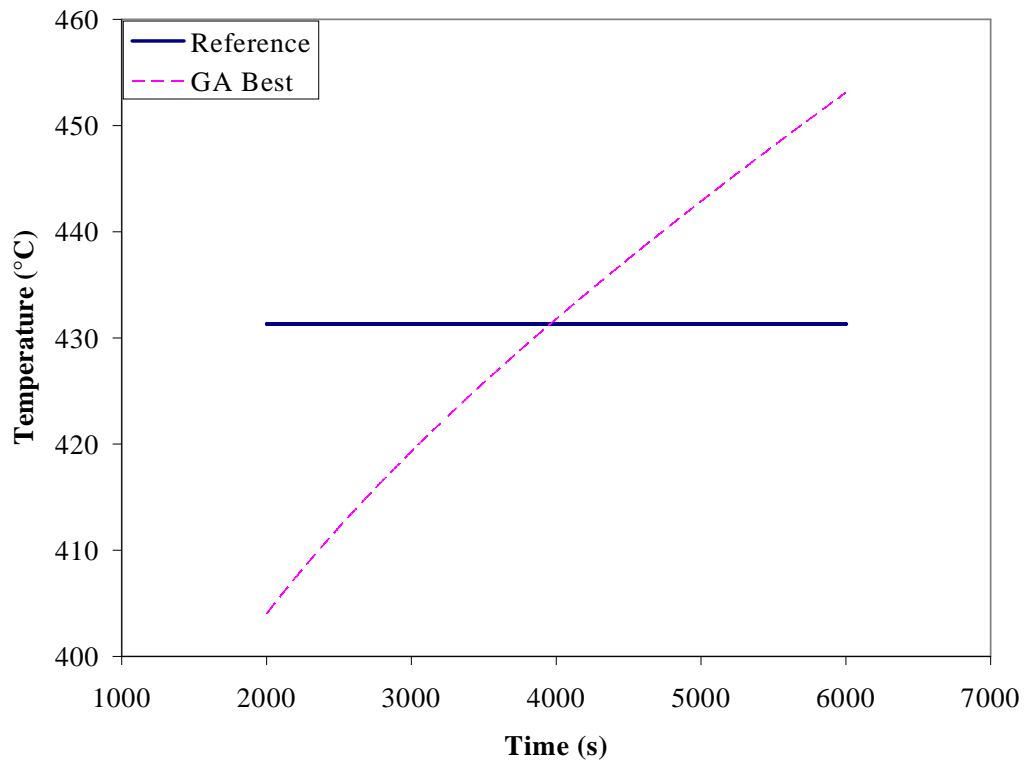
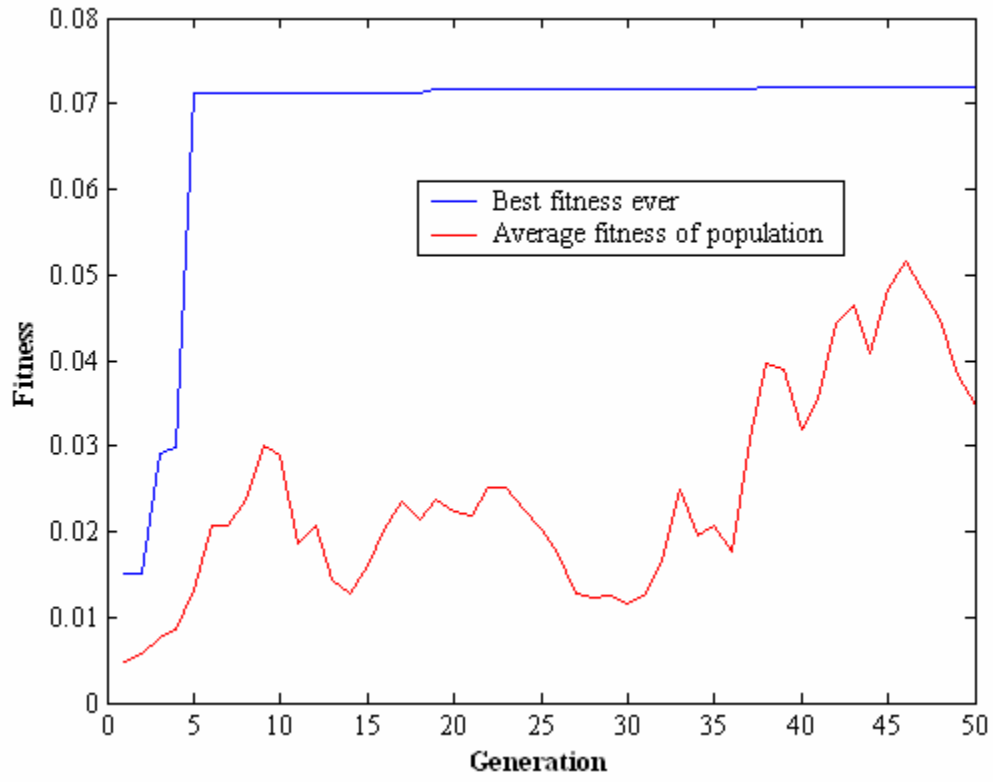
SR3_3_3_NC_b_5



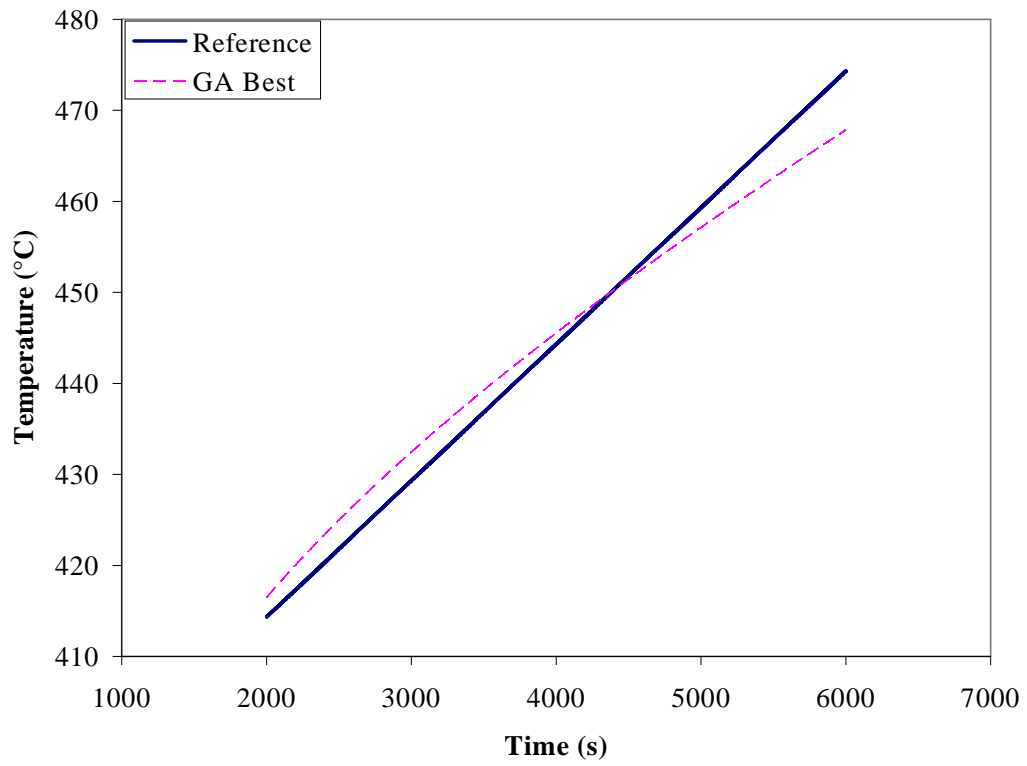
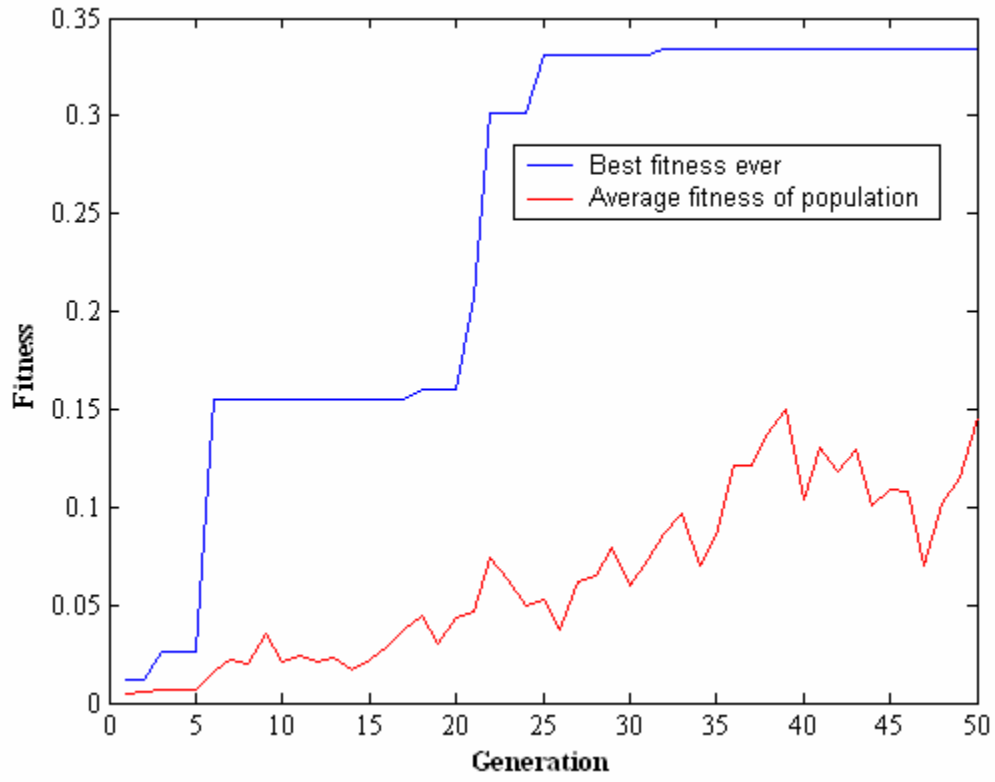
SR3_3_3_NC_c_1



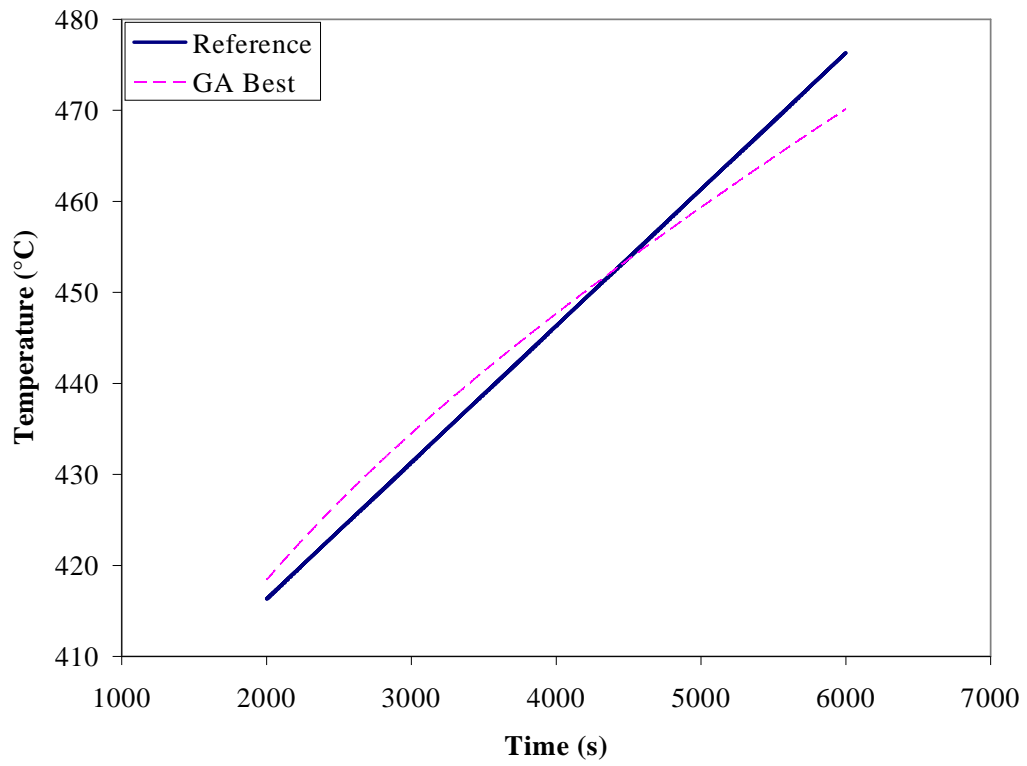
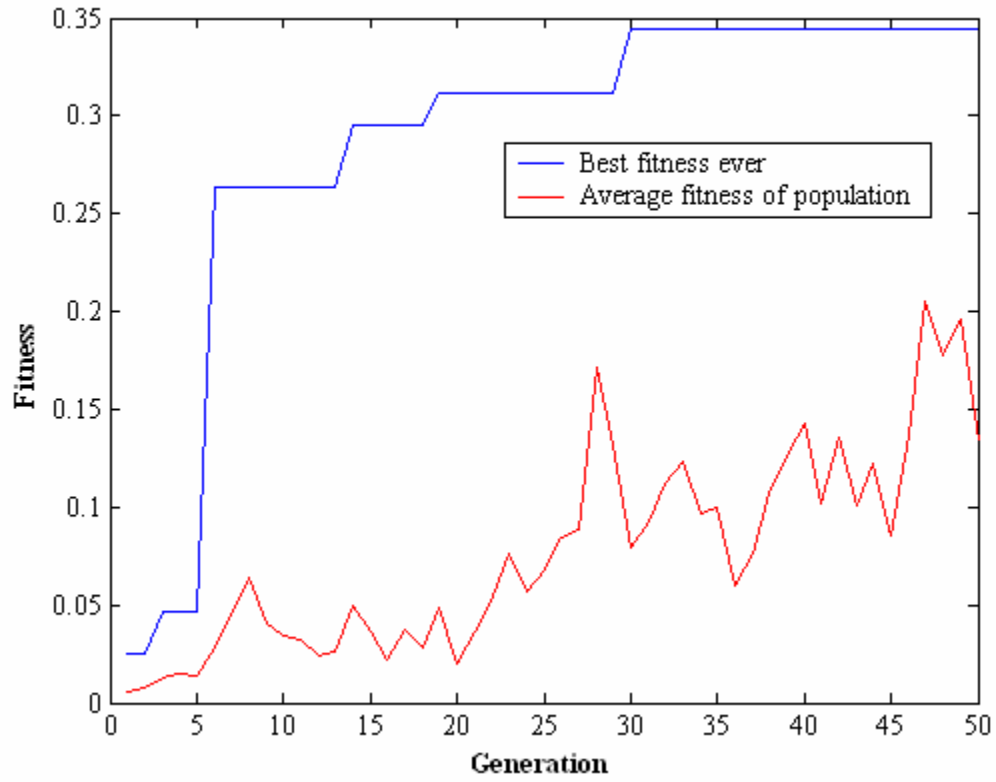
SR3_3_3_NC_d_1



SR3_3_3_NC_f_1



SR3_3_3_NC_g_1



Appendix A2

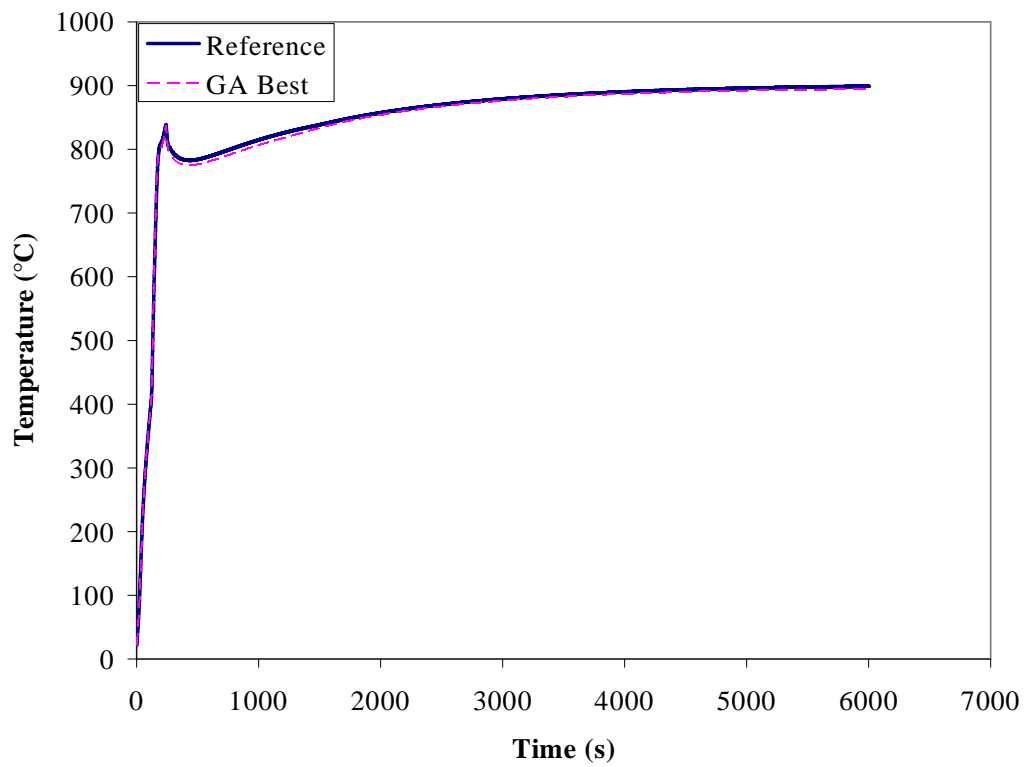
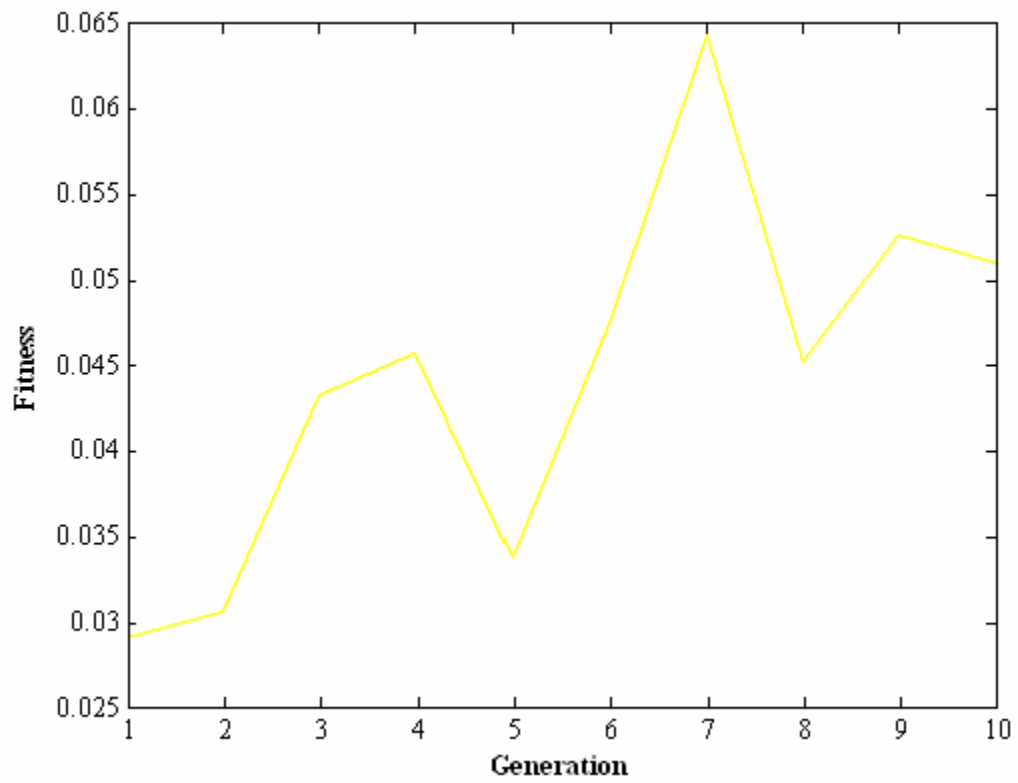
Simulation Number	Reference MLR	Reference Average HRR	Reference Vent	GA Best MLR	GA Best Average HRR	GA Best Vent	Bounds on MLR	Bounds on Vent	Notes on Simulation
SR3_3_3_ Fb_a_1	5432kW	1246 kW (240-6000s)	1m x 2m	5869 kW	1240 kW (240-6000s)	1.2m x 1.8m	1,000-10,000 kW	Width: 1m-2m, Height: 1m-3m	Population size of 10, 10 generations.*
SR3_3_3_ Fb_a_2	2900kW	1181 kW (240-6000s)	1m x 2m	2853 kW	1188 kW (240-6000s)	1.3m x 1.8m	1,000-7,000 kW	Width: 1m-2m, Height: 1m-2.9m	50 generations, 50 population size.*
SR3_3_3_ Fb_a_3	2456 kW	1144 kW (240-6000s)	1m x 2m	2462 kW	1135 kW (240-6000s)	.95m x 2.0m	1,000-7,000 kW	Width: .75m-2m, Height: 1m-2.9m	Population size of 50, 50 generations.*
SR3_3_3_ Fb_a_4	1303 kW	971 kW (240-6000s)	1m x 2m	1473 kW	1157 kW (240-6000s)	1.6m x 1.9m	1,000-7,000 kW	Width: .75m-2m, Height: 1m-2.9m	Population size of 50, 50 generations.*
SR3_3_3_ Fb_a_5	3000 kW	1187 kW (240-6000s)	1m x 2m	2993 kW	1187 kW (240-6000s)	1.0m x 1.9m	1,000-7,000 kW	Width: 0.5m-2m, Height: 1m-3m	Population size 25, 100 generations.
SR3_3_3_ Fb_a_6	1303 kW	971 kW (240-6000s)	1m x 2m	1507 kW	1194 kW (240-6000s)	1.3m x 2.1m	1,000-7,000 kW	Width: .5m-2m, Height: 1m-3.0m	Population size of 25, 50 generations.
SR3_3_3_ Fb_a_7	2900kW	1181 kW (240-6000s)	1m x 2m	2957 kW	1186 kW (240-6000s)	.96m x 2.0m	1,000-7,000 kW	Width: .5m-2m, Height: 1m-3m	Population size of 20, 50 generations.
SR3_3_3_ Fb_a_8	3000 kW	1188 kW (240-6000s)	1m x 2m	3484 kW	1262 kW (240-6000s)	.92m x 2.1m	200-7,000 kW	Width: .25m-2m, Height: 1m-3m	Population size of 20, 50 generations.
SR3_3_3_ Fb_b_1	2500kW	1043 kW (2000-6000s)	1m x 2m	2798 kW	1067 kW (2000-6000s)	1.0m x 2.0m	1,000-7,000 kW	Width: 1m-2m, Height 1m-2.9m	Population size of 100, 100 generations.
SR3_3_3_ Fb_b_2	2900kW	1074 kW (2000-6000s)	1m x 2m	2134 kW	1519 kW (2000-6000s)	1.5m x 2.5m	1,000-7,000 kW	Width: 1m-2m, Height: 1m-2.9m	Population size of 20, 100 generations.
SR3_3_3_ Fb_b_3	2900kW	1074 kW (2000-6000s)	1m x 2m	2630 kW	1833 kW (2000-6000s)	1.80 m x 2.67 m	1,000-7,000 kW	Width: .75m-2m Height: 1m-2.9m	Population size of 50 1000 generations.

Simulation Number	Reference MLR	Reference Average HRR	Reference Vent	GA Best MLR	GA Best Average HRR	GA Best Vent	Bounds on MLR	Bounds on Vent	Notes on Simulation
SR3_3_3_Fb_b_4	1700kW	960.4 kW (2000-6000s)	1m x 2m	2061 kW	960.1 KW (2000-6000s)	1.14m x 1.82m	1,000-7,000 kW	Width: .75m-2m, Height: 1m-2.9m	Population size of 50, 50 generations.
SR3_3_3_Fb_b_5	4654kW	1247 kW (2000-6000s)	1m x 2m	5060 kW	1298 kW (2000-6000s)	1.08m x 1.97m	200-7,000 kW	Width: .5m-2m, Height: 1m-3m	Population size of 25, 50 generations.
SR3_3_3_Fb_b_6	3000 kW	1081 kW (2000-6000s)	1m x 2m	2873 kW	1089 kW (2000-6000s)	1.33m x 1.79m	1,000-8,000 kW	Width: .5m-2m, Height: 1-2.9m	Population size of 50, 50 generations.
SR3_3_3_Fb_c_1	3000 kW	1081 kW (2000-6000s)	1m x 2m	2657 kW	1417 kW (2000-6000s)	2.0m x 1.9m	200-4,500 kW	Width: .75m-2m, Height: 1m-3m	Population size of 25, 25 generations.
SR3_3_3_Fb_d_1	3000 kW	1081 kW (2000-6000s)	1m x 2m	4497 kW	1385 kW (2000-6000s)	1.9m x 1.7m	200-4,500 kW	Width: .75m-2m, Height: 1m-3m	Population size of 25, 25 generations
SR3_3_3_Fb_e_1	5432kW	1146 kW (2000-6000s)	1m x 2m	6757 kW	1205 kW (2000-6000s)	1.6m x 1.6m	1,000-8,000 kW	Width: 1m-2m, Height: 1m-3m	Population size of 20, 20 generations.
SR3_3_3_Fb_e_2	5432kW	1146 kW (2000-6000s)	1m x 2m	7992 kW	1437 kW (2000-6000s)	1.3m x 2.0 m	1,000-8,000 kW	Width: 1m-2m, Height: 1m-2.9m	Population size of 50, 50 generations.
SR3_3_3_Fb_e_3	3000kW	1081 kW (2000-6000s)	1m x 2m	4487kW	1459 kW (2000-6000s)	2.0m x 1.8m	1,000-7,000 kW	Width: 1m-2m, Height: 1m-2.9m	Population size of 100, 100 generations.
SR3_3_3_Fb_e_4	1700 kW	960 kW (2000-6000s)	1m x 2m	5483 kW	1452 kW (2000-6000s)	1.8m x 1.8m	1,000-7,000kW	Width: 1m-2m Height: 1m-2.9m	Population size of 50, 50 generations.
SR3_3_3_Fb_e_5	1303 kW	908 kW (2000-6000s)	1m x 2m	6370 kW	1441 kW (2000-6000s)	1.64m x 1.82 m	1,000-7,000kW	Width: .75m-2m, Height: 1m-2.9m	Population size of 50, 50 generations.
SR3_3_3_Fb_e_6	1700 kW	960 kW (2000-6000s)	1m x 2m	5936 kW	1504 kW (2000-6000s)	1.61m x 1.92m	1,000-7,000kW	Width: .75m-2m, Height: 1m-2.9m	
SR3_3_3_Fb_f_1	3000kW	1081 kW (2000-6000s)	1m x 2m	2913 kW	1148 kW (2000-6000s)	1.1m x 2.0m	200-4,500 kW	Width: .75m-2m, Height: 1m-3m	Population size of 25, 25 generations.
SR3_3_3_Fb_g_1	3000 kW	1081 kW (2000-6000s)	1m x 2m	2508 kW	1066 kW (2000-6000s)	.75m x 2.3m	200-4,500 kW	Width: .75-2m, Height: 1m-3m	Population size of 25, 25 generations

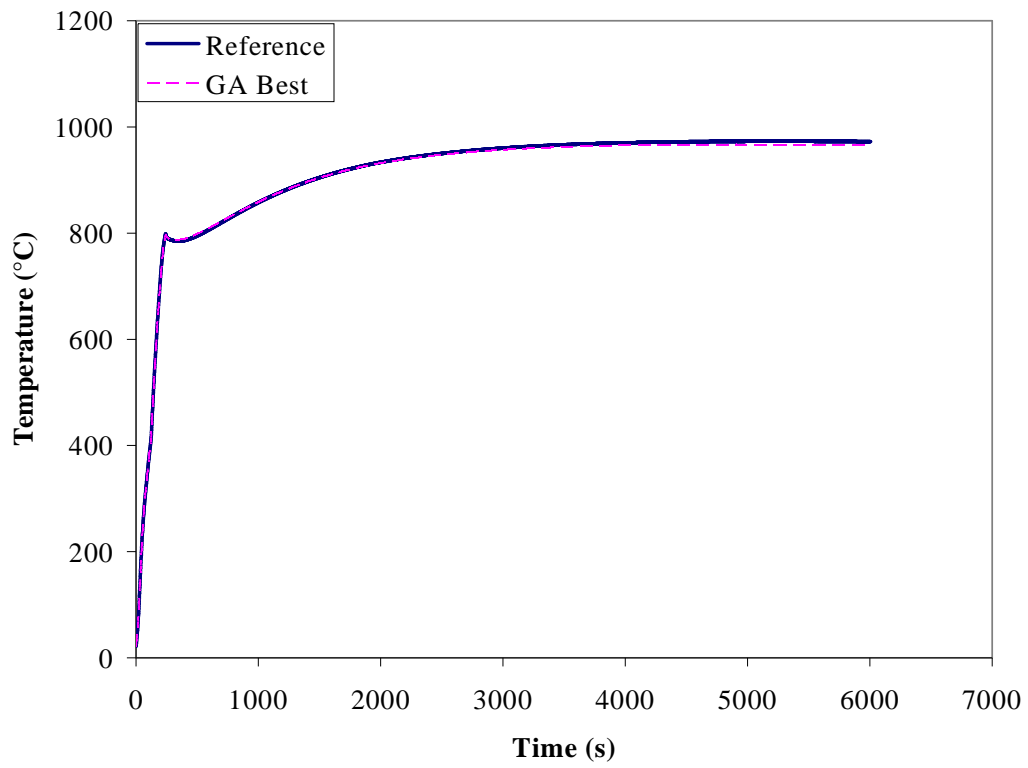
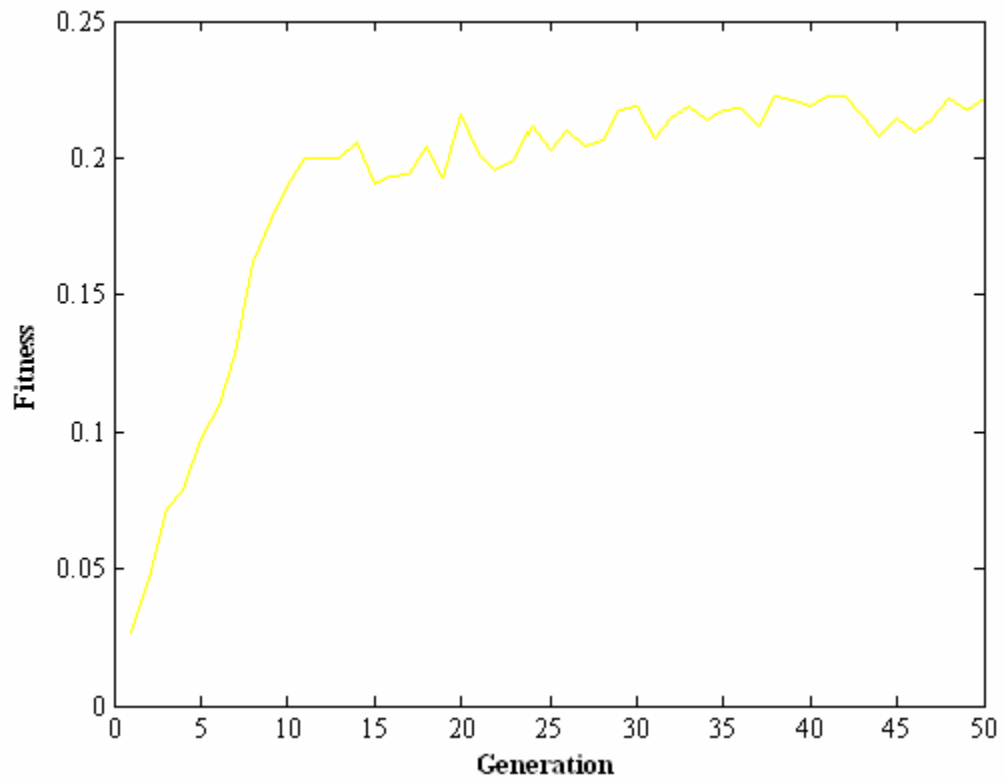
Simulation Number	Reference MLR	Reference Average HRR	Reference Vent	GA Best MLR	GA Best Average HRR	GA Best Vent	Bounds on MLR	Bounds on Vent	Notes on Simulation
SR3_3_3_Fb_h_1	1700kW.	960.4 kW (2000-6000s)	1m x 2m	4538 kW	1185 kW (2000-6000s)	1.01m x 2.04m	1,000-7,000 kW	Width: .75m-2m, Height: 1m-2.9m	Population size of 100, 100 generations.
SR3_3_3_Fb_h_2	1303 kW	908 kW (2000-6000s)	1m x 2m	3018 kW	841 kW (2000-6000s)	1.50m x 1.34m	1000-7,000 kW	Width: .75m-2m, Height: 1m-2.9m	50 generations 50 population size.
SR3_3_3_NC_b_1.	200 kW	200 kW (2000-6000s)	1m x 2m	205 kW	205 kW (2000-6000s)	1.28m x 1.94m	200-7,000 kW	Width, 0.25-2m, Height: 1-3m	Population size 20. 50 Generations.
SR3_3_3_NC_b_2.	600 kW	599 kW (2000-6000s)	1m x 2m	608 kW	607 kW (2000-6000s)	0.61m x 2.42m	200-7,000 kW	Width, 0.25-2m, Height: 1-3m	Population size 20. 50 Generations.
SR3_3_3_NC_b_3	1000 kW	973 kW (2000-6000s)	1m x 2m	1078 kW	1071 kW (2000-6000s)	1.54m x 2.12m	200-7,000 kW	Width, 0.25-2m, Height: 1-3m	Population size 20. 50 Generations.
SR3_3_3_NC_b_4	2000 kW	1222 kW (2000-6000s)	1m x 2m	1762 kW	1193 kW (2000-6000s)	1.02m x 1.99m	200-7,000 kW	Width, 0.25-2m, Height: 1-3m	Population size 20. 50 Generations.
SR3_3_3_NC_b_5	3000 kW	1271 kW (2000-6000s)	1m x 2m	4536 kW	1420 kW (2000-6000s)	1.95m x 1.53m	200-7,000 kW	Width, 0.25-2m, Height: 1-3m	Population size 20. 50 Generations.
SR3_3_3_NC_c_1	500 kW	499 kW (2000-6000s)	1m x 2m	2036 kW	434 kW (2000-6000s)	.71m x 1.03m	200-7,000 kW	Width, 0.25-2m, Height: 1-3m	Population size 20. 50 Generations.
SR3_3_3_NC_d_1	500 kW	499 kW (2000-6000s)	1m x 2m	1465 kW	366 kW (2000-6000s)	0.44m x 1.20m	200-7,000 kW	Width, 0.25-2m, Height: 1-3m	Population size 20. 50 Generations.
SR3_3_3_NC_f_1	500 kW	499 kW (2000-6000s)	1m x 2m	456 kW	456 kW (2000-6000s)	2.00m x 1.17m	200-7,000 kW	Width, 0.25-2m, Height: 1-3m	Population size 20. 50 Generations.
SR3_3_3_NC_g_1	500 kW	499 kW (2000-6000s)	1m x 2m	1434 kW	438 kW (2000-6000s)	0.79m x 1.00m	200-7,000 kW	Width, 0.25-2m, Height: 1-3m	Population size 20. 50 Generations.
SR10_10_3_Fb_a_1	4654kW	1507 kW (240-6000s)	1m x 2m	4330 kW	1531 kW (240-6000s)	1m x 2m	1,000-10,000 kW	Width: 1m-3m, Height: 1m-3m	Population size of 50, 200 generations.*
SR10_10_3_Fb_a_2	4654kW	1507 kW (240-6000s)	1m x 2m	4611.7 kW	1635 kW (240-6000s)	2.5m x 1.4m	1,000-10,000 kW	Width: 1m-3m, Height: 1m-3m	Population size of 100, 100 generations.*

Simulation Number	Reference MLR	Reference Average HRR	Reference Vent	GA Best MLR	GA Best Average HRR	GA Best Vent	Bounds on MLR	Bounds on Vent	Notes on Simulation
SR10_10_3_Fb_a_3	3987kW	1609 kW (240-6000s)	2.5m x 1.4m	3937 kW	1549 kW (240-6000s)	1.4m x 1.7m	1,000-10,000 kW	Width: 1m-3m, Height: 1m-3m	100 generations*
SR10_10_3_Fb_a_4	3987kW	1609 kW (240-6000s)	2.5m x 1.4m	3877.4 kW	1583 kW (240-6000s)	2.0m x 1.5m	1,000-10,000 kW	Width: 1m-3m, Height: 1m-3m	Population size 100, 200 generations.*
SR10_10_3_Fb_a_5	5432kW	1412 kW (240-6000s)	1m x 2m	7794 kW	1557.2 kW (240-6000s)	2.9m x 1.3m	1,000-10,000 kW	Width: 1m-3m, Height: 1m-3m	Population size of 20, 25 generations.*
SR10_10_3_Fb_a_6	5432kW	1412 kW (240-6000s)	1m x 2m	5728.9 kW	1419 kW (240-6000s)	1.2m x 1.8m	1,000-10,000 kW	Width: 1m-3m, Height: 1m-3m	Population size of 20, 500 generations.*
SR10_10_3_Fb_a_7	5432kW	1412 kW (240-6000s)	1m x 2m	5685 kW	1416 kW (240-6000s)	1.1m x 1.9m	1,000-10,000 kW	Width: 1m-3m, Height: 1m-3m	Population size of 20, 500 generations.*
SR10_10_3_Fb_a_8	2700 kW	1517 kW (240-6000s)	1m x 2m	2798 kW	1460 kW (240-6000s)	1.21m x 1.86m	1,000-10,000 kW	Width: 1m-3m, Height: 1m-3m	Population size 10. 100 Generations.*
SR10_10_3_Fb_b_1.	4654 kW 10m room	1307 kW (2000-6000s)	1m x 2m	3230 kW	1307 kW (2000-6000s)	1.63m x 1.56m	200-7,000 kW	Width: .5m-2m, Height: 1m-3m	Population size of 10, 25 generations.
SR10_10_3_Fb_e_1	2700kW	1517 kW (240-6000s)	1m x 2m	9994.0 kW	2104 kW (240-6000s)	1.0m x 3.0m	1000-10,000 kW	Width: 1m-3m, Height: 1m-3m	100 Generations. Fitness Function analyzed whole time frame.*
SR10_10_3_Fb_e_2	5700kW	1164 kW (2000-6000s)	1m x 2m	9994 kW	984 kW (2000-6000s)	1.7m x 1.5m	1000-10,000 kW	Width: 1m-3m, Height: 1m-3m	500 generations.

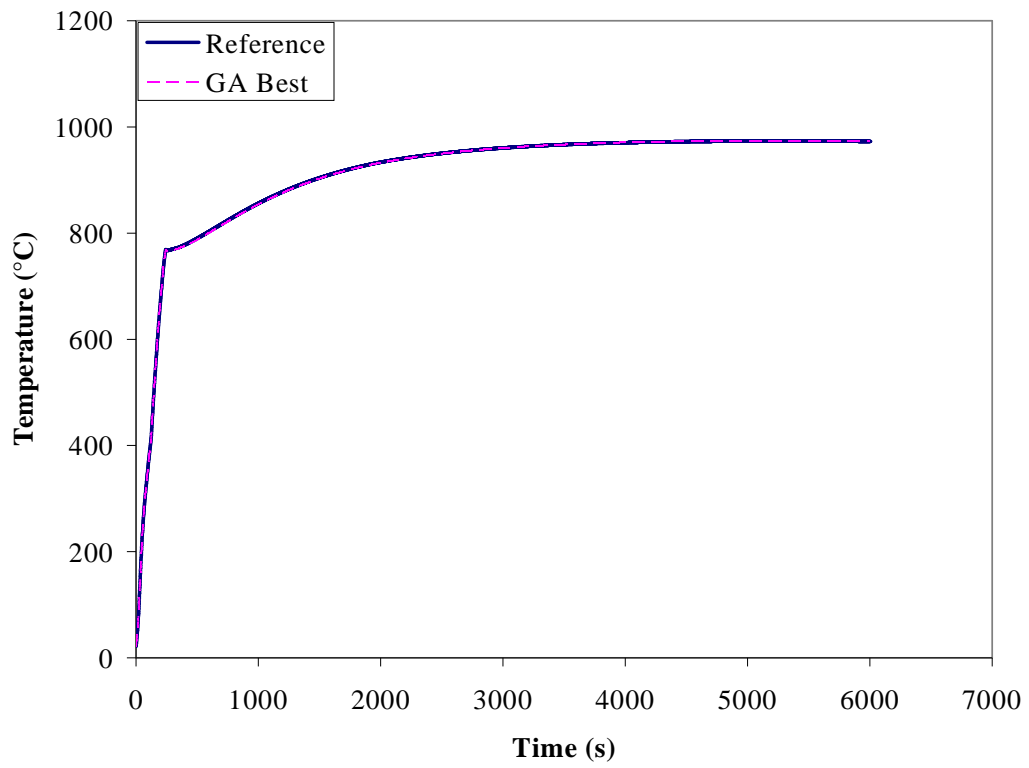
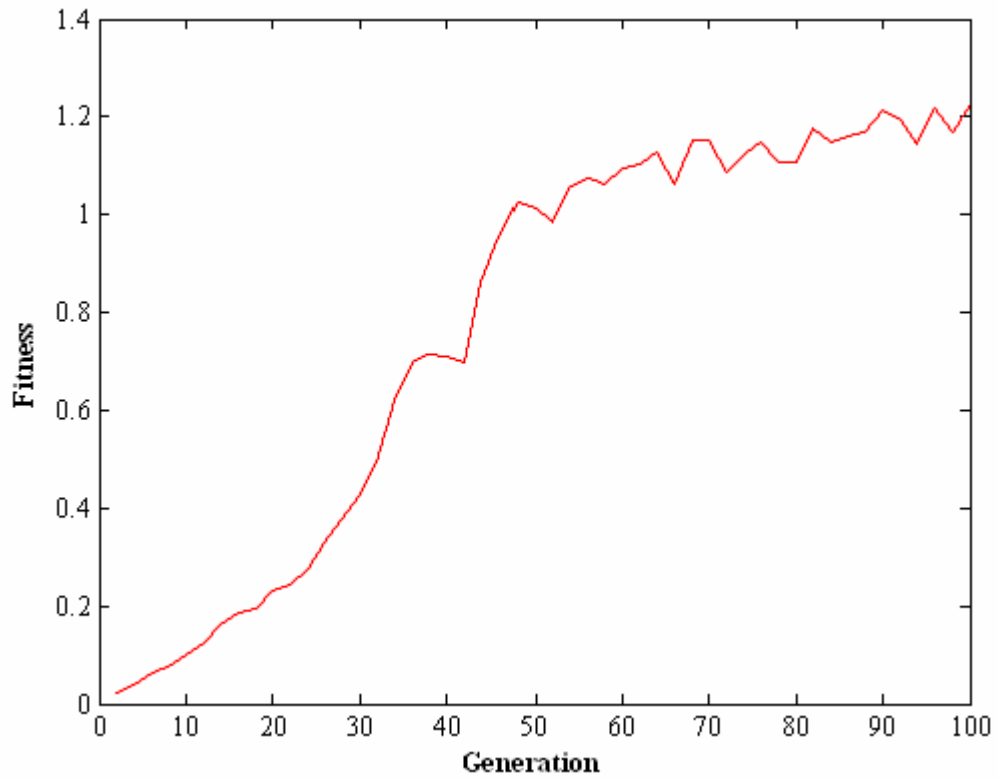
SR3_3_3_Fb_a_1



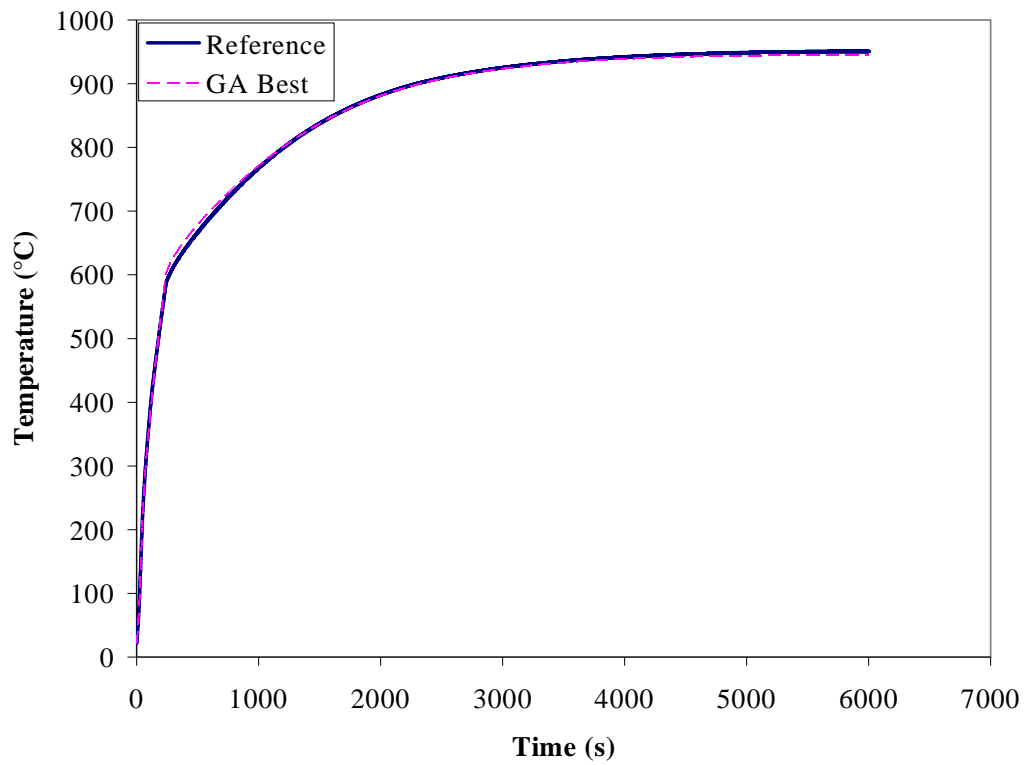
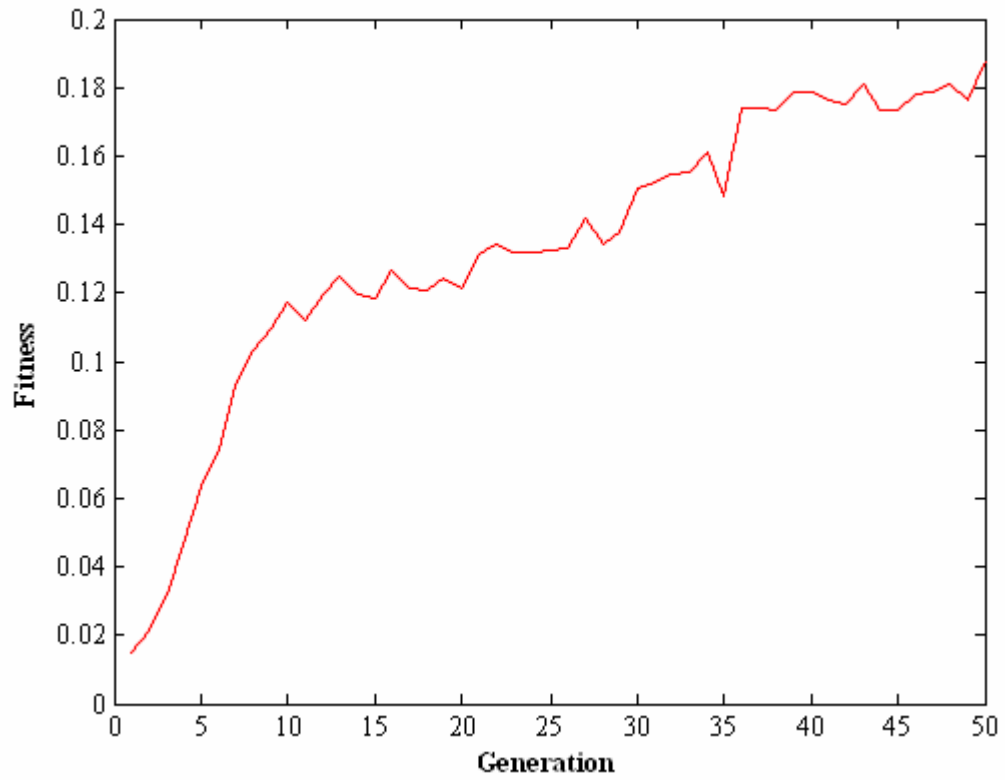
SR3_3_3_Fb_a_2



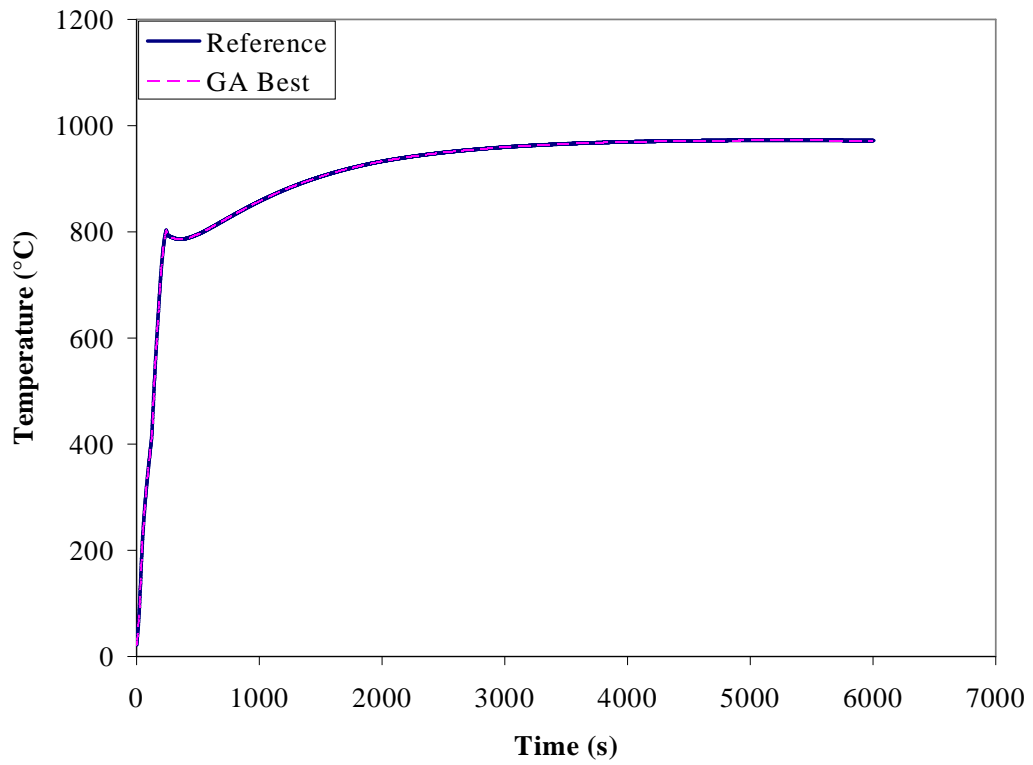
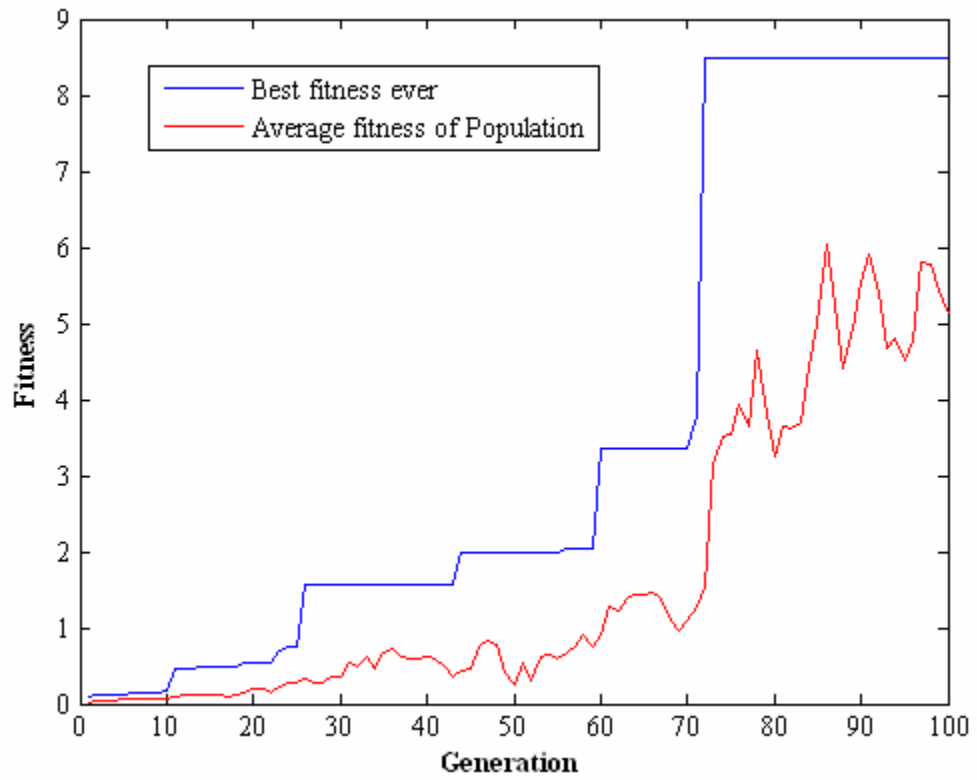
SR3_3_3_Fb_a_3



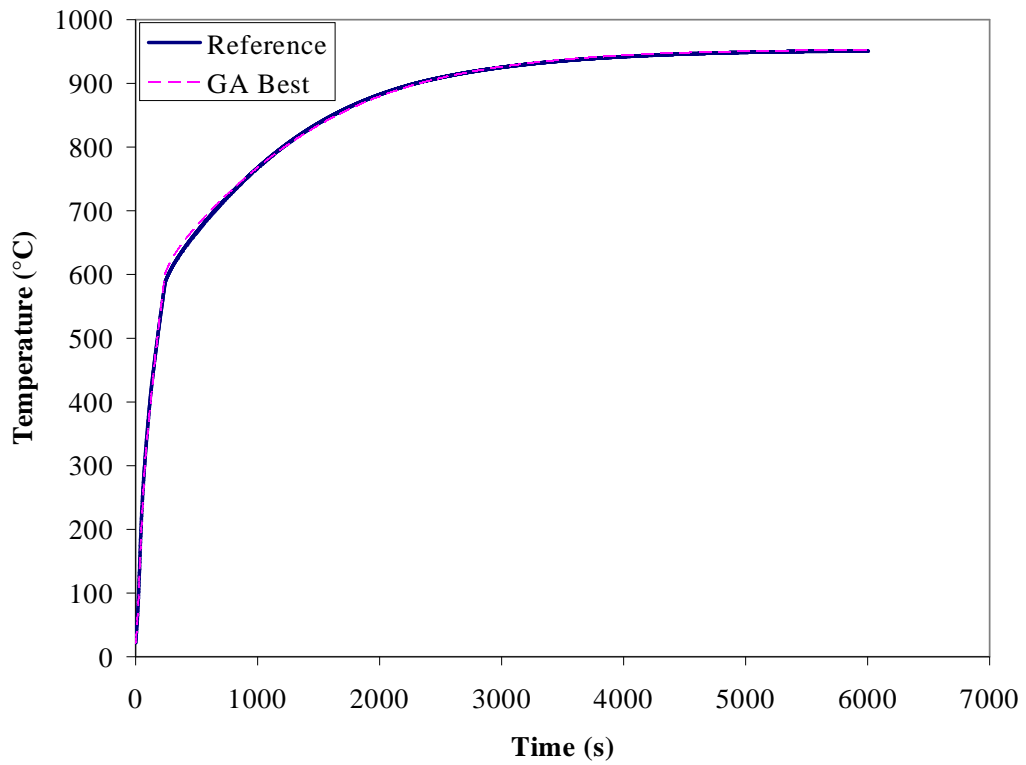
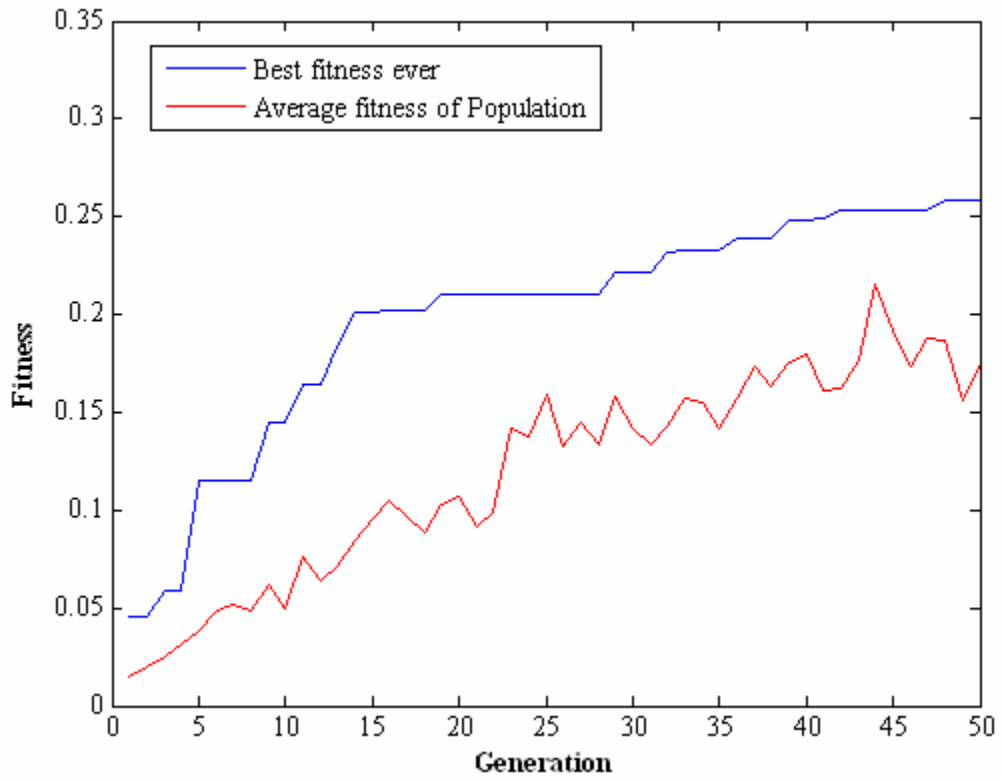
SR3_3_3_Fb_a_4



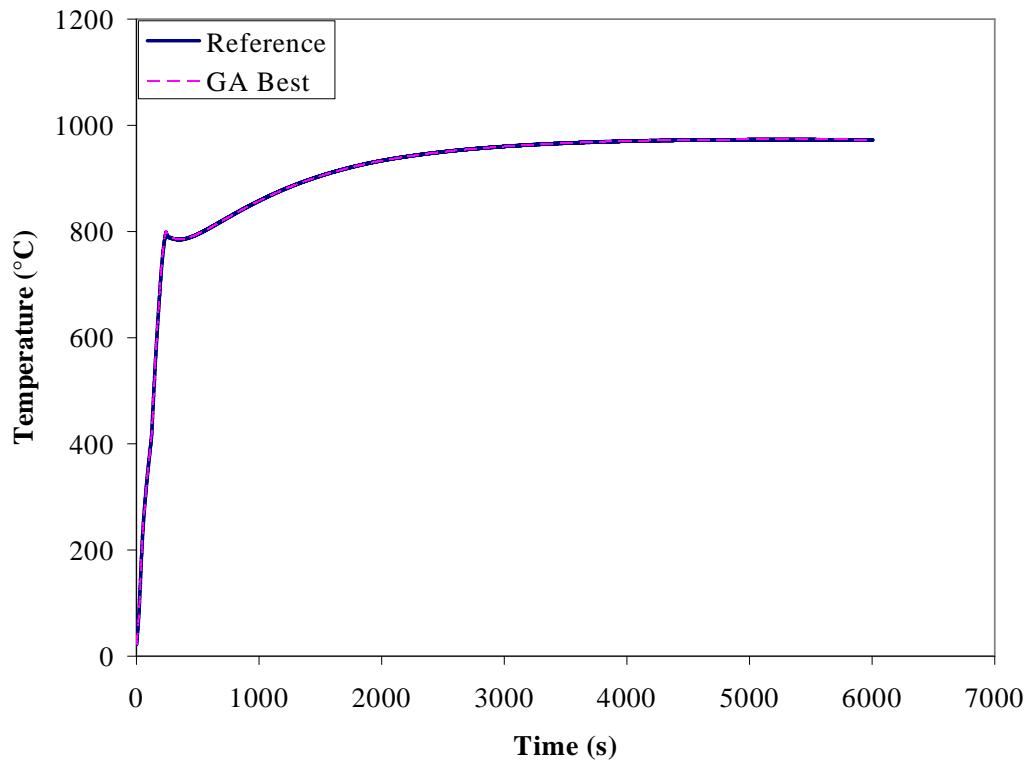
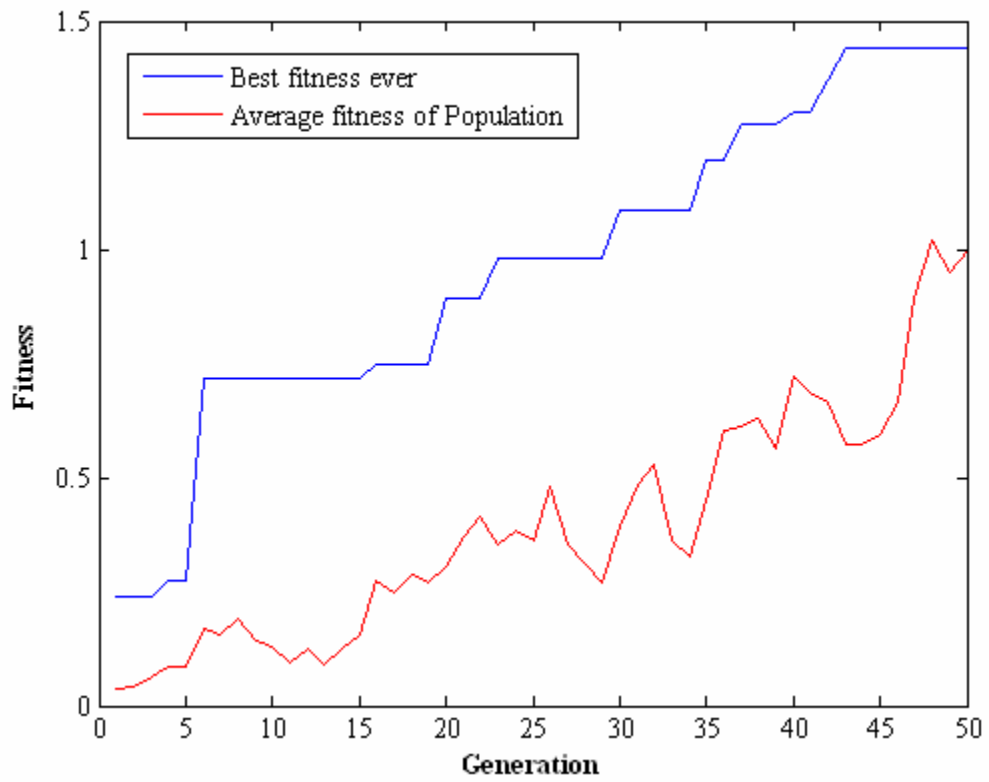
SR3_3_3_Fb_a_5



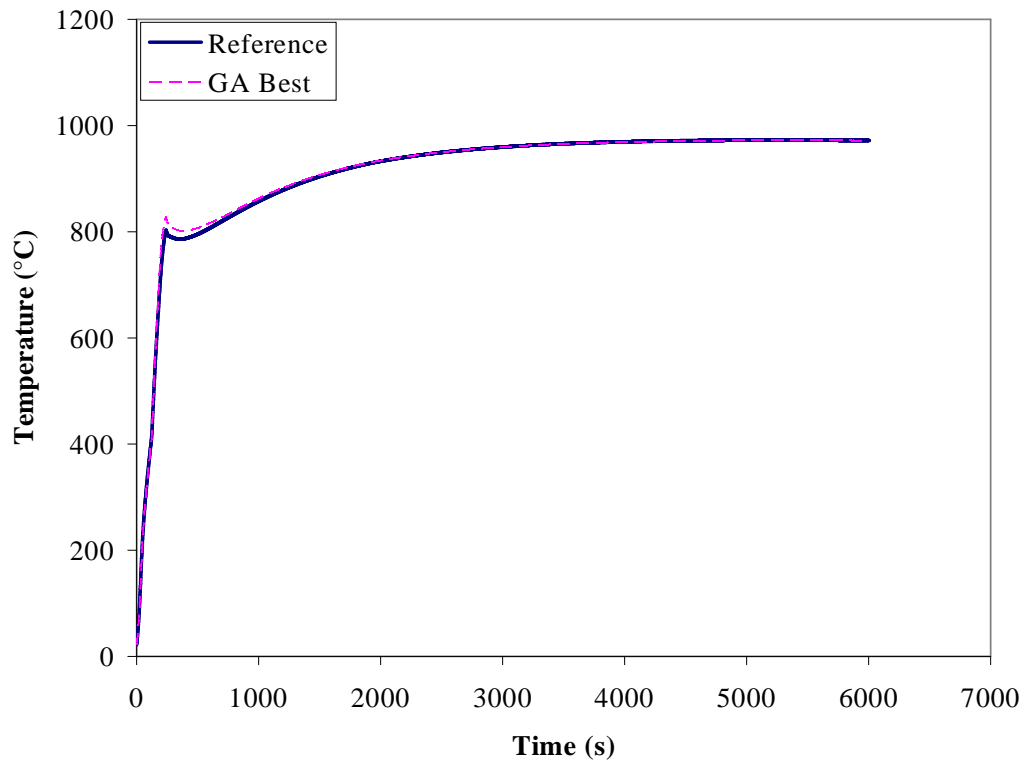
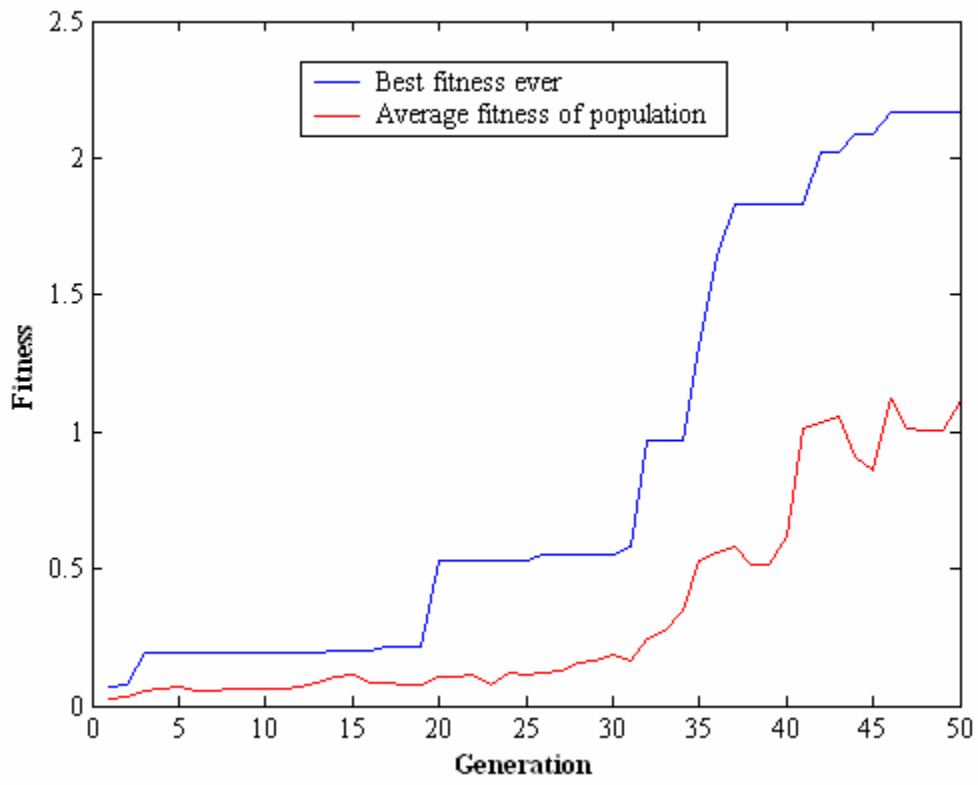
SR3_3_3_Fb_a_6



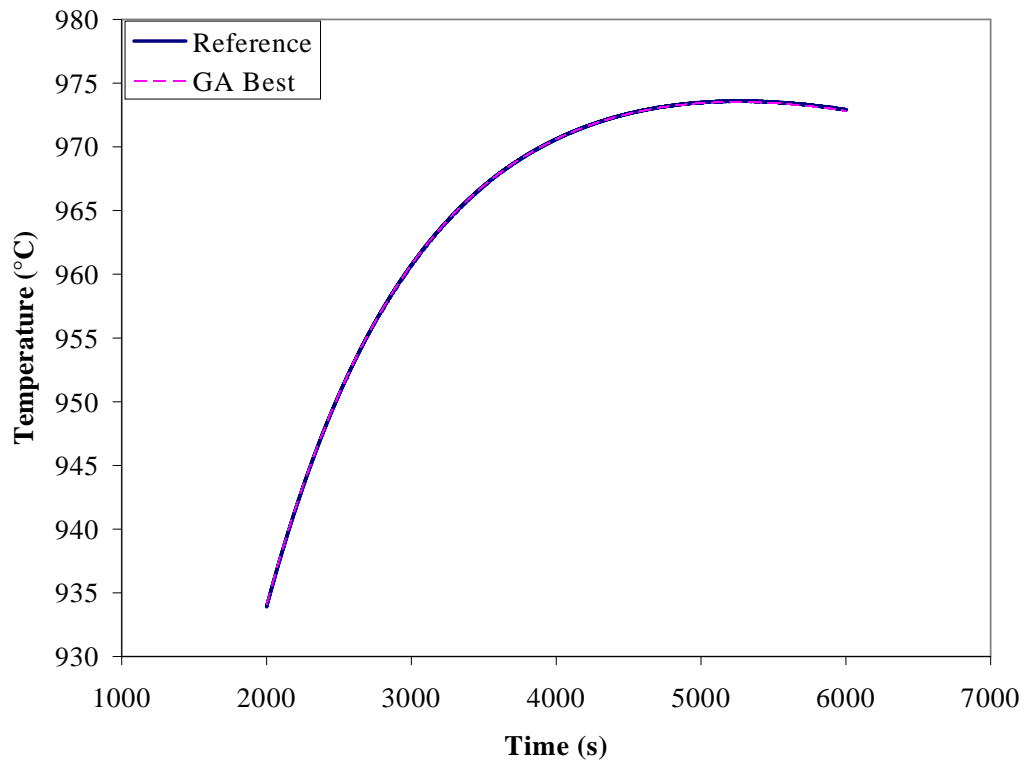
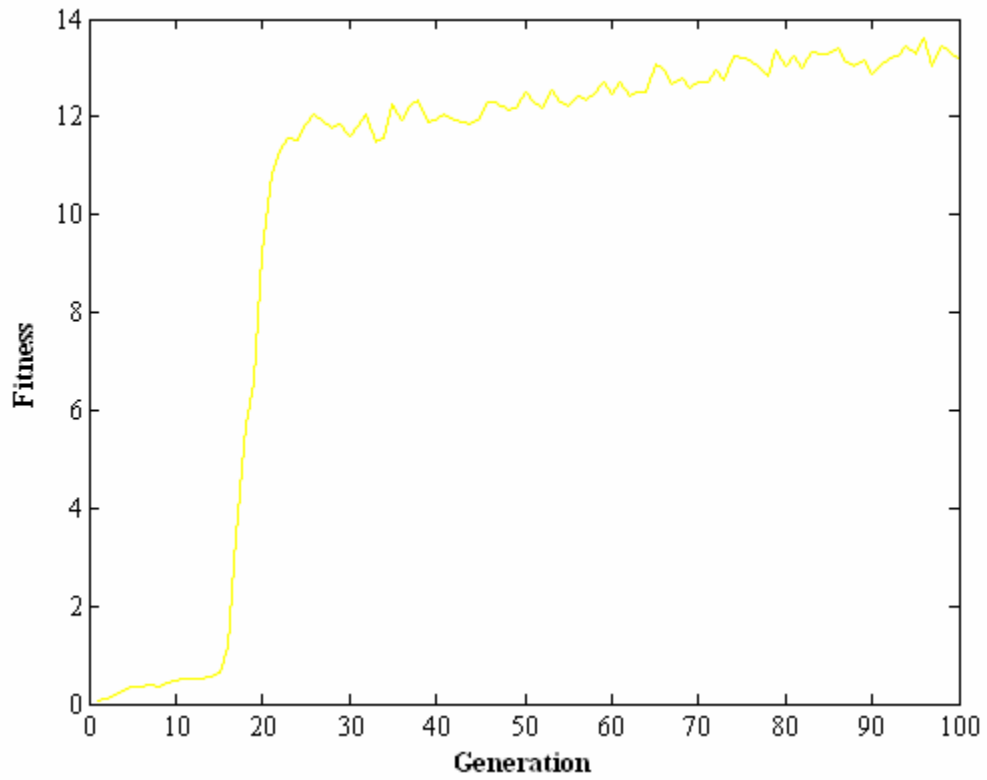
SR3_3_3_Fb_a_7



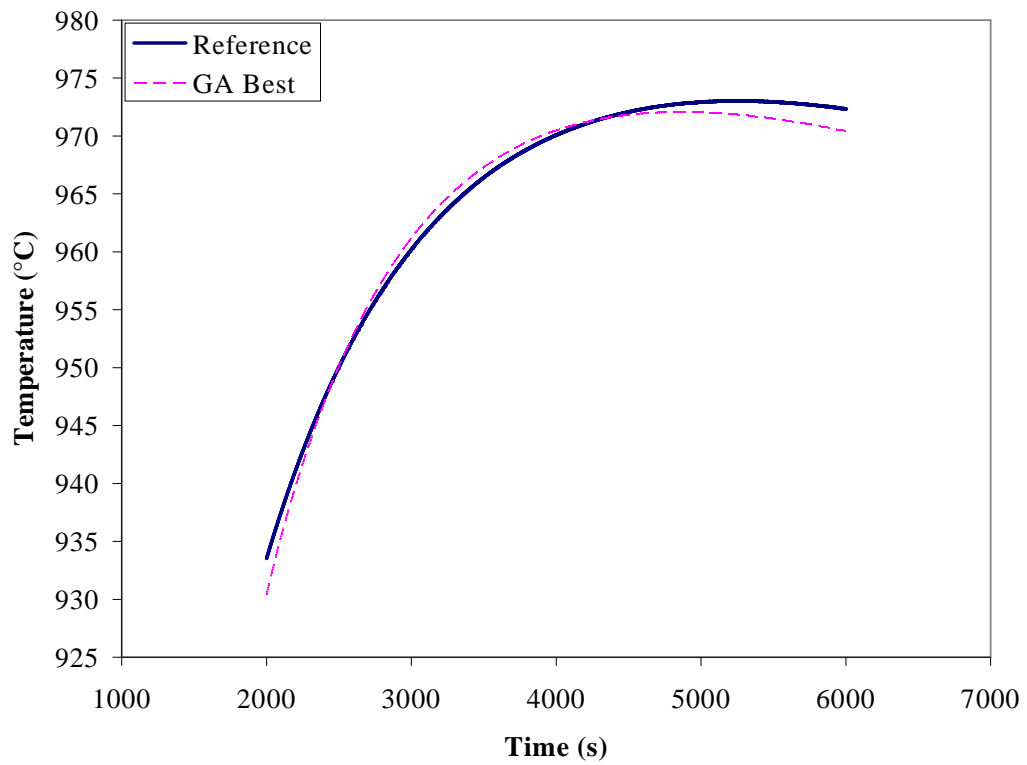
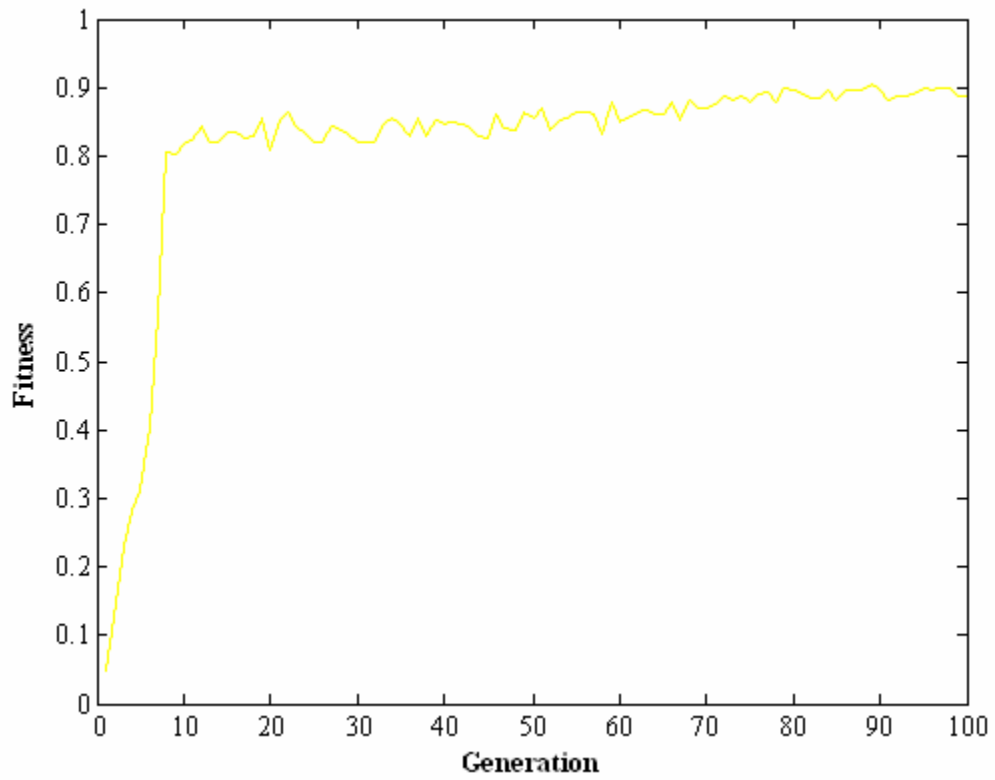
SR3_3_3_Fb_a_8



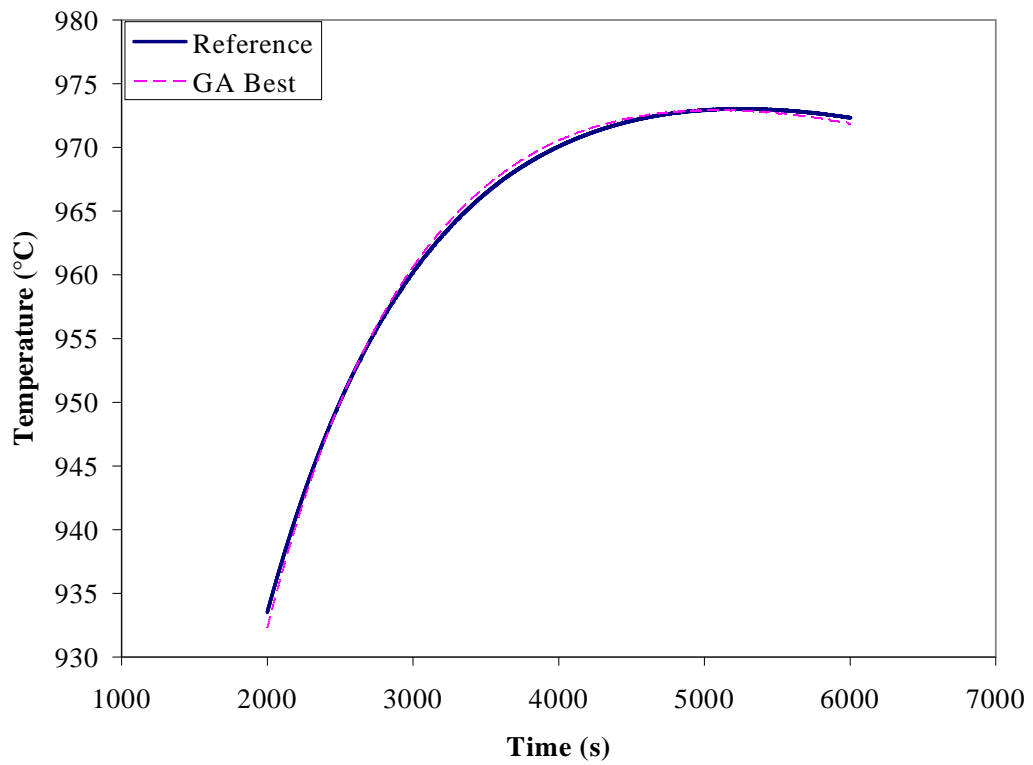
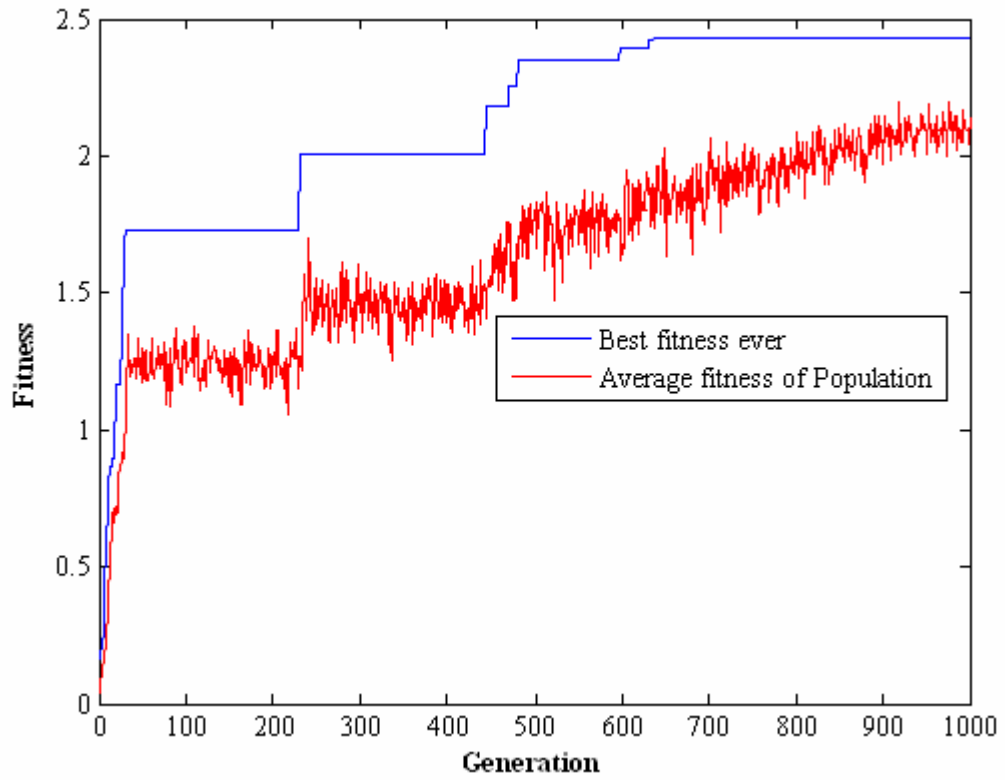
SR3_3_3_Fb_b_1



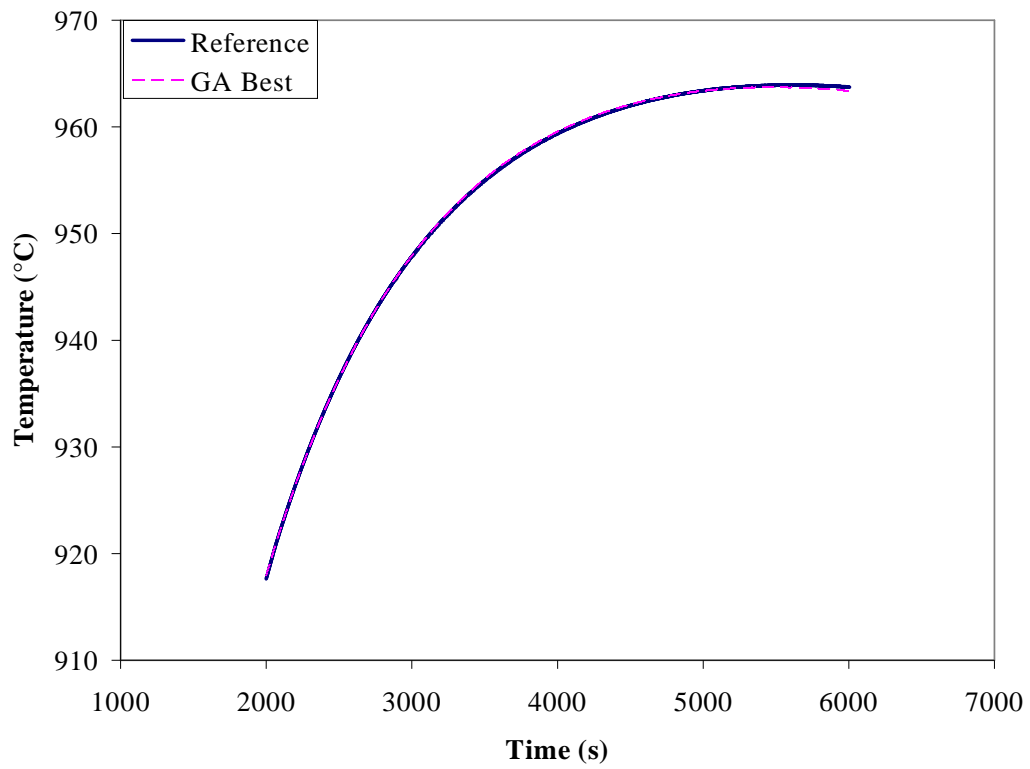
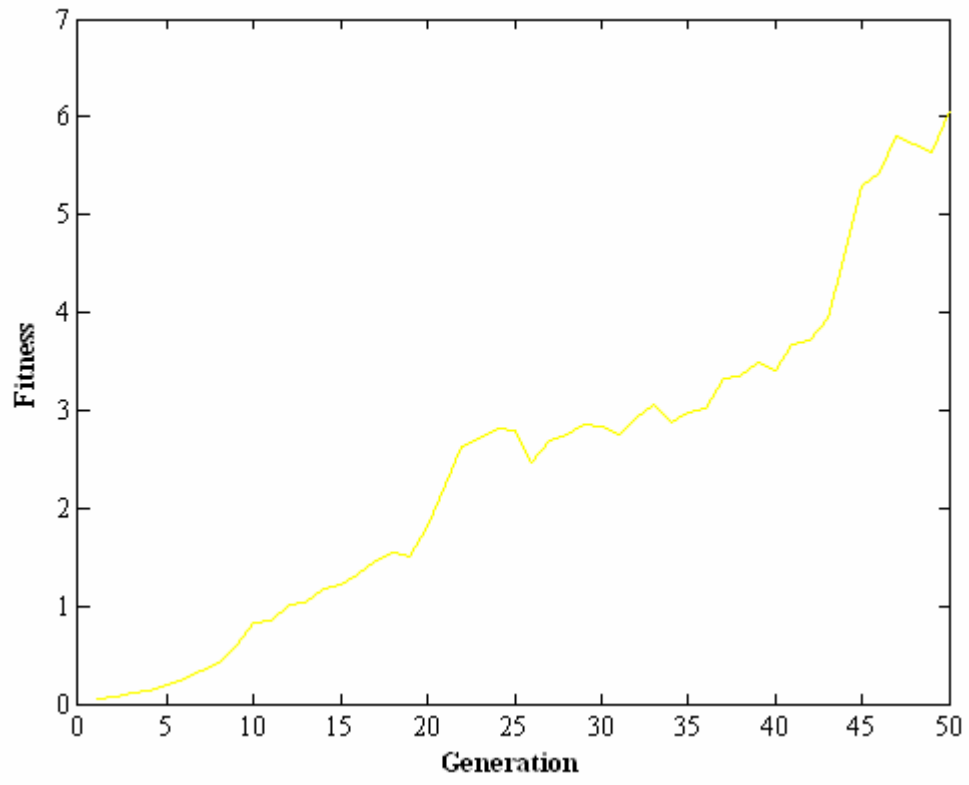
SR3_3_3_Fb_b_2



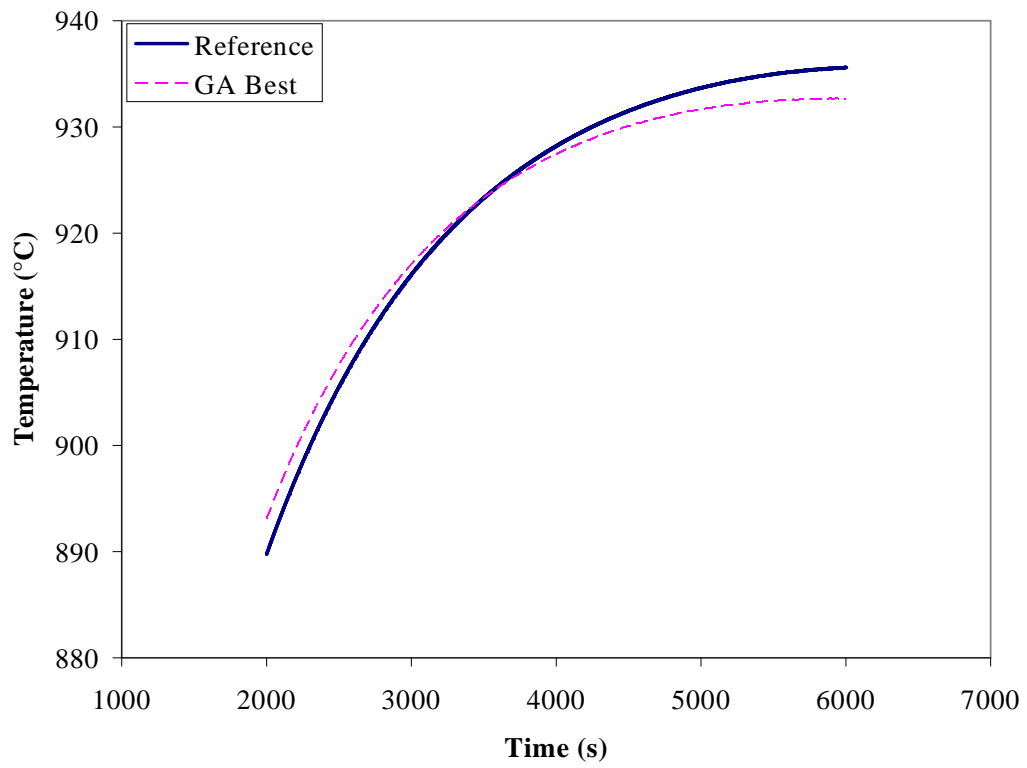
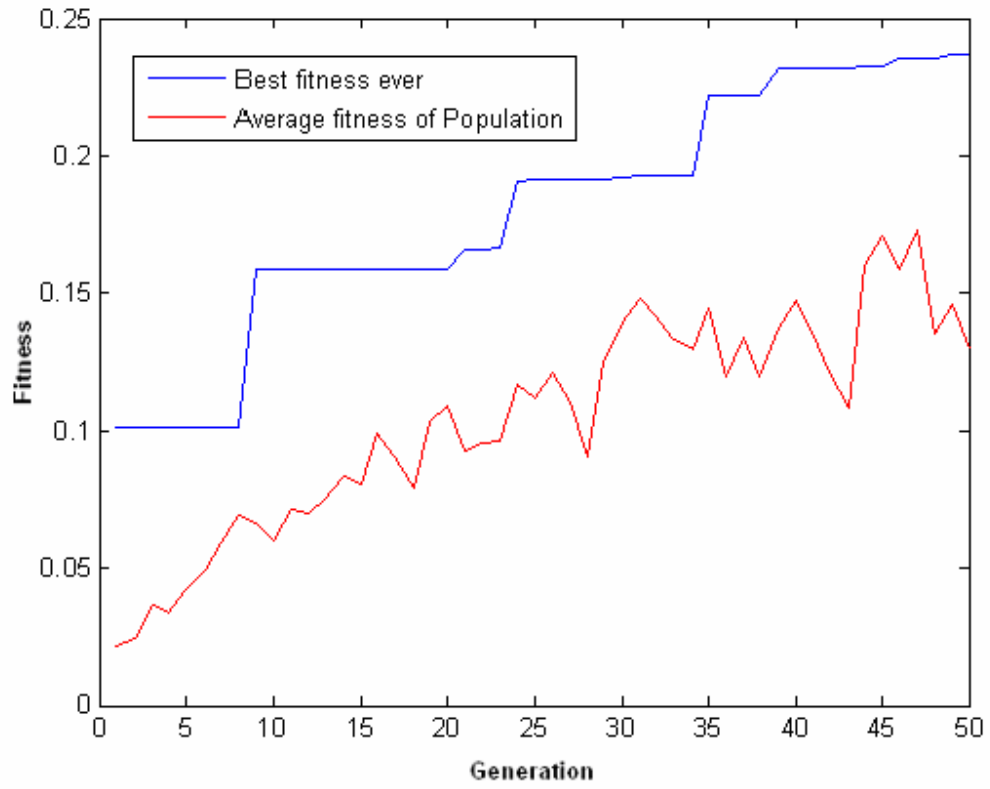
SR3_3_3_Fb_b_3



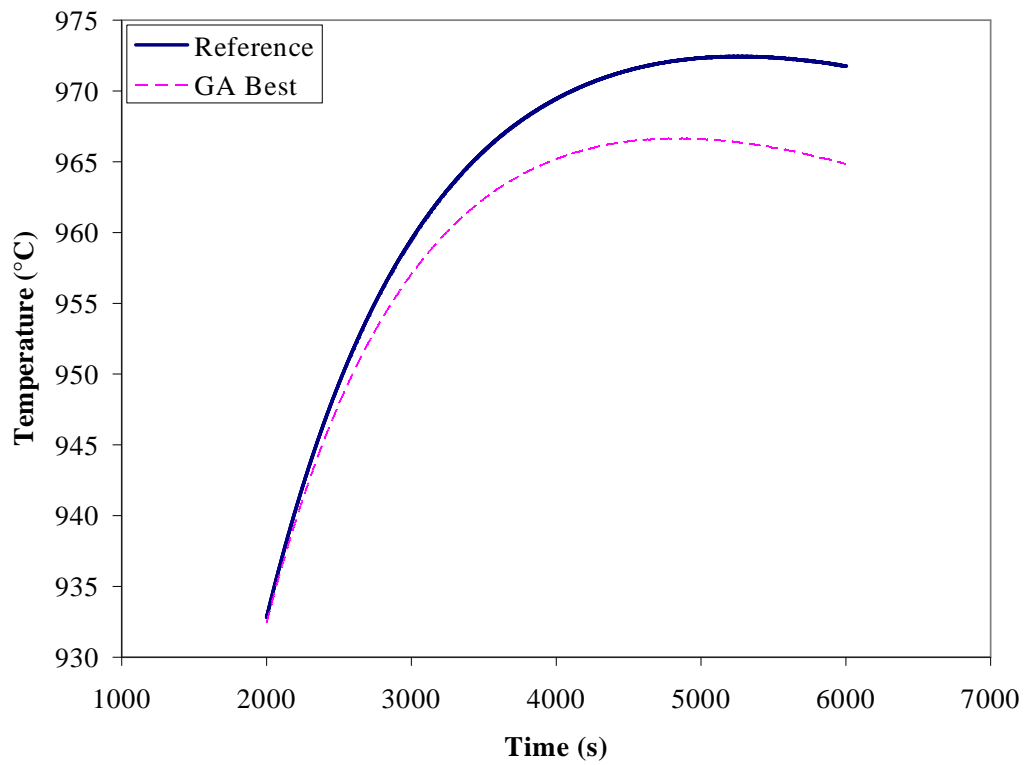
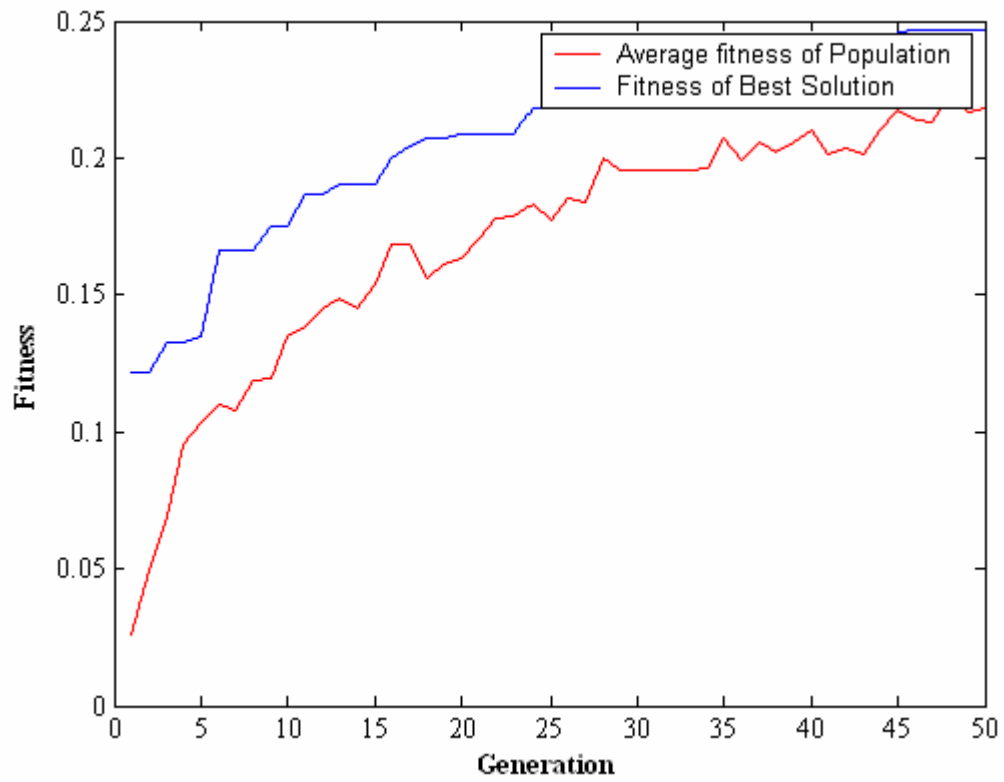
SR3_3_3_Fb_b_4



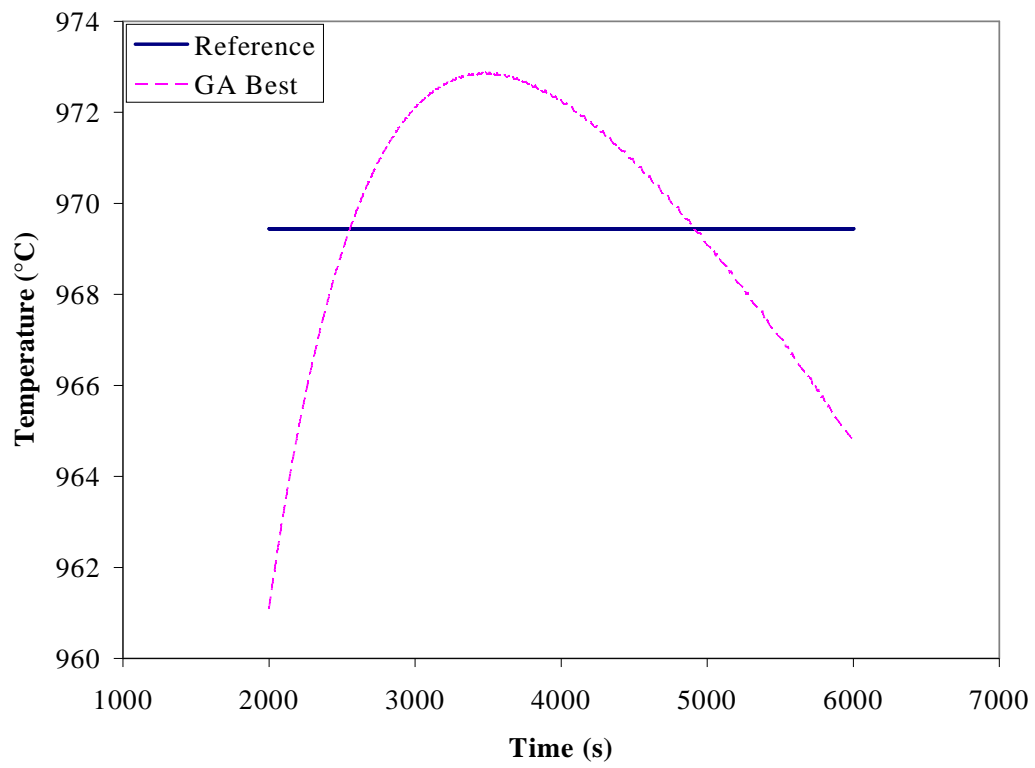
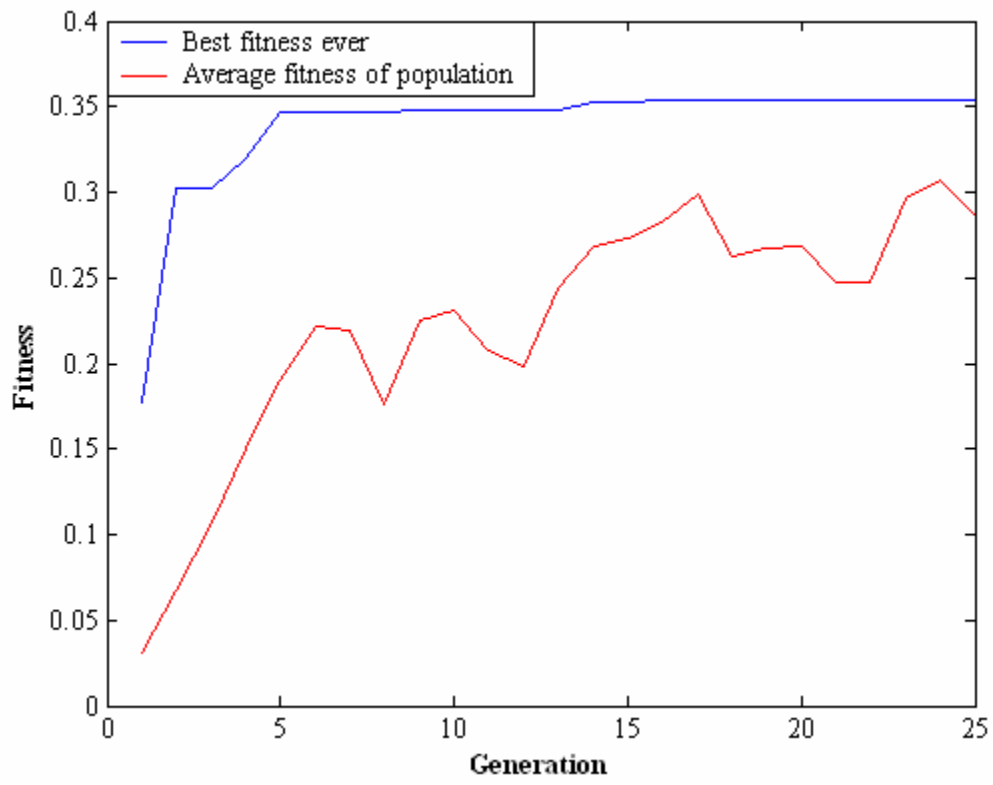
SR3_3_3_Fb_b_5



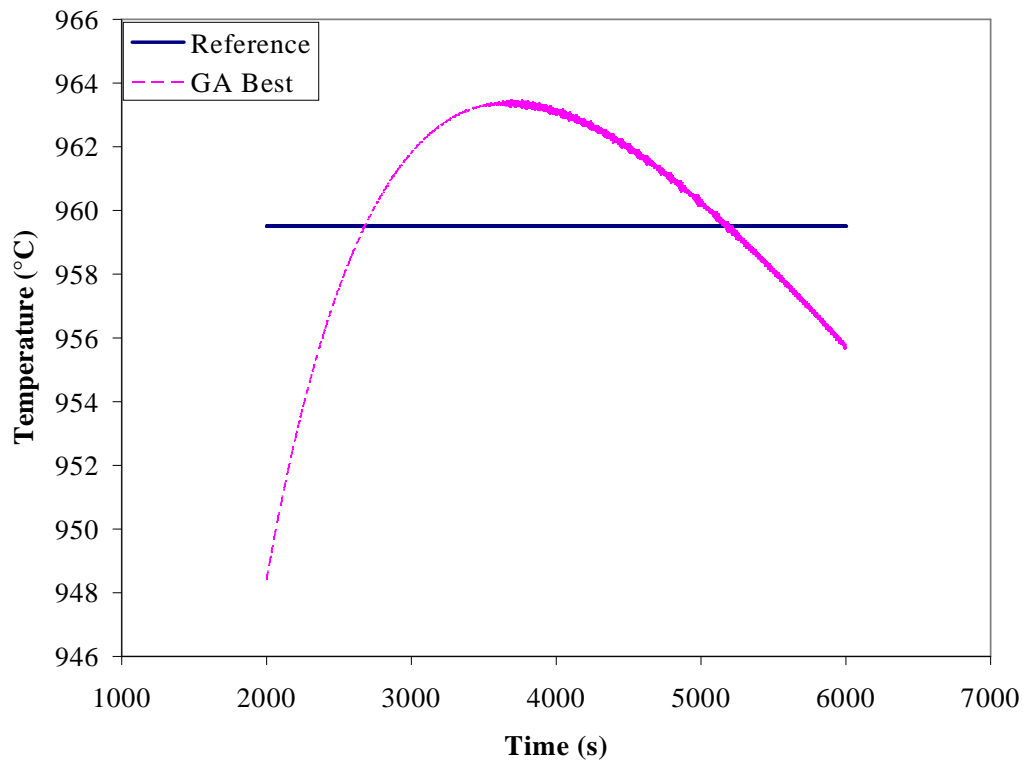
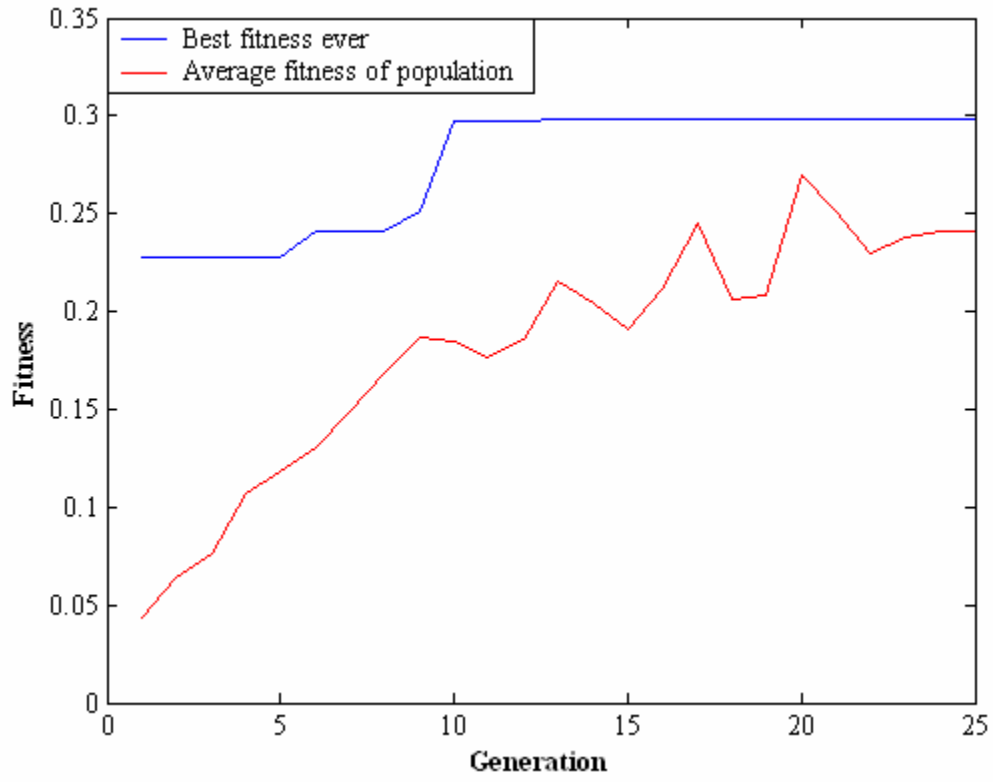
SR3_3_3_Fb_b_6



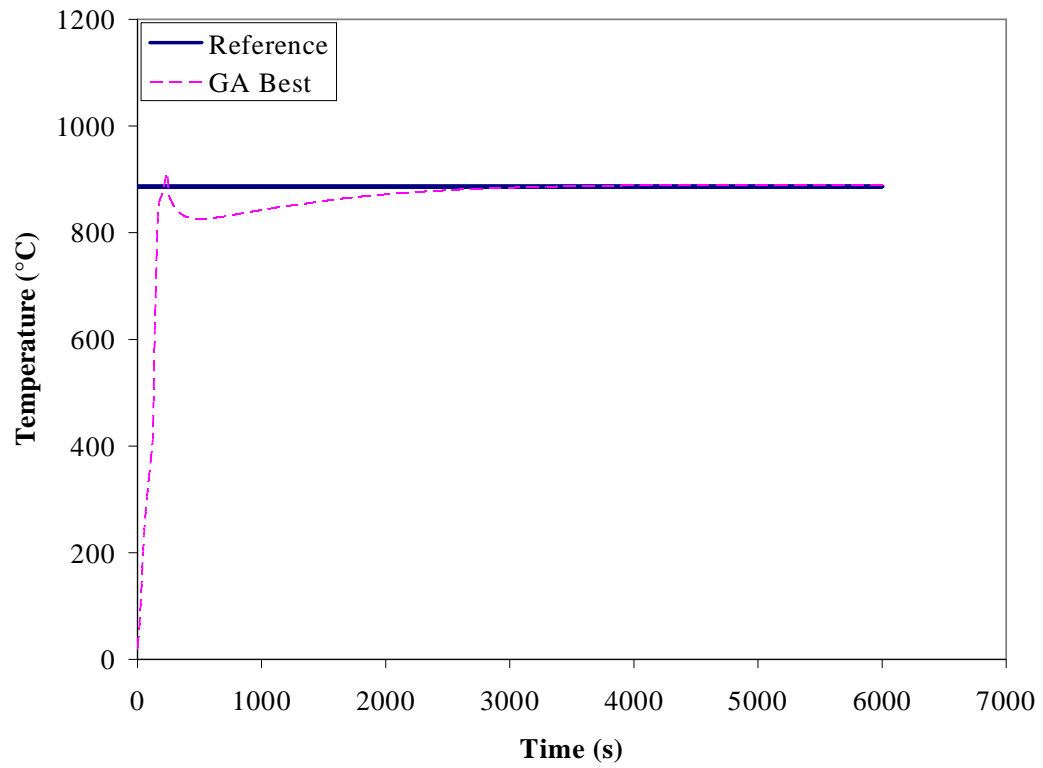
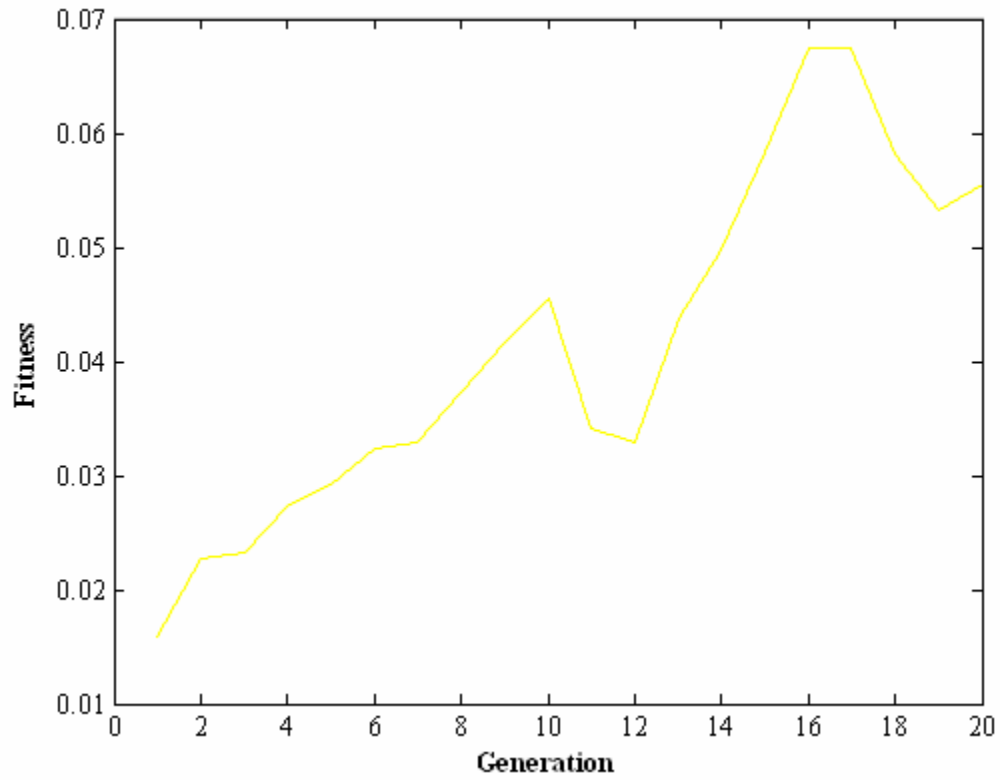
SR3_3_3_Fb_c_1



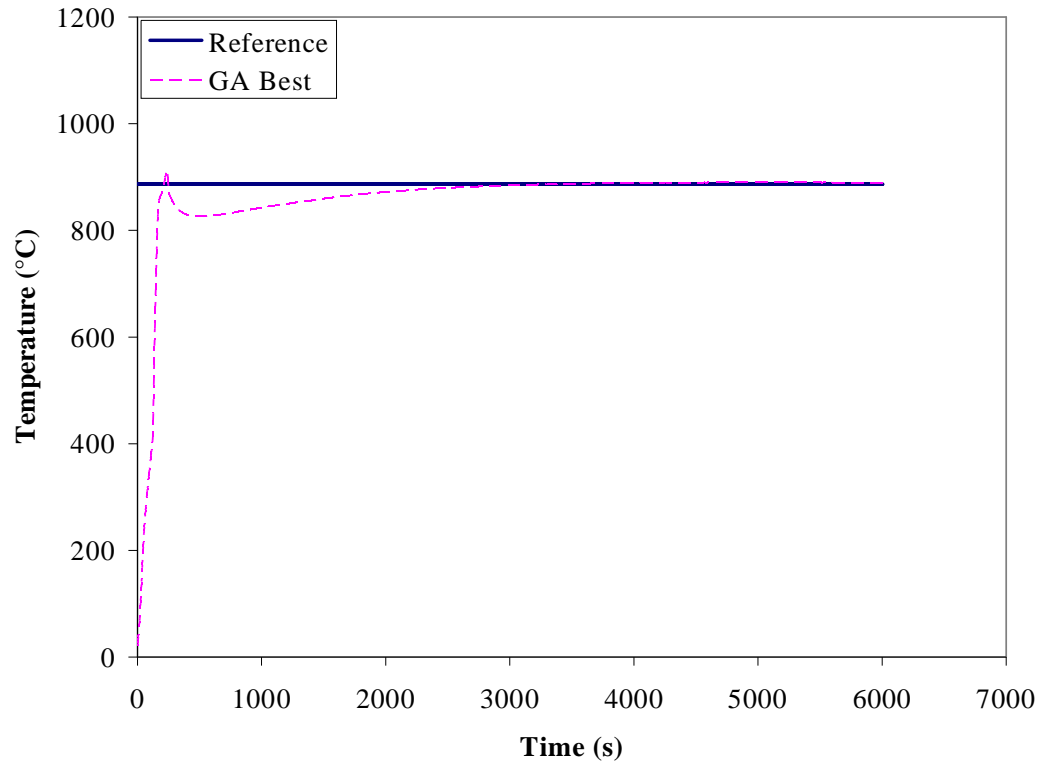
SR3_3_3_Fb_d_1



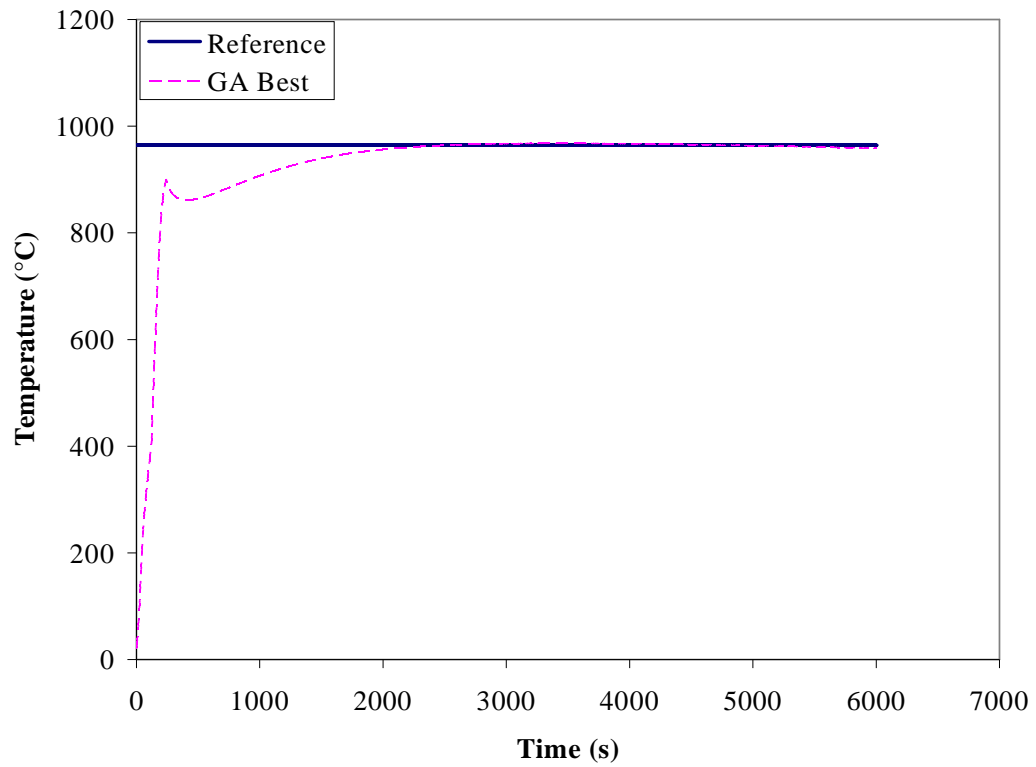
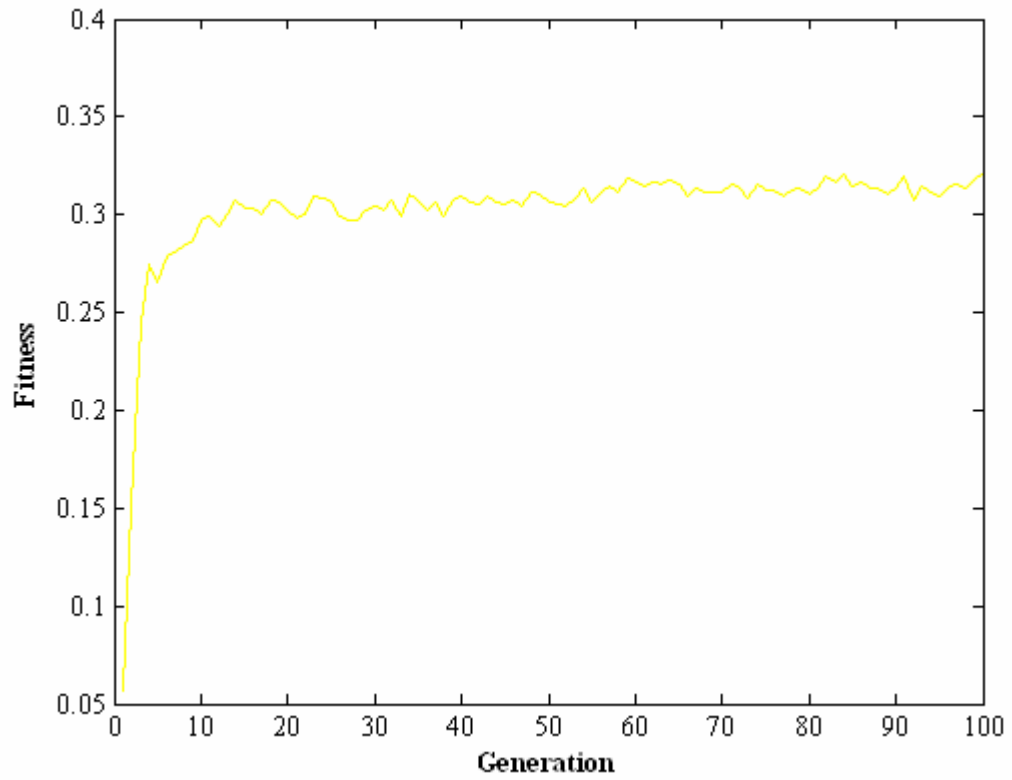
SR3_3_3_Fb_e_1



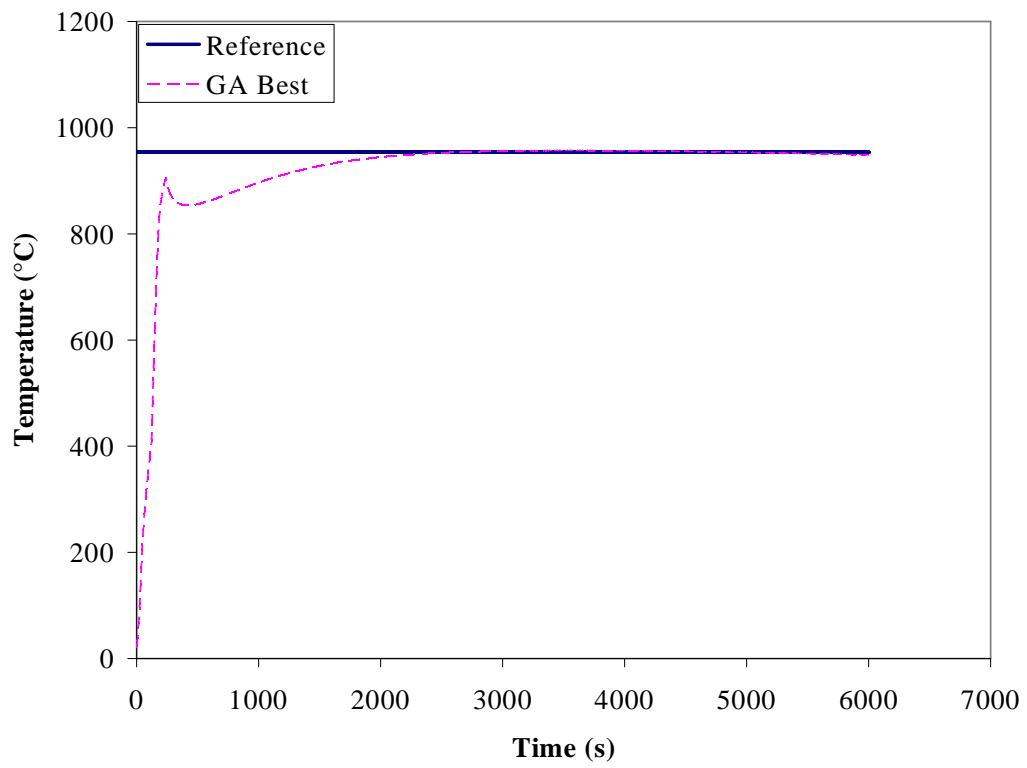
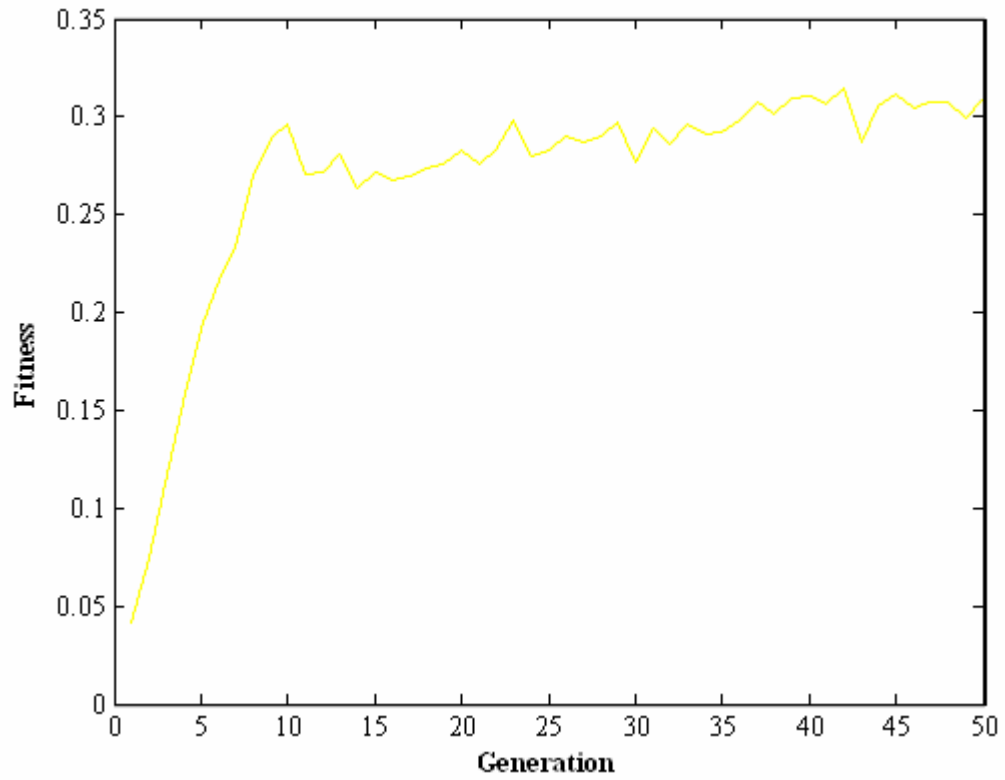
SR3_3_3_Fb_e_2



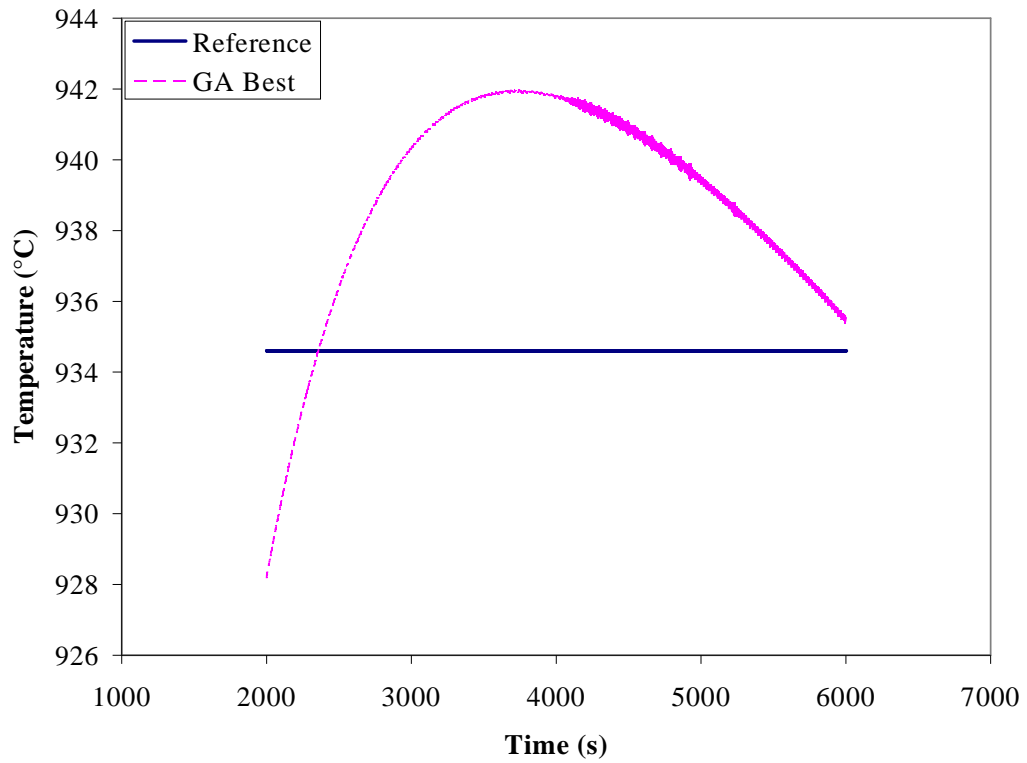
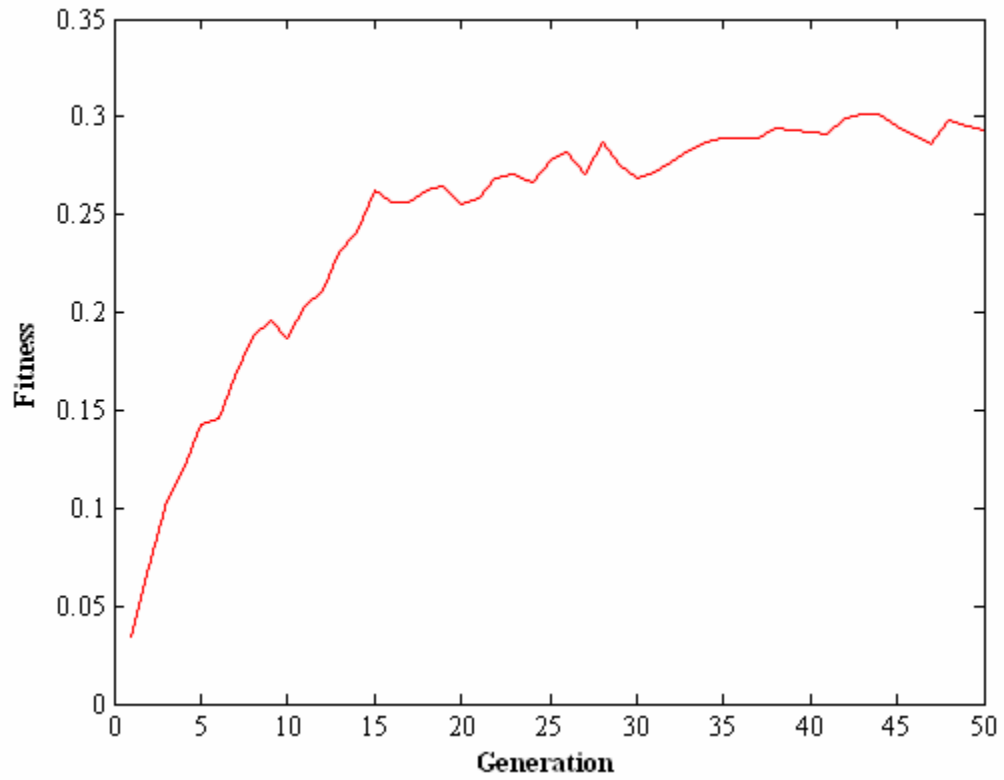
SR3_3_3_Fb_e_3



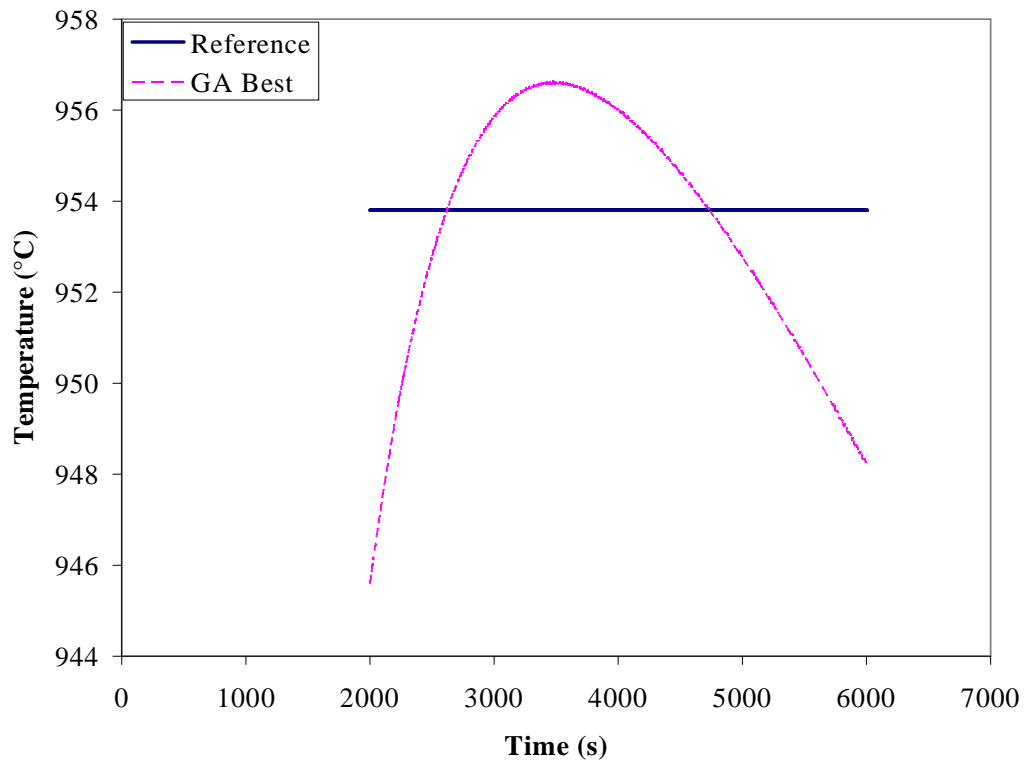
SR3_3_3_Fb_e_4



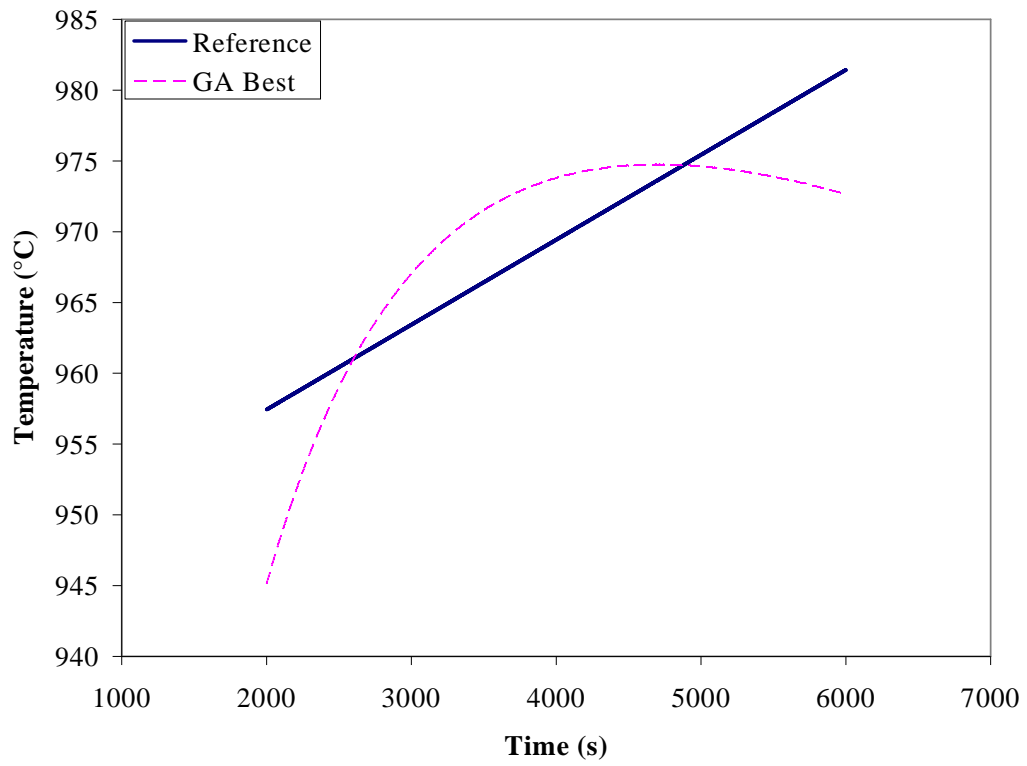
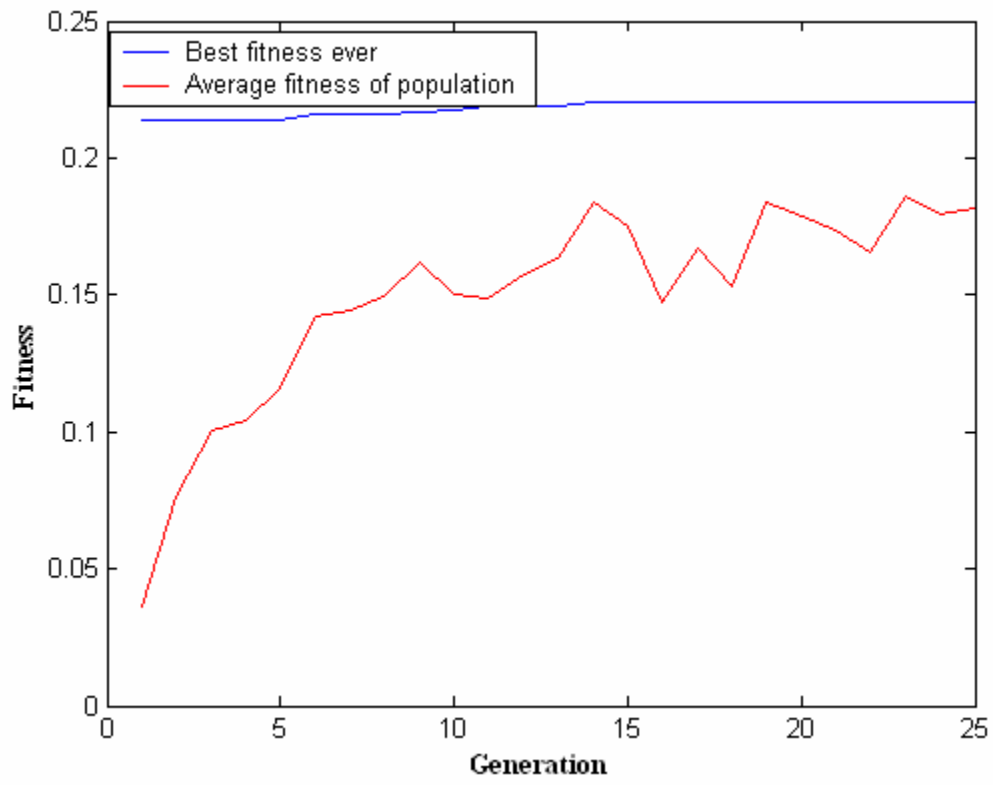
SR3_3_3_Fb_e_5



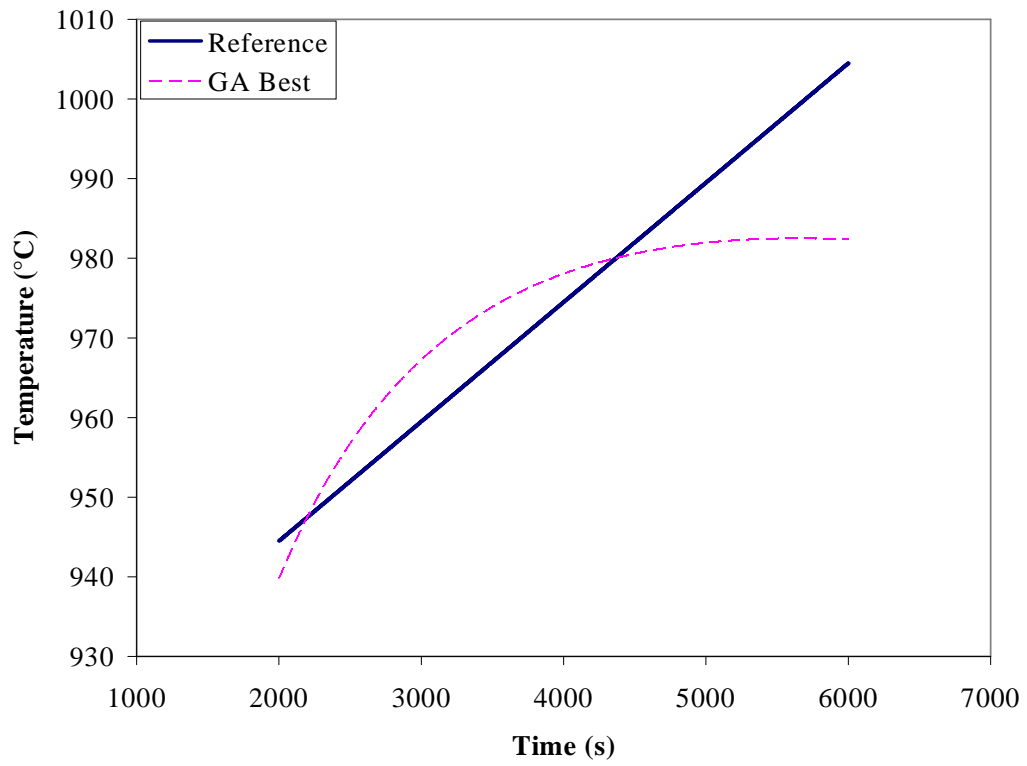
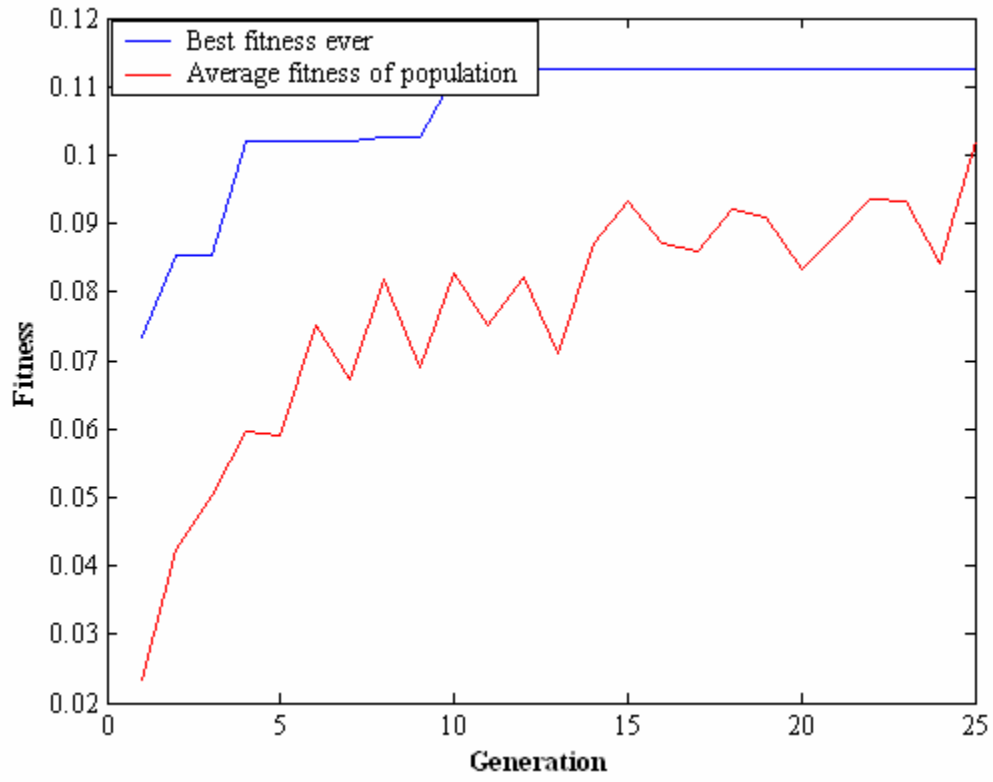
SR3_3_3_Fb_e_6



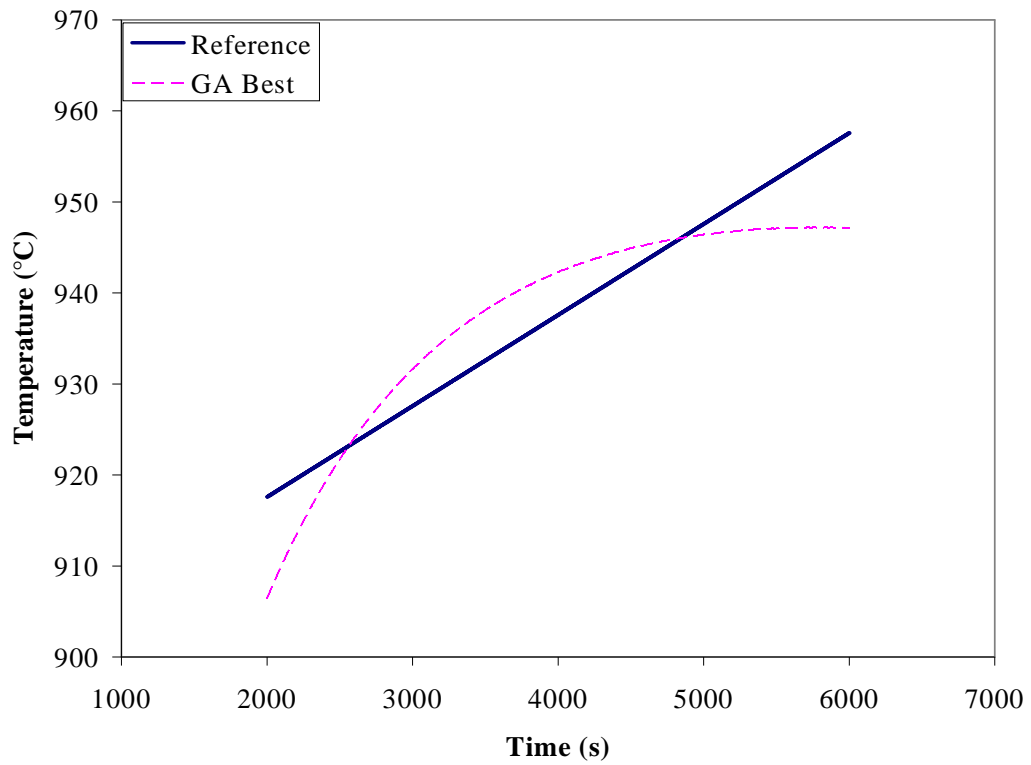
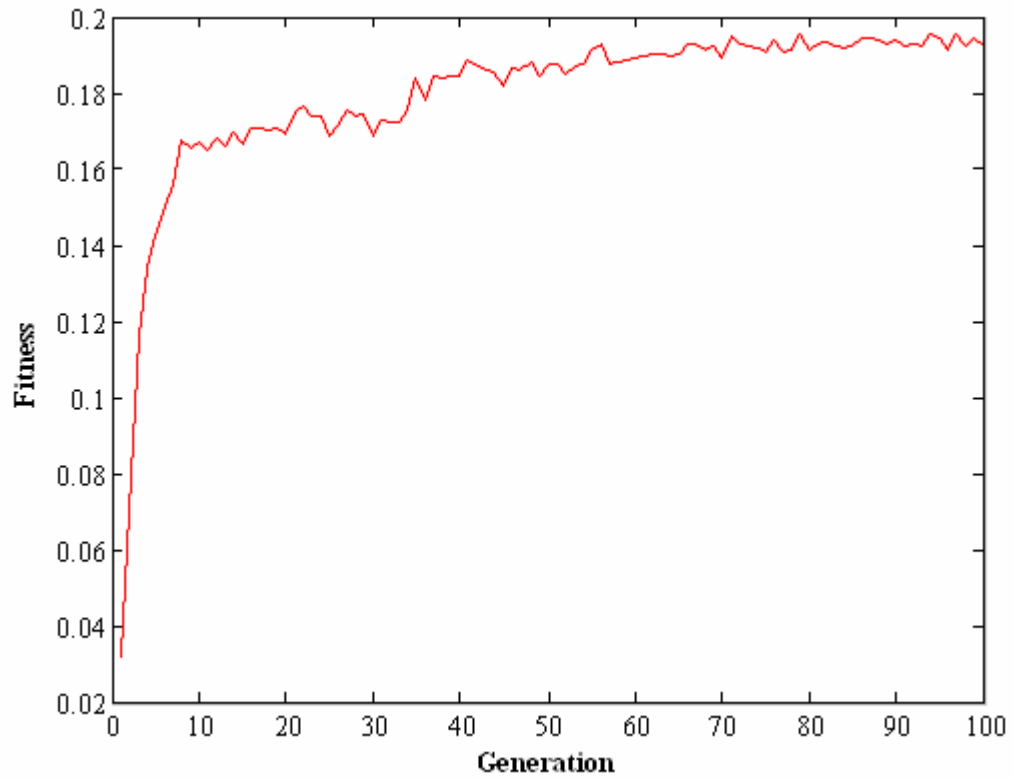
SR3_3_3_Fb_f_1



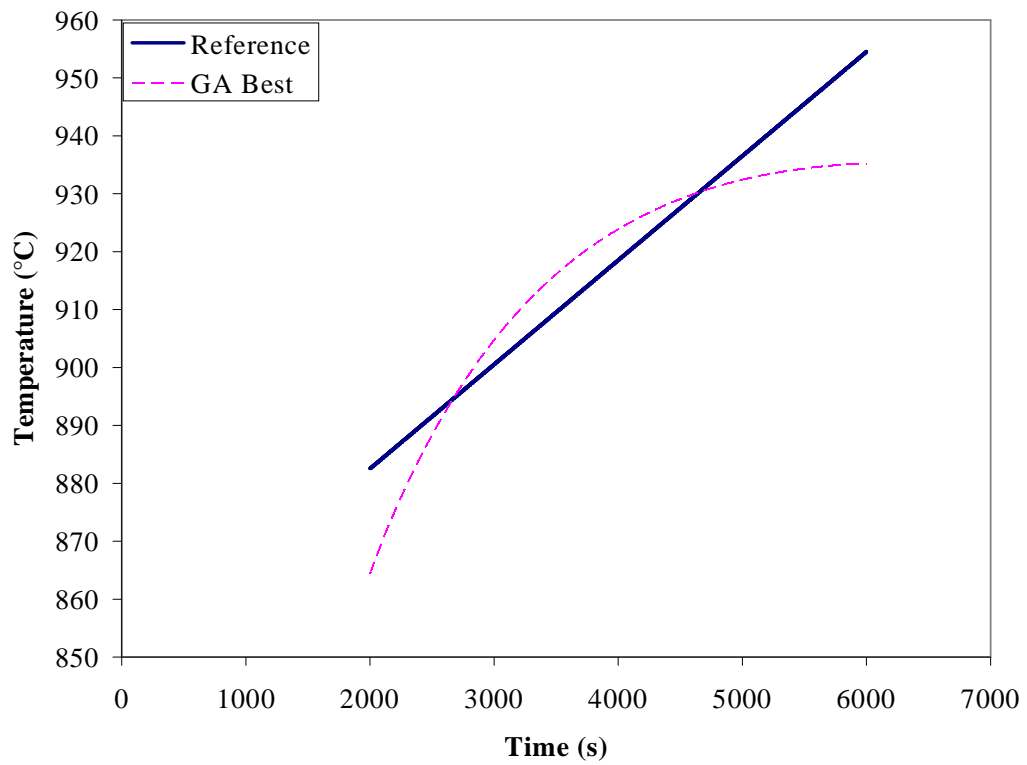
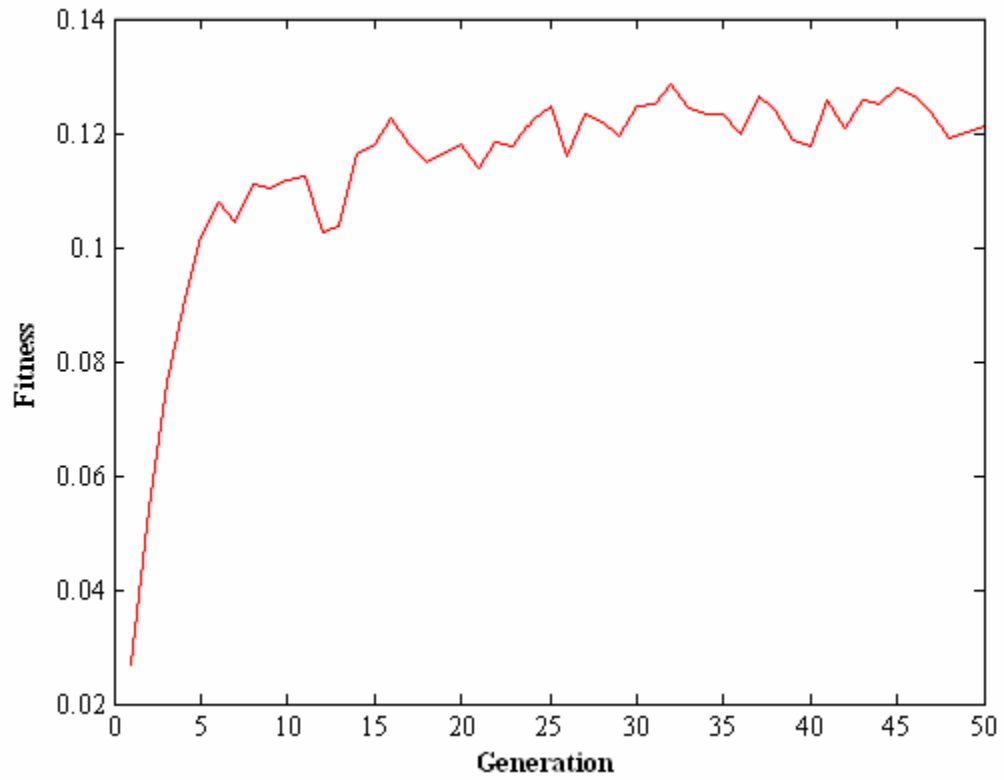
SR3_3_3_Fb_g_1



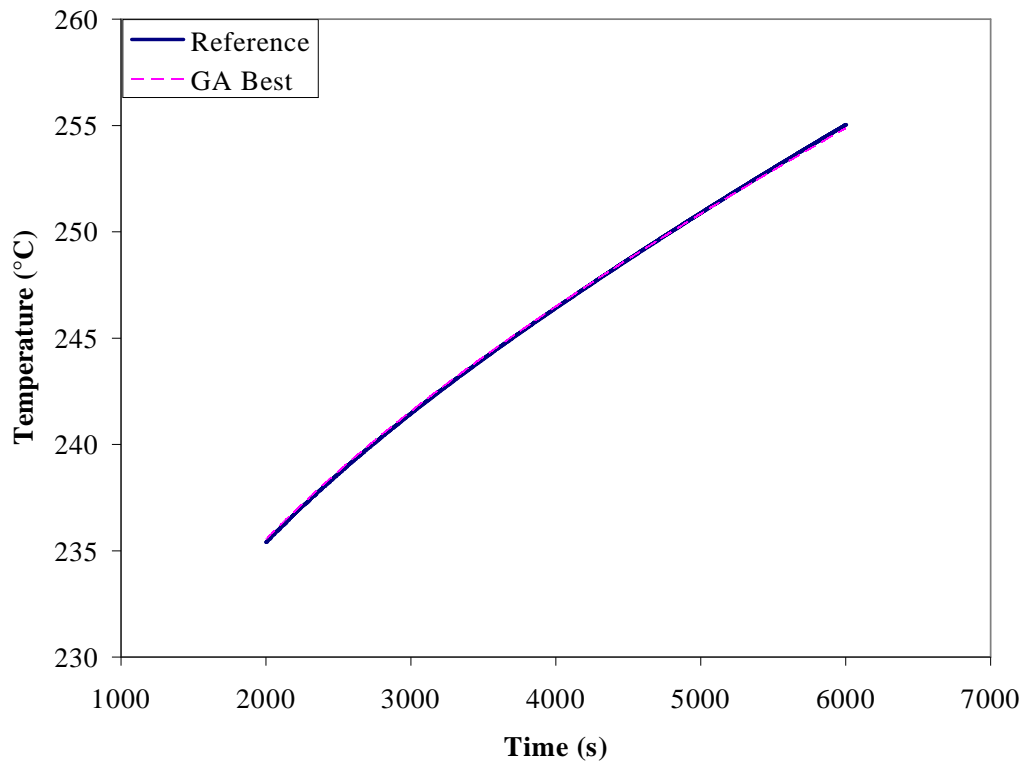
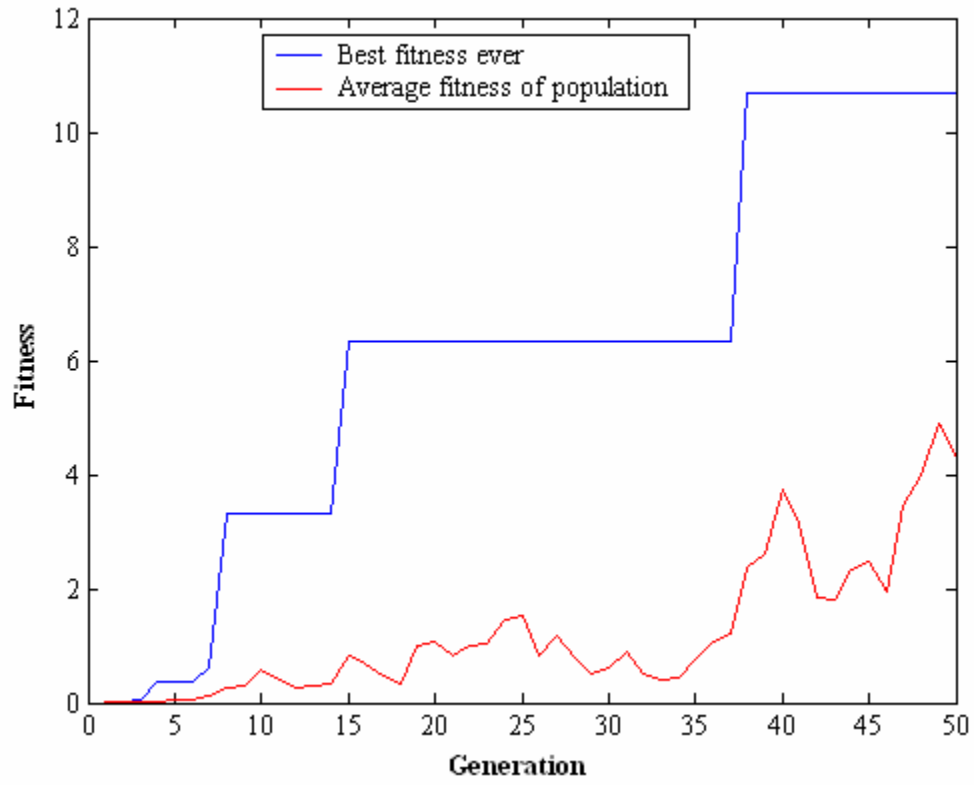
SR3_3_3_Fb_h_1



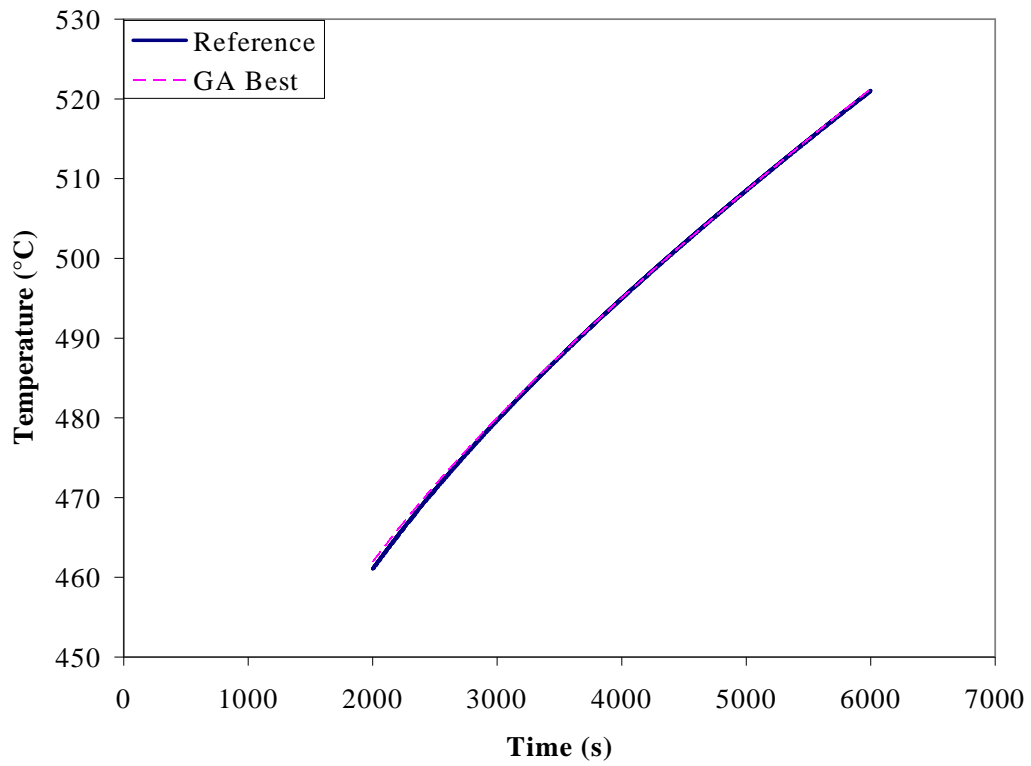
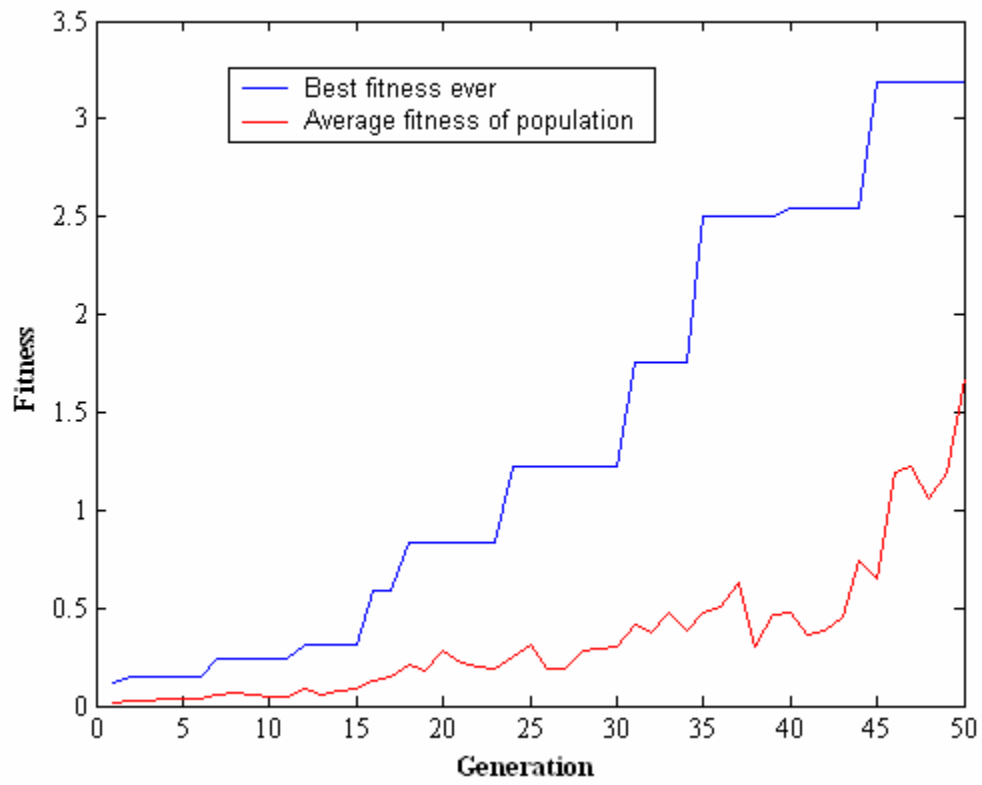
SR3_3_3_Fb_h_2



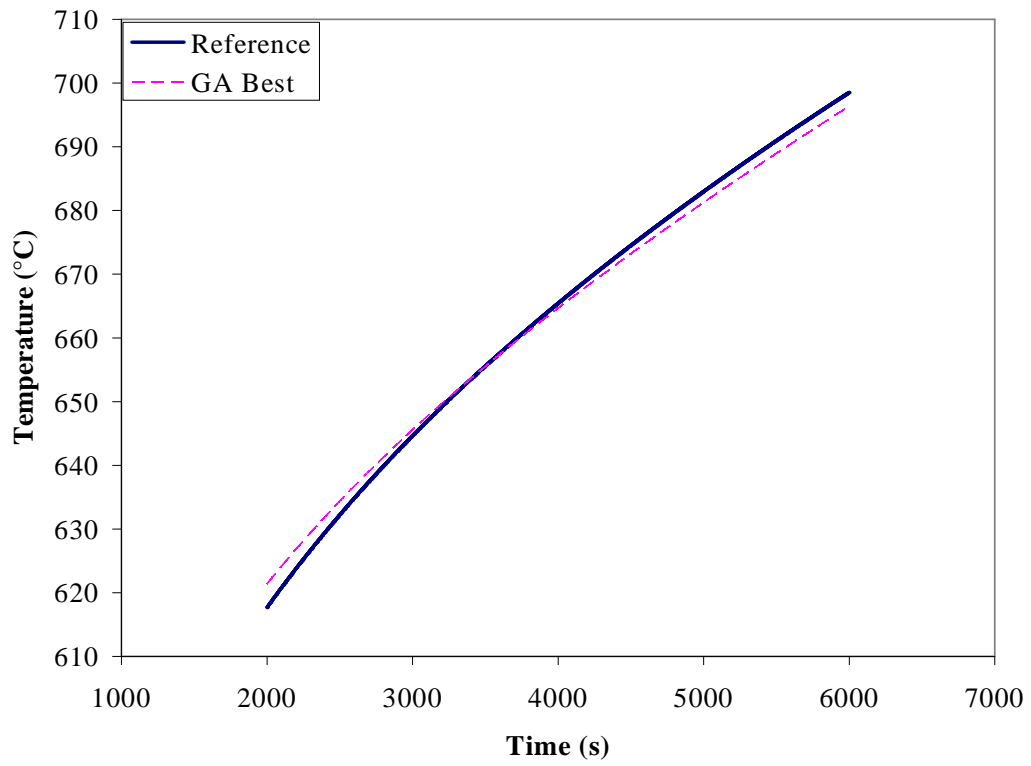
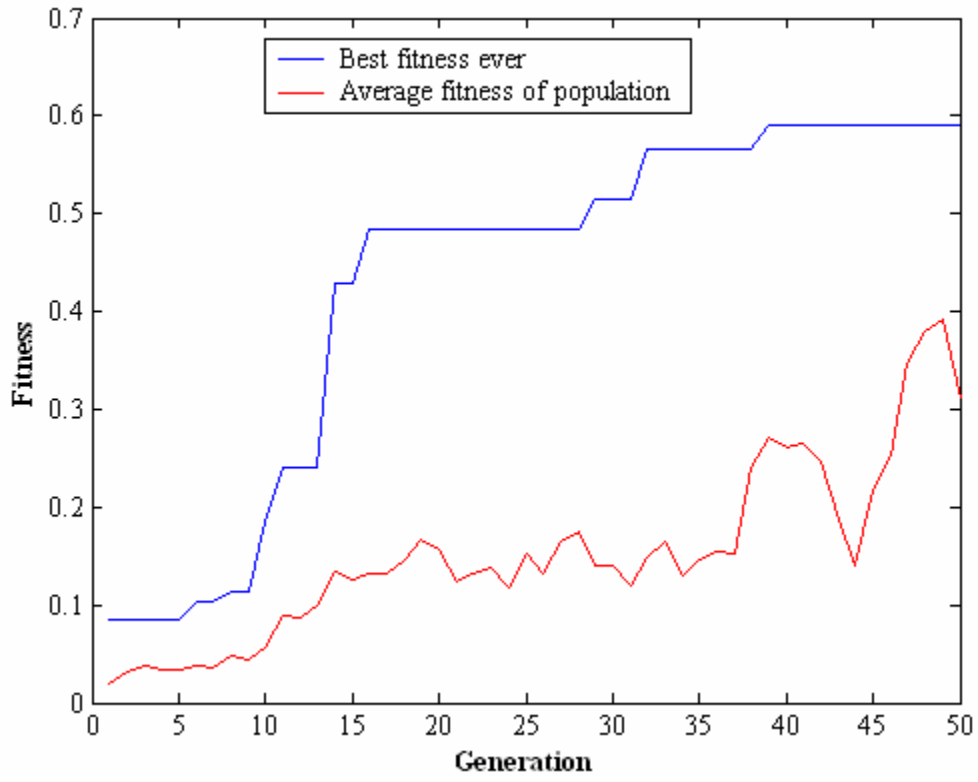
SR3_3_3_NC_b_1



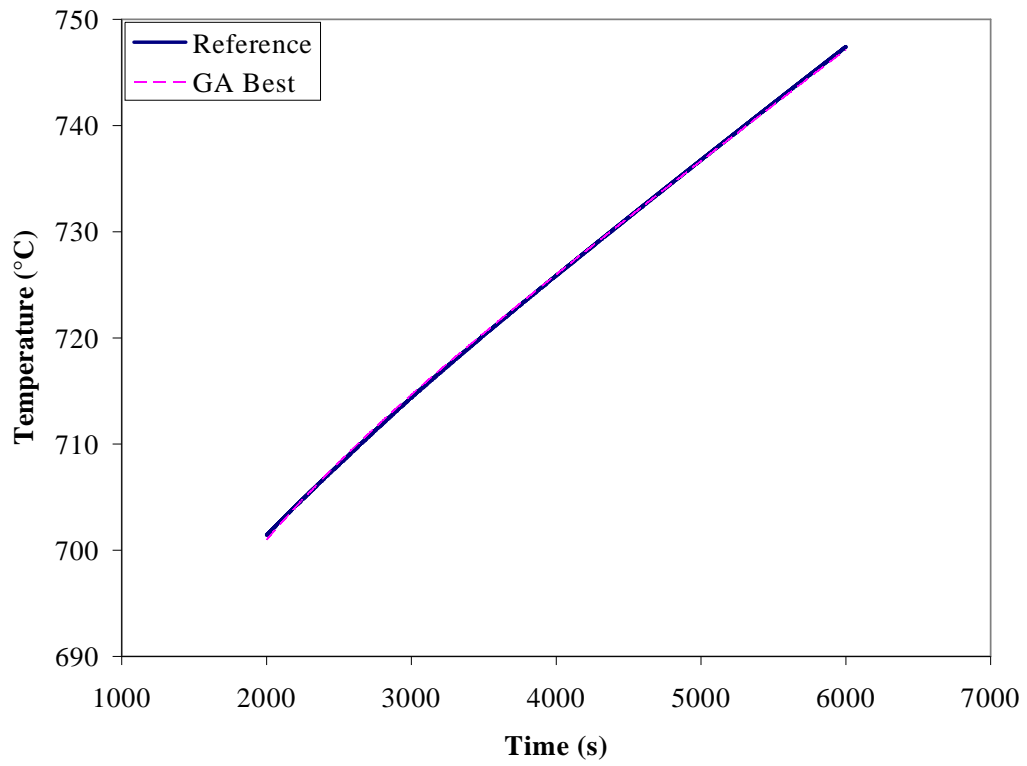
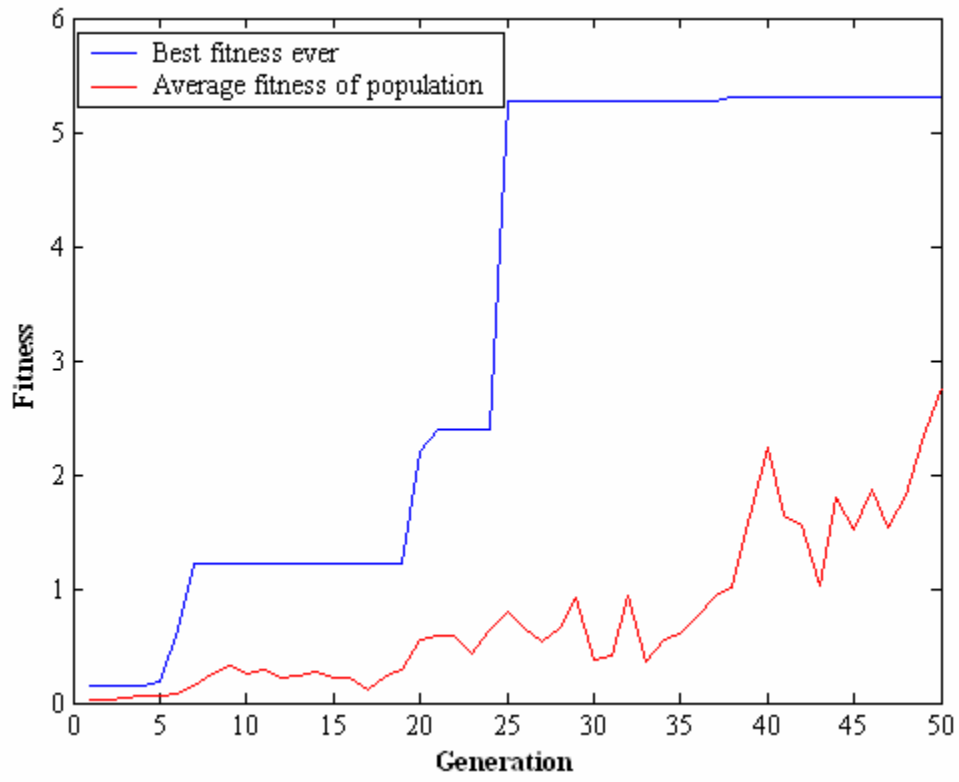
SR3_3_3_NC_b_2



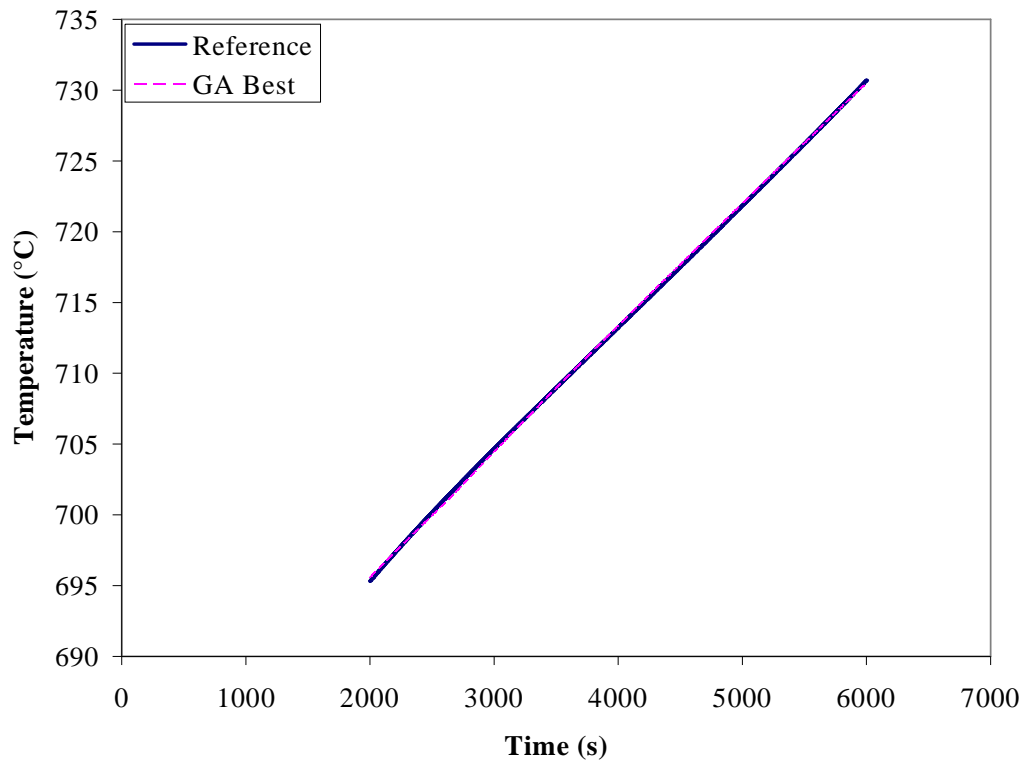
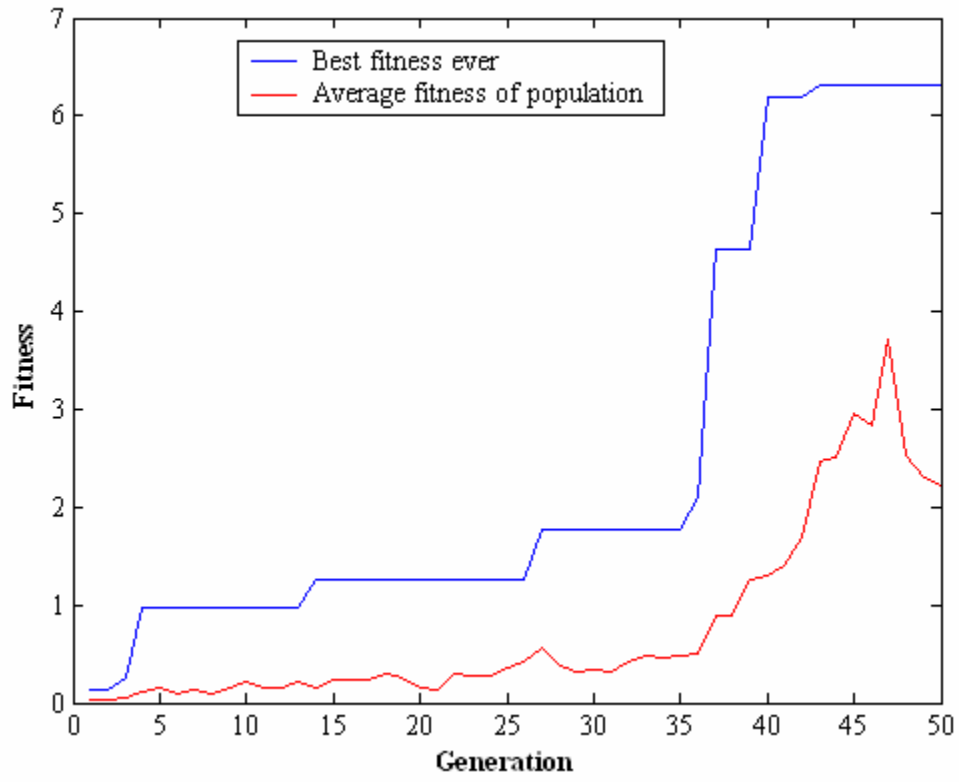
SR3_3_3_NC_b_3



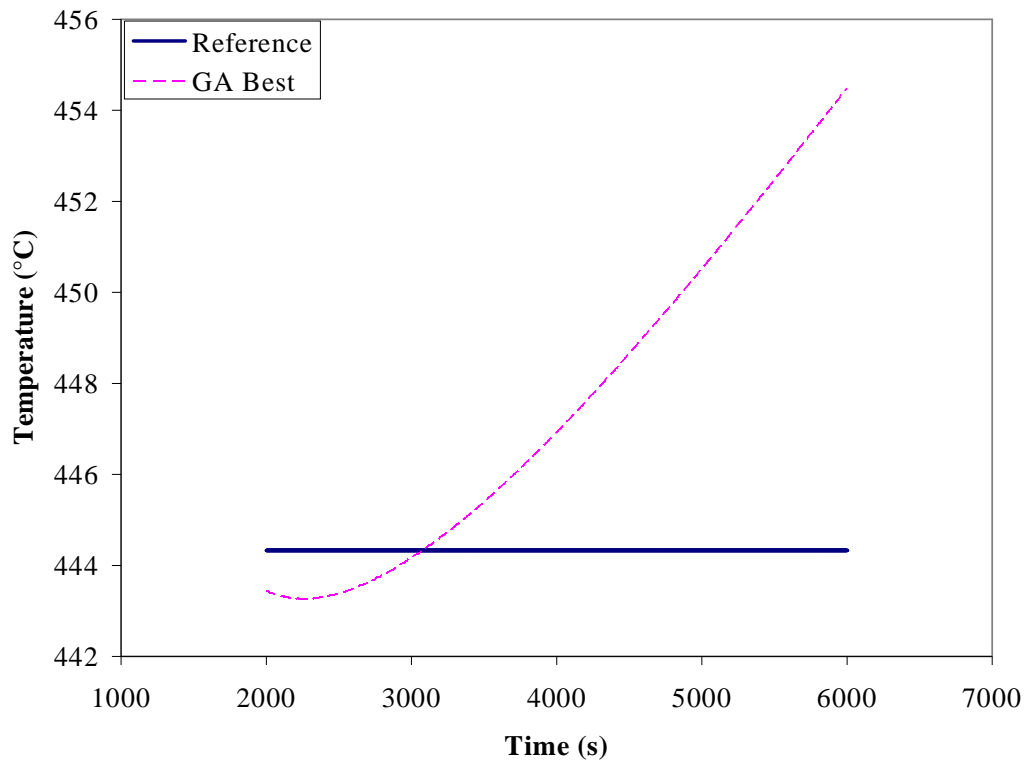
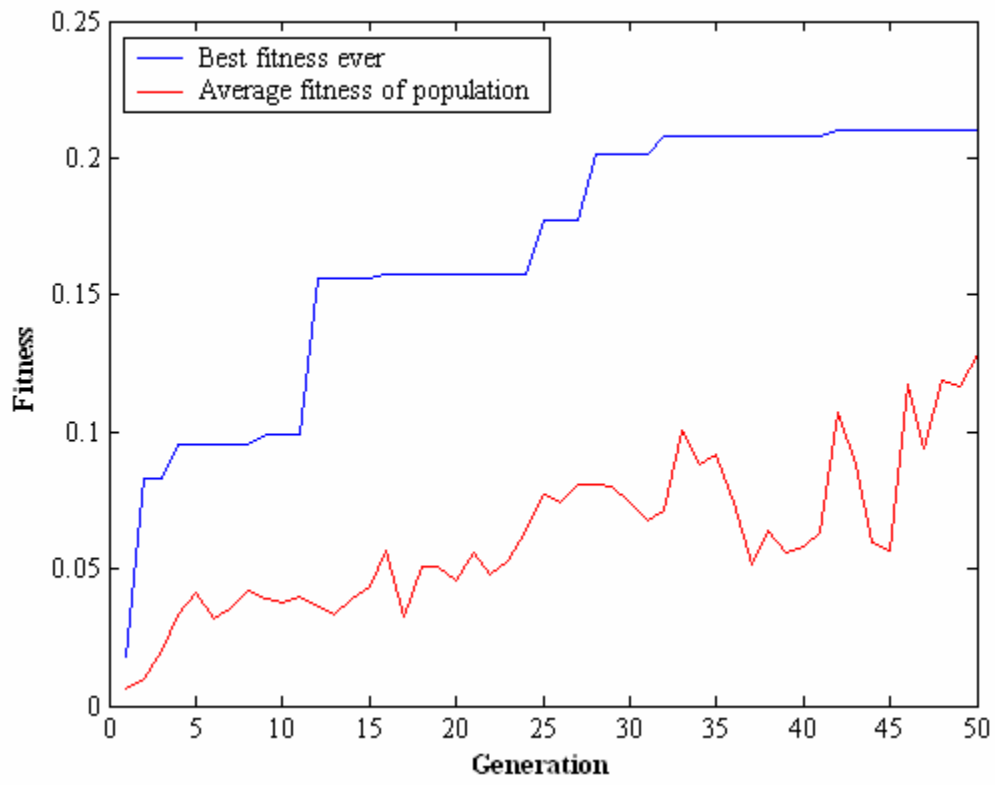
SR3_3_3_NC_b_4



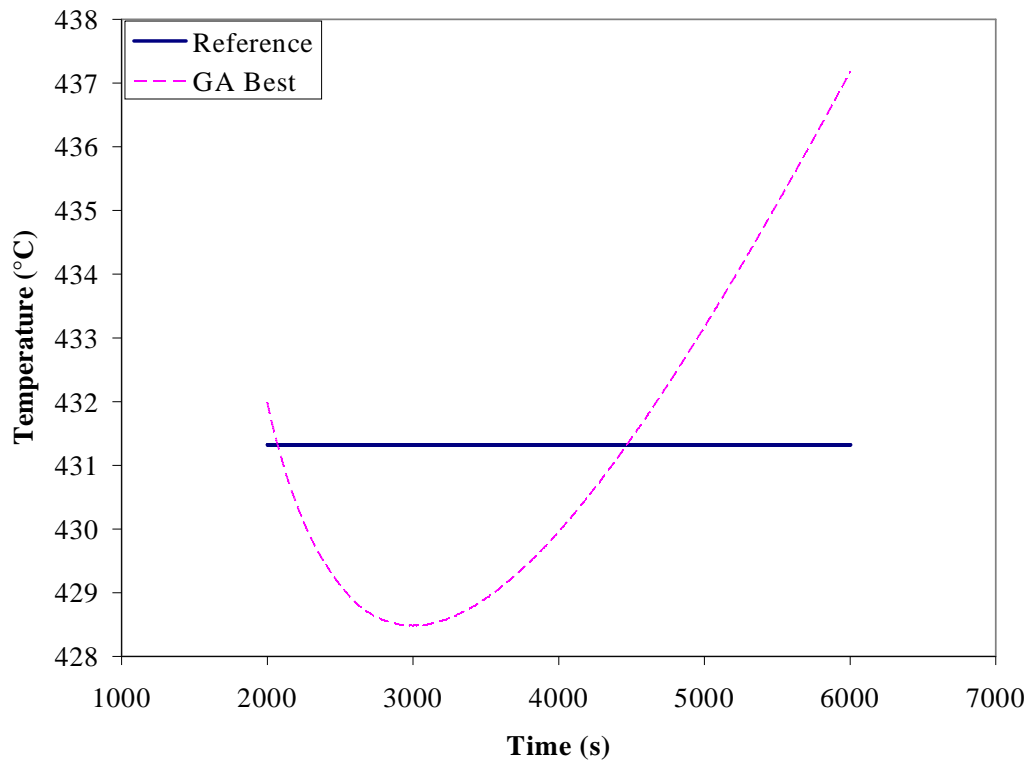
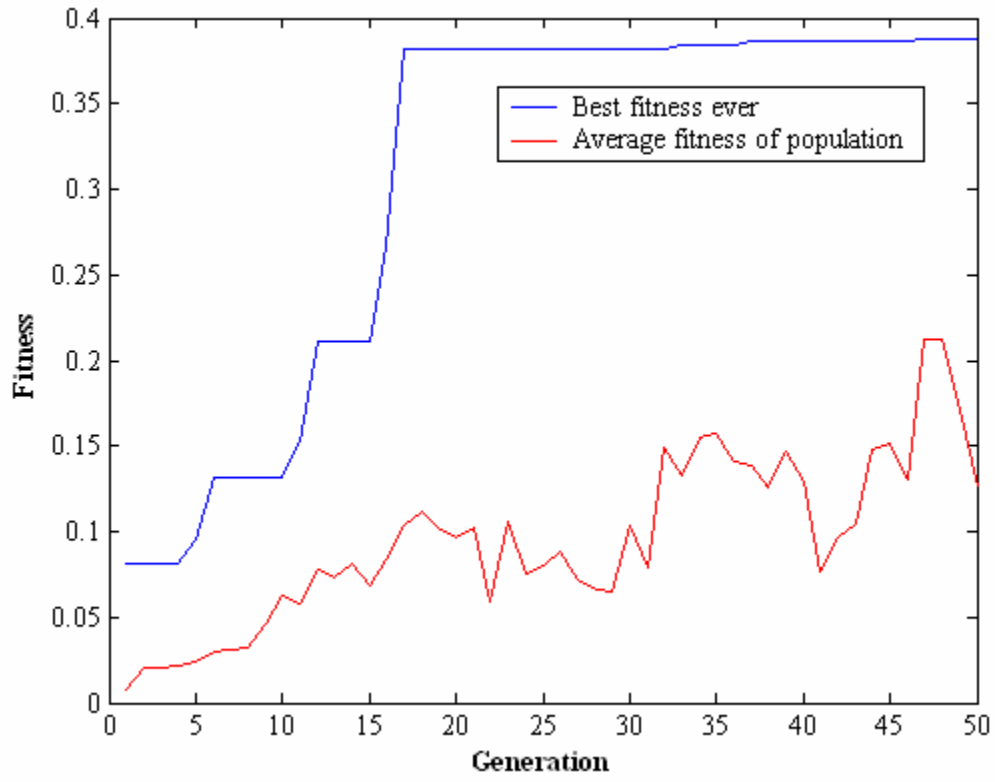
SR3_3_3_NC_b_5



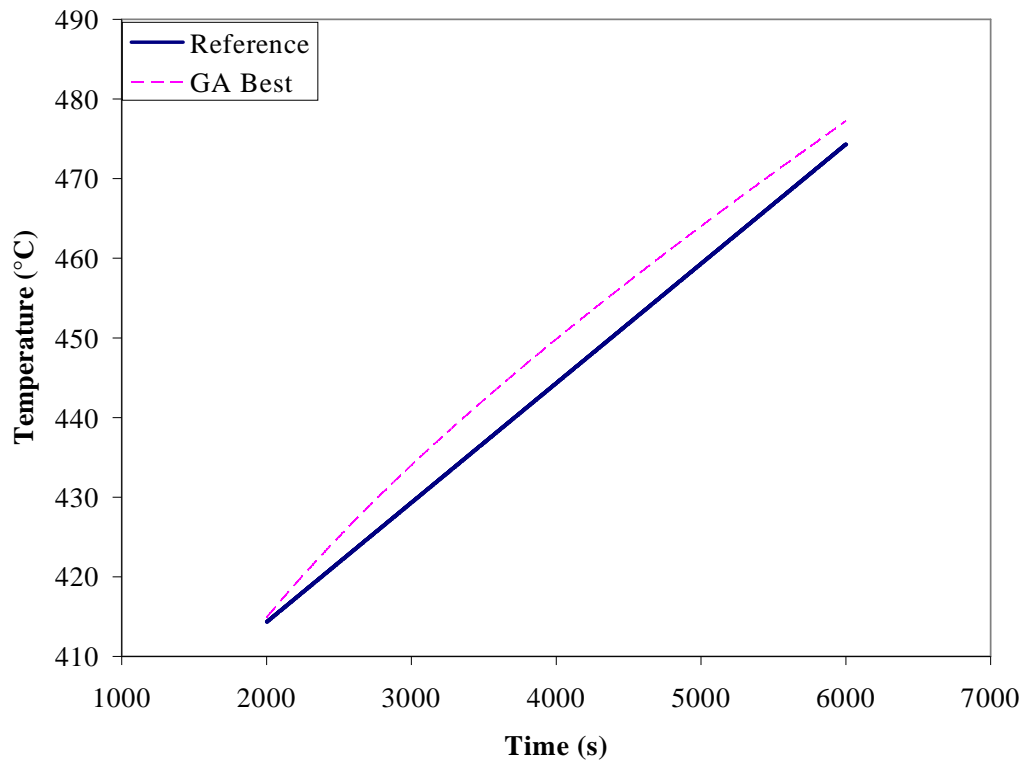
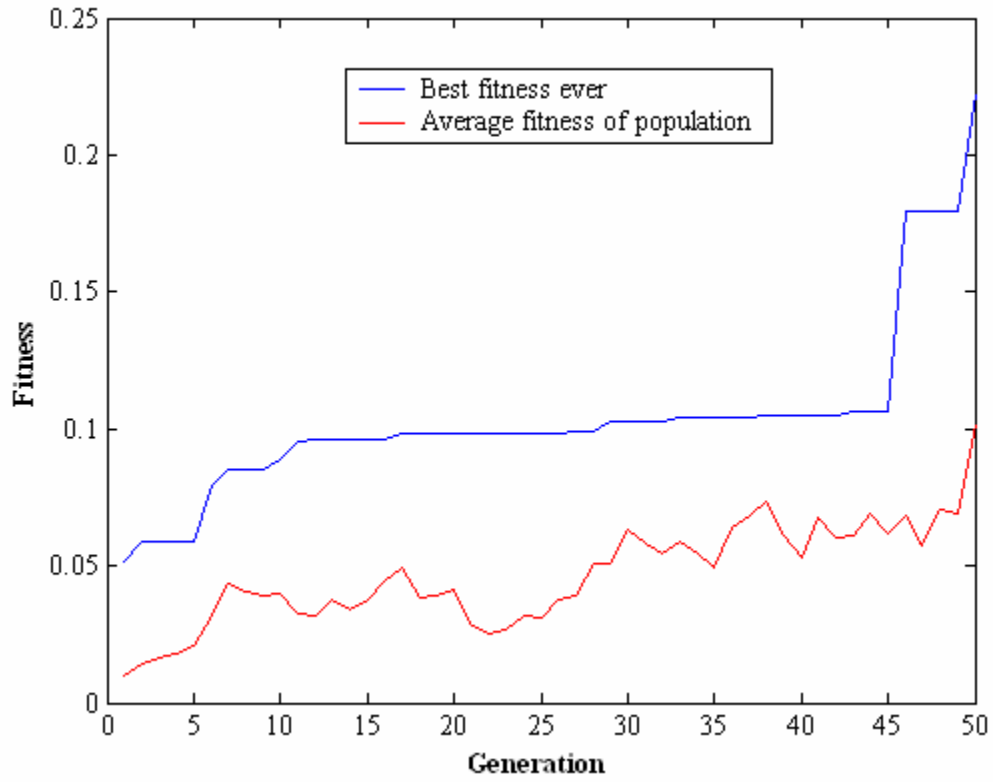
SR3_3_3_NC_c_1



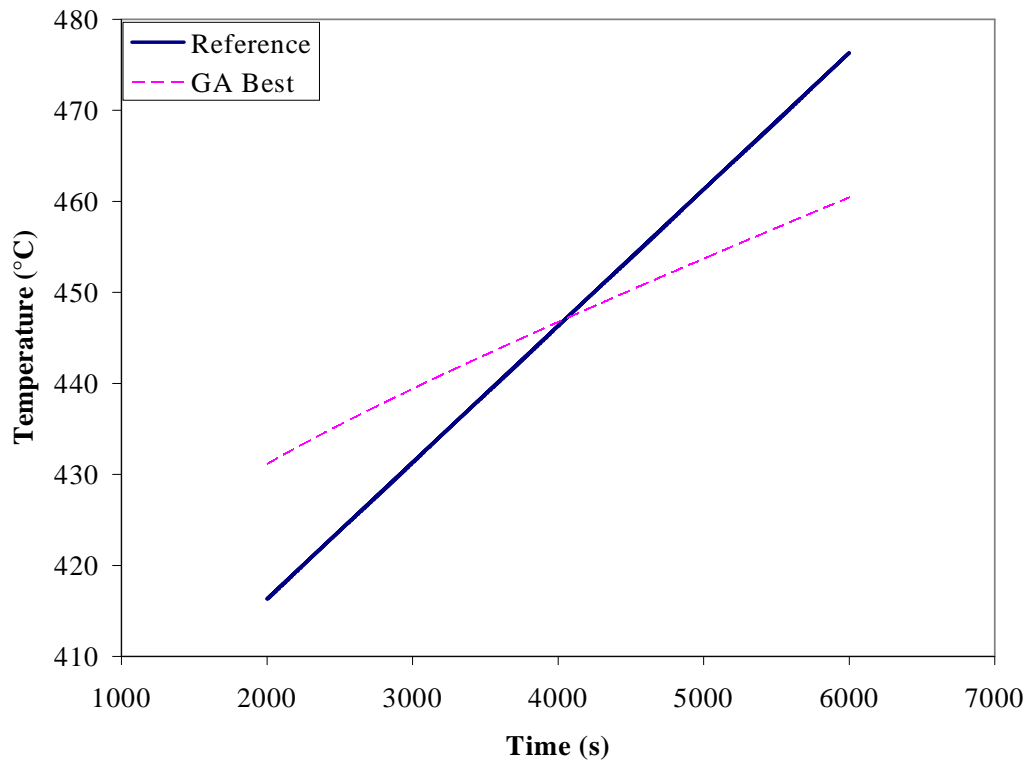
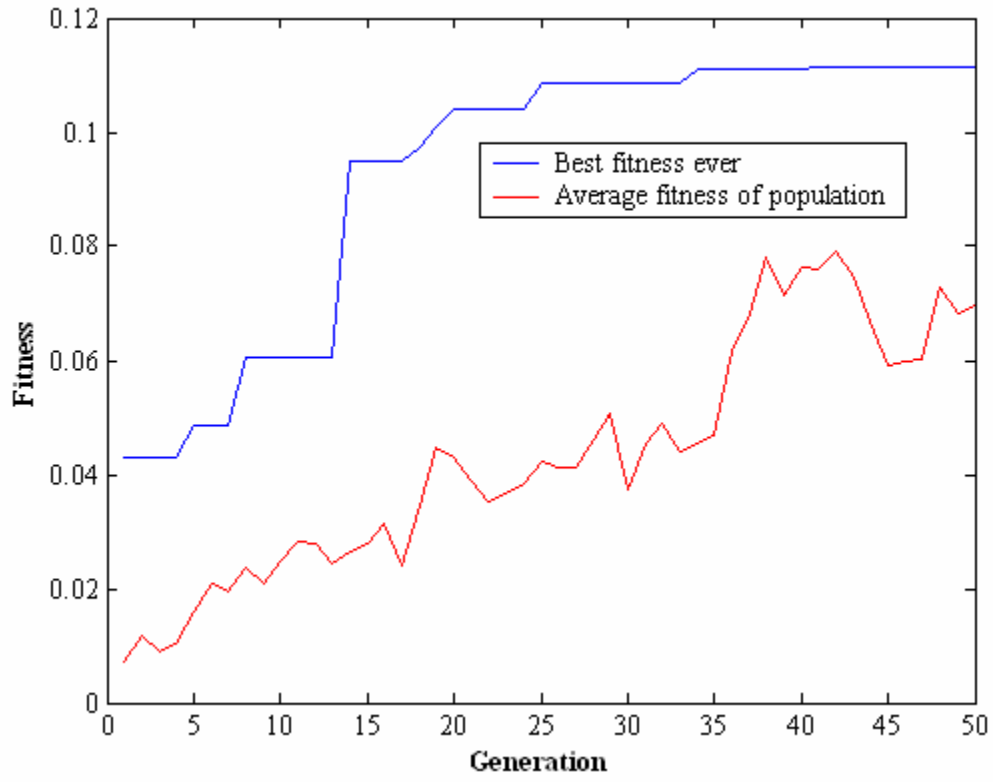
SR3_3_3_NC_d_1



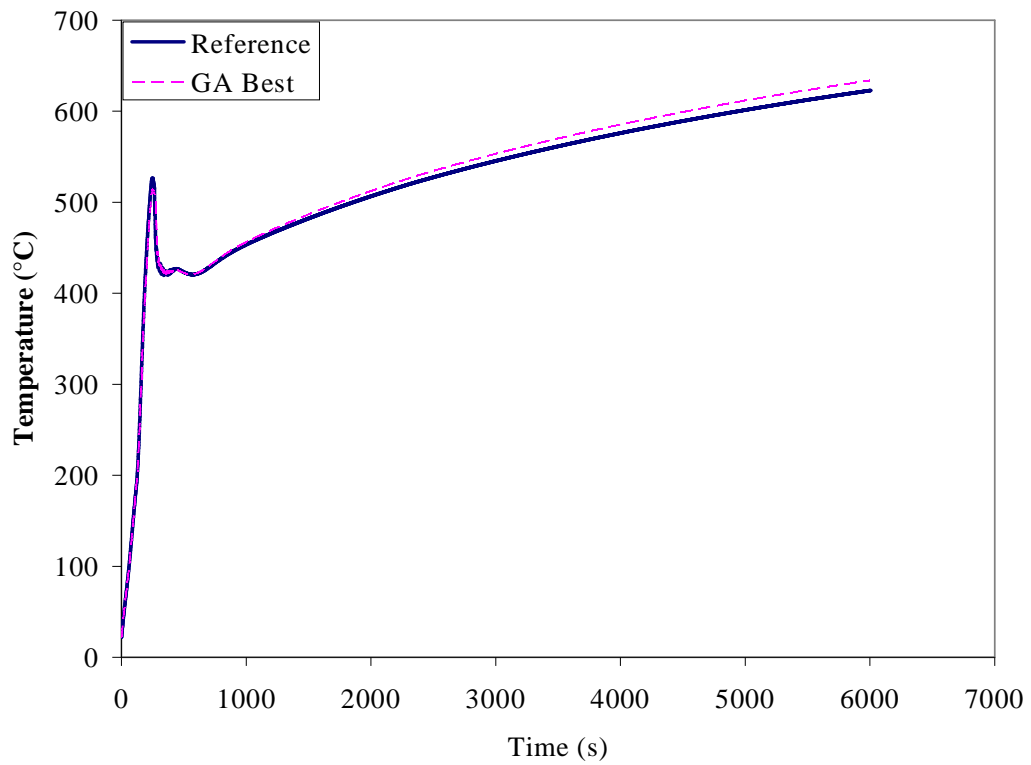
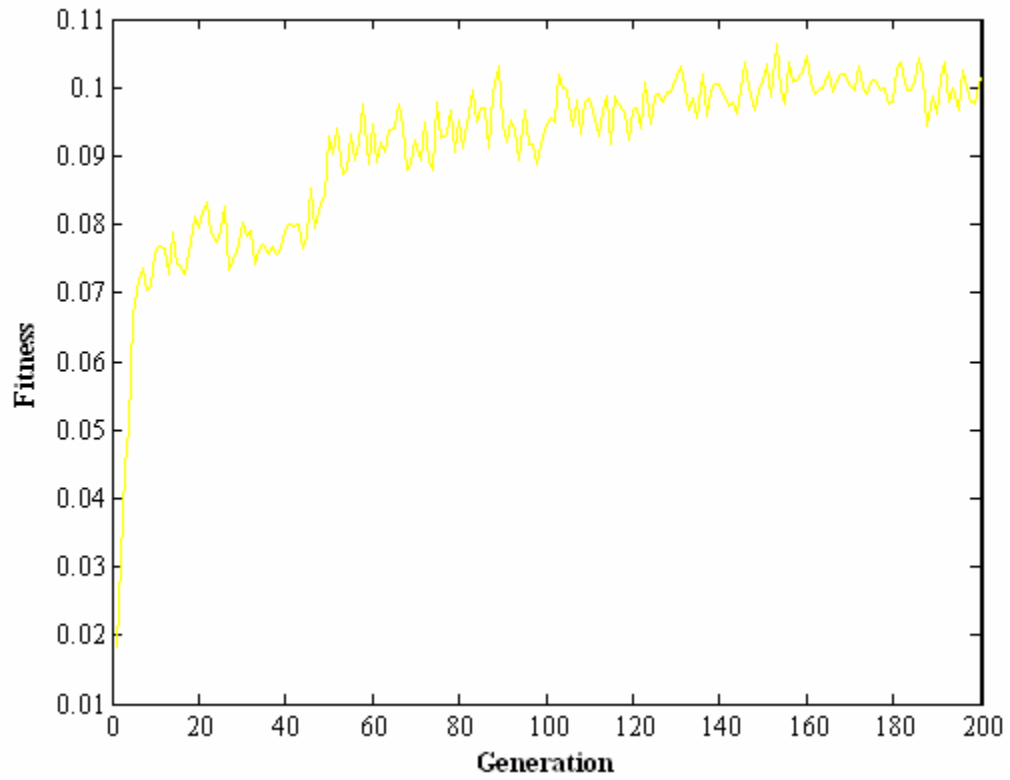
SR3_3_3_NC_f_1



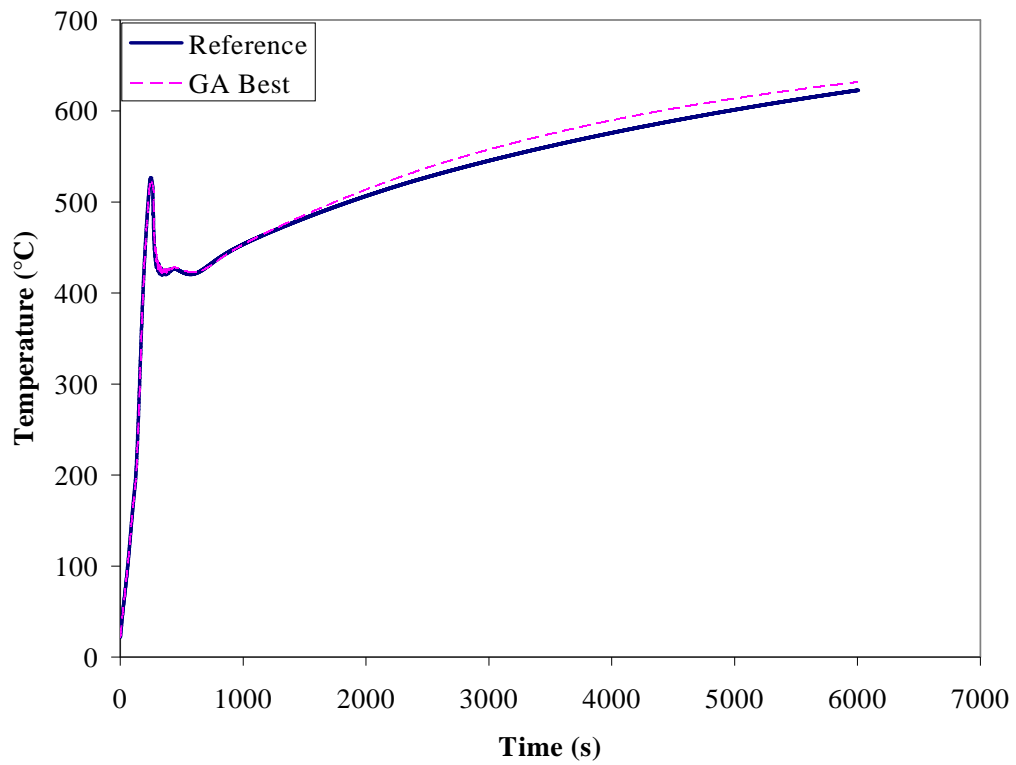
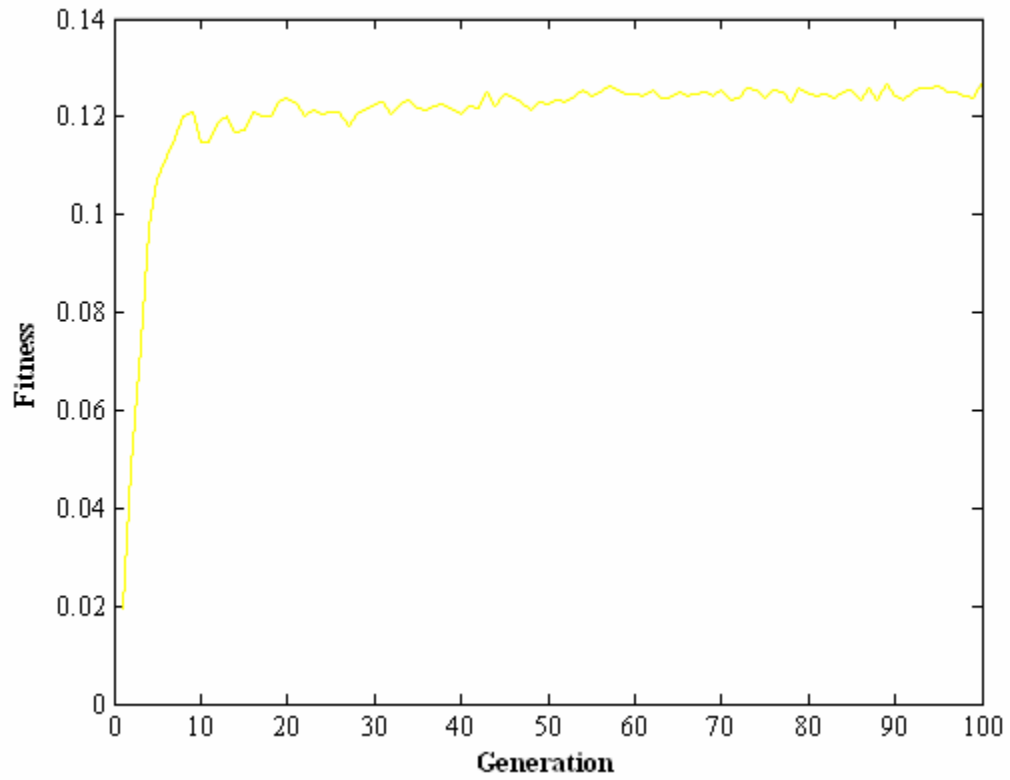
SR3_3_3_NC_g_1



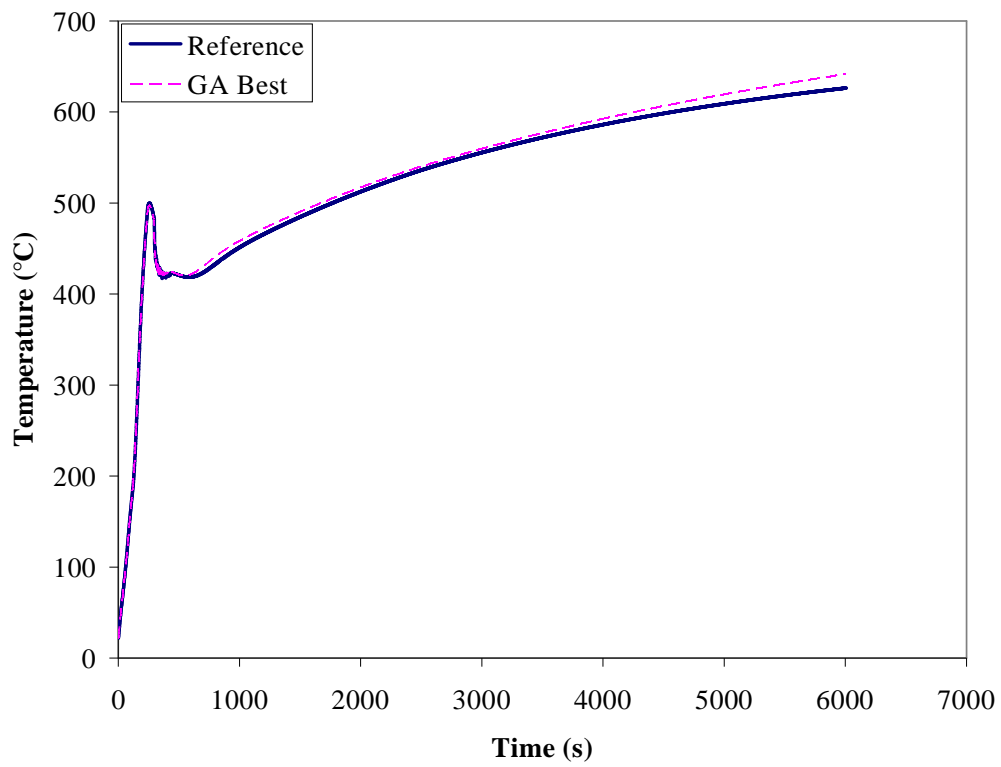
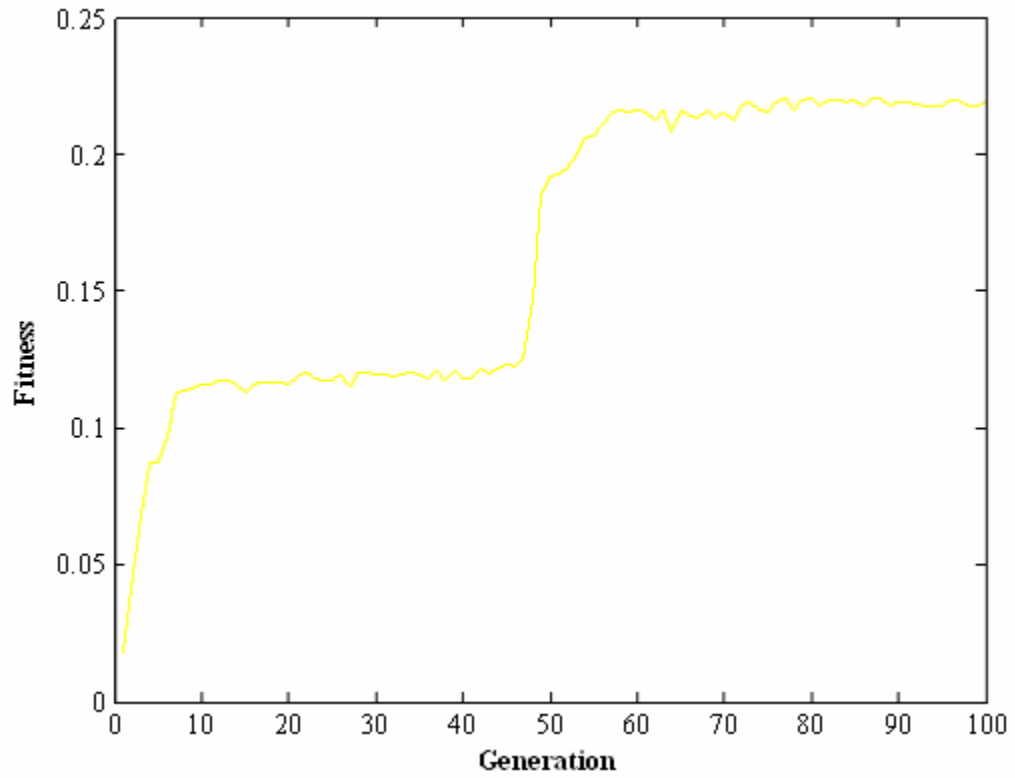
SR10_10_3_Fb_a_1



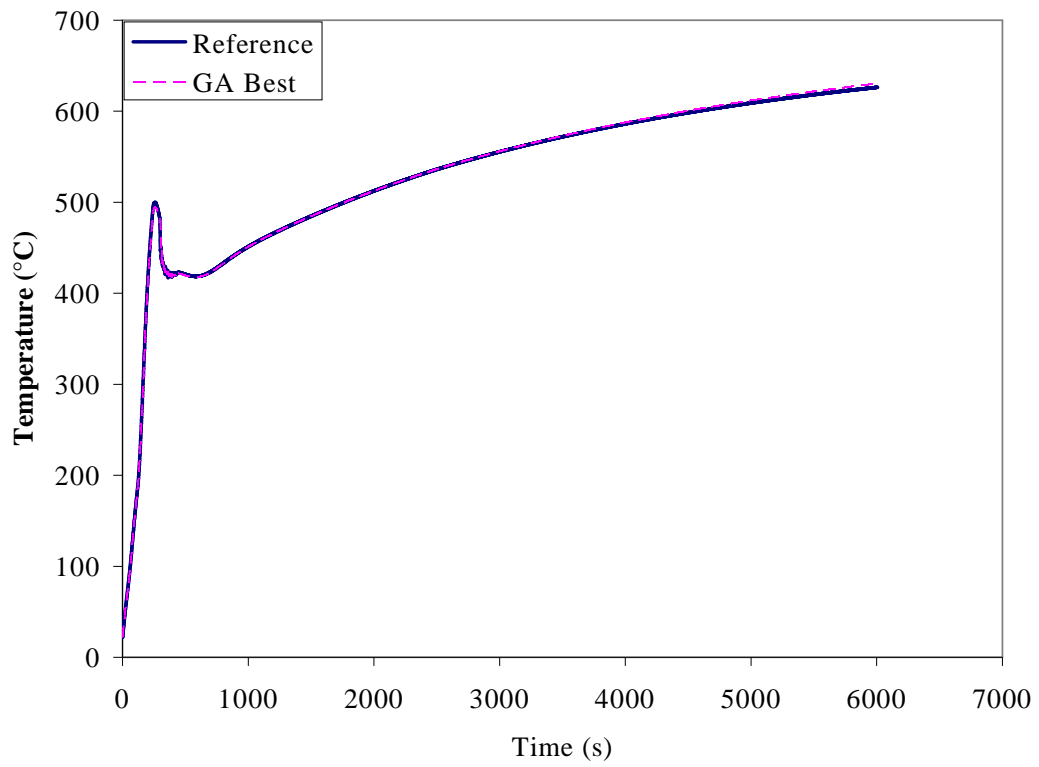
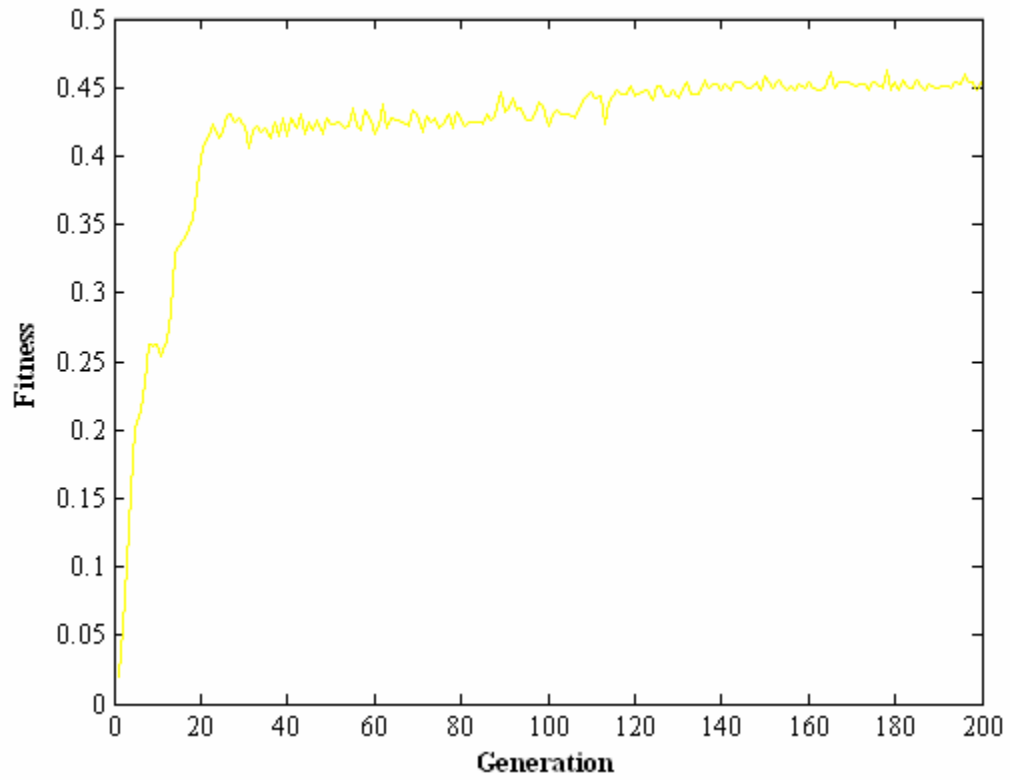
SR10_10_3_Fb_a_2



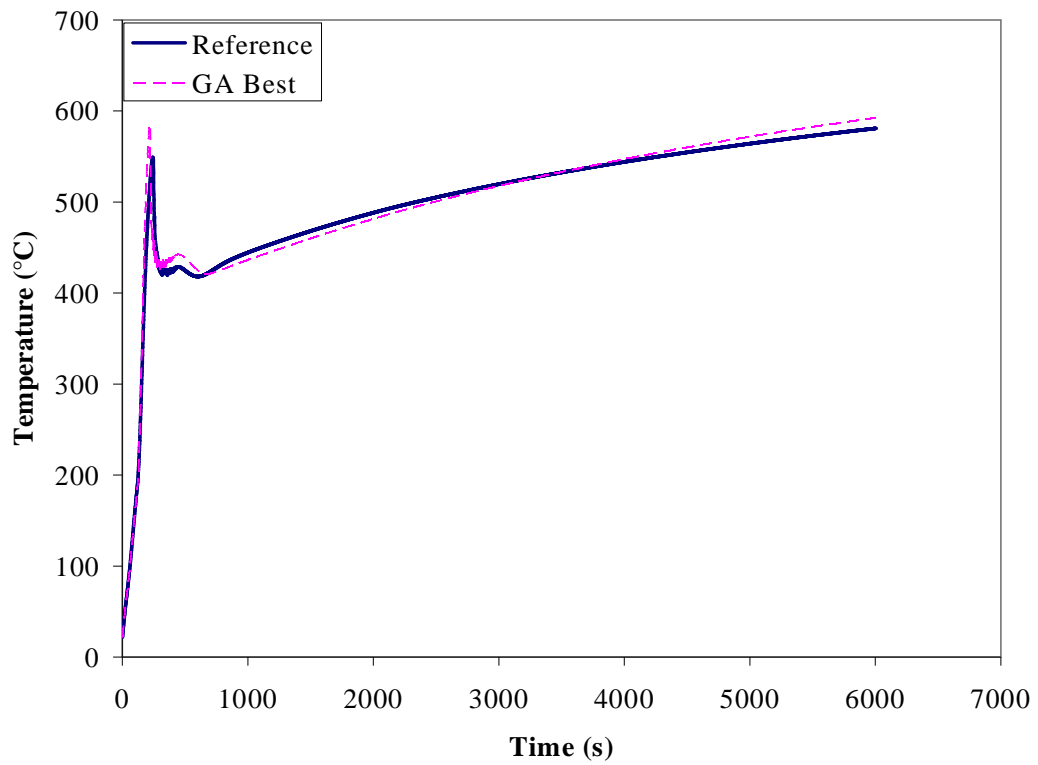
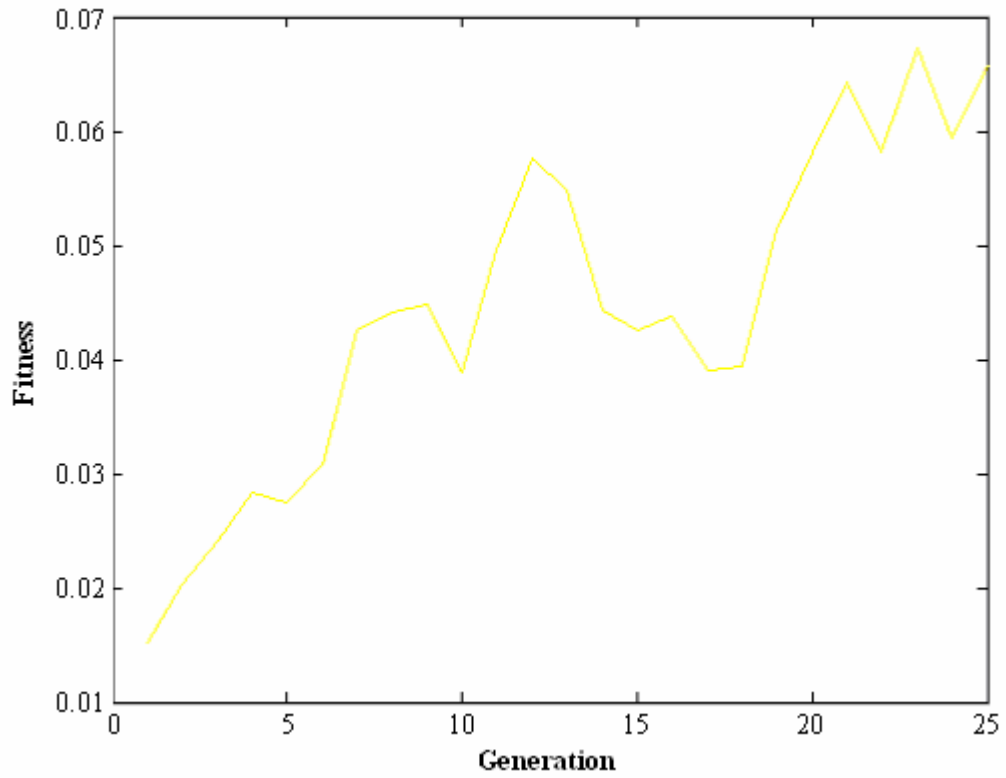
SR10_10_3_Fb_a_3



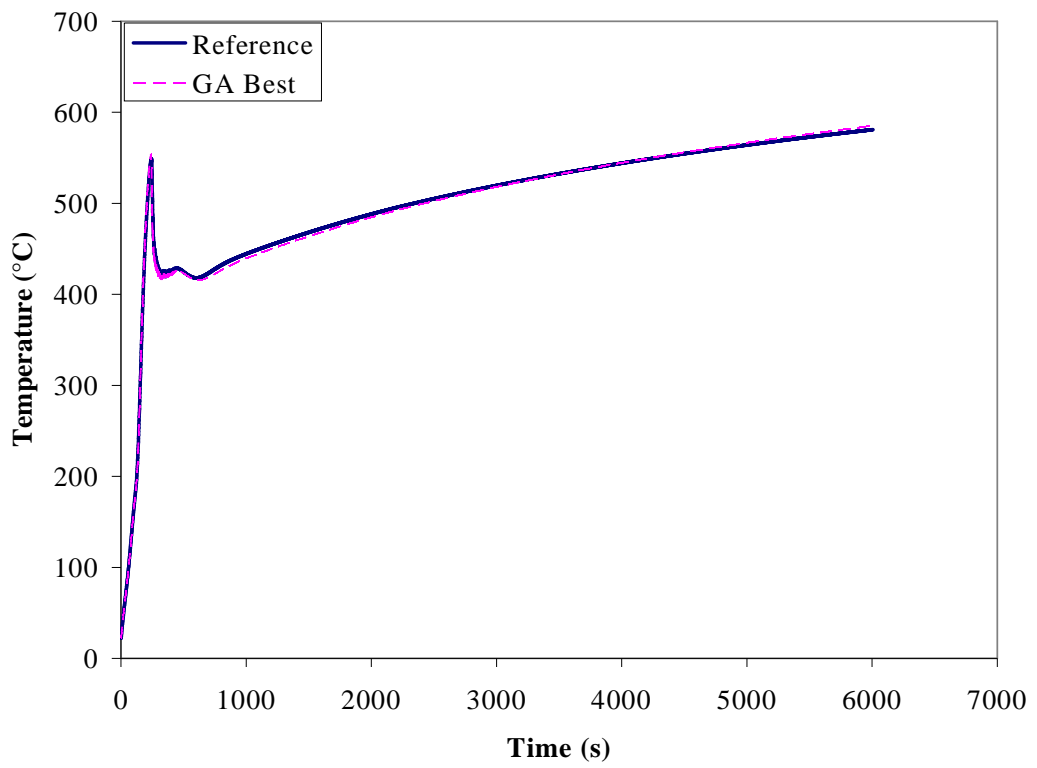
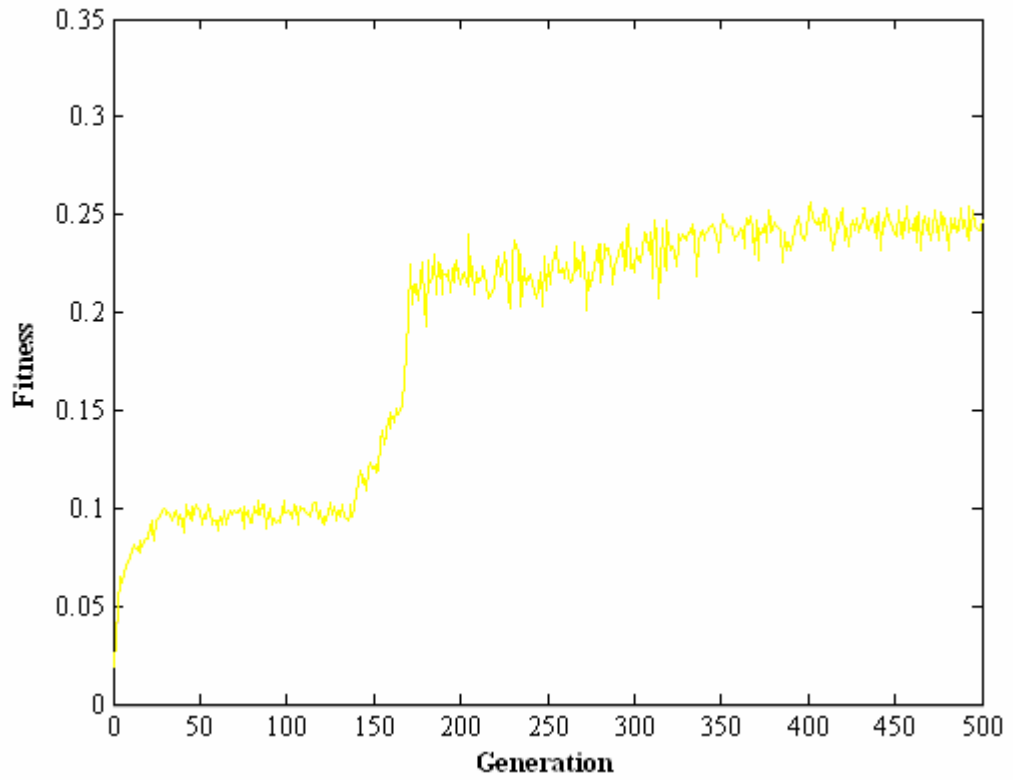
SR10_10_3_Fb_a_4



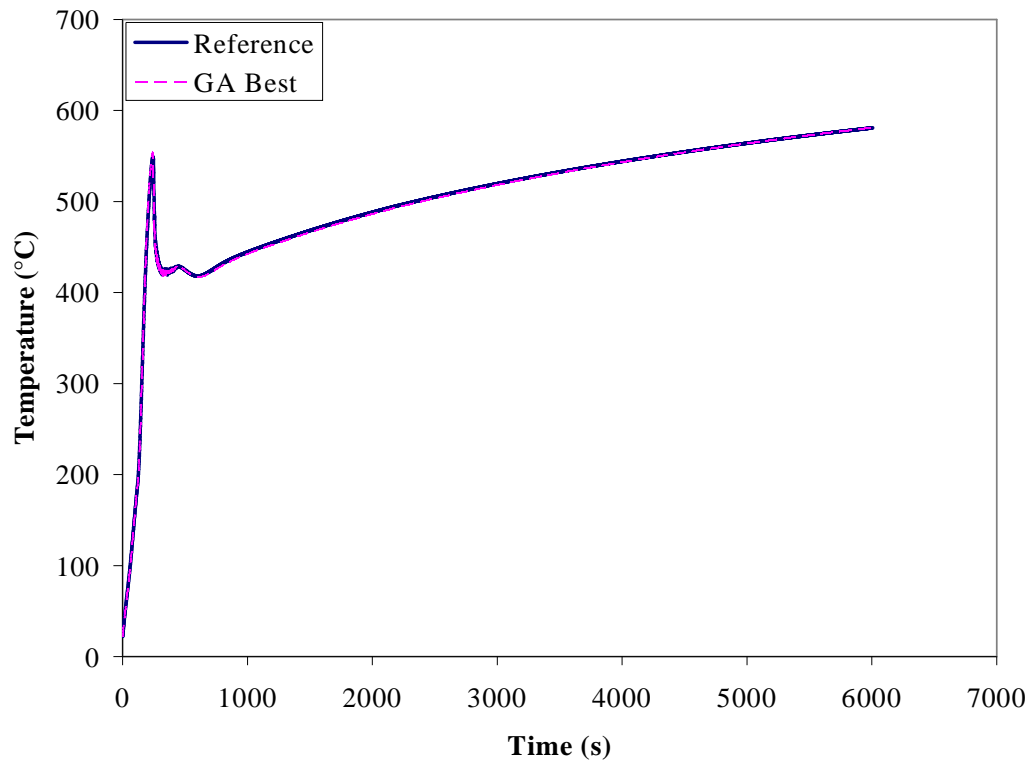
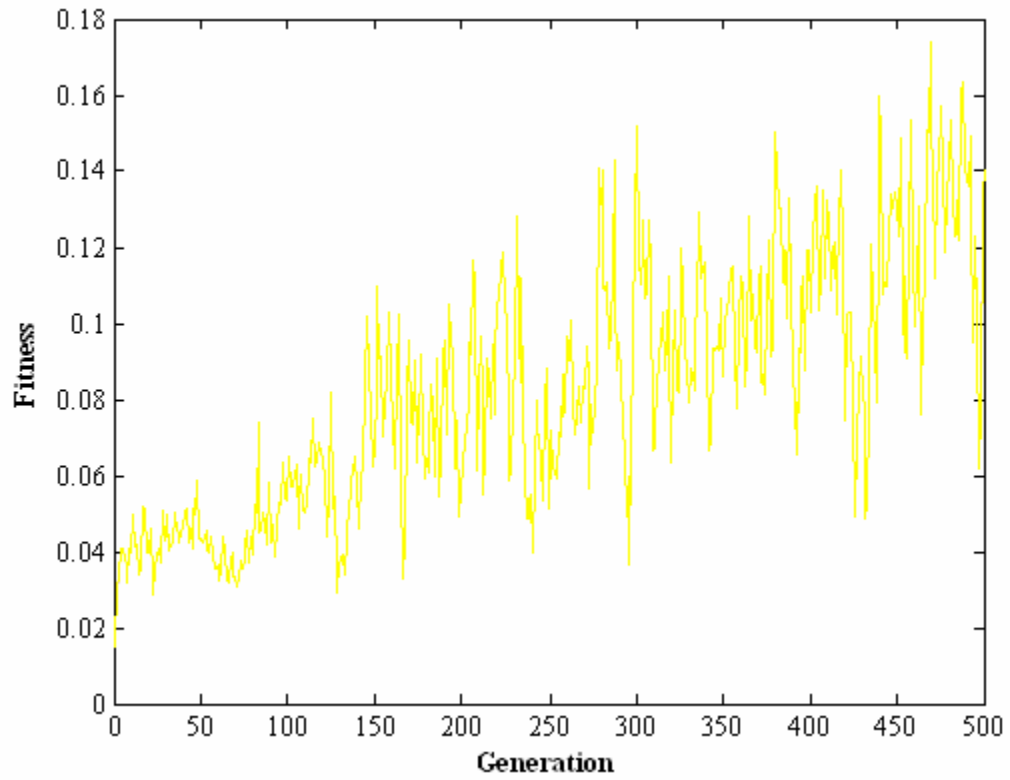
SR10_10_3_Fb_a_5



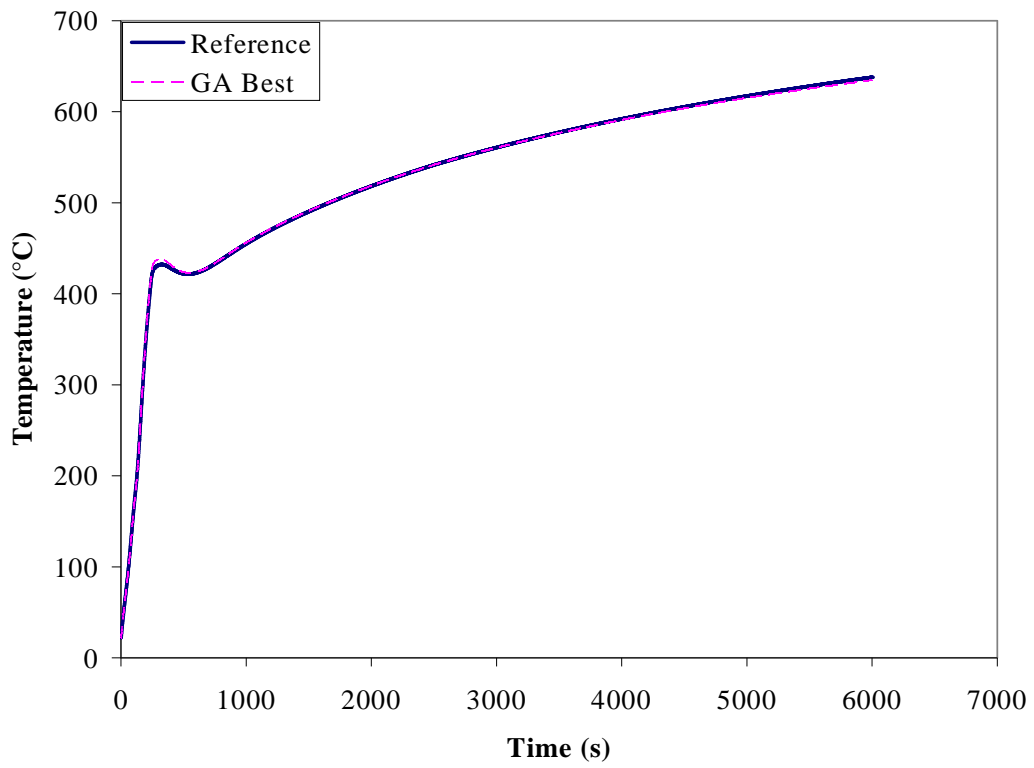
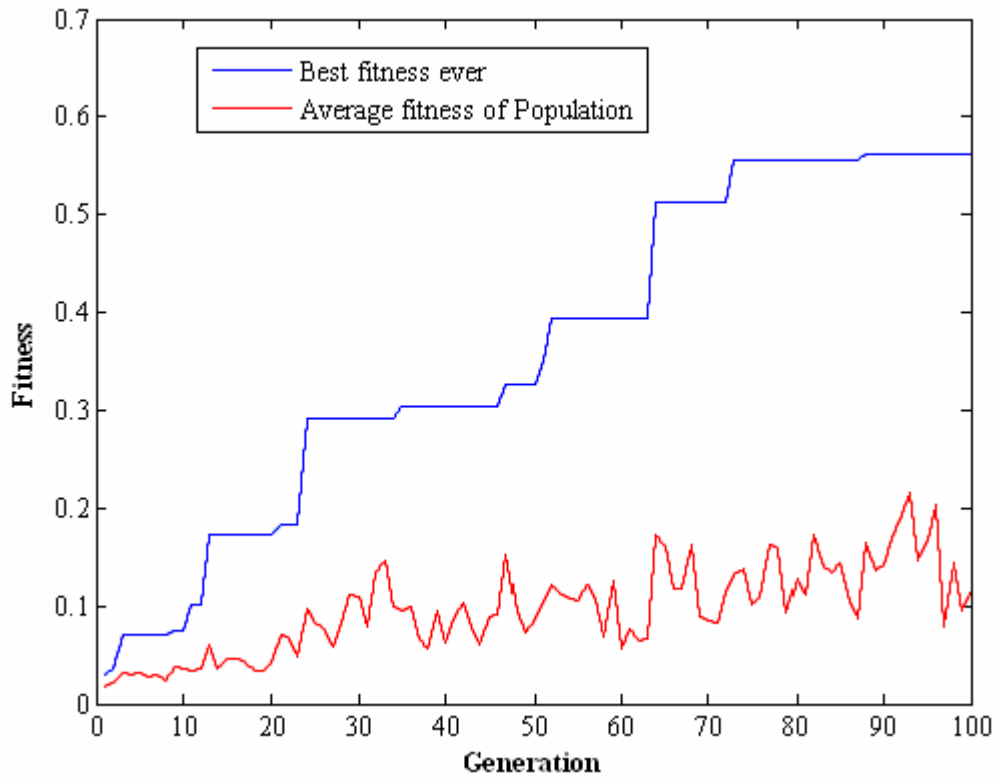
SR10_10_3_Fb_a_6



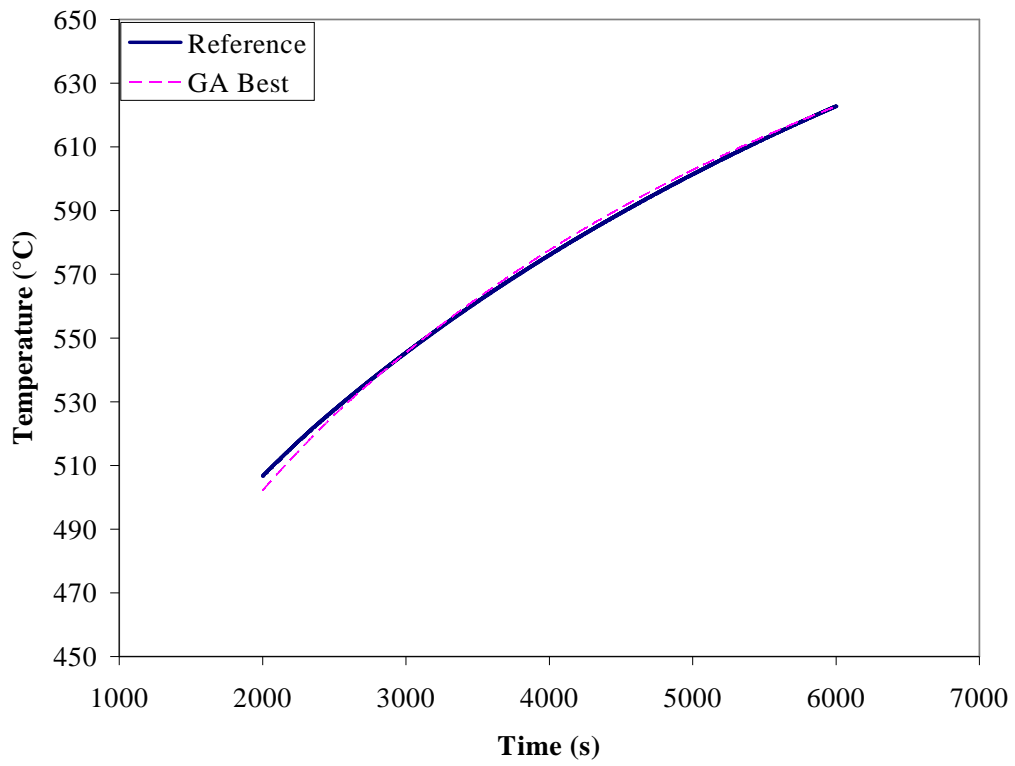
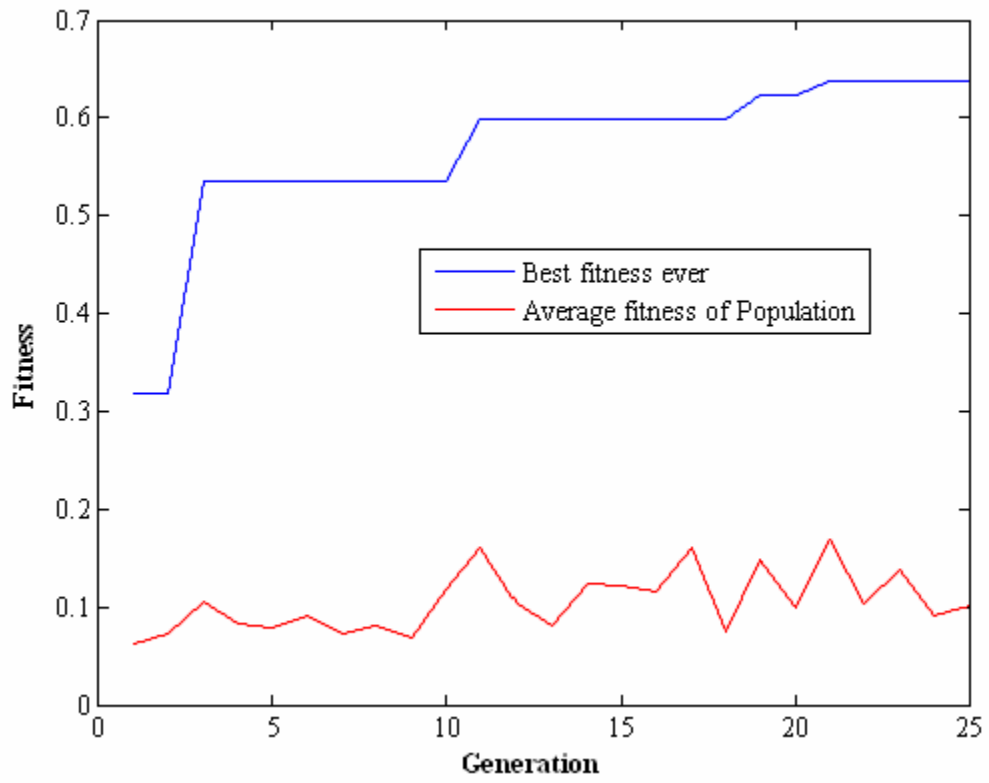
SR10_10_3_Fb_a_7



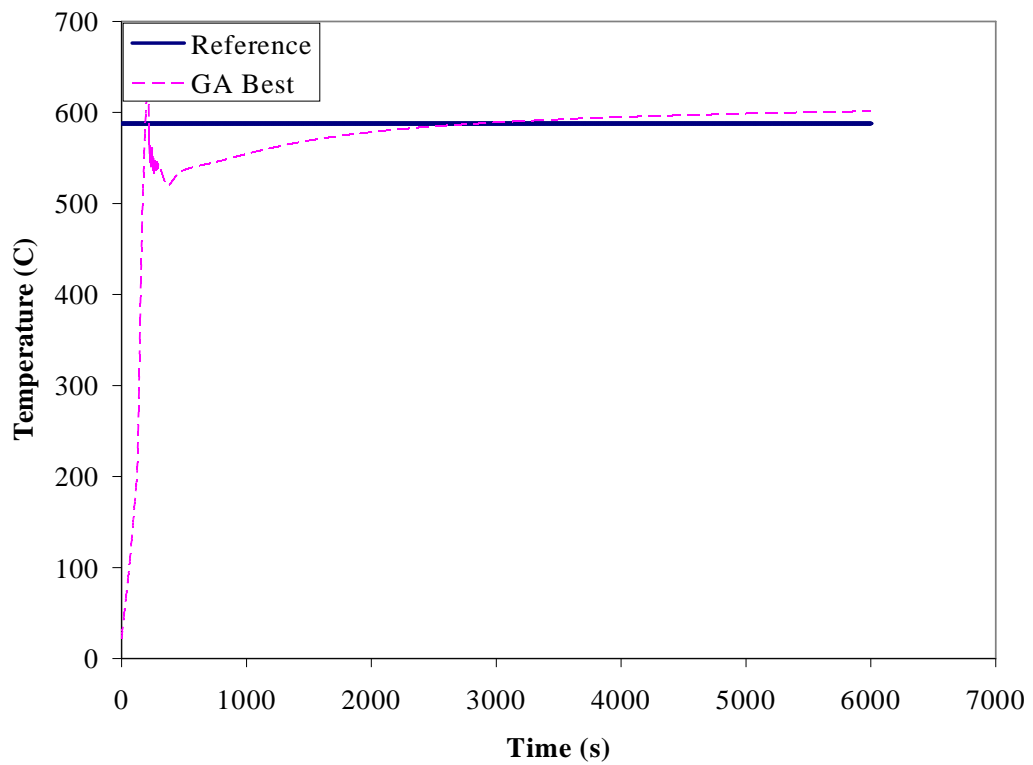
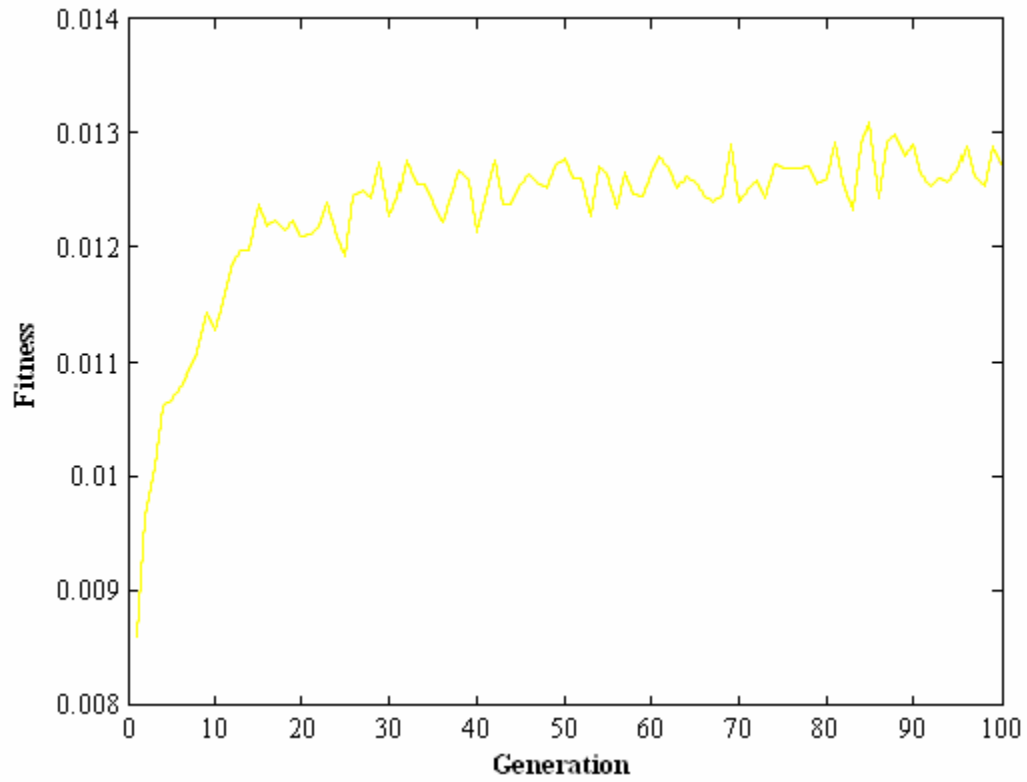
SR10_10_3_Fb_a_8



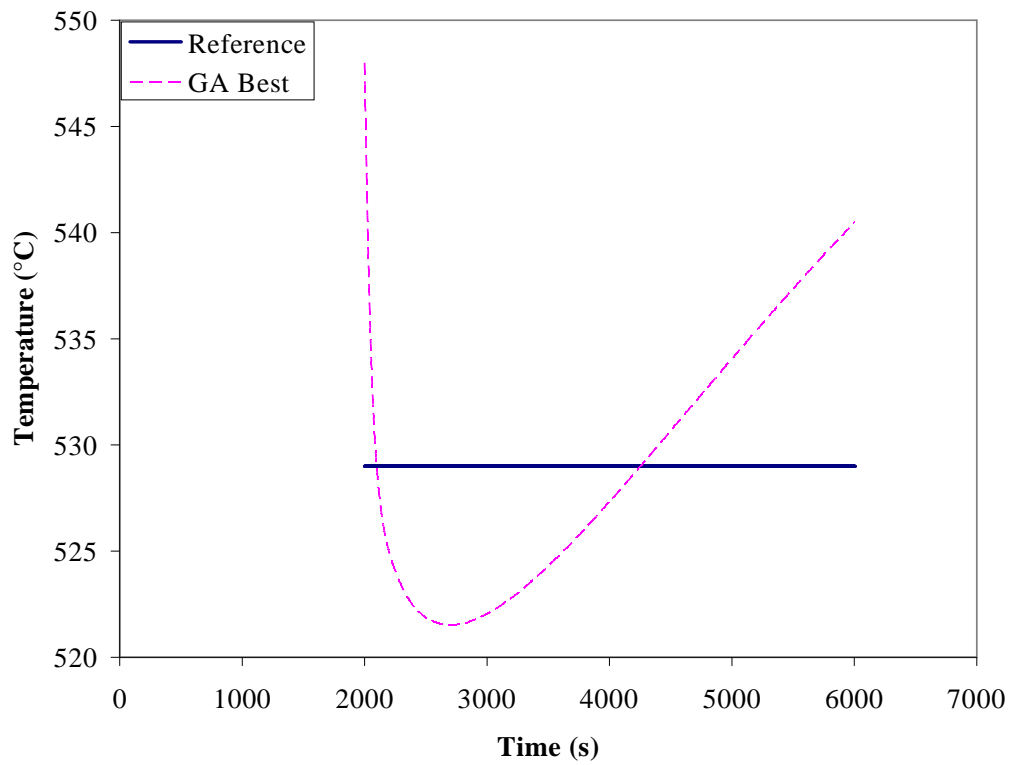
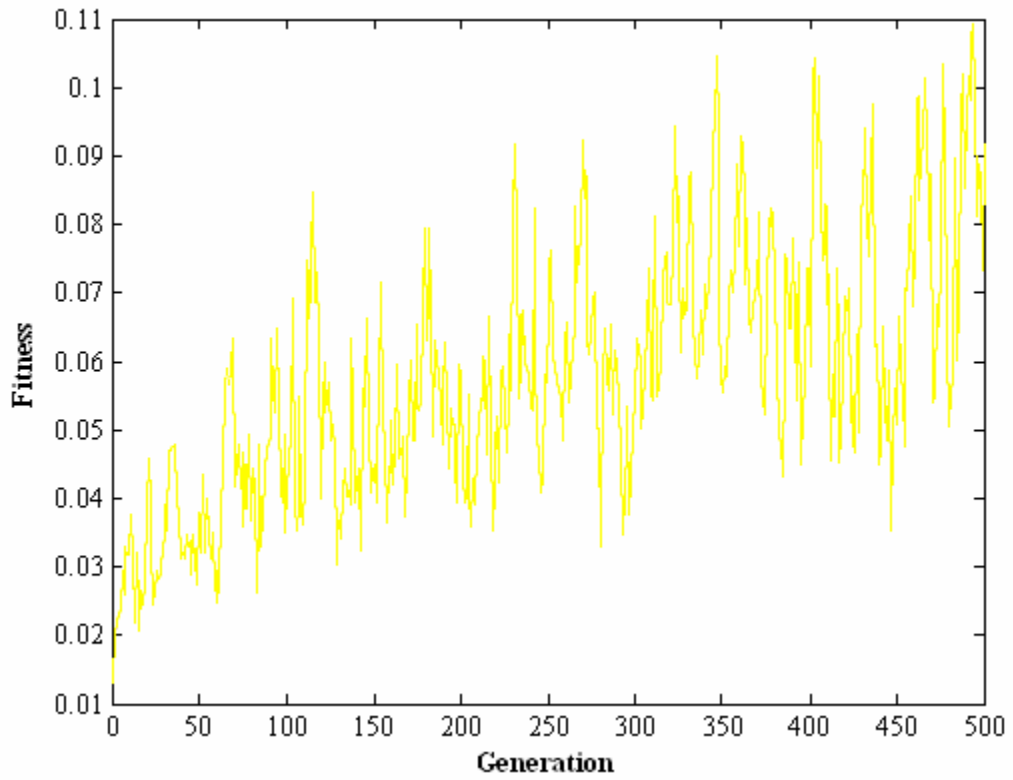
SR10_10_3_b_1



SR10_10_3_Fb_e_1



SR10_10_3_Fb_e_2



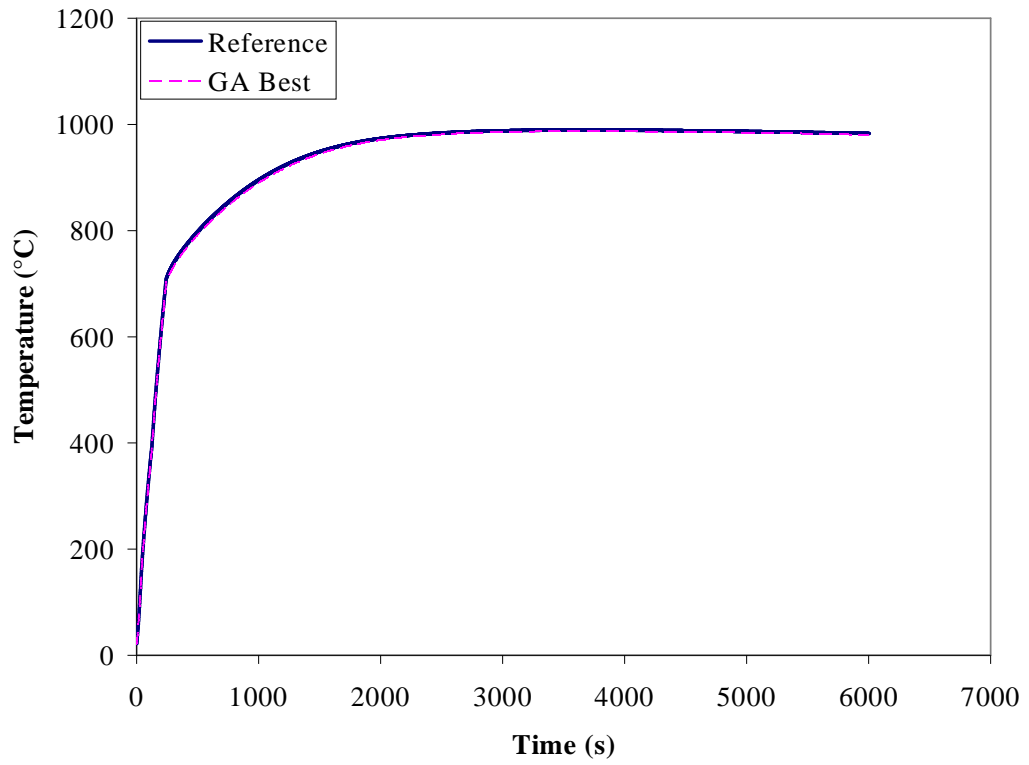
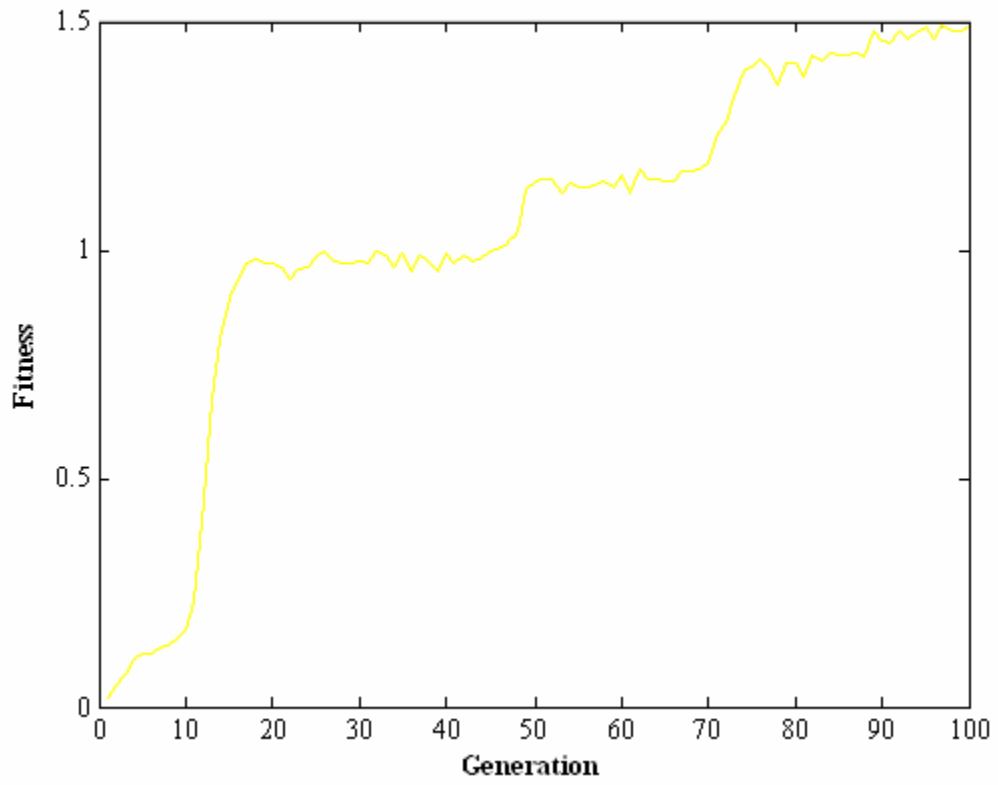
Appendix A3

Simulation Number	Reference MLR	Reference Average HRR	Reference Door	Reference Window	GA Best MLR	GA Best Average HRR	GA Best Door	GA Best Window	Bounds on MLR	Bounds on Door	Bounds of Window	Notes on Simulation
SR3_3_3_Fb_a_1	2300kW	1526 kW (240-6000s)	1m x 2m	1.0m wide. 1.5-2.5m high.	2303 kW	1555 kW (240-6000s)	0.97m x 2.09 m	1.0m wide. 1.08-2.49m high.	1,000-7,000 kW	Width: 0.75m-2m, Height: 1m-2.9m	Width 0-1m Upper end 1.5-3m Lower end 0-1.5m	Population size of 100, 100 generations *
SR3_3_3_Fb_a_2	3000 kW	1663 kW (240-6000s)	1m x 2m	1.0m wide. 1.5-2.5m high.	3003 kW	1669 kW (240-6000s)	1.00mx 2.61 m	.86m wide. 1.48m 1.88m high.	1000-6,000 kW	Width: 1m-2m, Height: 1m-2.9m	Width 0.5-1.5m Upper end 1.5-2.5m Lower end .5-1.5m	Population size of 25, 50 generations
SR3_3_3_Fb_a_3	3000 kW	1663 kW (240-6000s)	1m x 2m	1.0m wide. 1.5-2.5m high.	3061 kW	1667 kW (240-6000s)	1.03mx 2.48m	1.33 m wide. 1.50m - 1.88m high.	1,000-6,000 kW	Width: 1m-2m, Height: 1m-2.5m	Width 0.5 - 1.5m Upper end 1.5-3m Lower end 0-1.5m	Population size of 25. 25 generations Overall Reference Curve.*
SR3_3_3_Fb_b_1	2300kW	1432 kW (2000-6000s)	1m x 2m	1.0m wide. 1.5-2.5m high.	2423 kW	1510 kW (2000-6000s)	1.0m x 2.8 m	0m wide. 1.3m-2.9m high.	1,000-6,000 kW	Width: 1m-2m, Height: 1m-2.9m	Width 0-1m Upper end 1.5-3m Lower end 0-1.5m	Population size of 50, 50 generations
SR3_3_3_Fb_b_2	3000 kW	1671 kW (2000-6000s)	1m x 2m	1.0m wide. 1.5-2.5m high.	5162 kW	1647 kW (2000-6000s)	.71m x 1.64m	1.40m wide. 1.07m - 2.36m high.	200-6,000 kW	Width: 1m-2m, Height: 1m-2.0m	Width 0.5-1.5m Upper end 1.5-3m Lower 0-1.5m	Population size of 25, 50 generations
SR3_3_3_Fb_b_3	2300kW	1527 kW (2000-6000s)	1m x 2m	1.0m wide. 1.5-2.5m high.	2343 kW	1560 kW (2000-6000s)	1.24m x 1.25m	1.46m wide. 1.47m-2.46m high.	200-5,000 kW	Width: 1m-2m, Height: 1m-2.0m	Width 0.5-1.5m Upper end 1.5-2.5m Lower 0.5-1.5m	Population size of 25, 50 generations
SR3_3_3_Fb_b_4	5700kW	1809 kW (2000-6000s)	1m x 2m	1.0m wide. 1.5-2.5m high	2759 kW	1495 kW (2000-6000s)	1.24m x 1.29m	1.43m wide. 1.13m - 2.37m high.	200-6,000 kW	Width: 1m-2m, Height: 1m-2.0m	Width 0.5-1.5m Upper end 1.5-3m Lower 0-1.5m	Population size of 25, 50 generations
SR3_3_3_Fb_b_5	3000 kW	1539 kW (2000-6000s)	1m x 2m	1.0m wide. 1.5-2.5m high.	3118 kW	1552 kW (2000-6000s)	1.00m x 1.83m	.89m wide. 1.43m - 2.69m high.	200-5,000 kW	Width: 1m-2m, Height: 1m-2.5m	Width 0.5 -1.5m Upper end 1.5-3m Lower 0-1.5m	Population size of 20. 50 generations
SR3_3_3_Fb_c_1	3000kW	1539 kW (2000-6000s)	1m x 2m	1.0m wide. 1.5m-2.5m high	2786 kW	1421 kW (2000-6000s)	.69m x 2.15m	.72m wide. 1.08m-2.67m high	200-4,500 kW	Width: .5-2m wide. Height: 1-2.5m	Width 0 - 2.0m Upper end 1.5-3m Lower 0-1.5m	Population size of 25, 25 generations
SR3_3_3_Fb_d_1	3000 kW	1539 kW (2000-6000s)	1m x 2m	1.0m wide. 1.5m-2.5m high	3225 kW	1435 kW (2000-6000s)	.53m x 1.50m	1.24m wide. .96m - 2.48m high	200-4,500 kW	Width: .5-2m wide. Height: 1-2.5m	Width 0 - 2.0m Upper end 1.5-3m Lower 0-1.5m	Population size of 25. 25 generations

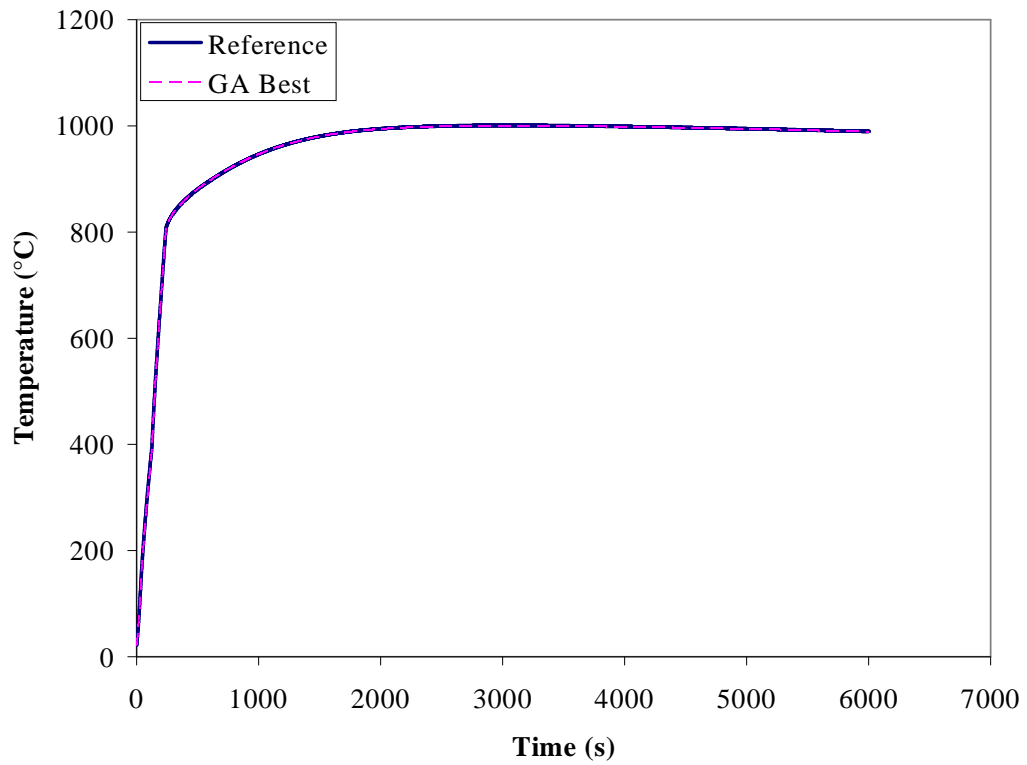
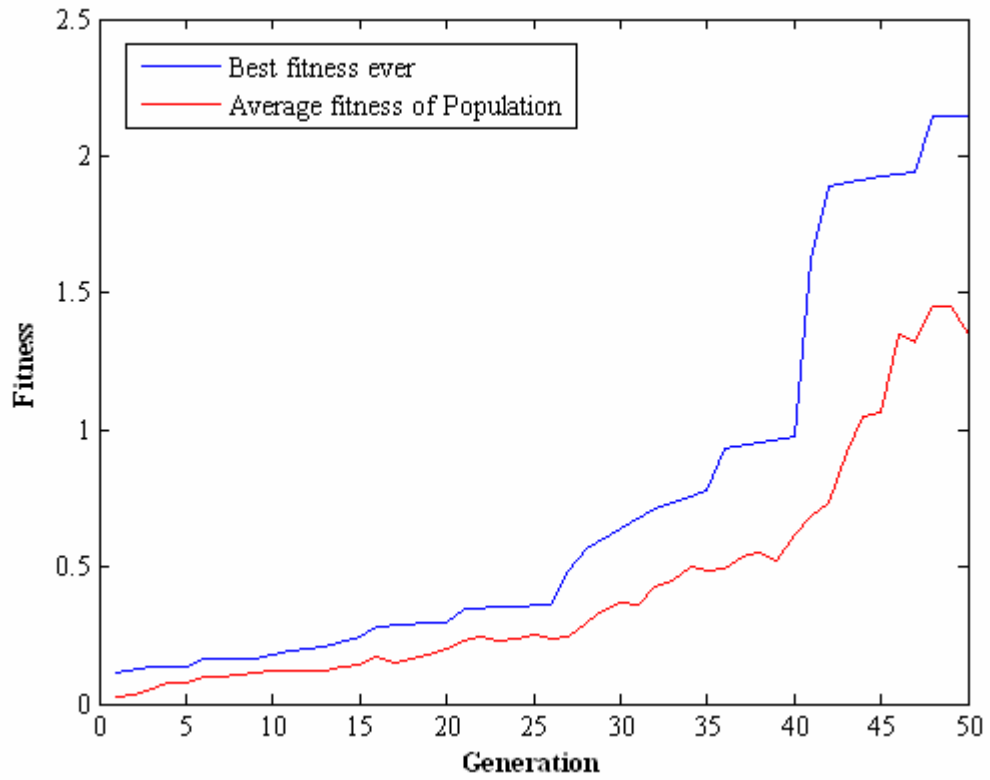
Simulation Number	Reference MLR	Reference Average HRR	Reference Door	Reference Window	GA Best MLR	GA Best Average HRR	GA Best Door	GA Best Window	Bounds on MLR	Bounds on Door	Bounds of Window	Notes on Simulation
SR3_3_3_Fb_e_1.	2300kW	1432 kW (2000-6000s)	1m x 2m	1.0m wide. 1.5-2.5m high.	3688 kW	2195 kW (2000-6000s)	1.1m x 2.9m	0.9m wide. 1.4m-2.9m high	1,000-6,000 kW	Width: 1m-2m, Height: 1m-2.9m	Width 0-1m Upper end 1.5-3m Lower end 0-1.5m	Population size of 50, 50 generations
SR3_3_3_Fb_e_2	2300kW	1527 kW (240-6000s)	1m x 2m	1.0m wide. 1.5-2.5m high.	5998 kW	2055 kW (240-6000s)	1.3m x 2.2 m	1.0m wide. 1.1m-2.2m high.	1,000-6,000 kW	Width: 1m-2m, Height: 1m-2.9m	Width 0-1m Upper end 1.5-3m Lower end 0-1.5m	Population size of 50. 50 generations Analyzed 0-6000s
SR3_3_3_Fb_e_3	2300kW	1432 kW (2000-6000s)	1m x 2m	1.0m wide. 1.5-2.5m high.	2572 kW	1433 kW (2000-6000s)	1.00m x 2.62	0.55 m wide. 1.16m-1.61m high.	1000-7,000 kW	Width: 1m-2m, Height: 1m-2.9m	Width 0.1 – 1m Upper end 1.5-3m Lower end 0-1.5m	Population size of 100, 100 generations
SR3_3_3_Fb_f_1	3000kW	1539 kW (2000-6000s)	1m x 2m	1.0m wide. 1.5m-2.5m high	3756 kW	1871 kW (2000-6000s)	1.22m x 2.26m	.67m wide. 1.02m - 2.898m high.	200-4,500 kW	Width: 0.5-2m Height: 1-2.5m	Width 0 – 2.0m Upper end 1.5-3m Lower end 0-1.5m	Population size of 25, 25 generations
SR3_3_3_Fb_h_1	2300kW	1432 kW (2000-6000s)	1m x 2m	1.0m wide. 1.5-2.5m high.	3064 kW	1364 kW (2000-6000s)	1.00 m x 1.34 m	0.56m wide. 1.13m-2.97m high.	1,000-6,000 kW	Width: 1m-2m, Height: 1m-2.9m	Width 0-1m Upper end 1.5-3m Lower end 0-1.5m	Population size of 100. 100 generations
SR3_3_3_NC_b_1	200 kW	200 kW (2000-6000s)	1m x 2m	1.0m wide. 1.5m-2.5m high	203 kW	203 kW (2000-6000s)	.65m x 1.85 m	1.86m wide 0.80m – 2.29m high.	200-6,000 kW	Width: 0.5-2m, Height: 1-2.5m	Width 0-2m Upper end 1.5-3m Lower end 0-1.5m	Population size 20, 50 generations
SR3_3_3_NC_b_2	600 kW	598 kW (2000-6000s)	1m x 2m	1.0m wide. 1.5-2.5m high.	549kW	548 kW (2000-6000s)	1.52 m x 2.10 m	1.13m wide. .61m - 1.92m high.	200-6,000 kW	Width: 0.5-2m, Height: 1-2.5m	Width 0-2m Upper end 1.5-3m Lower end 0-1.5m	Population size 20, 50 generations
SR3_3_3_NC_b_3	1000 kW	995 kW (2000-6000s)	1m x 2m	1.0m wide. 1.5-2.5m high.	909 kW	788 kW (2000-6000s)	.96m x 1.21m	0.18m wide. 1.32m - 2.60m high.	200-6,000 kW	Width: 0.5-2m, Height: 1-2.5m	Width 0-2m Upper end 1.5-3m Lower end 0-1.5m	Population size 20, 50 generations
SR3_3_3_NC_b_4	2000 kW	1638 kW (2000-6000s)	1m x 2m	1.0m wide. 1.5-2.5m high.	4263 kW	1952 kW (2000-6000s)	1.28 m x 1.93m	1.77m wide. 1.25m - 1.93m high.	200-6,000 kW	Width: 0.5-2m, Height: 1-2.5m	Width 0-2m Upper end 1.5-3m Lower end 0-1.5m	Population size 20, 50 generations
SR3_3_3_NC_b_5	3000 kW	1836 kW (2000-6000s)	1m x 2m	1.0m wide. 1.5-2.5m high.	3396 kW	1890 kW (2000-6000s)	1.07m x 1.96m	1.36m wide. 1.32m - 2.25m high.	200-6,000 kW	Width: 0.5-2m, Height: 1-2.5m	Width 0-2m Upper end 1.5-3m Lower end 0-1.5m	Population size 20, 50 generations

Simulation Number	Reference MLR	Reference Average HRR	Reference Door	Reference Window	GA Best MLR	GA Best Average HRR	GA Best Door	GA Best Window	Bounds on MLR	Bounds on Door	Bounds of Window	Notes on Simulation
SR3_3_3_ NC_c_1	500 kW	499 kW (2000-6000s)	1m x 2m	1.0m wide. 1.5-2.5m high.	540 kW	538 kW (2000-6000s)	.52m x 2.50m	.51m wide. .24m - 2.98m high.	200-6,000 kW	Width: 0.5m-2m, Height: 1m-2.5m	Width 0-2m Upper end 1.5-3m Lower end 0-1.5m	Population size of 20, 50 generations
SR3_3_3_ NC_d_1	500 kW	499 kW (2000-6000s)	1m x 2m	1.0m wide. 1.5-2.5m high.	574 kW	572 kW (2000-6000s)	2.00m x 2.42m	.39m wide. .14m - 2.39m high.	200-6,000 kW	Width: 0.5m-2m, Height: 1m-2.5m	Width 0-2m Upper end 1.5-3m Lower end 0-1.5m	Population size of 20, 50 generations
SR3_3_3_ NC_f_1	500 kW	499 kW (2000-6000s)	1m x 2m	1.0m wide. 1.5-2.5m high.	433 kW	432 kW (2000-6000s)	2.00m x 1.00m	.90m wide. 0m - 2.36m high.	200-6,000 kW	Width: 0.5m-2m, Height: 1m-2.5m	Width 0-2m Upper end 1.5-3m Lower end 0-1.5m	Population size of 20, 50 generations
SR3_3_3_ NC_g_1	500 kW	499 kW (2000-6000s)	1m x 2m	1.0m wide. 1.5-2.5m high.	629 kW	626 kW (2000-6000s)	1.74m x 1.00m	1.35m wide. 1.13m - 2.82m high.	200-6,000 kW	Width: 0.5m-2m, Height: 1m-2.5m	Width 0-2m Upper end 1.5-3m Lower end 0-1.5m	Population size of 20, 50 generations

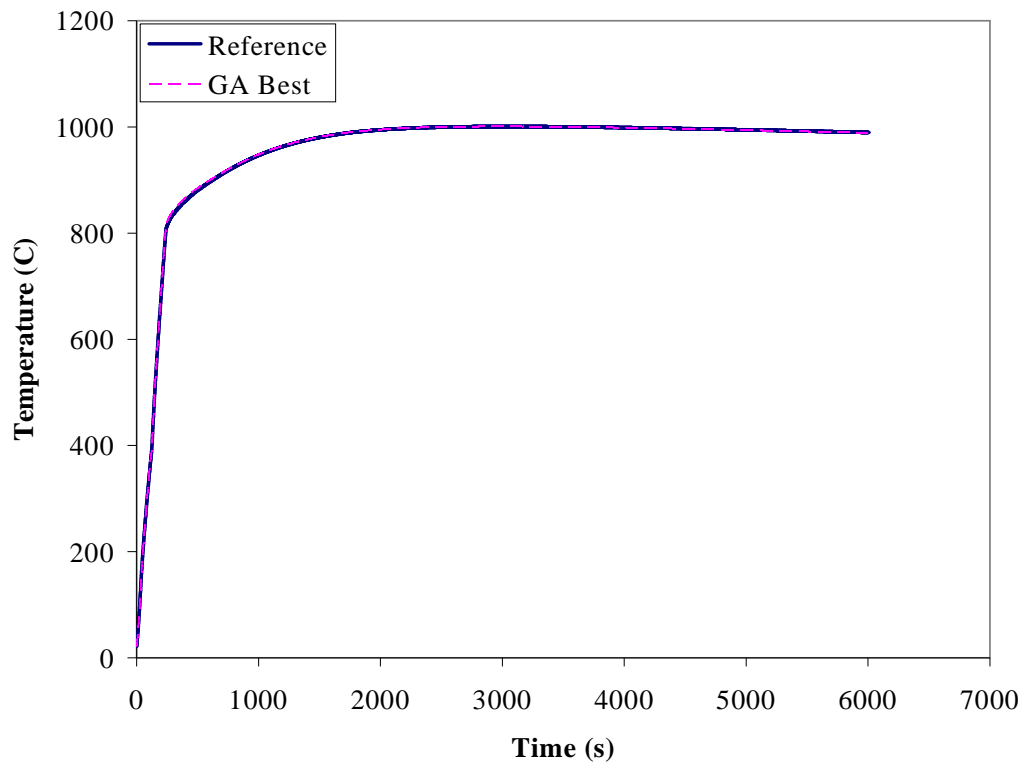
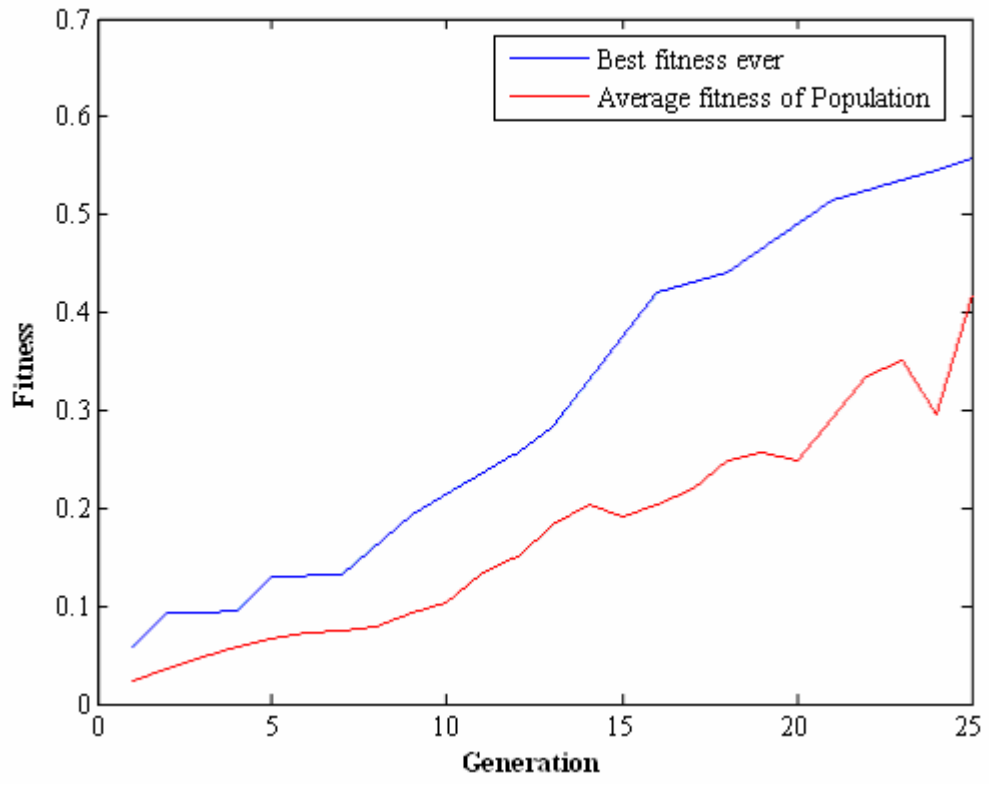
SR3_3_3_Fb_a_1



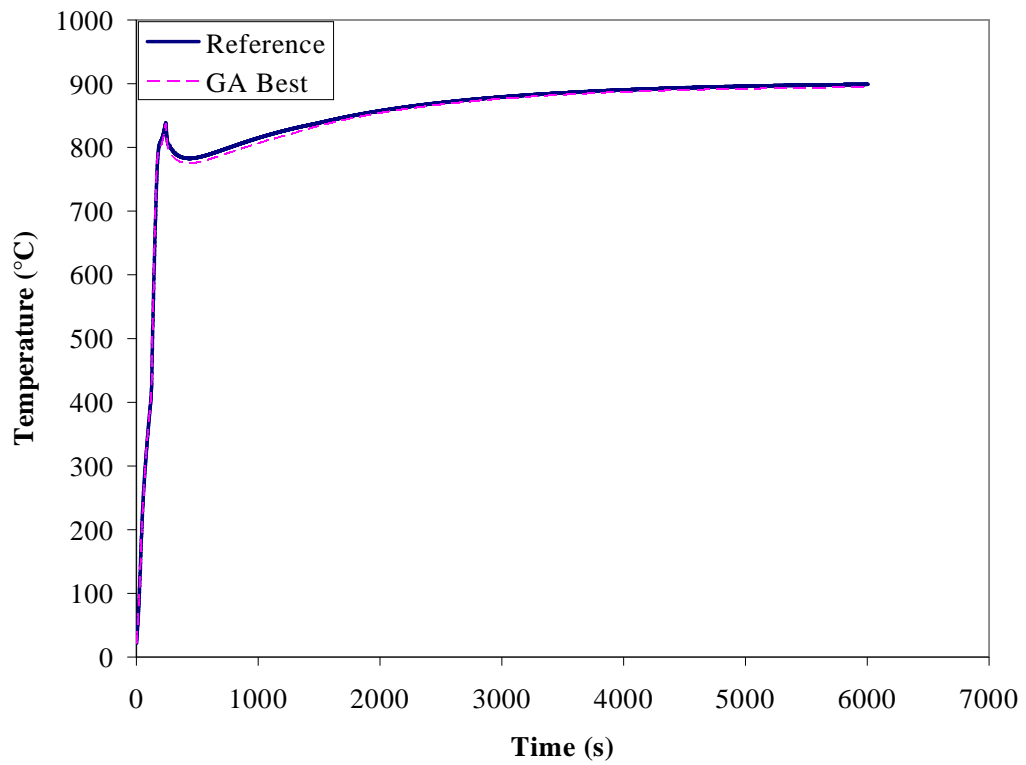
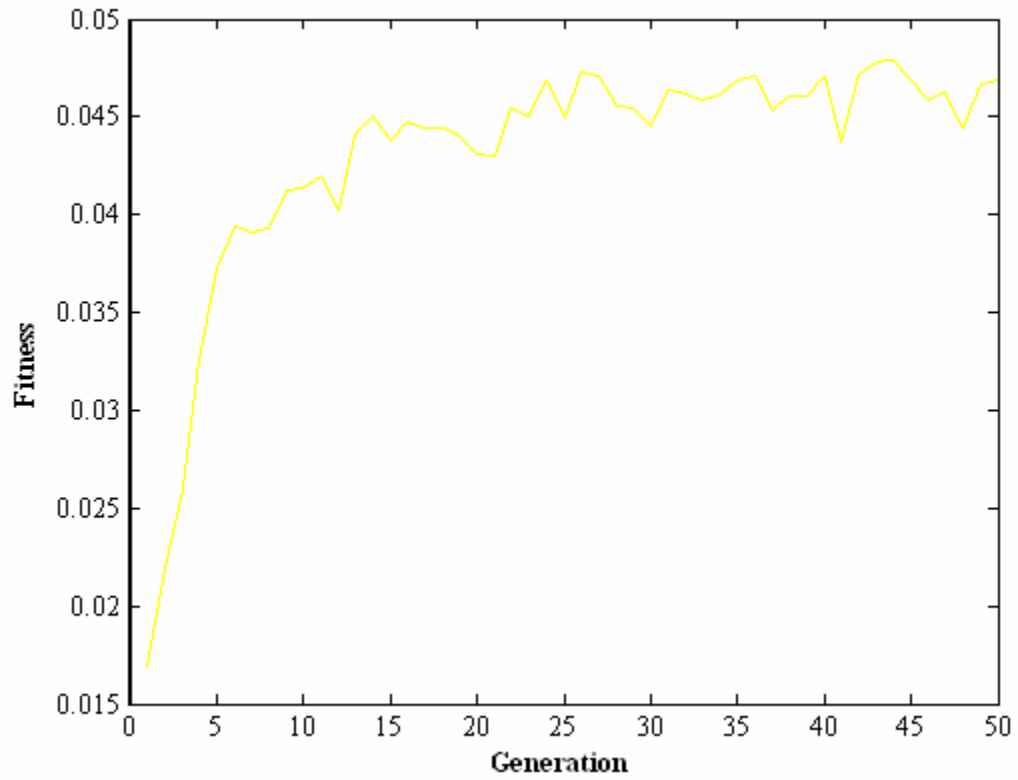
SR3_3_3_Fb_a_2



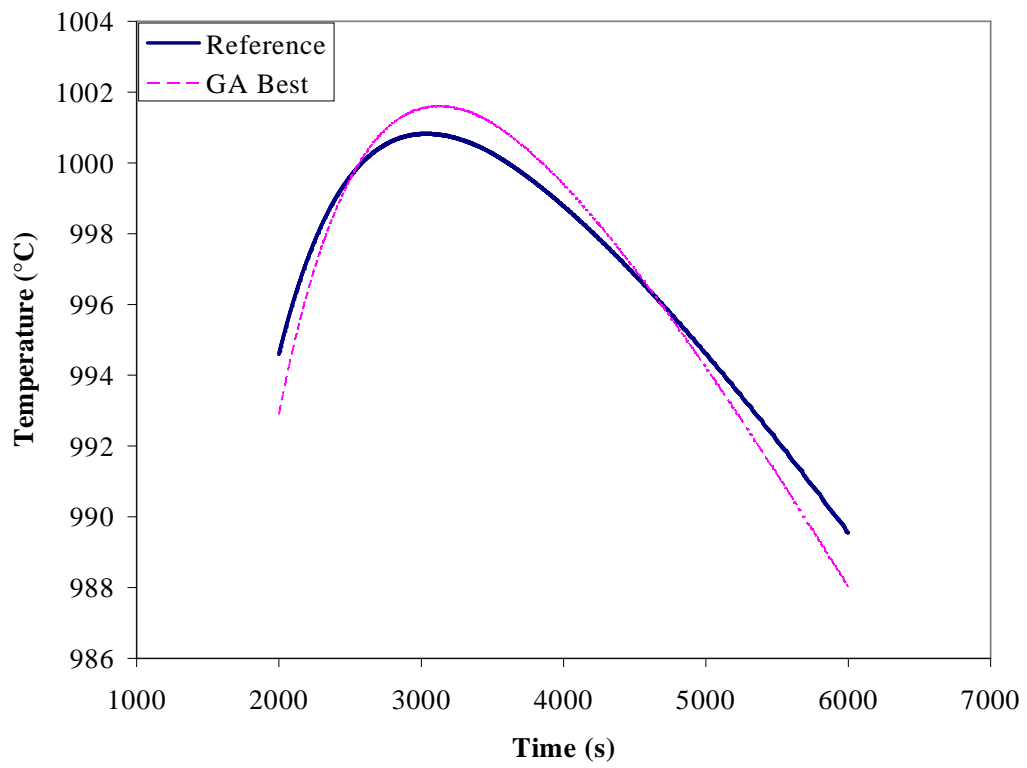
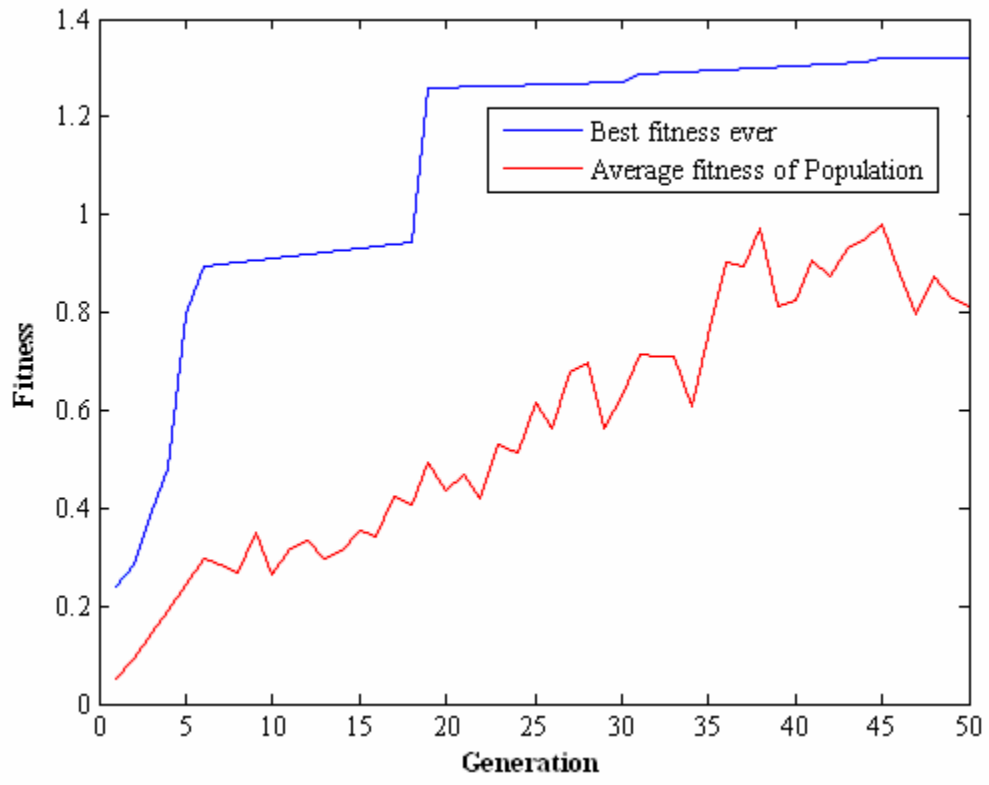
SR3_3_3_Fb_a_3



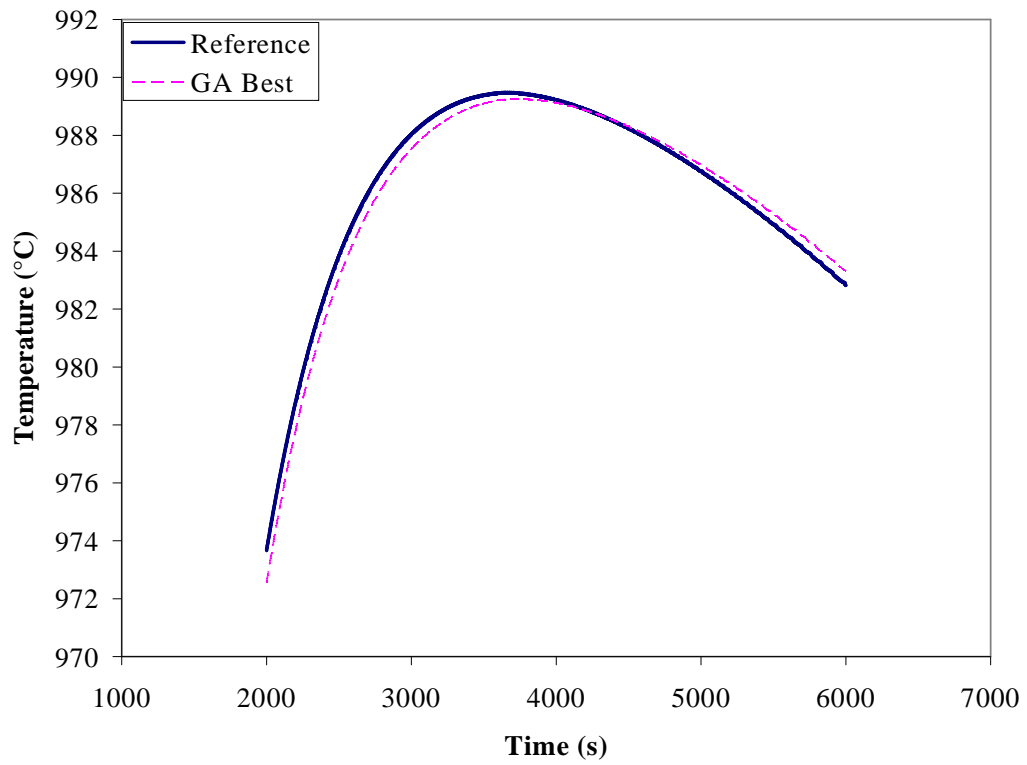
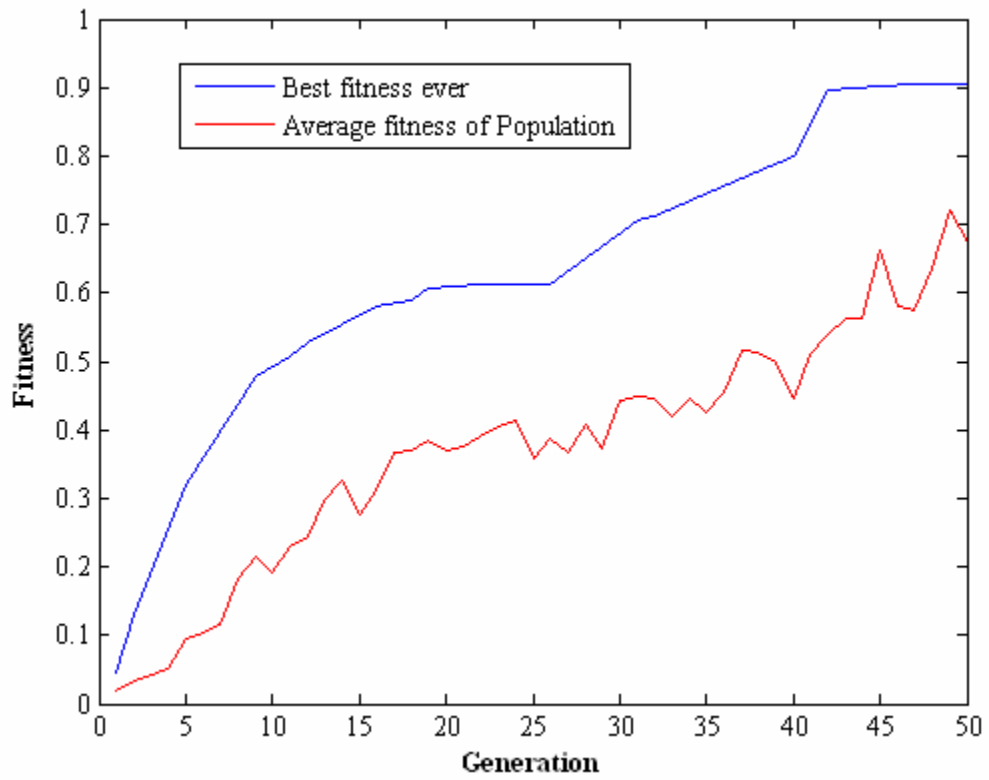
SR3_3_3_Fb_b_1



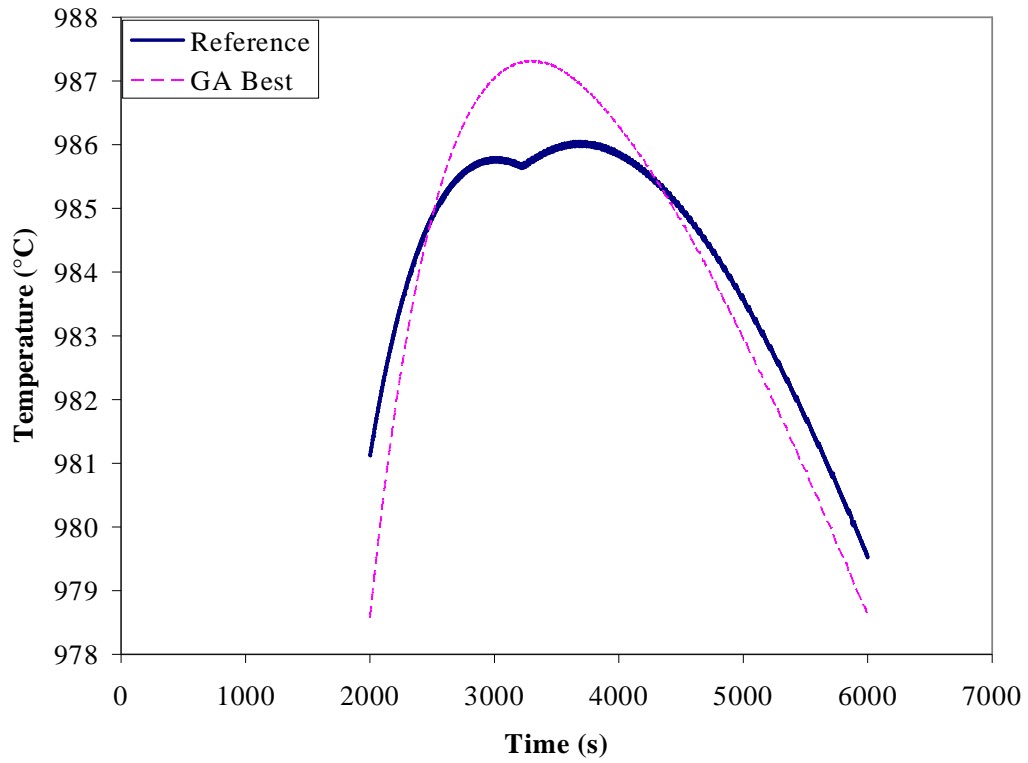
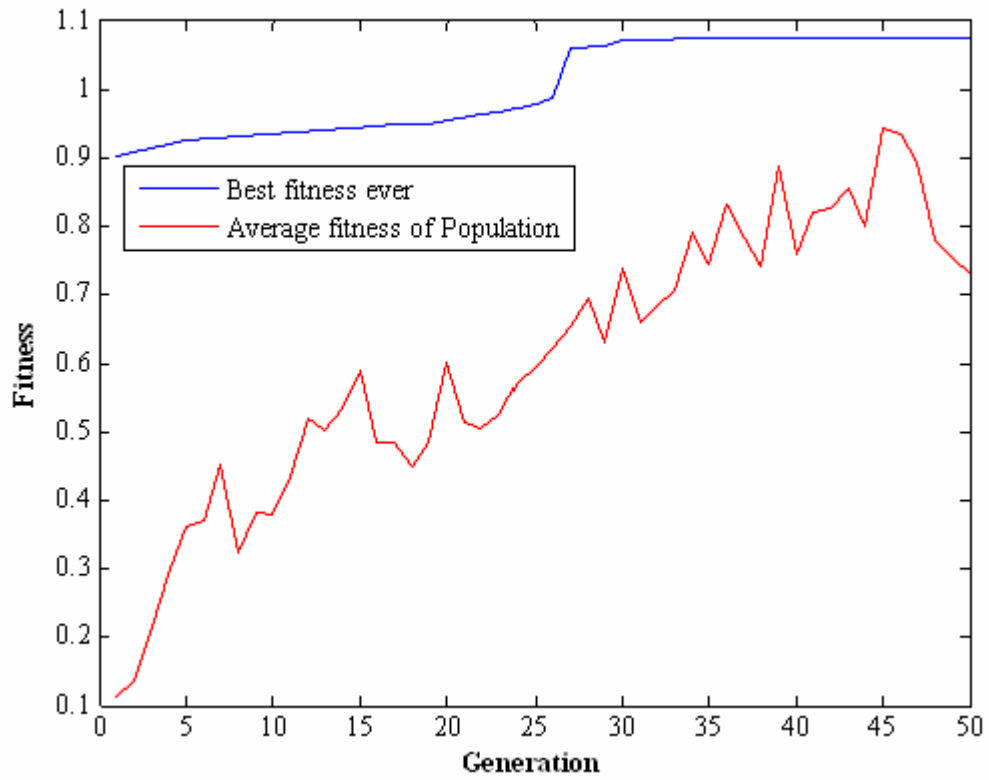
SR3_3_3_Fb_b_2



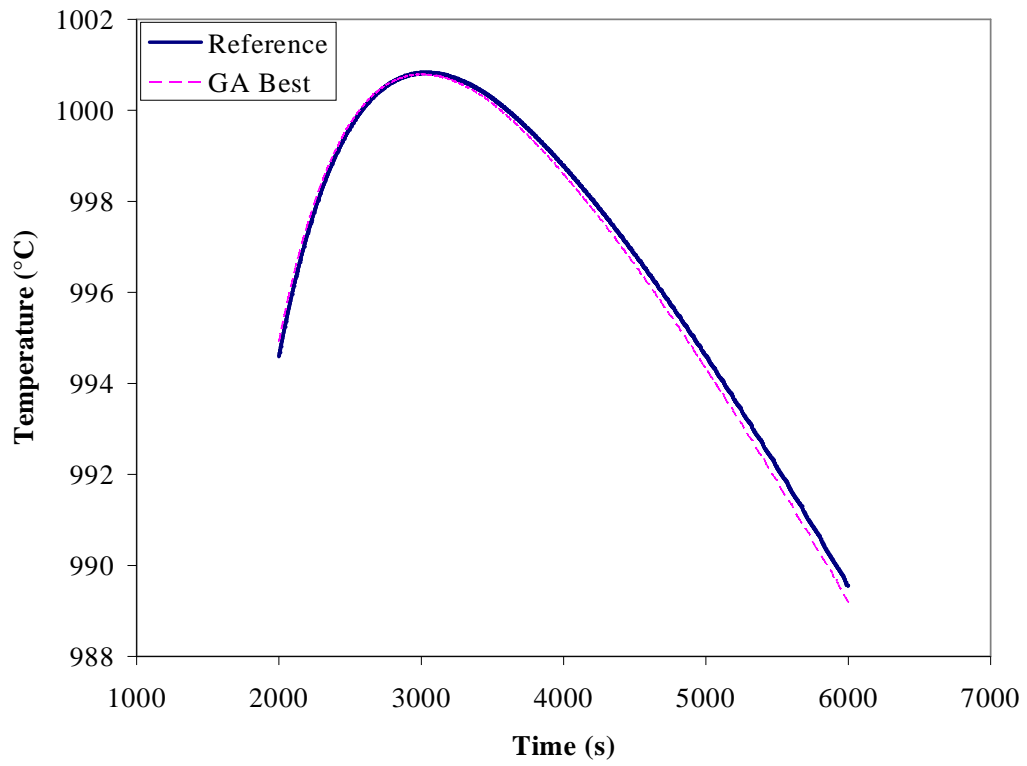
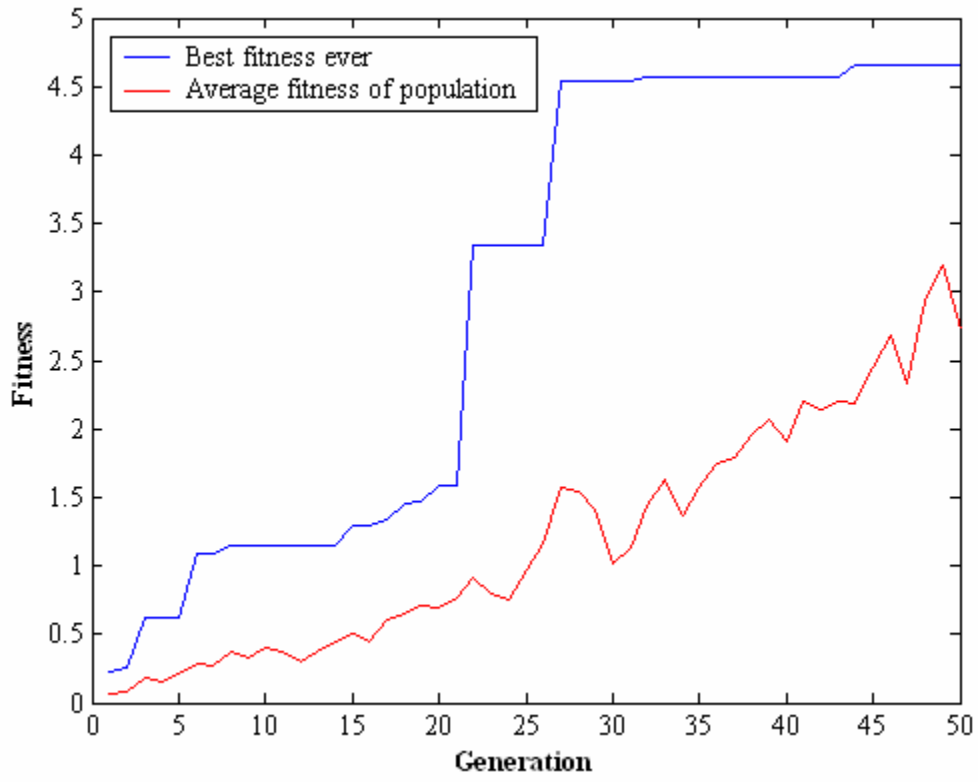
SR3_3_3_Fb_b_3



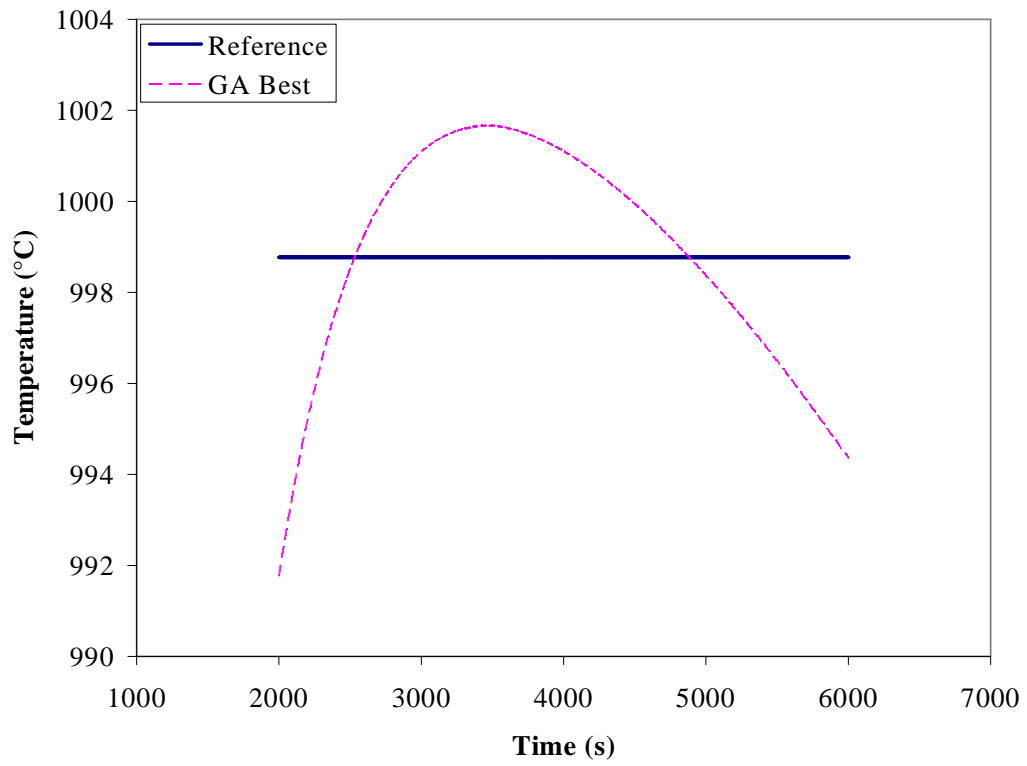
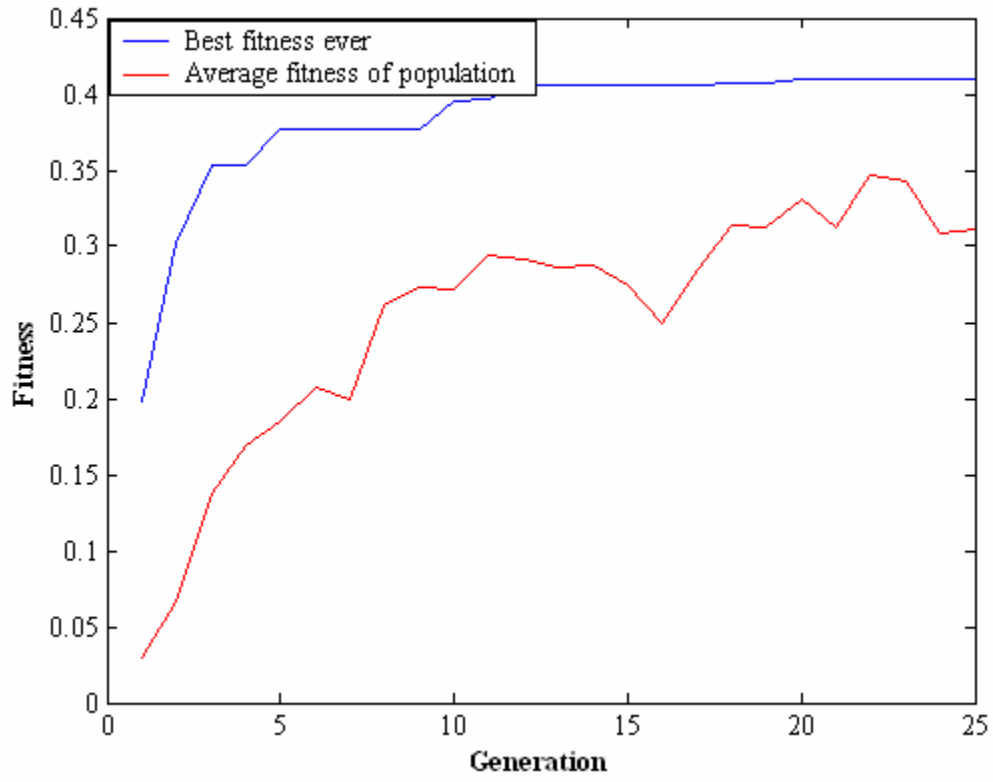
SR3_3_3_Fb_b_4



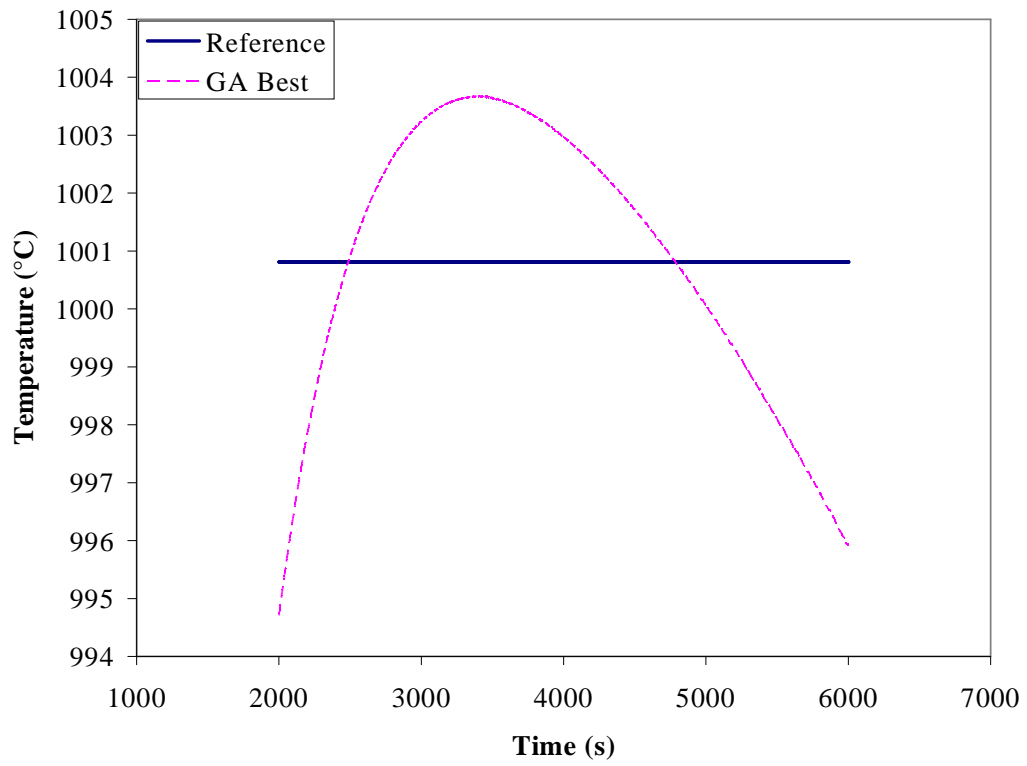
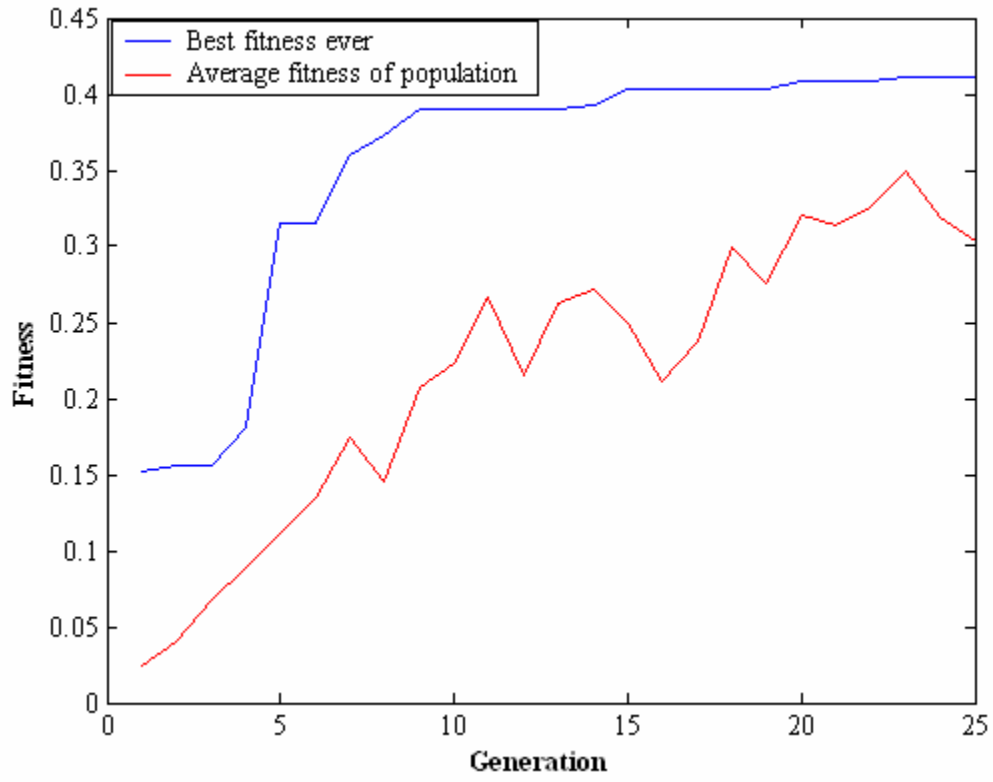
SR3_3_3_Fb_b_5



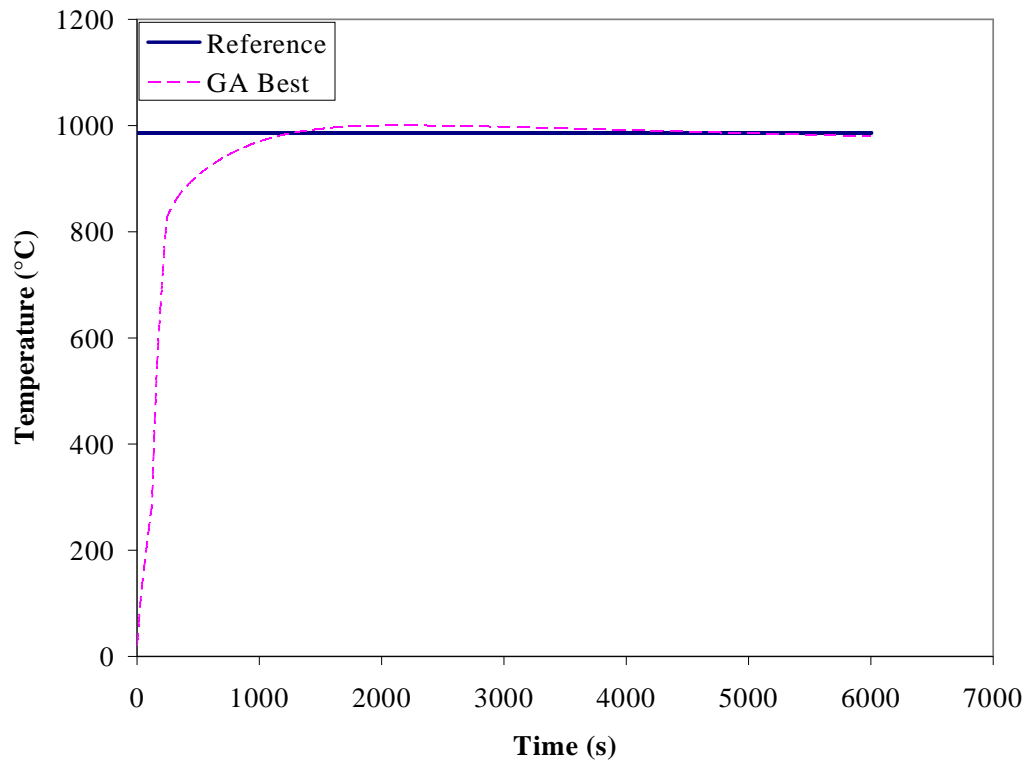
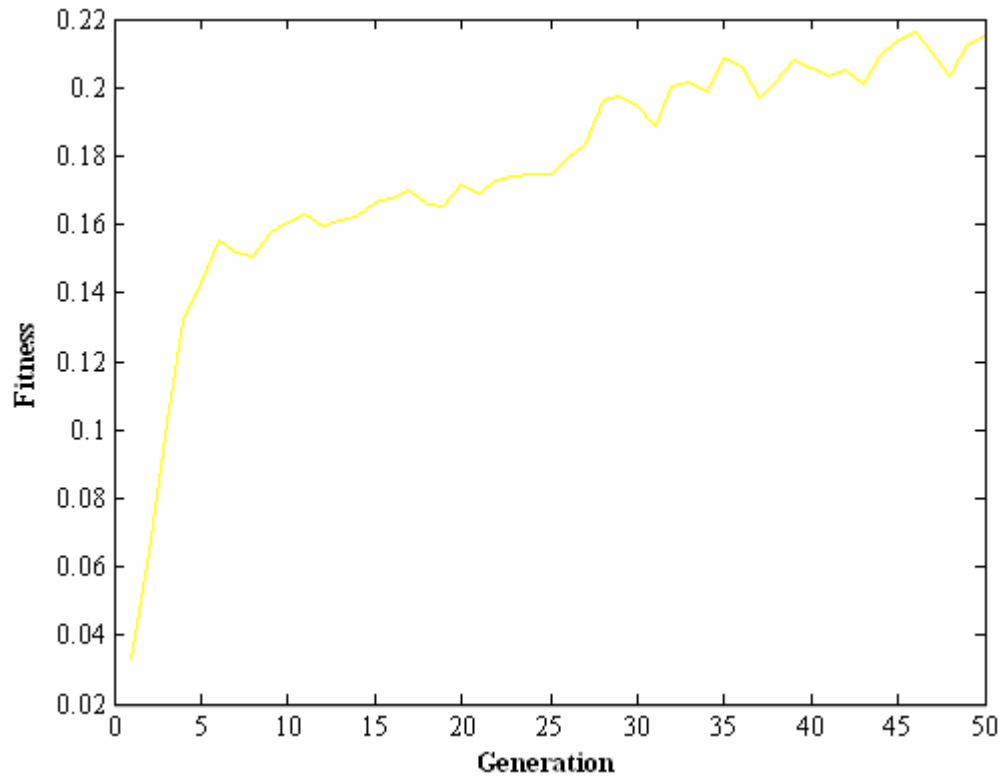
SR3_3_3_Fb_c_1



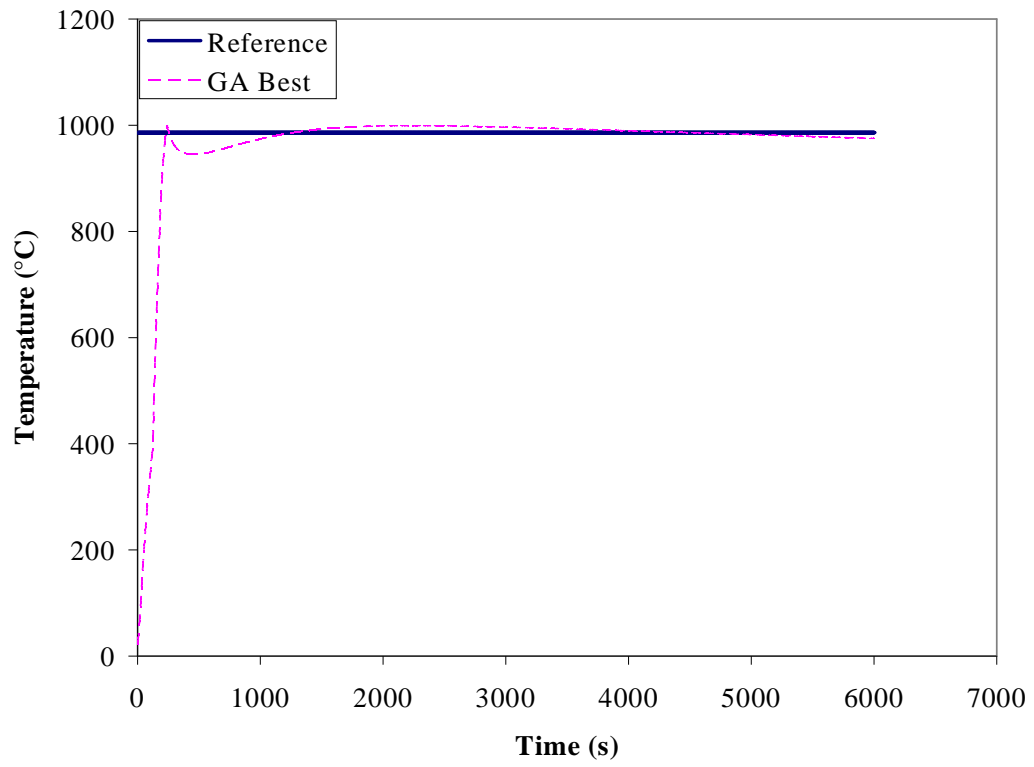
SR3_3_3_Fb_d_1



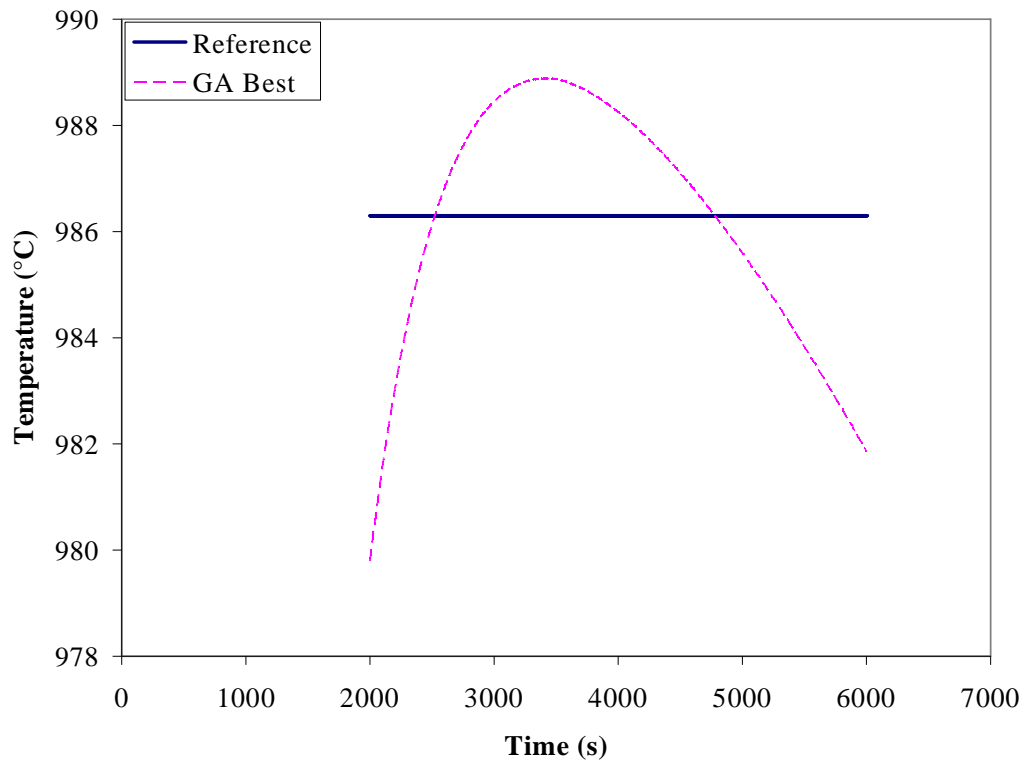
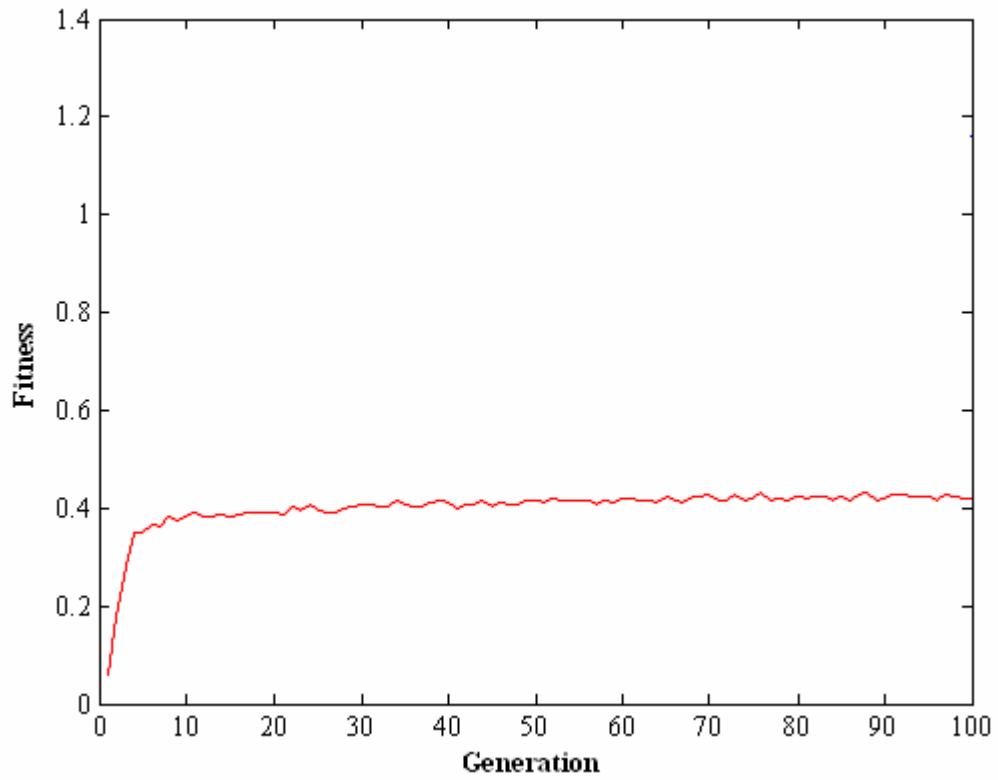
SR3_3_3_Fb_e_1



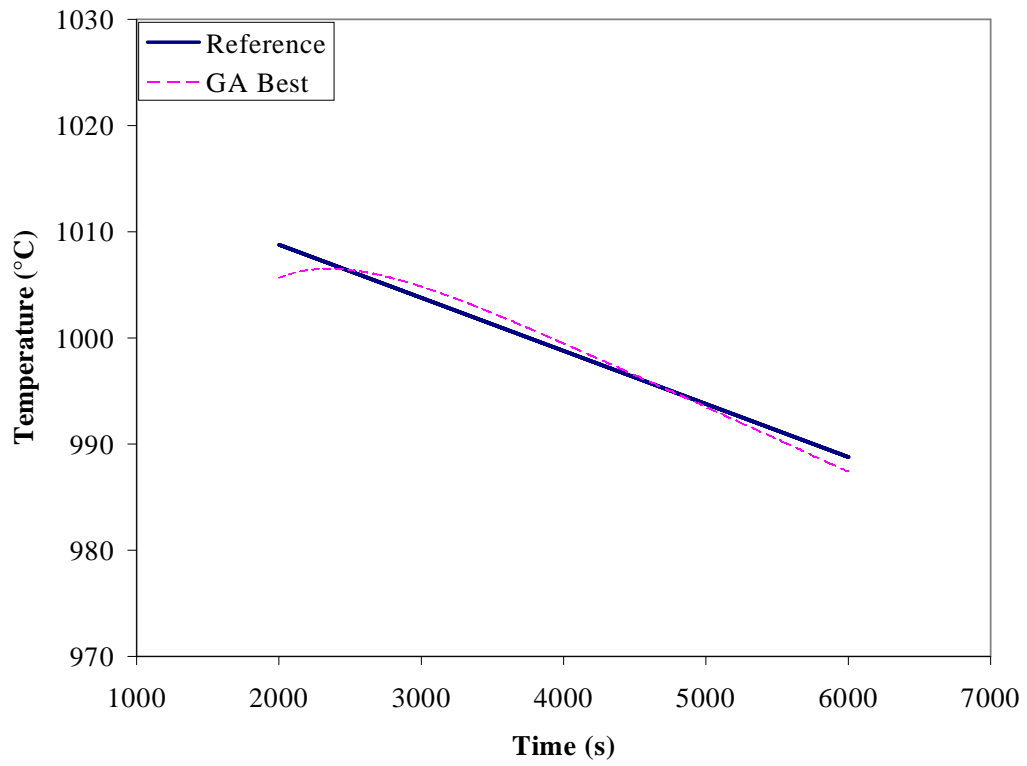
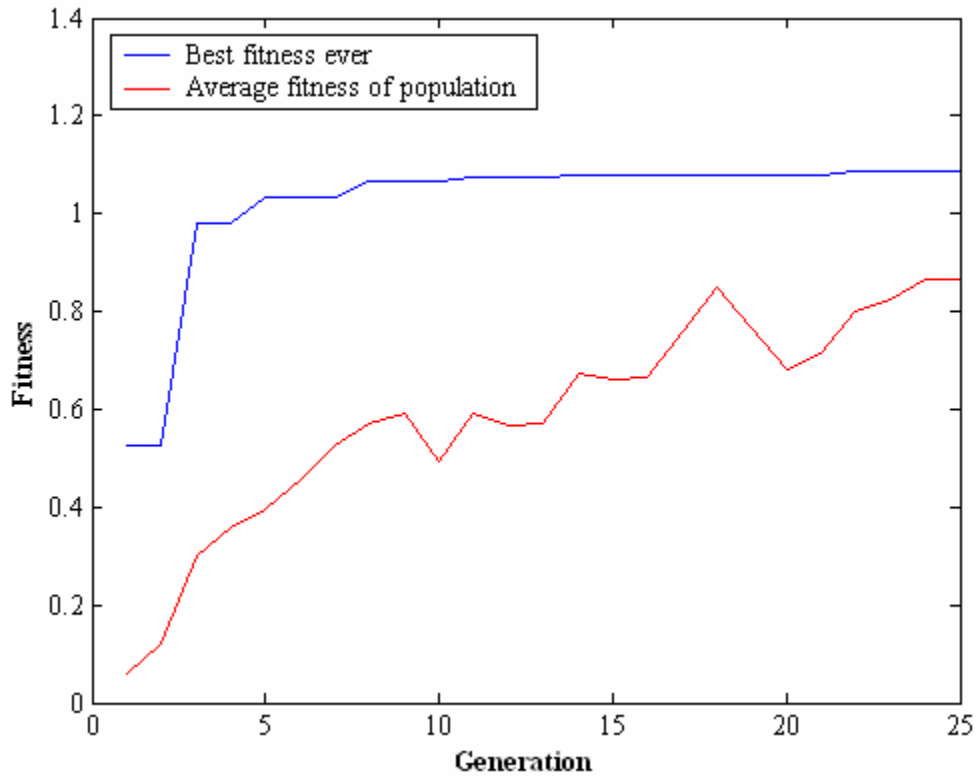
SR3_3_3_Fb_e_2



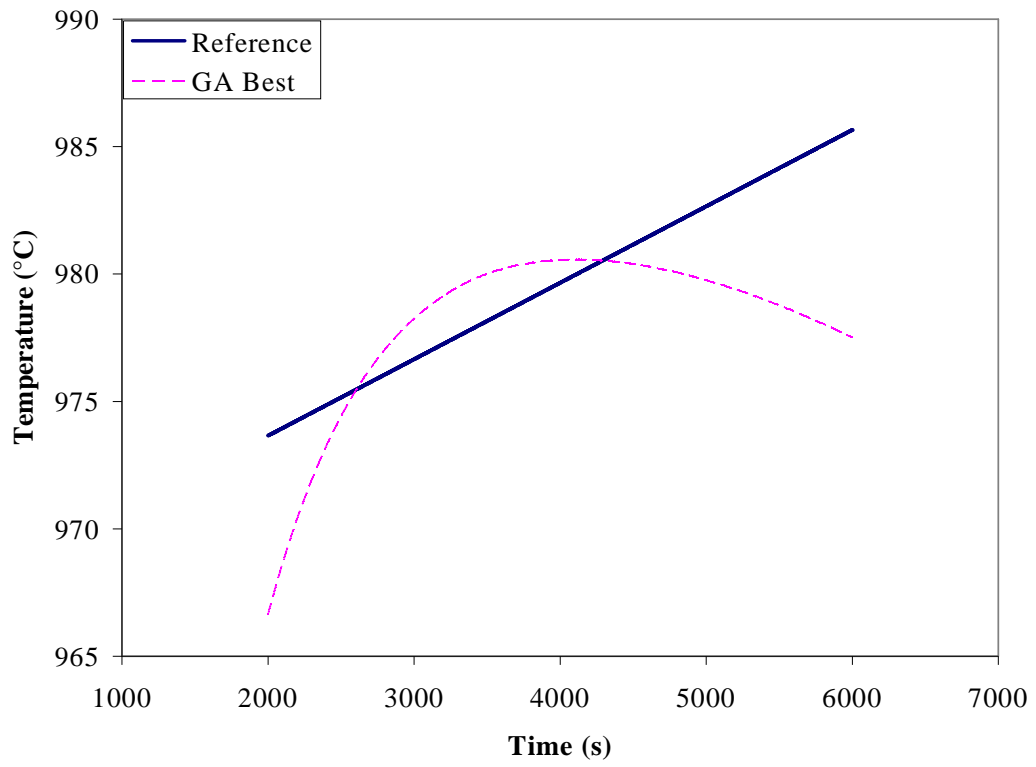
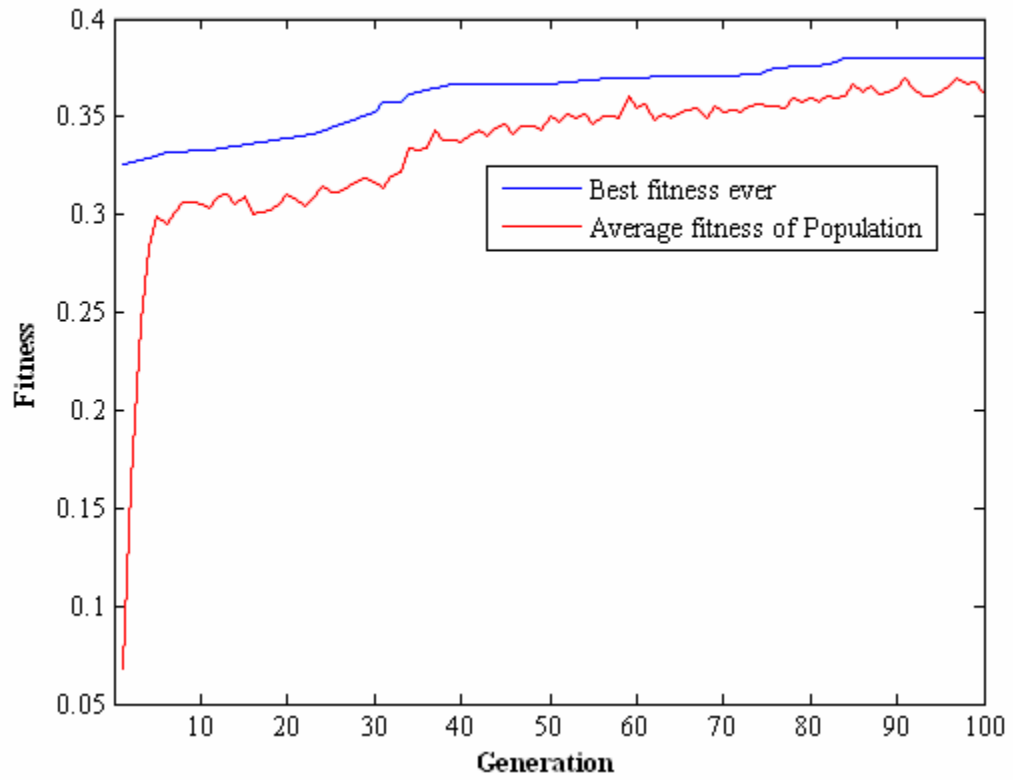
SR3_3_3_Fb_e_3



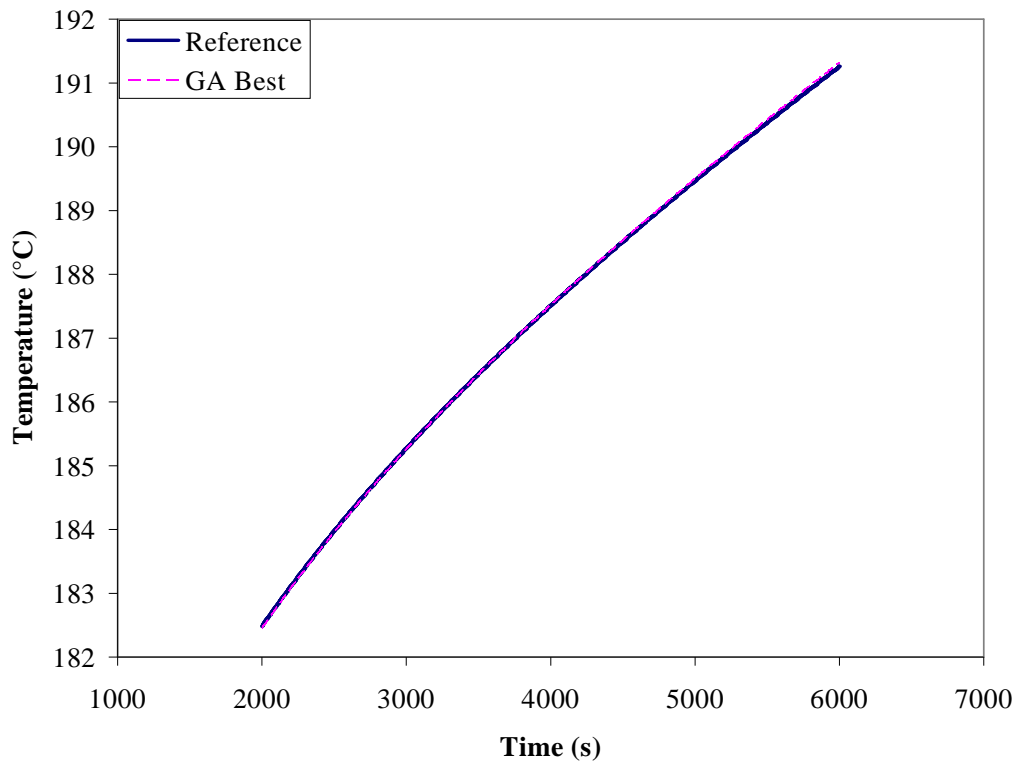
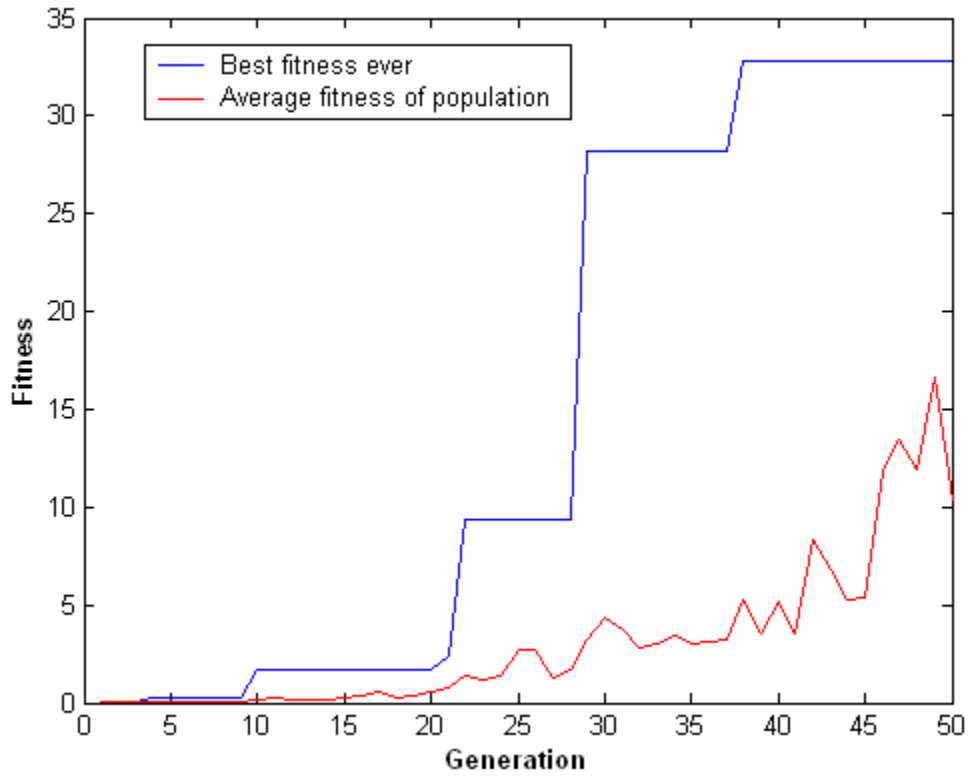
SR3_3_3_Fb_f_1



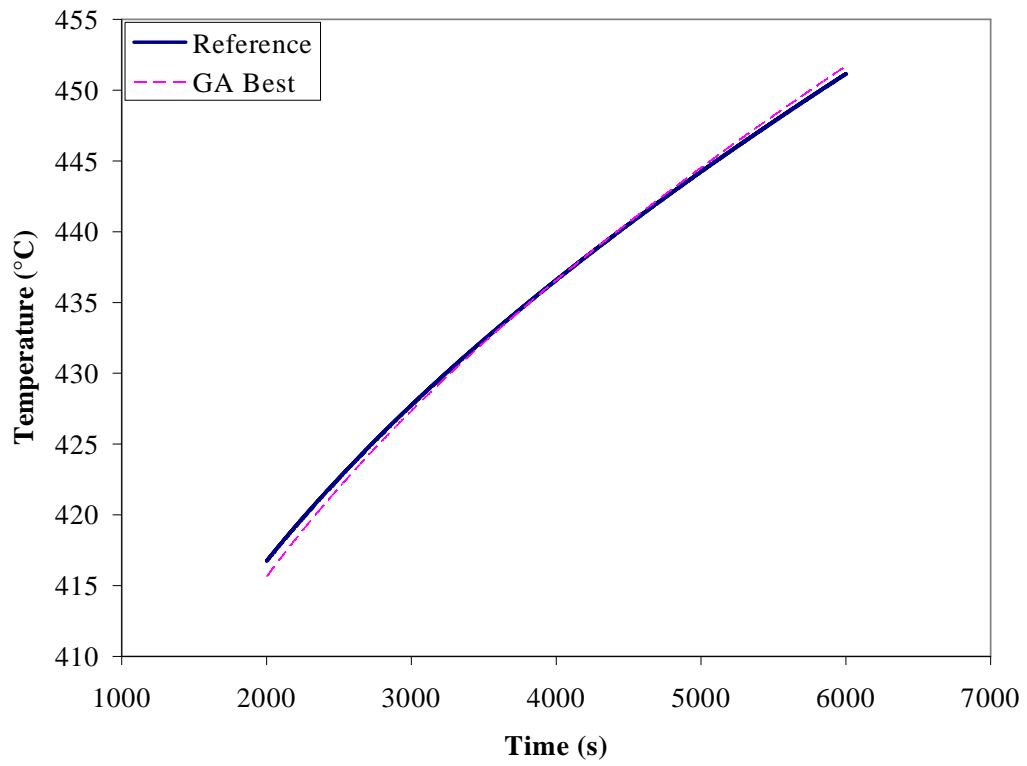
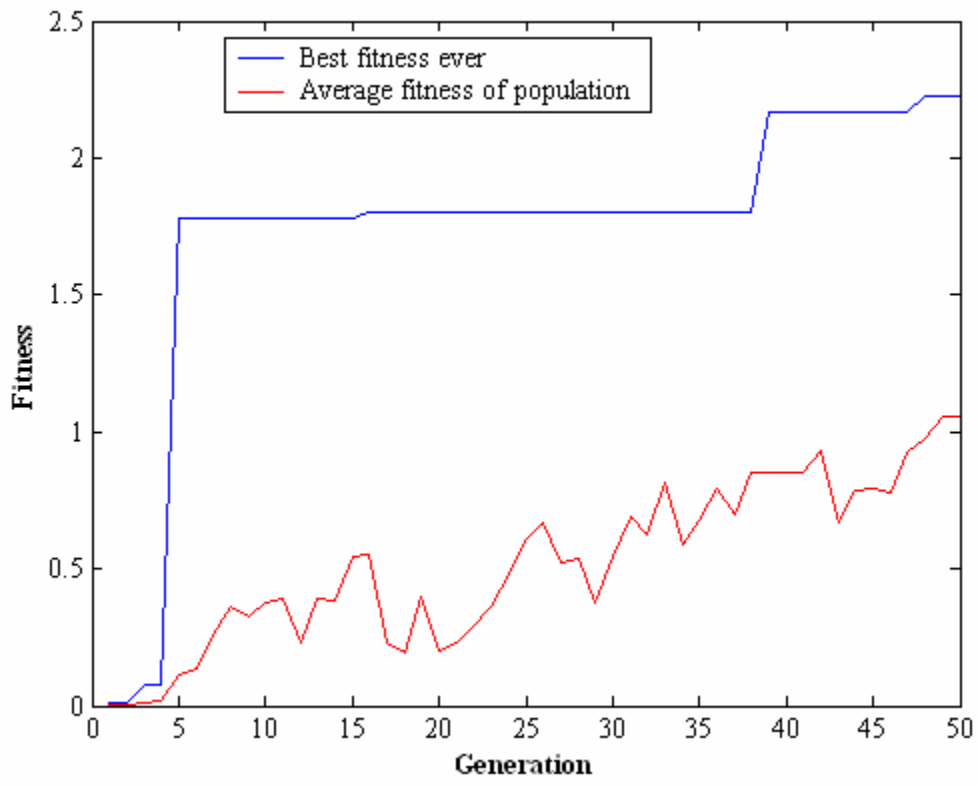
SR3_3_3_Fb_h_1



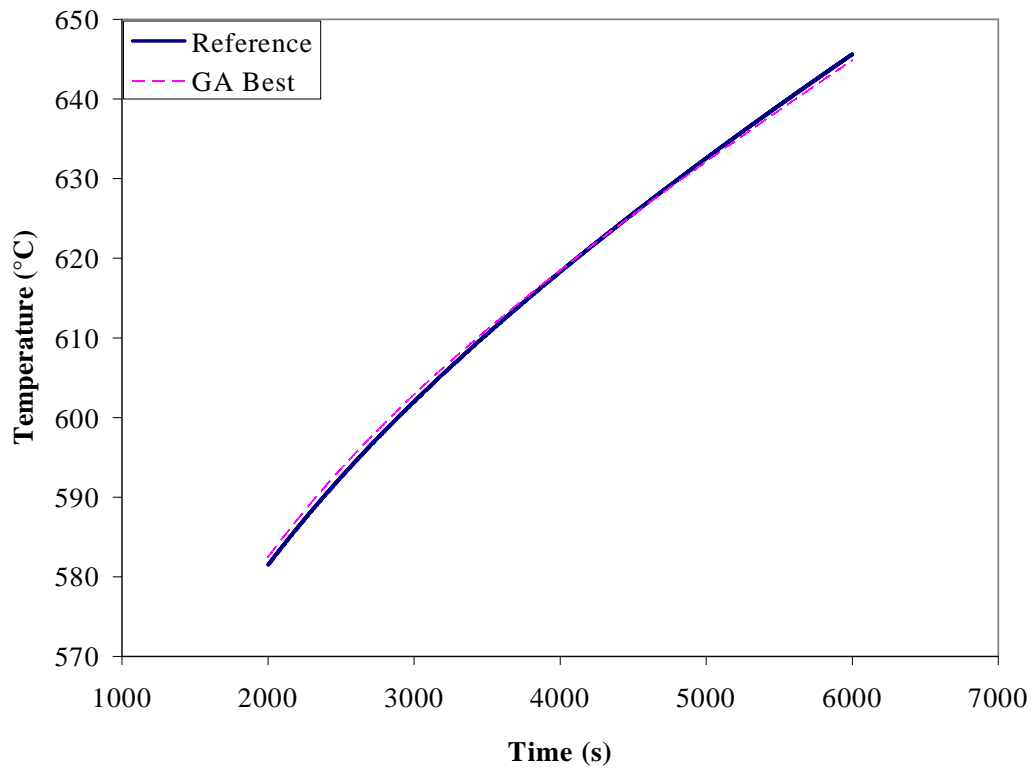
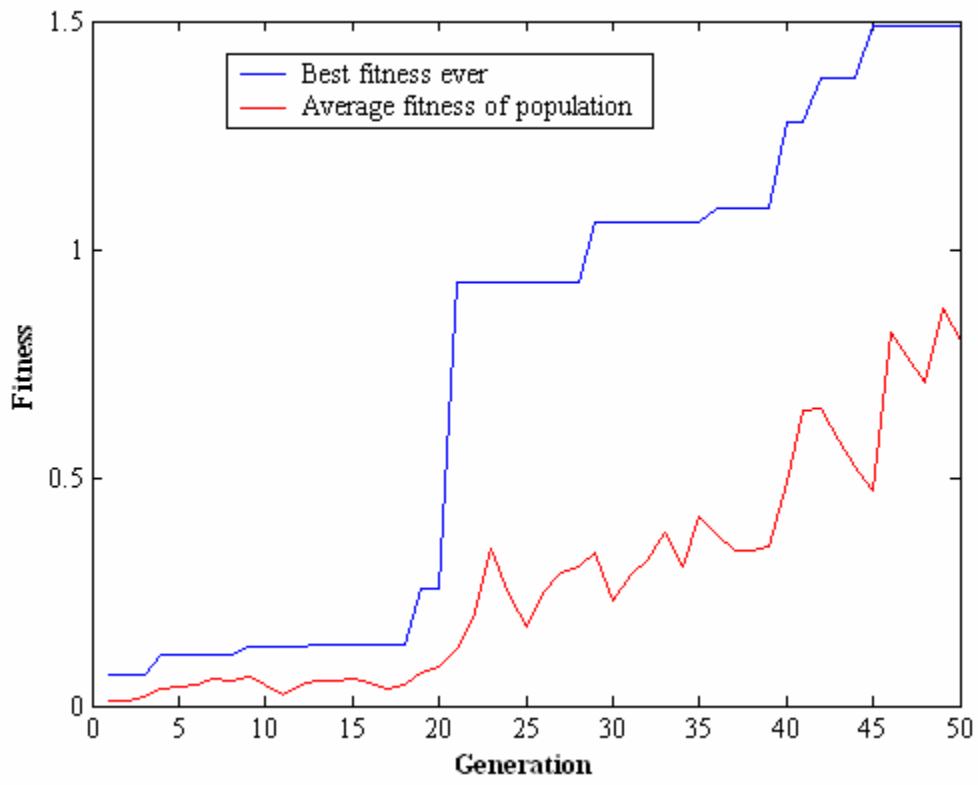
SR3_3_3_NC_b_1



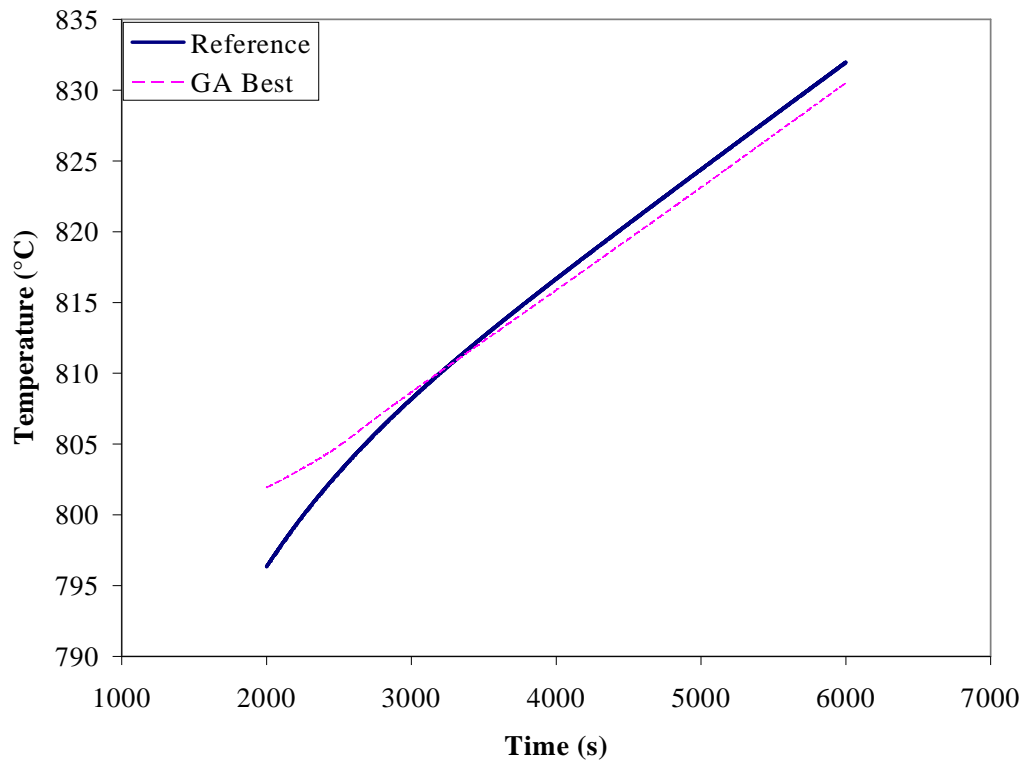
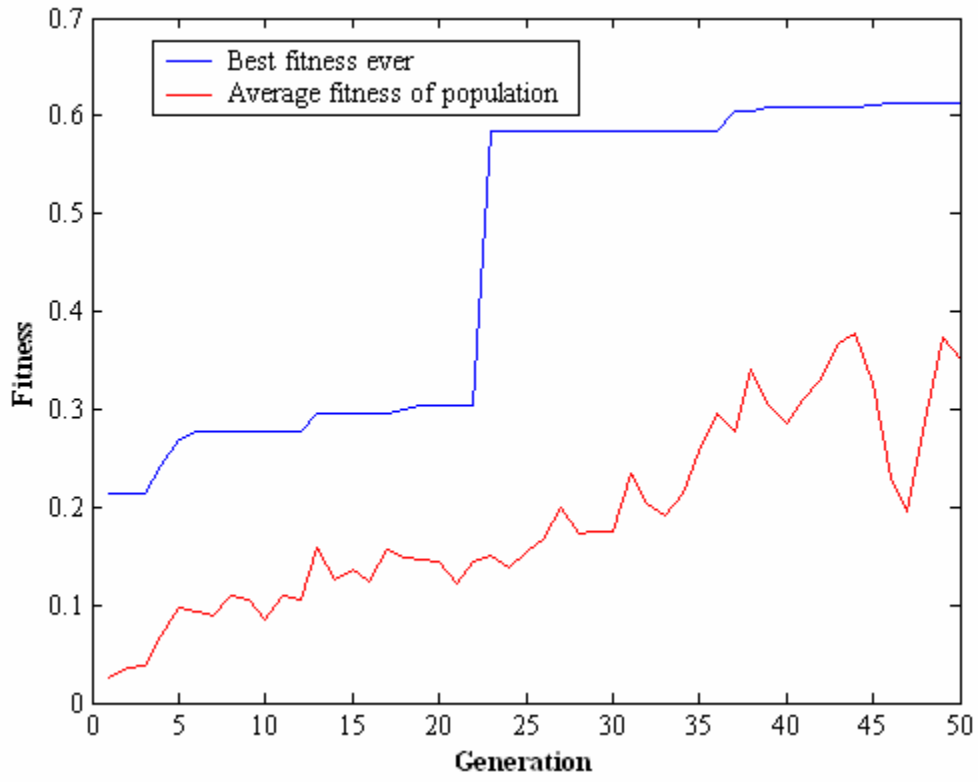
SR3_3_3_NC_b_2



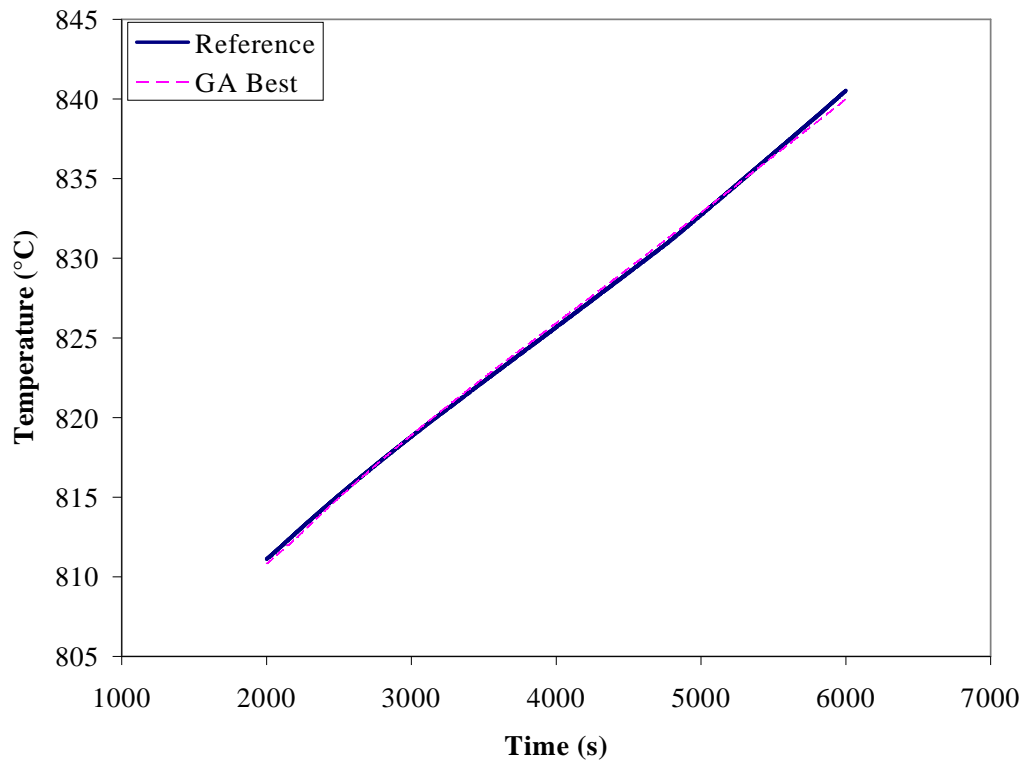
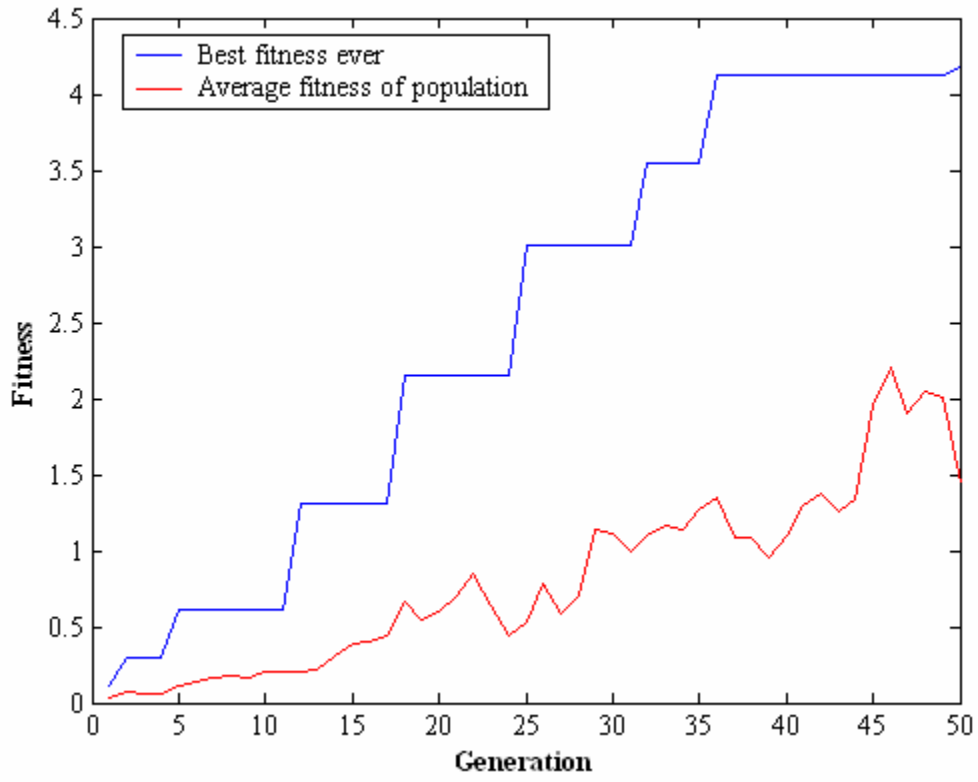
SR3_3_3_NC_b_3



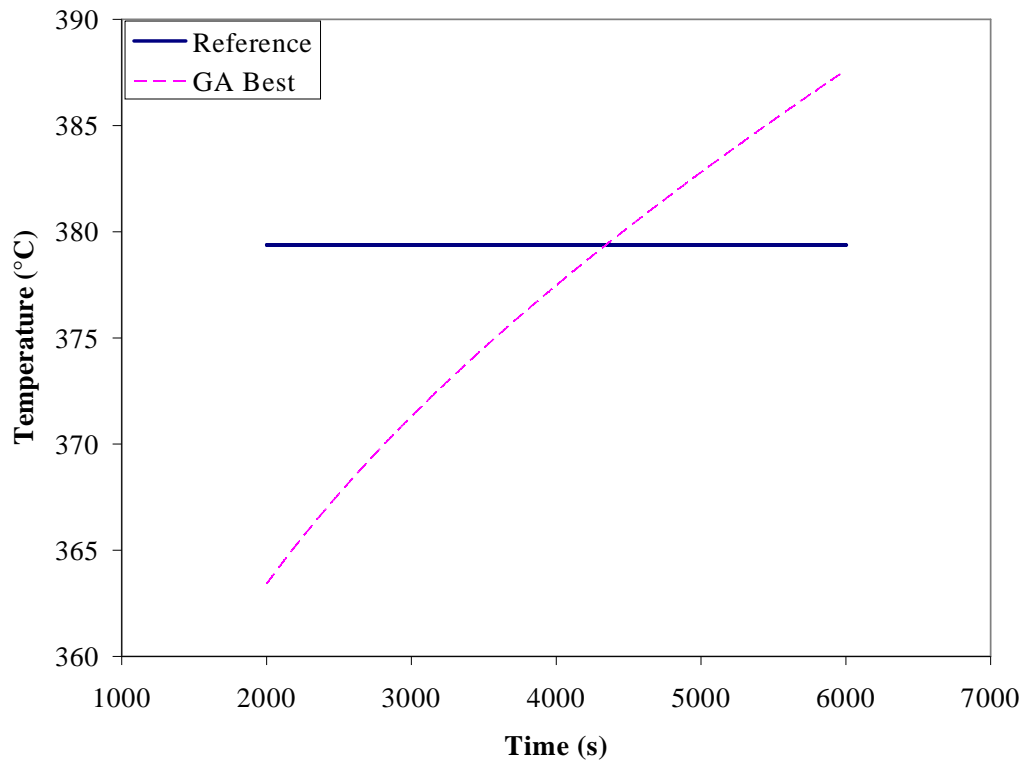
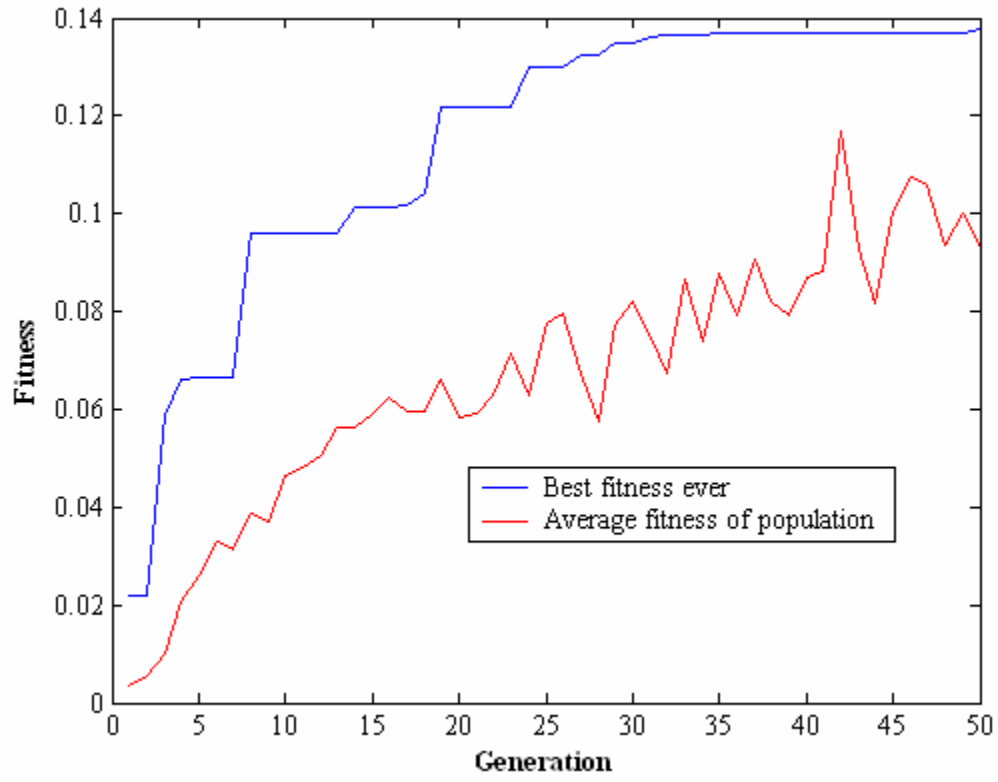
SR3_3_3_NC_b_4



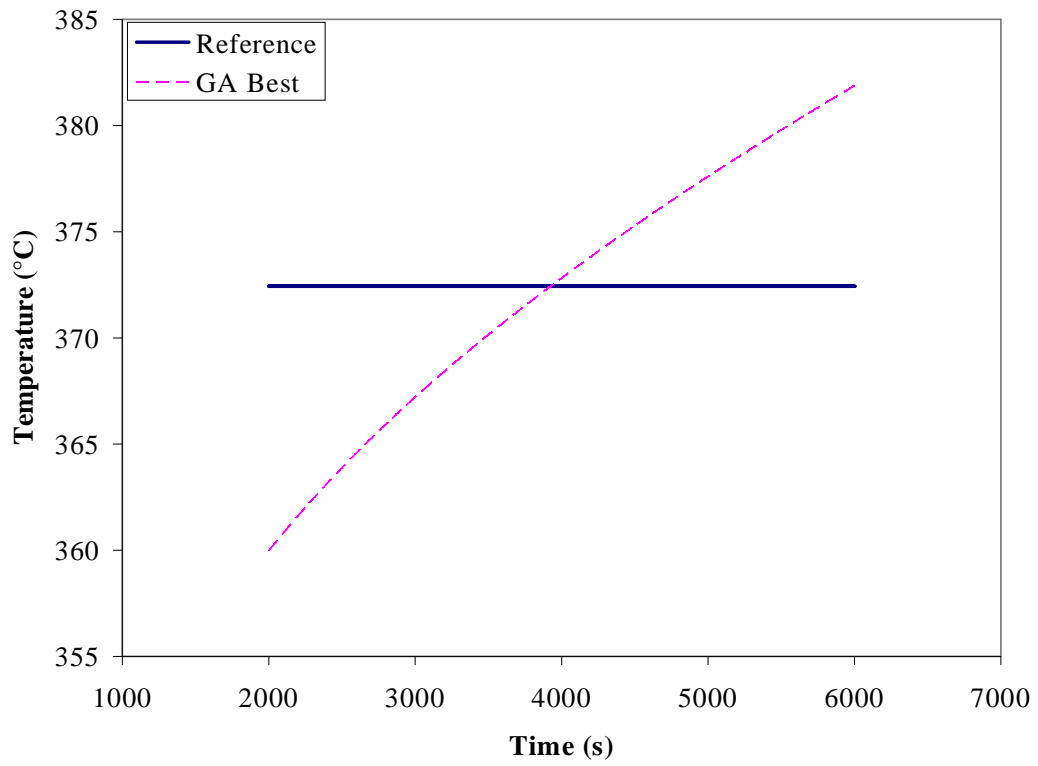
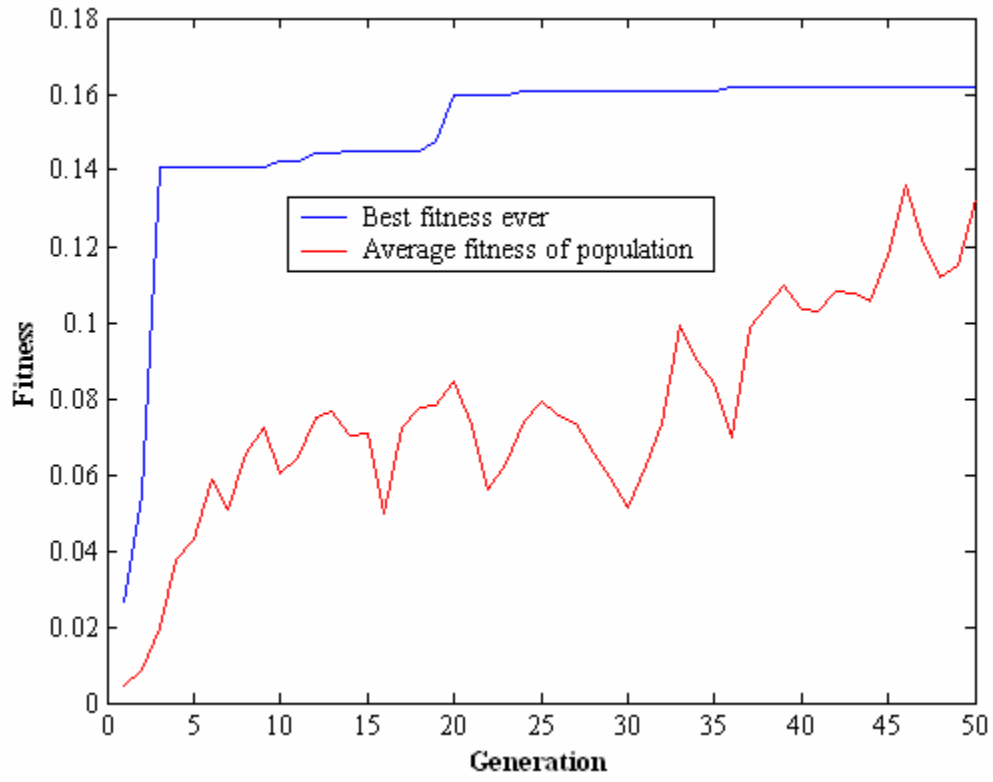
SR3_3_3_NC_b_5



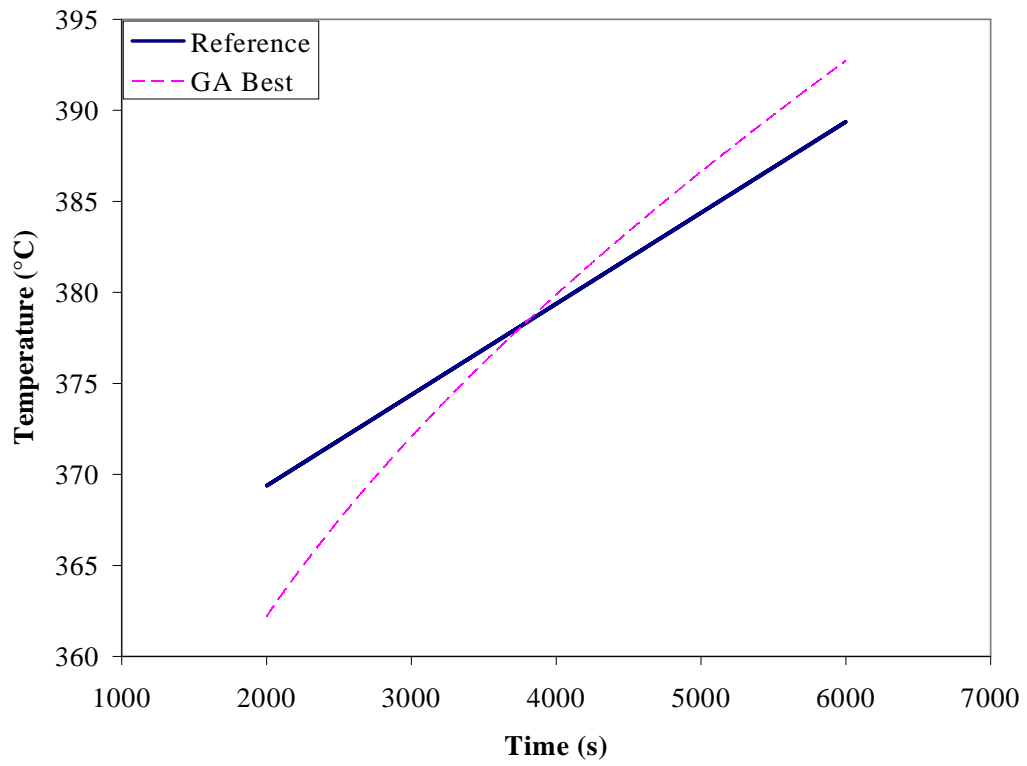
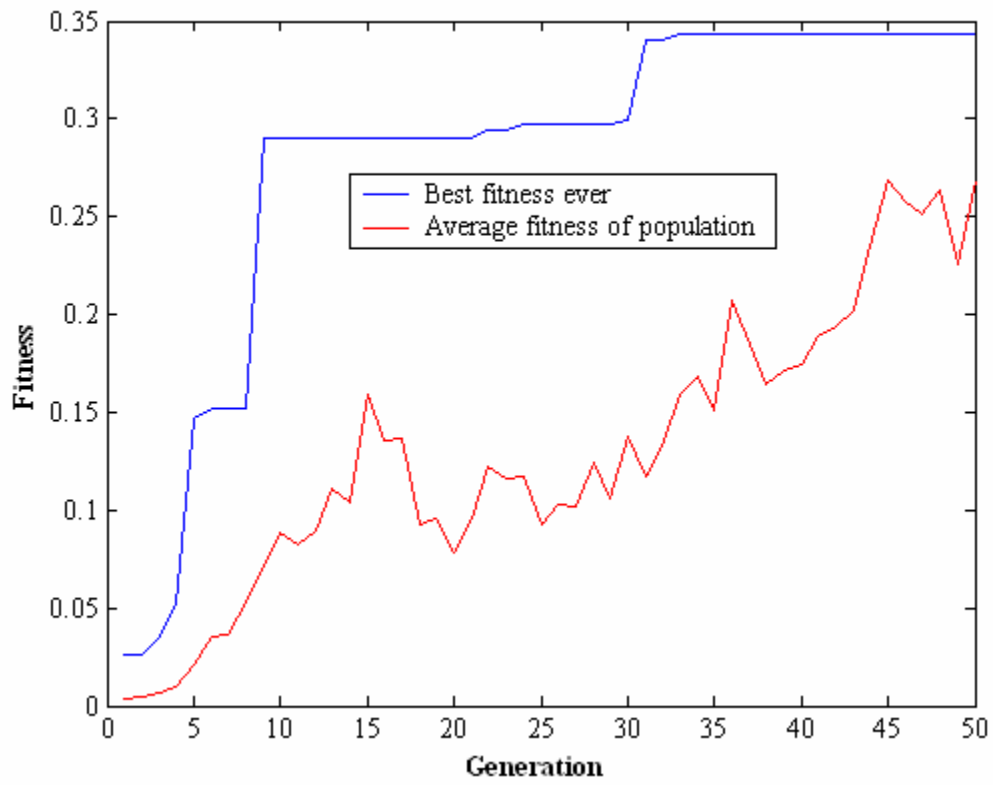
SR3_3_3_NC_c_1



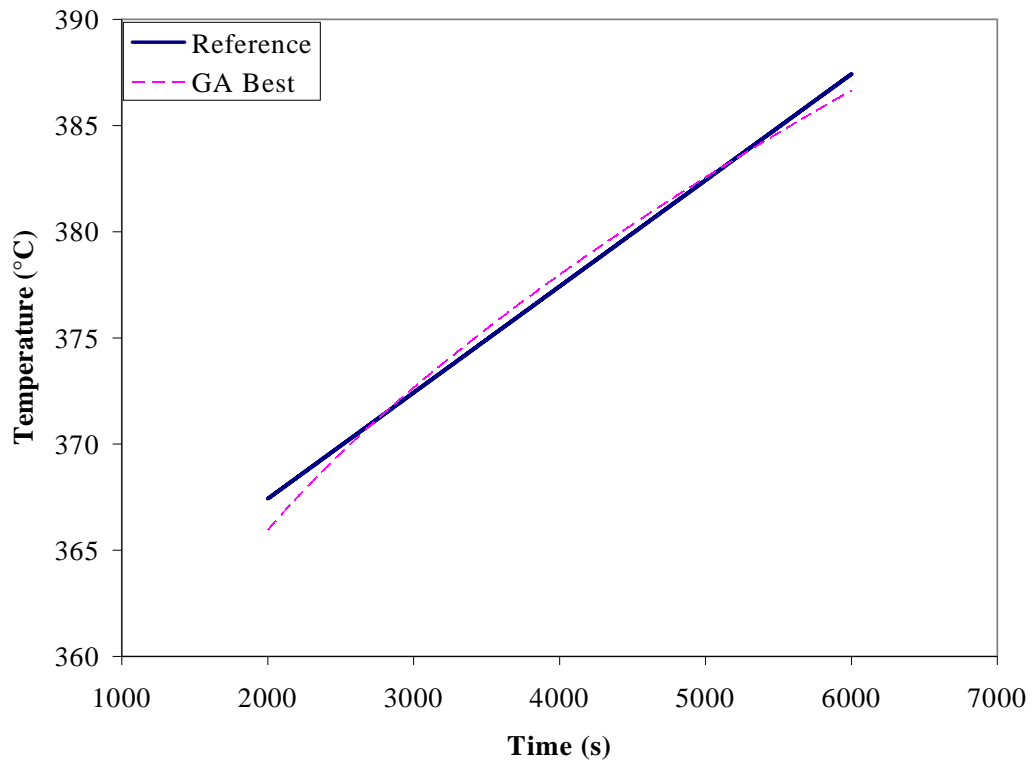
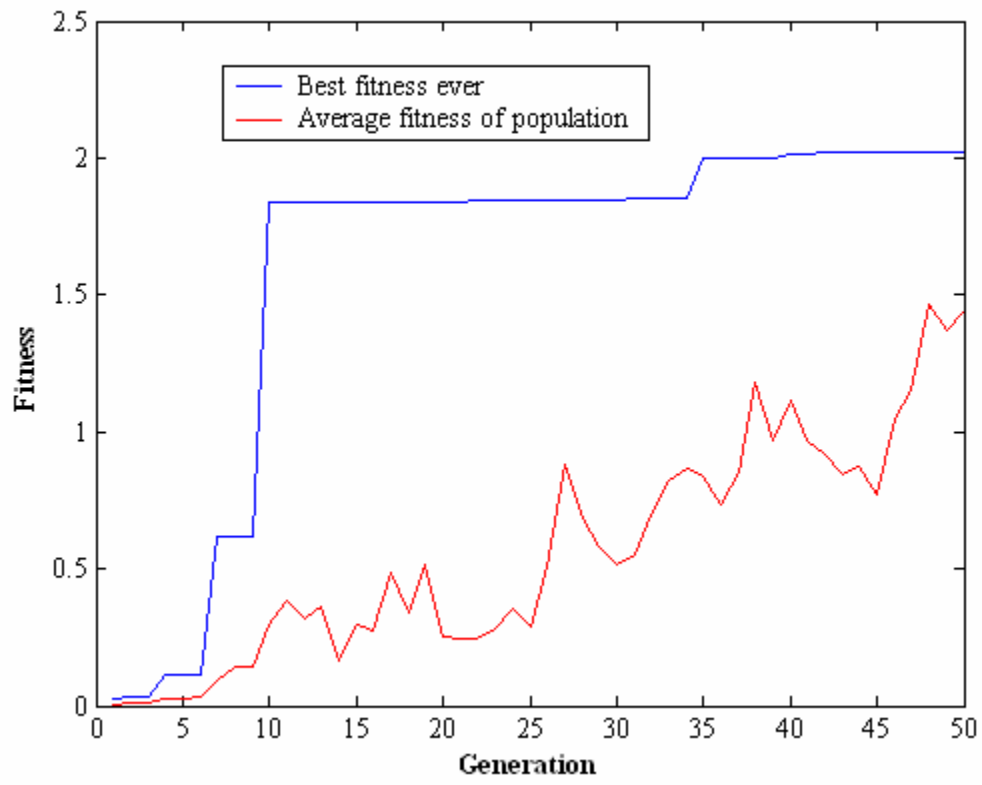
SR3_3_3_NC_d_1



SR3_3_3_NC_f_1



SR3_3_3_NC_g_1



Appendix A4

Appendix A4 is organized in the following manner:

MR_W#_letter_ #

Where MR (multiple rooms/compartments)

W# (Number of outside windows that are open)

W1_10_11 (window 1, 10 and 11 are open)

W1_10:18 (window 1, windows 10 through 18 are open)

W1:18 (all windows are open)

Letter	Meaning
a	Exact reference curve analyzed at steady state 2000-3000s from window W1.
b	Approximate steady reference curve with value taken instantaneously at 2500s.
c	Approximate sloped reference curve at 2500s.

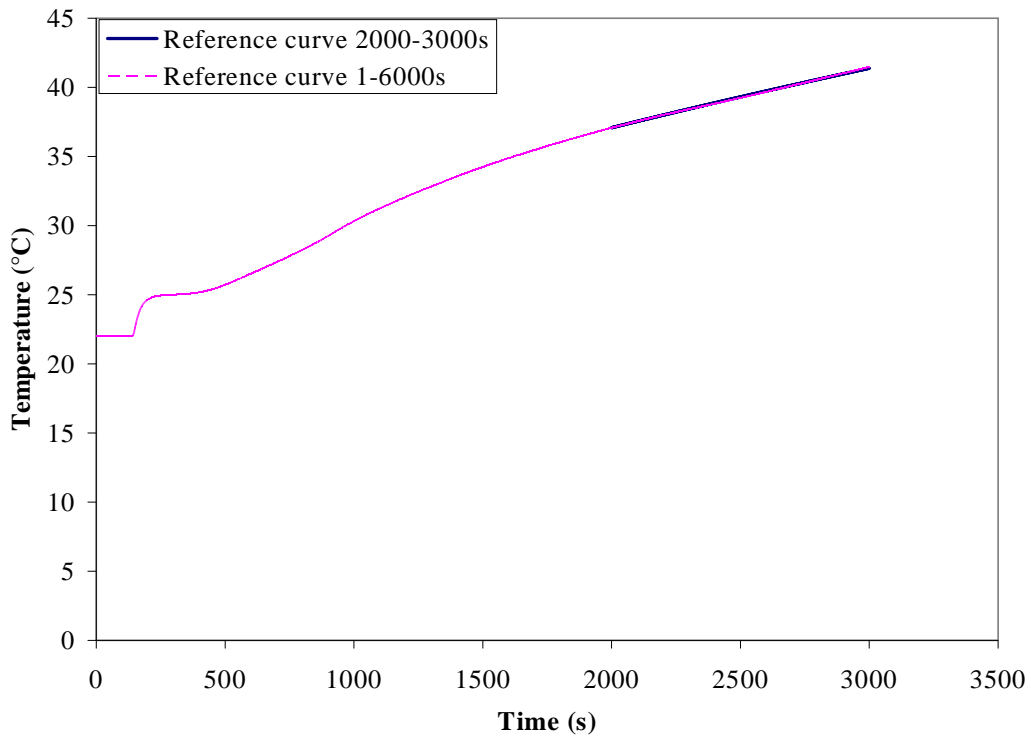


Figure 60. Simulation letter MR_a. Exact reference curve analyzed 2000-3000s.

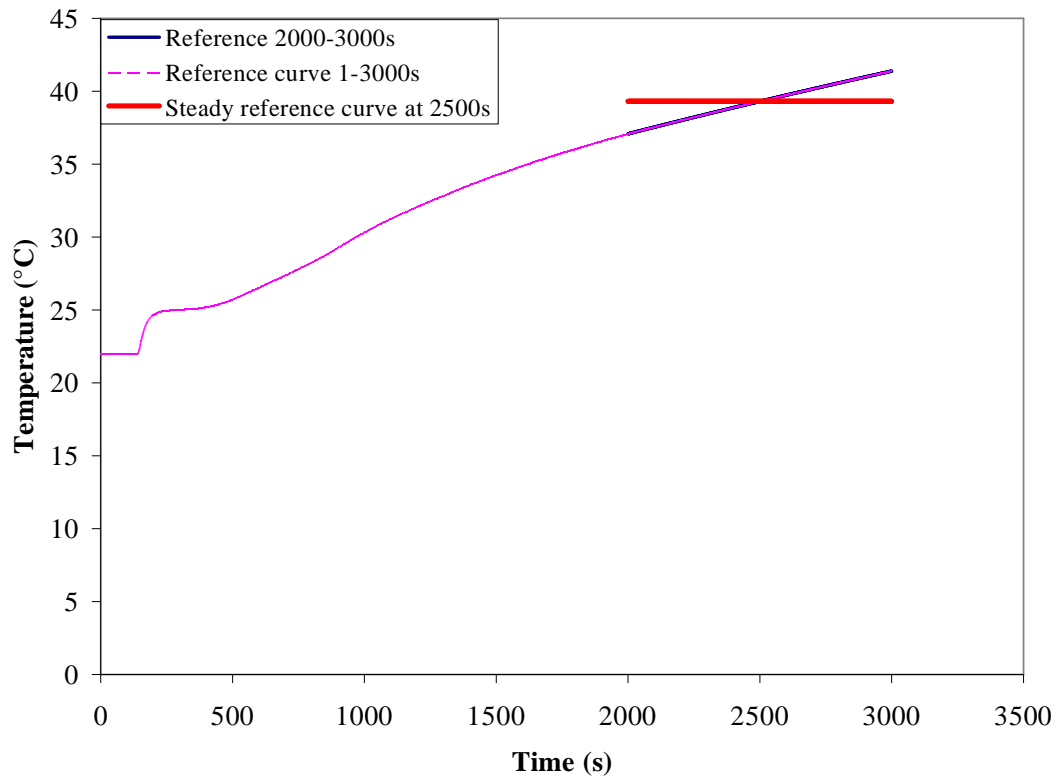
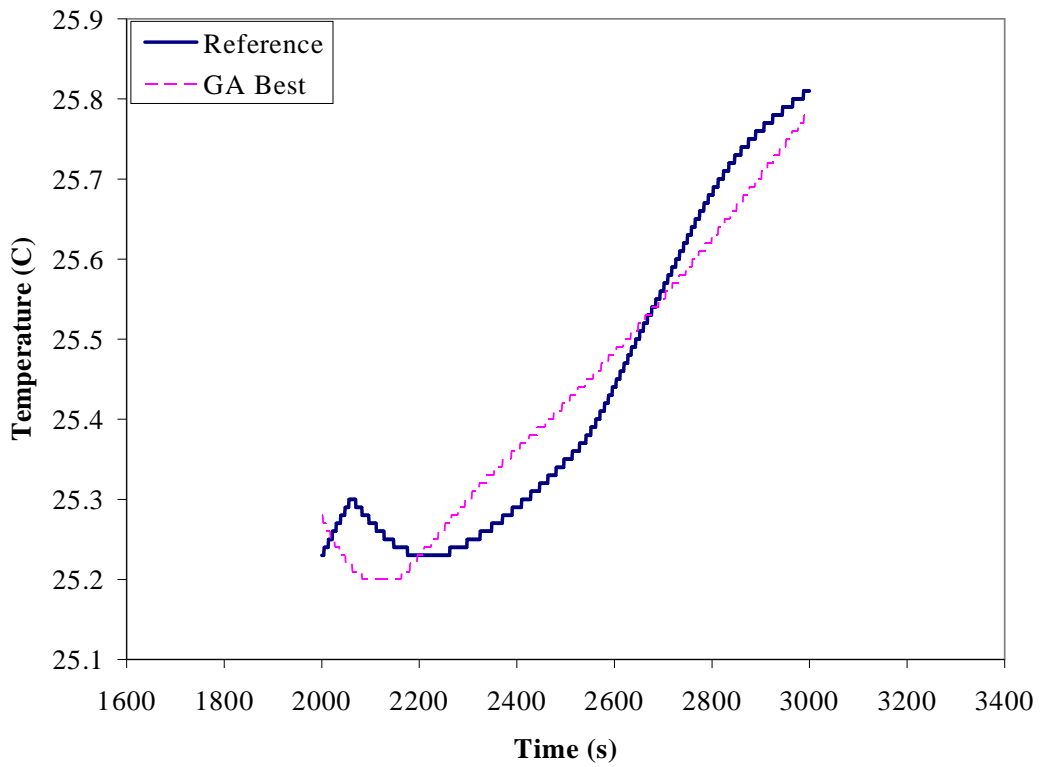
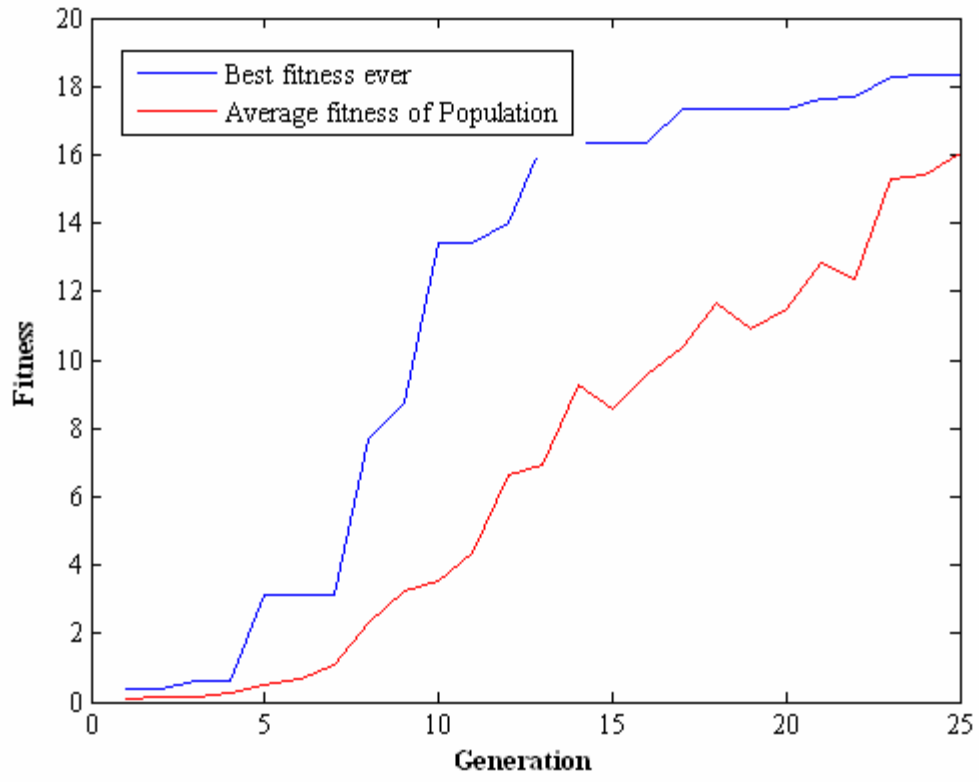


Figure 61. Simulation letter MR_b. Approximate steady reference curve with constant value taken at 2500s.

MR_W1_10_11_a_1: Total HRR is the total HRR added up in each compartment. The HRR's are averaged from 2000-3000s in increments of 200s.

Parameters	Reference Values	GA Best	Bounds	Notes
Mass Loss Rate	250 kW	571 kW	200- 5250 kW	Population size 25, 25 generations
Total HRR	243 kW	557 kW		
HRR Fire Room	241 kW	554 kW		
HRR Corridor	2 kW	3 kW		
HRR Room 1 (Analysis Window)	0 kW	0 kW		
HRR in all other rooms combined	0 kW	0 kW		
D1 width	1m	1.49m	.25m – 1.5m	
D2 width	1m	.78m	.25m – 1.5m	
D3 width	1m	.80m	.25m – 1.5m	
D4 width	1m	.93m	.25m – 1.5m	
D5 width	1m	1.21m	.25m – 1.5m	
D6 width	1m	.45m	.25m – 1.5m	
D7 width	1m	.65m	.25m – 1.5m	
D8 width	1m	.66m	.25m – 1.5m	
D9 width	1m	.76m	.25m – 1.5m	
D10 width	1m	.46m	.25m – 1.5m	
D11 width	1m	.56m	.25m – 1.5m	
D12 width	1m	1.49m	.25m – 1.5m	
D13 width	1m	.74m	.25m – 1.5m	
D14 width	1m	1.06m	.25m – 1.5m	
D15 width	1m	1.12m	.25m – 1.5m	
D16 width	1m	.75m	.25m – 1.5m	
D17 width	1m	1.16m	.25m – 1.5m	
D18 width	1m	.89m	.25m – 1.5m	

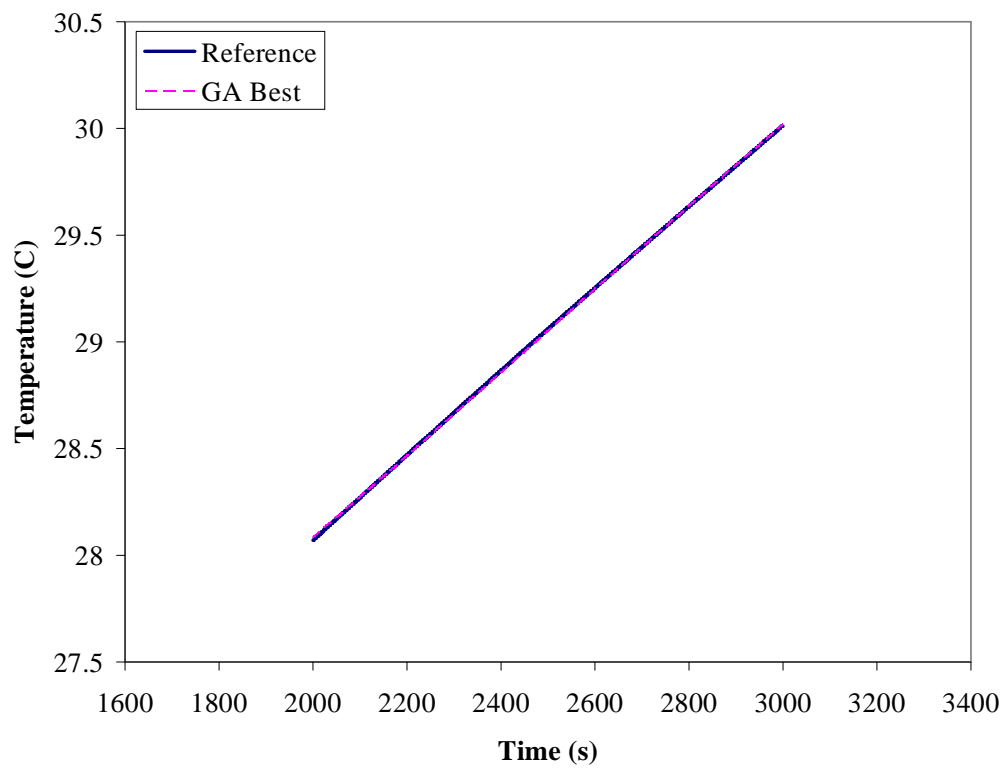
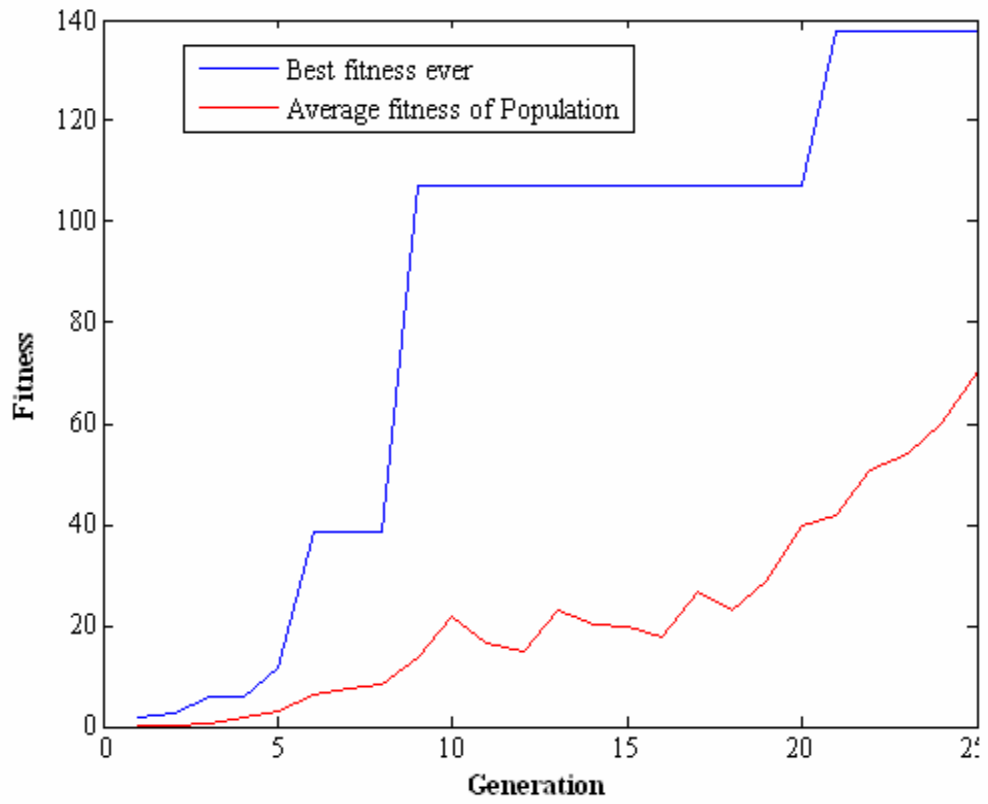
MR_W1_10_11_a_1



MR_W1_10_11_a_2: Total HRR is the total HRR added up in each compartment. The HRR's are averaged from 2000-3000s in increments of 200s.

Parameters	Reference Values	GA Best	Bounds	Notes
Mass Loss Rate	500 kW	492 kW	200- 5250 kW	Population size 25, 25 generations
Total HRR	487 kW	479 kW		
HRR Fire Room	482 kW	474 kW		
HRR Corridor	5 kW	5 kW		
HRR Room 1 (Analysis Window)	0 kW	0 kW		
HRR in all other rooms combined	0 kW	0 kW		
D1 width	1m	.88m	.25m – 1.5m	
D2 width	1m	1.45m	.25m – 1.5m	
D3 width	1m	1.07m	.25m – 1.5m	
D4 width	1m	.77m	.25m – 1.5m	
D5 width	1m	.51m	.25m – 1.5m	
D6 width	1m	.36m	.25m – 1.5m	
D7 width	1m	1.38m	.25m – 1.5m	
D8 width	1m	.43m	.25m – 1.5m	
D9 width	1m	.95m	.25m – 1.5m	
D10 width	1m	1.03m	.25m – 1.5m	
D11 width	1m	1.13m	.25m – 1.5m	
D12 width	1m	1.49m	.25m – 1.5m	
D13 width	1m	.67m	.25m – 1.5m	
D14 width	1m	.66m	.25m – 1.5m	
D15 width	1m	1.50m	.25m – 1.5m	
D16 width	1m	.88m	.25m – 1.5m	
D17 width	1m	.81m	.25m – 1.5m	
D18 width	1m	1.37m	.25m – 1.5m	

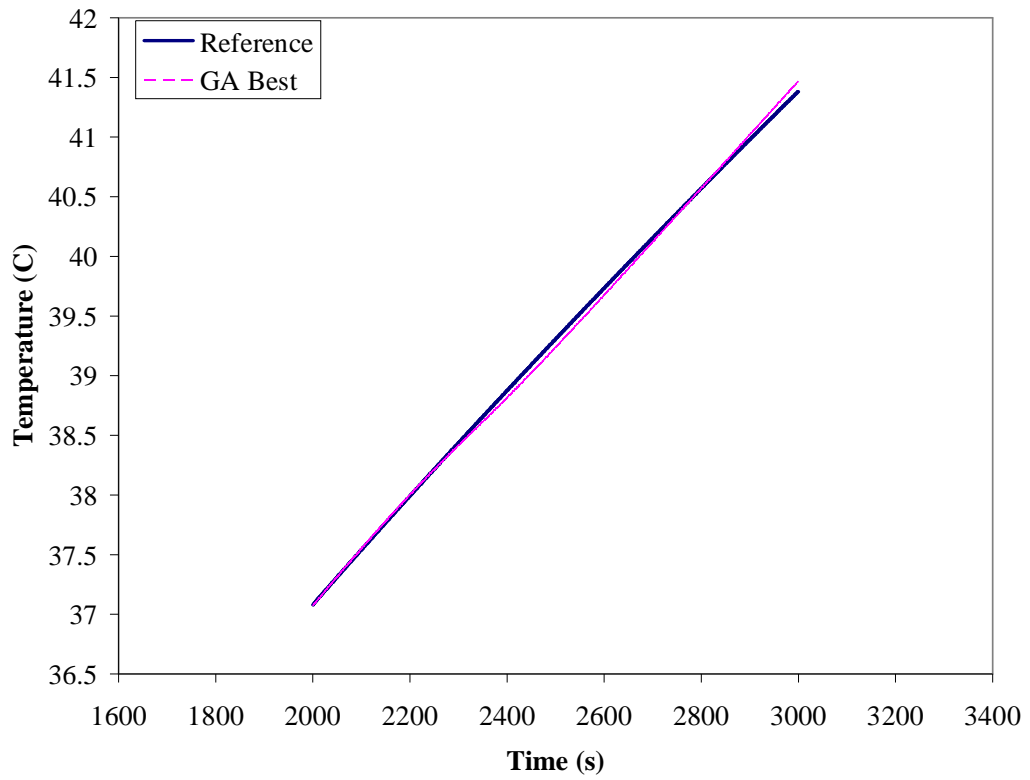
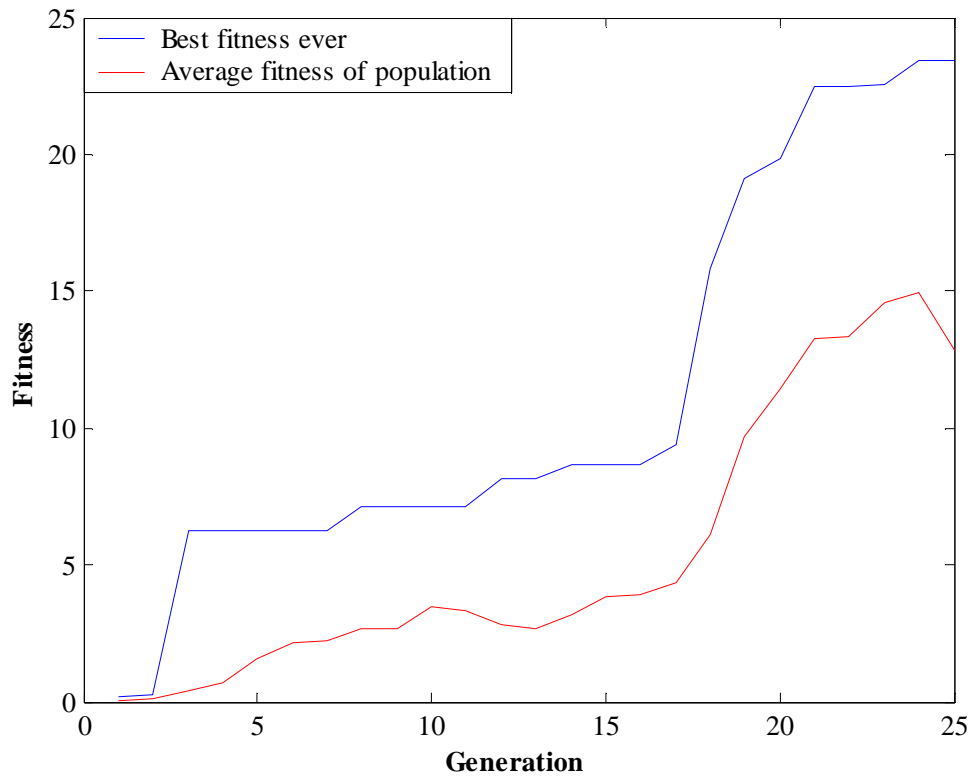
MR_W1_10_11_a_2



MR_W1_10_11_a_3: Total HRR is the total HRR added up in each compartment. The HRR's are averaged from 2000-3000s in increments of 200s.

Parameters	Reference Values	GA Best	Bounds	Notes
Mass Loss Rate	1000 kW	1186 kW	200- 6000 kW	Population size 25, 25 generations
Total HRR	995 kW	1145 kW		
HRR Fire Room	993 kW	1131 kW		
HRR Corridor	2 kW	14.5 kW		
HRR Room 1 (Analysis Window)	0 kW	0 kW		
HRR in all other rooms combined	0 kW	0 kW		
D1 width	1m	.56m	.25m – 1.5m	
D2 width	1m	.90m	.25m – 1.5m	
D3 width	1m	1.47m	.25m – 1.5m	
D4 width	1m	.95m	.25m – 1.5m	
D5 width	1m	.41m	.25m – 1.5m	
D6 width	1m	1.48m	.25m – 1.5m	
D7 width	1m	1.42m	.25m – 1.5m	
D8 width	1m	.92m	.25m – 1.5m	
D9 width	1m	1.22 m	.25m – 1.5m	
D10 width	1m	.97m	.25m – 1.5m	
D11 width	1m	.40m	.25m – 1.5m	
D12 width	1m	1.00m	.25m – 1.5m	
D13 width	1m	.93m	.25m – 1.5m	
D14 width	1m	.76m	.25m – 1.5m	
D15 width	1m	.98m	.25m – 1.5m	
D16 width	1m	1.28m	.25m – 1.5m	
D17 width	1m	.65m	.25m – 1.5m	
D18 width	1m	1.12m	.25m – 1.5m	

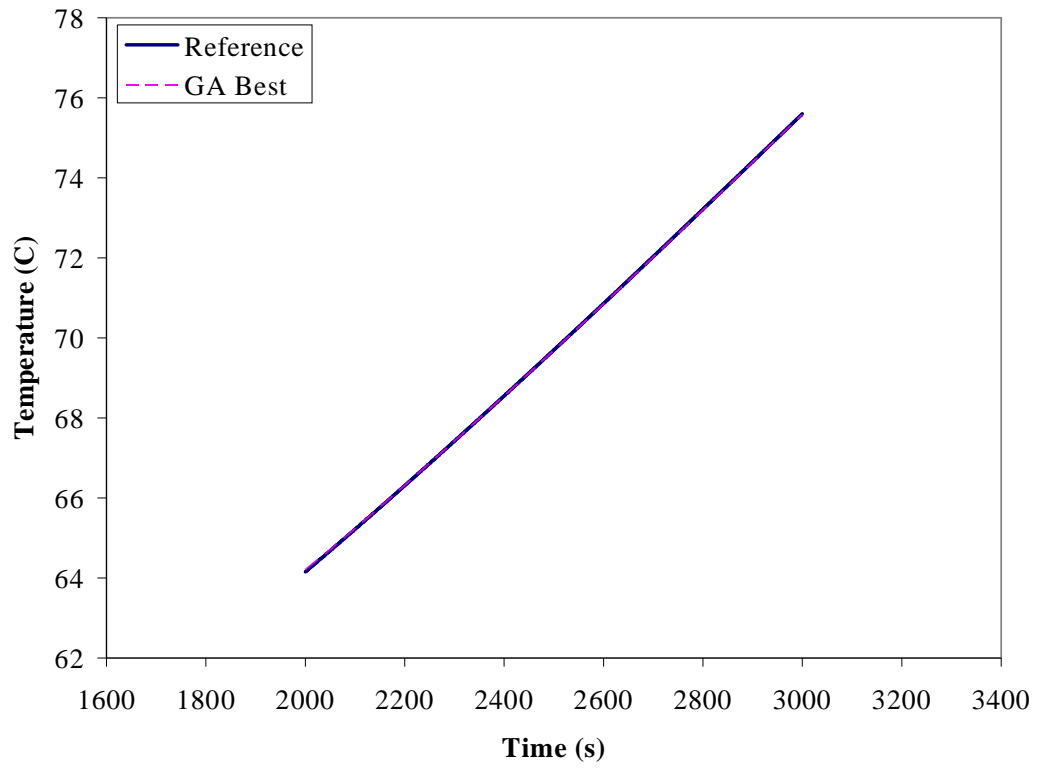
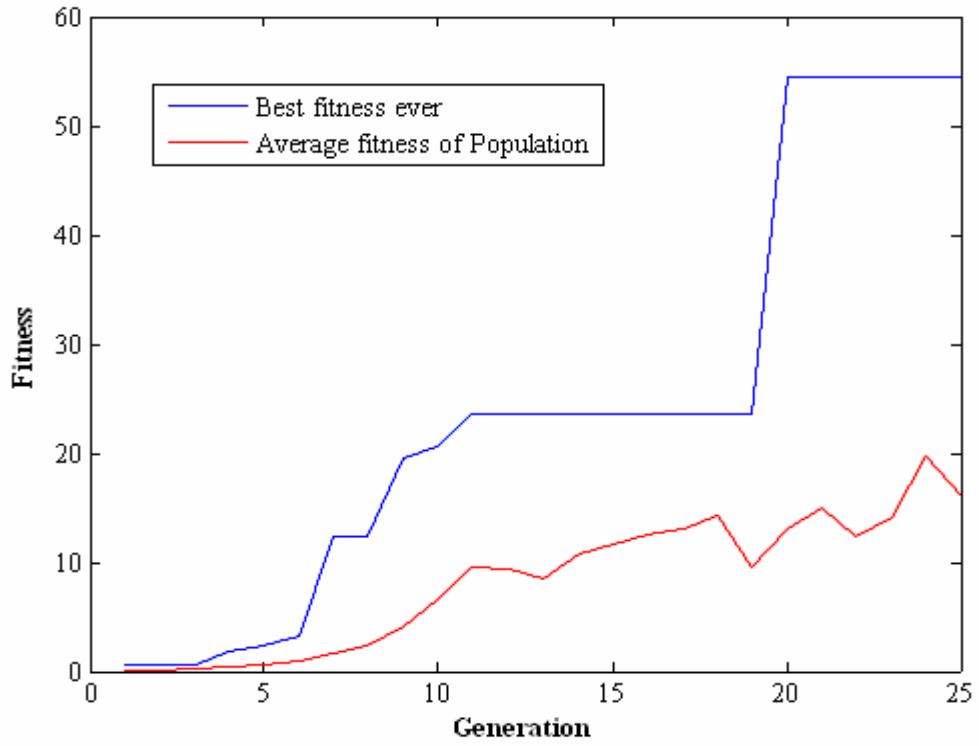
MR_W1_10_11_a_3



MR_W1_10_11_a_4: Total HRR is the total HRR added up in each compartment. The HRR's are averaged from 2000-3000s in increments of 200s.

Parameters	Reference Values	GA Best	Bounds	Notes
Mass Loss Rate	3000 kW	3050 kW	200- 5000 kW	Population size 25, 25 generations
Total HRR	1702 kW	1715 kW		
HRR Fire Room	1103 kW	1129 kW		
HRR Corridor	558 kW	546 kW		
HRR Room 1 (Analysis Window)	2 kW	2.5 kW		
HRR in all other rooms combined	40 kW	37 kW		
D1 width	1m	.99m	.25m – 1.5m	
D2 width	1m	.65m	.25m – 1.5m	
D3 width	1m	.78m	.25m – 1.5m	
D4 width	1m	.97m	.25m – 1.5m	
D5 width	1m	1.11m	.25m – 1.5m	
D6 width	1m	.38m	.25m – 1.5m	
D7 width	1m	.54m	.25m – 1.5m	
D8 width	1m	1.08m	.25m – 1.5m	
D9 width	1m	1.27m	.25m – 1.5m	
D10 width	1m	.94m	.25m – 1.5m	
D11 width	1m	.98m	.25m – 1.5m	
D12 width	1m	1.44m	.25m – 1.5m	
D13 width	1m	1.25m	.25m – 1.5m	
D14 width	1m	.25m	.25m – 1.5m	
D15 width	1m	1.02m	.25m – 1.5m	
D16 width	1m	1.23m	.25m – 1.5m	
D17 width	1m	1.41m	.25m – 1.5m	
D18 width	1m	.94m	.25m – 1.5m	

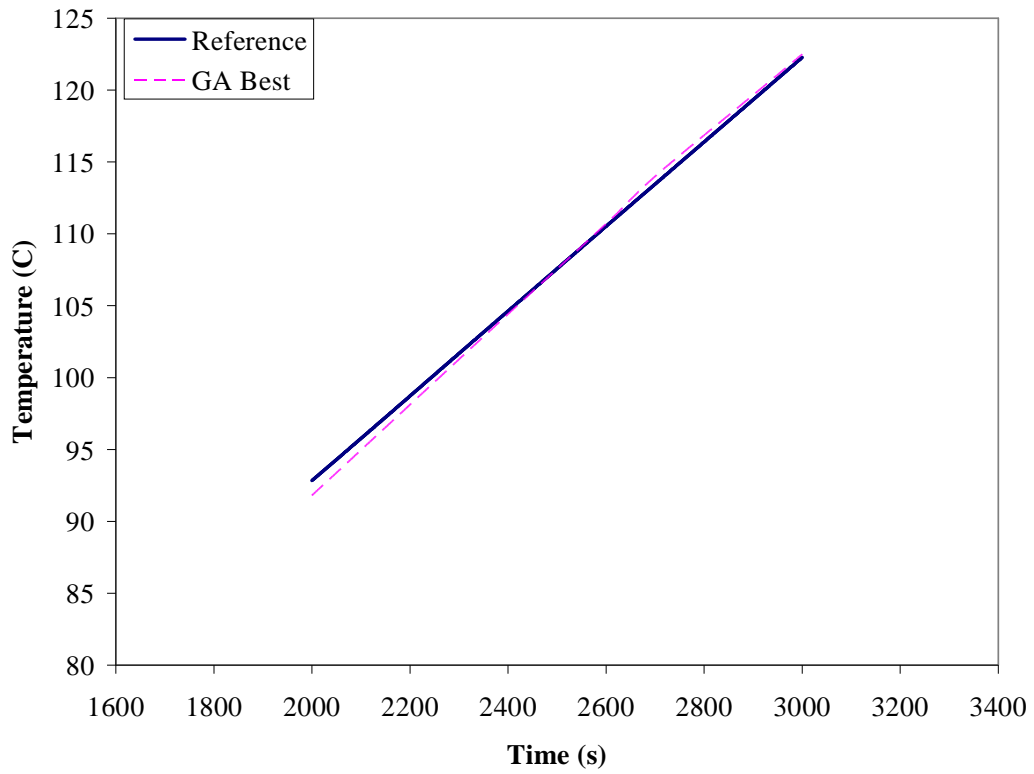
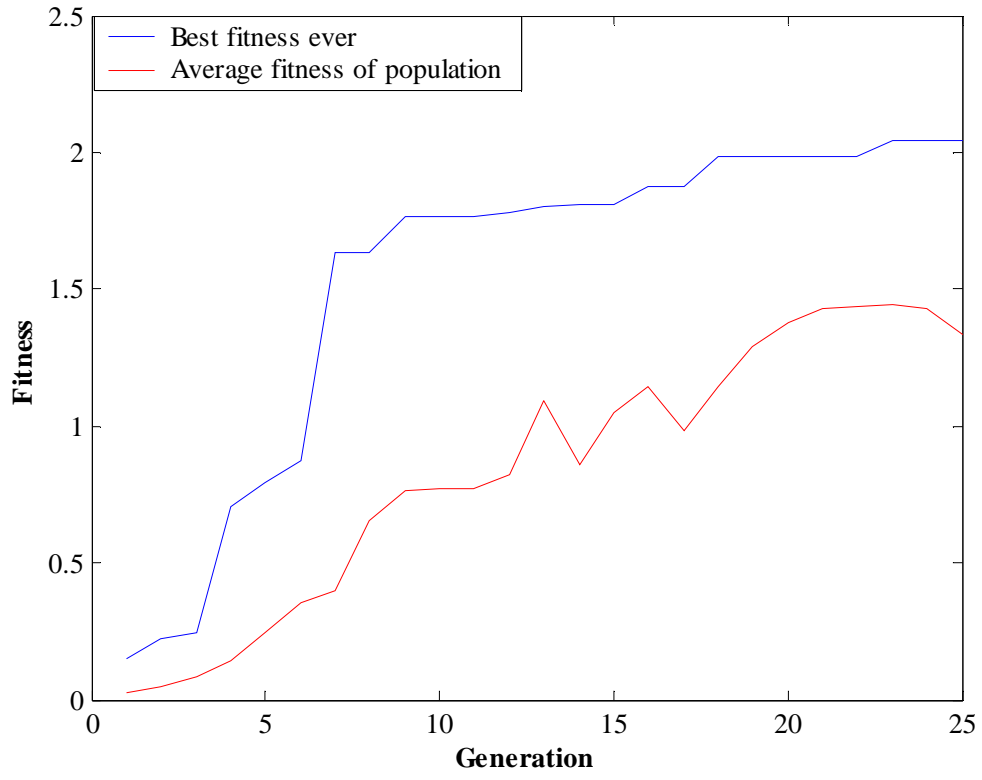
MR_W1_10_11_a_4



MR_W1_10_11_a_5: Total HRR is the total HRR added up in each compartment. The HRR's are averaged from 2000-3000s in increments of 200s.

Parameters	Reference Values	GA Best	Bounds	Notes
Mass Loss Rate	4000 kW	4163 kW	200- 6000 kW	Population size 25, 25 generations
Total HRR	2053 kW	1950kW		
HRR Fire Room	1038 kW	1069 kW		
HRR Corridor	665 kW	666 kW		
HRR Room 1 (Analysis Window)	23 kW	17 kW		
HRR in all other rooms combined	327 kW	199 kW		
D1 width	1m	1.37m	.25m – 1.5m	
D2 width	1m	.61m	.25m – 1.5m	
D3 width	1m	1.31m	.25m – 1.5m	
D4 width	1m	.78m	.25m – 1.5m	
D5 width	1m	.74m	.25m – 1.5m	
D6 width	1m	.91m	.25m – 1.5m	
D7 width	1m	.93m	.25m – 1.5m	
D8 width	1m	.25m	.25m – 1.5m	
D9 width	1m	1.01m	.25m – 1.5m	
D10 width	1m	.72m	.25m – 1.5m	
D11 width	1m	1.43m	.25m – 1.5m	
D12 width	1m	1.10m	.25m – 1.5m	
D13 width	1m	1.50m	.25m – 1.5m	
D14 width	1m	1.02m	.25m – 1.5m	
D15 width	1m	1.37m	.25m – 1.5m	
D16 width	1m	1.41m	.25m – 1.5m	
D17 width	1m	.43m	.25m – 1.5m	
D18 width	1m	1.05m	.25m – 1.5m	

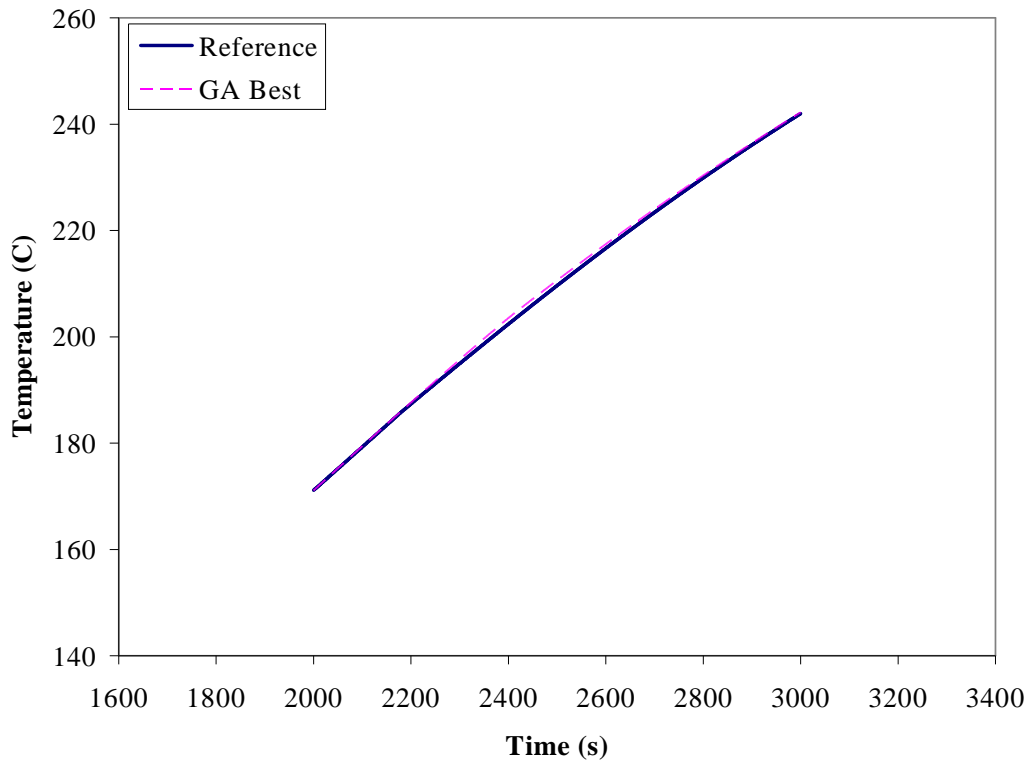
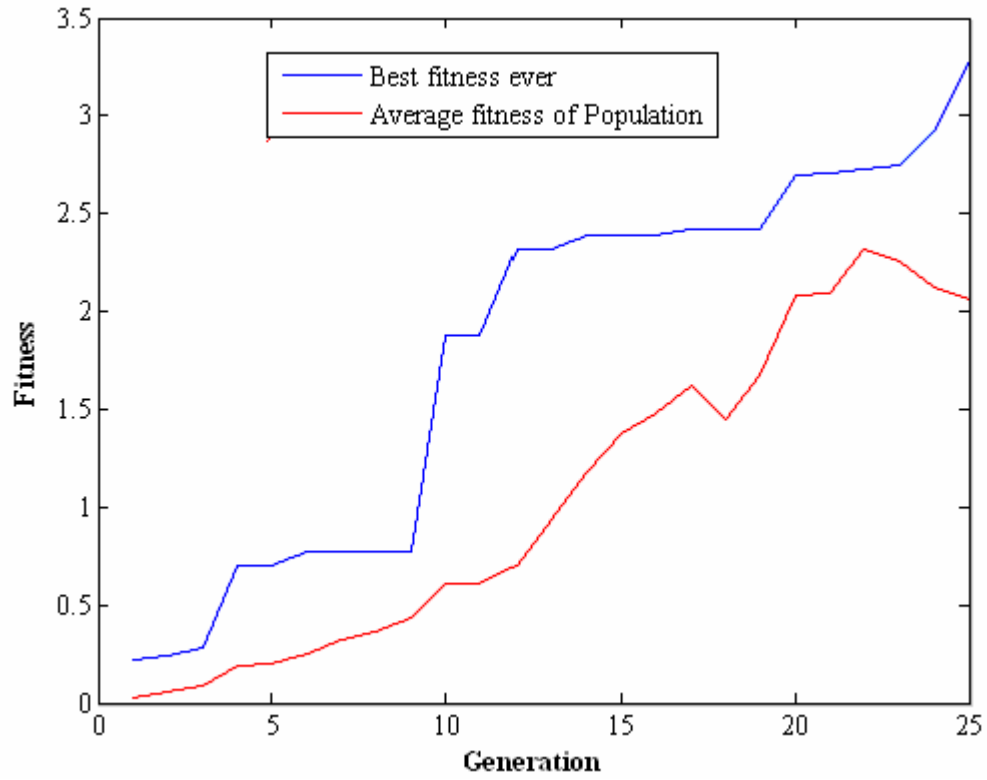
MR_W1_10_11_a_5



MR_W1_10_11_a_6: Total HRR is the total HRR added up in each compartment. The HRR's are averaged from 2000-3000s in increments of 200s.

Parameters	Reference Values	GA Best	Bounds	Notes
Mass Loss Rate	5000 kW	4722 kW	200- 5250 kW	Population size 25, 25 generations
Total HRR	2353 kW	2363 kW		
HRR Fire Room	916 kW	910 kW		
HRR Corridor	638 kW	675 kW		
HRR Room 1 (Analysis Window)	98 kW	183 kW		
HRR in all other rooms combined	701 kW	696 kW		
D1 width	1m	.56m	.25m – 1.5m	
D2 width	1m	.59m	.25m – 1.5m	
D3 width	1m	.50m	.25m – 1.5m	
D4 width	1m	1.02m	.25m – 1.5m	
D5 width	1m	.73m	.25m – 1.5m	
D6 width	1m	.64m	.25m – 1.5m	
D7 width	1m	1.16m	.25m – 1.5m	
D8 width	1m	1.30m	.25m – 1.5m	
D9 width	1m	.55m	.25m – 1.5m	
D10 width	1m	1.30m	.25m – 1.5m	
D11 width	1m	.98m	.25m – 1.5m	
D12 width	1m	.78m	.25m – 1.5m	
D13 width	1m	.83m	.25m – 1.5m	
D14 width	1m	.85m	.25m – 1.5m	
D15 width	1m	.98m	.25m – 1.5m	
D16 width	1m	.74m	.25m – 1.5m	
D17 width	1m	.77m	.25m – 1.5m	
D18 width	1m	1.33m	.25m – 1.5m	

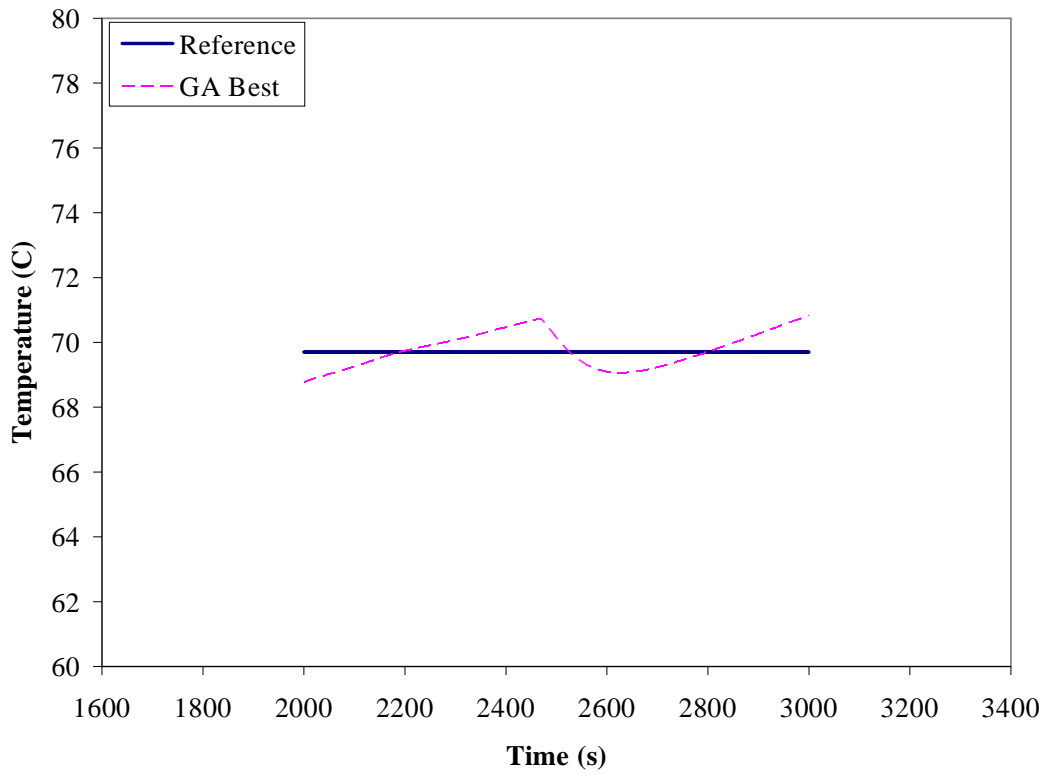
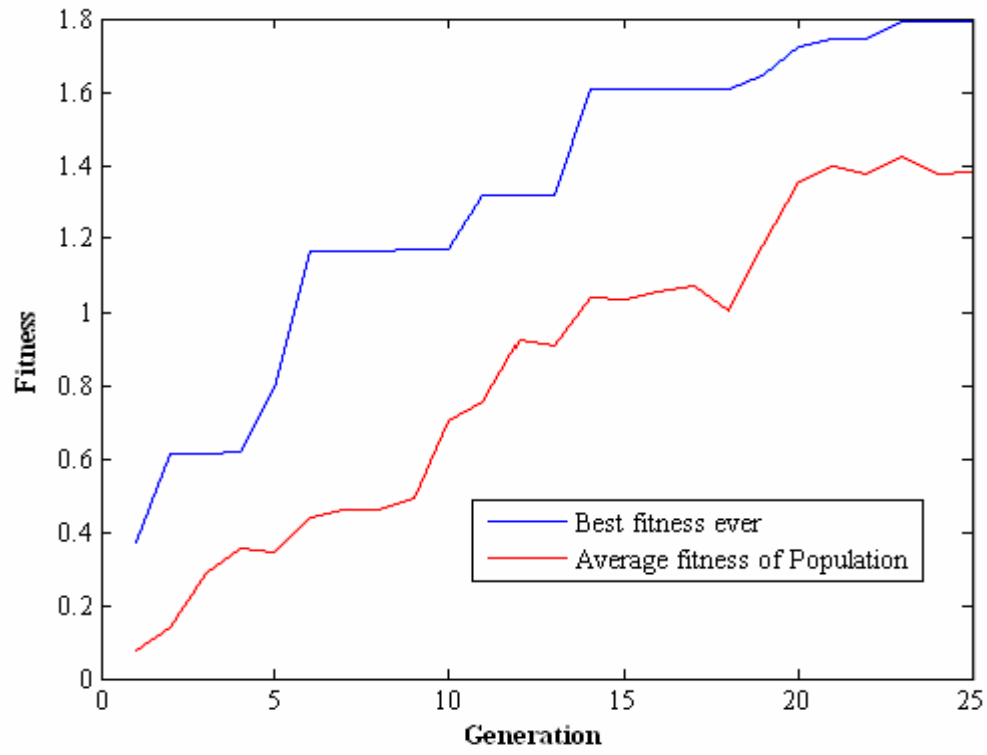
MR_W1_10_11_a_6



MR_W1_10_11_b_1: Total HRR is the total HRR added up in each compartment. The HRR's are averaged from 2000-3000s in increments of 200s.

Parameters	Reference Values	GA Best	Bounds	Notes
Mass Loss Rate	3000 kW	2377 kW	200- 5500 kW	Population size 25, 25 generations
Total HRR	1702 kW	1586 kW		
HRR Fire Room	1103 kW	1180 kW		
HRR Corridor	558 kW	405 kW		
HRR Room 1 (Analysis Window)	2 kW	0 kW		
HRR in all other rooms combined	40 kW	0 kW		
D1 width	1m	.53m	.25m – 1.5m	
D2 width	1m	.78m	.25m – 1.5m	
D3 width	1m	.77m	.25m – 1.5m	
D4 width	1m	.82m	.25m – 1.5m	
D5 width	1m	.59m	.25m – 1.5m	
D6 width	1m	.61m	.25m – 1.5m	
D7 width	1m	.77m	.25m – 1.5m	
D8 width	1m	.74m	.25m – 1.5m	
D9 width	1m	.91m	.25m – 1.5m	
D10 width	1m	1.28m	.25m – 1.5m	
D11 width	1m	.72m	.25m – 1.5m	
D12 width	1m	.40m	.25m – 1.5m	
D13 width	1m	.74m	.25m – 1.5m	
D14 width	1m	.94m	.25m – 1.5m	
D15 width	1m	.83m	.25m – 1.5m	
D16 width	1m	.74m	.25m – 1.5m	
D17 width	1m	1.07m	.25m – 1.5m	
D18 width	1m	.92m	.25m – 1.5m	

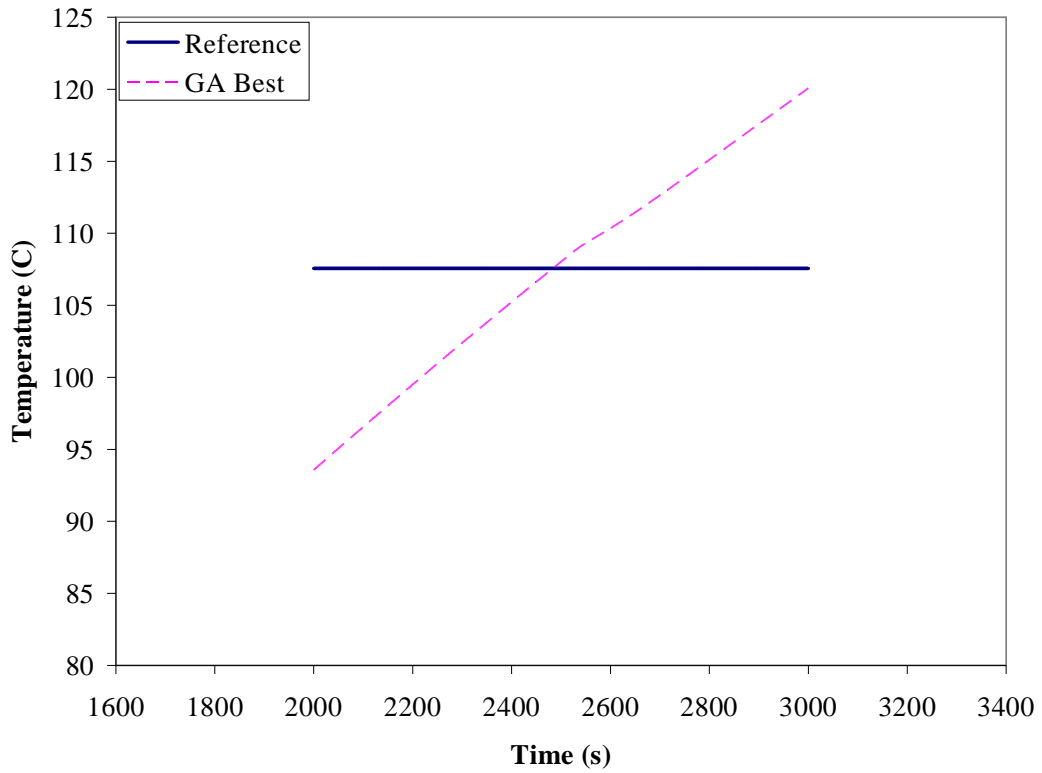
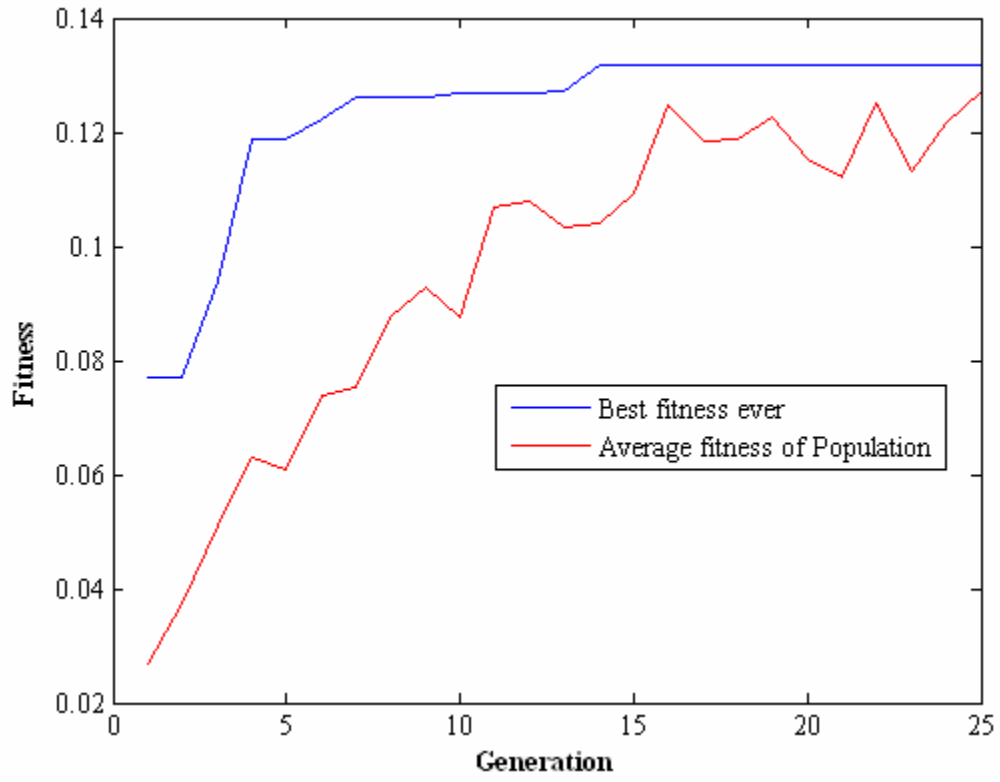
MR_W1_10_11_b_1



MR_W1_10_11_b_2: Total HRR is the total HRR added up in each compartment. The HRR's are averaged from 2000-3000s in increments of 200s.

Parameters	Reference Values	GA Best	Bounds	Notes
Mass Loss Rate	4000 kW	4707 kW	200- 5250 kW	Population size 25, 25 generations
Total HRR	2053 kW	1904 kW		
HRR Fire Room	1038 kW	1135 kW		
HRR Corridor	666 kW	509 kW		
HRR Room 1 (Analysis Window)	23 kW	28 kW		
HRR in all other rooms combined	327 kW	234 kW		
D1 width	1m	1.49m	.25m – 1.5m	
D2 width	1m	.63m	.25m – 1.5m	
D3 width	1m	.46m	.25m – 1.5m	
D4 width	1m	.29m	.25m – 1.5m	
D5 width	1m	.43m	.25m – 1.5m	
D6 width	1m	.69m	.25m – 1.5m	
D7 width	1m	.93m	.25m – 1.5m	
D8 width	1m	.30m	.25m – 1.5m	
D9 width	1m	1.50m	.25m – 1.5m	
D10 width	1m	.51m	.25m – 1.5m	
D11 width	1m	.54m	.25m – 1.5m	
D12 width	1m	.83m	.25m – 1.5m	
D13 width	1m	.88m	.25m – 1.5m	
D14 width	1m	.80m	.25m – 1.5m	
D15 width	1m	.89m	.25m – 1.5m	
D16 width	1m	.25m	.25m – 1.5m	
D17 width	1m	1.12m	.25m – 1.5m	
D18 width	1m	.42m	.25m – 1.5m	

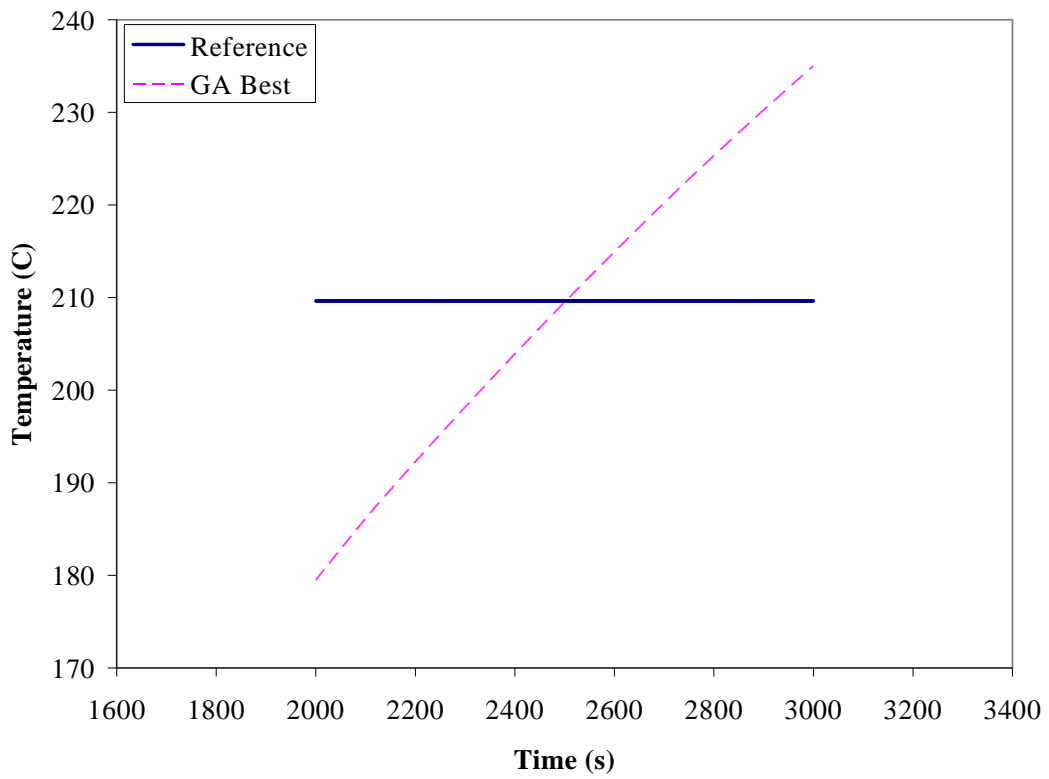
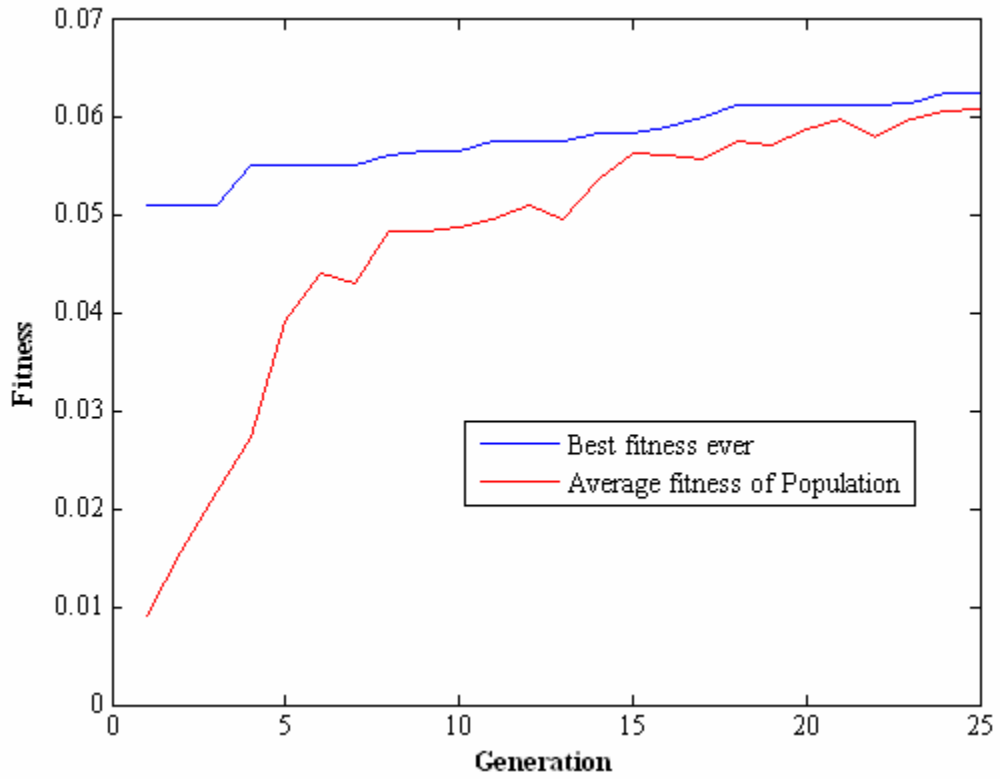
MR_W1_10_11_b_2



MR_W1_10_11_b_3: Total HRR is the total HRR added up in each compartment. The HRR's are averaged from 2000-3000s in increments of 200s.

Parameters	Reference Values	GA Best	Bounds	Notes
Mass Loss Rate	5000 kW	4962 kW	200- 5250 kW	Population size 25, 25 generations
Total HRR	2353 kW	2359 kW		
HRR Fire Room	916 kW	1027 kW		
HRR Corridor	638 kW	641 kW		
HRR Room 1 (Analysis Window)	198 kW	96 kW		
HRR in all other rooms combined	701 kW	596 kW		
D1 width	1m	1.13m	.25m – 1.5m	
D2 width	1m	1.07m	.25m – 1.5m	
D3 width	1m	.36m	.25m – 1.5m	
D4 width	1m	.26m	.25m – 1.5m	
D5 width	1m	.97m	.25m – 1.5m	
D6 width	1m	1.03m	.25m – 1.5m	
D7 width	1m	.29m	.25m – 1.5m	
D8 width	1m	.36m	.25m – 1.5m	
D9 width	1m	.47m	.25m – 1.5m	
D10 width	1m	.95m	.25m – 1.5m	
D11 width	1m	.68m	.25m – 1.5m	
D12 width	1m	1.43m	.25m – 1.5m	
D13 width	1m	.26m	.25m – 1.5m	
D14 width	1m	.78m	.25m – 1.5m	
D15 width	1m	1.30m	.25m – 1.5m	
D16 width	1m	.25m	.25m – 1.5m	
D17 width	1m	1.26m	.25m – 1.5m	
D18 width	1m	.32m	.25m – 1.5m	

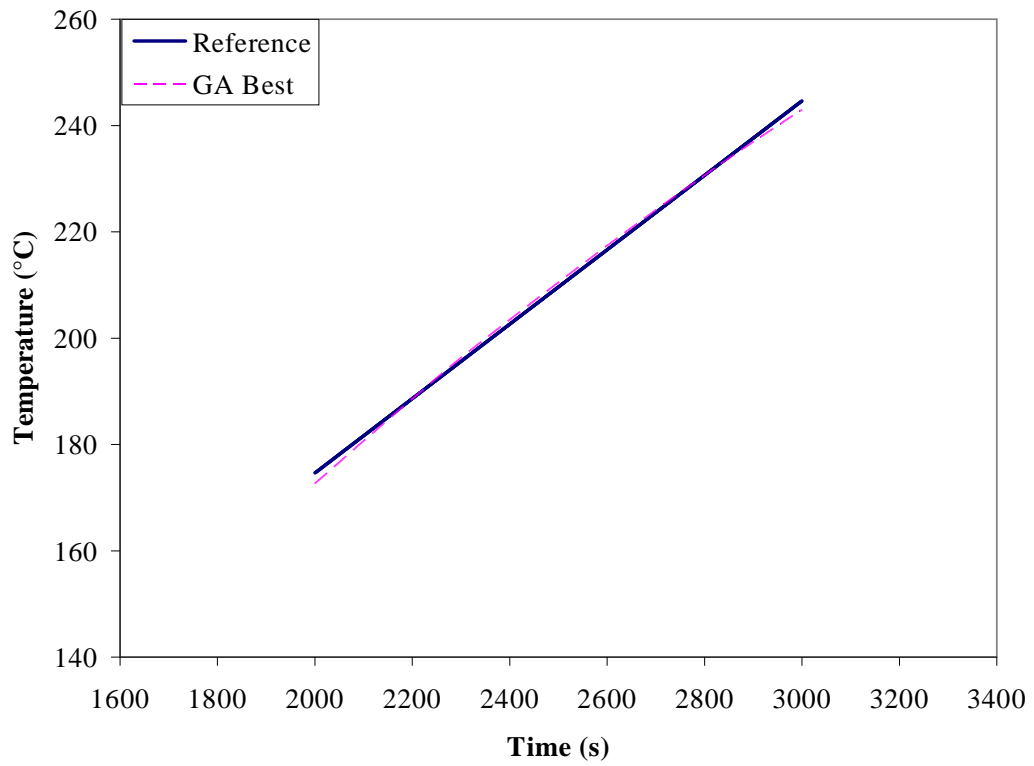
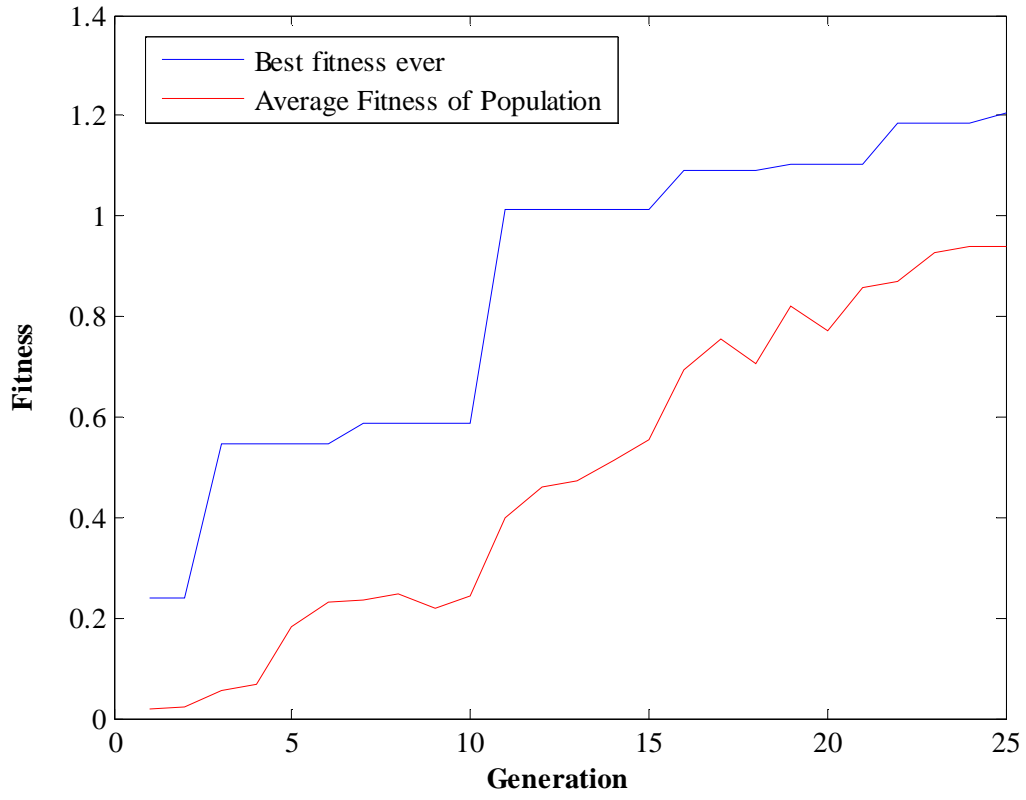
MR_W1_10_11_b_3



MR_W1_10_11_c_1: Total HRR is the total HRR added up in each compartment. The HRR's are averaged from 2000-3000s in increments of 200s.

Parameters	Reference Values	GA Best	Bounds	Notes
Mass Loss Rate	5000 kW	4930 kW	200- 5250 kW	Population size 25, 25 generations
Total HRR	2321 kW	2341 kW		
HRR Fire Room	815 kW	949 kW		
HRR Corridor	581 kW	640 kW		
HRR Room 1 (Analysis Window)	125 kW	90 kW		
HRR in all other rooms combined	800 kW	662 kW		
D1 width	1m	.72m	.25m – 1.5m	
D2 width	1m	.77m	.25m – 1.5m	
D3 width	1m	.72m	.25m – 1.5m	
D4 width	1m	.78m	.25m – 1.5m	
D5 width	1m	.67m	.25m – 1.5m	
D6 width	1m	1.20m	.25m – 1.5m	
D7 width	1m	.38m	.25m – 1.5m	
D8 width	1m	.88m	.25m – 1.5m	
D9 width	1m	.67m	.25m – 1.5m	
D10 width	1m	1.04m	.25m – 1.5m	
D11 width	1m	.93m	.25m – 1.5m	
D12 width	1m	.85m	.25m – 1.5m	
D13 width	1m	1.16m	.25m – 1.5m	
D14 width	1m	1.17m	.25m – 1.5m	
D15 width	1m	.60m	.25m – 1.5m	
D16 width	1m	1.16m	.25m – 1.5m	
D17 width	1m	.89m	.25m – 1.5m	
D18 width	1m	1.20m	.25m – 1.5m	

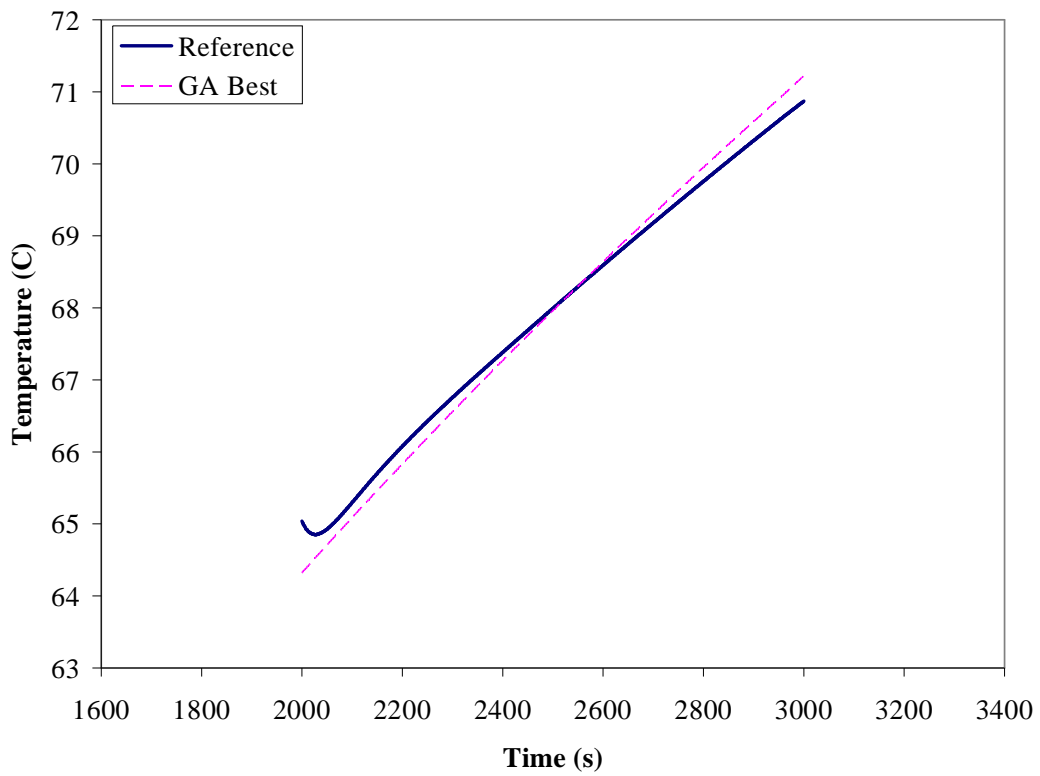
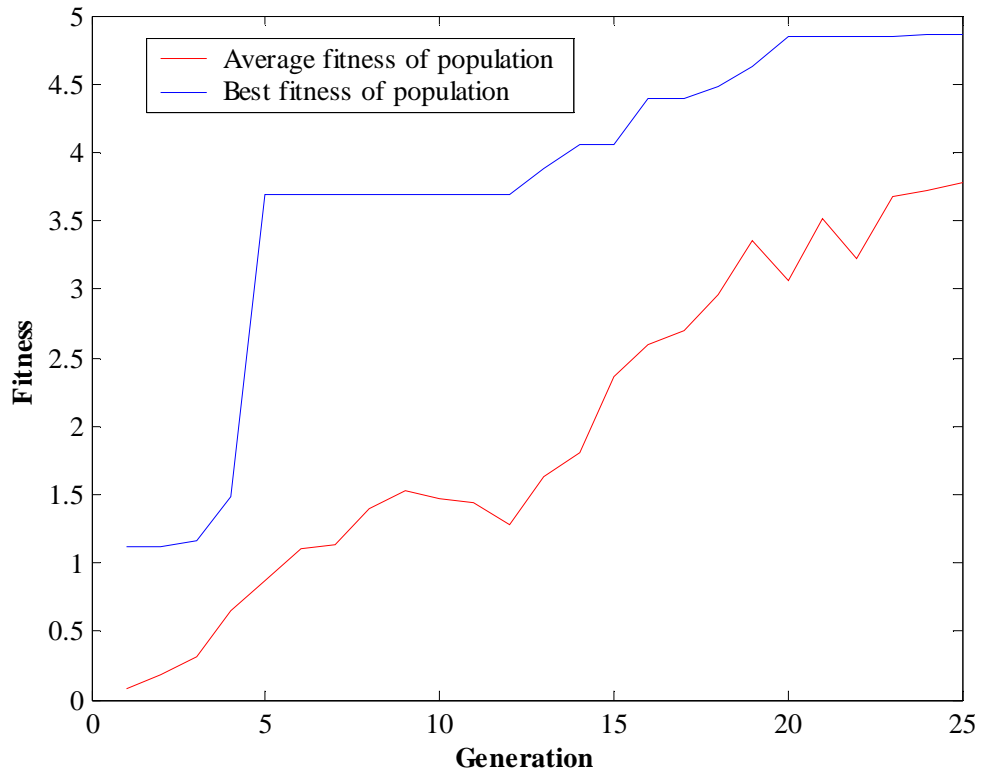
MR_W1_10_11_c_1



MR_W1_W10:18_a_1: Total HRR is the total HRR added up in each compartment. The HRR's are averaged from 2000-3000s in increments of 200s.

Parameters	Reference Values	GA Best	Bounds	Notes
Mass Loss Rate	3000 kW	3216 kW	200- 7000 kW	Population size 25, 25 generations
Total HRR	2015 kW	2160 kW		
HRR Fire Room	1592 kW	1655 kW		
HRR Corridor	423 kW	498 kW		
HRR Room 1 (Analysis Window)	0 kW	1 kW		
HRR in all other rooms combined	0 kW	5 kW		
D1 width	1m	.71m	.25m – 1.5m	
D2 width	1m	1.01m	.25m – 1.5m	
D3 width	1m	.49m	.25m – 1.5m	
D4 width	1m	.27m	.25m – 1.5m	
D5 width	1m	.55m	.25m – 1.5m	
D6 width	1m	1.02m	.25m – 1.5m	
D7 width	1m	.53m	.25m – 1.5m	
D8 width	1m	1.30m	.25m – 1.5m	
D9 width	1m	.85m	.25m – 1.5m	
D10 width	1m	1.16m	.25m – 1.5m	
D11 width	1m	.55m	.25m – 1.5m	
D12 width	1m	1.18m	.25m – 1.5m	
D13 width	1m	.99m	.25m – 1.5m	
D14 width	1m	.28m	.25m – 1.5m	
D15 width	1m	.99m	.25m – 1.5m	
D16 width	1m	1.08m	.25m – 1.5m	
D17 width	1m	1.44m	.25m – 1.5m	
D18 width	1m	.34m	.25m – 1.5m	

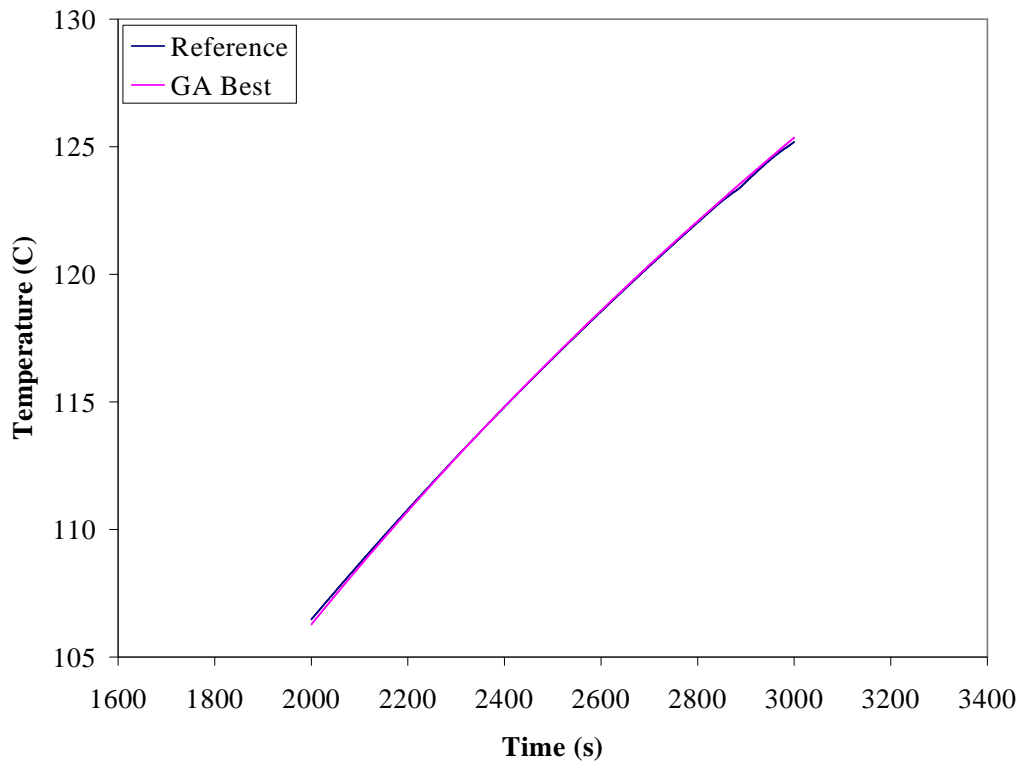
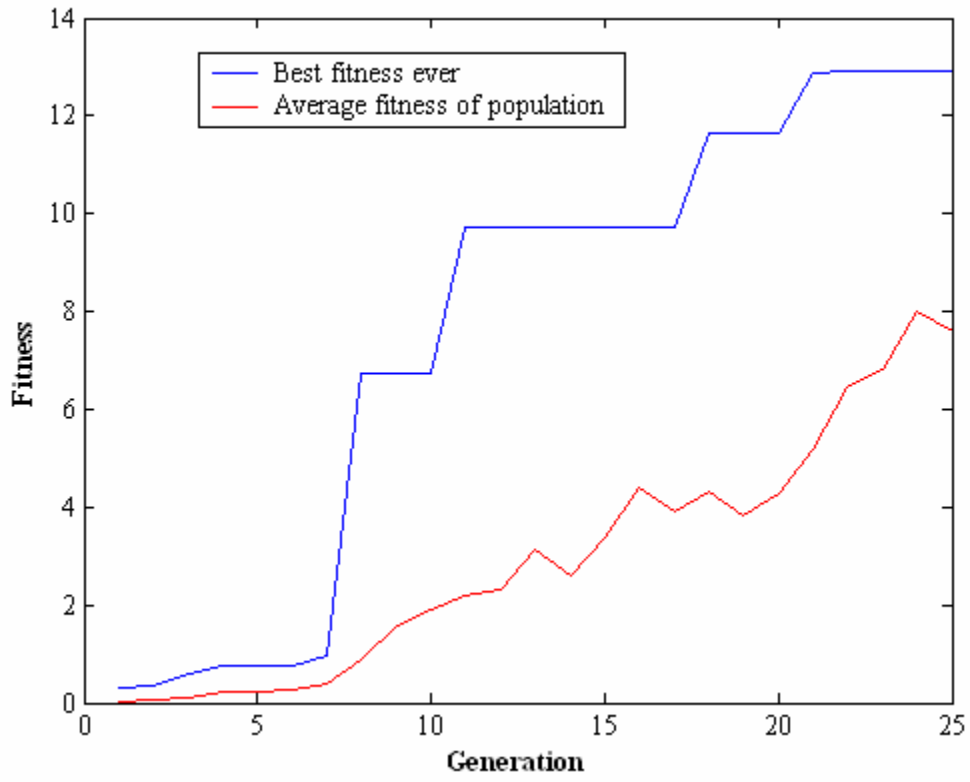
MR_W1_W10:18_a_1



MR_W1_W10:18_a_2: Total HRR is the total HRR added up in each compartment. The HRR's are averaged from 2000-3000s in increments of 200s.

Parameters	Reference Values	GA Best	Bounds	Notes
Mass Loss Rate	5000 kW	5678 kW	200- 7000 kW	Population size 25, 25 generations
Total HRR	2717 kW	2793 kW		
HRR Fire Room	1626 kW	1677 kW		
HRR Corridor	800 kW	708 kW		
HRR Room 1 (Analysis Window)	23 kW	29 kW		
HRR in all other rooms combined	269 kW	379 kW		
D1 width	1m	.73m	.25m – 1.5m	
D2 width	1m	1.38m	.25m – 1.5m	
D3 width	1m	.43m	.25m – 1.5m	
D4 width	1m	1.23m	.25m – 1.5m	
D5 width	1m	.49m	.25m – 1.5m	
D6 width	1m	.92m	.25m – 1.5m	
D7 width	1m	.30m	.25m – 1.5m	
D8 width	1m	.77m	.25m – 1.5m	
D9 width	1m	1.02m	.25m – 1.5m	
D10 width	1m	.81m	.25m – 1.5m	
D11 width	1m	1.44m	.25m – 1.5m	
D12 width	1m	1.37m	.25m – 1.5m	
D13 width	1m	.67m	.25m – 1.5m	
D14 width	1m	.56m	.25m – 1.5m	
D15 width	1m	.74m	.25m – 1.5m	
D16 width	1m	1.09m	.25m – 1.5m	
D17 width	1m	.35m	.25m – 1.5m	
D18 width	1m	.84m	.25m – 1.5m	

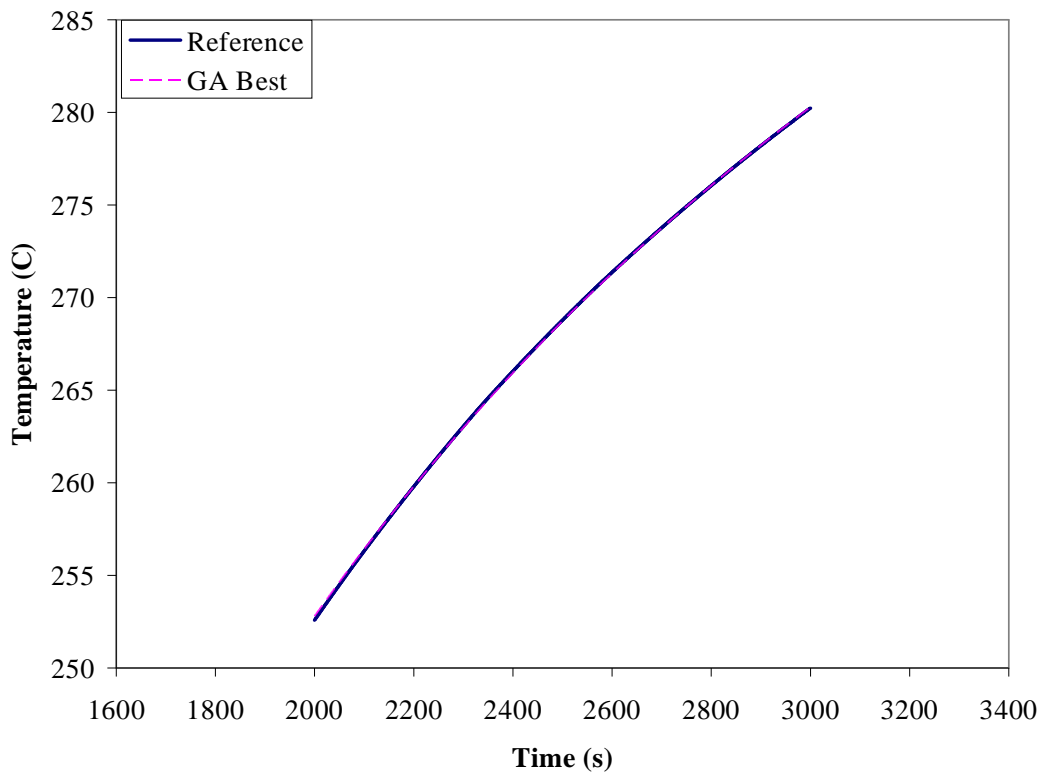
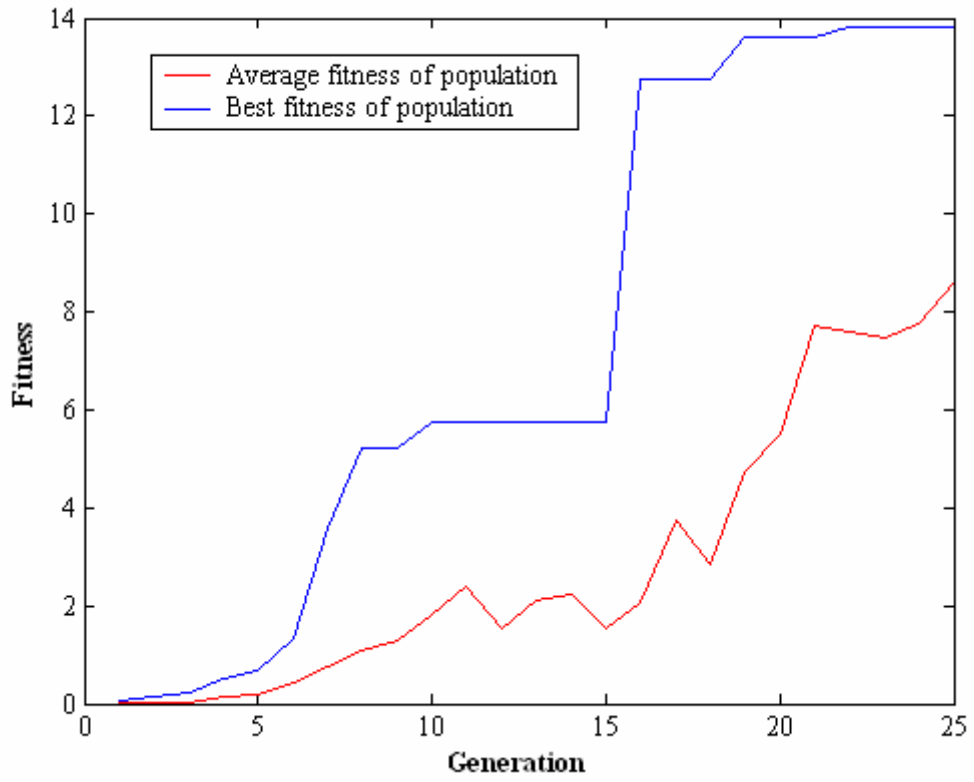
MR_W1_W10:18_a_2



MR_W1_W10:18_a_3: Total HRR is the total HRR added up in each compartment. The HRR's are averaged from 2000-3000s in increments of 200s.

Parameters	Reference Values	GA Best	Bounds	Notes
Mass Loss Rate	7000 kW	6144 kW	200- 7000 kW	Population size 25, 25 generations
Total HRR	3402 kW	3222 kW		
HRR Fire Room	1734 kW	1754 kW		
HRR Corridor	817 kW	855 kW		
HRR Room 1 (Analysis Window)	79 kW	74 kW		
HRR in all other rooms combined	772 kW	539 kW		
D1 width	1m	1.47m	.25m – 1.5m	
D2 width	1m	.67m	.25m – 1.5m	
D3 width	1m	1.50m	.25m – 1.5m	
D4 width	1m	1.50m	.25m – 1.5m	
D5 width	1m	1.50m	.25m – 1.5m	
D6 width	1m	.36m	.25m – 1.5m	
D7 width	1m	.71m	.25m – 1.5m	
D8 width	1m	1.30m	.25m – 1.5m	
D9 width	1m	.93m	.25m – 1.5m	
D10 width	1m	1.12m	.25m – 1.5m	
D11 width	1m	1.11m	.25m – 1.5m	
D12 width	1m	1.11m	.25m – 1.5m	
D13 width	1m	.97m	.25m – 1.5m	
D14 width	1m	.50m	.25m – 1.5m	
D15 width	1m	.63m	.25m – 1.5m	
D16 width	1m	.46m	.25m – 1.5m	
D17 width	1m	1.50m	.25m – 1.5m	
D18 width	1m	1.06m	.25m – 1.5m	

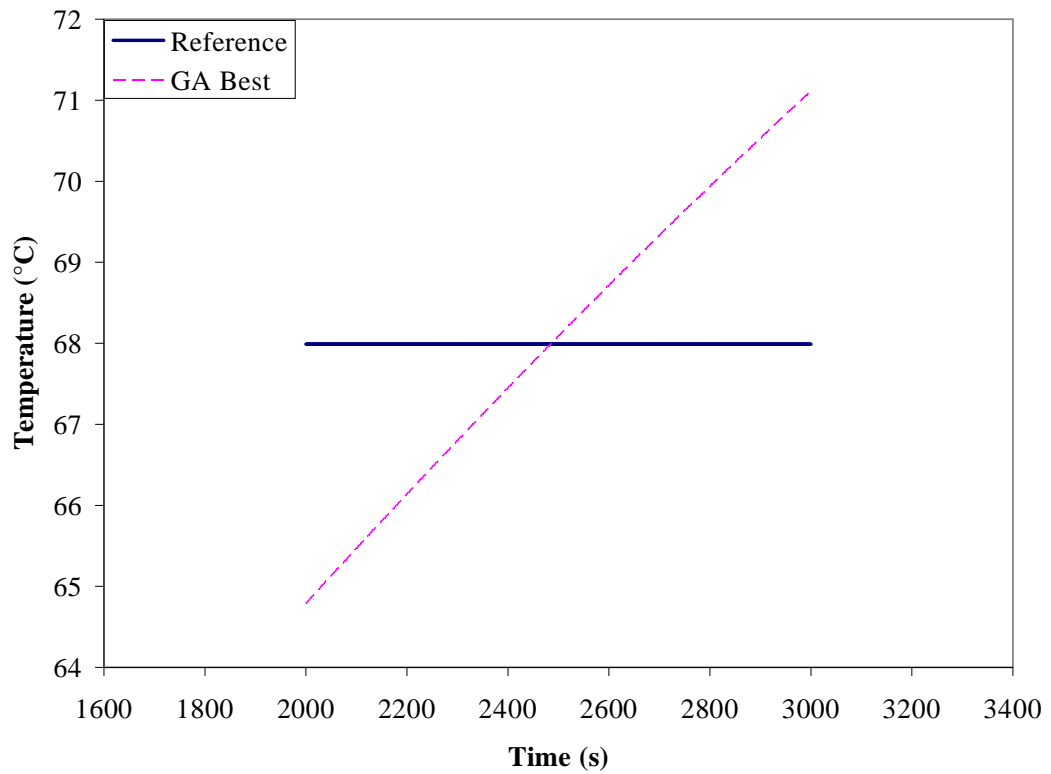
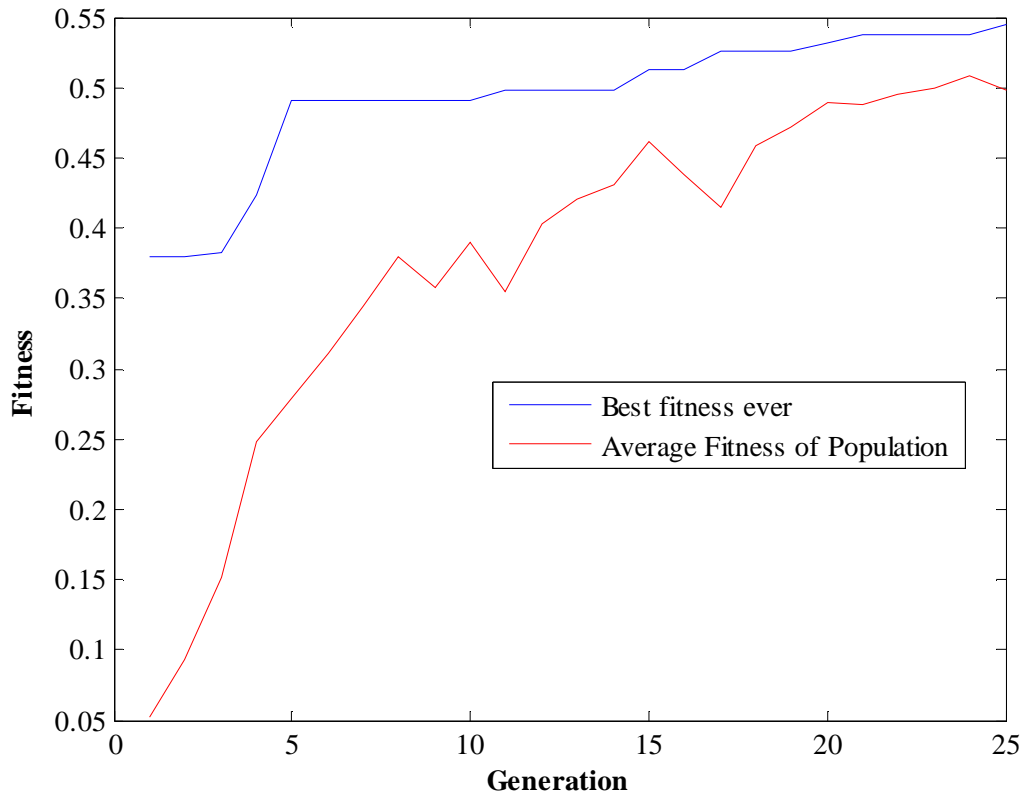
MR_W1_W10:18_a_3



MR_W1_W10:18_b_1: Total HRR is the total HRR added up in each compartment. The HRR's are averaged from 2000-3000s in increments of 200s.

Parameters	Reference Values	GA Best	Bounds	Notes
Mass Loss Rate	3000 kW	3035 kW	200- 7000 kW	Population size 25, 25 generations
Total HRR	2015 kW	2097 kW		
HRR Fire Room	1592 kW	1642 kW		
HRR Corridor	423 kW	450 kW		
HRR Room 1 (Analysis Window)	0 kW	0 kW		
HRR in all other rooms combined	0 kW	5 kW		
D1 width	1m	.76m	0.25m – 1.5m	
D2 width	1m	1.01m	0.25m – 1.5m	
D3 width	1m	.56m	0.25m – 1.5m	
D4 width	1m	.33m	0.25m – 1.5m	
D5 width	1m	1.15m	0.25m – 1.5m	
D6 width	1m	1.05m	0.25m – 1.5m	
D7 width	1m	.70m	0.25m – 1.5m	
D8 width	1m	1.28m	0.25m – 1.5m	
D9 width	1m	.37m	0.25m – 1.5m	
D10 width	1m	1.19m	0.25m – 1.5m	
D11 width	1m	.55m	0.25m – 1.5m	
D12 width	1m	1.17m	0.25m – 1.5m	
D13 width	1m	.98m	0.25m – 1.5m	
D14 width	1m	.29m	0.25m – 1.5m	
D15 width	1m	.95m	0.25m – 1.5m	
D16 width	1m	1.04m	0.25m – 1.5m	
D17 width	1m	1.44m	0.25m – 1.5m	
D18 width	1m	.35m	0.25m – 1.5m	

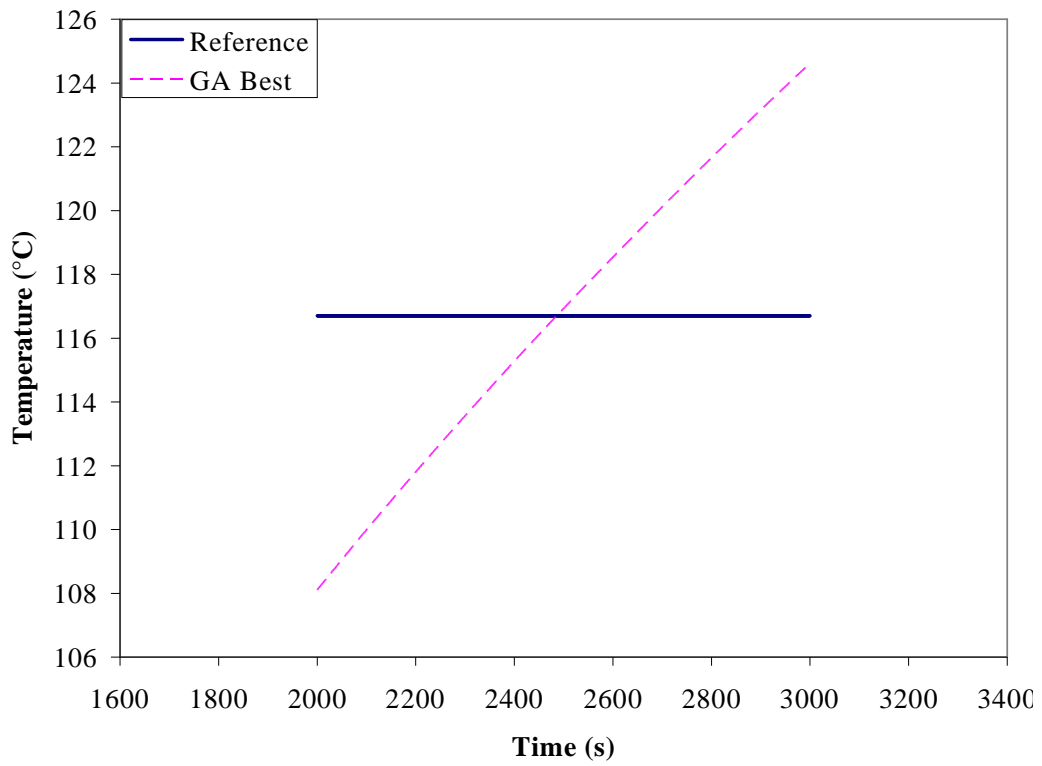
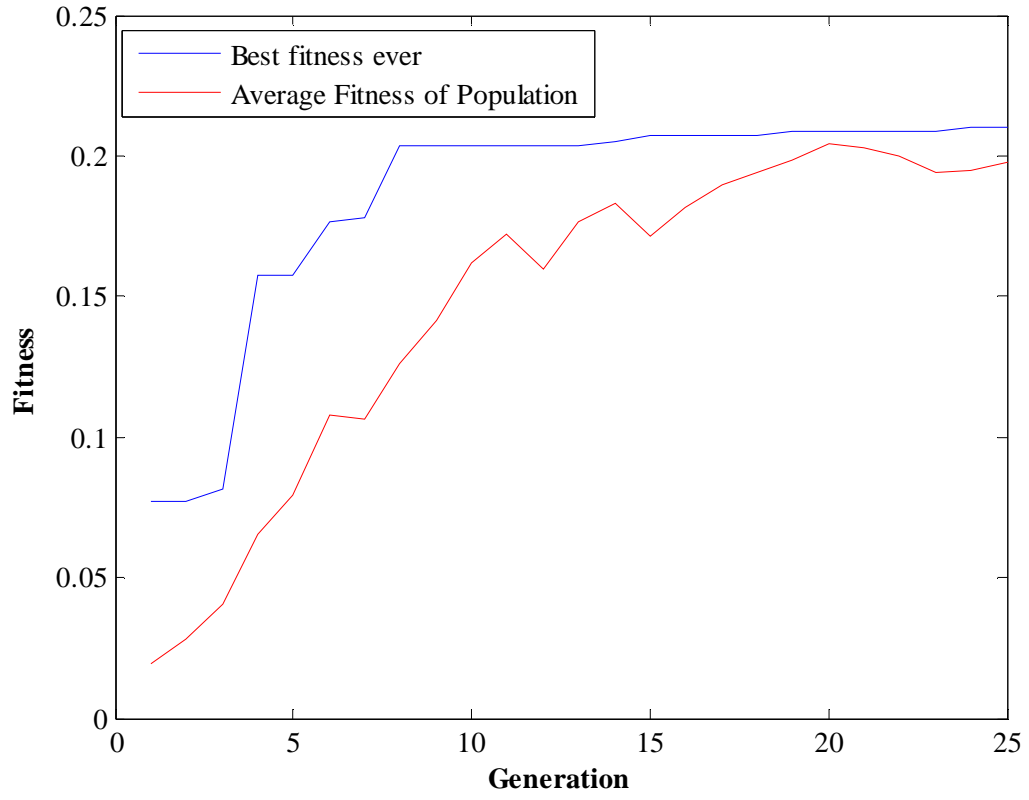
MR_W1_W10:18_b_1



MR_W1_W10:18_b_2: Total HRR is the total HRR added up in each compartment. The HRR's are averaged from 2000-3000s in increments of 200s.

Parameters	Reference Values	GA Best	Bounds	Notes
Mass Loss Rate	5000 kW	5511 kW	200- 7000 kW	Population size 25, 25 generations
Total HRR	2717 kW	3190 kW		
HRR Fire Room	1626 kW	1828 kW		
HRR Corridor	800 kW	947 kW		
HRR Room 1 (Analysis Window)	23 kW	21 kW		
HRR in all other rooms combined	269 kW	394 kW		
D1 width	1m	.72m	0.25 m – 1.5m	
D2 width	1m	.50m	0.25 m – 1.5m	
D3 width	1m	.28m	0.25 m – 1.5m	
D4 width	1m	.66m	0.25 m – 1.5m	
D5 width	1m	0.97m	0.25 m – 1.5m	
D6 width	1m	0.28m	0.25 m – 1.5m	
D7 width	1m	1.04m	0.25 m – 1.5m	
D8 width	1m	1.20m	0.25 m – 1.5m	
D9 width	1m	.72m	0.25 m – 1.5m	
D10 width	1m	1.35m	0.25 m – 1.5m	
D11 width	1m	1.38 m	0.25 m – 1.5m	
D12 width	1m	1.49m	0.25 m – 1.5m	
D13 width	1m	1.36m	0.25 m – 1.5m	
D14 width	1m	.58m	0.25 m – 1.5m	
D15 width	1m	1.39 m	0.25 m – 1.5m	
D16 width	1m	1.29m	0.25 m – 1.5m	
D17 width	1m	0.99m	0.25 m – 1.5m	
D18 width	1m	1.38m	0.25 m – 1.5m	

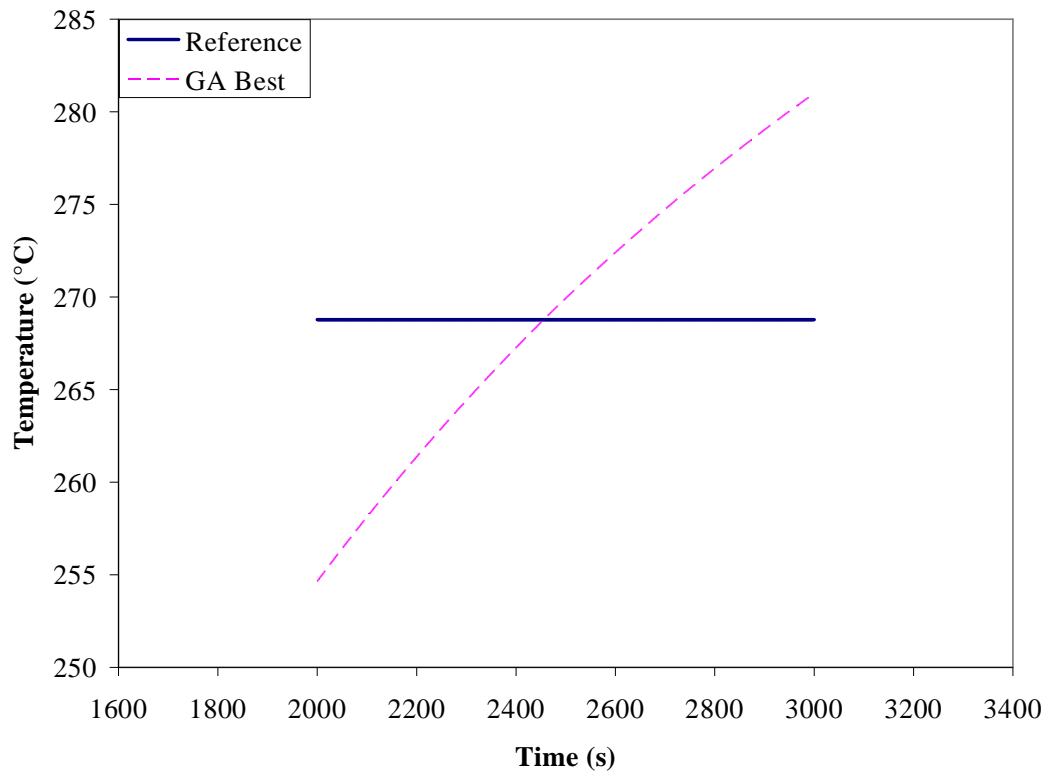
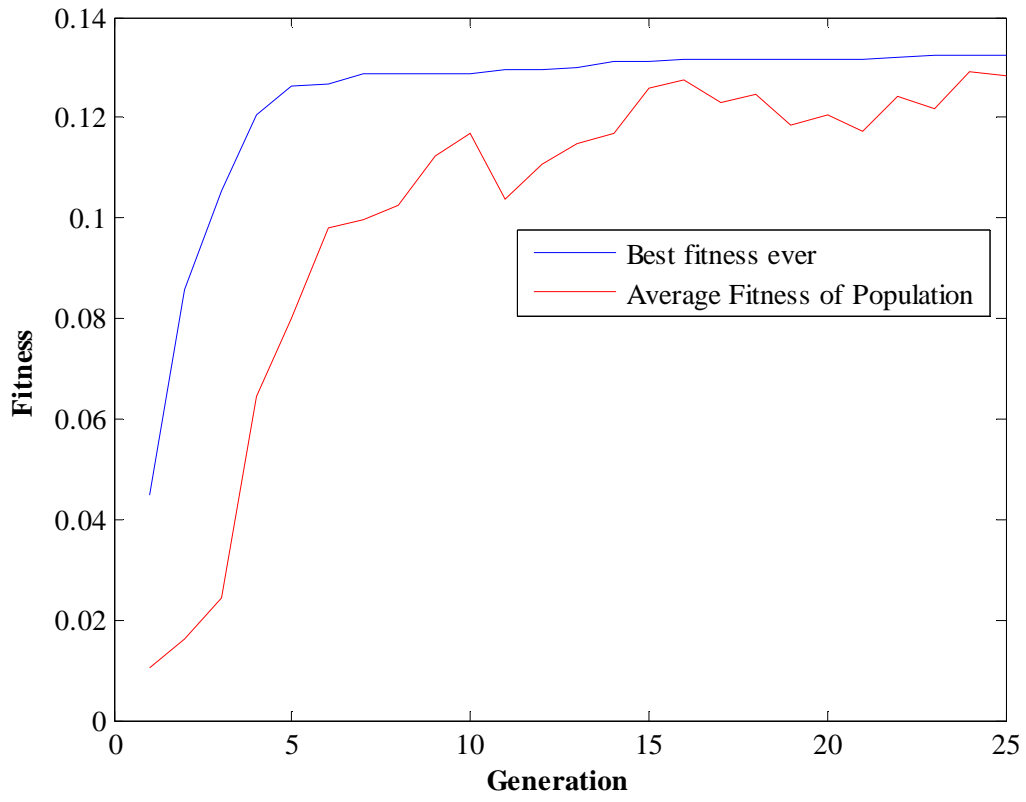
MR_W1_W10:18_b_2



MR_W1_W10:18_b_3: Total HRR is the total HRR added up in each compartment. The HRR's are averaged from 2000-3000s in increments of 200s.

Parameters	Reference Values	GA Best	Bounds	Notes
Mass Loss Rate	7000 kW	6037 kW	200- 7000 kW	Population size 25, 25 generations
Total HRR	3402 kW	3242 kW		
HRR Fire Room	1734 kW	1800 kW		
HRR Corridor	817 kW	868 kW		
HRR Room 1 (Analysis Window)	79 kW	73 kW		
HRR in all other rooms combined	771 kW	502 kW		
D1 width	1m	1.46m	0.25 m – 1.5m	
D2 width	1m	1.40m	0.25 m – 1.5m	
D3 width	1m	.91m	0.25 m – 1.5m	
D4 width	1m	.25m	0.25 m – 1.5m	
D5 width	1m	1.21m	0.25 m – 1.5m	
D6 width	1m	.27m	0.25 m – 1.5m	
D7 width	1m	1.07m	0.25 m – 1.5m	
D8 width	1m	.88m	0.25 m – 1.5m	
D9 width	1m	.48m	0.25 m – 1.5m	
D10 width	1m	1.15m	0.25 m – 1.5m	
D11	1m	.88m	0.25 m – 1.5m	
D12	1m	1.27m	0.25 m – 1.5m	
D13	1m	.74m	0.25 m – 1.5m	
D14	1m	.76m	0.25 m – 1.5m	
D15	1m	.57m	0.25 m – 1.5m	
D16	1m	.55m	0.25 m – 1.5m	
D17	1m	1.21m	0.25 m – 1.5m	
D18	1m	1.01m	0.25 m – 1.5m	

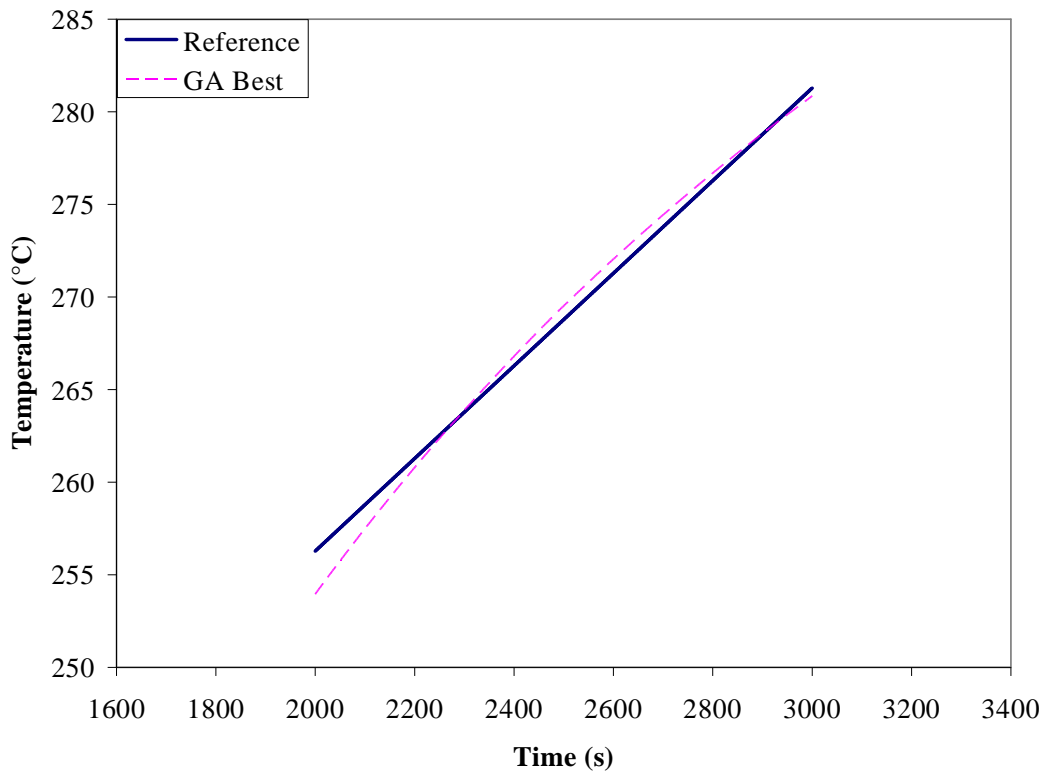
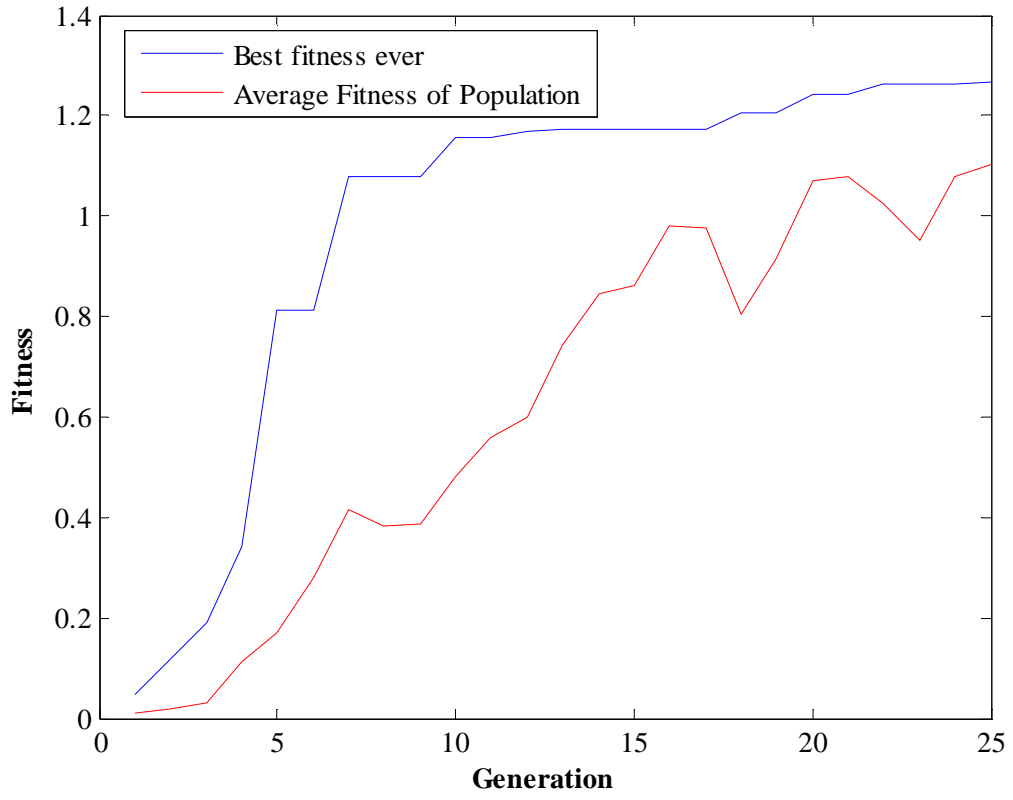
MR_W1_W10:18_b_3



MR_W1_W10:18_c_1: Total HRR is the total HRR added up in each compartment. The HRR's are averaged from 2000-3000s in increments of 200s.

Parameters	Reference Values	GA Best	Bounds	Notes
Mass Loss Rate	7000 kW	6027 kW	200- 7000 kW	Population size 25, 25 generations
Total HRR	3363 kW	3213 kW		
HRR Fire Room	1686 kW	1778 kW		
HRR Corridor	787 kW	867 kW		
HRR Room 1 (Analysis Window)	82 kW	73 kW		
HRR in all other rooms combined	808 kW	496 kW		
D1 width	1m	1.46m	0.25 m – 1.5m	
D2 width	1m	1.40m	0.25 m – 1.5m	
D3 width	1m	.89m	0.25m – 1.5m	
D4 width	1m	.85m	0.25m – 1.5m	
D5 width	1m	1.16m	0.25m – 1.5m	
D6 width	1m	.28m	0.25m – 1.5m	
D7 width	1m	.75m	0.25m – 1.5m	
D8 width	1m	.29m	0.25m – 1.5m	
D9 width	1m	.67m	0.25m – 1.5m	
D10 width	1m	1.15m	0.25m – 1.5m	
D11	1m	.90m	0.25m – 1.5m	
D12	1m	1.27m	0.25m – 1.5m	
D13	1m	.68m	0.25m – 1.5m	
D14	1m	.76m	0.25m – 1.5m	
D15	1m	.56m	0.25m – 1.5m	
D16	1m	.31m	0.25m – 1.5m	
D17	1m	1.27m	0.25m – 1.5m	
D18	1m	1.16m	0.25m – 1.5m	

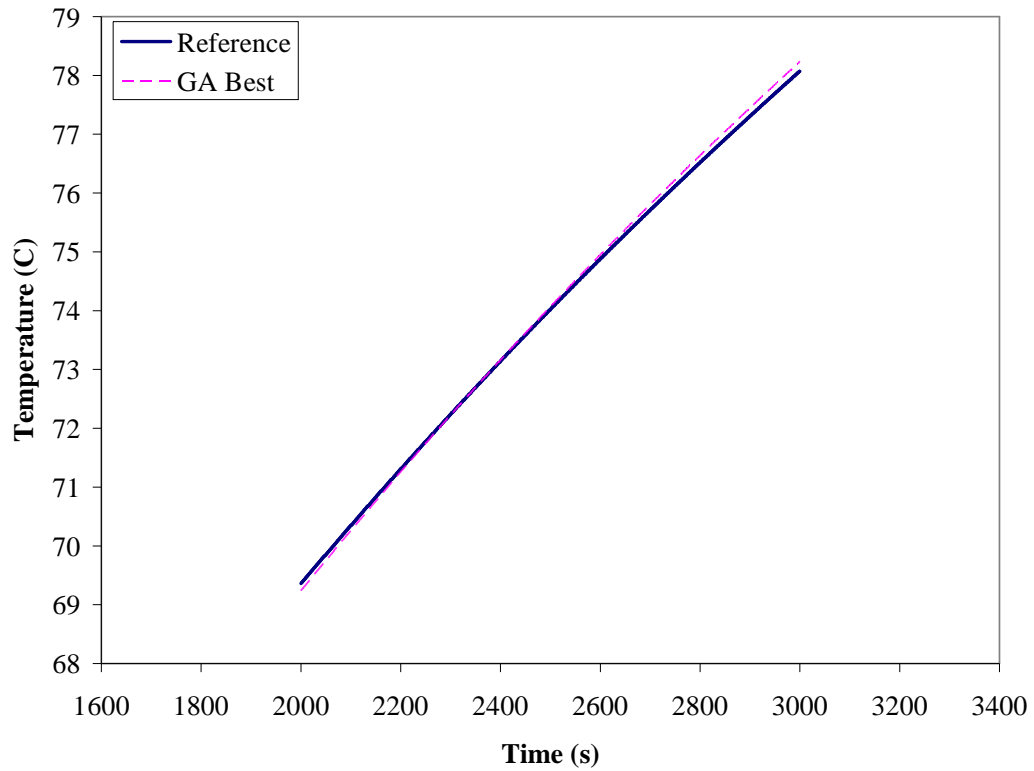
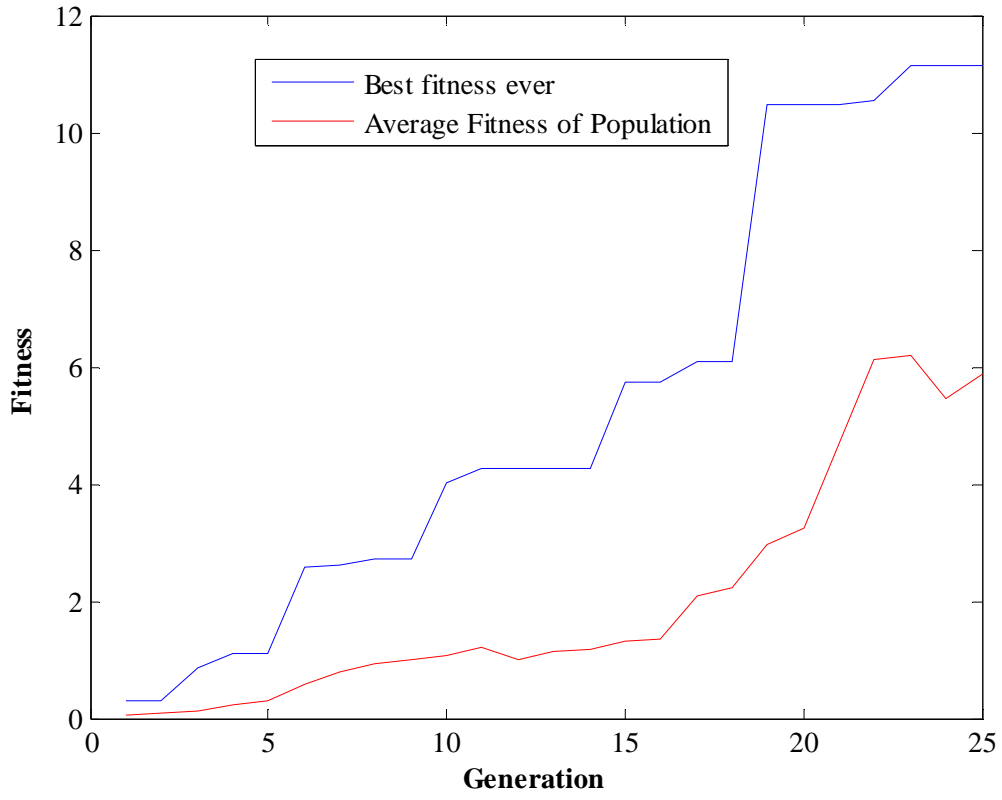
MR_W1_W10:18_c_1



MR_W1:18_a_1: Total HRR is the total HRR added up in each compartment. The HRR's are averaged from 2000-3000s in increments of 200s.

Parameters	Reference Values	GA Best	Bounds	Notes
Mass Loss Rate	3000 kW	4472 kW	200- 7000 kW	Population size 25, 25 generations
Total HRR	2176 kW	2954 kW		
HRR Fire Room	1819 kW	2054 kW		
HRR Corridor	357 kW	772 kW		
HRR Room 1 (Analysis Window)	0 kW	5 kW		
HRR in all other rooms combined	0 kW	122 kW		
D1 width	1m	.48m	0m – 1.5m	
D2 width	1m	.87m	0m – 1.5m	
D3 width	1m	.11m	0m – 1.5m	
D4 width	1m	.33m	0m – 1.5m	
D5 width	1m	1.29m	0m – 1.5m	
D6 width	1m	.36m	0m – 1.5m	
D7 width	1m	.83m	0m – 1.5m	
D8 width	1m	.79m	0m – 1.5m	
D9 width	1m	1.07m	0m – 1.5m	
D10 width	1m	1.33m	0m – 1.5m	
D11 width	1m	.45m	0m – 1.5m	
D12 width	1m	1.17m	0m – 1.5m	
D13 width	1m	1.17	0m – 1.5m	
D14 width	1m	.49m	0m – 1.5m	
D15 width	1m	1.28m	0m – 1.5m	
D16 width	1m	.99m	0m – 1.5m	
D17 width	1m	.84m	0m – 1.5m	
D18 width	1m	.81m	0m – 1.5m	

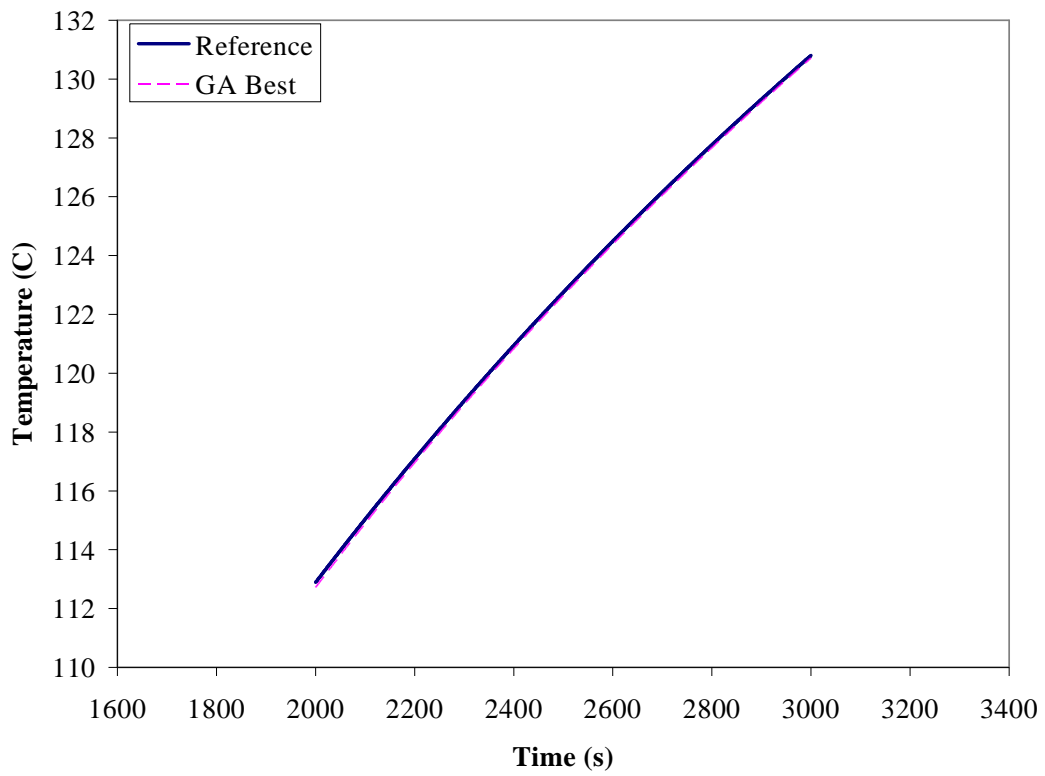
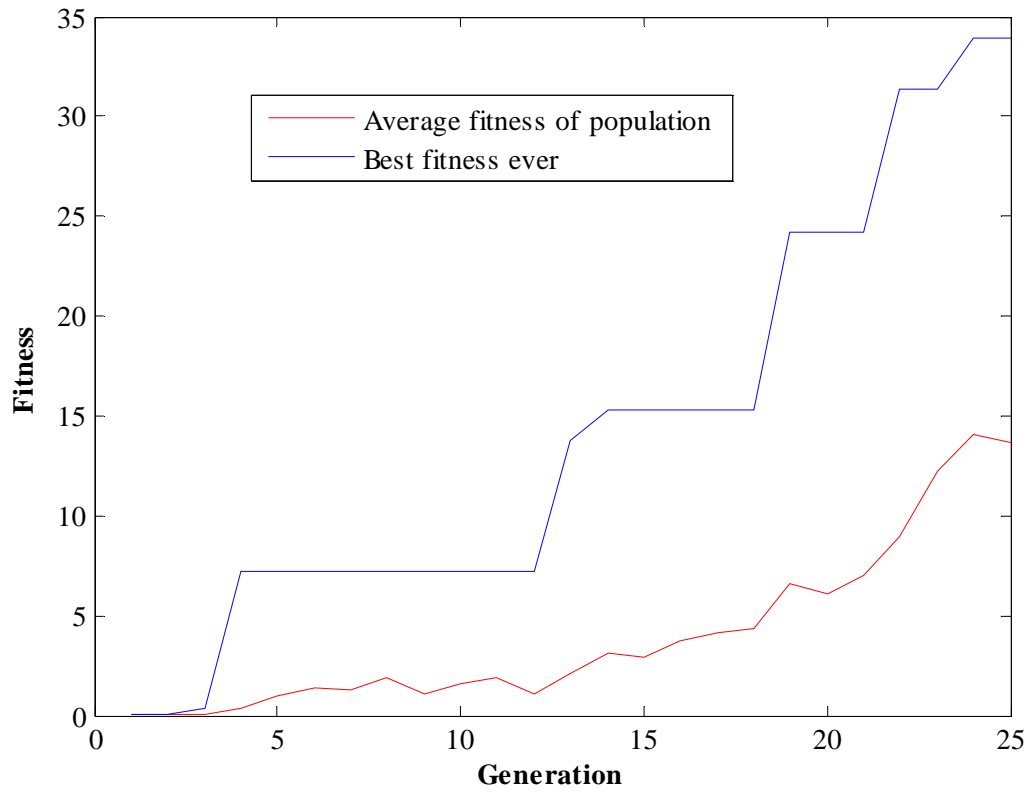
MR_W1:18_a_1



MR_W1:18_a_2: Total HRR is the total HRR added up in each compartment. The HRR's are averaged from 2000-3000s in increments of 200s.

Parameters	Reference Values	GA Best	Bounds	Notes
Mass Loss Rate	5000 kW	6175 kW	200- 5250 kW	Population size 25, 25 generations
Total HRR	2971 kW	3562 kW		
HRR Fire Room	2012 kW	2128 kW		
HRR Corridor	766 kW	860 kW		
HRR Room 1 (Analysis Window)	12 kW	19 kW		
HRR in all other rooms combined	182 kW	555 kW		
D1 width	1m	.30m	0m – 1.5m	
D2 width	1m	.22m	0m – 1.5m	
D3 width	1m	.93m	0m – 1.5m	
D4 width	1m	.36m	0m – 1.5m	
D5 width	1m	.74m	0m – 1.5m	
D6 width	1m	.03m	0m – 1.5m	
D7 width	1m	.83m	0m – 1.5m	
D8 width	1m	.60m	0m – 1.5m	
D9 width	1m	0.23m	0m – 1.5m	
D10 width	1m	1.19m	0m – 1.5m	
D11 width	1m	1.28m	0m – 1.5m	
D12 width	1m	.07m	0m – 1.5m	
D13 width	1m	1.50m	0m – 1.5m	
D14 width	1m	.90m	0m – 1.5m	
D15 width	1m	.57m	0m – 1.5m	
D16 width	1m	.46m	0m – 1.5m	
D17 width	1m	.68m	0m – 1.5m	
D18 width	1m	.37m	0m – 1.5m	

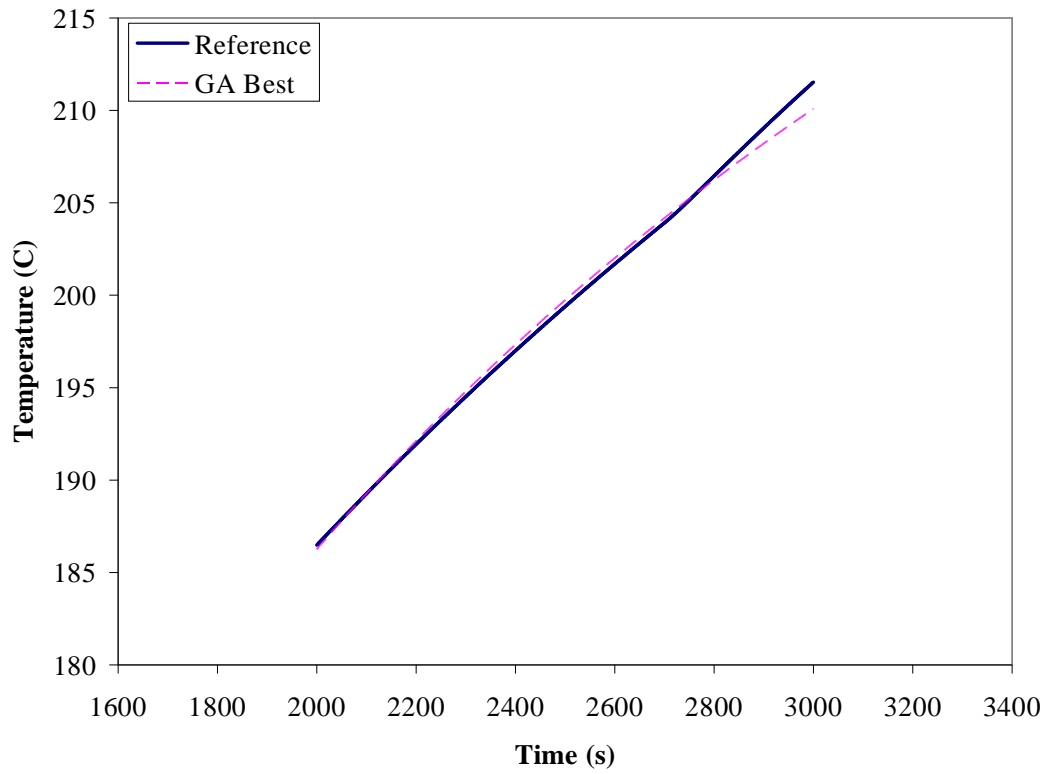
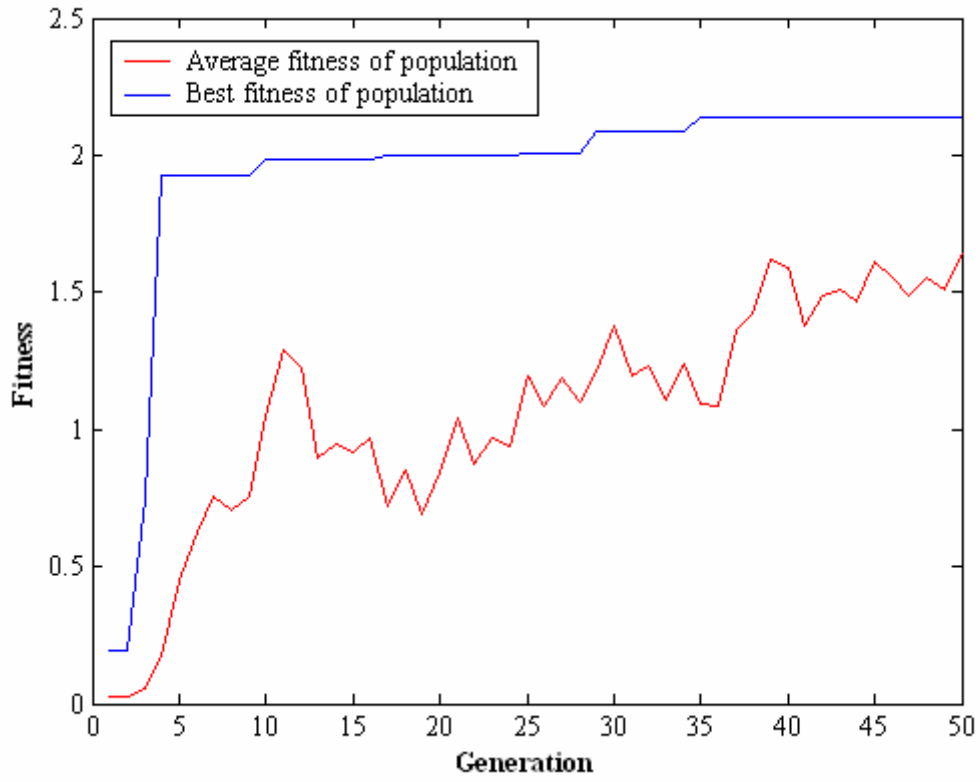
MR_W1:18_a_2



MR_W1:18_a_3: Total HRR is the total HRR added up in each compartment. The HRR's are averaged from 2000-3000s in increments of 200s.

Parameters	Reference Values	GA Best	Bounds	Notes
Mass Loss Rate	7000 kW	5863 kW	200- 7000 kW	Population size 25, 50 generations
Total HRR	3732 kW	3555 kW		
HRR Fire Room	2074 kW	2159 kW		
HRR Corridor	979 kW	910 kW		
HRR Room 1 (Analysis Window)	40 kW	36 kW		
HRR in all other rooms combined	639 kW	450 kW		
D1 width	1m	1.28m	0m – 1.5m	
D2 width	1m	1.31m	0m – 1.5m	
D3 width	1m	1.44m	0m – 1.5m	
D4 width	1m	.53m	0m – 1.5m	
D5 width	1m	1.33m	0m – 1.5m	
D6 width	1m	.31m	0m – 1.5m	
D7 width	1m	1.37m	0m – 1.5m	
D8 width	1m	.86m	0m – 1.5m	
D9 width	1m	1.28m	0m – 1.5m	
D10 width	1m	1.29m	0m – 1.5m	
D11 width	1m	.90m	0m – 1.5m	
D12 width	1m	1.14m	0m – 1.5m	
D13 width	1m	.71m	0m – 1.5m	
D14 width	1m	.97m	0m – 1.5m	
D15 width	1m	.79m	0m – 1.5m	
D16 width	1m	.44m	0m – 1.5m	
D17 width	1m	1.50m	0m – 1.5m	
D18 width	1m	1.03m	0m – 1.5m	

MR_W1:18_a_3



Appendix A5

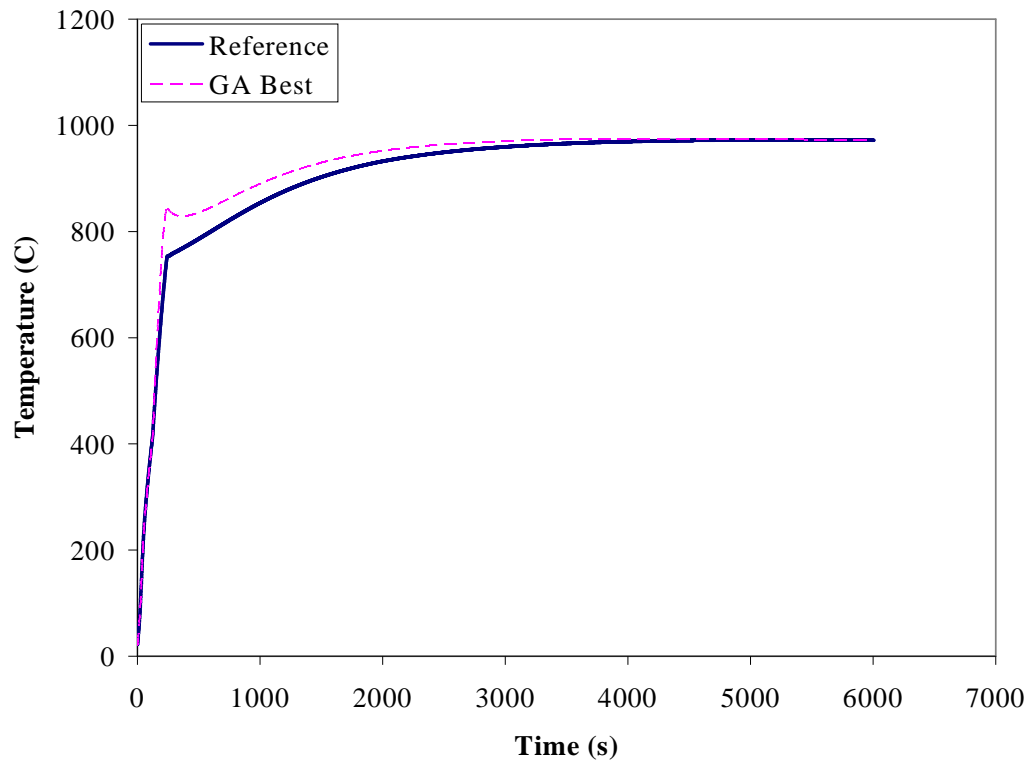
Studies on the affect of population size and the number of generations

*For the population size studies a 3m x 3m x 3m compartment composed of hard and flexible fiber board was analyzed. The fire was ramped up to 720 kW at 120s, and then a steady fire was specified from 240-6000s. All simulations analyzed the entire reference curve from 1-6000s. Varying population sizes and generations were then analyzed.

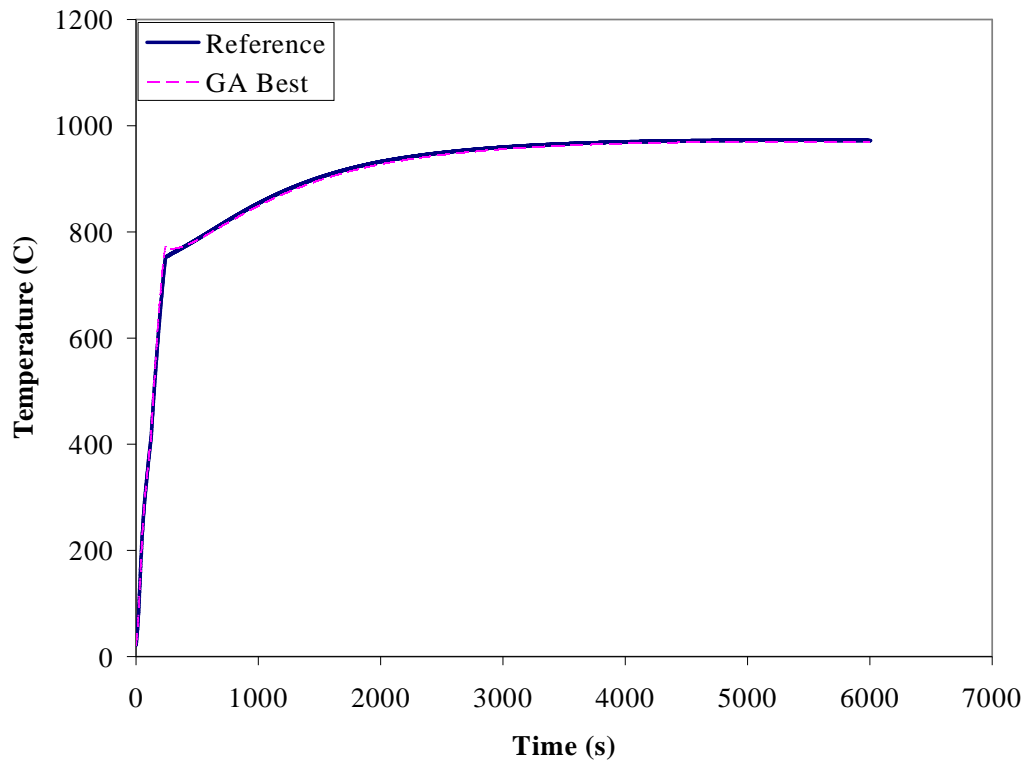
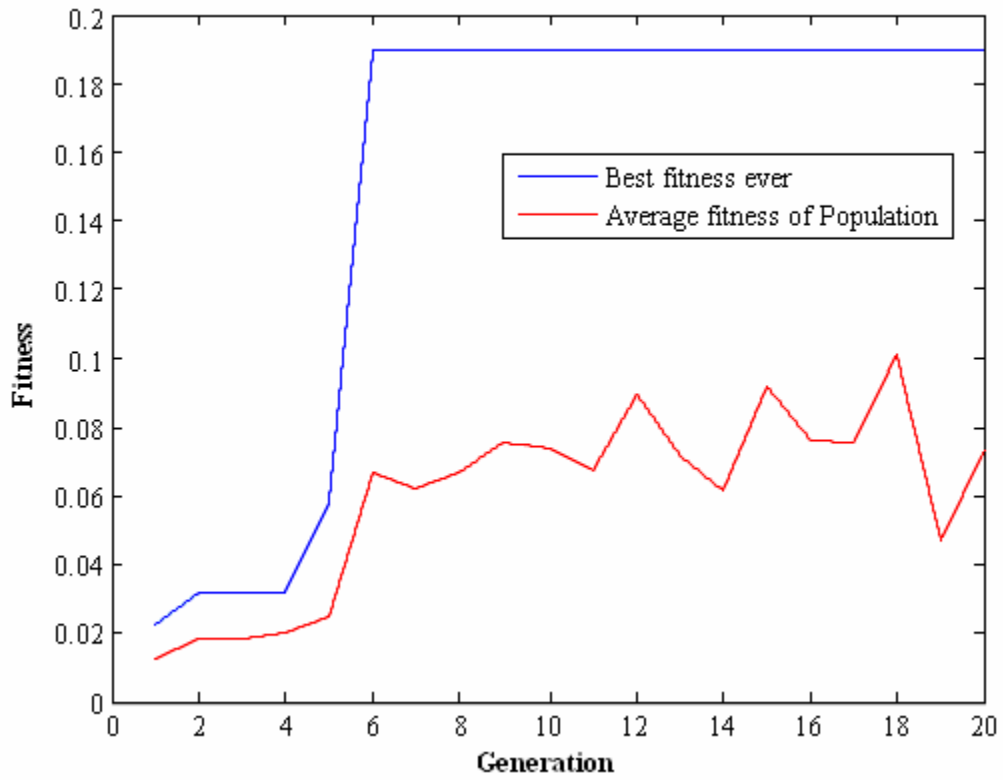
Simulation Number	Reference MLR	Reference Average HRR	Reference Vent	GA Best MLR	GA Best Average HRR	GA Best Vent	Bounds on MLR	Bounds on Vent	Notes on Simulation
SR3_3_3_Fb_a_1	2300kW	1129 kW (240-6000s)	1m x 2m	3475 kW	1387 kW (240-6000s)	1.23m x 2.02m	500-7,000 kW	Width: 0.5m-2m, Height: 1m-3m	Population size of 5, 1 generation.
SR3_3_3_Fb_a_2	2300kW	1129 kW (240-6000s)	1m x 2m	2576 kW	1123 kW (240-6000s)	1.06m x 1.90m	500-7,000 kW	Width: 0.5m-2m, Height: 1m-3m	Population size of 5, 20 generations.
SR3_3_3_Fb_a_3	2300kW	1129 kW (240-6000s)	1m x 2m	2405 kW	1155 kW (240-6000s)	1.31m x 1.81m	500-7,000 kW	Width: 0.5m-2m, Height: 1m-3m	Population size of 5, 50 generations
SR3_3_3_Fb_a_4	2300kW	1129 kW (240-6000s)	1m x 2m	2505 kW	1155 kW (240-6000s)	1.14m x 1.90m	500-7,000 kW	Width: 0.5m-2m, Height: 1m-3m	Population size of 5, 100 generations
SR3_3_3_Fb_a_5	2300kW	1129 kW (240-6000s)	1m x 2m	2465 kW	1191 kW (240-6000s)	.78m x 2.32m	500-7,000 kW	Width: 0.5m-2m, Height: 1m-3m	Population size of 25, 1 generation.
SR3_3_3_Fb_a_6	2300kW	1129 kW (240-6000s)	1m x 2m	2347 kW	1112 kW (240-6000s)	.87m x 2.09m	500-7,000 kW	Width: 0.5m-2m, Height: 1m-3m	Population size of 25, 20 generations.
SR3_3_3_Fb_a_7	2300kW	1129 kW (240-6000s)	1m x 2m	2300.4 kW	1129 kW (240-6000s)	1.00m x 2.00m	500-7,000kW	Width: 0.5m-2.0m, Height: 1m-3m	Population size of 25, 50 generations
SR3_3_3_Fb_a_8	2300kW	1129 kW (240-6000s)	1m x 2m	2299.9 kW	1129 kW (240-6000s)	1.003 m x 1.999 m	500-7,000 kW	Width: 0.5m-2.0m, Height: 1m-3m	Population size of 25, 100 generations.
SR3_3_3_Fb_a_9	2300kW	1129 kW (240-6000s)	1m x 2m	2201 kW	1250 kW (240-6000s)	1.31m x 2.00m	500-7,000 kW	Width: 0.5m-2.0m, Height: 1m-3m	Population size of 100, 1 generations.

Simulation Number	Reference MLR	Reference Average HRR	Reference Vent	GA Best MLR	GA Best Average HRR	GA Best Vent	Bounds on HRR	Bounds on Vent	Notes on Simulation
SR3_3_3_Fb_a_10	2300kW	1129 kW (240-6000s)	1m x 2m	2295 kW	1155 kW (240-6000s)	1.24m x 1.87m	500-7,000 kW	Width: 0.5m-2.0m, Height: 1m-3m	Population size of 100, 20 generations.
SR3_3_3_Fb_a_11	2300kW	1129 kW (240-6000s)	1m x 2m	2292kW	1128.3 kW (240-6000s)	.99m x 2.01m	500-7,000 kW	Width: 0.5m-2.0m, Height: 1m-3m	100 population size, 50 Generations
SR3_3_3_Fb_a_14	2300kW	1129 kW (240-6000s)	1m x 2m	2327 kW	1123 kW (240-6000s)	.90m x 2.08m	500-7,000 kW	Width: 0.5m-2.0m, Height: 1m-3m	100 population size 100 generations.

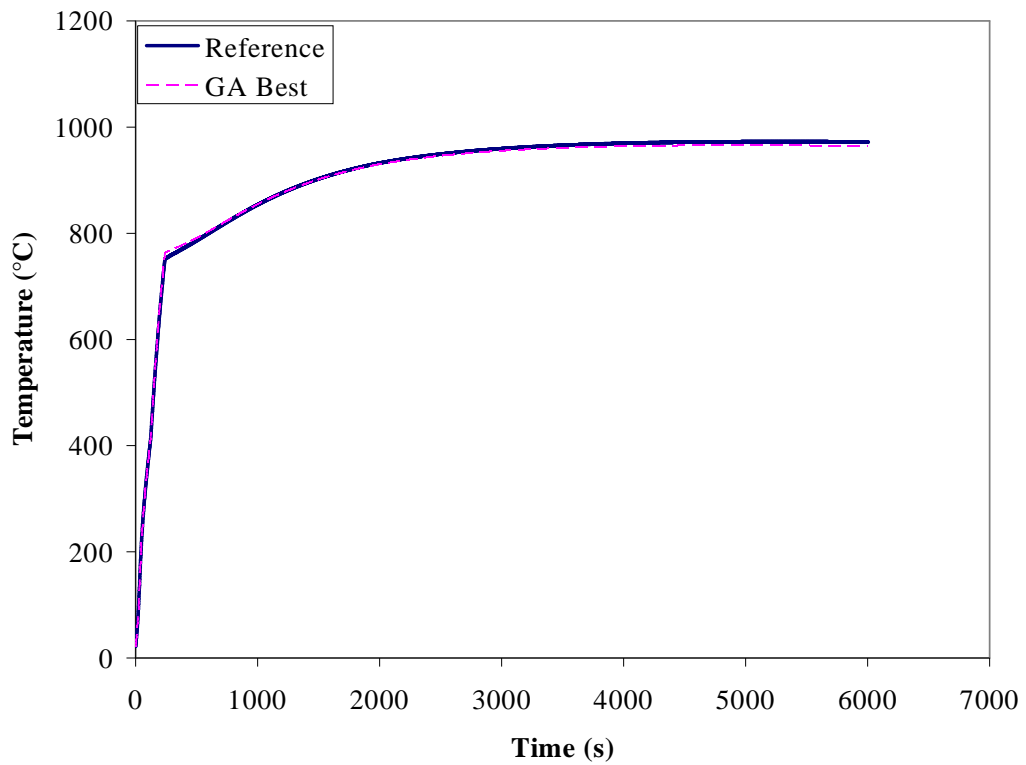
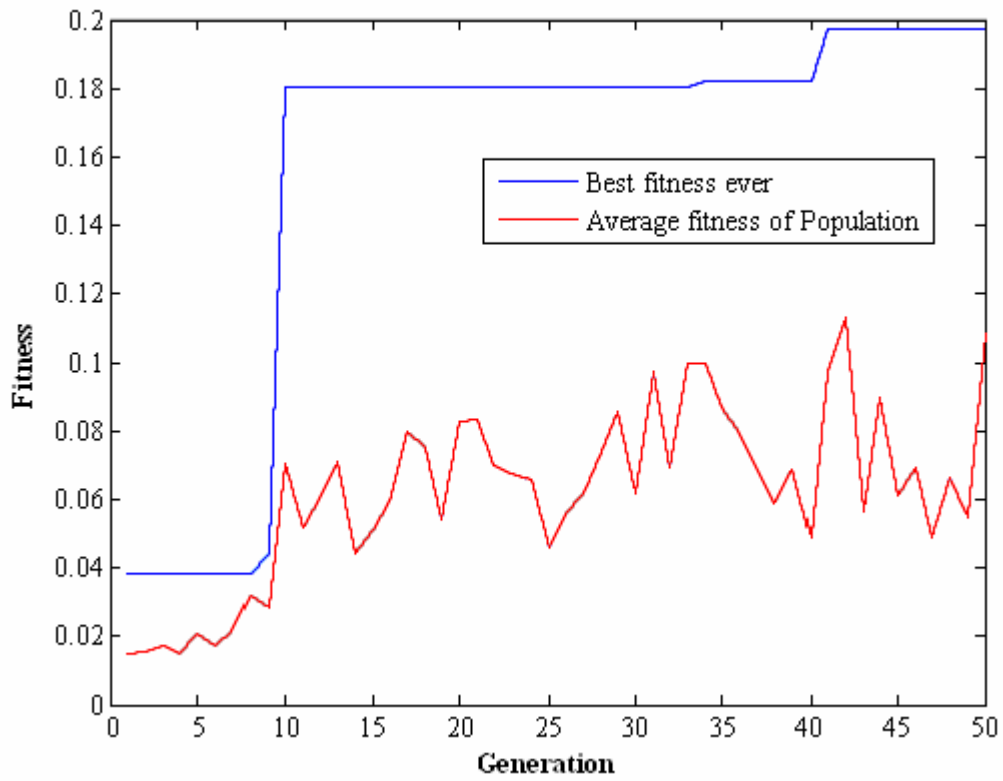
SR3_3_3_Fb_a_1



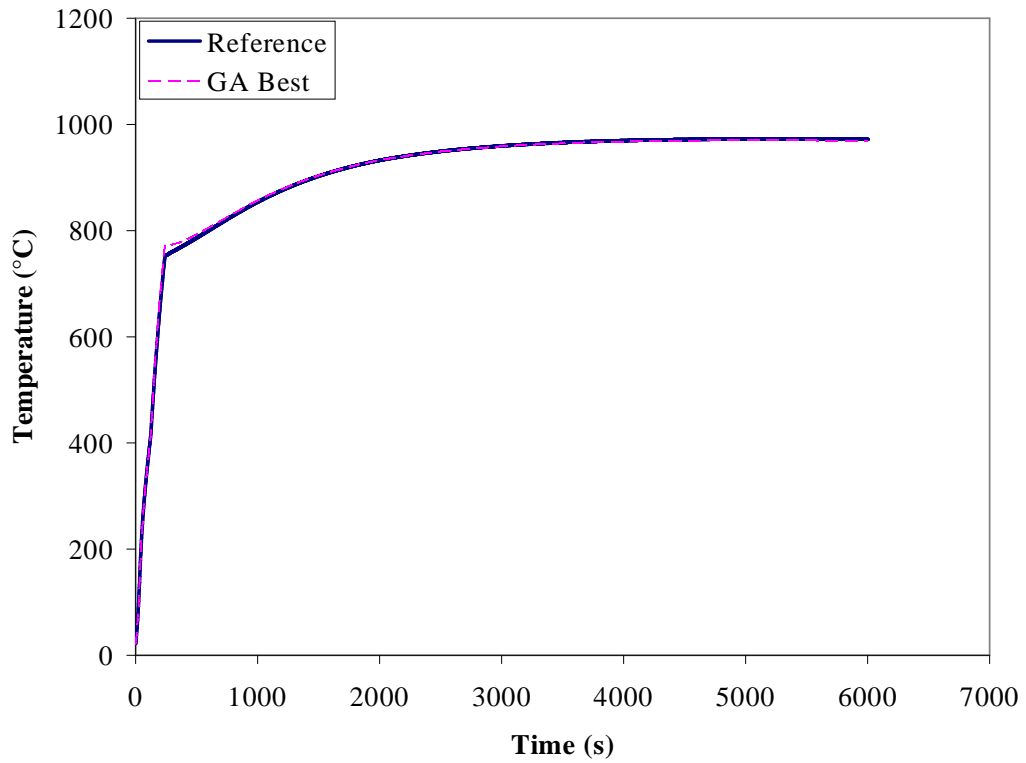
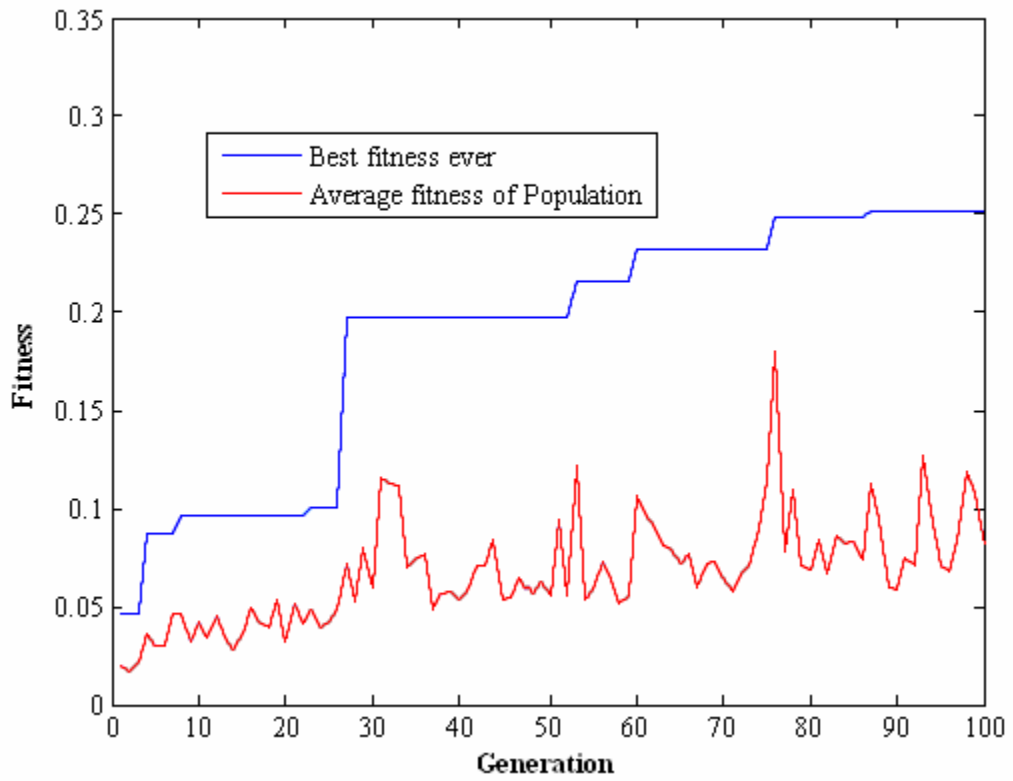
SR3_3_3_Fb_a_2



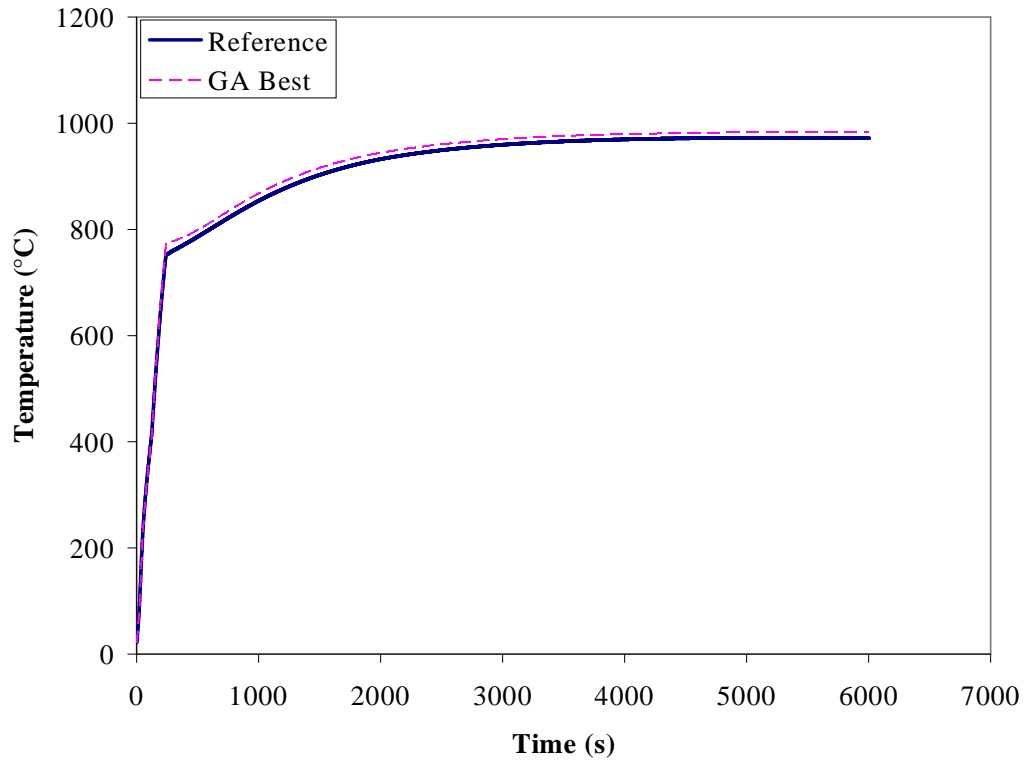
SR3_3_3_Fb_a_3



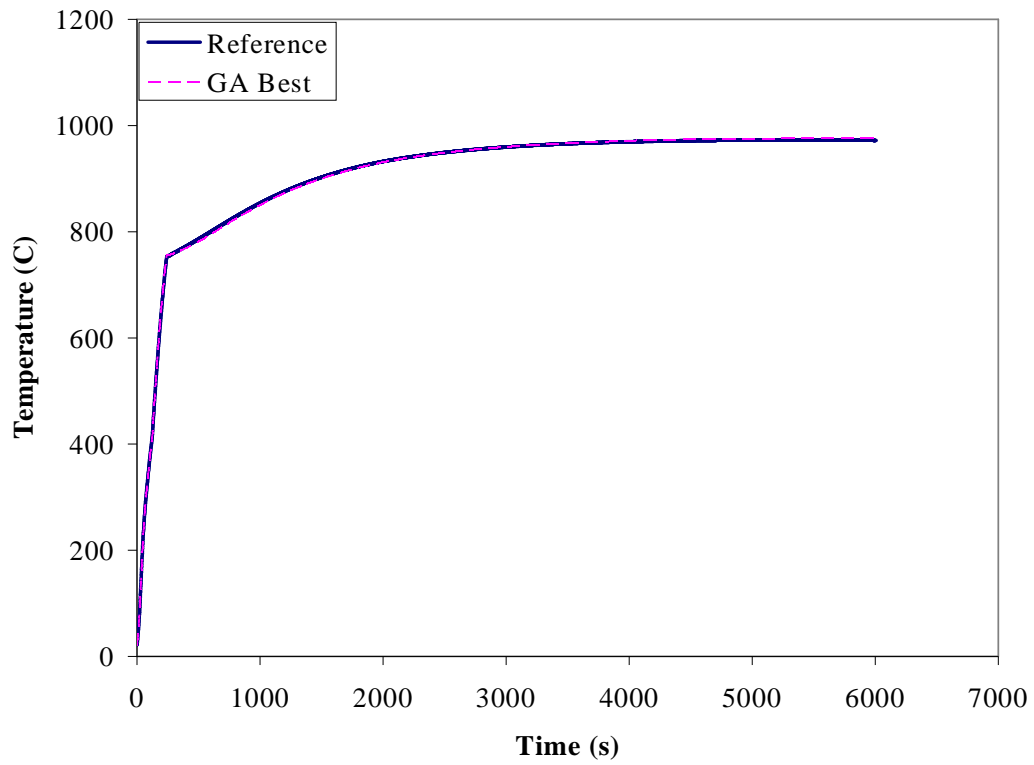
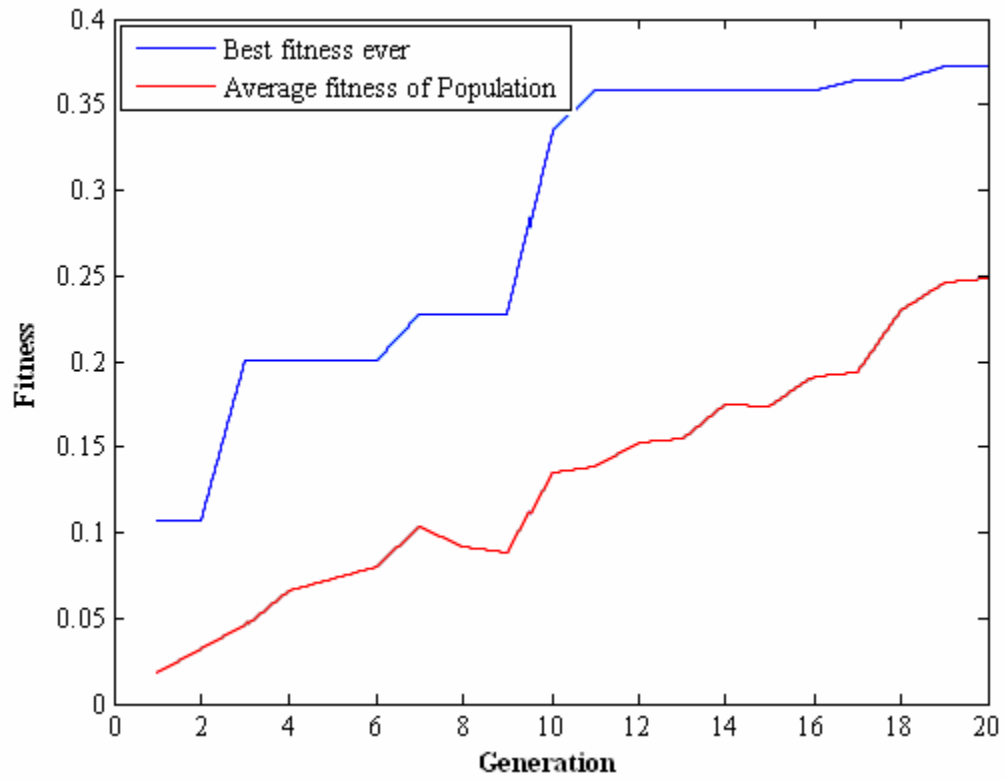
SR3_3_3_Fb_a_4



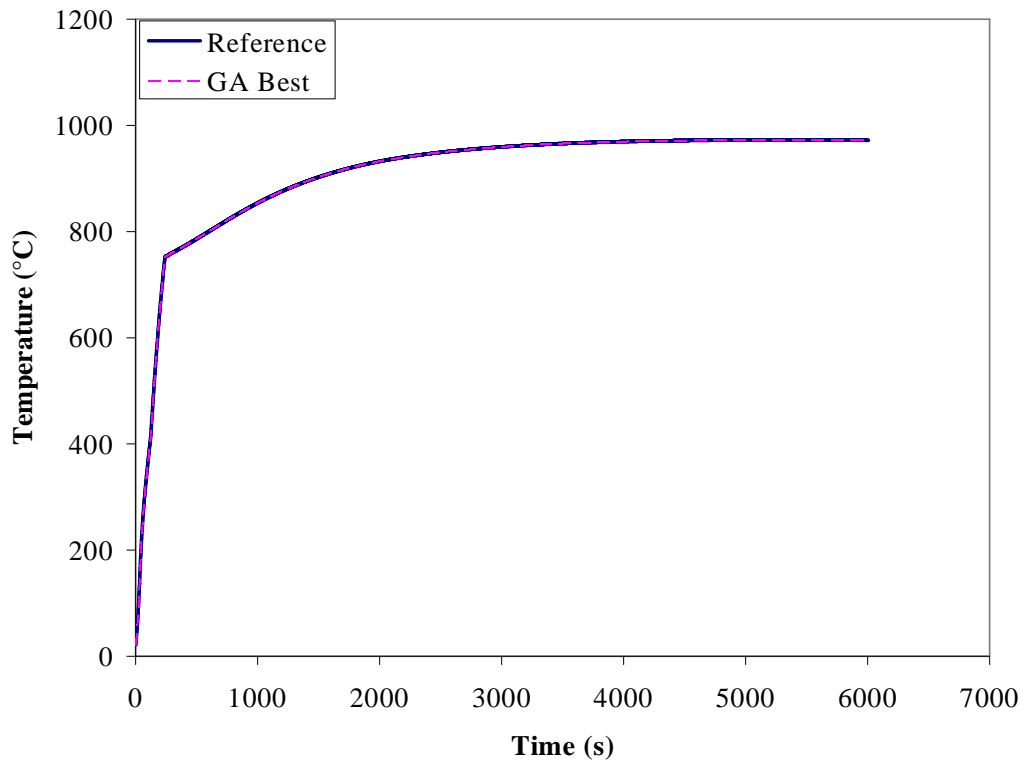
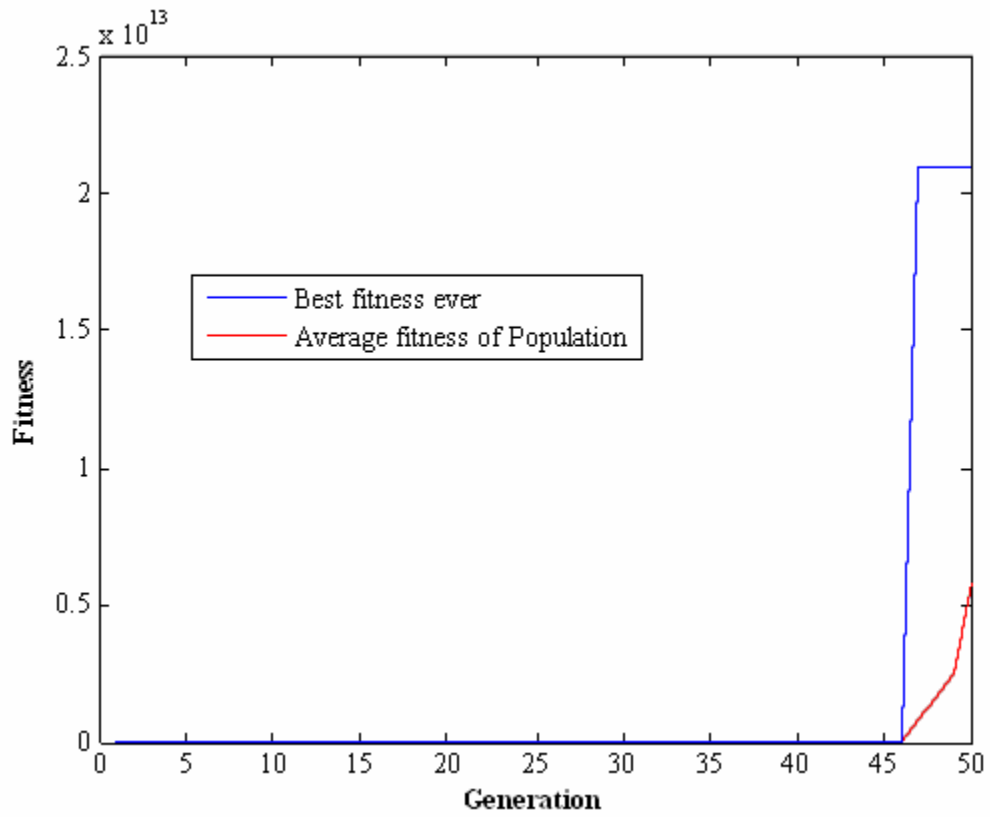
SR3_3_3_Fb_a_5



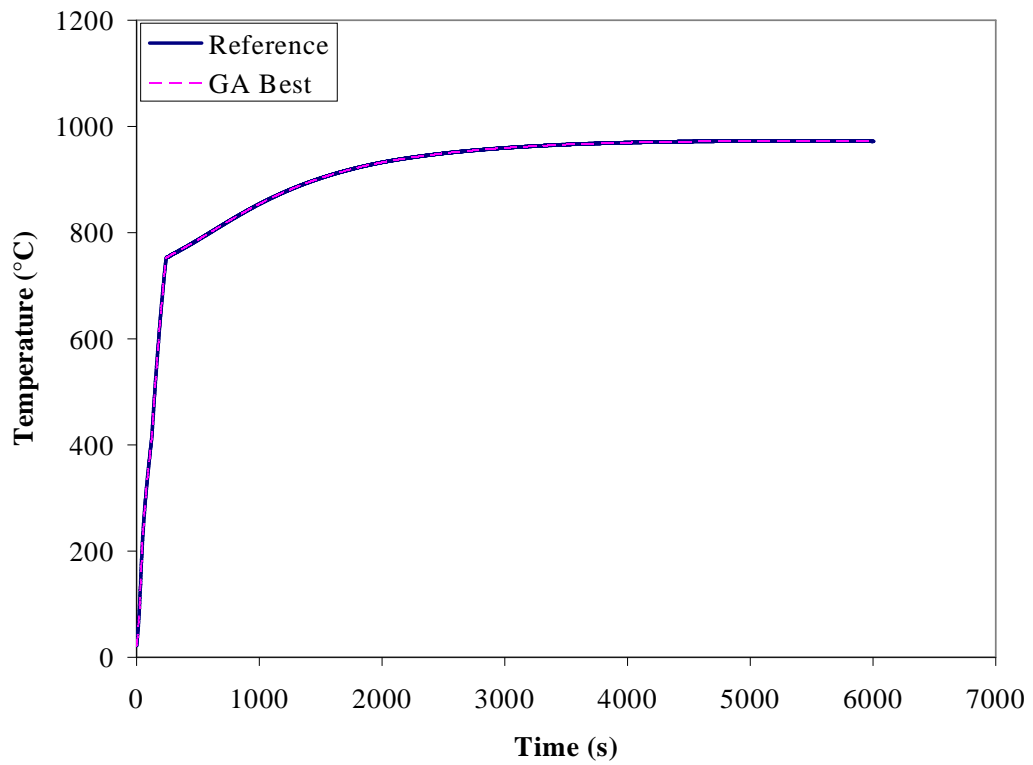
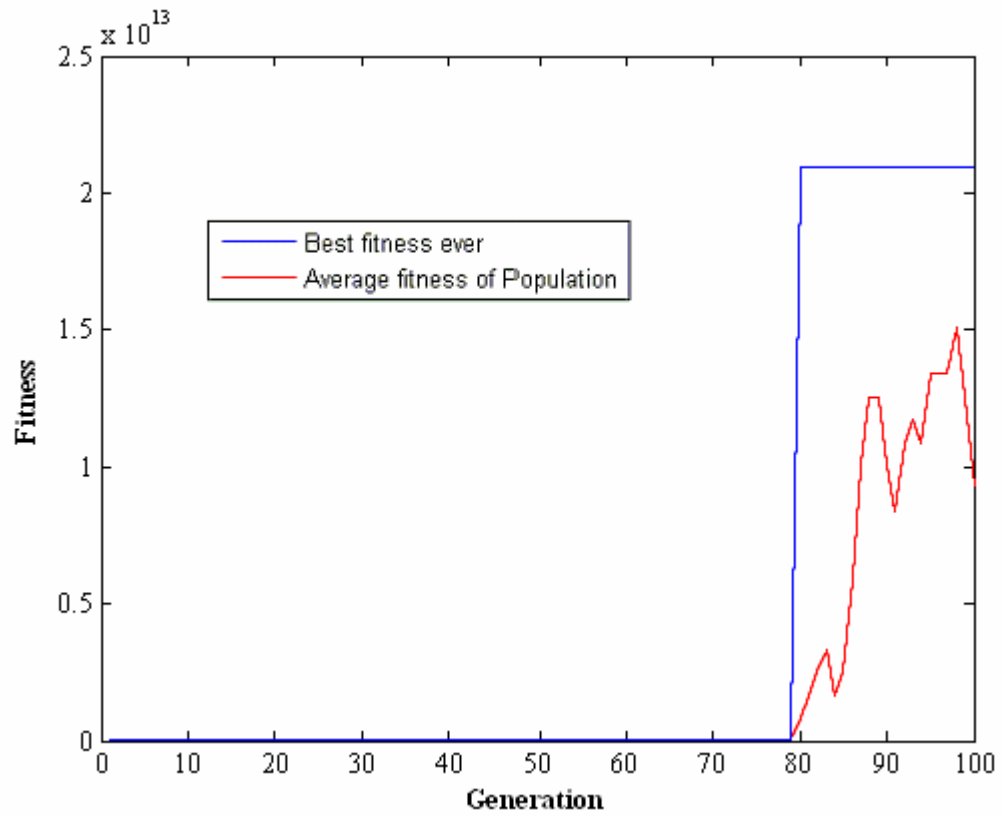
SR3_3_3_Fb_a_6



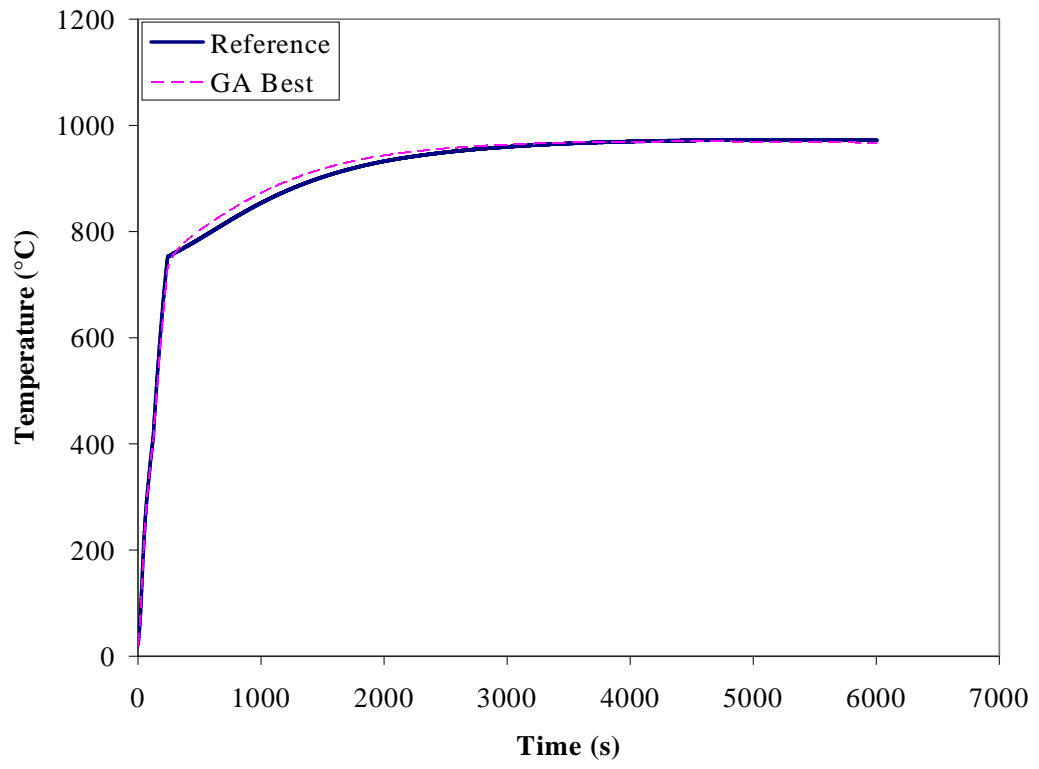
SR3_3_3_Fb_a_7



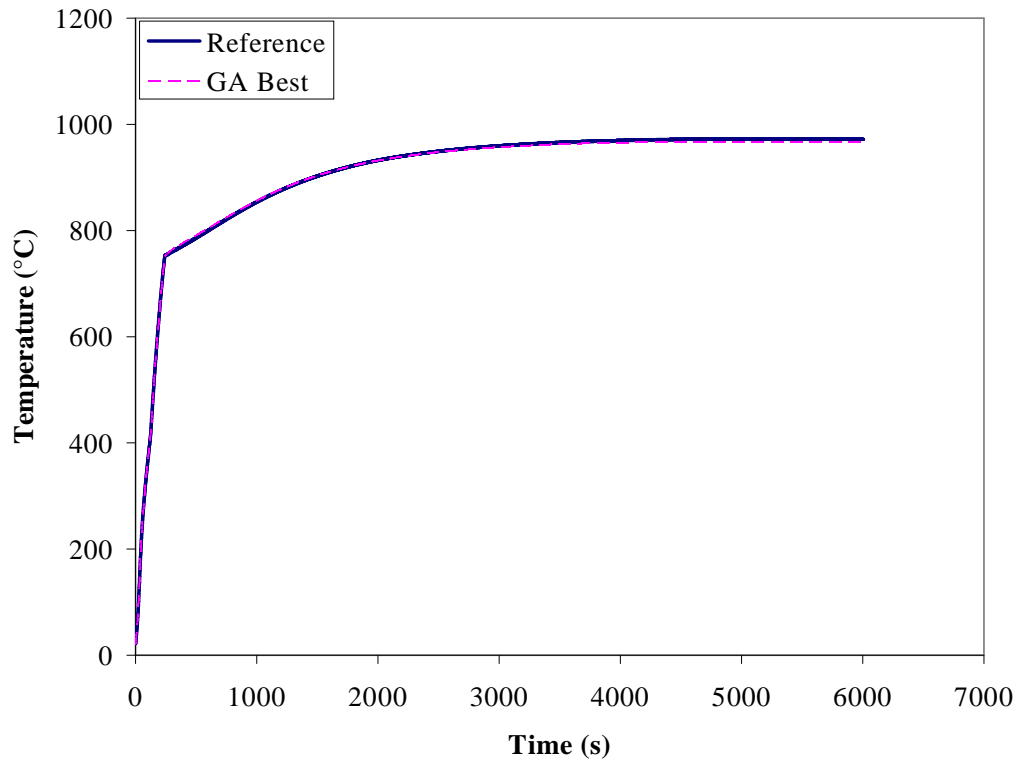
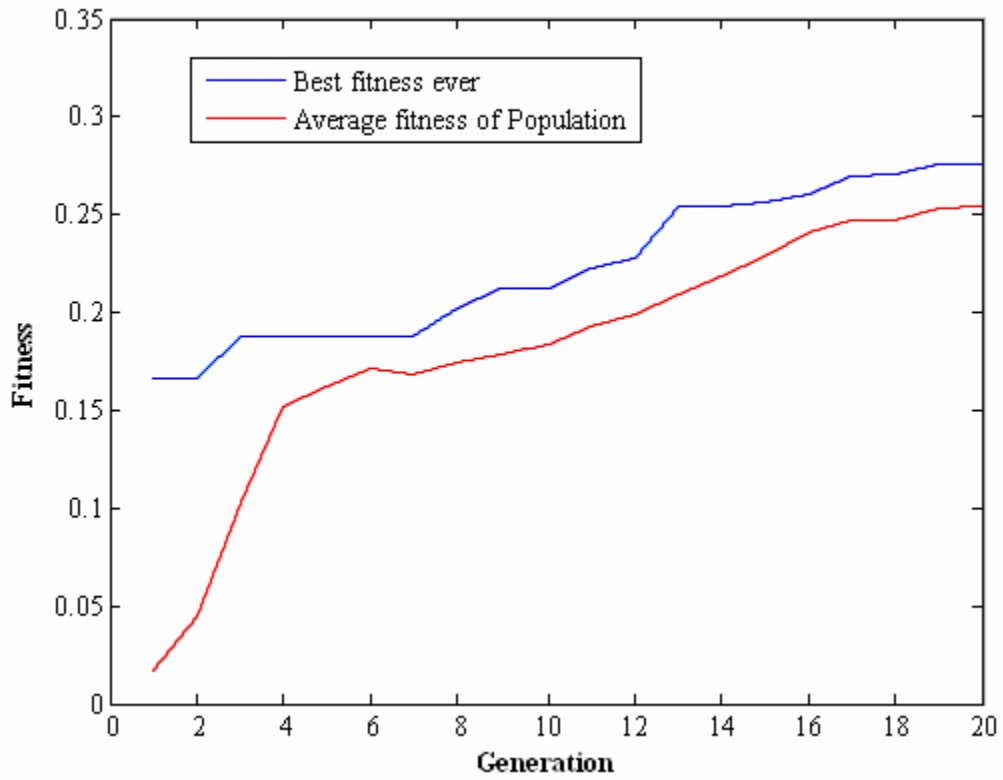
SR3_3_3_Fb_a_8



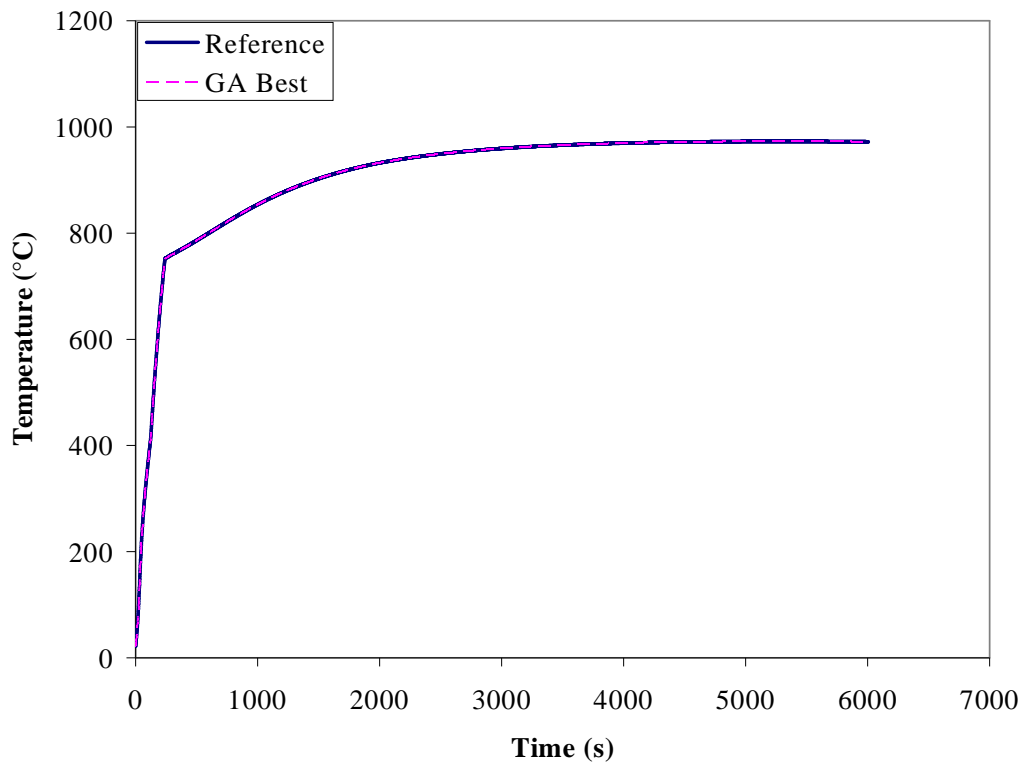
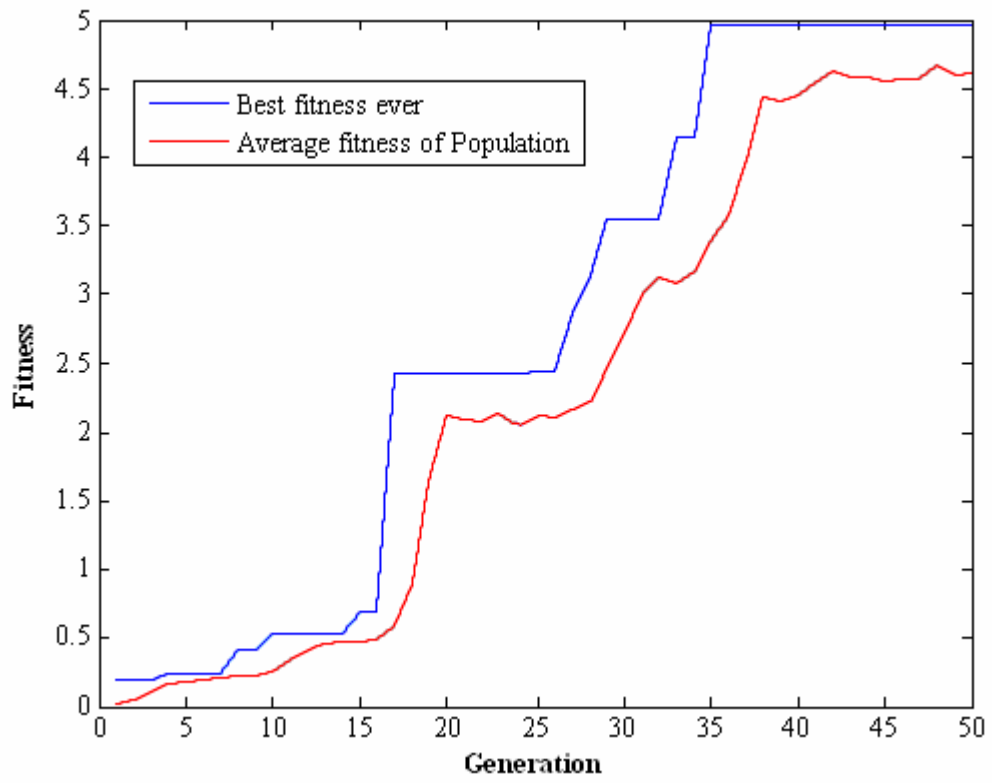
SR3_3_3_Fb_a_9



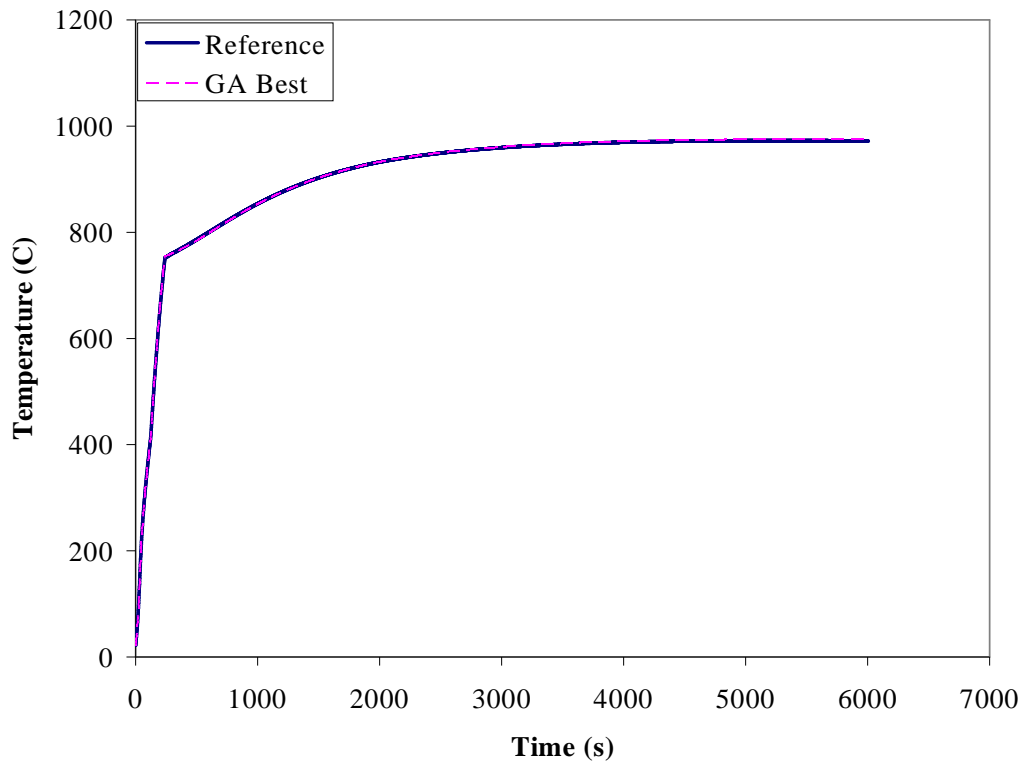
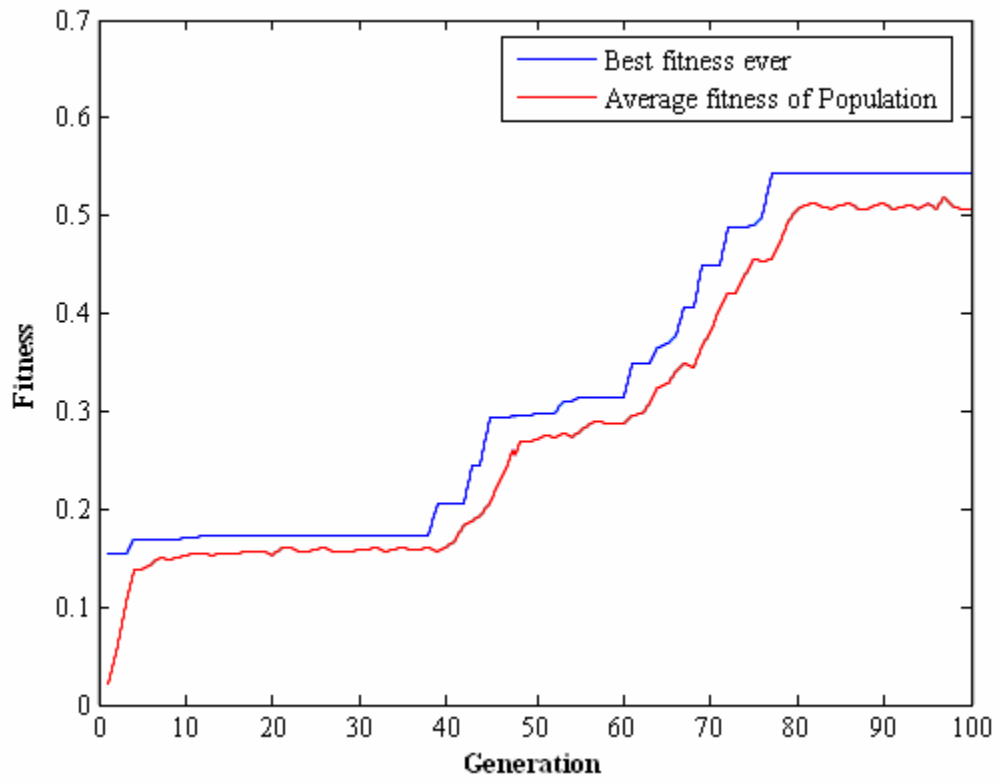
SR3_3_3_Fb_a_10



SR3_3_3_Fb_a_11



SR3_3_3_Fb_a_12



Appendix A6

All simulations are where three windows are open, window 1, window 10 and window 11.

FDS_Room1_letter

Smoke coming out of room 1 is analyzed.

FDS_FR_letter

Smoke coming out of fire room is analyzed

Letter	Meaning
a	Only Parameter is MLR
b	Approximate steady reference Curve taken from FDS at 600s into the simulation. Reference curve and IFM analyzed from 400-800s.
c	Approximate steady reference Curve taken from FDS at 1400s into the simulation. Reference curve and IFM analyzed from 400-800s.

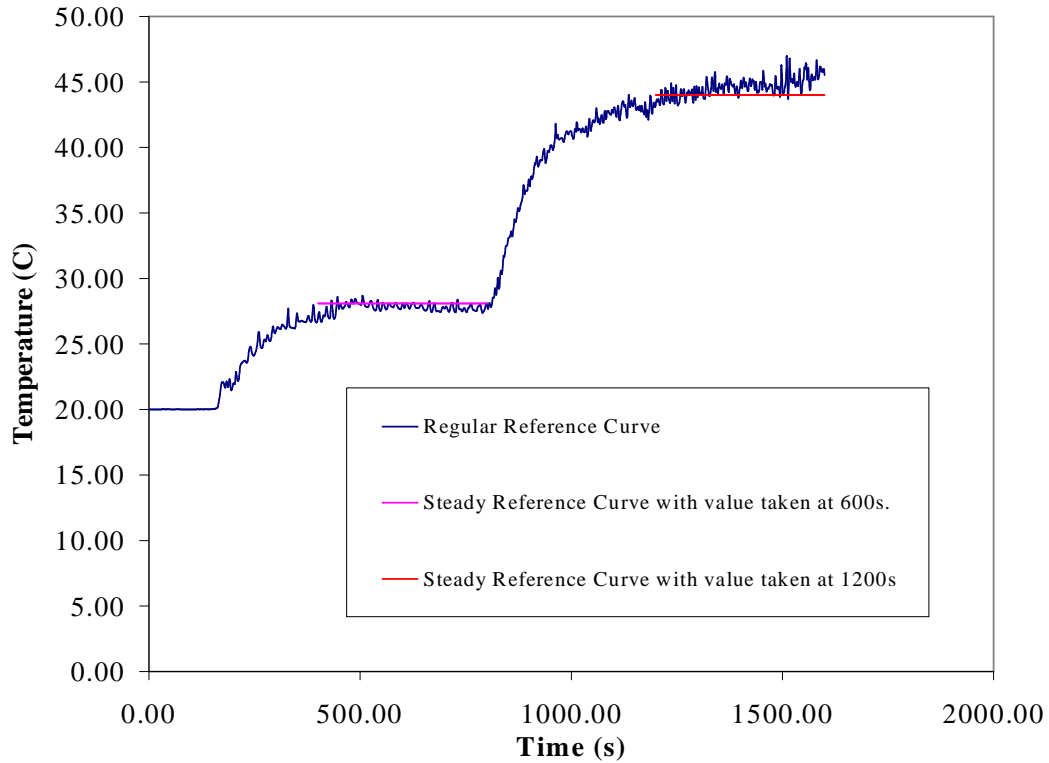
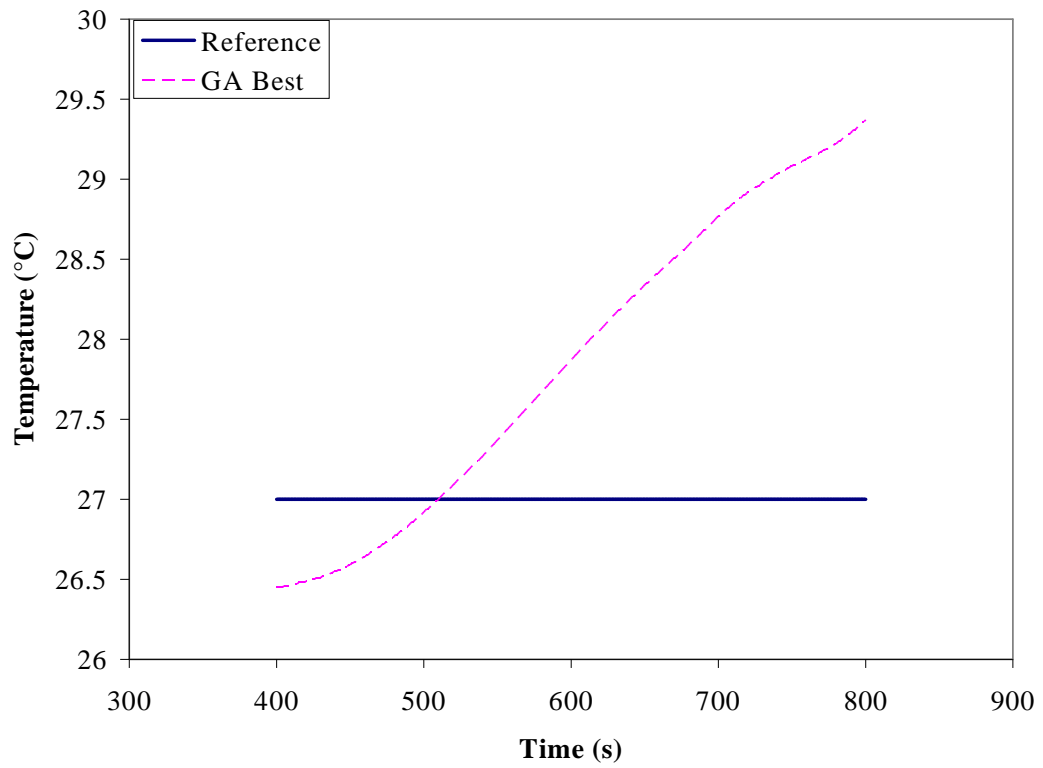
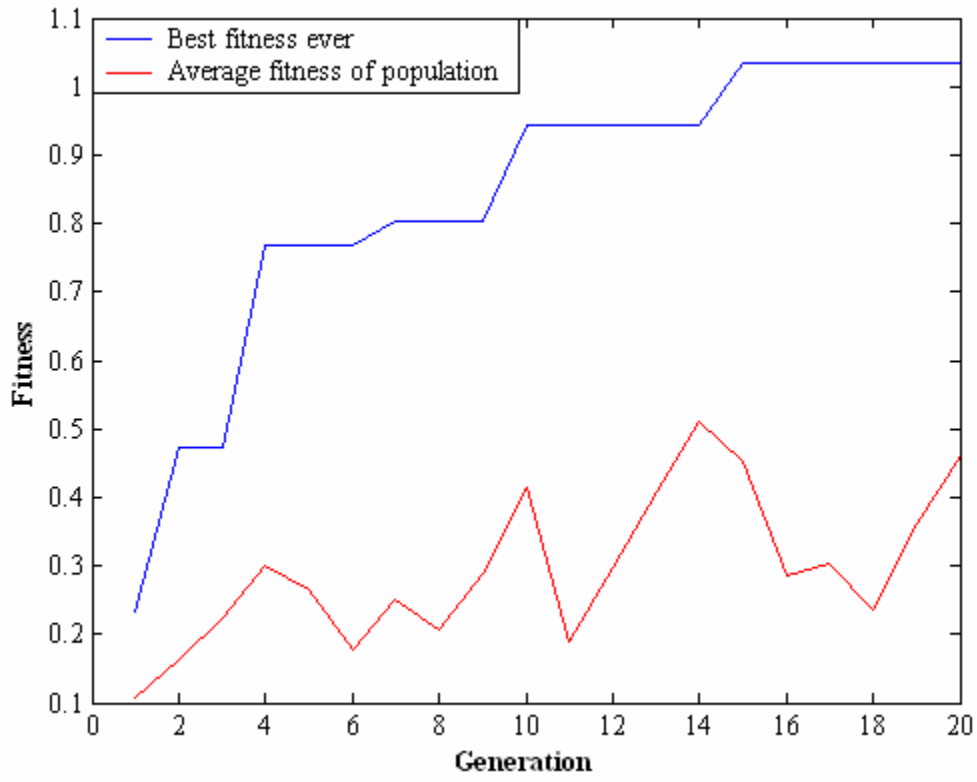


Figure 62. Sample reference curve for FDS multi-compartment tests.

FDS_Room1_a1.

Parameters	Reference Values	GA Best	Bounds	Notes
Mass Loss Rate	1000 kW	2266 kW	200- 6000 kW	Population size 10, 20 generations. FDS temperature is 28 °C at 600s.
Total HRR	992 kW	2146 kW		
HRR Fire Room	988 kW	2101 kW		
HRR Corridor	0 kW	45 kW		
HRR Room 1 (Analysis Window)	0 kW	0 kW		
HRR in all other rooms combined	NA	0 kW		

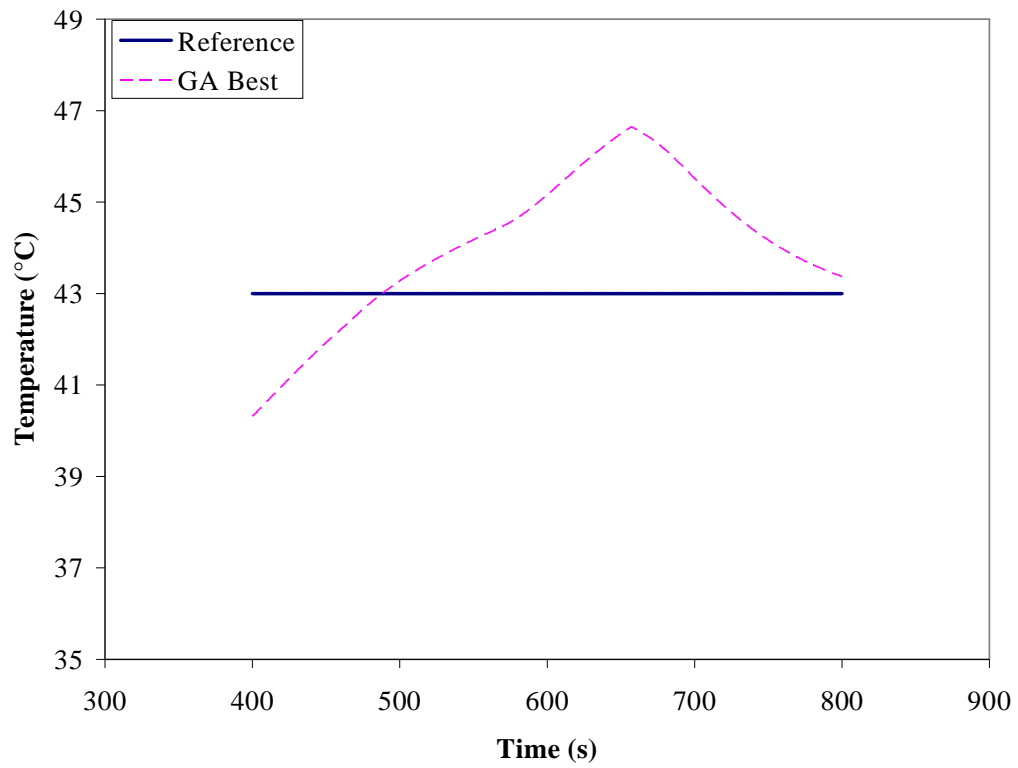
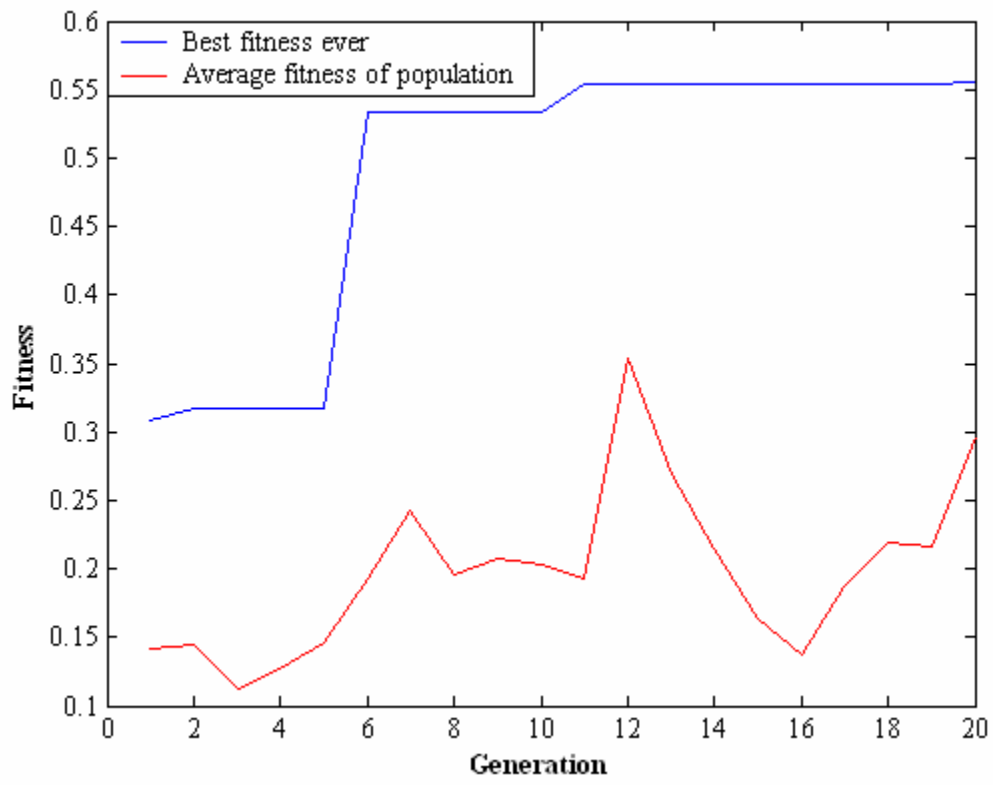
FDS_Room1_a1



FDS_Room1_a2

Parameters	Reference Values	GA Best	Bounds	Notes
Mass Loss Rate	3000 kW	3668 kW	200- 6000 kW	Population size 10, 20 generations. FDS temperature was 43°C at 600s
Total HRR	2476 kW	2782 kW		
HRR Fire Room	2301 kW	2402 kW		
HRR Corridor	78 kW	380 kW		
HRR Room 1 (Analysis Window)	0 kW	0 kW		
HRR in all other rooms combined	NA	0 kW		

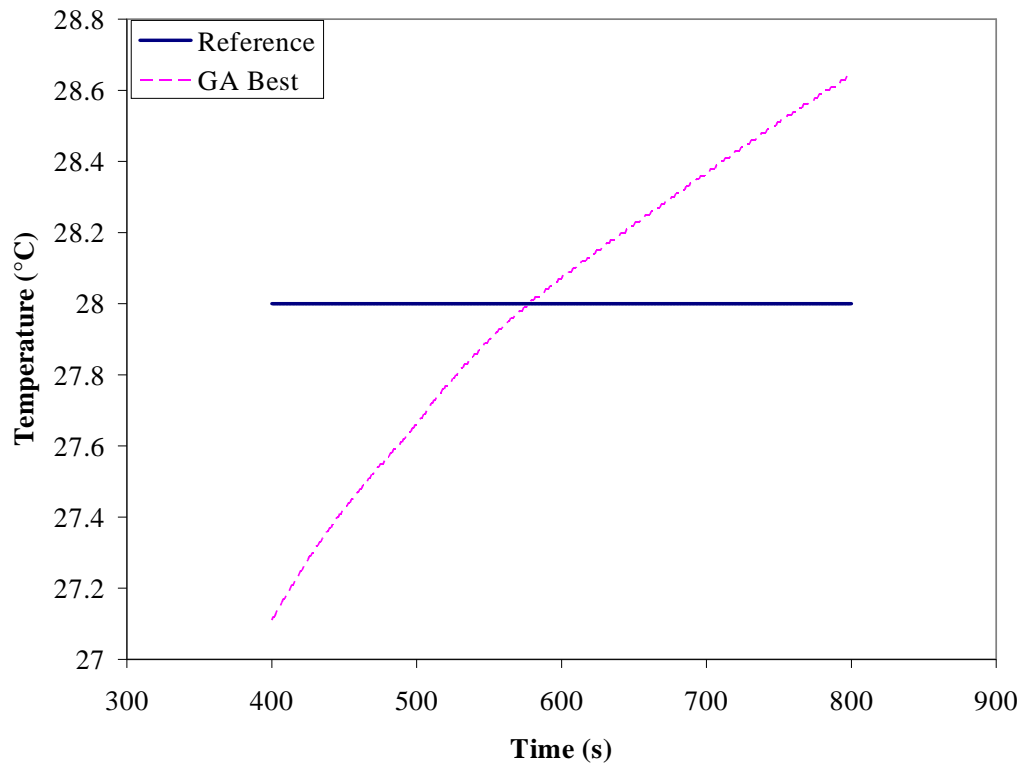
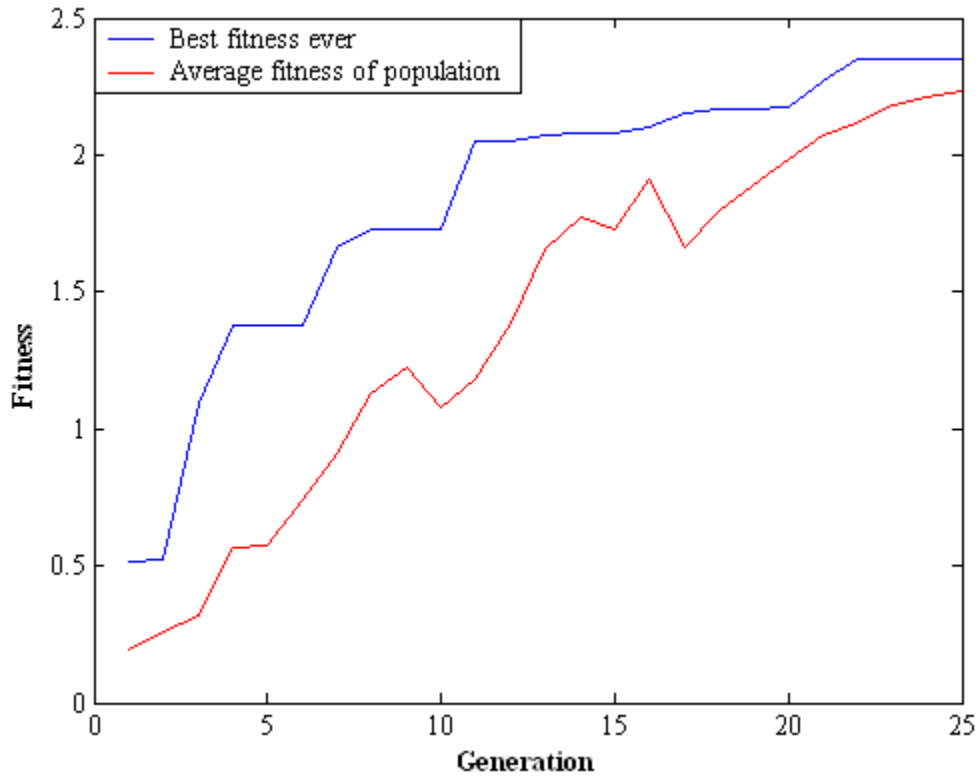
FDS_Room1_a2



FDS_Room1_b1.

Parameters	Reference Values	GA Best	Bounds	Notes
Mass Loss Rate	1000 kW	5400 kW	200- 6000 kW	Population size 25, 25 generations. FDS temperature was 28 °C at 600s.
Total HRR	992 kW	2165 kW		
HRR Fire Room	988 kW	1727 kW		
HRR Corridor	0 kW	434 kW		
HRR Room 1 (Analysis Window)	0 kW	0 kW		
HRR in all other rooms combined	NA	4 kW		
D1 width	1m	.63m	.05-1m	
D2 width	1m	.05m	.05-1m	
D3 width	1m	.97m	.05-1m	
D4 width	1m	.05m	.05-1m	
D5 width	1m	.85m	.05-1m	
D6 width	1m	.84m	.05-1m	
D7 width	1m	.23m	.05-1m	
D8 width	1m	.62m	.05-1m	
D9 width	1m	.63m	.05-1m	
D10 width	1m	.37m	.05-1m	
D11 width	1m	.83m	.05-1m	
D12 width	1m	1.00m	.05-1m	
D13 width	1m	.11m	.05-1m	
D14 width	1m	.33m	.05-1m	
D15 width	1m	.86m	.05-1m	
D16 width	1m	.53m	.05-1m	
D17 width	1m	1.00m	.05-1m	
D18 width	1m	.90m	.05-1m	

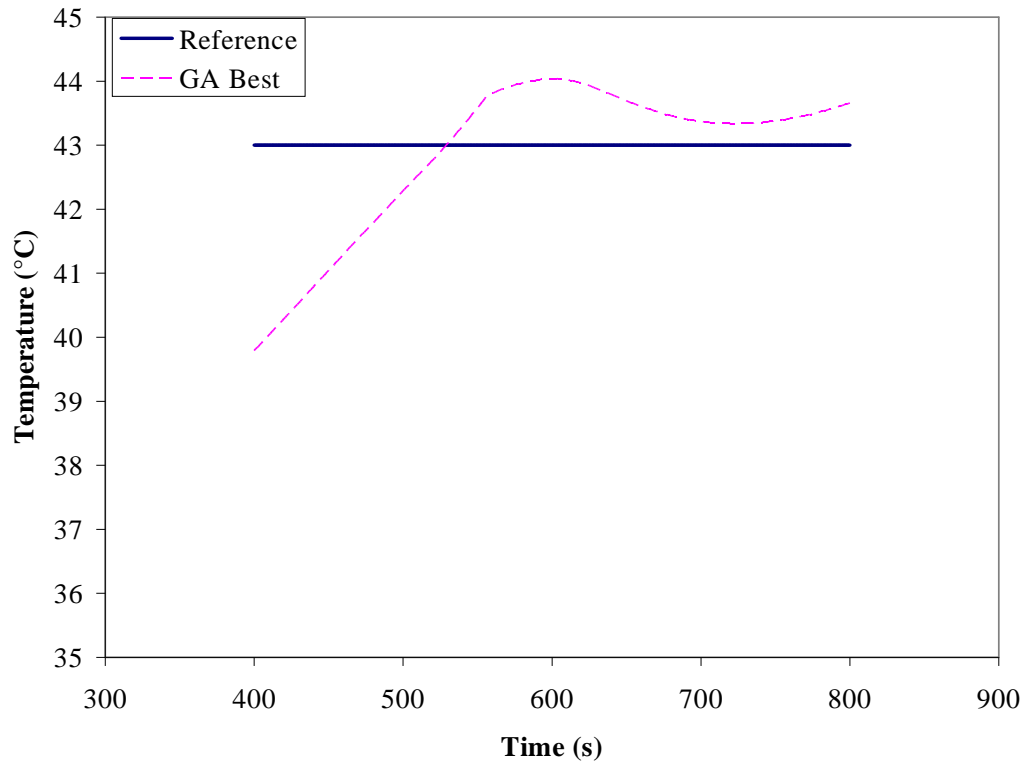
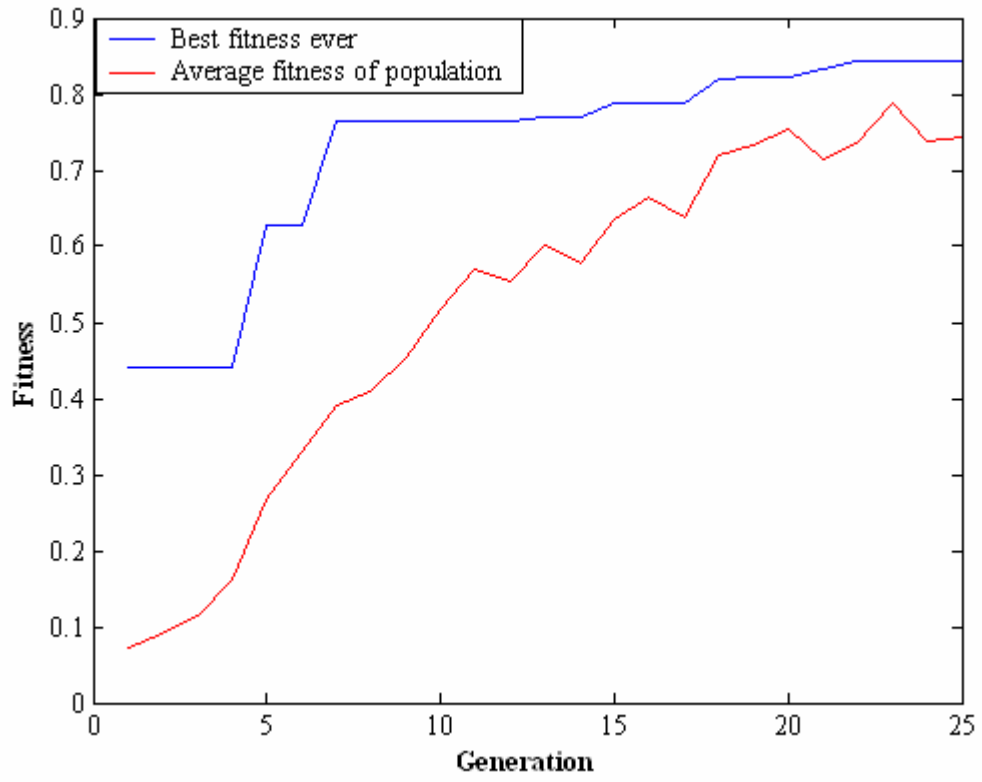
FDS_Room1_b1



FDS_Room1_b2

Parameters	Reference Values	GA Best	Bounds	Notes
Mass Loss Rate	3000 kW	5408 kW	200- 6000 kW	Population size 25, 25 generations. FDS temperature was 43°C at 600s.
Total HRR	2476 kW	2624 kW		
HRR Fire Room	2301 kW	2042 kW		
HRR Corridor	78 kW	567 kW		
HRR Room 1 (Analysis Window)	0 kW	2 kW		
HRR in all other rooms combined	NA	13 kW		
D1 width	1m	.88m	.05-1m	
D2 width	1m	.25m	.05-1m	
D3 width	1m	.24m	.05-1m	
D4 width	1m	.52m	.05-1m	
D5 width	1m	.56m	.05-1m	
D6 width	1m	1.00m	.05-1m	
D7 width	1m	1.00m	.05-1m	
D8 width	1m	.60m	.05-1m	
D9 width	1m	.13m	.05-1m	
D10 width	1m	.51m	.05-1m	
D11 width	1m	.53m	.05-1m	
D12 width	1m	1.00m	.05-1m	
D13 width	1m	.06m	.05-1m	
D14 width	1m	.05m	.05-1m	
D15 width	1m	.45m	.05-1m	
D16 width	1m	.98m	.05-1m	
D17 width	1m	.09m	.05-1m	
D18 width	1m	.84m	.05-1m	

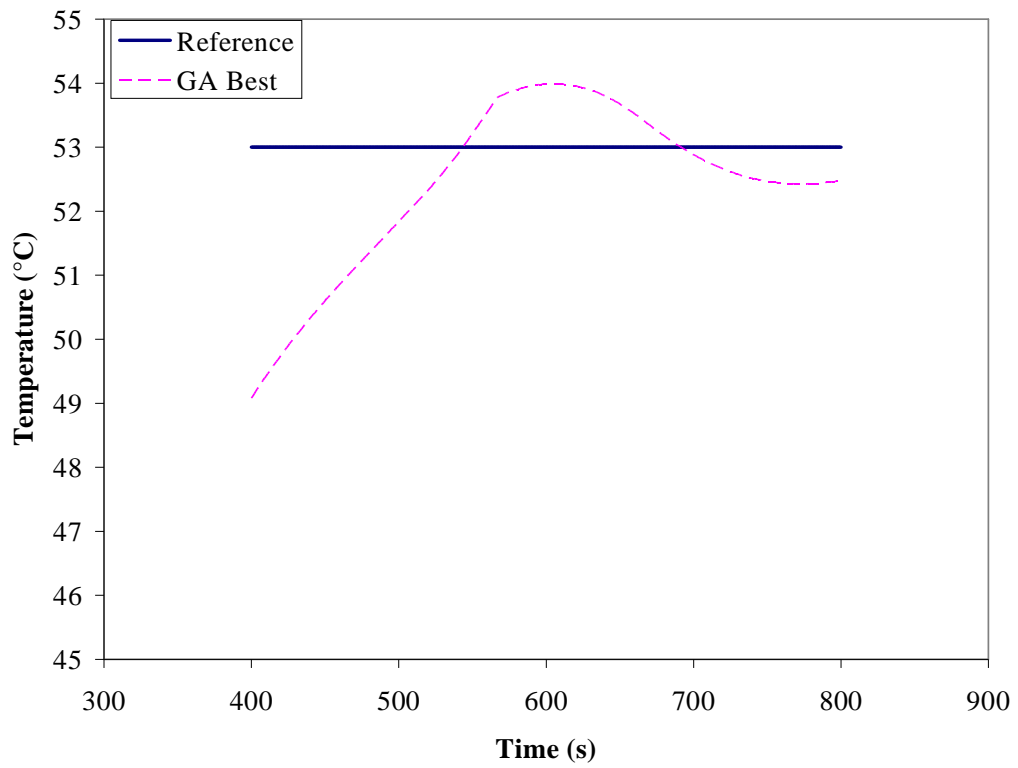
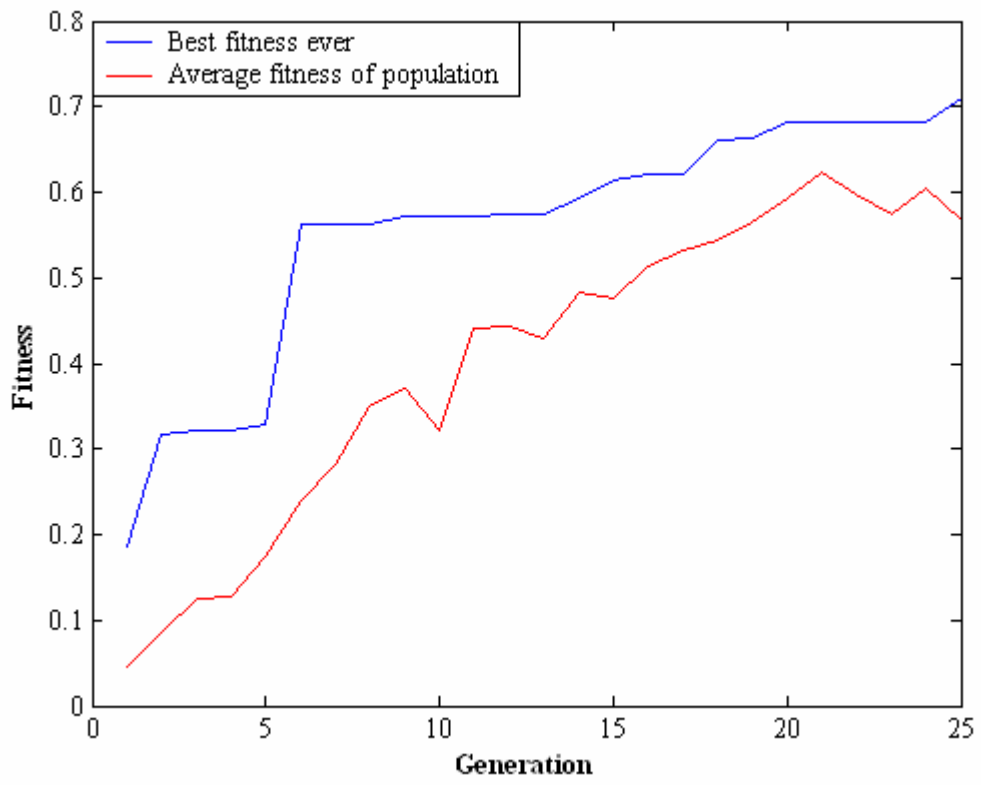
FDS_Room1_b2



FDS_Room1_b3

Parameters	Reference Values	GA Best	Bounds	Notes
Mass Loss Rate	6000 kW	4489 kW	200- 6000 kW	Population size 25, 25 generations. FDS temperature was 53°C at 1400s.
Total HRR	3654 kW	2988 kW		
HRR Fire Room	3376 kW	2389 kW		
HRR Corridor	244 kW	583 kW		
HRR Room 1 (Analysis Window)	0 kW	2 kW		
HRR in all other rooms combined	NA			
D1 width	1m	.79m	.05-1m	
D2 width	1m	.86m	.05-1m	
D3 width	1m	.33m	.05-1m	
D4 width	1m	.29m	.05-1m	
D5 width	1m	.24m	.05-1m	
D6 width	1m	1.00m	.05-1m	
D7 width	1m	.29m	.05-1m	
D8 width	1m	.82m	.05-1m	
D9 width	1m	1.00m	.05-1m	
D10 width	1m	.89m	.05-1m	
D11 width	1m	.46m	.05-1m	
D12 width	1m	.35m	.05-1m	
D13 width	1m	.97m	.05-1m	
D14 width	1m	.05m	.05-1m	
D15 width	1m	.96m	.05-1m	
D16 width	1m	.94m	.05-1m	
D17 width	1m	.95m	.05-1m	
D18 width	1m	.14m	.05-1m	

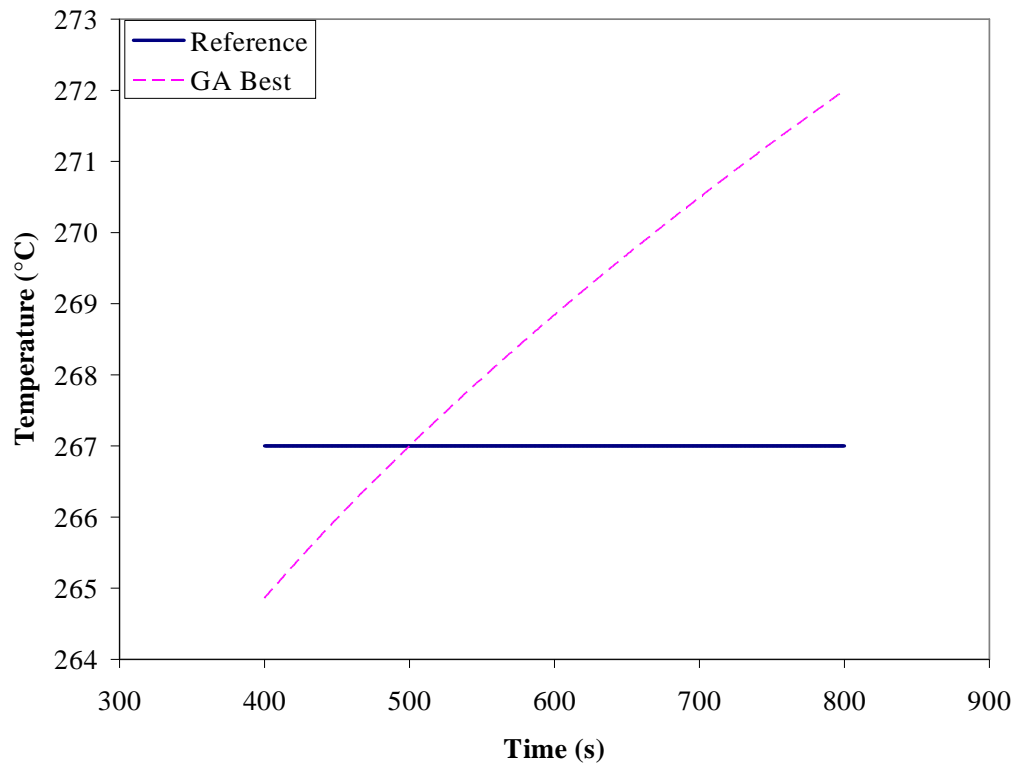
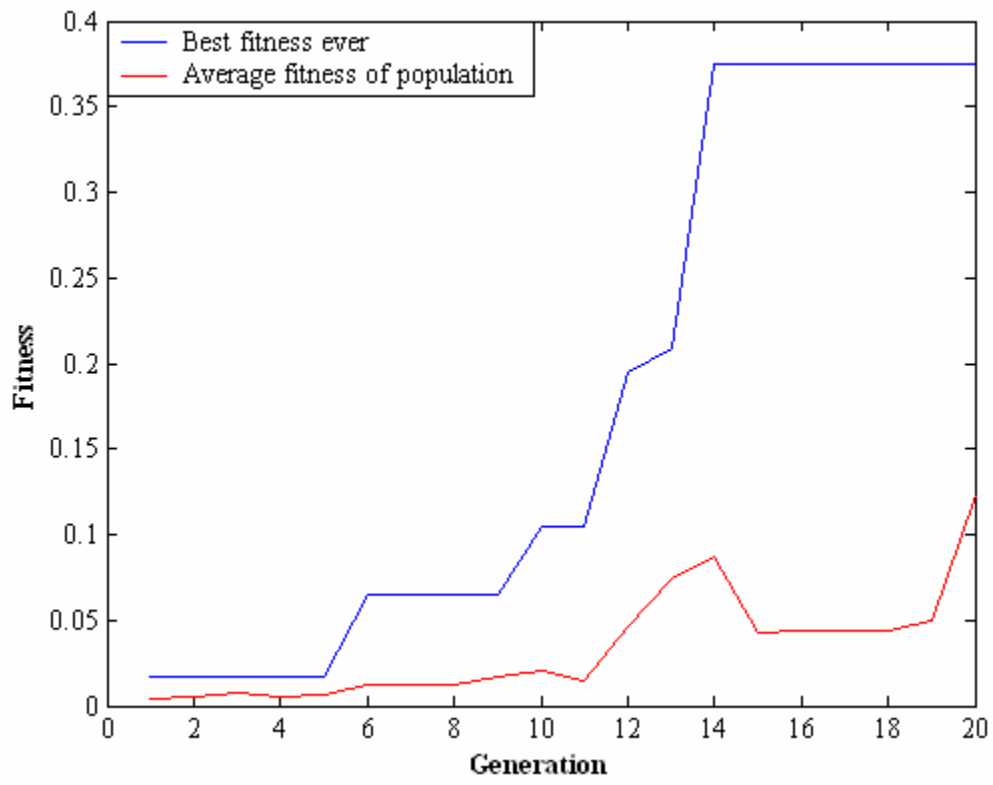
FDS_Room1_b3



FDS_FR_a1.

Parameters	Reference Values	GA Best	Bounds	Notes
Mass Loss Rate	1000 kW	450 kW	200- 6000 kW	Population size 10, 20 generations. FDS temperature was 267 °C at 600s.
Total HRR	992 kW	439 kW		
HRR Fire Room	988 kW	437 kW		
HRR Corridor	0 kW	2 kW		
HRR Room 1 (Analysis Window)	0 kW	0 kW		
HRR in all other rooms combined	NA	0 kW		

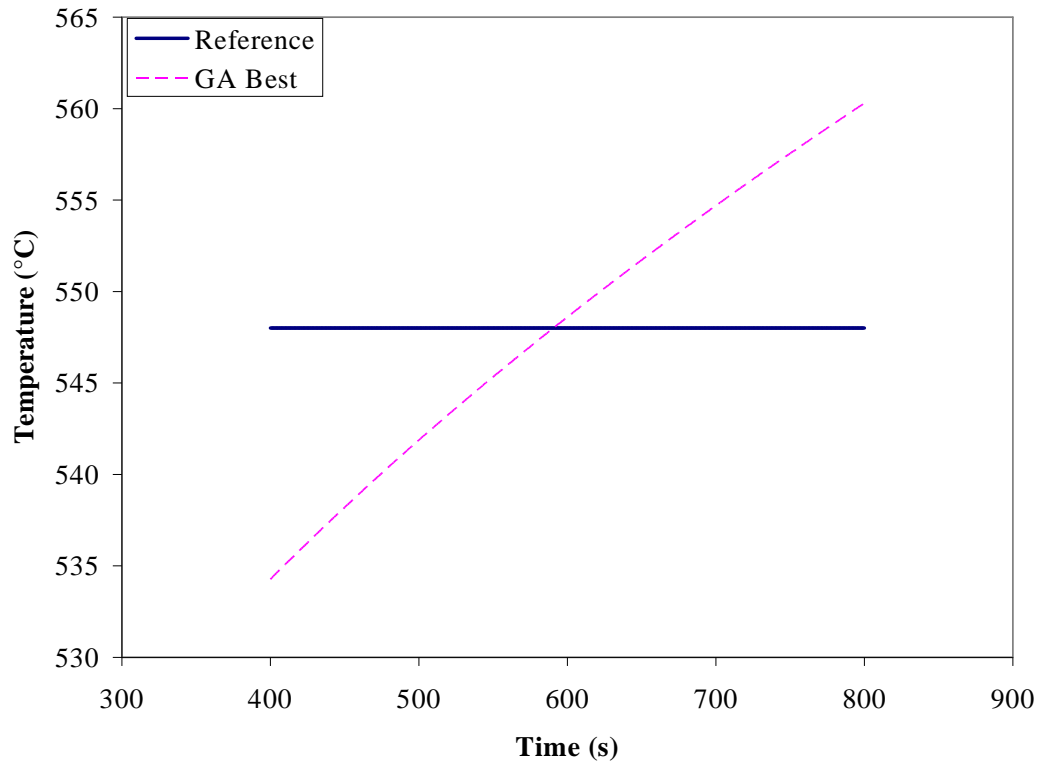
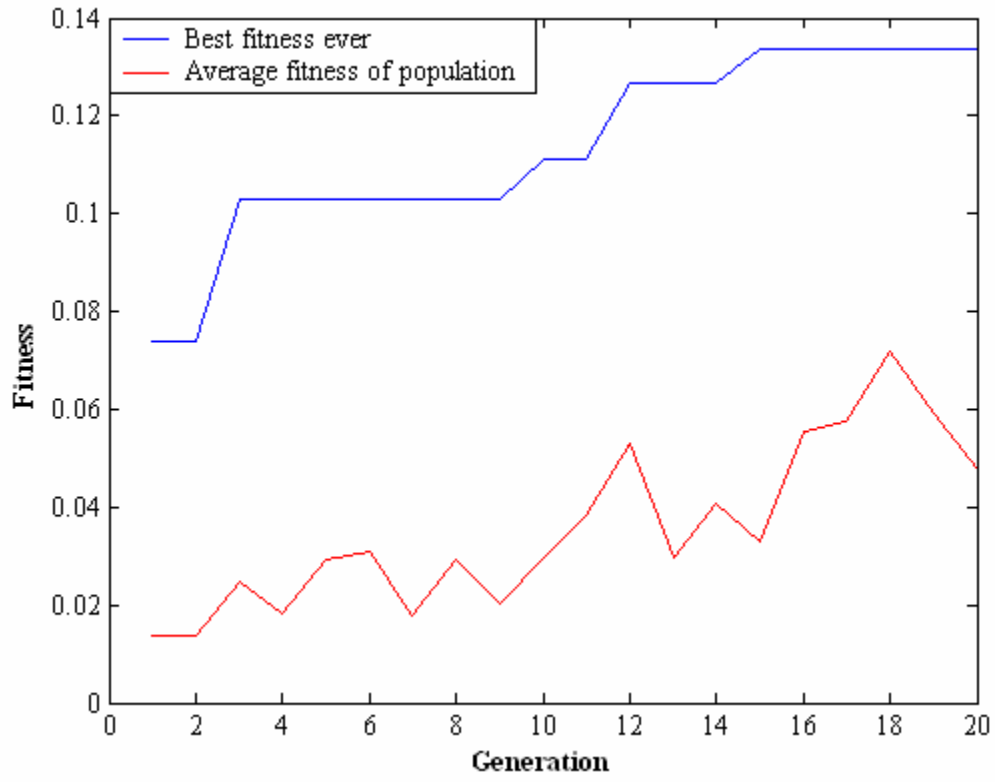
FDS_FR_a1



FDS_FR_a2

Parameters	Reference Values	GA Best	Bounds	Notes
Mass Loss Rate	3000 kW	1483 kW	200- 6000 kW	Population size 10, 20 generations. FDS temperature was 548 °C at 600s.
Total HRR	2476 kW	1479 kW		
HRR Fire Room	2301 kW	1478 kW		
HRR Corridor	78 kW	1 kW		
HRR Room 1 (Analysis Window)	0 kW	0 kW		
HRR in all other rooms combined	NA	0 kW		

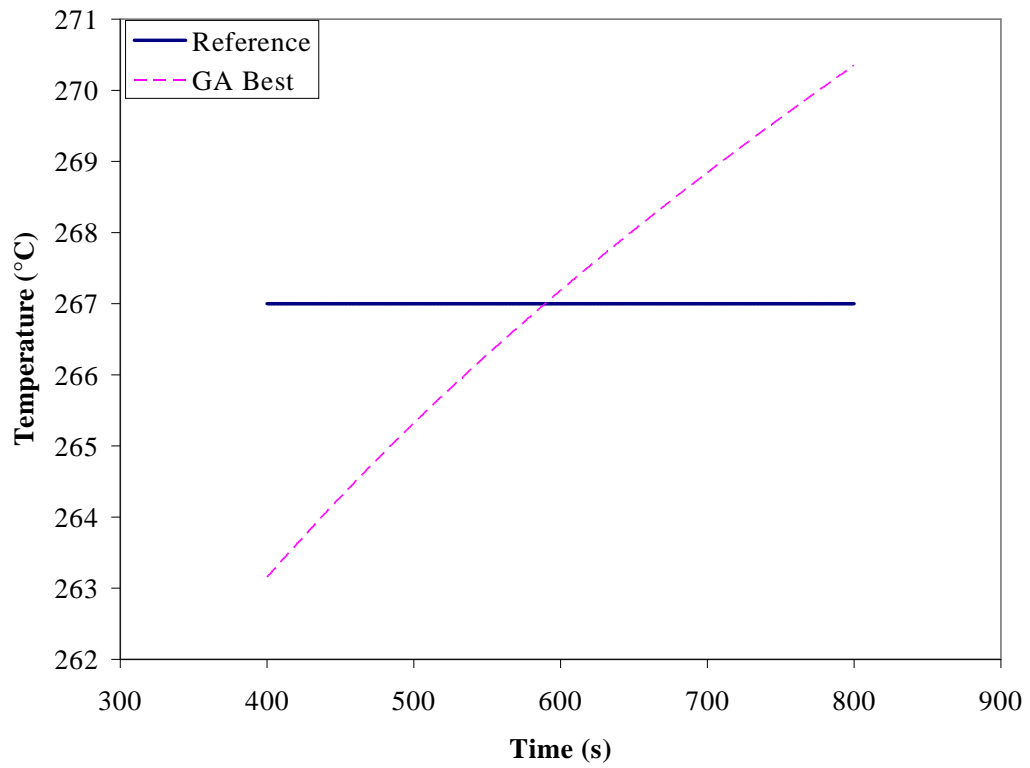
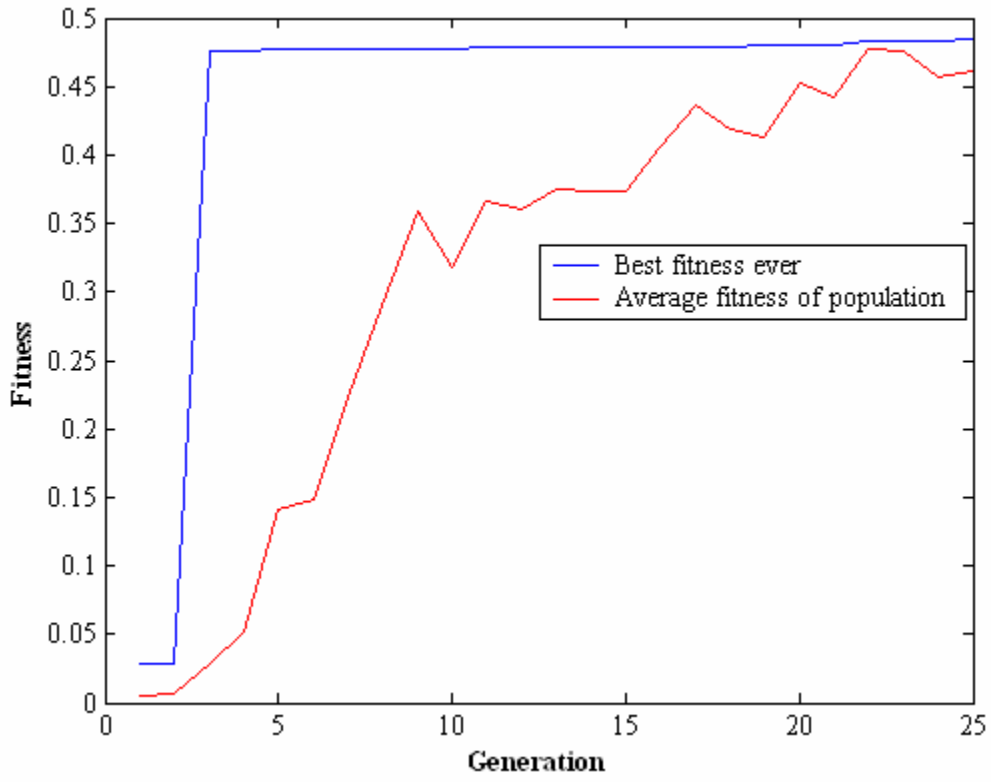
FDS_FR_a2



FDS_FR_b1.

Parameters	Reference Values	GA Best	Bounds	Notes
Mass Loss Rate	1000 kW	439 kW	200- 6000 kW	Population size 25, 25 generations. FDS temperature was 267°C at 600s.
Total HRR	992 kW	429 kW		
HRR Fire Room	988 kW	427 kW		
HRR Corridor	0 kW	2 kW		
HRR Room 1 (Analysis Window)	0 kW	0 kW		
HRR in all other rooms combined	NA	0kW		
D1 width	1m	.17m	.05-1m	
D2 width	1m	.98m	.05-1m	
D3 width	1m	.92m	.05-1m	
D4 width	1m	.76m	.05-1m	
D5 width	1m	1.00m	.05-1m	
D6 width	1m	.67m	.05-1m	
D7 width	1m	.43m	.05-1m	
D8 width	1m	.50m	.05-1m	
D9 width	1m	.31m	.05-1m	
D10 width	1m	.86m	.05-1m	
D11 width	1m	.81m	.05-1m	
D12 width	1m	.93m	.05-1m	
D13 width	1m	.95m	.05-1m	
D14 width	1m	1.00m	.05-1m	
D15 width	1m	1.00m	.05-1m	
D16 width	1m	.77m	.05-1m	
D17 width	1m	.96m	.05-1m	
D18 width	1m	.54m	.05-1m	

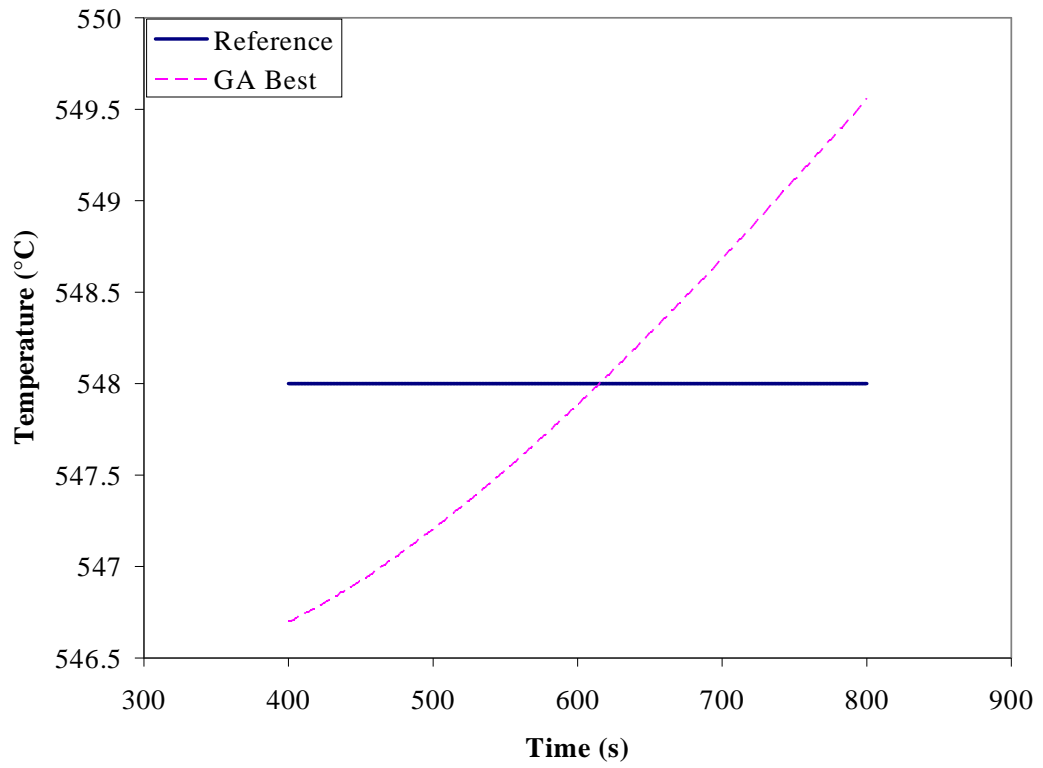
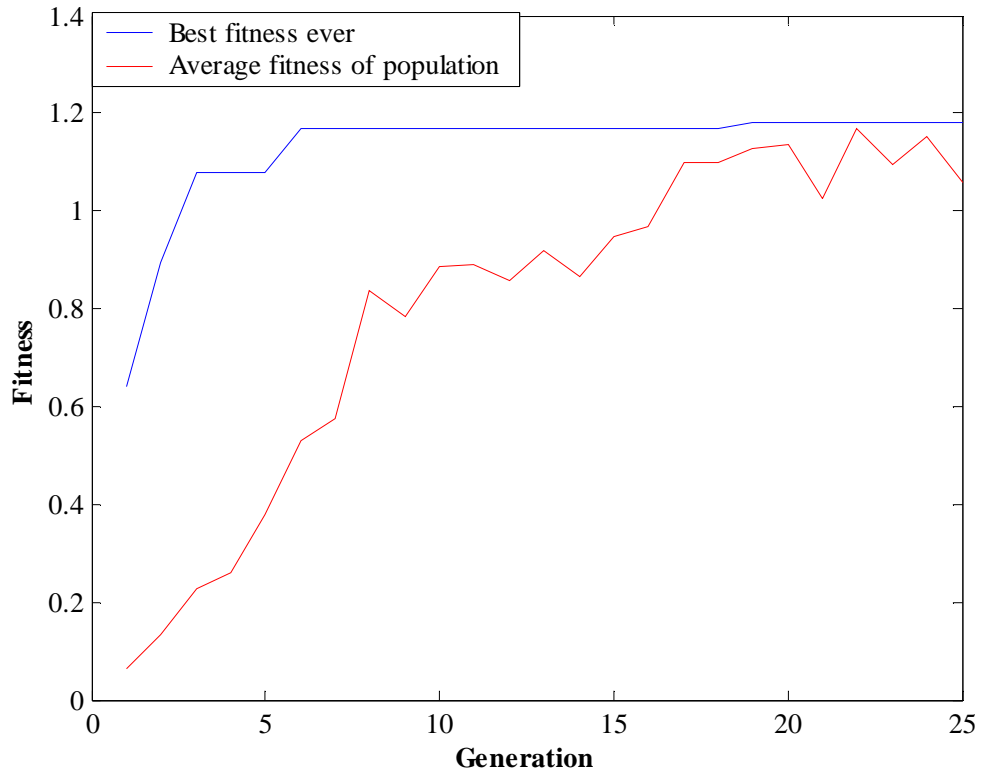
FDS_FR_b1



FDS_FR_b2

Parameters	Reference Values	GA Best	Bounds	Notes
Mass Loss Rate	3000 kW	2287 kW	200- 6000 kW	Population size 25, 25 generations. FDS temperature was 548°C at 600s.
Total HRR	2476 kW	1434 kW		
HRR Fire Room	2301 kW	1392 kW		
HRR Corridor	78 kW	42 kW		
HRR Room 1 (Analysis Window)	0 kW	0 kW		
HRR in all other rooms combined	NA			
D1 width	1m	.76m	.05-1m	
D2 width	1m	.38m	.05-1m	
D3 width	1m	.61m	.05-1m	
D4 width	1m	.82m	.05-1m	
D5 width	1m	.85m	.05-1m	
D6 width	1m	.62m	.05-1m	
D7 width	1m	.70m	.05-1m	
D8 width	1m	.37m	.05-1m	
D9 width	1m	.84m	.05-1m	
D10 width	1m	.19m	.05-1m	
D11 width	1m	.96m	.05-1m	
D12 width	1m	.92m	.05-1m	
D13 width	1m	.31m	.05-1m	
D14 width	1m	.95m	.05-1m	
D15 width	1m	.60m	.05-1m	
D16 width	1m	.55m	.05-1m	
D17 width	1m	.41m	.05-1m	
D18 width	1m	.44m	.05-1m	

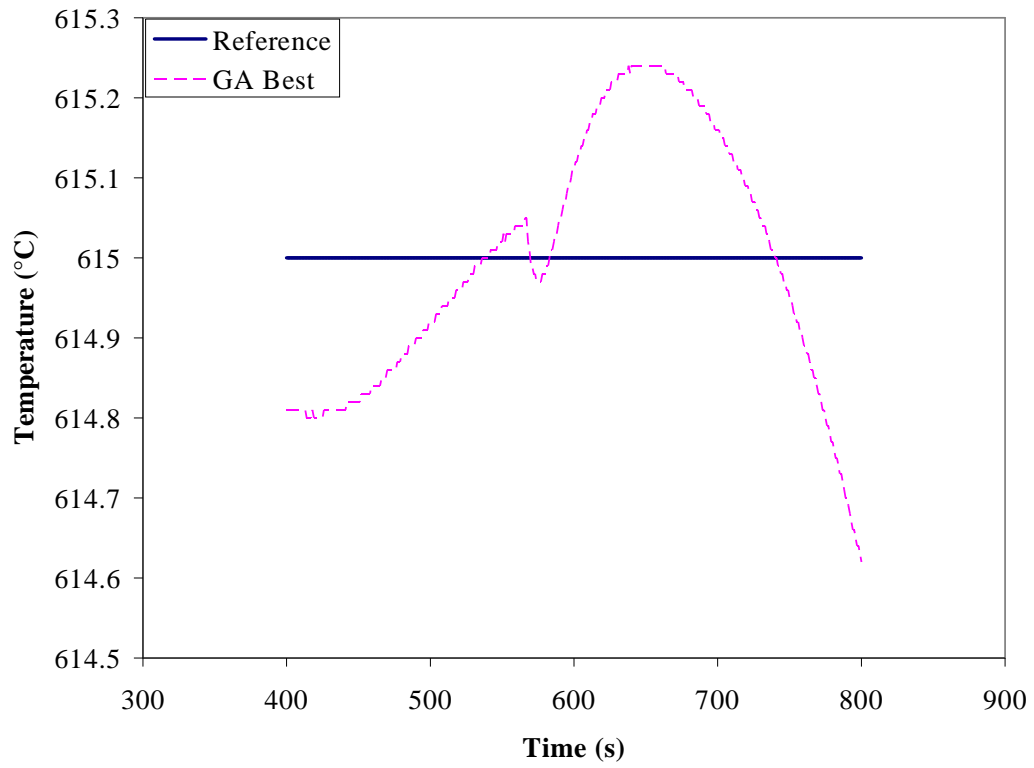
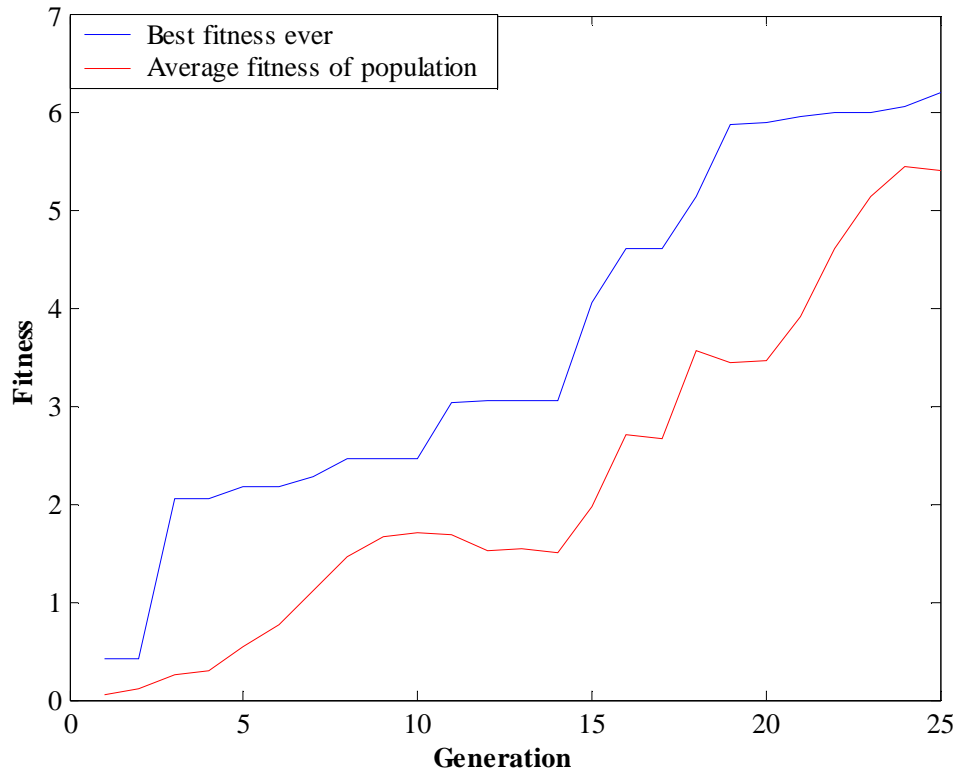
FDS_FR_b2



FDS_FR_b3

Parameters	Reference Values	GA Best	Bounds	Notes
Mass Loss Rate	6000 kW	4994 kW	200- 6000 kW	Population size 25, 25 generations. Temperature at 1200s is 578 °C. However 615 °C was used, to be more representative of the overall temperature profile.
Total HRR	3654 kW	2516 kW		
HRR Fire Room	3376 kW	2016 kW		
HRR Corridor	244 kW	494 kW		
HRR Room 1 (Analysis Window)	0 kW	0 kW		
HRR in all other rooms combined	NA	6 kW		
D1 width	1m	.44m	.05m-1.0m	
D2 width	1m	.49m	.05m-1.0m	
D3 width	1m	.73m	.05m-1.0m	
D4 width	1m	.63m	.05m-1.0m	
D5 width	1m	.51m	.05m-1.0m	
D6 width	1m	.36m	.05m-1.0m	
D7 width	1m	.05m	.05m-1.0m	
D8 width	1m	.98m	.05m-1.0m	
D9 width	1m	.60m	.05m-1.0m	
D10 width	1m	.49m	.05m-1.0m	
D11 width	1m	.84m	.05m-1.0m	
D12 width	1m	.51m	.05m-1.0m	
D13 width	1m	.51m	.05m-1.0m	
D14 width	1m	.31m	.05m-1.0m	
D15 width	1m	.45m	.05m-1.0m	
D16 width	1m	.58m	.05m-1.0m	
D17 width	1m	.53m	.05m-1.0m	
D18 width	1m	.71m	.05m-1.0m	

FDS_FR_b3



Appendix A6 continued. BRI and FDS direct comparisons.

1MW FDS and BRI

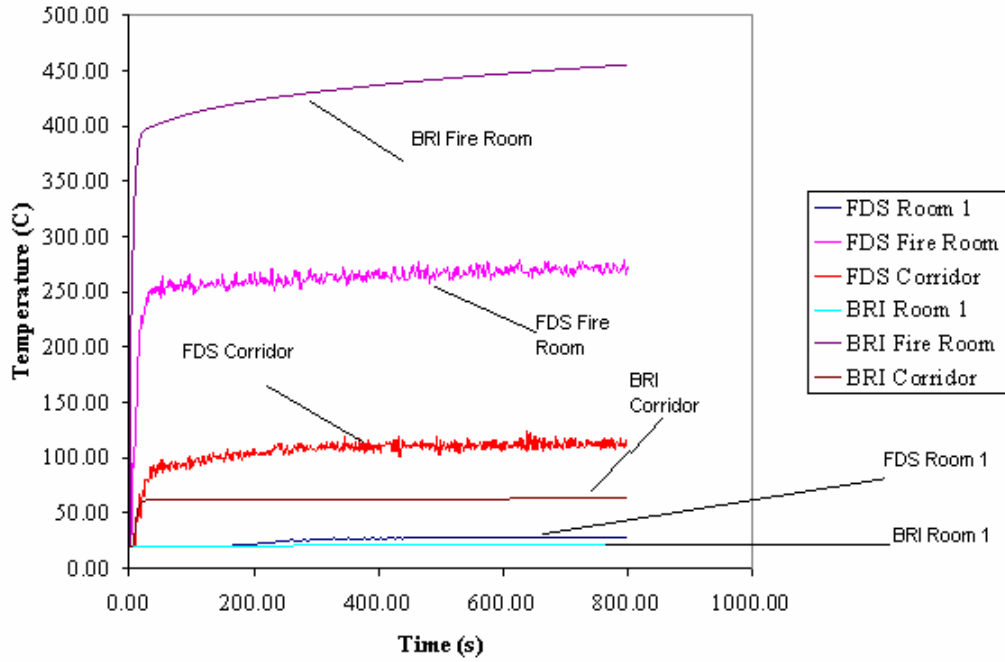


Figure 63. Upper Layer Temperatures for BRI and FDS for 1MW MLR.

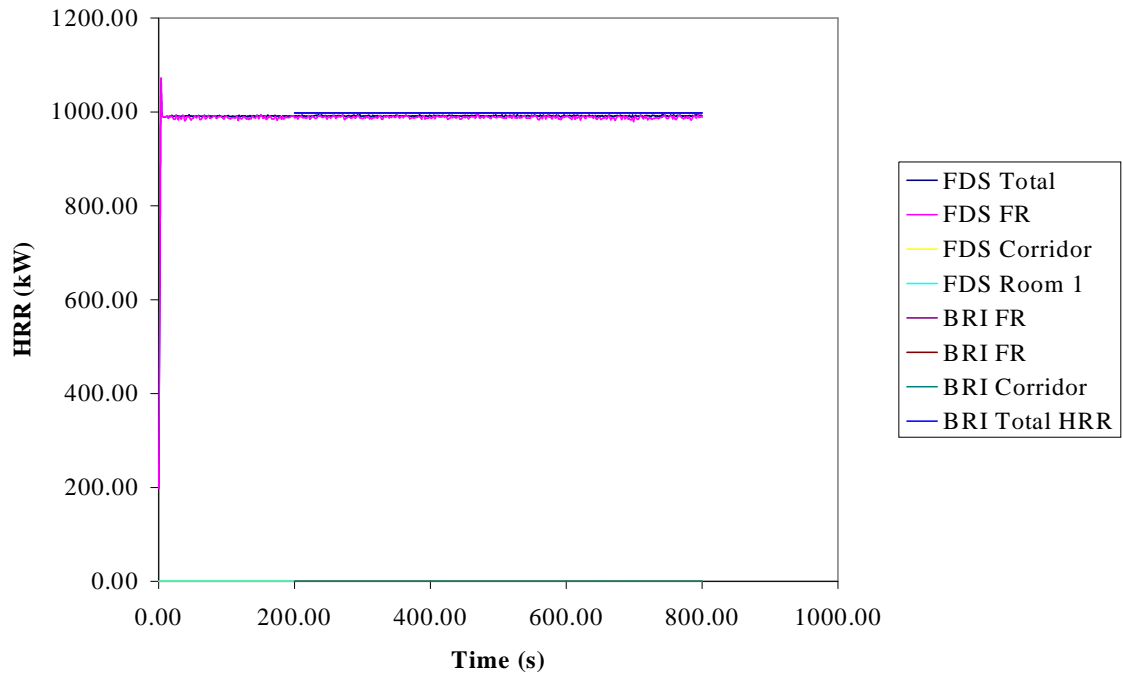


Figure 64. HRR Comparisons for BRI and FDS 1MW MLR.

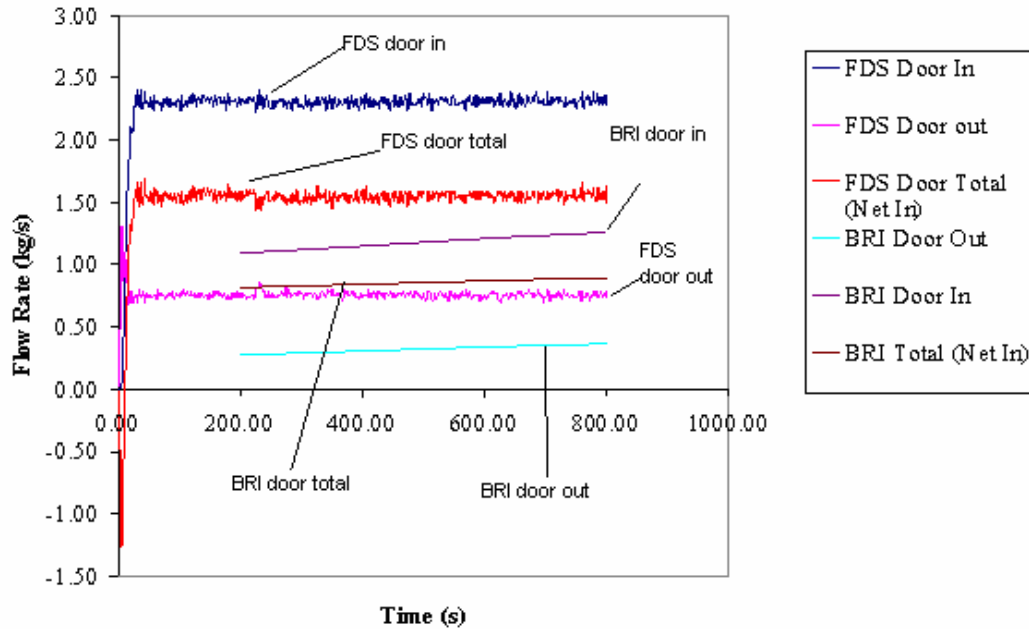


Figure 65. Mass Flow Rates through door for FDS and BRI.

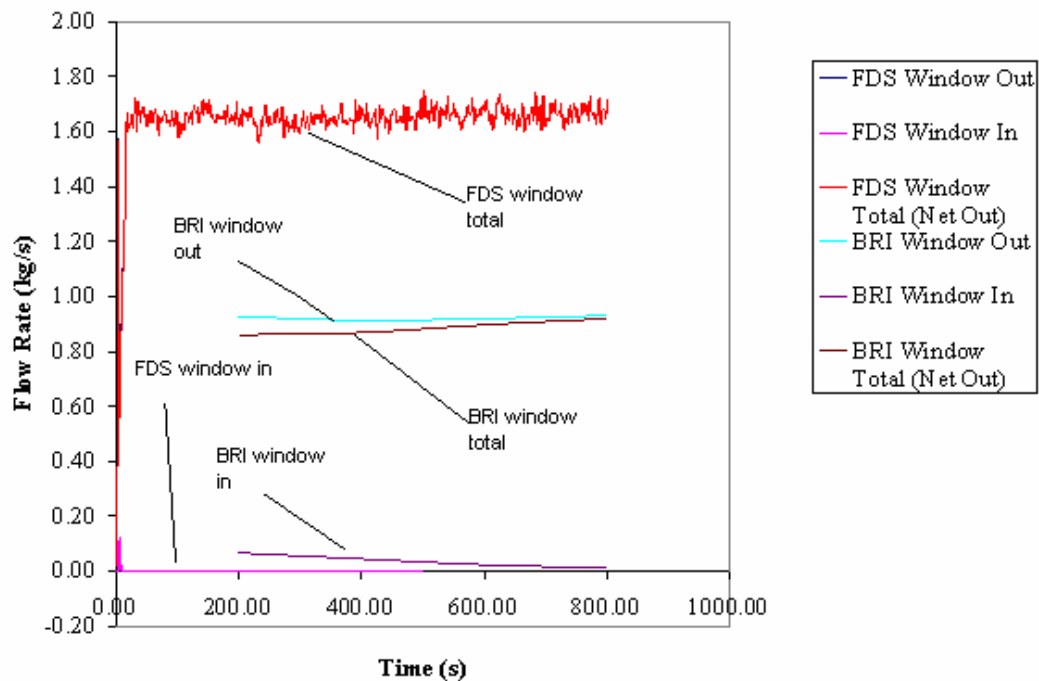


Figure 66. Mass flow rates through window for BRI and FDS 1MW MLR.

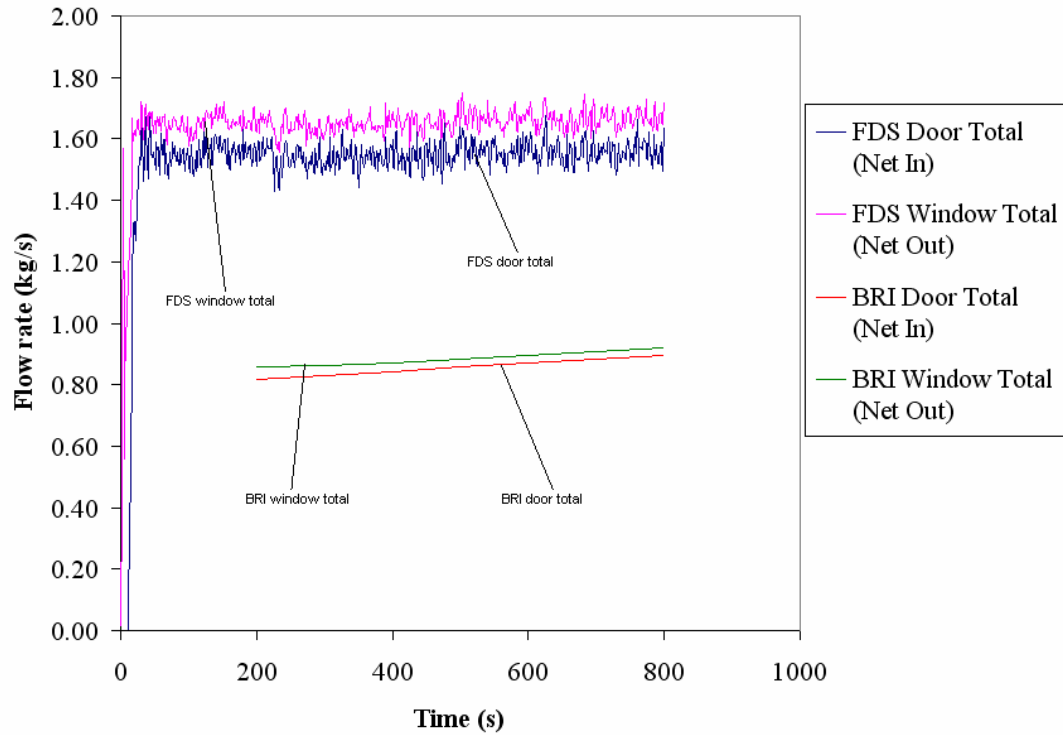


Figure 67. Total Mass Flow Rates through door and window for FDS and BRI 1MW MLR.

3MW FDS and BRI

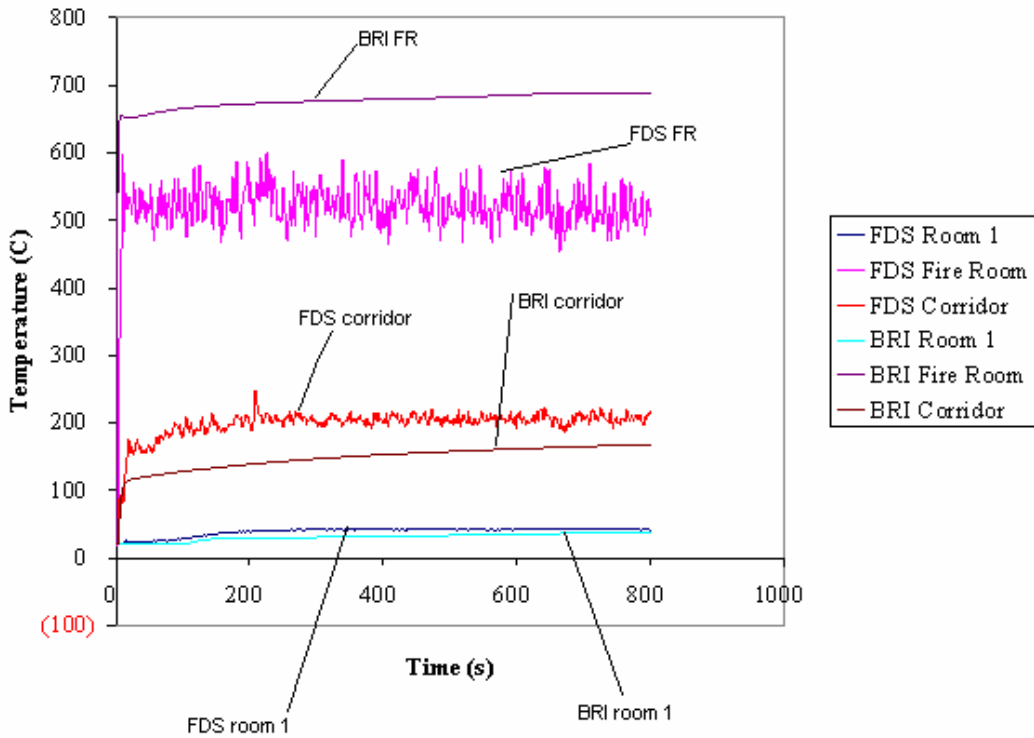


Figure 68. Upper layer temperature profile for BRI and FDS 3MW MLR.

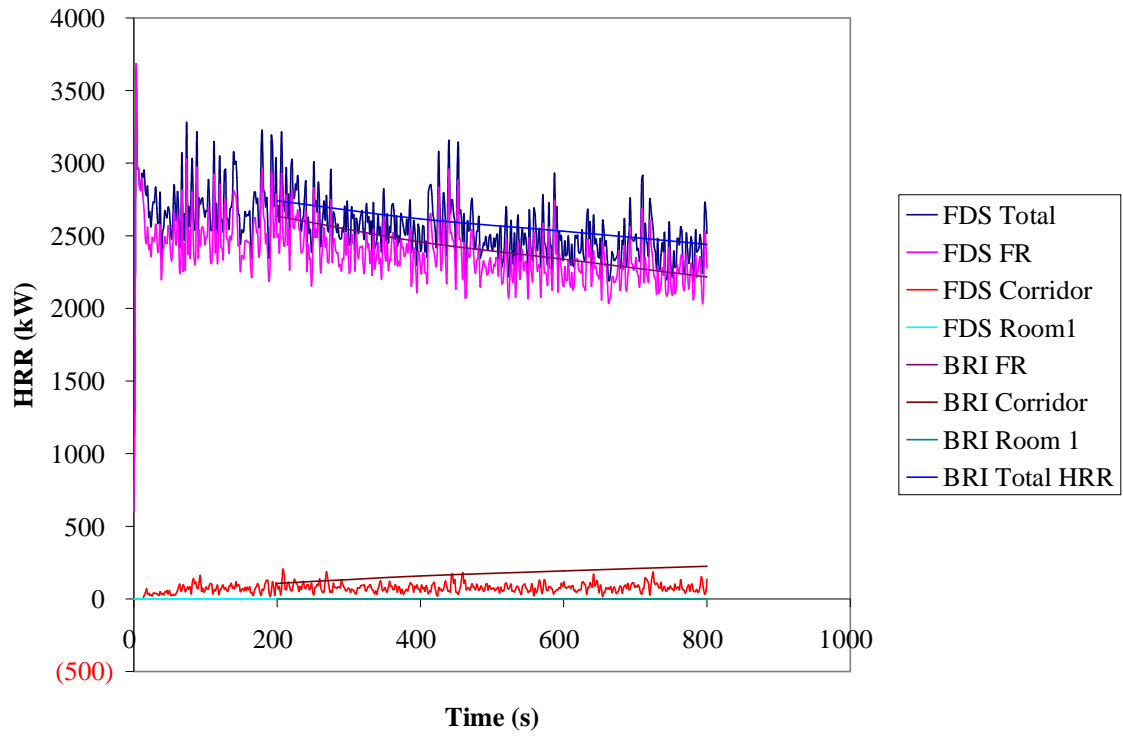


Figure 69. HRR comparisons for FDS and BRI for 3MW MLR.

Appendix B

Sample BRI2002 input files and sample IFM code structure.

Single Compartment Input File (3m x 3m x 3m)

```
Single Compartment
October 2006
01
Single Compartment
  6000.      1.      120.0      1.0
  1
    4.0
  1
1 (FIRE ROOM)      1      0.0      3.0      1      27      28      1
  0.0      3.00      3.00      0.0
  1      2      1      1.0      2.0      0.0      0
9999
9999
  1
  4      1
    0.0      120.0      240.0      6000.0
    0.0      720.0      3000      3000
    0.0      1.44      6.00      6.00
    0.0      0.0      0.0      0.0
  4
  1      1
    22.0      50.0
  0
  1
    22.0      50.0
  1
    0.0      10.0      0.33
    0.0
  0
9999
```

IFM Algorithm Calling function for single compartment

```
clear all;
clc;

tic
%This is the bounds on the Mass loss rate
bounds=[1000 4500]
initPop=initializega(1,bounds,'testFitness_final');
initPop

% Runs the GA for the default crossover and mutation functions
[Y endPop bPop trace] = ga(bounds,'testFitness_final',[],initPop,[1e-6 1
0],'maxGenTerm',1);

Y
endPop
toc
plot(trace(:,1),trace(:,2),'b-')
hold on
plot(trace(:,1),trace(:,3),'r-')
xlabel('Generation'); ylabel('Fitness')
legend('Best fitness ever', 'Average fitness of population')
%The blue line is a track of the best solution, the red line is a track of the
%average of the population
```

IFM Algorithm Evaluation Function for single compartment

```
function [sol, val] = testFitness_final(sol,options)
Y=xlsread('TEMPSM.xls');

MLR=sol(1);
b=MLR/500;
filename=[num2str(1)]
fid = fopen(filename, 'w')
fprintf(fid, '\n    0.0    720.0    %5.0f    %5.0f\n    0.0    1.44    %5.2f    %5.2f',
MLR, MLR, b(1), b(1));
fclose(fid);
!copy1.bat;
cd CMD_test;
!BRI.bat;
```

```
%each trial solutions temperature curve
[a]=dlmread('tempm.dat','0',[4 0 6003 1]);
cd c:\;
cd C:\HRR_with_CMD_Final;
%fitness assigned to each trial solution
val = (sqrt(sum((a(:,2)-Y(:,2)).^2)/(length((a(:,2))))))^-1;
```

Multiple Compartment Input File (4.5m x 4.5m x 3m rooms, one corridor 3.5m x 40.5m long)

SAMPLE BUILDING

2002.10.28

Multiple Compartment

0001

	800.0	1.0	200.0	1.0					
1	3.00								
19									
1W			1	0.0	3.00	1	11	11	1
	0.0	4.50	4.50						
2W			1	0.0	3.00	1	11	11	1
	0.0	4.50	4.50						
3W			1	0.0	3.00	1	11	11	1
	0.0	4.50	4.50						
4W			1	0.0	3.00	1	11	11	1
	0.0	4.50	4.50						
5W			1	0.0	3.00	1	11	11	1
	0.0	4.50	4.50						
6W			1	0.0	3.00	1	11	11	1
	0.0	4.50	4.50						
7W			1	0.0	3.00	1	11	11	1
	0.0	4.50	4.50						
8W			1	0.0	3.00	1	11	11	1
	0.0	4.50	4.50						
9W			1	0.0	3.00	1	11	11	1
	0.0	4.50	4.50						
10E (fire room)			1	0.0	3.00	1	11	11	1
	0.0	4.50	4.50						
11E			1	0.0	3.00	1	11	11	1
	0.0	4.50	4.50						
12E			1	0.0	3.00	1	11	11	1
	0.0	4.50	4.50						
13E			1	0.0	3.00	1	11	11	1
	0.0	4.50	4.50						
14E			1	0.0	3.00	1	11	11	1
	0.0	4.50	4.50						
15E			1	0.0	3.00	1	11	11	1
	0.0	4.50	4.50						
16E			1	0.0	3.00	1	11	11	1
	0.0	4.50	4.50						
17E			1	0.0	3.00	1	11	11	1
	0.0	4.50	4.50						
18E			1	0.0	3.00	1	11	11	1
	0.0	4.50	4.50						
19			1	0.0	3.00	1	11	11	1
	0.0	3.50	40.5						
1	19	1	0.63	2.00	0.0				0
1	20	1	1.0	2.50	1.5				0
2	19	1	0.05	2.00	0.0				0
2	20	1	0.0	2.50	1.5				0
3	19	1	0.97	2.00	0.0				0
3	20	1	0.0	2.50	1.5				0

4	19	1	0.10	2.00	0.0	0
4	20	1	0.0	2.50	1.5	0
5	19	1	0.84	2.00	0.0	0
5	20	1	0.0	2.50	1.5	0
6	19	1	0.80	2.00	0.0	0
6	20	1	0.0	2.50	1.5	0
7	19	1	0.23	2.00	0.0	0
7	20	1	0.0	2.50	1.5	0
8	19	1	1.00	2.00	0.0	0
8	20	1	0.0	2.50	1.5	0
9	19	1	1.00	2.00	0.0	0
9	20	1	0.0	2.50	1.5	0
10	19	1	0.37	2.00	0.0	0
10	21	1	1.0	2.50	1.5	0
11	19	1	0.83	2.00	0.0	0
11	21	1	1.0	2.50	1.5	0
12	19	1	0.67	2.00	0.0	0
12	21	1	0.0	2.50	1.5	0
13	19	1	0.23	2.00	0.0	0
13	21	1	0.0	2.50	1.5	0
14	19	1	0.33	2.00	0.0	0
14	21	1	0.0	2.50	1.5	0
15	19	1	0.66	2.00	0.0	0
15	21	1	0.0	2.50	1.5	0
16	19	1	0.53	2.00	0.0	0
16	21	1	0.0	2.50	1.5	0
17	19	1	0.47	2.00	0.0	0
17	21	1	0.0	2.50	1.5	0
18	19	1	0.90	2.00	0.0	0
18	21	1	0.0	2.50	1.5	0
9999						
9999						
10						
4	1					
	0.0	120.0	240.0	3000.0		
	5401	5401	5401	5401		
	10.80	10.80	10.80	10.80		
	0.0	0.0	0.0	0.0		
4						
1	1					
	20.0	50.0				
0						
1						
	20.0	50.0				
2						
	0.0	0.00	0.00			
	0.0					
0						
9999						

IFM Calling Function for Multiple Compartments

```
clear all;
clc;

tic
%First row is the Mass loss rate, next 18 rows are the bounds on the door widths.
bounds= [200 5250; ones(18,1)*[.25 1.5]];
initPop=initializega(1,bounds,'testFitness_final');
initPop;

% Now let's run the ga using all default genetic operators and mutations.
[Y endPop bPop trace] = ga(bounds,'testFitness_final',[],initPop,[1e-6 1
1],'maxGenTerm',1);

endPop'
Y'
toc
plot(trace(:,1),trace(:,2),'b-')
hold on
plot(trace(:,1),trace(:,3),'r-')
xlabel('Generation'); ylabel('Fitness')
legend('Best fitness ever', 'Average fitness of population')
%The blue line is a track of the best solution, the red is a track of the
%average of the population
```

IFM Evaluation Function for Multiple Compartments

```
function [sol, val] = testFitness_final(sol,options)
Y=xlsread('TEMPSM.xls');

MLR=sol(1);
b=MLR/500;
d1=sol(2);
d2=sol(3);
d3=sol(4);
d4=sol(5);
d5=sol(6);
d6=sol(7);
d7=sol(8);
d8=sol(9);
d9=sol(10);
d10=sol(11);
d11=sol(12);
```

```

d12=sol(13);
d13=sol(14);
d14=sol(15);
d15=sol(16);
d16=sol(17);
d17=sol(18);
d18=sol(19);

```

```

filename=['inppartFire.dat'];
fid = fopen(filename, 'w');
fprintf(fid, '\n %5.0f %5.0f %5.0f %5.0f\n %5.2f %5.2f %5.2f
%5.2f', MLR,MLR,MLR, MLR, b(1), b(1), b(1), b(1));
fclose(fid);
filename2=['inppartVent.dat'];
fid2=fopen(filename2, 'w');
% Using %4.2f, %3.2f, %2.2f, %1.2f, or %0.2f all give the same result as long as the
% parameter is smaller than 5 digits i.e. less than 10.00
%(period counted as a digit in fprintf)
fprintf(fid2, ' 1 19 1 %4.2f 2.00 0.0 0', d1);
fclose(fid2);
fid2=fopen(filename2, 'a');
fprintf(fid2, '\n 1 20 1 1.0 2.50 1.5 0');
fclose(fid2);
fid2=fopen(filename2, 'a');
fprintf(fid2, '\n 2 19 1 %4.2f 2.00 0.0 0', d2);
fclose(fid2);
fid2=fopen(filename2, 'a');
fprintf(fid2, '\n 2 20 1 0.0 2.50 1.5 0');
fclose(fid2);
fid2=fopen(filename2, 'a');
fprintf(fid2, '\n 3 19 1 %4.2f 2.00 0.0 0', d3);
fclose(fid2);
fid2=fopen(filename2, 'a');
fprintf(fid2, '\n 3 20 1 0.0 2.50 1.5 0');
fclose(fid2);
fid2=fopen(filename2, 'a');
fprintf(fid2, '\n 4 19 1 %4.2f 2.00 0.0 0', d4);
fclose(fid2);
fid2=fopen(filename2, 'a');
fprintf(fid2, '\n 4 20 1 0.0 2.50 1.5 0');
fclose(fid2);
fid2=fopen(filename2, 'a');
fprintf(fid2, '\n 5 19 1 %4.2f 2.00 0.0 0', d5);
fclose(fid2);
fid2=fopen(filename2, 'a');

```

```

fprintf(fid2, '\n 5 20 1 0.0 2.50 1.5 0');
fclose(fid2);
fid2=fopen(filename2, 'a');
fprintf(fid2, '\n 6 19 1 %4.2f 2.00 0.0 0, d6);
fclose(fid2);
fid2=fopen(filename2, 'a');
fprintf(fid2, '\n 6 20 1 0.0 2.50 1.5 0');
fclose(fid2);
fid2=fopen(filename2, 'a');
fprintf(fid2, '\n 7 19 1 %4.2f 2.00 0.0 0, d7);
fclose(fid2);
fid2=fopen(filename2, 'a');
fprintf(fid2, '\n 7 20 1 0.0 2.50 1.5 0');
fclose(fid2);
fid2=fopen(filename2, 'a');
fprintf(fid2, '\n 8 19 1 %4.2f 2.00 0.0 0, d8);
fclose(fid2);
fid2=fopen(filename2, 'a');
fprintf(fid2, '\n 8 20 1 0.0 2.50 1.5 0');
fclose(fid2);
fid2=fopen(filename2, 'a');
fprintf(fid2, '\n 9 19 1 %4.2f 2.00 0.0 0, d9);
fclose(fid2);
fid2=fopen(filename2, 'a');
fprintf(fid2, '\n 9 20 1 0.0 2.50 1.5 0');
fclose(fid2);
fid2=fopen(filename2, 'a');
fprintf(fid2, '\n 10 19 1 %4.2f 2.00 0.0 0, d10);
fclose(fid2);
fid2=fopen(filename2, 'a');
fprintf(fid2, '\n 10 21 1 1.0 2.50 1.5 0');
fclose(fid2);
fid2=fopen(filename2, 'a');
fprintf(fid2, '\n 11 19 1 %4.2f 2.00 0.0 0, d11);
fclose(fid2);
fid2=fopen(filename2, 'a');
fprintf(fid2, '\n 11 21 1 1.0 2.50 1.5 0');
fclose(fid2);
fid2=fopen(filename2, 'a');
fprintf(fid2, '\n 12 19 1 %4.2f 2.00 0.0 0, d12);
fclose(fid2);
fid2=fopen(filename2, 'a');
fprintf(fid2, '\n 12 21 1 0.0 2.50 1.5 0');
fclose(fid2);
fid2=fopen(filename2, 'a');
fprintf(fid2, '\n 13 19 1 %4.2f 2.00 0.0 0, d13);

```

```

fclose(fid2);
fid2=fopen(filename2, 'a');
fprintf(fid2, '\n 13 21 1 0.0 2.50 1.5 0');
fclose(fid2);
fid2=fopen(filename2, 'a');
fprintf(fid2, '\n 14 19 1 %4.2f 2.00 0.0 0', d14);
fclose(fid2);
fid2=fopen(filename2, 'a');
fprintf(fid2, '\n 14 21 1 0.0 2.50 1.5 0');
fclose(fid2);
fid2=fopen(filename2, 'a');
fprintf(fid2, '\n 15 19 1 %4.2f 2.00 0.0 0', d15);
fclose(fid2);
fid2=fopen(filename2, 'a');
fprintf(fid2, '\n 15 21 1 0.0 2.50 1.5 0');
fclose(fid2);
fid2=fopen(filename2, 'a');
fprintf(fid2, '\n 16 19 1 %4.2f 2.00 0.0 0', d16);
fclose(fid2);
fid2=fopen(filename2, 'a');
fprintf(fid2, '\n 16 21 1 0.0 2.50 1.5 0');
fclose(fid2);
fid2=fopen(filename2, 'a');
fprintf(fid2, '\n 17 19 1 %4.2f 2.00 0.0 0', d17);
fclose(fid2);
fid2=fopen(filename2, 'a');
fprintf(fid2, '\n 17 21 1 0.0 2.50 1.5 0');
fclose(fid2);
fid2=fopen(filename2, 'a');
fprintf(fid2, '\n 18 19 1 %4.2f 2.00 0.0 0', d18);
fclose(fid2);

fid2=fopen(filename2, 'a');
fprintf(fid2, '\n 18 21 1 0.0 2.50 1.5 0');
fclose(fid2);
!copy1.bat
cd CMD_test;
!BRI.bat
[a]=dlmread('tempm.dat','0',[4 0 3003 1]);
cd c:\;
cd C:\HRR_multi_compartment_doors;
val = (sqrt(sum((a(2000:3000,2)-Y(2000:3000,2)).^2)/(length((a(2000:3000,2))))))^(-1);

```

Bibliography

- [1] J.R. Hall, Jr. and A.E. Cote. "An overview of the fire problem and fire protection." In *Fire Protection Handbook*. 19th ed. Vol. 1. National Fire Protection Association. 2003, pp 2-1, 2-36.
- [2] T. Wakamatsu. Ed. "BRI2002: Two layer zone smoke transport model." *Fire Science and Technology*. Vol 23, No. 1 (Special Issue). 2004.
- [3] W.D. Davis, and G.P. Forney. "A sensor-driven fire model version 1.1," National Institute of Standards and Technology, NISTIR 6705. Jan 2001.
- [4] W.S. Lee, and S.K. Lee. "The estimation of fire location and heat release rate by using sequential inverse method," *Journal of the Chinese Society of Mechanical Engineers*. Vol 26, No. 2. pp. 201-207. 2005.
- [5] R.F. Richards, R.T. Ribail, A. W. Bakkom, and O.A. Plumb. "Fire detection, location and heat release rate through inverse problem solution. Part I: Theory," *Fire Safety Journal*. Vol. 28. pp. 323-350. 1997.
- [6] R.F. Richards, R.T. Ribail, A. W. Bakkom, and O.A. Plumb. "Fire detection, location and heat release rate through inverse problem solution. Part II: Experiment," *Fire Safety Journal*. Vol. 28. pp. 351-378. 1997.
- [7] D. Berry, A. Usmani, J. Torero, A. Tate, S. McLaughlin, S. Potter, A. Trew, R. Baxter, M. Bull, and M. Atkinson. "FireGrid: Integrated emergency response and fire safety engineering for the future built environment." Available: <http://www.firegrid.org/>. Accessed [June 23, 2007].
- [8] S. Wang, M. Berentsen, and T. Kaiser. "Signal processing algorithms for fire localization using temperature sensor arrays," *Fire Safety Journal* 40 (2005) pp. 689-697.
- [9] National Institute of Standards and Technology. *CFAST/FAST Version 6 Software*. Available at <http://fast.nist.gov/>. 2007.
- [10] H. Zhou, K. Cen, and J. Fan. "Multi-objective optimization of the coal combustion performance with artificial neural networks and genetic algorithms," *International Journal of Energy Research* 2005. pp. 29:499-510.
- [11] M Zhong, W. Xing, F. Weicheng, L. Peide, and C. Baozhi. "Airflow optimizing control research based on genetic algorithm during mine fire period." *Journal of Fire Sciences*. vol. 21 pp. 131. 2003.

- [12] L. Yang, B.F. Jones, and S. Hang. "A fuzzy multi-objective programming for optimization of fire station locations through genetic algorithms," *European Journal of Operational Research*. Vol 181. pp. 903-315. 2007.
- [13] Z. Zhao. "Steel columns under fire-a neural network based strength model," *Advances in Engineering Software*. Vol. 37. pp. 97-105. 2006.
- [14] G. Rein, C. Lautenberger, and A.C. Fernandez-Pello. "Application of genetic algorithms and thermogravimetry to determine the kinetics of polyurethane foam in smoldering combustion," *Combustion and Flame*. Vol. 146. 2006. pp. 95-108.
- [15] C. Lautenberger, G. Rein, and A.C. Fernandez-Pello. "The application of a genetic algorithm to estimate material properties for fire modeling from bench-scale fire test data," *Fire Safety Journal* 41 (2006) pp. 204-214.
- [16] B. Karlsson and J. Quintiere. "A Qualitative Description of Enclosure Fires." In *Enclosure Fire Dynamics*. CRC Press, 2000, pp.11-46.
- [17] A. Trouve. ENFP425, "Fire Modeling." ENFP425, Module 1. Fire Protection Engineering, University of Maryland. 2006.
- [18] R. Peacock. Personal Communication. National Institute of Standards and Technology. November 2006.
- [19] D. Madryzkowski, and W.D. Halton. "Cook County administration building fire, 69 West Washington, Chicago, Illinois, October 17, 2003: Heat release rate experiments and FDS simulations." National Institute of Standards and Technology. NIST Special Publication SP-1021. July 2004.
- [20] National Fire Protection Association. *NFPA92B: Standard for Smoke Management Systems in Malls, Atria and Large Areas*. 2000 ed. Quincy, MA.
- [21] W.D Walton, and P.H. Thomas. "Estimating Temperatures in Compartment Fires." In *SFPE Handbook of Fire Protection Engineering*. 3rd ed. 2002, pp3-171, 3-188.
- [22] "Optimization." Available: http://en.wikipedia.org/wiki/Category:Optimization_algorithms. Accessed June 27, 2007.
- [23] E.B. Magrab, S. Azarm, B. Balachandran, J.H. Duncan, K.E. Herold, G.C. Walsh. "Optimization," in *An Engineer's Guide to Matlab*, 2nd ed. New Jersey: Pearson Prentice Hall, 2005. pp 603-639.

- [24] C.R. Houck, and J.A. Joines. “A genetic algorithm for function optimization: A matlab implementation,”
<http://www.ie.ncsu.edu/mirage/GAToolBox/gaot/papers/gaot.ps>. Accessed [January 9, 2007].